

A11100 989903

NATL INST OF STANDARDS & TECH R.I.C.



A11100989903

/NBS monograph  
QC100 .U558 V100;1967 C.1 NBS-PUB-C 1959

# TRACE CHARACTERIZATION

## CHEMICAL AND PHYSICAL



U.S. DEPARTMENT OF COMMERCE

NATIONAL BUREAU OF STANDARDS

MONOGRAPH 100







UNITED STATES DEPARTMENT OF COMMERCE  
Alexander B. Trowbridge, *Acting Secretary*  
NATIONAL BUREAU OF STANDARDS · A. V. Astin, *Director*

# TRACE CHARACTERIZATION

## Chemical and Physical

W. Wayne Meinke and Bourdon F. Scribner, Editors

Institute for Materials Research  
National Bureau of Standards  
Washington, D.C. 20234

Based on lectures and discussions of the  
1st Materials Research Symposium  
held at the NBS, Gaithersburg, Maryland  
October 3-7, 1966



National Bureau of Standards Monograph 100

Issued April 28, 1967

---

For sale by the Superintendent of Documents, U.S. Government Printing Office  
Washington, D.C. 20402 - Price \$4.50

National Bureau of Standards

AUG 16 1967

134,824

QC

100

.U556

cop.2

circ.

### ABSTRACT

A symposium on Trace Characterization, Chemical and Physical was held at the National Bureau of Standards October 3-7, 1966. This volume contains the texts of invited lectures, and summaries by the rapporteurs of the contributed papers and discussion sessions. Topics covered include trace characterization and the properties of materials; electrical measurements; electrochemical methods; optical and x-ray spectroscopy; x-ray diffraction; optical methods; chemical spectrophotometry; nuclear methods; mass spectroscopy; preconcentration; sampling and reagents; and electron and optical microscopy.

**Key Words:** Trace characterization, electrochemical methods, x-ray spectroscopy, nuclear methods, electron and optical microscopy, optical spectroscopy, symposium on trace characterization.

**Library of Congress Catalog Card Number: 66-62907**

## FOREWORD

Development and improvement of measurement techniques for the characterization of materials by chemical and physical means is a prime responsibility of the Institute for Materials Research of the National Bureau of Standards. The Institute carries out this responsibility by serving as a focal point for development of measurement methodology and by encouraging the dissemination of relevant information. Measurement methodology is the essential forerunner to critically evaluated data on materials of importance to the advance of industry and commerce, one of the major missions of the Institute for Materials Research.

“Trace Characterization—Chemical and Physical,” the first annual symposium of the Institute for Materials Research, was held October 3–7, 1966, in the new NBS Laboratories at Gaithersburg, Maryland. Over 600 scientists representing industry, government, and university from the United States and from many other countries attended in order to take advantage of this excellent opportunity for dialogue between specialists of varying backgrounds and interests.

This volume contains the invited papers presented at the Symposium, together with summaries of the contributed papers and ensuing discussions by the rapporteurs. Symposia such as this one and those that will follow are tailored to provide an opportunity for interdisciplinary discussions of the state of the art in the broad spectrum of competences in materials science represented at the National Bureau of Standards.

GORDON K. TEAL, *Director*  
Institute for Materials Research.



## PREFACE

This book represents the formal report of the first materials research symposium of the NBS Institute for Materials Research, which was held at the new site of the National Bureau of Standards in Gaithersburg, Maryland, from October 3 through October 7, 1966. The subject of the symposium was "Trace Characterization—Chemical and Physical."

The Symposium was intended to bring together the leading authorities both from within the United States and from abroad in the many different fields which contribute to the physical and chemical characterization of materials, and especially to the detection and determination of trace amounts of defects and "foreign" substances. It was envisioned that this meeting would provide a forum for the examination of the successes and shortcomings of the present understanding of materials characterization and for the comparative evaluation of experimental methods and techniques. Its purpose was accordingly to improve the effectiveness of materials research (1) by summarizing the present capabilities and the future potential of the more useful tools for trace characterization of materials, and (2) by prompting the exchange of knowledge among the various disciplines upon which a complete and meaningful characterization depends.

In the past there have been a number of symposia which have focused on one or another specific aspect of trace characterization. Unfortunately, these symposia have often mirrored a rather parochial point of view and have encouraged the exhaustive study of one particular area of competence without a corresponding attempt to establish the exact status of that competence within the broad field of trace characterization. For this symposium, therefore, we made a serious effort to bring together the several groups whose experimental techniques and competences differ but who could find a common ground in meaningful discussions about trace characterizations. Emphasis was placed on a broad view of materials research as an interdisciplinary effort, and a special attempt was made to establish lines of communication among the specialists—chemists and physicists—engaged in the several aspects of materials characterization.

In general, the morning sessions were devoted to one-hour invited lectures by outstanding authorities in the field. The introductory lecture stressed the important relationship between trace composition and the properties of materials. The remaining sessions were devoted to a close examination of the "state of the art" and the future promise of the more useful tools for trace characterization. Among the specialties

considered were electrical and electrochemical measurements; nuclear methods; optical, mass, absorption, and x-ray spectroscopy; electron and x-ray diffraction; microscopy; and methods for sampling and preconcentration.

The contributed papers, numbering about 90, were distributed in preprint form to all registrants. Instead of an oral presentation of these papers, a summary of the salient points was given by a rapporteur who was, in each case, also an outstanding expert in the particular area under discussion. The afternoon sessions were, in general, given over to these rapporteur summaries and to discussions in which the rapporteur, the authors of the contributed papers, and the audience participated. Included in this volume are the texts of the invited papers and summaries of the contributed papers and discussions. A detailed listing of the contributed papers is given in an appendix.

An undertaking of such a magnitude would not have been possible without the wholehearted cooperation and assistance of a large group of people within the Institute for Materials Research and the National Bureau of Standards. Many of these individuals served on Symposium committees; their names will be found in the list of committees given in the appendix to this book. Particular thanks are due Dr. Roger G. Bates, Assistant General Chairman, Dr. John K. Taylor, Arrangements Chairman, and Dr. David H. Freeman, Social Chairman of the Symposium. The members of the Program Committee are to be commended for their highly effective planning and directing of the scientific program and their assistance in the publication of this book. The NBS Office of Technical Information under the direction of W. R. Tilley, with special help from R. T. Cook and J. E. Carpenter and their coworkers, gave invaluable assistance in many phases of the effort varying from the initial publicity brochures and programs to this final publication of the manuscripts. Within the Analytical Chemistry Division special thanks are due to R. Boreni and especially to Mrs. Rosemary Maddock who, more than anyone else, has provided the coordinating effort that has made early publication of this volume a reality.

W. WAYNE MEINKE  
BOURDON F. SCRIBNER.

December 15, 1966

**1st Materials Research Symposium**  
**Trace Characterization, Chemical and Physical**

**General Chairman**

W. Wayne Meinke  
Analytical Chemistry Division, NBS Institute for Materials Research

**Program Committee Chairman**

Bourdon F. Scribner  
Analytical Chemistry Division, NBS Institute for Materials Research

**Session Chairmen**

(Institute for Materials Research—National Bureau of Standards)  
(Washington, D.C. 20234)

Trace Characterization and the Properties of Materials	W. Wayne Meinke Analytical Chemistry Division
Electrical Measurements	Robert L. Parker Metallurgy Division
Electrochemical Methods	John K. Taylor Analytical Chemistry Division
Optical and X-ray Spectroscopy	Marvin Margoshes Analytical Chemistry Division
X-ray Diffraction	Ernest Ambler Inorganic Materials Division
Physical Optical Methods	Hans Frederikse Inorganic Materials Division
Chemical Spectrophotometry	Oscar Menis Analytical Chemistry Division
Nuclear Methods	James R. DeVoe Analytical Chemistry Division
Mass Spectroscopy	Bourdon F. Scribner Analytical Chemistry Division
Preconcentration, Sampling, and Reagents	David H. Freeman Analytical Chemistry Division
Electron and Optical Microscopy	John B. Wachtman, Jr. Inorganic Materials Division



## CONTENTS

	Page
Foreword.....	iii
Preface.....	v
Session subjects and chairmen.....	vii
INTRODUCTION.....	1
TRACE CHARACTERIZATION AND THE PROPERTIES OF MATERIALS	
<i>Hannay, N. B.</i> , Lecturer	
Introduction.....	5
Characterization.....	6
The Relation of Properties to Composition and Structure.....	7
Electrical Properties.....	7
Semiconductors.....	7
Metals.....	10
Superconductors.....	14
Ionic Conductivity.....	14
Optical Properties.....	15
Alkali Halides.....	16
Luminescence.....	17
Magnetic Properties.....	18
Mechanical Properties.....	19
Structural Transformations.....	24
Chemical Reactivity.....	29
Radiation Effects in Solids.....	33
Surfaces.....	35
Characterization and Properties.....	36
References.....	38
ELECTRICAL MEASUREMENTS FOR TRACE CHARACTERIZATION	
<i>Weisberg, L. R.</i> , Lecturer	
Introduction.....	39
Value of Electrical Measurements for Analysis.....	39
Criteria for Analytical Use.....	39
Characteristics of Electrical Measurements.....	40
Applications of Electrical Measurements.....	42
Fundamental Principles and Apparatus.....	50
Fundamentals.....	50
Resistivity.....	53
Residual Resistivity.....	57
Hall Effect.....	60
Thermally Stimulated Currents (TSC).....	63
Summary and Conclusions.....	65
References.....	67

## ELECTRICAL MEASUREMENTS—Contributed Papers and Discussion

*Powell, R. L., Rapporteur*

	Page
Introduction.....	69
Contributed Papers.....	71
Discussion.....	73
References.....	74

## TRACE CHARACTERIZATION BY ELECTROCHEMICAL METHODS

*Laitinen, H. A., Lecturer*

Introduction.....	75
Methods Based on Passage of Faradaic Current.....	76
Measurement of Current as Related to Concentration.....	76
Classical Polarography.....	76
“Tast” Polarography or Intermittent Polarography.....	78
Derivative Polarography.....	79
Pulse Polarography.....	80
Square Wave Polarography.....	84
Alternating Current Polarography.....	85
Radiopolarography.....	86
Catalytic Currents in Polarography.....	88
Adsorption Effects in Polarography.....	88
Measurements of Current at Electrodes of Constant Area (Voltammetry).....	88
Steady state methods.....	88
Single sweep and cyclic voltammetry.....	89
Voltage step chronoamperometry.....	90
Chronopotentiometry.....	90
Coulometry.....	91
Coulometry at Constant Potential.....	91
Coulometry at Constant Current.....	92
Coulometry of Surface Layers.....	92
Thin Layer Coulometry.....	92
Coulometric Titration.....	93
Chronocoulometry.....	94
Galvanic Analysis.....	95
Coulostatic Analysis.....	95
Stripping Analysis.....	96
Electrolytic Concentration.....	101
Methods Based on Electrodes at Equilibrium.....	101
Direct Potentiometry.....	101
Electrodes of the First Class.....	101
Electrodes of Second and Third Classes.....	102
Glass Electrodes.....	102
Liquid Ion Exchange Membrane Electrode.....	103
Precipitate-Impregnated Membrane Electrodes.....	103
Precision Null-Point Potentiometry.....	103
Methods in Which Faradaic Current is Unimportant.....	104
Conductance.....	104
High Frequency Admittance.....	104
Double Layer Capacitance Measurements.....	105
Summary.....	105
References.....	107

## ELECTROCHEMICAL METHODS—Contributed Papers and Discussion

*Osteryoung, R. A., Rapporteur*

Page

Introduction.....	111
Contributed Papers.....	112
Discussion.....	119
References.....	120

## OPTICAL AND X-RAY SPECTROSCOPY

*Addink, N. W. H., Lecturer*

Introduction.....	121
Flame Emission and Absorption.....	122
Experimental Test of Theoretical Considerations.....	122
Theoretical Considerations Concerning the Influence of Temperature.....	125
Comparison of Absorption and Emission.....	129
Analysis of Multicomponent Systems in Solution.....	129
Future Prospects.....	129
Classical Emission Spectral Analysis.....	130
The Arc.....	130
General Considerations.....	130
The Significance of the Rate of Evaporation, Sideward Losses and the Temperature of Column and Mantle.....	133
Additions before Arcing.....	134
Limits of Detection.....	134
Impurities Present in Graphite Electrodes.....	136
Other Methods of Evaporation and Excitation.....	136
The Spark.....	136
Future Prospects.....	138
X-Ray Fluorescence and Microprobe Analysis.....	139
X-Ray Fluorescence.....	139
General Considerations.....	139
Non-linear Working Curves.....	141
Thin Layers.....	141
Factors Bearing on Fluorescence Energies.....	142
Microprobe Analysis.....	143
Future Prospects (General).....	143
Final Conclusions.....	144
Future Prospects (General).....	146
Acknowledgments.....	146
References.....	147

## OPTICAL AND X-RAY SPECTROSCOPY—Contributed Papers and Discussion

*Kaiser, H., Rapporteur*

Introduction.....	149
Contributed Papers.....	149
Nomenclature.....	152
Limit of Detection.....	153
References.....	164

## EFFECTS OF TRACE IMPURITIES ON X-RAY DIFFRACTION

*Chikawa, J. and Newkirk, J. B. Lecturers*

Introduction.....	165
X-Ray Diffraction Topography.....	166
Experimental Methods.....	167
Berg-Barrett.....	167
Double Crystal.....	168

	Page
Scanning Transmission.....	169
Anomalous Transmission.....	171
Causes of Contrast.....	171
Homogeneous Dilation and Tilt Contrast.....	172
Direct Image.....	173
Dynamical Images.....	173
The Effects of Impurity on Dislocation Images.....	175
Imperfections Produced From Trace Impurities.....	179
Precipitates.....	180
Impurity Segregation: Non-Uniform Impurity Distribution.....	182
Lattice Parameter Variations Due to Impurities.....	186
Double Crystal Method.....	187
Moire Patterns.....	189
Effect of Impurities on Integrated Intensity of X-ray Diffraction.....	191
Integrated Diffracted Intensity in Reflection.....	192
Impurity Effect on Anomalous Transmission.....	193
Impurity Effect on Electron Density Distribution.....	195
Electron Density Map—Difference Method.....	195
Precise Determination of Structure Factors by Means of Pendellösung Fringes...	196
Other Effects of Impurities.....	198
Influence of Impurities on Phase Stability.....	198
Influence of Impurities on Solid State Reaction Kinetics.....	199
Summary.....	199
Acknowledgements.....	199
References.....	199
<b>X-RAY DIFFRACTION—Contributed Papers and Discussion</b>	
<i>Peiser, H. S., Rapporteur</i>	
Introduction.....	203
Contributed Papers.....	205
Discussion.....	208
References.....	209
<b>PHYSICAL OPTICAL METHODS—Contributed Papers and Discussion</b>	
<i>Frederikse, H. P. R., Rapporteur</i>	
Introduction.....	211
Invited and Contributed Papers.....	212
References.....	214
<b>CHEMICAL SPECTROPHOTOMETRY IN TRACE CHARACTERIZATION</b>	
<i>West, T. S., Lecturer</i>	
Introduction.....	215
Molecular-Absorption Spectrophotometry.....	217
Selectivity of Reaction.....	217
Mechanism of Colour Production.....	219
Identity of Liganding Atom.....	220
Steric Hindrance in Organic Reagents.....	221
Chelate-Cage Reagent Molecules.....	222
Formation of Ternary Complexes.....	224
Methods of Ternary Complex Formation.....	224
The Alizarin Complexan-Lanthanon System for Fluoride Ion.....	225
The Bis[diphenanthroline-silver(I)] BPR Ternary System, etc.....	227
Sensitivity of Reaction.....	230
The Sensitivity Barrier.....	231

	Page
Surmounting the Sensitivity Barrier.....	232
Evolution of Amplification Reaction.....	233
Evolution of Kinetochromic Spectrophotometry.....	234
Molecular Absorption Spectrophotometry in the Future.....	237
Molecular Fluorescence Spectrophotometry (Spectrofluorimetry).....	237
Absorption Re-emission Processes.....	239
Phosphorescence and the Triplet State.....	242
Extinction of Fluorescence.....	243
Quenching Processes.....	243
Chemical Reaction.....	243
Intermolecular Collision and Temperature Effect.....	243
Viscosity of Medium.....	244
Nature of Solvent Medium.....	244
Charge-transfer Processes.....	244
Dissolved Cations and Ionic Strength.....	245
Effect of Dissolved Oxygen.....	245
Radiative Quenching and Delayed Fluorescence.....	245
Non-Quenching Extinction Processes.....	246
Instrumentation.....	247
Choice of Instrument.....	248
Physical Laws Governing Fluorescence Emission.....	249
Basic Differences Between Fluorimetry and Absorbance.....	252
Reagents for Spectrofluorimetric Analysis.....	252
Character of Reacting Cation.....	253
Nature of Fluorogenic Reagents.....	254
Aliphatic Compounds.....	254
Aromatic Compounds.....	254
Molecular Configuration.....	255
Steric Effects.....	256
Principal Types of Fluorogenic Reagent.....	257
Fluorescence Energy Transfer Systems.....	258
Fluorometric Reagents in Practice.....	258
Assessment of Molecular Fluorescence Spectrophotometry as an Analytical Technique.....	259
Prospects for the Future.....	266
Atomic Absorption Spectrophotometry.....	266
Presentation of Atoms for Analysis.....	267
The Atom Furnace Reservoir.....	267
Flame Reservoirs.....	268
Processes in Flames.....	268
Nebulisation of Solutions.....	270
Other Atom Reservoirs.....	271
Hollow Cathode Sputtering.....	271
Electric Discharge and Plasma Jets.....	271
Atomic Spectra and the Hollow Cathode Lamp.....	272
Necessity for Monochromator.....	273
Multi-element Lamps.....	273
Monochromated Continuum Sources.....	274
Spectral Discharge Lamps.....	274
Microwave-powered Sources, etc.....	275
Types of Burner.....	275
Long Flames.....	276
Types of Flame Medium.....	277

	Page
Conventional Flames.....	277
The Nitrous Oxide-Acetylene Flame.....	278
Types of Hollow Cathode Lamp.....	278
High Intensity Hollow Cathode Lamps.....	279
Analytical Relationships in Atomic-Absorption Spectrophotometry.....	279
Choice of Wavelength.....	279
Assessment of Atomic-Absorption Spectrophotometry as an Analytical Trace Technique.....	280
Future Developments in Atomic-Absorption Spectrophotometry.....	283
Atomic Fluorescence Spectrophotometry.....	284
Types of Atomic Fluorescence Lines.....	286
Analytical Relationships in Atomic-Fluorescence Spectrophotometry.....	287
Instrumentation.....	289
General Arrangement.....	289
Types of Burner.....	289
Fuel Gases.....	290
Excitation Sources for Atomic Fluorescence Spectrophotometry.....	291
Spectral Discharge Lamps and Microwave-powered Sources.....	291
Continuum Sources.....	292
Sensitivity and Selectivity of Atomic Fluorescence Spectrophotometry.....	292
Determination of Selenium and Tellurium.....	294
Assessment of Atomic Fluorescence Spectrophotometry as an Analytical Technique.....	295
Future Developments in Atomic-Fluorescence Spectrophotometry.....	297
References.....	298
 CHEMICAL SPECTROPHOTOMETRY—Contributed Papers and Discussion	
<i>Menis, Oscar, Rapporteur</i>	
Introduction.....	303
Contributed Papers.....	303
Discussion.....	305
References.....	306
 RADIOACTIVITY TECHNIQUES IN TRACE CHARACTERIZATION	
<i>Smales, A. A., Lecturer</i>	
Introduction.....	307
Activation Analysis.....	307
General Principles.....	307
Activating Agents and Irradiation Facilities.....	310
Slow neutrons.....	310
Fast neutrons.....	316
Gamma photons.....	317
Charged particles.....	320
Prompt Radiation Techniques.....	322
Radiochemical Separations.....	323
Instrumentation.....	325
Accuracy and Precision.....	326
Position of Activation Analysis Relative to other "Trace Characterisation" Methods.....	326
Analysis Using Radioactive Tracers.....	327
Introduction.....	327
Isotopic Methods.....	328
Single isotope dilution.....	328
Stoichiometric isotope dilution.....	329

Page

Isotopic exchange.....	330
Non-isotopic Methods.....	331
Isotope derivative and derivative dilution.....	331
Isotope displacement.....	332
Radiorelease.....	332
Radiometric Titration.....	333
Assessment of Radioactive Trace Methods.....	333
Avoidance of Analysis by Means of Tracers.....	334
Concluding Remarks.....	335
Acknowledgements.....	335
References.....	335
<b>NUCLEAR METHODS—Contributed Papers and Discussion</b>	
<i>Guinn, V. P., Rapporteur</i>	
Neutron Activation Analysis.....	337
Thermal-Neutron.....	337
Fast-Neutron.....	340
Photonuclear Activation Analysis.....	342
Charged-Particle Activation Analysis.....	344
Other Activation Analysis Topics.....	345
Other Nuclear Methods.....	346
References.....	346
<b>SPARK SOURCE MASS SPECTROMETRIC ANALYSIS OF SOLIDS</b>	
<i>Ahearn, A. J., Lecturer</i>	
Introduction.....	347
Mass Spectrometry with Spark Source.....	348
Analytical Capabilities of Spark Source Technique.....	350
Factors Limiting Detection Sensitivity.....	351
Diffuse Background.....	351
Line Background.....	355
Factors Limiting Accuracy of Analysis.....	358
Transmission Stability of Instrument.....	359
Reciprocity Fulfillment.....	359
Emulsion Sensitivity—Dependence on Element.....	359
Calibration of Emulsion.....	360
Spark Source Ionization Pattern.....	360
Integration of Ion Intensity Profile.....	360
The Relative Sensitivity Problem.....	361
Ion Samples versus Standard Solid Samples.....	362
Precision Capabilities of Spark Source Technique.....	366
The Homogeneity Problem.....	370
Standard Sample Needs and Possibilities.....	371
Summary.....	372
Conclusion.....	373
References.....	374
<b>MASS SPECTROSCOPY—Contributed Papers and Discussion</b>	
<i>Owens, E. B., Rapporteur</i>	
Introduction.....	377
Analytical Applications.....	377
The State of the Art—Improving Accuracy.....	378
Sensitivity Coefficients.....	379
Photoplate Evaluation.....	380
Ion Charge Distribution.....	381

	Page
Computer Use in Calculations.....	381
Molecules Found in Spark Spectra.....	381
Quantitative Mass Spectrography.....	382
Comments from the Authors and Discussion from the Floor.....	382
References .....	384
PRECONCENTRATION IN TRACE ANALYSIS	
<i>Minczewski, J., Lecturer</i>	
Introduction.....	385
Preparation of Sample.....	387
The Analyzed Materials and Sample.....	387
The Technique of Work.....	390
Hermetization of Operations.....	390
Laboratory Vessels and Containers.....	391
Reagents.....	395
Concentration and Separation of Traces.....	396
Masking.....	397
Precipitation and Coprecipitation.....	398
Extraction.....	402
Chromatography.....	406
Volatility.....	409
Zone Melting.....	412
Final Remarks.....	413
Acknowledgements.....	414
References.....	414
PRECONCENTRATION, SAMPLING, AND REAGENTS—Contributed Papers and Discussion	
<i>Morrison, G. H., Rapporteur</i>	
Introduction.....	417
Preconcentration and Separation Methods.....	419
Reagents.....	421
Sampling and Sample Preparation.....	422
Discussion.....	424
References.....	425
THE STUDY OF CRYSTAL IMPERFECTIONS BY MEANS OF OPTICAL METHODS AND BY MEANS OF ELECTRON MICROSCOPY AND ELEC- TRON DIFFRACTION	
<i>Amelinckx, S., Lecturer</i>	
Introduction.....	427
Historical Survey.....	428
Structural Defects.....	431
Dislocations.....	431
Definition, Displacement Vector.....	431
Burgers Circuit—Burgers Vector.....	432
Dislocation Loops.....	433
Displacement Fields.....	435
Stress Fields—Cottrell Interaction.....	437
Energy of a Dislocation.....	437
Force on a Dislocation; Motion of Dislocations.....	438
Forces Between Dislocations.....	440
Multiplication of Dislocations.....	440
Stacking Faults. Partial Dislocations.....	441
Arrays of Dislocations.....	443

	Page
Polygonization.....	445
Observation Methods.....	447
Surface Methods.....	447
Growth Spirals.....	447
Evaporation Spirals.....	449
Etching.....	450
Bulk Methods.....	455
Decoration.....	455
Birefringence.....	467
Electron Microscopy and Electron Diffraction.....	468
Transmission Electron Microscopy.....	468
Introduction.....	468
Principle of the Method.....	469
Specimen Preparation.....	470
Electron Diffraction in Perfect Crystals.....	471
Kikuchi lines—Determination of $s$ .....	472
Extinction Contours.....	474
Thickness contours.....	474
Inclination or Bend Contours.....	475
Contrast at Dislocations.....	477
Origin of the Contrast.....	477
Determination of the Direction of the Burgers Vector. Extinction Conditions...	479
Determination of the Sign of the Dislocations (i.e., the Sense of the Burgers Vector).....	483
Determination of the Length of the Burgers Vector.....	483
Dislocations Inclined with Respect to the Foil; Oscillating Contrast.....	487
Dislocations Seen End On.....	487
Stacking Faults.....	490
Types of Stacking Faults.....	490
In f.c.c. Crystals.....	490
In h.c.p. Crystals.....	492
Antiphase Boundaries; Periodic Antiphase Boundaries and Stacking Faults...	493
Origin of the Contrast.....	493
Some Properties of Stacking Fault Fringes.....	496
Displacement Vector Determination.....	497
Determination of the Type of Stacking Fault.....	497
In f.c.c. Crystals.....	497
Hexagonal Close Packed Crystals.....	500
The Measurement of Stacking Fault Energies.....	501
Ribbons.....	501
Extended Nodes.....	504
Other Methods Based on Electron Microscopy.....	508
Contrast at Slip Traces.....	508
Point Defects and Dislocations.....	509
Processes Giving Rise to Point Defect Clusters.....	510
Quenching.....	510
Irradiation.....	511
Plastic Deformation.....	511
Deviations From Stoichiometry.....	511
Nature of the Defect Clusters.....	512
Dislocation Loops.....	512
Stacking Fault Tetrahedra.....	514
Cavities.....	516
Helices.....	516

	Page
Methods to Determine the Character of the Loops.....	516
The Geometrical Method.....	517
The Tilting Method.....	520
Loops Seen Edge On.....	520
Stacking Fault Method.....	521
The Burgers Vector Method.....	522
Domain Boundaries.....	524
Ferroelectric Domains.....	524
Anti-ferromagnetic Domain Boundaries.....	527
Domains Due to Interstitial Ordering.....	527
Ferromagnetic Domain Walls.....	528
Other Planar Defects.....	531
Direct Lattice Resolution.....	531
Moiré Patterns.....	532
The Effect of the Presence of Defects on the Diffraction Pattern.....	537
Discussion.....	538
Acknowledgements.....	540
References.....	540
<b>ELECTRON AND OPTICAL MICROSCOPY—Contributed Papers and Discussion</b>	
<i>Wilsdorf, H. G. F., Rapporteur</i>	
Introduction.....	547
Contributed Papers.....	549
Discussion.....	557
References.....	559
APPENDIX I. List of contributed papers.....	561
APPENDIX II. Symposium committees.....	567
INDEX.....	569

# TRACE CHARACTERIZATION

## Chemical and Physical

### INTRODUCTION

**W. WAYNE MEINKE and BOURDON F. SCRIBNER**

*Institute for Materials Research  
National Bureau of Standards  
Washington, D.C. 20234*

The problem of the meaningful measurement of "traces," be they chemical contaminants or physical defects, has become critical during the past few years as the field of materials research has developed and matured. One to two decades ago the appellation "spectroscopically pure" was sufficient to characterize materials for almost any use, whether in research or in technology. More recently, however, development of special preparation techniques for high-purity materials and the discovery of unique properties in these highly-purified materials has resulted in a situation where our capabilities for preparation and our demands in utilization have often far outstripped our ability to characterize.

Furthermore, there exists at the present time a multitude of methods and techniques which have the potential for developing characterization information. Many of these methods depend upon physical principles originally discovered and investigated without regard for possible analytical applications. They often require specialized equipment and understanding and have remained the concern of special groups of scientists. Each usually serves an important analytical function, and thus many of these competences have become highly developed and self-sufficient—with their own disciples, their own vocabulary, their own symposia, and their own societies. Each group explores in depth the potentialities of its own area and develops elaborate programs for remedying its own deficiencies and limitations.

Unfortunately, interest in cross-fertilization with other parallel competences is often minimal. Specific symposia dedicated to a given competence rarely permit time for a glimpse of alternate modes of operation. Competing sessions at general meetings discourage the broadening which is so important in the development of a proper perspective.

What the practitioner of any area of characterization should understand is that the ultimate user of his information does not care whether the effort has come from chemistry or physics, from spectroscopy, electrochemistry, or nuclear techniques. Nor is he concerned with whether the result has emanated from a highly developed competence

with decades of experience and tradition or from a newly discovered and newly exploited principle of nature. Rather, he wants accurate characterization information for certain critical aspects of his material so that he can assure consistent reproduction of this material.

Eleven years ago this need was recognized in the biomedical field and resulted in a conference on Trace Analysis sponsored by the Sloan-Kettering Institute and the New York Academy of Sciences. This symposium covered what might be called the "chemical" methods of trace characterization and emphasized the application of these techniques to the elements of biomedical significance at the parts per million level. The papers for this symposium have been published [1]<sup>1</sup> and form a very useful reference.

In the past decade the areas of solid state physics and chemistry have developed rapidly, with greatly expanded requirements for sensitivity and accuracy, which have intensified this demand for development of the best in many types of characterization methods. Two books [2, 3] have appeared which present, side by side, the case for several of the most important methods. Detailed reviews and bibliographies [4] giving reference to the original literature form excellent source material for further exploration of the subject.

The approach of the present volume has been somewhat different. Rather than emphasize an exhaustive treatment, we suggested that the invited papers consist of candid reports on the present status of efforts in trace characterization in all pertinent categories of the particular subject area, together with a forecast of the future potential. In addition, we proposed that the papers should contain some discussion of basic principles, but we regarded the critical evaluation of the field to be of primary importance. Furthermore, we suggested that the correct emphasis could perhaps be achieved by considering that the author was summarizing the "state of the art" in his specialty for the benefit of experts in the other fields.

Selection of the topics evidently had to be arbitrary, but the subjects chosen included most of the areas which today give the major promise for future improvements in trace characterization.

This volume then brings together state of the art summaries in most of the areas pertinent today for trace characterization. The authors have distilled the experience of many years into their papers and have also provided a glimpse of problems to be faced in the future. In addition, the summaries by the rapporteurs of contributed papers and discussions bring attention to current research in characterization and round out the treatment of each subject. Consequently, it is our hope that this book will provide guidance in materials characterization both for the present and for a number of years to come.

---

<sup>1</sup> Figures in brackets indicate the literature references at the end of this Introduction.

**References**

- [1] Yoe, John H., and Koch, Henry J., Jr., Eds., Trace Analysis, John Wiley & Sons, New York, 1957.
- [2] Cali, J. Paul, Ed., Trace Analysis of Semiconductor Materials, MacMillan Co., New York, 1964.
- [3] Morrison, George H., Ed., Trace Analysis, Physical Methods, Interscience, New York, 1965.
- [4] See for example Anal. Chem. **38**, No. 5, Annual Reviews (1966).



# TRACE CHARACTERIZATION AND THE PROPERTIES OF MATERIALS

N. B. HANNAY

*Bell Telephone Laboratories, Incorporated  
Murray Hill, New Jersey 07971*

## 1. Introduction

The rapid growth of solid-state science and technology in recent years has brought with it a surge of interest in the materials sciences. Physicists interested in the fundamental properties of solids have discovered that it is absolutely vital for them to have available research materials with a high degree of chemical purity and structural perfection. And, at the same time, in nearly every area of engineering there is a demand for better materials, to do things which are within the limits of present scientific knowledge but which require materials control or properties not generally attainable. To illustrate the dependence of engineering on progress in materials, a survey of a solid-state device development organization recently showed that over 75 percent of the people were engaged in materials work of one sort or another. Contrast this to the situation a few years ago, when materials work was rather incidental to the development of electron tubes, the forerunner of modern solid-state devices.

While the overall dependence of solid-state science and technology on the quality and control of materials is now well recognized, non-materials people often fail to distinguish between two clear and distinct aspects of the materials work. Not only must the materials scientist seek preparative methods, but he also needs methods for characterizing his materials as to purity and perfection, in order to make meaningful both the advancement of preparative methods and investigations of properties.

What is characterization? A definition has been proposed in a recent study of characterization by a committee of the Materials Advisory Board [1]<sup>1</sup> and it is this:

“Characterization describes those features of the composition and structure of a material that are significant for a particular preparation, study of properties, or use, and suffice for reproduction of the material.”

---

<sup>1</sup> Figures in brackets indicate the literature references at the end of this paper.

The preparation of a material should not have to be included in its characterization, because it is not a property of the material; lacking perfection in our methods of characterization, however, we may still have to specify preparation method, as a substitute for true characterization. Also, the properties of a material should not have to be included in its characterization, because the properties result from the composition and structure. Again, however, the lack of sufficiently good methods for determining this composition and structure may require us to fall back on the specification of certain properties in the characterization of a material. Eventually, however, one hopes to understand properties in terms of composition and structure, and to eliminate the need for a description of properties, as well as of the method of preparation, in characterization.

This symposium focuses attention on the growing awareness of the necessity for developing and using better methods for characterizing solids. It is concerned with one large segment of characterization—the identification and determination of very small concentrations of chemical impurities or structural imperfections. Many of the most interesting properties of solids depend directly upon these small concentrations of impurities and defects, and the illustration of this is a principal theme of this paper.

## II. Characterization

In simple terms our definition of characterization means “what atoms are present, and where are they.” This is all that is required, in principle, for complete characterization.

A closer examination of what is required to specify the atoms present and their location shows the complexity of the problem, however. Again looking at the findings of the Materials Advisory Board study, it is convenient to divide characterization into three main categories: the chemical composition, the major structural parameters of the solid, and the deviations of the structure from the ideal, i.e., the structural imperfections. This symposium is concerned with many aspects of the first of these categories, composition, and with the third, crystal imperfections.

Under composition we seek the identification of impurities, and this includes both their valence state and their state of chemical combination; we include also the determination of the concentration of minor phases, as well as their location and homogeneity. Finally, we require information about surface impurities.

Under structural imperfections we include point defects, or agglomerates of point defects; vacancies, interstitials, and antistructure defects fall into this category. Also, we include line defects, or dislocations, and the characterization of these may be complex as it includes geometrical information, such as the Burgers vector and the orientation, as well as dislocation density, impurity atmospheres, etc. Finally we include area

defects, and there are many kinds of these—grain boundaries, twin boundaries, stacking faults, interphase boundaries—with geometry and impurity atmospheres to be characterized.

But this is not the whole story, unfortunately. Large categories of materials fall outside the limits implied by the terms we have used to define composition and structural imperfections. Polycrystalline inorganic solids require much additional information for a complete characterization, including details of grain geometry and composition, additional phases present, geometry, surface details, and many other features. Perhaps even more complicated are organic macromolecular solids, as the characterization of polymers involves questions of molecular weight distribution, chain branching and tacticity, solid additions and plasticizers, cross-links, network topology, copolymers, polyblends, crystallinity, free volume, and a host of other characterization parameters.

Our aim in this article is to provide perspective for characterization, by relating it to the properties of solids. Perhaps we can visualize this relationship by considering [2] the process of transforming, say, a pile of ore into a useful item of hardware:

Raw Material → Useful Material → Study of Properties → Uses

The step from raw materials to useful materials involves both the preparation and characterization of the latter. We will here focus our attention on the inter-relationship between “useful materials” and the properties. As stated in our introduction, the ultimate goal of materials work, and therefore of characterization, is to achieve certain properties; from a scientific standpoint it is the fundamental understanding of properties in terms of composition and structure that is the goal, and from an engineering standpoint it is the achievement of properties needed for a particular end-use.

### III. The Relation of Properties to Composition and Structure

We shall discuss the role of “trace impurities”—both chemical and structural—by giving some examples of their relation to the properties of various kinds of solids. A perception of this relationship will then make almost self-evident our concluding remarks about the need for improved characterization.

#### A. ELECTRICAL PROPERTIES [3]

##### 1. *Semiconductors*

The electrical properties of semiconductors [4] offer a by-now familiar, but nevertheless classic example of a profound effect of traces of chemical impurities on physical properties. It is the experience with semiconductors, more than anything else, which has supplied the impetus

to much of the work on the purification, crystal growth, and characterization of the solid-state materials of today.

Most semiconductor phenomena depend vitally upon the impurity content of the material. Concentrations of electrically active chemical impurities in the range  $10^{-6}$  to much less than  $10^{-9}$  determine the electrical properties, and in compound semiconductors the point defects (vacancies, interstitials) can be equally important. In a small number of semiconductors, notably silicon and germanium, purities in the  $10^{-9}$  range or better have been achieved, and the whole spectrum of impurity-dependent phenomena has been quantitatively studied. As a result germanium and silicon are very well understood in a fundamental way. (Effects due to point defects are perhaps less well understood than the effects due to impurities.) In other semiconductors the need for similarly high purities is recognized, but there have been varying degrees of success in the effort to achieve high purities. The understanding of a semiconductor is, in general, proportional to the degree of purification which has been achieved with that material.

In such semiconductors as germanium and silicon, the carrier (conduction electrons and holes) concentrations are determined primarily by the concentrations of Group III and Group V impurities present in the material. In compound semiconductors other impurities function similarly as simple donors and acceptors. A large number of semiconductor phenomena depend directly upon the carrier concentration. These include: transport properties, such as electrical conductivity, thermoelectricity and Hall effect; many optical properties, such as electroluminescence, photoconductivity, and some optical absorption effects; and a variety of other phenomena, such as  $p$ - $n$  junction behavior, chemical interactions among impurities and imperfections, and so on. The electron and hole concentrations may also be affected by the concentrations of point defects associated with nonstoichiometry, in the case of many compound semiconductors. Any concentration of donor and acceptor impurities (or point defects) which is at least as great as the intrinsic carrier concentration will be significant. Thus in silicon at room temperature the carrier concentrations will be determined by the donor and acceptor impurities present if they exceed about one part in  $10^{11}$ , and in germanium the corresponding figure is roughly one part in  $10^9$ . These semiconductor phenomena depend primarily upon the number of simple donors and acceptors present, but not, in general, upon their chemical identity.

Another set of phenomena includes those properties which depend more specifically upon the identity of impurities, whether they be ordinary donors and acceptors, or electrically active in a more subtle way. Several important properties are related to the ionization energies of the donors and acceptors, i.e., the work required to remove an electron from a donor in the lattice to a large distance, or to add an electron to an

acceptor. These include the temperature dependence of the electrical conductivity, Hall effect, threshold for photoconductivity, and optical absorption by impurity centers. The ionization energies will usually vary even among chemically similar impurities, the differences sometimes being very small, and sometimes large. Hole-electron recombination processes, trapping and luminescence characteristically depend upon the electronic energies for the center at which the recombination occurs. Recombination processes in germanium and silicon are sensitive to even smaller concentrations of certain impurities than are the carrier dependent phenomena mentioned earlier. Thus the minority carrier lifetime in germanium is reduced one to two orders of magnitude by concentrations of transition metal impurities, such as nickel, at the  $10^{-9}$  level.

Much of the effort that has gone into semiconductor materials has been associated with the identification and control of trace impurities and structural imperfections. In the relatively simple and well-controlled semiconductors silicon and germanium, the concentrations of these centers are usually small, and the problem has been to develop characterization tools of sufficiently high sensitivity. In many compound semiconductors, the variety of defects of importance in a given sample may be much larger, and the main problem is to sort them out to a degree which permits an understanding of the electrical properties. This is illustrated in Figure 1 for pure PbS; the concentrations of several of species are shown as a function of the sulfur pressure in equilibrium with a sample of a given defect concentration. The full line shows the experimentally accessible parameter, the majority carrier concentration; it can be seen that this falls far short of revealing the entire chemical composition. This is a relatively simple situation, as far as compound semiconductors go, because no impurities or interstitials have been assumed to be present. Practical cases will therefore be even more complicated and the extent of the information needed for

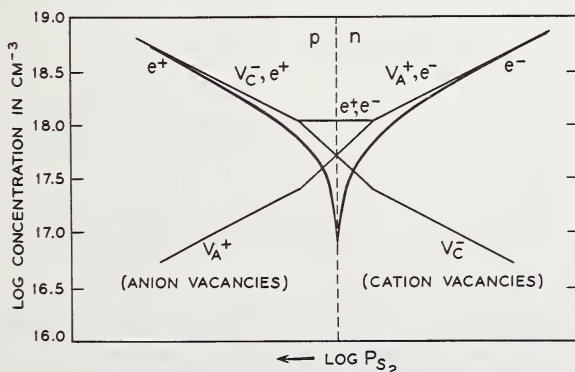


Figure 1. Concentrations of defects expected in PbS as a function of sulfur pressure. Full line gives experimental values for carrier concentrations,  $|n - p|$ . After Hannay [4].

complete characterization should be apparent. Only a few compound semiconductors among the many which show this kind of nonstoichiometry have had even the major features of their composition worked out, due to the difficulty in determining the various defect concentrations [5].

## 2. Metals

Turning next to the study of metals, we note that the last few years have seen an upsurge in the effort to unravel the basic electronic structure of metals. The key to this effort has been the attainment in a number of metals of a sufficient level of chemical purity and of crystalline perfection to permit the measurement of quantities which are useful in revealing this electronic structure [6].

The relationship between purity and electrical resistivity is one of the most direct effects of chemical purity and crystal perfection in metals. Impurities and imperfections increase the resistivity of metals, because they act as scattering centers for electrons and therefore reduce the mean free path of the electrons, i.e., the average distance an electron travels between collisions with these centers or with phonons (lattice vibrations). An ideally pure, perfect metal would have its resistivity determined only by the lattice vibrations. It would show a zero resistivity at 0 °K, increasing as  $T^5$  at slightly higher temperatures because of the lattice vibrations, as shown in Figure 2. Impure samples would show a higher resistivity, because of the increased electron scattering by impurities and defects. The effect of impurities on the resistivity of copper is shown in Figure 3. The resistivity exhibits a linear dependence upon the concentration of chemical impurities, and there are very great differences between impurities in their effects on resistivity; Fe in Cu at 4.2 °K is an extreme case. Table 1 also compares the effect on resistivity of several impurities and structural imperfections.

TABLE 1. Approximate contributions of impurities and defects to the resistivity of copper.

( $10^6 \times \Delta\rho/\%$  impurity or defect, ohm cm/%)

<i>Chemical Impurities</i>		<i>Physical Defects</i>	
Ag	0.2	Vacancies	1.3
Ni	2	Interstitials	5
Fe	20		
Sn	5	Dislocations, 0.4 to $3 \times 10^{-14} N$	
Sb	9	where $N = \text{cm of dislocation/cm}^3$ .	

The low temperature resistivity is often used as a practical measure of purity in metals. As Figure 2 shows, at liquid helium temperatures most of the resistivity is due to impurities and imperfections, even in quite pure materials; at room temperature the resistivity is primarily

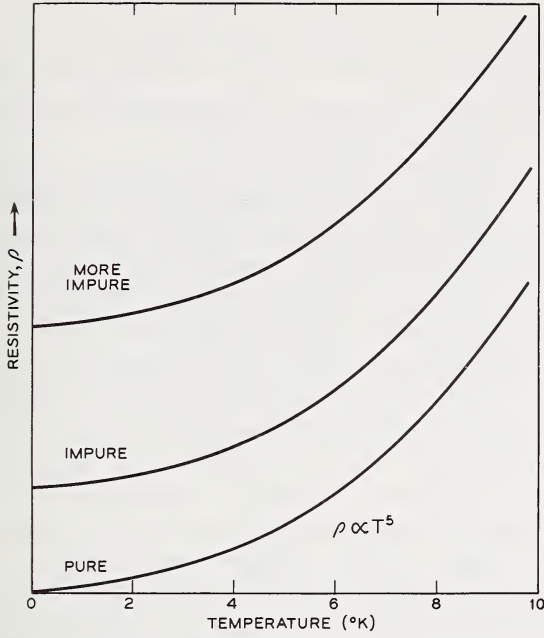


Figure 2. Schematic of resistivity of a metal at low temperatures [6].

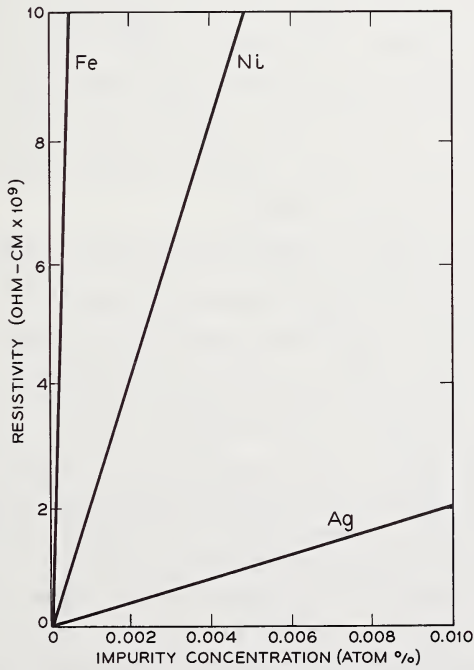


Figure 3. Resistivity of copper with impurities (4.2 °K) [6].

determined by the lattice vibrations. Thus the higher the "resistance ratio",  $R_{298^\circ\text{K}}/R_{4.2^\circ\text{K}}$ , the purer the metal is both chemically and structurally. The resistance ratio is a figure of merit which lumps together the effects of chemical impurities and structural imperfections, without regard to their individual importance.

A number of phenomena are useful in studies of the band structure and Fermi surfaces of metals; among them are magneto-resistance, Hall effect, magneto-acoustic absorption, cyclotron resonance, deHaas-vanAlphen effect, thermoelectric power, anomalous skin effect, helicon waves and Alfvén waves. One can see in a general way why these effects necessitate materials of very high purity. Several of the phenomena, for example, involve the use of a magnetic field, which causes the electrons in the metal to move in circular (cyclotron) orbits in a plane perpendicular to the field direction. In order to interact with the lattice in all possible ways, the electron must complete at least one orbit before it is scattered. Scattering results from interaction of the electron with chemical impurities and crystal imperfections. One seeks therefore to use high magnetic fields in order to reduce the size of the orbit, and to use high purity materials to reduce scattering. It turns out that the purity demands are quite stringent, as there is a practical limit to the magnetic field strengths which are available, and the only recourse in making the measurements feasible is to reduce the resistivity by increasing the purity and crystal perfection. Resistivities below about  $10^{-9}$  ohm cm (at low temperatures) are generally necessary for these kinds of measurements. One can see from Table 1 that to achieve these resistivities in copper, purities in the order of half a part per million for iron are required, and within an order of magnitude of this for other elements. Copper was one of the first metals for which the Fermi surface was determined in detail, and this has been followed by similar work in a number of other metals.

Resistance ratios that have been achieved for a number of metals in which purification efforts have been most successful are shown in Table 2. Generally speaking resistance ratios of a few thousand are required in order to make fundamental Fermi surface studies.

The effect of point defects, as distinct from chemical impurities, can be studied in material of sufficient chemical purity by quenching-in the defects. Concentrations of the defects in excess of the equilibrium number are achieved by rapid cooling from some high temperature at which the equilibrium concentration is considerably larger. Figure 4 shows the resistivity changes due to "frozen-in" vacancies in gold, after quenching from various temperatures,  $T_q$  [7]. Equilibrium concentrations of vacancies in metals are of the order of 10 ppm at 1000 °K, since the formation energies are of the order of one eV and the vacancy concentration  $[V] \cong N \exp(-E_v/kT)$ , where  $N$  is the number of lattice sites in a cubic centimeter.

TABLE 2. Resistance ratios of some purified metals. ( $R_{298}/R_{4.2}$ ).  
(after W. A. Reed)

Al	26,000	Nb	5,000
Be	3,300	Ni	4,000
Bi	500	Pb	100,000
Cd	38,000	Pd	5,000
Cu	25,000	Pt	1,600
Cs	2,000	Rb	2,500
Fe	5,500	Re	55,000
Ga	100,000	Sn	100,000
K	12,000	Ta	15,000
Li	4,000	W	80,000
Mg	> 100,000	Zn	40,000
Mo	12,000		

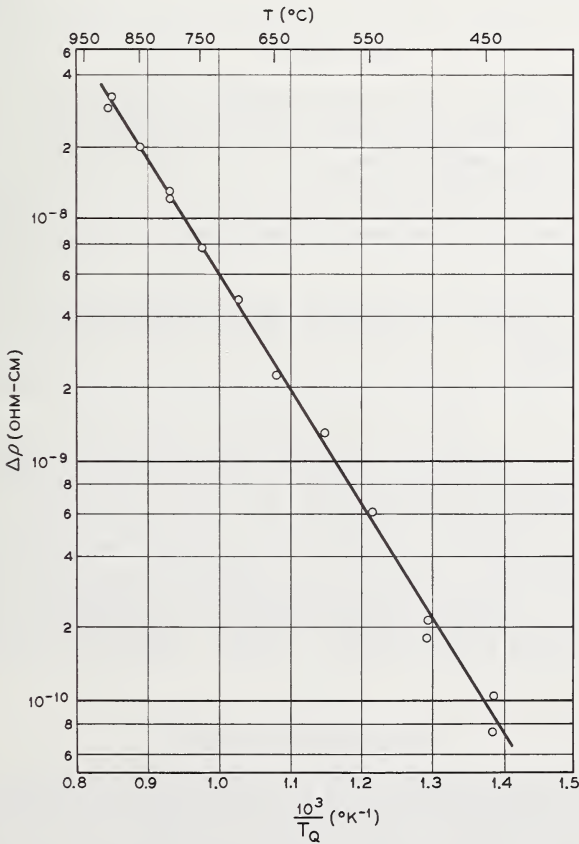


Figure 4. Change in resistivity of gold after quenching from various temperatures ( $T_Q$ ).  
After Swalin [7].

### 3. Superconductors

A number of effects in superconductors arise from impurity concentrations of a few percent or a few tenths of a percent; thus the superconducting transition temperature of various metals and alloys is decreased by the addition of rare earth metals.

It has also been discovered that very much smaller impurity concentrations can be of great significance in superconductors. Thus when molybdenum is sufficiently pure it becomes superconducting below about 1 °K [8]. The transition temperatures for a number of samples prepared in different ways are shown in Table 3.

TABLE 3. Superconducting transition temperatures for various samples of molybdenum.

Supplier	Transition temperature
(1) Johnson Matthey. "Specpure" Quality measured as received. The measurements showed the ac resistance of this sample to be at least several-fold greater than the rest of the samples.	°K None
(2) Johnson Matthey. "Specpure" Molten 15 seconds in arc furnace.	0.58
(3) Johnson Matthey. "Specpure" Molten 3 minutes in arc furnace.	0.92

A quantitative analytical characterization of these samples was not possible, although the most significant impurity in determining the transition temperature is iron, in the parts per million range. One part per million of added iron is sufficient to prevent the quantitative measurement of the isotope effect in molybdenum, the isotope effect being the change in superconducting transition temperature between the separate isotopes of an element. Similar behavior is found in other cases.

### 4. Ionic Conductivity

In insulating ionic compounds, the free electron and hole concentrations may be so low that the electrical conductivity is dominated by ionic motions, despite their much smaller mobilities [3]. The mobility is closely related to the ionic diffusion coefficient, by the Einstein relationship. Since diffusion in ionic compounds usually proceeds via a vacancy

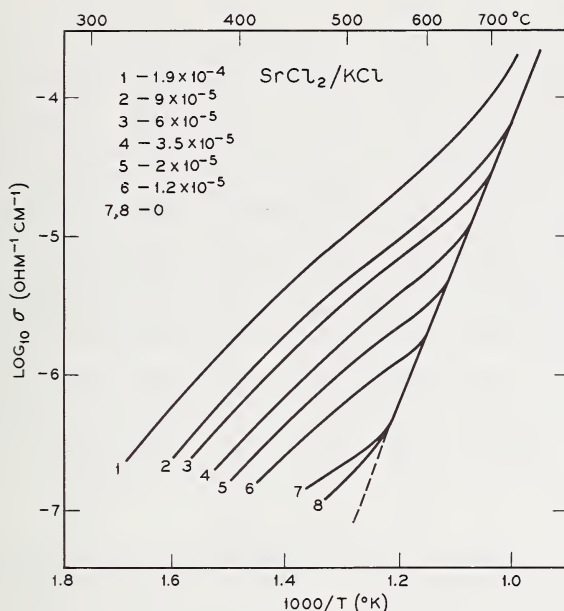


Figure 5. Ionic conductivity of KCl with added  $\text{SrCl}_2$ .

or interstitial mechanism, the diffusivity, and therefore the conductivity, depend directly upon the point defect concentration, and any changes in this concentration will be reflected directly in these quantities.

It is, in fact, quite possible to change the point defect concentration by simple chemical means, using the principle of charge compensation. If a divalent cation is added to an alkali halide, for example, for every added impurity ion there appears in the crystal a cation vacancy, to preserve the overall charge neutrality of the crystal. This is shown in Figure 5, which shows the effect of adding  $\text{SrCl}_2$  to KCl. At high temperatures the intrinsic, equilibrium concentration of vacancies outweighs the contribution of the impurities, but at lower temperatures the conductivity is raised by the extra vacancies introduced with the  $\text{Sr}^{2+}$ .

In other ionic compounds (for example, silver halides) interstitial cations dominate the conductivity. Anions can also be important.

### B. OPTICAL PROPERTIES

Optical properties of solids are sometimes closely related to electrical properties [3]. We noted in the preceding section that absorption, luminescence, and photoconductivity in semiconductors may be due to the same impurities or defects which determine the electrical properties. Similar kinds of centers affect the optical behavior of insulators.

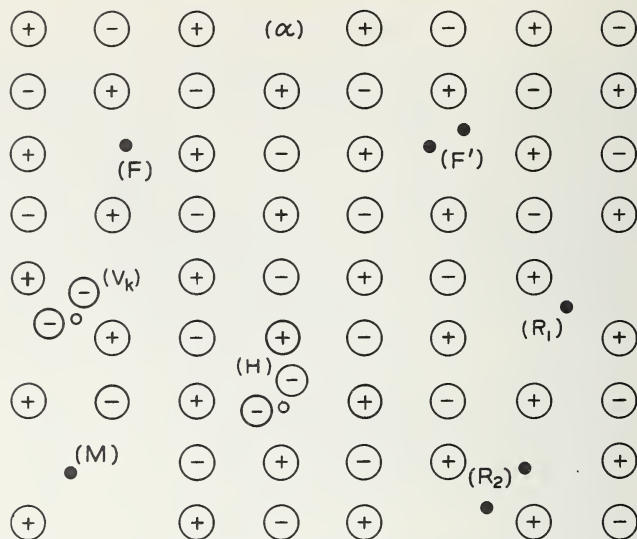


Figure 6. Models for defects in alkali halides (○ holes, ● electrons).

### 1. Alkali Halides

Perhaps the most studied of these effects in insulators is the absorption in alkali halides arising from "color centers." Proposed models for a number of these are shown in Figure 6 [3]. Each kind of center has a characteristic absorption spectrum, and the intensity of the absorption is proportional to the concentration of the center. It is also possible to convert some of the centers into others. Thus if the *F*-center, which is

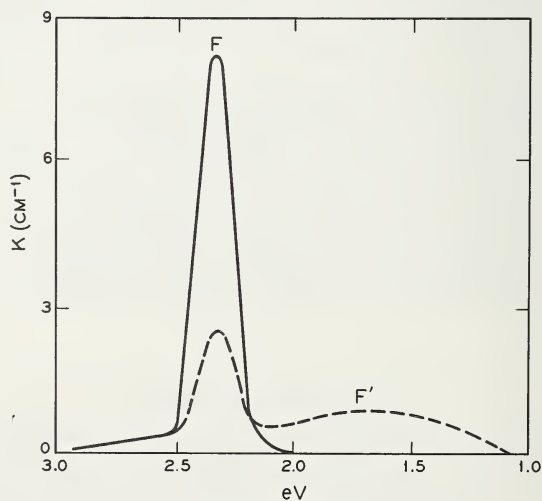


Figure 7. Conversion of *F*-center into *F'*-center by irradiation. Full line is *F*-band before irradiation, dashed line shows absorption spectrum after irradiation.

an anion vacancy with a trapped electron, is irradiated at a wavelength corresponding to the peak of its absorption, the peak gradually decreases in size and at the same time the  $F'$ -band, peaked at a different wavelength, grows (Fig. 7). The reason for this can be seen from Figure 6. The  $F'$ -center differs from the  $F$ -center only in the number of attached electrons; the absorption in the  $F$ -band, or "bleaching," ionizes the center, releasing an electron which wanders through the crystal until it is trapped, either at another ionized  $F$ -center or at an un-ionized  $F$ -center. In the latter event it produces an  $F'$ -center, with *two* trapped electrons.

The absorption of light by simple chemical impurities or point defects in semiconductors frequently leads to ionization, in a manner essentially like the absorption due to  $F$ -centers in the alkali halides. The photoconductivity arising from this impurity ionization, as well as the absorption process itself, have been the subjects of intensive study in semiconductors and have yielded much fundamental information about defect centers.

## 2. Luminescence

In the preceding section we referred to recombination processes for electrons and holes in semiconductors. Whenever electrons or holes occupy states lying higher in energy than states which are empty, transitions will tend to occur so that the system can return to the equilibrium condition; the characteristic decay time for this process is the "lifetime." This recombination may involve, for example, the return of a conduction band electron to an empty state in the valence band or on an impurity, or of an electron from a filled impurity state to an empty state in the valence band or on an impurity. It can occur with the loss of the excess energy to the lattice as heat, or as a radiative process — "luminescence." A variety of methods may be used to raise the electrons initially to the higher-lying states. These include electron bombardment, optical excitation, electric field excitation, and excitation by a chemical reaction. Thus electron bombardment furnishes the excitation for the active screen materials ("phosphors") of cathode ray tubes, and optical and electric-field excitation are the principal means used in lasers.

Phosphors are extremely sensitive to trace impurities [3]. These may function as "activators," "co-activators," and "poisons." Many of the important phosphors are very difficult to control chemically, not only because of this dependency upon traces of chemical impurities but also because of tendencies toward nonstoichiometry and effects due to the resulting lattice imperfections. A large effort has gone into the understanding and control of the chemistry of phosphors, much of it limited in effectiveness by insufficiently good characterization methods.

The role of activators in two primary classes of phosphors may be understood as follows. In the class illustrated by thallium-activated alkali halides, the thallos ions, which are randomly distributed on cation sites, are raised to excited electronic states by the absorption of energy

in the excitation process. These then decay to their ground states with the emission of radiation. In sulfide phosphors, such as ZnS:Ag, ZnS:Cu, and CdS:Ag, the excitation produces free electrons and holes. The hole is captured by the impurity center, with the emission of radiation. A later capture of a conduction electron restores the center to a neutral condition and prepares it again to perform its function in the luminescence process.

"Poisons" are impurities which provide unwanted recombination paths for the holes and electrons. It has been demonstrated in germanium and silicon that recombination centers at concentrations of less than  $10^{-9}$  can have very large effects, and so the detection and removal of poisons, or recombination centers, can be a major challenge; impurities in sulfide phosphors in the ppm range have been shown to act as poisons.

"Co-activator" impurities may function in more than one manner. One, certainly, is to facilitate the incorporation into the crystal of the activator impurities by providing charge compensation. Thus the addition of trivalent cations to a II-IV compound improves the solubility of the monovalent activators, and the addition of monovalent anions ( $\text{Cl}^-$ ,  $\text{Br}^-$ ) does the same. Another way a second impurity, or co-activator, can function is to modify the energy level of the activator impurity.

The interaction of two impurities, in relation to luminescence, has been examined in detail in the electroluminescent material GaP [9]. In this case the recombination leading to luminescence involves holes and electrons *both* bound to impurity centers, as distinct from the mode described above involving a free carrier and an impurity center. An electron on a donor impurity and a hole on a nearby acceptor impurity recombine with the emission of light. The wavelength depends upon the energy of interaction of the two charged impurities, and this in turn depends upon their distance of separation. Since this is restricted to certain values by the geometry of the crystal lattice (nearest neighbors, next-nearest, etc.) the impurity separation distances have certain, discrete, allowable values. Assuming random distribution of the two impurities on their allowed lattice sites, a theoretical calculation of the positions and intensities of the luminescence spectrum can be made by simply calculating the coulombic interaction energy; the observed spectra show a series of lines in quite good agreement with these values, as shown in Figure 8. In this case we see that the important information about impurities involves not only their identities and concentrations, but also (the distribution of) their distances of separation.

### C. MAGNETIC PROPERTIES

While many of the important magnetic properties of solids are bulk effects, there has been increasing realization that there are important

phenomena which depend upon impurity concentrations well below the tenths of a percent range. A good example of such an effect is the ferromagnetic resonance line width in yttrium iron garnet (YIG) [10]. The line width at low temperatures has been found to be about 6 oersteds in normal single crystal YIG, prepared from ordinary yttrium oxide, which contains significant concentrations of various rare earth impurities. The spin-lattice relaxation times of these rare earth ions are such that they can appreciably affect the line widths in YIG. An extensive purification program led to the reduction of the rare earth impurity content to less than 0.1 ppm, and YIG made from this material showed ferromagnetic resonance line widths of the order 0.1 oersteds, about a fifty-fold reduction. Still further improvements were achieved by the removal of silicon down to the ppm range; this tetravalent impurity reduces an equal amount of the host crystal ferric ions to ferrous because of charge compensation, and these divalent irons also contribute to the relaxation rate. The net result of this further purification was to reduce low-temperature line widths by another order of magnitude (Fig. 9).

Interstitial impurities, such as carbon, nitrogen, hydrogen and sulfur, have important effects on bulk magnetic properties [11]. In soft iron, concentrations of these impurities in the hundredths or even thousandths of a percent can change the permeability by one to two orders of magnitude. Also, aging effects in iron are dependent upon small traces of nitrogen. Figure 10 shows that the permeability of iron containing 0.001% nitrogen hardly changes with aging whereas material with 0.005% nitrogen showed a marked decrease in permeability upon aging. The reduction is due to the precipitation of nitride from a supersaturated solution, as the solubility limit at room temperature is of the order of 0.001%. The effect can be reversed by heating to higher temperatures, as the nitride solubility increases with temperature.

#### D. MECHANICAL PROPERTIES

The mechanical properties of solids are critically dependent upon structural imperfections. The electronic properties discussed in the

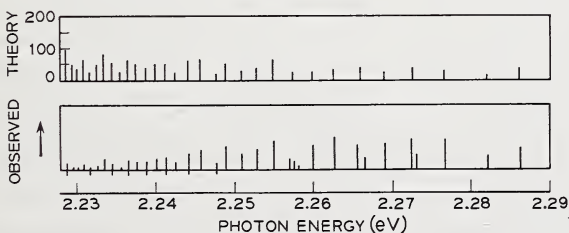


Figure 8. Observed and calculated frequencies and intensities for some of the emission lines in GaP.

## TRACE CHARACTERIZATION

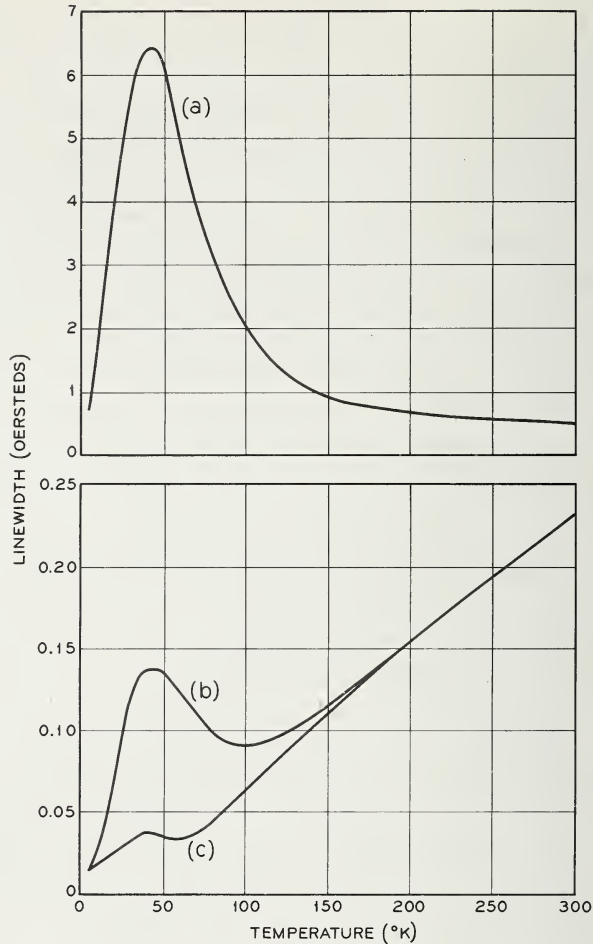


Figure 9. Ferromagnetic resonance line width in YIG. (a) normal YIG, (b) rare earth impurities removed, (c) silicon removed. After G. H. Morrison, "Trace Analysis," Interscience Publishers, New York (1965).

preceding sections have been seen to depend importantly upon chemical impurities, and to a somewhat lesser extent upon point defects. Line defects—dislocations—also affect some electronic properties but are of less immediate concern. On the other hand, they are of paramount importance to the mechanical properties. Chemical impurities sometimes play a major role here, while point defects are less important. Area defects are of several kinds; those which constitute gross discontinuities, such as interphase boundaries or grain boundaries, have major significance for most properties; the more subtle area defects, such as tilt boundaries, twist boundaries, twins, and stacking faults are often outweighed in their effects by other structural imperfections, and we will not be greatly concerned with them in this review.

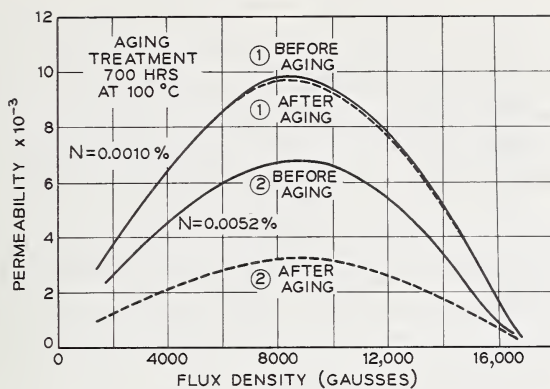


Figure 10. Effect of nitrogen on permeability of Fe. After Schumacher [11].

It has long been recognized that the strengths of real crystals fall orders of magnitude short of those expected for a perfect crystal, which should have an ultimate strength limited only by the magnitude of the chemical bonding forces holding the solid together. It is, of course, well known that dislocations provide the mechanism by which plastic deformation occurs at yield stresses far below this theoretical limit. Dislocation-free whiskers of certain metals have been observed to show elastic strains of more than a percent, at least two orders of magnitude higher than the values for ordinary samples of the metals, before yielding. It has also been possible to prepare large dislocation-free samples of silicon and germanium, and to investigate their yield behavior [12]. Results for dislocation-free germanium as well as for samples containing various dislocation densities are shown in Figure 11. It can be seen that dislocation densities of the order of  $10^6/\text{cm}^2$  virtually eliminate the upper yield point (dislocation densities of this magnitude are somewhat lower than those found in ordinary samples of metals).

While very pure, nearly perfect crystals show exceptional yield strengths, the presence of just a few dislocations will decrease the yield point well *below* that of an ordinary metal, because the dislocation allows an easy slip mechanism and therefore plastic flow, and there is no strengthening mechanism to prevent this deformation. Several mechanisms can block this slip resulting from individual dislocations, and thereby lead to the actual strengths observed in practical metals, which are intermediate between theoretical strengths for perfect crystals and those with relatively few dislocations. One strengthening mechanism is the mechanical blocking of dislocation motion by small particles of a second phase (iron carbide in steel, for example). Grain boundaries can also block dislocation motion. Solute impurity atoms provide still another mechanism. They tend to collect in the vicinity of dislocations, where the lattice is somewhat expanded, during the formation of the metal at high temperatures which allow impurity mobility; at lower

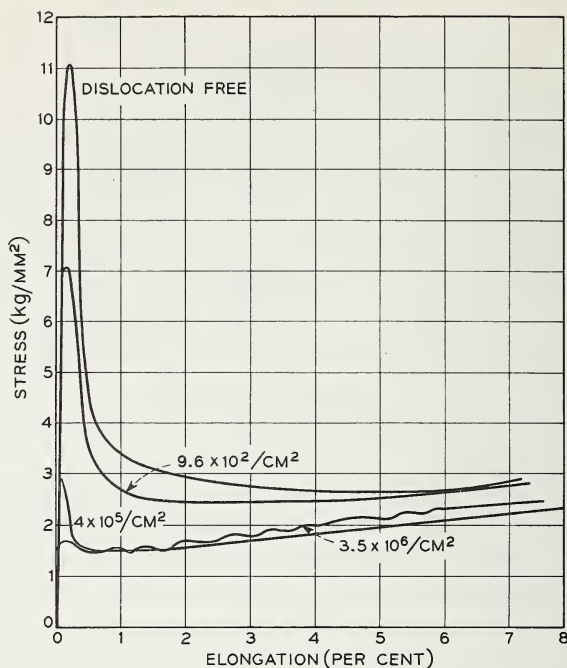


Figure 11. Tensile deformation of Ge for various initial dislocation densities. After Patel and Chaudhuri [12].

temperatures they are immobile, and this impurity cloud pins the dislocation because the dislocation cannot move away from the impurities without an increase in energy. Finally, when dislocations are present in sufficient number, they can become interlocked and this accounts, for example, for the work-hardening of even very pure metals.

It is apparent that the elucidation of mechanical strength depends upon the control and characterization of the material with respect to line and area defects and chemical impurities. The advent of very pure and nearly perfect materials has at least partly opened the door on fundamental studies of mechanical properties, and on the practical realization of a number of mechanical properties which have long been desired but were apparently beyond reach. We shall be interested in both aspects.

Looking first at some of the fundamental studies permitted by the availability of high purity materials with low defect concentrations, we saw in Figure 11 the effects of dislocations in the absence of chemical impurities. The effect on the mechanical properties of a chemical impurity, oxygen, has also been studied. Unless precautions are taken in the preparation, silicon can contain appreciable quantities of dissolved oxygen, which occupies an interstitial position bonded to two adjacent silicon atoms. When the solid is heated at an appropriate temperature, the oxygen clusters into  $-\text{SiO}_4-$  units, and at higher temperatures into

SiO<sub>2</sub> aggregates. Since the oxygen can be electrically active, electrical conductivity measurements reflect the changes in the structure of the defect centers. There is also a change in the infra-red absorption spectrum as each condition has a characteristic absorption behavior. The maximum yield strength is also decreased substantially by the heat treatment, and concentrations of a part per million or below are significant [13].

Extensive studies have been carried out on high-purity lead, to show the effects of chemical impurities [11]. Among the properties measured were stress-strain, for "pure" lead and for material with small amounts of added silver (Fig. 12). The initial slope is steeper, reflecting a stiffening of the lattice, and an increase in tensile strength clearly results. The effect is due to the formation of a precipitated phase (recall our earlier remarks about the interaction of dislocations and a second phase); the solid solubility of silver in lead has been exceeded at these concentrations. In Figure 13 another property of lead is shown, the dependence of tensile strength upon time, with and without added arsenic. It is evident that a very small impurity addition rapidly accelerates the age hardening of lead.

The recent progress in metal purification has had important implications for the practical applications of metals, especially the refractories, which present great difficulties in fabrication [6]. Most of these effects are due to interstitial impurities such as oxygen, carbon, and nitrogen, and frequently these are bound chemically so strongly that their removal is difficult. When the purification is achieved, however, very large

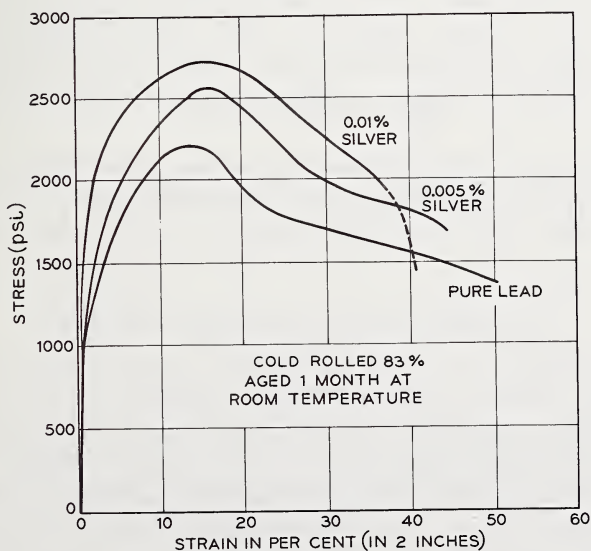


Figure 12. Stress-strain in Pb. After Schumacher [11].

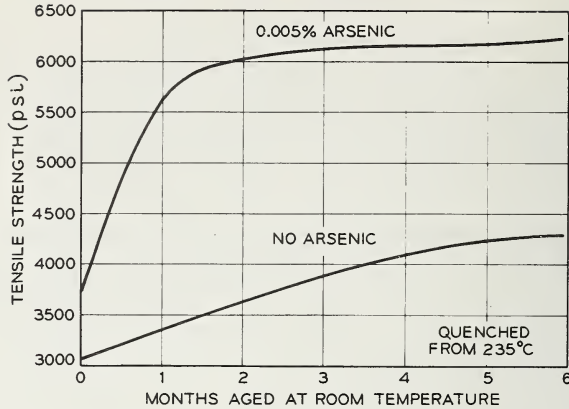


Figure 13. Age hardening of Pb. After Schumacher [11].

changes occur, and the material can frequently be worked easily. The brittleness of ordinary tungsten is associated with impurities at around 200 ppm; with impurity concentrations reduced below about 10 ppm, tungsten becomes ductile. Other refractory metals behave in a similar way, upon purification. Among these is beryllium, as shown in Figure 14. The extreme difficulty in fabricating ordinary beryllium is well known, and the development of such ductility is remarkable. The impurity content of this bar, which has been bent by hand at room temperature, is of the order of a few ppm. Still another example is titanium, which, like beryllium, holds oxygen tenaciously. An order of magnitude reduction in yield stress results from extensive zone refining. The change in ductility with purity is shown in Figure 15 for two samples of iron; one was vacuum melted, the other vacuum melted and zone-refined. Despite the somewhat larger grain size of the latter (which would be expected to reduce ductility, in general), it had a much greater elongation.

In many of the studies of high-purity metals, including some we have made reference to, chemical analyses are available only on the less pure samples. The need for characterization of the pure materials is apparent.

#### E. STRUCTURAL TRANSFORMATIONS [14]

Closely related to mechanical properties are structural transformations. Many of these depend on atom movements in the solid phase. The two primary mechanisms for diffusion in single crystals are provided by the motion of interstitial atoms, and by vacancy diffusion. In the latter case we observe that vacancy motion in a given direction is equivalent to the flow of host atoms on normally-occupied lattice sites (or of substitutional impurities) in the opposite direction. Obviously, then, the



Figure 14. Ductility of pure Be. After Schaub and Cabane, *Compt. Rend.* **257**, (2), 444 (1963).

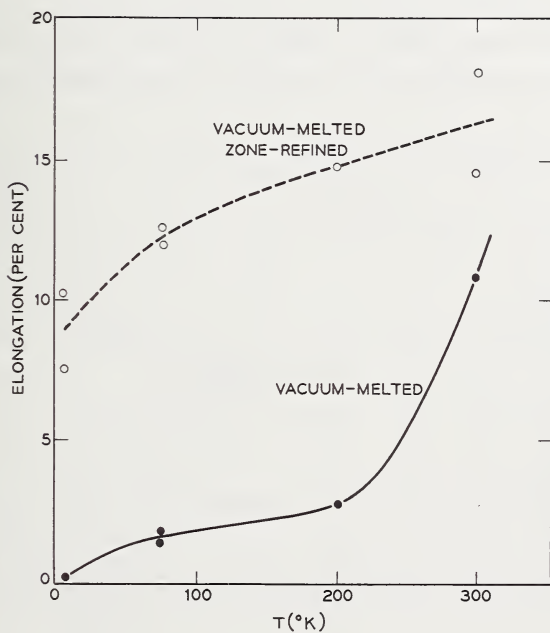


Figure 15. Ductility of pure Fe.

point defect concentration is of immediate concern in diffusion-controlled phenomena. We saw an example of this in Section III.A.4, in our discussion of ionic conductivity in alkali halides.

When grain boundaries, dislocations, etc. are present they may greatly accelerate the diffusion rates. The general expansion and disruption

of the lattice along grain boundaries results in high vacancy concentrations and increased inter-atomic spacings, and these increase diffusivities, as shown in Figure 16 [15]. Dislocations can provide sinks or sources for vacancies, and this also results in a change in diffusion rates.

At any temperature above 0 °K, there will be an equilibrium number of vacancies and interstitials in any solid, and this can be calculated simply from elementary statistical considerations, providing we know the energy required to displace an atom from its normal substitutional site to an interstitial position, or to form the vacancy by breaking bonds and removing an atom to the surface (there is an overall increase in entropy which results from the disorder associated with point defect formations, and an expenditure of energy to form the defects; at equilibrium the free energy is at its minimum). As noted earlier, vacancy concentrations are of the order of  $10^{-5}$  in many metals. Point defects can also be introduced in a controlled way, in compounds, by suitable additions, and our earlier discussion of ionic conductivity in alkali halides illustrated how this can be brought about.

We now consider the general problem of structural transformations in solids and their relationship to diffusion process. The development of a new structure, or phase, when the free energy change for such a trans-

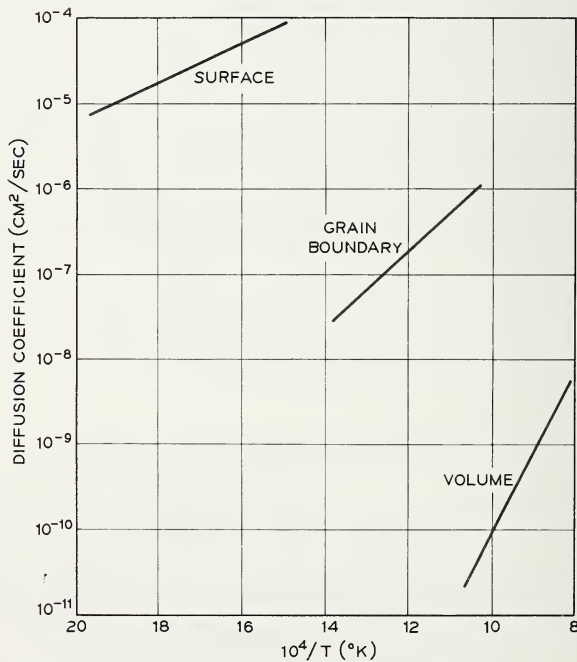


Figure 16. Comparison of volume, surface and grain boundary diffusion, for self-diffusion of Ag. After Brophy et al. [15].

formation is favorable, involves two stages, nucleation and growth. Nucleation may be homogenous, and result from fluctuations within a uniform solid. It may also be heterogeneous, being facilitated by the presence of impurity inclusions, grain boundaries, dislocations, etc., for several reasons: homogeneous nucleation must overcome the extra free energy required to form the new surfaces associated with the nuclei of the new structure, and if a grain boundary is already present, the interfacial energy of this existing boundary is available to help overcome the free energy required for nuclei to form. Also, grain boundaries and dislocations help relieve the stresses accompanying the nucleation processes, and these stresses also involve a free energy increase which must be overcome. Impurity inclusions in grain boundaries also may catalyze a nucleation process.

The second stage of a transformation is growth, and this results from diffusion. In special cases the motion required is so small—of the order of a lattice spacing or less—than this stage does not influence the kinetics of the overall process. A notable example of a “diffusionless” transformation is the martensitic, in steels. In general, however, the diffusion processes discussed above govern the growth rate.

A specific transformation system which illustrates both nucleation and growth, as well as the role of defects, is provided by the precipitation of lithium from a supersaturated solution in silicon [16]. The results are shown in Figure 17; the amount precipitated is seen to depend on  $t^{3/2}$  for the major part of the precipitation. This implies a spherically symmetric diffusion to the nuclei of precipitated lithium, and therefore indicates something about the nature of the nuclei. A different time dependence would result from different geometries—dislocations, for example, which are common nucleation sites for precipitation (in fact, this provides a useful method for characterizing dislocations, by dislocation “decoration”). The four curves are for different samples, and the variations in rate reflect differences in the number of nucleation centers. Sample 2 originally had too few nucleation centers to show any perceptible precipitation, and so the sample was then exposed to high energy electron bombardment. This produces a profusion of point defects in solids, and the much faster rate of precipitation observed after the bombardment, together with the spherical symmetry found for the diffusion field, imply that these defects provided the initial nucleation centers.

The rate of growth of the nuclei in a transformation may be altered by any factors which change diffusion rates. The introduction of vacancies, by bombardment or by the addition of appropriate chemical impurities (see Fig. 5), can lead to changes in the diffusion rate. Also the presence of a second chemical impurity which interacts with the diffusing species can change the diffusion rate. Thus the precipitation rate of lithium in silicon containing oxygen is greatly reduced, as shown

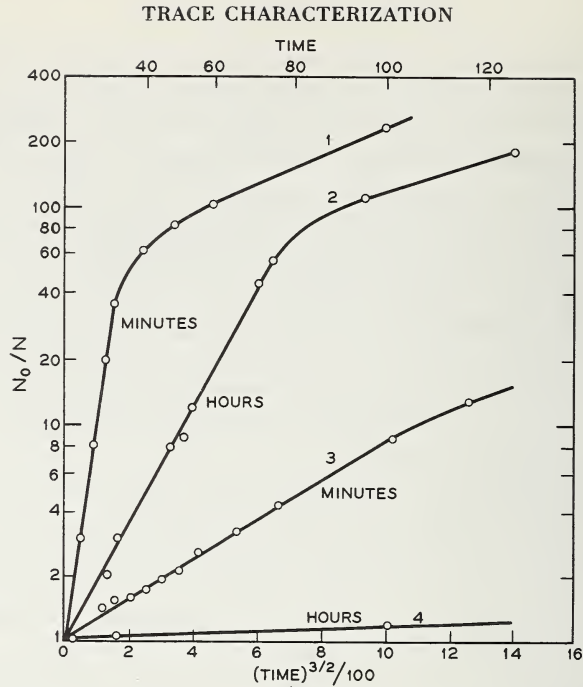


Figure 17. Precipitation of Li in Si (four samples with different concentrations of nucleation centers). After Hannay [4].

in Figure 18, by an interaction of Li with the oxygen; this interaction immobilizes a large fraction of the interstitial Li and effectively prevents it from diffusing, as long as the interaction for any given interstitial Li persists [17]. The diffusion coefficient is reduced by a factor representing the fraction of Li which is un-bound, and therefore gives the equilibrium constant for the reaction between Li and O. The effectiveness of dislocations as nucleation centers for precipitation is shown by the data of Figure 19.

Precipitation has been discussed as an example, to illustrate the nucleation and growth features of a transformation, but other kinds of transformations depend upon the same general principles, and the role of impurities and structural defects is common to all. Many transformations are of very great technological importance, and semi-empirical means have been used to achieve the desired practical results. An understanding of basic processes in properly characterized materials could accelerate this process. Thus the realization of the role of solid state diffusion in sintering, together with an understanding of the principles by which trace additions of chemical impurities can interact with the host compound through the charge compensation mechanism to increase vacancy concentrations, have pointed the way to controlled alteration of sintering rates. Likewise, recrystallization and grain growth rates, so important in metallurgical processing, have been

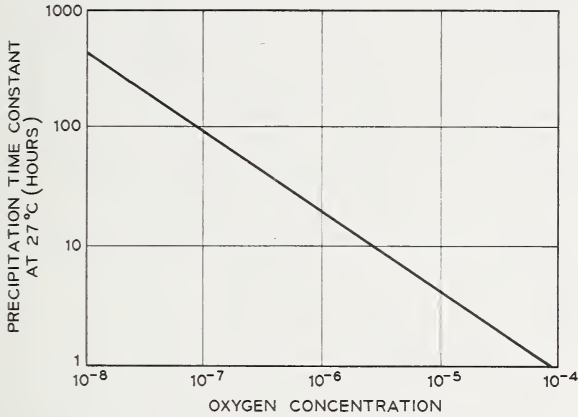


Figure 18. Precipitation of Li in Si containing oxygen. After Pell [17].

explored in terms of chemical purity. Figure 20 shows the recrystallization rate of aluminum, with various concentrations of added copper, and reveals the extreme sensitivity to impurities [6]. It has even been possible, in high purity metals, to study the migration of individual grain boundaries. They have been found to be affected in an important way by such factors as the angle between adjoining crystallites, certain angles providing special points of juncture between crystallites where the crystal structures become more or less continuous. The addition of an impurity reduces the migration rate for these special boundaries less than for randomly oriented boundaries. While it is not yet possible to give a complete account of grain boundary motion in fundamental terms, because of the lack of data in high purity systems, the realization of the necessity for high purity, well-characterized materials is a major step forward.

#### F. CHEMICAL REACTIVITY [18]

Ordinarily one thinks of chemical reactions mainly in terms of gas and liquid phase reactions. There are also certain important solid phase reactions, however. Conspicuous among these are corrosion, or tarnish reactions, between a solid and either a gaseous or liquid reactant. The mechanism by which such a reaction continues again involves material transport in the solid phase, as the reaction would otherwise soon stop as the product of the reaction began to develop at the interface and separate the two reactants. This was demonstrated first in the classic

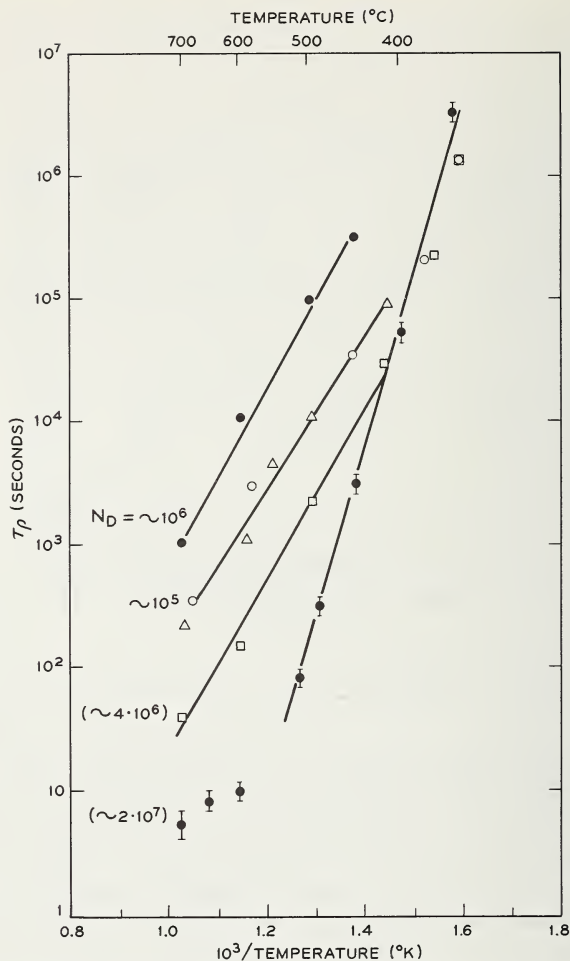


Figure 19. Precipitation of Cu in Ge, showing effect of dislocation density ( $N_D$ ). After Hannay [4].

experiment of Wagner, on the sulfiding of silver (Fig. 21). He demonstrated that after reaction, block II of the  $\text{Ag}_2\text{S}$  had gained weight, block I of  $\text{Ag}_2\text{S}$  was unchanged, and the block of Ag had lost weight, providing clear evidence that silver had diffused through the product phase, with the continuing reaction occurring at the sulfur- $\text{Ag}_2\text{S}$  interface.

Many other tarnish reactions can be understood in the same terms, and this has led to an understanding of the kinetics of film growth. Among the most studied of such systems is the oxidation of copper, which, like the oxidation of a number of other metals, follows the parabolic law (film thickness proportional to  $t^{1/2}$ ) characteristic of tarnish reactions which are rate-limited by diffusion through the product film. In the oxidation of copper, copper diffuses by a vacancy mechanism to

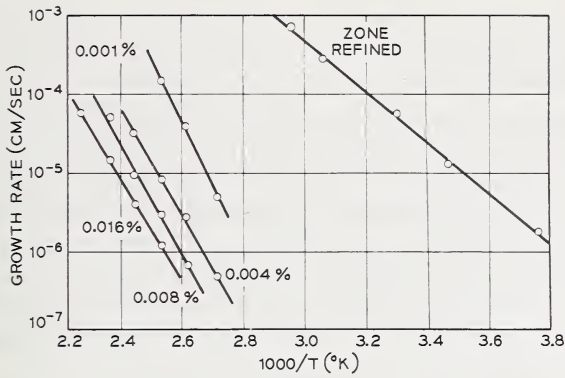


Figure 20. Effect of Cu on grain growth rates in Al [6].

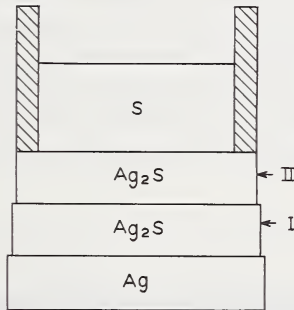


Figure 21. Experiment to show mechanism of the tarnish reaction sulfiding of silver.

the outer surface, where reaction occurs. More generally, vacancies or interstitials might contribute to a tarnish reaction, and either (or both) cation or anion motion might be involved.

A solid-solid reaction can be understood in the same terms. Thus in the addition reaction of  $MgO$  and  $Al_2O_3$  to form the spinel  $MgAlO_4$ , both  $Al^{3+}$  and  $Mg^{2+}$  diffuse, and in the double decomposition of  $CuX + BaO$  to form  $BaX_2$  and  $Cu_2O$ , the correlation of chemical reactivity and point defect concentration (as measured by ionic conductivity) has been well established. Thus in solid-state reactions, as well as in tarnish reactions, chemical control of point defect concentrations can alter diffusion rates and therefore, also, the chemical reaction rates. For example, in the reaction of silver with bromine to form  $AgBr$ , the addition of small amounts of  $Cd$  to the  $Ag$  accelerates the reaction because the divalent cation,  $Cd^{2+}$ , in the product phase introduces an equal concentration of cation vacancies, for charge compensation. This reduces the concentration of interstitial silver, the diffusing species.

Corrosion reactions between a solid and a liquid or vapor often reveal another effect of structural imperfections, the enhanced reactivity of

the solid in the places where the lattice is disrupted. Grain boundaries, for example, may react in this way. Another reason for their enhanced reactivity is that they may collect chemical impurities, for reasons discussed earlier, and therefore represent a different composition chemically. Even a single dislocation produces a sufficient disordering of the lattice to enhance reactivity, and this has been taken advantage of in the detection of dislocations through the "etch pits" developed on the surface at the points where dislocations intersect the surface, as a result of chemical etching. Figure 22 shows the 1-to-1 correspondence in position of these etch pits with the points of intersection with the surface of the dislocations, as revealed by "decoration" (discussed in the previous section) for a sample of silicon [19].

As just noted, grain boundary effects can accelerate the corrosion of solids. Even more subtle variations or inhomogeneities in impurity content between slightly separated regions of the solid can also increase the rate of corrosion, producing "local action cells". These operate much like an ordinary storage battery; the driving force for the passage of current, which is accompanied by the dissolution of metal in the local regions that are anodic, is provided by the difference in chemical potential between regions of the solid with somewhat different impurity contents.



Figure 22. Termination of dislocations in etch pits. Copper has been precipitated on silicon dislocations, with photograph taken by transmitted infrared. After Dash [19].

Another familiar solid phase chemical reaction is the photographic process. In the development of the latent image, metallic silver is nucleated in the silver halide. There must be a mechanism for the transport of silver ions to the sites where metallic silver is formed, and this is believed to be interstitial diffusion. Dislocations or grain boundaries may play a role, by providing preferred deposition sites. Chemical impurities also are clearly important, as indicated by the role of sensitizers. Sulfur sensitization, for instance, apparently involves the formation of  $\text{Ag}_2\text{S}$  at the surfaces of crystallites, where they act as hole-traps and promote the formation of the interstitial silver needed to continue the image formation.

In decomposition reactions nucleation of the product phase is important (note the resemblance of chemical reactions to transformations, in the importance of both nucleation and growth stages). The thermal decomposition of  $\text{KMnO}_4$ , for example, is enhanced by pre-irradiation, which shortens the induction time for the reaction (Fig. 23). The irradiation produces cation vacancies and interstitials, which then recombine with the release of energy. The local heating decomposes nearby  $\text{MnO}_4^-$  ions and increases the number of nuclei of the reaction product, and the increase in nucleation sites effectively shortens the induction period.

### G. RADIATION EFFECTS IN SOLIDS

We have already had occasion to mention a number of solid state phenomena dependent upon irradiation. A primary effect of irradiation often is to produce point defects, and we have seen how these can promote transformations or chemical reactions, either by supplying nucleation sites or by increasing diffusion rates. In Figure 24 we show

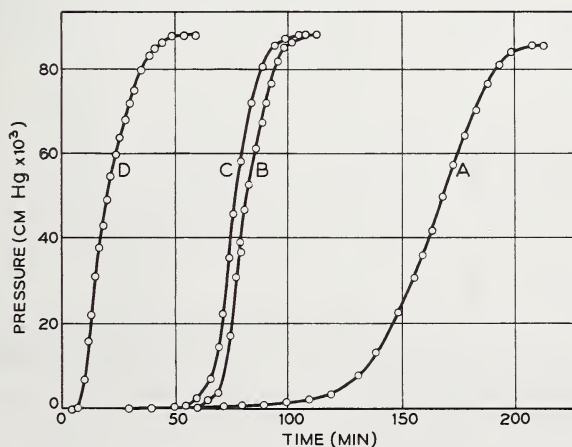


Figure 23. Shortening of induction period for thermal decomposition of  $\text{KMnO}_4$ , by irradiation.

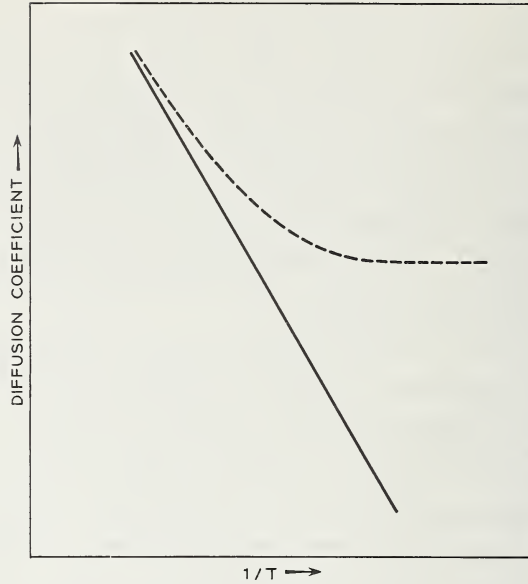


Figure 24. Schematic of enhanced diffusion under irradiation: solid line is normal diffusion, dashed line is enhanced rate in steady-state condition during bombardment.

schematically how the diffusion coefficient can be enhanced by irradiation leading to vacancy formation. In the steady state, a concentration of vacancies above that intrinsic to the crystal is produced in the low temperature region.

A profusion of complex centers can be produced by irradiation, in addition to simple vacancies and interstitials. For example centers have been identified in silicon [20] containing small amounts of oxygen or of phosphorous corresponding to the following structures:



In silicon with very low aluminum concentrations,  $\sim 10^{-7}$ , electron bombardment produces interstitial  $\text{Al}^{2+}$ . The mechanism suggested is the primary production of vacancies and interstitial silicon, with later displacement of the (substitutional) Al by the interstitial Si as it diffuses through the lattice. Many other radiation damage centers are known, also.

H. SURFACES

We have mainly been concerned with bulk properties of solids, but it is obvious that many properties associated with the surface are of equal interest, and that the characterization of surface impurities and defects is vital to progress in these areas. It is only within very recent years that techniques for the analysis of surfaces have become available, and already the rewards to be expected from their further development are apparent. Techniques have been developed for the preparation and maintenance for appreciable times of atomically clean surfaces, for half a dozen or so materials. With this have also come techniques for surface characterization, of both the clean surfaces and those with adsorbed gases. Among these are flash desorption, field emission and field ion microscopy, low energy electron diffraction (LEED), and high resolution electron microscopy. LEED, for example, shows details of structure of the surface layers. While Ni atoms on a clean Ni surface reflect the arrangement in the bulk, the two or three top layers in silicon and germanium show a complex rearrangement of the surface, with displacement of atoms both sideward and normal to the surface (Fig. 25a). In an ionic compound, such as LiF, the anions and cations may be displaced differently. With adsorbed gases, surface structures develop which may be quite unexpected. Thus, while iodine on silicon behaves in the expected manner, oxygen on nickel does not (Fig. 25b). The relationship of the surface features, as shown by these new characterization techniques, to the physical and chemical properties, largely remains to be established.

One vast area of interest in chemistry is adsorption and catalysis on solid surfaces. Few major problems have so eluded efforts to gain a

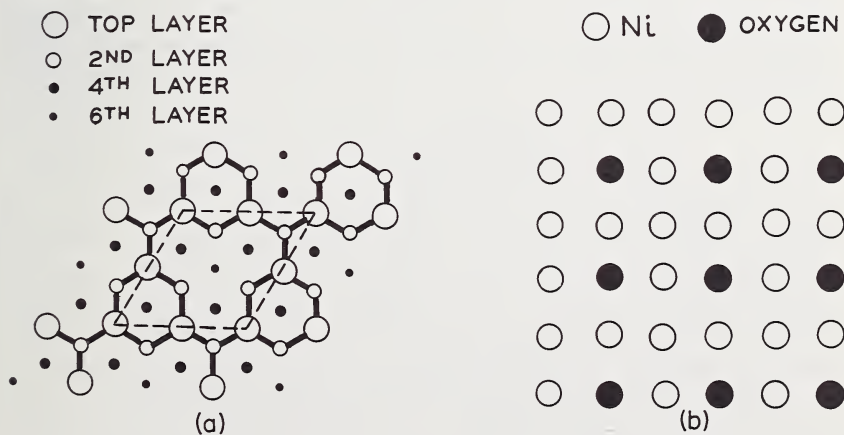


Figure 25. (a) "Reconstructed" surface layers of clean silicon, (b) (100) face of Ni with one-quarter coverage by oxygen (only the top layer is shown).

fundamental understanding as has the role of the solid in the catalysis of chemical reactions. The new techniques for the characterization of surfaces offer promise for the elucidation of the nature of the adsorbed layer, and this is clearly a key feature in the understanding of catalysis. Many attempts have been made also to relate the nature of the bulk solid to its role as a catalyst, and while certain factors are found to be highly suggestive, their generality has yet to be established and exceptions can be found. One such factor is the electronic structure of the solid, and among the clues that have been noted is the semiconducting nature of a number of nonmetallic catalysts. This is thought to be related to the transfer of electrons back and forth between the solid and the adsorbed reacting species. The Fermi level in the solid determines the ability for this to occur, and this in turn is determined by the chemical composition, in the usual manner for semiconductors. This is illustrated by the oxidation of CO to CO<sub>2</sub> on NiO. The addition of monovalent ions, such as Li<sup>+</sup>, converts an equal number of divalent nickel ions to trivalent ions, making the material more *p*-type and lowering the Fermi level. The addition of trivalent ions, such as Cr<sup>3+</sup>, removes trivalent Ni<sup>3+</sup>. The effect of these additions on the activation energy for the reaction is shown in Figure 26 [21].

Another example of the possible relation of the chemical and defect composition to the catalytic activity is provided by studies of the H<sub>2</sub>—D<sub>2</sub> exchange reaction on MgO. The catalyst can be activated by irradiation with  $\gamma$ -rays. Electron spin resonance was used to measure the concentration of *V*<sub>1</sub>-centers and there was found to be a strong correlation between catalytic activity and *V*<sub>1</sub>-concentration as the activity induced by the irradiation decayed, as shown in Figure 27 [22].

#### IV. Characterization and Properties

We have reviewed, in a way which was necessarily sketchy, some of the relationships between the physical and chemical properties of solids, and the trace quantities of chemical impurities or structural imperfec-

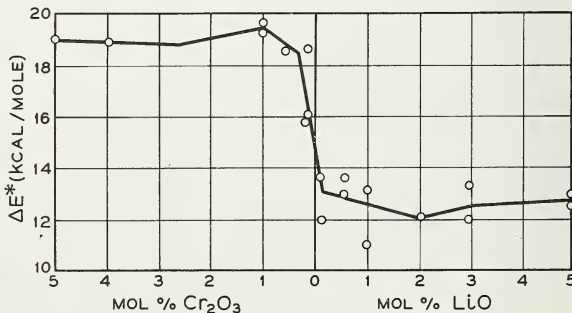


Figure 26. Activation energy for the oxidation of CO on NiO with added impurities. After Schwab [21].

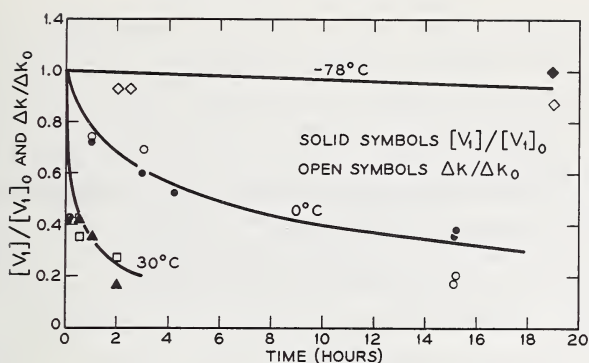


Figure 27. Annealing curves for ultraviolet-irradiated MgO. Ordinates show  $V_1$ -concentration and catalytic rate constant, following the irradiation. After Lunsford [22].

tions which are present in every real material. As we noted earlier, a primary goal of materials preparation and characterization is to facilitate the development and understanding of these relationships. We see constantly examples in all areas of solid state science and technology where our ability to control or comprehend properties is limited by our inability to do a good enough job of characterization.

We have endeavored, in our choice of examples to illustrate the relationships between properties and trace impurities and structural defects, to bring out a few of the areas where improvements in characterization are needed. In the area of electronic materials, for example, the efforts to study and utilize new semiconducting compounds, of fundamental research interest or with promising electrical or optical properties for the rapidly growing array of new semiconductor devices, would be greatly aided by better techniques for extremely low concentration of chemical impurities. Magnetic materials research and development is hampered by our rather crude techniques for determining valence state. Equally poor techniques for stoichiometry determination affect work with many compounds of interest as electronic materials. Surface effects are of great importance in devices for integrated circuits, and here again our characterization techniques are quite inadequate.

In the area of structural materials we have a pressing national need for new materials, with improved capability for high-temperature performance, or which have high strengths combined with light weights. We have already noted the intimate dependence of the mechanical properties of the refractory metals, which of course are of particular interest for such applications, on purity and perfection, and we are led to compare our relatively poor analytical techniques for the light elements, such as carbon, nitrogen, and oxygen, with the predominant role of these impurities in the refractory metals. Another pressing national need in the materials area has to do with the degradation of materials. Corrosion and oxidation are extremely costly—for example, 25% of our

steel production has been said to be for the replacement of corroded equipment—and it often is impurity dependent. Polymeric materials degrade, and we are so unable to characterize them, as a class, that our approaches to the control of polymer degradation often have to be Edisonian. Radiation damage phenomena involving defects in solids are important in materials ranging in application from nuclear reactors to electronic devices in satellites.

Thus we find that all areas of solid state research and technology have broad regions where we are limited by the materials we have available and our ability to control them chemically and structurally. It is apparent that improved characterization is an indispensable part of the materials work needed to permit further advances in these areas.

## V. References

- [1] Report of the Committee on Characterization of Materials, of the Materials Advisory Board (to be published).
- [2] After H. W. Leverenz.
- [3] See, for example, C. Kittel, "Introduction to Solid State Physics," John Wiley & Sons, New York (1956); A. J. Dekker, "Solid States Physics," Prentice-Hall, Englewood Cliffs, N.J. (1957).
- [4] See, for example, "Semiconductors," N. B. Hannay, Ed., Reinhold Publ. Corp., New York (1959).
- [5] "Chemistry of Imperfect Crystals," F. A. Kroger, Interscience, New York (1964).
- [6] See, for example, "Ultra-High Purity Metals," The American Society for Metals, Metals Park, Ohio (1962).
- [7] See "Thermodynamics of Solids," R. A. Swalin, John Wiley & Sons, New York (1962).
- [8] B. T. Matthias, T. H. Geballe, E. Corenzwit, and G. W. Hull, Jr., *Phys. Rev.* **129**, 1025 (1963).
- [9] D. G. Thomas, M. Gershenson, and F. A. Trumbore, *Phys. Rev.* **133**, A269 (1964).
- [10] E. G. Spencer and J. P. Remeika, *Proc. Intermag. Conf.*, T-159, IEEE, Washington, D.C. April, 1964.
- [11] See, for example, E. E. Schumacher, *Trans. AIME* **188**, 1097 (1950).
- [12] J. R. Patel and A. R. Chaudhuri, *J. Appl. Phys.* **34**, 2788 (1963).
- [13] J. R. Patel, *Discussions Faraday Soc.*, No. 38, (1964).
- [14] See, for example, "Introduction to Solids," L. V. Azaroff, McGraw-Hill, New York (1960).
- [15] See "The Structure and Properties of Materials," (Vol. 2—"Thermodynamics of Structure"), J. H. Brophy, R. M. Rose, and J. Wulff, John Wiley & Sons, New York (1964).
- [16] F. J. Morin and H. Reiss, *J. Phys. Chem. Solids*, **3**, 196 (1957).
- [17] E. M. Pell, in *Symposium on Solid-State Physics and Telecommunications*, Brussels, 1958. Désirant and Michiels, Ed., Academic Press, New York (1960).
- [18] See, for example, "Reactivity of Solids," J. H. de Boer Ed., Elsevier Publ. Co., Amsterdam (1961); "Chemistry of the Solid State," W. E. Garner, Ed., Butterworths Scientific Publications, London, (1955).
- [19] W. C. Dash, *J. Appl. Phys.* **27**, 1193 (1956).
- [20] "Radiation Damage in Semiconductors," Paris, 1964. Academic Press, New York (1965).
- [21] G. M. Schwab, "Semiconductor Surface Physics," Univ. of Pennsylvania Press, Philadelphia (1957).
- [22] J. H. Lunsford, *J. Phys. Chem.* **68**, 2312 (1964).

# ELECTRICAL MEASUREMENTS FOR TRACE CHARACTERIZATION

LEONARD R. WEISBERG

*RCA Laboratories, Princeton, New Jersey 08540*

## I. Introduction

The use of electrical measurements for trace characterization has evoked considerable interest in recent years [1-3].<sup>1</sup> There is little question that if electrical measurement apparatus were available commercially today in a form where the sample could be inserted, a button pushed, and the results presented on a chart, these techniques might already be in wide use. However, this is still in the future, since they are really laboratory methods. The doubt justifiably arises in the minds of analytical chemists whether or not these techniques are of value, or if they might involve more effort than they are worth. In short, this is a question of complexity versus utility.

This is certainly an important question, and to answer it better, this paper is divided into two distinct parts. In the first part, the value of electrical measurements to the analytical chemist will be discussed. In the second part, the fundamental principles of these methods will be reviewed, and techniques and apparatus necessary to carry out these measurements will be described. It will be seen that the simplicity of both the apparatus and interpretation is an important feature of these techniques.

It is particularly significant here that this is the first of a series of symposia on Materials Research. The electrical measurements to be discussed were spawned in and by materials research; and, as will be seen later, the interrelationship of analysis with materials research determines whether or not they should be used in an analytical laboratory.

## II. Value of Electrical Measurements for Analysis

### A. CRITERIA FOR ANALYTICAL USE

We first consider what the criteria are for introducing new instruments into an analytical laboratory. We can determine this by examining those instrumental techniques that are presently in use, which include instruments for emission spectrography, mass spectrography, electron spin resonance, nuclear magnetic resonance, electron probe microanalysis,

---

<sup>1</sup>Figures in brackets indicate the literature references at the end of this paper.

and electron microscopy. What are the common features of these instruments?

Their most outstanding feature is that they are enormously expensive—their prices range between \$25,000 and \$100,000. In fact, none of these techniques were acceptable until they became expensive—i.e. until a large effort had been invested in engineering and automating their operation. Thus, we can conclude that cost is not an important factor here, and instead that the first criterion for a new measurement technique is *simplicity of use*.

The second most important feature is that each measurement has *special advantages*, that extend the range or speed of analysis over previous instruments. This is clearly manifest in the above mentioned instruments. For example, the mass spectrograph can detect a very wide range of impurities at one to two orders of magnitude lower concentration than the emission spectrograph.

The third common feature is that each instrument is *self-sufficient*, i.e. that the defects can be specifically identified in any given matrix, without requiring supporting information. Therefore, each instrument can provide a *meaningful* characterization by itself.

## B. CHARACTERISTICS OF ELECTRICAL MEASUREMENTS

How well do electrical measurements fulfill these three criteria: simplicity, special advantages, and self-sufficiency? Let us consider the advantages and disadvantages of electrical measurements in this light.

First, we consider the question of *simplicity*. Here we mean both simplicity of measurement, and simplicity of interpretation. There are many electrical properties known that are dependent upon the presence of impurities. Some of these are listed in Table 1, and are also discussed in the paper by N. B. Hannay of this conference. However, for most of these, the effects are not well enough established to permit either simple measurement or interpretation. In many cases, results can be ambiguous, especially when the material is structure sensitive. For example, it is well established that impurities can affect the superconductive transition temperature. However, even if one were told that there were three samples of  $\text{Nb}_3\text{Sn}$ , with transition temperatures of 18 °K, 17 °K, and 16 °K, one could draw no specific conclusions concerning their impurity concentrations since this variation could be caused by lattice defects. The same sort of problem exists with dielectric relaxation, space charge limited currents, cyclotron resonance, internal friction, and magneto-acoustic absorption. Magnetic properties are so highly structure sensitive and dependent on major constituents that trace impurities are not easily detected, except in special cases. However, these methods should not be considered out of the question. As further research is carried out, some of these methods might attain great

utility. For example, later in this book, papers are given on trace characterization by measuring dielectric properties, and by thermoelectric measurements.

Thus, for routine and simple use in an analytical laboratory, one should presently consider only the first four properties listed in Table 1. Each of these requires simple apparatus, and can be constructed using commercially available instruments. The cost of constructing any of these should be below \$5,000, and require perhaps about a month to build and put into operation. Finally, these four techniques cover the full gamut of electrical properties, including metals, semiconductors, and insulators.

We next consider *self-sufficiency*. Unfortunately, the main disadvantage of these electrical measurement techniques is that they are non-specific—i.e. in general, impurities are *not* identified by the measurement. Effects of different impurities can be separated in some electrical measurements, but in these cases, the electrical behavior of the impurity is a function of its matrix. In fact, when effects from different impurities are not separated, only the dominant impurities are then detected, and this is a masking problem that can't be avoided. Next, since it is generally not known which impurity provides the effect, unambiguous impurity concentrations cannot be determined using electrical measurements. Finally, lattice defects can produce electrical effects similar to those of impurities, and many impurities are not electrically active, which prevents absolute impurity measurements. Instead, electrical measurements must be used as an analytical tool in conjunction with other main analytical methods. In fact, these measurements

TABLE 1. Impurity Dependent Electrical Properties.

Resistivity
Residual Resistivity
Hall Effect
Thermally Stimulated Currents
Space Charge Limited Currents
Thermoelectric Power
Dielectric Relaxation
Piezoelectricity
Internal Friction
Cyclotron Resonance
Magneto-Acoustic Absorption
Superconducting Properties
Critical Temperature
Critical Current
Magnetic Properties
Permeability
Ferromagnetic Resonance Line Width

must be calibrated at higher impurity concentrations versus standard analytical procedure, before their results can be extrapolated to low concentrations. They can never independently provide a meaningful characterization of trace impurities. Thus, electrical measurements fail the criterion of self-sufficiency.

Turning to the last criterion, *special advantages*, here electrical measurements excel, surpassing all other analytical methods in several respects, listed in Table 2. Their sensitivity is outstanding, easily entering the part-per-billion range (i.e., 1 atom in  $10^9$ ). This is the most important feature of electrical measurements, and by itself justifies their use. In addition, their relative precision is very high, within 10%, which is especially important when comparing impurity concentrations between samples. Next, they are non-destructive to the sample—i.e., the sample is not consumed during the measurement process. Finally, the analysis requires a relatively short time—typically from 1 to 100 minutes. The combination of these four properties fully satisfies the last criterion.

### C. APPLICATIONS OF ELECTRICAL MEASUREMENTS

We have discussed that four electrical measurements, resistivity, residual resistivity, Hall effect, and thermally stimulated currents, only *partially* satisfy criteria for widespread use in an analytical laboratory. However, because of their special advantages, they still have potential value in an analytical laboratory, and the question that arises concerns exactly where they can be used.

The answer to this question can be found by referring again to the

TABLE 2. Advantages of electrical measurements.

- (1) Very High Sensitivity (to 1 part in  $10^9$ )
- (2) High Relative Precision (10%)
- (3) High Speed (1 to 100 min.)
- (4) Non-Destructive to Sample

underlying theme of this Symposium—materials research. Since these electrical measurements were spawned by materials research, we must ask the materials researchers where these techniques have been most useful. Experience here has disclosed three main applications: determination of *over-all purity*, *monitoring purification*, and delineating *impurity distribution*. In none of these applications is the identification of an impurity essential. These three applications are best described by presenting some case histories taken from the annals of materials research, where use of electrical measurements have played a crucial role. It will be seen that, in general, electrical measurements are most important at very low impurity concentrations, where many other analytical techniques fail.

*Example 1: General Principles—Purity of Water*

First, for illustration, we will consider an example familiar to all analytical chemists—the determination of water purity by resistivity measurements. This example clearly illustrates all the features, both good and bad, described above for electrical measurements.

Pure water has a resistivity of about  $3 \times 10^7$  ohm-cm at 18 °C, and the resistivity decreases approximately in direct proportion to the ionic concentration, as shown in Figure 1. The resistivity of a water sample is determined by dipping commercially available electrodes into the sample, and reading the resistivity or conductivity from a standard bridge circuit. Analytical results can be found within a minute, with a detection limit below 1 ppm, and an accuracy of a few percent, without destroying the sample. The apparatus costs only about \$100.

The disadvantages are also clearly shown here. Not all impurities affect the conductivity of water equally, (e.g.,  $\text{Li}^+$  has a mobility an order of magnitude below  $\text{H}^+$ ) and some provide almost no ions at all, such as organic impurities. Thus, the analysis measures only the general *minimum* impurity content, and also no knowledge is derived concerning the identity of the impurities.

Even though the measurement does not fully characterize the purity of water, the value of the measurement is manifest. One merely has to ask how much time the analytical chemist would have to spend to continually check the purity of water before carrying out other tests, or

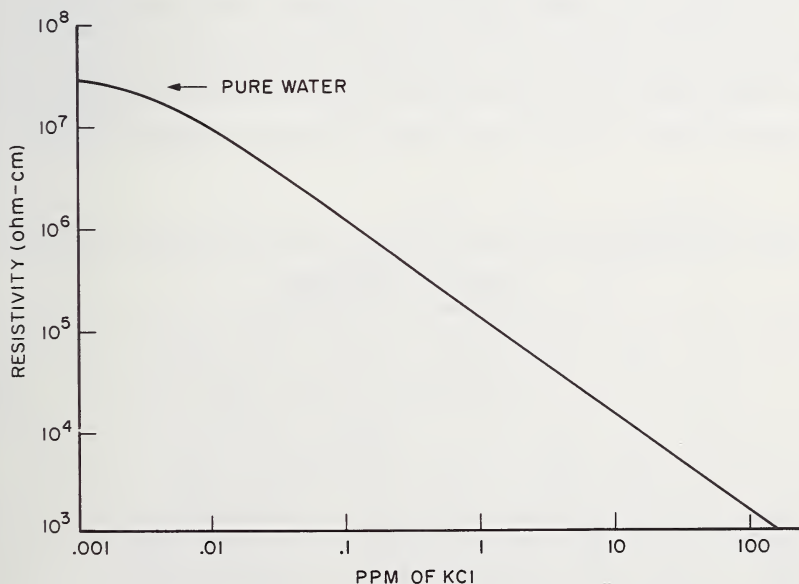


Figure 1. Variation of resistivity with impurity concentration in water at room temperature. (ppm = parts in  $10^6$ ).

to continually determine if a water distillation apparatus was functioning properly. Countless hours have been saved through the years by the use of this method.

*Example 2: Purification of Gallium and Aluminum*

One of the most annoying problems in materials research is to perform a careful purification procedure, and then not know whether or not it worked. Indeed, this problem is encountered quite regularly in the ultrapurification of metals, when the total impurity concentration is reduced below the order of 1 ppm. At this level, there is no convenient analytical technique to rapidly detect a broad range of impurities for a large number of samples. Therefore, progress in purification is badly impeded. For example, if one is using a chemical treatment to clean material, one would like to know whether one, three, or ten treatments are necessary, or even harmful. Another purification treatment is to directionally solidify or zone refine a material in a boat. One hopes that impurities are swept to the tail end of the ingot, but this procedure must be monitored.

In the purification of gallium and aluminum, *residual resistivity measurements* (described later) played a very important role. In the case of gallium, the procedure used was directional freezing. Subsequent to freezing, samples were removed from the ingot for emission spectrographic analysis [4], and the results found are shown in Table 3. Despite very careful emission spectrographic analysis, no variation at all could be seen along the ingot. However, referring to the last column of the table, use of residual resistivity measurements clearly showed that the front end of the ingot was, indeed, purer than the tail end, even though the difference was less than a factor of two. Use of residual resistivity measurements actually saved *months* of work in gallium purification.

TABLE 3. Variation of impurity content (in ppm) along a directionally solidified gallium bar.

(After Kramer and Foster [4])

	Cu	Sn	Pb	Hg	Zn	Al	Fe	Mg	Ca	Si	$\frac{R_{300}}{R_{4.2}}$
Front	0.1	nd*	nd	nd	nd	0.1	nd	0.01	0.1	nd	44,000
Middle	0.1	nd	nd	nd	nd	0.1	nd	0.01	0.1	nd	39,000
Tail	0.1	nd	nd	nd	nd	0.1	nd	0.01	0.1	nd	30,000

\*Not detected.

In the above method, the zone refined ingot must be sectioned to provide samples for measurements. However, this can be avoided. The ingot can be preserved by placing electrical leads along its length [5, 6], as shown in Figure 2. Current is passed through the bar, and the resistivity of any section is determined from the potential drop between sets of leads. The results for the variation of residual resistivity in zone refined aluminum [5, 6] is shown in Figure 3. Again, the effect of purification is clearly demonstrated.

### *Example 3: Impurity Distribution in Germanium*

In the above examples, the high sensitivity of electrical measurements was the major factor determining their use. In the example here, the *high relative precision* of the measurement technique is the significant feature. The dependence of resistivity of germanium on the impurity content is shown in Figure 4, where a donor is an impurity that can contribute a conduction electron to the solid. This figure is quite similar to Figure 1, and this is not accidental, but occurs because impurities in a semiconductor are very analogous to ions in a solution. Not only is the extreme sensitivity manifest here, but above 1 part in  $10^9$ , the resistivity varies linearly with impurity concentration. The resistivity is easily measured to a relative precision of 2%.

The control of impurity distributions in semiconductors is an extremely important problem, not only technologically, but also since it can provide important information concerning the fundamentals of crystal growth mechanisms. To impart desired characteristics to a semiconductor, selected impurities are deliberately added to the semiconductor. In growth from the melt, the impurity can be added to the melt before growth, but then the impurity is segregated to the tail end of the ingot.

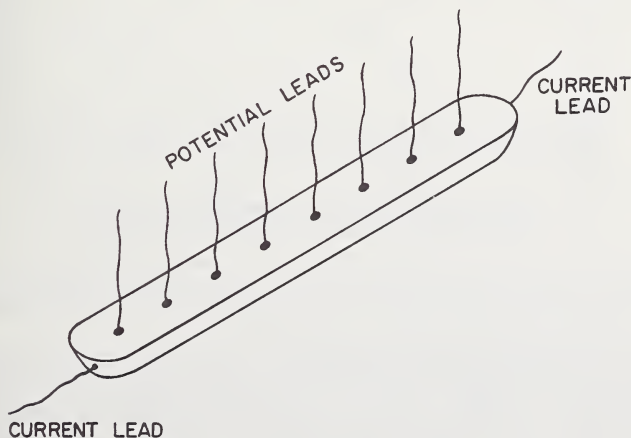


Figure 2. Position of current and potential leads on an ingot for residual resistivity measurements.

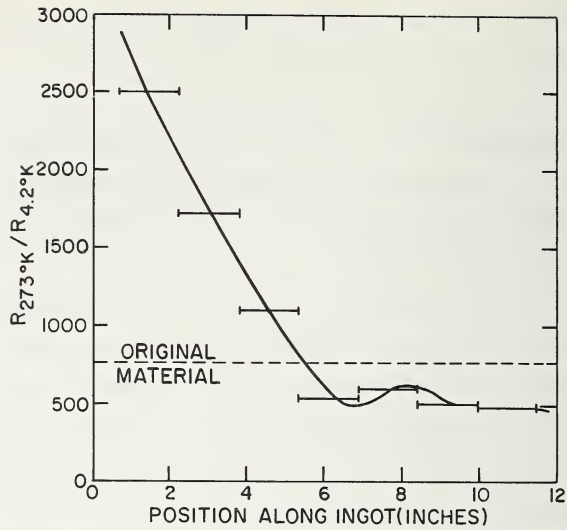


Figure 3. Residual resistance ratio of aluminum, zone refined with 20 passes of two zones.

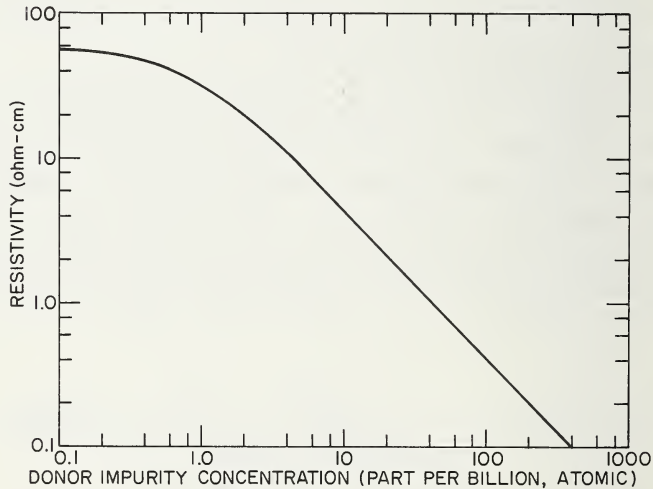


Figure 4. Variation of resistivity with donor impurity concentration in germanium at room temperature (parts per billion = parts in  $10^9$ ).

While this may be desirable if one is purifying, it is *undesirable* if one tries to achieve highly uniform properties.

After growth, the impurity distribution along the entire length of the crystal can be rapidly and accurately determined by measuring the resistivity [7], as is shown [8] in Figure 5, curve (a). By using special growth techniques to correct for the impurity segregation [8], the impurity distribution was then held constant to within about 20% over a 20 cm portion of the ingot, as shown in Figure 5, curve (b). Comparing Figure

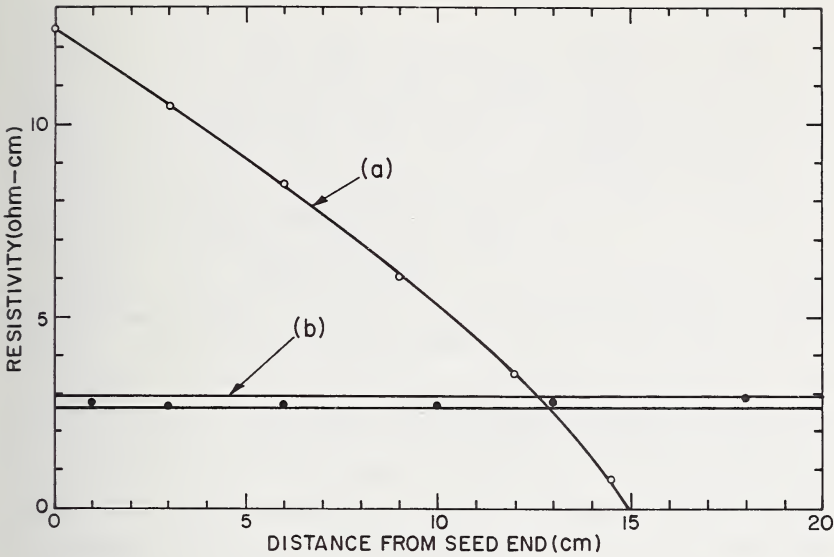


Figure 5. Variation of impurity concentration, as revealed by resistivity measurements, along the length of a single crystal of germanium grown by (a) ordinary Czochralski method, and (b) special Czochralski method.

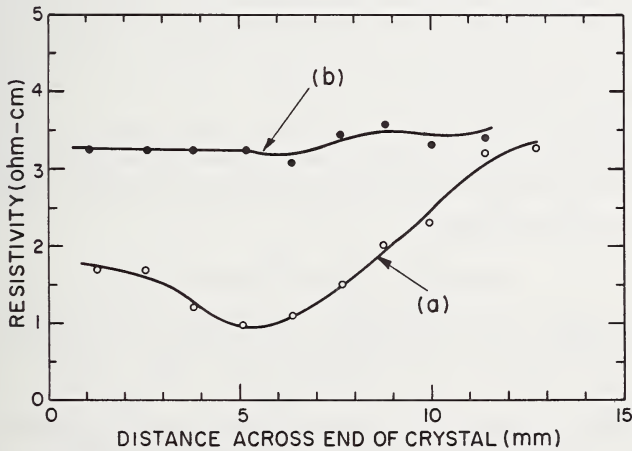


Figure 6. Radial variation in impurity concentration, revealed by resistivity measurements, in a germanium single crystal (a) before and (b) after optimizing the thermal gradient.

5 to Figure 4, it is seen that the impurity concentration was easily measured here to a high relative precision in the range of 5 to 50 parts in  $10^9$ . Indeed, the corrected impurity distribution (Fig. 5, curve (b)), was actually measured to be held constant to 2 parts in  $10^9$  over a 20 cm length! This remarkable measurement cannot be even approached by ordinary analytical techniques.

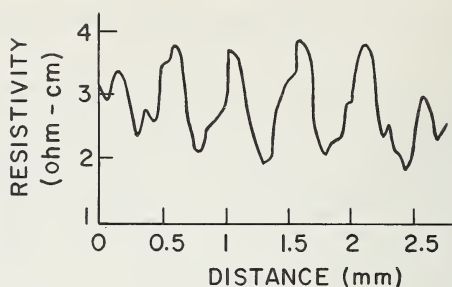


Figure 7. Fluctuation in impurity concentration in germanium as revealed by resistivity measurements.

Let us turn up the "magnification" a bit further. In Figure 6 is shown the radial variation of resistivity, before and after correction [8]. One division in Figure 5 is equivalent to  $2/3$  of the entire Figure 6, so that we are seeing here impurity variations over a fine scale. Even smaller variations can be seen. In Figure 7 is shown a periodic fluctuation in impurity distribution [9], again detected by resistivity measurements. The points in Figure 6 are so far apart that this effect would have gone unnoticed! Note that impurity variations can be seen in distances as small as 0.1 mm in the impurity concentration range below 1 ppm. Furthermore, the ingot is not damaged by the measurement. Such a measurement by ordinary analytical techniques would be a hopeless task. Even electron microprobe analysis would not work here, because the impurity concentrations are too low.

Once again, the point here is that not only were many man-months saved by these measurements, but also that an analytical laboratory could well be overwhelmed by confrontation with such a task, without using resistivity measurements.

#### *Example 4: Over-all Purity in GaAs*

The purpose of this example is to illustrate how electrical measurements are enhanced by coupling them with standard analytical techniques.

Hall effect measurements (discussed later) are more difficult to perform than resistivity measurements, but provide a more direct measurement of the impurity concentration. They are quite important in semiconductors in accurately surveying the overall purity.

In 1958, Hall measurements indicated that 0.1 to 100 ppm of impurities were in GaAs, and varied from sample to sample. The impurity level could not be controlled since the impurity source was unknown. Sulfur was suspected to be the major impurity, since it is a major impurity in the arsenic. Accordingly, a considerable time of unrewarding effort was spent developing a sufficiently sensitive wet chemical method to detect sulfur, but this just showed that sulfur was *not* the suspected impurity.

It was also obvious that tracking down other suspected impurities by quantitative analytical procedures would be too time consuming. Instead, semiquantitative emission spectrographic data was accumulated on nearly 100 samples of GaAs, and compared to the Hall effect electrical data [10]. The result is shown in Figure 8, in which it is seen that a one-to-one correspondence existed between the concentration of silicon and the electron-carrier concentration.

Using this result, the entire course of the GaAs research program was altered, since the Hall effect measurement could then provide meaningful and highly accurate information concerning the purity of the samples. A Hall measurement can be carried out in about 30 minutes, and provides a measure of the silicon concentration at and below 1 ppm to an accuracy of  $\pm 20\%$ , using a sample weighing about 1/2 gram, and not destroying the sample. Several crystals were grown per week, and several samples were removed for analysis from each crystal. It is easily seen that performing highly accurate quantitative analysis in this low concentration range could be problematical for an analytical laboratory, if Hall measurements were unavailable.

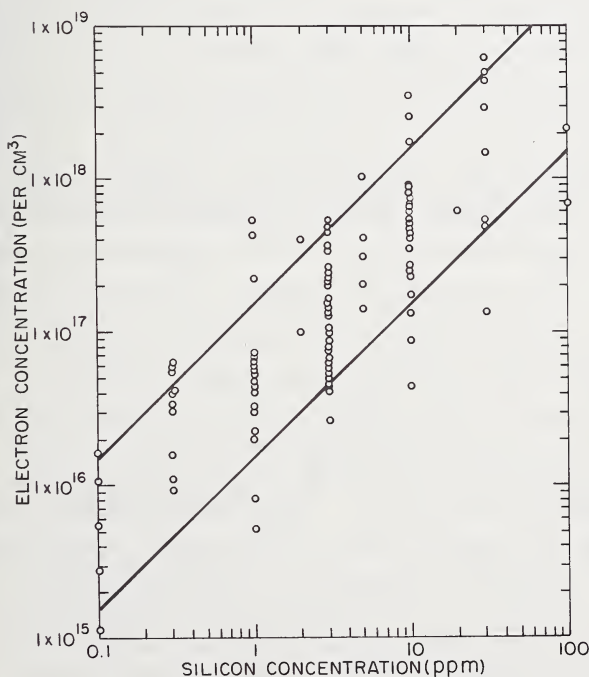


Figure 8. Variation of electron concentration with silicon concentration in GaAs single crystals. Horizontal separation of solid lines indicate limits of accuracy of semi-quantitative emission spectrographic analysis for silicon (ppm = parts in  $10^6$ ).

### III. Fundamental Principles and Apparatus

#### A. FUNDAMENTALS

Each electrical measurement is useful for only a particular class of materials depending upon its electrical resistivity, as indicated in Table 4. This difference is not superficial, but is related to the way the impurities affect the electrical properties, which differs in each case, as is also shown in Table 4.

TABLE 4. Detection of impurities by their electrical effect in materials of different resistivities ( $\rho$ ).

Method	Material	Effect of impurities
(1) Residual resistivity	Metals ( $\rho < 10^{-4}$ )	Scatters current carriers (lowers mobility).
(2) Resistivity, Hall effect	Semiconductors ( $10^{-4} < \rho < 10^4$ )	Adds current carriers (electrons, holes, ions).
(3) Thermally stimulated currents	Insulators ( $\rho > 10^4$ )	Traps current carriers.

In *metals*, there are so many electrons ordinarily present that they swamp out any electrons possibly contributed by trace impurities. Instead, the important feature is that the impurities can scatter electrons, thus raising the electrical resistivity. However, the lattice itself also scatters electrons, and this effect dominates at room temperature. By reducing the temperature to liquid helium temperature (4.2 °K), the effect of scattering of electrons by the lattice is reduced to the point where it no longer dominates. Then, as shown in Figure 9, the resistivity is determined by the scattering of the electrons from the impurity atoms. The purer the material, the higher is the electron mobility, and the smaller is the resistivity. It was noticed 100 years ago by Matthiessen that the resistivity due to the addition of impurities is approximately temperature independent. Thus, the presence of impurities usually provides a low temperature limit to the resistivity, and this limit is termed the *residual resistivity*. The measurement of resistivity (or conductivity) at 4.2 °K thus provides a sensitive measure of impurity concentration.

In *semiconductors*, in contrast, there are relatively few electrons present, and each electron added by impurities has an appreciable effect, so

that a direct correlation exists between electrically active impurity concentration and resistivity. Impurities in semiconductors can be fruitfully compared to ions in solution. This is clearly seen by comparing Figure 1 for impurities in water to Figure 4 for impurities in germanium.

Concerning *insulators*, there are almost no current carriers available at all, and trace impurities far outnumber the current carriers, which is the reverse of the condition for metals and semiconductors. However, in insulators, impurities can act as traps, i.e., they can capture a current carrier for a certain length of time before releasing it. This occurs because the ionization energies are large and the ionization constants are small. One then utilizes the trapping effect of impurities to detect their presence.

Thus, the fundamental quantities affecting the electrical measurements are the concentration per  $\text{cm}^3$  of current carriers,  $n$ , the mobility of the carriers,  $\mu$ , and the concentration of electrons released by traps,  $n_T$ . In general, the relation between the resistivity  $\rho$ ,  $n$ , and  $\mu$  is given by

$$n = 1/(\rho e \mu) \quad (1)$$

where  $e$  is the electronic charge. We must distinguish between the electron concentration  $n$  and the impurity concentration  $N$ . In a metal, as mentioned above,  $n$  is constant with impurity concentration, so that  $\rho$  is inversely proportional to  $\mu$ , and  $\mu$  is inversely related to the impurity concentration  $N$ . Unfortunately there is no general expression relating  $\mu$  and  $N$ , since the impurity scattering depends upon the particular impurity and the lattice it is in. Therefore, the residual resistivity gives only a general and relative measure of the impurity content. One

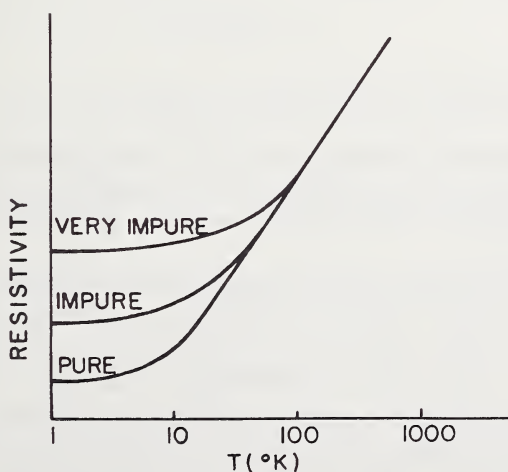


Figure 9. Variation of resistivity with temperature in a metal.

other restriction on its use should be noted—it cannot be used for metallic *alloys*. The presence of the alloying element scatters electrons, and this masks the presence of trace impurities.

For semiconductors, the situation is simpler. To a first approximation, one can assume that  $\mu$  is a constant independent of impurity concentration. Then  $n$  varies inversely with  $\rho$ , and since the impurity concentration  $N=n$ ,  $N$  then is inversely proportional to  $\rho$ . However, it is not always true that  $\mu$  is independent of  $N$ .

This problem of assuming constant mobility can be eliminated by using the Hall effect. An interesting analogy can be drawn between a Hall effect and a pH measurement. A pH measurement determines the concentration of ions in a solution, while a Hall measurement determines the concentration of charge carriers in a solid. However, the method of measurement is completely different. Here one adds a magnetic field  $H$  across the sample of thickness  $t$ , and passes a current through the sample. The magnetic field deflects the current causing a transverse voltage, the Hall voltage  $V_H$ , to be set up across the sample, and this voltage is easily measured. As shown in standard deriviations [11], the concentration of current carriers, and hence the impurity concentration, is given by:

$$n = IH 10^{-8}/V_H et \quad (2)$$

where  $V_H$  is expressed in volts,  $t$  is the sample thickness expressed in cm,  $I$  is the current through the sample in amps,  $e = 1.6 \times 10^{-19}$  coulombs, and  $H$  is the magnetic field in gauss. By comparing Eqs. (1) and (2), it is obvious that measurements of both the Hall effect and the conductivity provides the Hall mobility  $\mu$  of the dominant species:

$$\mu = 1/(nep) \quad (3)$$

When  $\rho$  is expressed in ohm-cm,  $\mu$  is expressed in the convenient laboratory units of cm<sup>2</sup>/volt-sec. The mobility serves as an additional measure of the impurity concentration of a semiconductor both at room temperature, and especially at low temperatures (e.g. 77 °K). This is demonstrated in Figure 10 for the case of germanium at room temperature.

In the case of *insulators*, the important feature is that the escape of charge carriers from a trap is a temperature activated process, and varies as  $\exp(-E/kT)$ , where  $E$  is the activation or ionization energy associated with each trap,  $k$  is Boltzmann's constant, and  $T$  is the absolute temperature. If a trap is filled at low temperatures (e.g. below 78 °K), the carriers cannot escape except after very long times (hours or even days). Thus, one can "charge up" the traps by shining light on the sample at 78° K. Then, as the temperature is raised, a

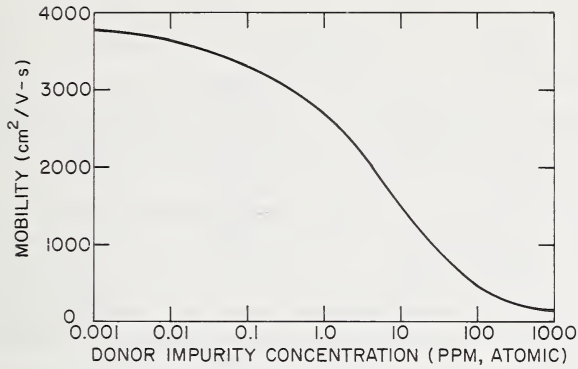


Figure 10. Variation of electron Hall mobility with donor impurity concentration in germanium at room temperature (ppm = parts in  $10^6$ ).

temperature is reached at which the electron can escape rapidly. When the electrons escape from each type of impurities, a current can suddenly flow in the sample if a voltage is applied, called the thermally stimulated current (TSC), causing a "TSC peak" in the variation of current versus temperature.

As the sample is heated, the current flows during a TSC peak for a given length of time. By integration of the area under the TSC peak, the total number of electrons that have flowed through the sample can be counted. However, this is not the number of electrons that originally escaped from the traps. The ratio of electrons that escaped to those that were actually counted is measured by generating a known concentration of electron-hole pairs  $N_{PC}$  in the sample per unit volume per sec. This is accomplished by shining a calibrated light source on it and measuring the photocurrent  $\Delta I$ . The trap (i.e. impurity) concentration  $N$  per  $\text{cm}^3$  is then given by:

$$N = N_{TSC} N_{PC} / \Delta I \quad (4)$$

where  $N_{TSC}$  is the number of electrons derived from the integration of the area under the TSC peak. Although this measurement is somewhat more complex than the previous methods, this is a very powerful and useful tool.

We proceed below to the apparatus needed for the four measurement techniques.

## B. RESISTIVITY

The sample to be measured can be either liquid or solid, and monocrystalline or polycrystalline, unless electrical barriers are known to form at internal boundaries. The main problem exists in making good contacts to the specimen [12], i.e. both ohmic and low resistance. For

purposes of discussion here, a contact is ohmic when its resistance is independent of direction and magnitude of the current. All measurements of conductivity should be carried out at least twice, with the current flowing in each direction to check for such spurious effects. In liquids, to minimize polarization and related effects, AC measurements are required.

The method employed for the measurement depends on the resistance of the formed contact. If the contact resistance is negligible with respect to the sample, then only two contacts are needed to the specimen. The resistance is determined by measuring the current flowing through the sample when a known voltage is applied. A commercial resistivity meter can be used for this measurement if high accuracy is not essential. Alternatively, the sample can be placed in a resistivity bridge. The resistivity  $\rho$  is found from the resistance  $R$  by the relation

$$\rho = AR/L \quad (5)$$

where  $L$  is the separation between the contacts,  $A$  is the cross-sectional area, and it is assumed that this area is constant throughout the sample.

It is possible to determine resistivities without knowing the sample dimensions, such as for irregularly shaped specimens, by using a four-point *resistivity probe*, as shown in Figure 11. For many materials, all that is necessary is to press the probe against the sample, independent of the shape and size of the sample, provided the sample is large enough with respect to the probe spacing, so the sample can be assumed infinite. The current is passed between the outer two probes, and the voltage measured between the inner two. The resistivity is given by

$$\rho = 2\pi dV/I \quad (6)$$

where  $d$  is the spacing between each pair of adjacent electrodes,  $V$  is the voltage and  $I$  the current. Probes with very small spacings can be constructed. In Figure 11, the contacting wires can be 0.003 in. diameter tungsten wires with sharp points, and the spacing  $d$  can be 0.010 in. With such a small probe, one can detect variations in resistivity at different positions throughout a sample (e.g., see Fig. 5). One simplifying feature here is that four-point probes for resistivity measurements are now commercially available, such as from the Dumas Company or the Fels Company (England).

A preferred method of measuring variations in resistivity along a sample is to use a resistivity "scan" procedure [7]. As shown in Figure 12, the current is passed thru the sample, while a probe moves along the surface to measure the potential drop. This measurement is easily automated by measuring the potential drop on a recorder, and have

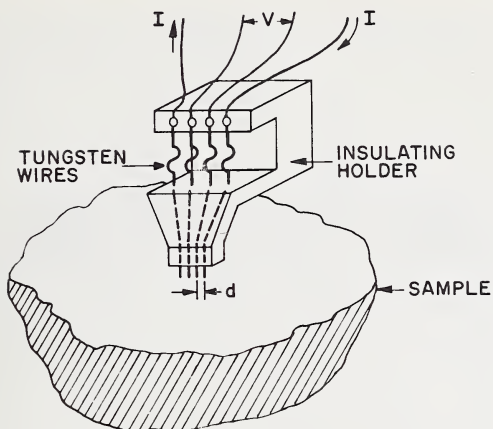


Figure 11. Four-point probe resistivity measurement.

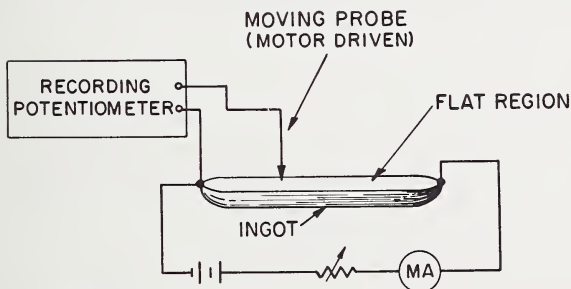


Figure 12. Resistivity scan method of measuring resistivity variation along an ingot.

a motor drive move the probe along the sample. If the impurities are distributed uniformly, the line drawn by the recorder will be linear, and any deviation from linearity indicates a non-uniformity. This is the type of method used to obtain the resistivity variations shown in Figures 5, 6, and 7.

For those cases where the contact resistance is comparable to or greater than the sample resistance, the four-contact potential-drop method must be used, as shown in Figure 13. In a bar-shaped sample, current leads are placed at the ends of the sample, and two voltage contacts along the sample. If negligible current is drawn in the potential leads, their contact resistance will not affect the measurement. This can be accomplished by using a null-type instrument such as a potentiometer to measure the voltage, or else a very high input impedance DC voltmeter. The conductivity is again given by Eq. (5), except that  $L$  is now the separation between the voltage probes.

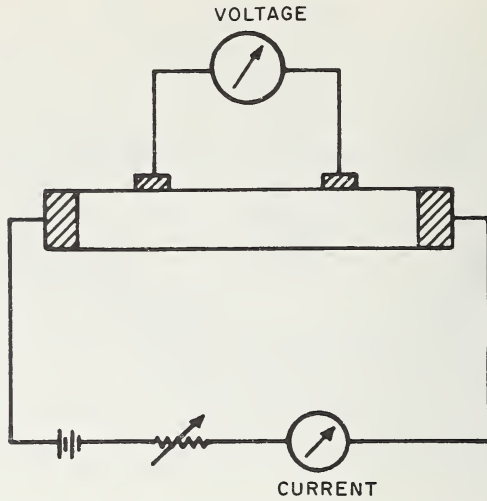


Figure 13. Four-contact potential drop measurement of resistivity.

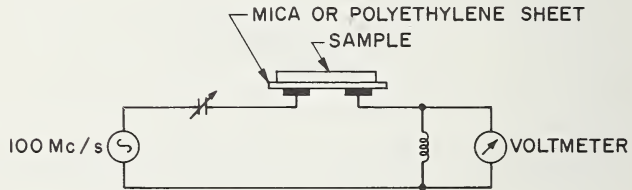


Figure 14. Contactless measurement of resistivity by capacitance coupling. After Nishizawa et al., [13].

One of the detrimental features of the above measurement techniques is that the sample must be directly contacted. This increases the difficulty of automating resistivity measurements. It would be helpful to have contactless measurement methods, and indeed it is possible to measure resistivity without contacting the specimen at all by using AC methods. In one such scheme [13], shown in Figure 14, two capacitive contacts are made to the specimen by placing it against two electrodes covered with a very thin sheet of mica or polyethylene sheet. The two electrodes are connected to a circuit having an inductance, variable capacitor, and a high frequency (100 Mc/s) voltage source. As the capacitor is varied close to resonance, the voltage drop across the inductance goes through a maximum. By calibrating this voltage with

known resistances, the resistivity can be determined directly. This particular system is applicable for samples with resistivities in the range  $10\text{--}10^4$  ohm-cm.

### C. RESIDUAL RESISTIVITY

In practice, instead of using the residual resistivity directly to measure impurity content, one employs the ratio of resistance at room temperature to that at liquid helium temperature. This minimizes extraneous factors in the measurement such as sample geometry and shape [5]. It is even unnecessary then to measure the electrode spacing or sample dimensions. Furthermore, use of the ratio minimizes effects due to anisotropy, such as in gallium [14].

The resistivity can be measured to a precision of a few per cent by using the simple four-contact potential drop method of measurement (see Fig. 13). The current is supplied from a battery, in series with controlling resistors, ammeter, and reversing switch. Because of the low resistances that must be measured at low temperatures, a DC voltmeter having a high sensitivity must be used, such as the Keithley 148 Nanovoltmeter that has a sensitivity of  $10^{-9}$  V. The potential should be measured with the current flowing in the forward and reverse directions to detect and eliminate extraneous effects such as thermoelectric voltages. For a 1 mm-diameter wire-shaped sample of gallium [12], typical values of the current and voltage at room temperature are 10 ma and  $10^{-5}$  V, and at 4.2 °K are 2 amps and  $10^{-7}$  V.

Since measurements are made at only one low temperature, 4.2 °K, the required cryogenic apparatus is quite simple. In most cases, the storage Dewar itself in which liquid helium is supplied can be used directly, provided the sample and sample holder are small enough to fit directly into its mouth.

A typical sample holder for measuring three small wire samples simultaneously is shown in Figure 15. The Teflon mounting piece is attached to the end of a 6 mm diameter thin (0.2 mm) wall stainless steel tube, 80 cm long. Two 0.018-in. and two 0.012-in. diam. copper wires pass through the tube to the Teflon piece for current and potential leads, respectively. Contact to the sample is made with coiled silver wires. The holder can be inserted directly into a Dewar with a 3/4-in. bore entrance tube. Before immersion in the helium, the holder is first precooled by immersion in liquid nitrogen. The helium consumption is then only 200 cc for each dip of the holder.

It is also possible to measure the resistivity of a sample without making any contacts, and this can be very important since it facilitates automation of the measurement. This method depends upon the characteristic decay of magnetically induced eddy currents [15]. The apparatus involved is shown schematically in Figure 16. For a

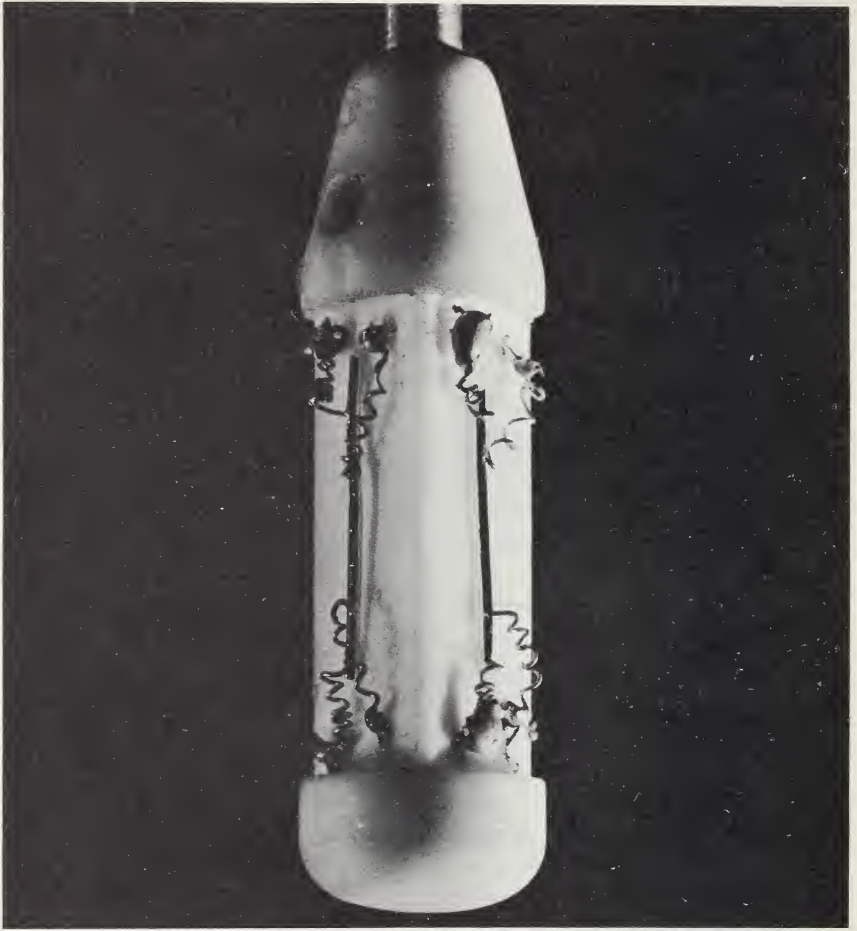


Figure 15. Sample holder for measuring the residual resistivity of three wire specimens simultaneously. Two mounted gallium wire specimens are shown each having a 1 mm diameter.

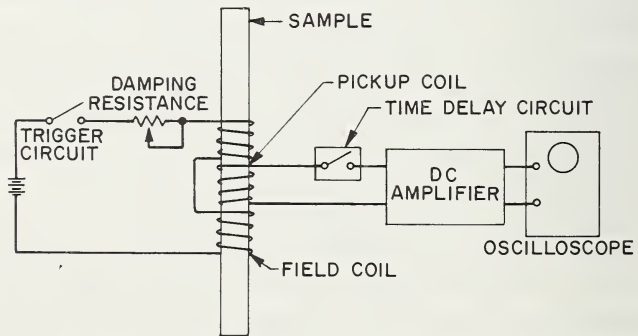


Figure 16. Contactless measurement of residual resistivity by inductive coupling using eddy current decay.

cylindrical specimen with radius  $R$  cm, the time constant  $\gamma$  of the exponential decay is related to the resistivity by the equation

$$\rho = \frac{2.17\mu R^2 10^{-9}}{\gamma} \text{ ohm-cm} \quad (9)$$

where  $\mu$  is the permeability ( $\mu=1$  for non-magnetic materials). The decay of eddy currents induced in the specimen by suddenly removing the magnetic field is displayed on an oscilloscope and photographed. With this method, an accuracy comparable to that of the four-contact method can be achieved, and resolution to a few millimeters along a sample is possible. However, this method may give spurious results with anisotropic metals, and to measure iron, a separate magnetic field must be applied to saturate the iron.

Resistivity data has already been accumulated on a wide variety of metals. The resistance ratios achieved for seventeen metals are listed in Table 5. Copper has been studied most completely, and the separate effects of specific elements on the residual resistivity have been determined for copper [16-18], aluminum [17, 18], gallium [4, 14], and indium [17], among others. Some difficulty has been found with gaseous impurities such as oxygen, since they can react with other impurities and reduce their effect on the resistivity [19, 20]. For example, the copper with the highest resistivity ratio was not the purest sample [21].

The variation of the resistivity ratio with impurity content in copper, for example, is quite pronounced. It increases from about 10 for a purity of 99.9% to 1000 for 99.999%, and to about  $10^4$  for the highest purity copper [21]. For this reason, residual resistivity measurements

TABLE 5. Resistance ratios of some high-purity metals.

Element	$R_{300}/R_{4.2}$	Element	$R_{300}/R_{4.2}$
Ag	740	Ni	2,200
Al	26,000	Pd	7,500
Be	3,300	Pt	1,600
Bi	500	Re	55,000
Cd	38,000	Sb	830
Cu	8,000	Sn	28,000
Ga	40,000	W	80,000
In	17,000	Zn	40,000
Mo	12,000		

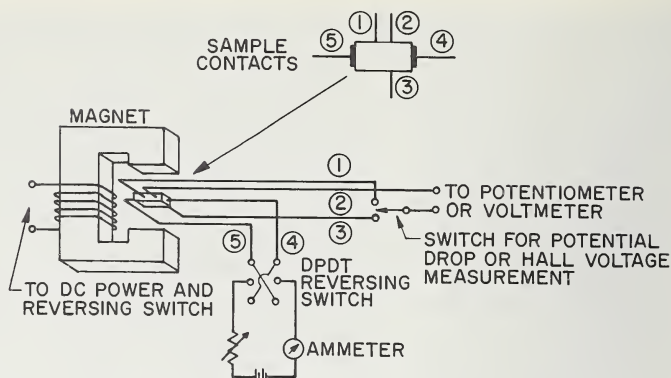


Figure 17. Apparatus for measuring the Hall effect and resistivity.

have been used frequently to monitor the purification of a metal, e.g. to determine if a particular purification procedure is effective, as discussed in Section IIC. This is especially important when impurity contents are below the spectrographically detectable limits.

The growing importance of the residual resistance in characterizing the purity of metals is clearly manifest by the increasing tendency of manufacturers of high purity metals to specify the resistivity ratios of their materials as the analytical standard reference.

#### D. HALL EFFECT

The apparatus for the usual DC Hall effect measurement is shown in Figure 17, together with the resistivity measurement. Ohmic contacts are placed on the sample as shown. The resistivity is measured by the potential drop method, discussed also in the previous section. The magnetic field of one or two thousand gauss can be produced by either an electromagnet, or a high field permanent magnet.

Two voltages are measured, the Hall voltage, across contacts 2 and 3 (Fig. 17), and the potential drop for resistivity, across contacts 1 and 2. In the voltage measurement, one should draw no current to avoid effects due to contact resistance. It is preferable to use a potentiometer, but if a DC voltmeter is used, its input resistance should be much larger than the sum of the sample and contact resistances. Typically, the range of voltages extends from several microvolts to several millivolts.

In Hall voltage measurements, several spurious potentials can arise. The largest of these is the potential due to the misalignment of the Hall probes (contacts 2 and 3), which are on opposite edges of the sample. To eliminate these effects, one measures the Hall voltage four times: first with the original direction of current and field, second with the current reversed, third with the current and field reversed,

and fourth with just the field reversed. The Hall voltage is then derived by adding the first and third, subtracting the second and fourth, and dividing by four.

At times, a sample with the convenient parallelepiped shape shown in Figure 17 cannot be used. However, it is still possible to make Hall and resistivity measurements on a disk-type sample having an arbitrary shape using the van der Pauw method [22]. Referring to Figure 18, four contacts  $a$ ,  $b$ ,  $c$ ,  $d$ , are placed around the edge of the disk. A known voltage is applied first to contacts  $c$  and  $d$  and the current is measured between contacts  $a$  and  $b$ , giving a "cross" resistance  $R_{abcd}$ . Similarly,  $R_{bcda}$  is measured, and the resistivity is obtained from

$$\rho = \frac{\pi t}{\ln 2} \frac{(R_{abcd} + R_{bcda})}{2} f \quad (7)$$

where  $t$  is the thickness of the disk, and  $f$  is a correction factor which must be included if the two resistances are not equal. Values for the correction factor  $f$  are given by van der Pauw [22]. Next, a magnetic field is applied, and the change in the "cross" resistance  $\Delta R_{bdxac}$  is measured. The carrier concentration  $n$  is given by:

$$n = H/et\Delta R_{bdxac}. \quad (8)$$

In some semiconductors (having an energy band gap of only one or two tenths of an electron volt), the intrinsic number of electrons and holes swamp out the carriers due to impurities, so that room temperature Hall measurements no longer measure impurity effects. In such cases, appropriate Hall data can still be acquired by immersing the sample in liquid nitrogen. Lowering the temperature to 77 °K freezes out the intrinsic carriers, but does not appreciably affect the carriers introduced by impurities. Furthermore, lowering the temperature has the additional advantage of reducing scattering of holes and electrons by the lattice, so that the Hall mobility provides a more accurate

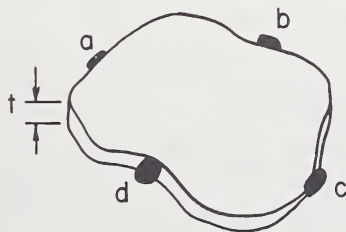


Figure 18. Typical sample and contact positions for van der Pauw measurement of resistivity and Hall effect.

measurement of the total electrically active impurities. A container for the liquid nitrogen, small enough to fit between the pole pieces of the magnet, can easily be fabricated from a block of "Styrofoam" plastic.

The most complete Hall effect studies have been carried out on the elemental semiconductors, germanium and silicon. In these materials, electrically active impurity concentrations well below 1 ppm are commonly achieved, so that most other analytical techniques are difficult. A full Hall effect analysis involves high precision techniques, and also includes measurements as a function of temperature [23]. The accuracy and sensitivity achievable is shown in Table 6 for the case of silicon.

TABLE 6. Impurity concentrations in two silicon specimens  
(After C. A. Klein and W. D. Straub [23])

Specimen	Floating-zone grown	Pulled from quartz crucible
Resistivity (ohm-cm)	1330	53
Net impurity conc. (from Hall effect)	$0.2 \pm 0.001$ atoms in $10^9$	$5.0 \pm 0.02$ atoms in $10^9$

Note the very low impurity concentration involved here. It is again clear that these results cannot be matched by other analytical techniques. In favorable cases, the temperature variation of the carrier concentration provides the ionization energy of the impurity, and hence can be used to identify a specific impurity.

Another example of the widespread use of Hall measurements in semiconductors is the case of the III-V compounds [24]. As mentioned before, the mobility also serves to measure the impurity content. The variation of mobility has been determined for GaAs [10, 25], InP [25], AlSb [25], InSb [26], etc., and the Hall mobility has been used specifically to monitor purity, for example in the preparation of GaAs single crystals [27]. Similarly, for many other classes of solid inorganic semiconductors, the Hall effect has been widely employed, and its use as an analytical tool will continue to grow.

## E. THERMALLY STIMULATED CURRENTS (TSC)

The sample to be analyzed must have a low enough dark conductivity for the TSC to be measured. Practically, the conductivity must be below roughly  $10^{-6}$  mho/cm at the temperature of measurement, and it is this limitation that bars the application of this technique to most semiconductors. An experimental advantage of TSC measurements is that single crystalline samples are not required, and even amorphous materials (such as selenium films) can be analyzed for trace impurities. However, the disadvantage of the technique is that ohmic contacts must be made to the specimen, which is not always possible, such as with organic samples.

It is usually sufficient to cool the sample to only 77 °K, unless traps with values of  $E$  less than 0.15 eV are to be measured. Thus, as shown in Figure 19, only a simple liquid nitrogen Dewar is required, with provision for heating and cooling the sample between 77 °K and 400 °K at predetermined rates such as 0.1 to 0.5 °C/sec. For example, if the sample holder has sufficient mass, the nitrogen can be removed, and the heating rate of the sample will be quite uniform. A thermocouple is used to measure the temperature of either the sample holder, or preferably the sample itself by attaching it directly to one of the current contacts. The Dewar or sample chamber must be light-tight, with a window provided to shine light onto the specimen, as shown in Figure 19.

The electrical measurements are also simple, since only current need be measured. Only two contacts to the sample are required (see Fig. 19). A known voltage, usually 1 to 100 V, is supplied from a battery, and a very high sensitivity ammeter is placed in series with the sam-

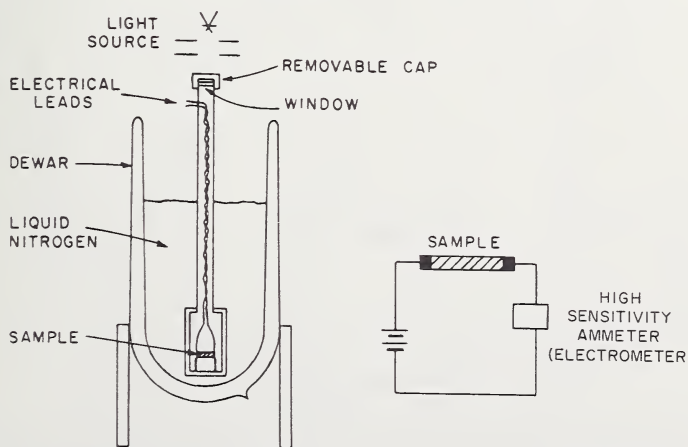


Figure 19. Apparatus for thermally stimulated current measurements.

ple, such as a Keithly 610 Electrometer or a Cary Model 31 vibrating reed Electrometer. It is convenient to use an  $X$ - $Y$  recorder (e.g. Moseley Autograf), with the output from the electrometer placed on the  $Y$ -axis, and the output from the thermocouple on the  $X$ -axis.

Next, a light source is required that has a variable and calibrated intensity. An incandescent lamp can be used, and variations in light intensity are conveniently obtained with neutral wire mesh filters. The light source must have a wavelength greater than that corresponding to the band gap of the insulator.

Three separate measurements are preferably carried out sequentially over the range of temperature of interest: dark conductivity, TSC, and photoconductivity. The measurement of dark conductivity provides the base line to which the other two measurements are referred. First, the sample is cooled to liquid nitrogen temperature, during which the dark conductivity is measured, as shown in Figure 20. At 77 °K, the sample is illuminated with a very bright light source, such as a focused

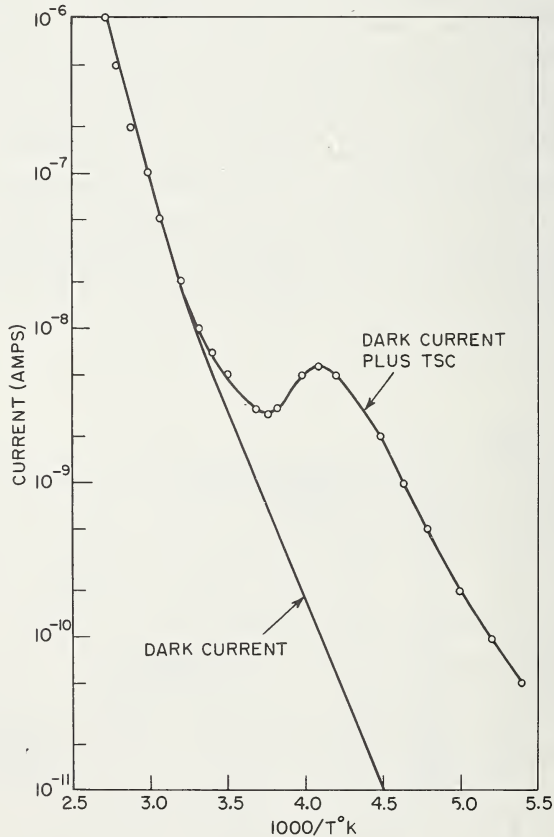


Figure 20. Variation of current with temperature with 100 V applied to GaAs crystal: dark current, and dark current plus thermally stimulated current (TSC).

microscope lamp. This floods the sample with holes and electrons, and fills the traps.

Second, the light is turned off, and the sample is heated in the dark. As the temperature is increased, a current is measured in excess of the normal dark current, contributed by carriers freed from the traps, and this is the TSC (see Fig. 20). Upon subtracting the dark current, one obtains the TSC peaks shown in Figure 21. Finally, the gain is measured by continuously shining a light having a known intensity on the sample over the entire temperature range. The excess current as compared to the dark current is the photocurrent.

TSC measurements have been applied to a wide variety of insulators and semi-insulators, such as CdS [28], ZnS [29], CdSe [30],  $\text{HgI}_2$  [31], and GaAs [32, 33]. Figure 21 shows results for GaAs. Typical TSC peaks for an insulator are shown in Figure 22, where the existence of at least seven traps can be distinguished and their variation in concentration from sample to sample is shown. The temperature of the TSC peak can aid in identifying an impurity. At present, most traps in most materials are of unknown origin. In years to come, an increasing number of traps will be identified with specific impurities and lattice defects, and TSC measurements will then be of even greater utility.

#### IV. Summary and Conclusions

The advantages and disadvantages of electrical measurements for trace characterization were reviewed in relation to an analytical chemist's criteria for accepting new analytical techniques. Of many possible electrical measurements, only four are believed to be presently suitable

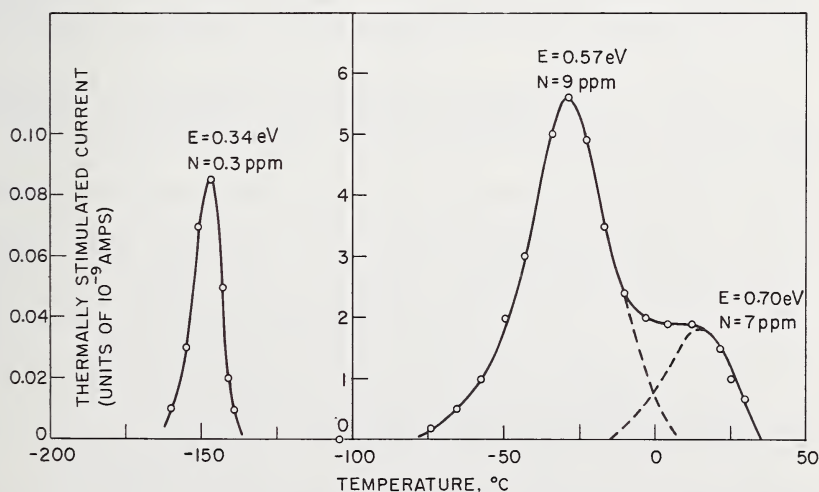


Figure 21. TSC current peaks derived from Figure 20 by subtracting the dark current. Values attached to peaks are activation energies  $E$  and trap concentrations in atomic ppm (ppm = parts in 10<sup>6</sup>).

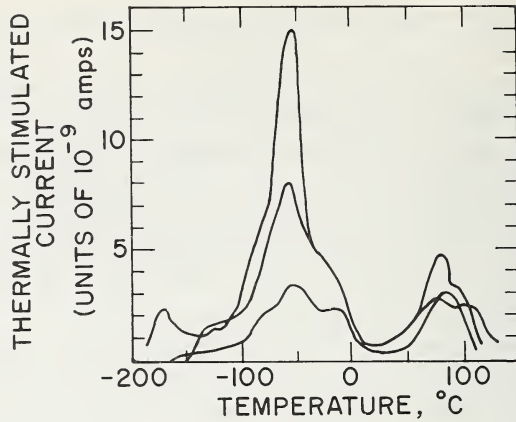


Figure 22. Thermally stimulated current curves for three different CdS crystals. After R. H. Bube, *Photoconductivity of Solids*, John Wiley, New York, 1960, p. 298.

for routine application in an analytical laboratory: resistivity, residual resistivity, Hall effect, and possibly thermally stimulated currents. These are characterized by very high sensitivity and relative precision, but are non-specific. Therefore, they are most useful for providing a general measure of purity, monitoring purification, and determining impurity distributions. Some case histories were presented in which their application was especially rewarding, including purification of gallium and aluminum, impurity distributions in germanium, and research on GaAs. Results were achieved that are impossible using other analytical techniques. The underlying principles and main features of apparatus for these measurements were described. The simplicity of both the apparatus and the interpretation is a significant feature of electrical measurements.

A key feature of these electrical measurement techniques is that they were spawned in and by materials research, and achieved their greatest potential when applied in this direction. It can be concluded that analytical laboratories that are *not* closely connected to a materials research laboratory working on metals or semiconductors will have little use for these techniques at the present. In contrast, analytical laboratories dealing with materials research on pure metals would find residual resistivity measurements of immediate benefit. If automated equipment were made commercially available, these techniques would be in widespread use, as indicated in the paper in this conference by A. F. Clark et al. from the National Bureau of Standards.

In the case of semiconductors, apparatus for resistivity measurements is simple to build, and should definitely be useful. Depending upon problems that arise, Hall effect measurements are less ambiguous, and can also be of help. Use of these measurements should find their way into analytical laboratories over the next decade.

The question of potential application is less clear for insulators. The method of thermally stimulated currents is very powerful, but still has some pitfalls. Furthermore, present techniques require that good electrical contacts be made to the sample, which, in the case of many organic materials, cannot be done. The ultimate potential of this technique for analysis must still be determined. For example, contactless methods of measurement for organics should be considered here.

Finally, besides the above-mentioned limitation of these methods of organics, it is also noted that these methods have been mostly used for solids, although liquids are not excluded (e.g. water).

## V. References

- [1] Weisberg, L. R., in *Trace Analysis: Physical Methods*, G. H. Morrison, Ed., John Wiley, New York, 1965 pp. 511-543.
- [2] Weisberg, L. R., *Annals N. Y. Acad. Sciences* **137**, 360 (1966).
- [3] Weisberg, L. R., *Anal. Chemistry* **38**, 31A (1966).
- [4] Kramer, R. A., and Foster, L. M., in *Preparation of III-V Compounds*, R. K. Willardson and H. L. Goering, Eds., *Compound Semiconductors*, Reinhold, New York, 1962, Vol. 1, p. 146.
- [5] Kunzler, J. E., and Wernick, J. H., *Trans. AIME* **212**, 856 (1958).
- [6] Wernick, J. H., Dorsi, D., and Byrnes, J. J., *J. Electrochem. Soc.* **106**, 245 (1959).
- [7] Valdes, L. B., in *Transistor Technology*, Vol. I, D. Van Nostrand, Princeton, 1958, p. 131.
- [8] Nelson, H., in *Transistors I*, RCA Laboratories, Princeton, 1956, pp. 66-76.
- [9] Ueda, H., *J. Phys. Soc. Japan* **16**, 61 (1961): also see ref. 7, 125-131.
- [10] Weisberg, L. R., Rosi, F. D., and Herkart, P. G., in *Properties of Elemental and Compound Semiconductors*, H. D. Gatos, Ed. *Metallurgical Society Conferences* Vol. 5, Interscience, New York, 1960, pp. 54. 56.
- [11] See, for example, Lindberg, O., *Proc. I.R.E.* **40**, 1414 (1952).
- [12] Bridgers, H. E., Scaff, J. H., and Shive, J. N., Eds. *Transistor Technology*, Vol. 1, D. Van Nostrand, Princeton, 1958, pp. 10-12, 53-58, 136, 141-145, 149-150, 264-274, 323 ff.
- [13] Nishizawa, J., et al., in *Ultrapurification of Semiconductor Materials*, M. S. Brooks and J. K. Kennedy, Eds., Macmillan, New York, p. 636 (1962).
- [14] Weisberg, L. R., and Josephs, R. M., *Phys. Rev.* **124**, 36 (1961).
- [15] Bean, C. P., DeBlois, R. W., and Nesbitt, L. B., *J. Appl. Phys.* **30**, 1976 (1959).
- [16] Smart, J. S., Jr., and Smith, A. A., *Trans. AIME* **152**, 103 (1943).
- [17] Chanin, G. et al., *Phys. Rev.* **114**, 719 (1959).
- [18] Vassel, C. R., *J. Phys. Chem. Solids* **7**, 90 (1958).
- [19] Smart, J. S., Jr., and Smith, A. A., *Trans. AIME* **147**, 48 (1942).
- [20] Redman, J. K., et al., *Bull. Am. Phys. Soc. Series II*, **4**, 150 (1959).
- [21] Kunzler, J. E., in *Ultra-High-Purity Metals*, American Society for Metals, Metals Park, Ohio, 1962, p. 171.
- [22] van de Pauw, L. J., *Philips Research Repts.* **13**, 1 (1958).
- [23] Klein, C. A., and Straub, W. D., in *Ultrapurification of Semiconductor Materials*, M. S. Brooks and J. K. Kennedy, Eds., Macmillan, New York, 1962, p. 397.
- [24] Reid, F. J., in *Preparation of III-V Compounds*, R. K. Willardson and H. L. Goering, Eds. *Compound Semiconductors*, Vol. 1 Reinhold, New York 1962, p. 158.

- [25] Reid, F. J., and Willardson, R. K., *J. Electronics and Control* **5**, 54 (1958).
- [26] Rupprecht, H., Weber, R., and Weiss, H., *Z. Naturforsch.* **15a**, 783 (1960).
- [27] Ekstrom, L., and Weisberg, L. R., *J. Electrochem. Soc.* **109**, 321 (1962).
- [28] Bube, R. H., *J. Chem. Phys.* **23**, 18 (1955).
- [29] Bube, R. H., *Phys. Rev.* **83**, 393 (1951).
- [30] Bube, R. H., and Barton, L. A., *J. Chem. Phys.* **29**, 128 (1958).
- [31] Bube, R. H., *Phys. Rev.* **106**, 703 (1957).
- [32] Bube, R. H., *J. Appl. Phys.* **31**, 315 (1960).
- [33] Blanc, J., Bube, R. H., and Weisberg, L. R., *J. Phys. Chem. Solids* **25**, 225 (1964).

# ELECTRICAL MEASUREMENTS

## Contributed Papers and Discussion

ROBERT L. POWELL

*Institute for Materials Research  
National Bureau of Standards  
Boulder, Colorado 80302*

### I. Introduction

The contributed papers on electrical methods for trace characterization have been made much simpler to summarize by the thorough review given by Dr. Weisberg. In addition to his general discussion, he covered in detail the advantages and disadvantages and economic aspects of four of the more useful methods utilizing the electrical properties: electrical resistivity near room temperature, electrical resistivity at very low temperatures (residual resistivity), Hall effect, and thermally-stimulated currents. The first two properties are especially practical for characterizing metals and semiconductors; the third, for semiconductors; and the fourth, for insulators. In January of this year, he published a review article in *Analytical Chemistry* [1]<sup>1</sup>; last year he contributed a chapter to Morrison's book, *Trace Analysis* [2]. The latter article is particularly useful because of numerous examples and an extensive bibliography.

Before commenting on the contributed papers of this session, let us review what is desired in the way of microscopic characterization by solid-state scientists and engineers. It is realized that the total request is quite impractical at the present. The information generally necessary to completely determine the properties of solids includes knowledge of the following:

- A. Impurity levels—type and concentrations—  
     $10^{-6}$  to  $10^{-8}$  for metals, and  $10^{-6}$  to  $10^{-10}$  for semiconductors  
    and insulators.
- B. Location of chemical impurities—  
    in solid solution—interstitial, substitutional, ordered or  
    disordered.  
    segregated—isolated or grouped in macroscopic inclusions.

---

<sup>1</sup> Figures in brackets indicate the literature references at the end of this paper.

- C. Location and concentration of physical imperfections —  
point imperfections such as vacancies, linear imperfections such as dislocations, or area imperfections such as grain boundaries.
- D. Ionic state of chemical impurities —  
Ionized in various valence states, neutralized, or in complex chemical compounds.

All of the above deviations from the ideal crystalline solid may be critically important to the observed magnitude or behavior of one physical property or another. But present analytic tools are a long way from being able to supply the necessary detailed characterization. Therefore, the highly sensitive, low-detection limit, but very nonspecific, electrical methods must often be used for many materials with trace imperfections which tax the detection powers of other methods.

At present electrical methods are usually employed only where the appropriate measuring systems are already in existence for carrying out other research programs. In general, there are no packaged measurement systems available commercially for making trace characterizations using electrical property methods. However, several of us in the field are trying to remedy this defect by designing general purpose equipment. Publication of reports with detailed construction drawings, wiring diagrams, and instructions should make the methods more generally available to those presently inexperienced in electrical measurements.

It is potentially possible to use many different properties as a means of characterizing materials, particularly solids. Consideration of the various properties may be systematized by enumerating the relevant external force fields, variable environments, and observed responses. For example, the external force fields may include electrical field (either dc or ac), magnetic field, thermal gradient, or mechanical strain. All force fields may occur in specimens with various environments such as different temperatures or pressures. The measured response signal may be, for example, electrical potential drop, electrical current, temperature gradient, thermal current, or static electrical charge. Of the many possible combinations only a few are reasonable as properties that may be used for characterization. An example of one simple combination is the electrical resistance which involves measurement of the electrical current caused by an electrical field along a specimen with a variable or fixed temperature environment. The Hall effect is more complicated for it involves measurement of a potential gradient across a specimen when a magnetic field is imposed that is perpendicular both to a line joining the potential probes and to the electrical current flowing through the specimen. Both the electrical resistivity and the Hall effect properties are usually strongly temperature dependent. Both of these properties were discussed in Weisberg's talk and are described in more detail in the paper by Clark et al, and in the paper by Bullis.

## II. Contributed Papers

The dielectric constant indicates the magnitude of electrical surface charges, or rather the variation of them, when an alternating electrical field is imposed upon an insulating crystal. The paper by Professor Smakula briefly discusses this property.

Two other examples of the many possible combinations are 1) the piezoelectric effect where one measures the resultant electric field across a sample that has a strain field imposed on it, and 2) the thermoelectric effect where one determines the electric potential difference set up along a specimen in the presence of a thermal gradient. The latter effect is the subject of the paper by Sparks and Powell.

In the abstract of Professor Smakula's paper he has indicated the potential usefulness of measurements of the complex dielectric constant for characterizing imperfections in insulating crystals. For an introduction to the concepts used in dielectric studies, J. C. Anderson [3] has recently written a good short book addressed to a general scientific audience. Research and advances in this field have not equalled those in the science and technology of semiconductors. For general information, progress in dielectrics is well reviewed in an annual series [4]. Though not unknown (e.g., page 45 of vol. 5 of reference [4]), remarks on the specific effects of chemical impurities, physical imperfections, or inclusions are relatively rare. One example of a direct study of the effects of imperfections is the thesis on heterogeneous mixtures by de Loor [5].

Electrical resistivity is the simplest physical property to understand and was well covered by Weisberg earlier. The expressions used for resistivity (or conductivity) are different for semiconductors and metals. For semiconductors the conductivity (inverse of resistivity) is given by

$$\sigma = \sum_i n_i z_i \mu_i$$

where  $n_i$  is the concentration of carriers,  $z_i$  is their charge, and  $\mu_i$  is their mobility. The concentration and mobility are generally functions of temperature. For many semiconductors, the mobility is independent of the concentration of carriers. Therefore, the conductivity at a fixed temperature will be, for those semiconductors, directly proportional to the concentration of carriers and, therefore, to the concentration of "effective" impurities. Weisberg has given several pertinent examples both in his talk and in his earlier papers [1, 2].

Temperature dependence of the conductivity indicates the variation of carrier concentration and, therefore, the ionization energy of the impurities. This measurement is fairly specific for different impurities. However, the experimental determination of resistivity over a wide range of temperatures is relatively difficult and, therefore, the method is not

widely used. For some semiconductors it is necessary to go to liquid nitrogen (77 °K) or liquid helium (4 °K) temperatures to reliably measure impurity effects.

For pure metals the carrier concentration does not change with temperature and does not change significantly with trace impurity variations. However, the mobility, or rather the inverse concepts of time-of-relaxation and mean-free-path, depend strongly on temperature at moderate temperatures and on imperfection concentration at low temperatures. The expression used for analyzing electrical resistivity is:

$$\rho_0 = \sum_i n_i \rho_{0i}$$

where  $n_i$  is again the impurity concentration and  $\rho_{0i}$  is the specific residual resistance of each type of imperfection. For many types of chemical imperfections

$$\rho_{0i} = a_i + b_i(\Delta z)^2.$$

where  $a_i$  depends primarily on ionic volume differences and  $\Delta z$  indicates the valence difference between the host and impurity ions. Ferromagnetic metals have a very strong effect on the residual resistivity of many metals. A recent book by Meaden [6] gives a very good introductory discussion of the electrical resistivity of metals which is useful for the general scientist or engineer. He has a particularly good chapter on the resistivity changes caused by chemical or physical imperfections.

For some time the change of resistance between 0° and 20° or 100 °C has been used industrially as a measure of the purity of aluminum and copper wires. However, the ratio of the residual resistance,  $R_0$ , to the 0 °C resistance is a much more accurate indicator of the effective purity. Although use of liquid helium was in the past a barrier for many laboratories, it should not be one any longer since helium is so widely available. The instrumentation required for residual resistance measurements is quite simple. For these reasons measurements of the residual resistance ratio,  $R_{0\text{ }^\circ\text{C}}/R_{0\text{ }^\circ\text{K}}$ , should become more widespread as a good indicator of trace impurities in pure metals. It is already widely used to trace the effects of radiation damage and subsequent annealing and as a method for production control of high purity metals.

Weisberg described several ways to measure the electrical resistance of metals or semiconductors. They are briefly the two lead, four lead with separate potential probes, generalized four probe, capacitive coupling, and inductive coupling methods. The first is usable for high resistance wires; the second, for low resistance specimens or wires; the third, for thin films or sheets; the fourth, for very high resistivity ( $10-10^4$  ohm-cm) plates; and the last for very low resistivity bulk samples. The latter method, referred to as the eddy current decay

method has been used extensively at our laboratories in Boulder to test metals for the Standard Reference Materials Program of the National Bureau of Standards. The metals tested include high-purity gold, copper, platinum and zinc. The methods are described in the paper by Moulder, Clark, and Gniewek. They are relatively easy to use and should become widely utilized as production controls in the preparation of high purity metals.

For reasons too lengthy to explain here, Hall-effect methods are not suitable for metals, but they are of tremendous importance for characterizing semiconductors. Dr. Bullis gives in his paper a very good review of the physical concepts and experimental problems of these methods.

Of the many additional possible properties, one more of great usefulness for metallic wires is described in the paper by Sparks and Powell. That is the thermoelectric power. Again, this method is quite simple and utilizes inexpensive equipment. Liquid helium is again preferable for obtaining one of the junction temperatures. A review of thermoelectric properties, including the influences of imperfections, has been given in the small book by MacDonald [7]. The thermoelectric power of metals is sensitive to minute concentrations of physical imperfections or chemical impurities. However, unlike the electrical resistivity, the total thermoelectric power is *not* a simple additive property. Rather the total is given by

$$S = \frac{\sum n_i \rho_i S_i}{\rho_{\text{total}}}$$

where  $S_i$  is the specific thermoelectric power of a given impurity and the other terms have their usual definition.

The paper by Sparks and Powell gives several examples of the application of thermoelectric power measurements to the characterization of metal wires, both industrial wires and pure metals of the Standard Reference Materials Program. When combined with resistivity measurements, the two methods can give fairly good indications of the specific impurities, if the specific  $S_i$  and  $\rho_i$  are known from previous controlled experiments. John Cochrane (Johnson, Matthey, & Co.) has used this method to analyze and estimate the concentration of separate specific impurities in high-purity platinum.

### III. Discussion

Questions from the audience were numerous. Among those answered by the authors' panel were:

1. Can one determine the specific concentration of impurities in pure lead (say 5 ppm impurities) by electrical measurements? Yes, moderately well, if both electrical resistivity and thermoelectric power

are measured, the specific components are known from control experiments, and a general idea of the main impurities is given.

2. Have electrical methods been used for trace characterization of biological materials? No, not very much, though there are some isolated exceptions.

3. What effect does oxygen have on the electrical properties of germanium and silicon? The effects are complicated. The chemical state of the oxygen ions is important;  $O_2$  and  $O_4$  complexes and oxygen chains each act differently. The state of the oxygen atoms will depend on annealing times and temperatures. The various chemical changes can be followed by measurements of resistivity and Hall effect.

4. Can trace impurities be detected in binary alloys? Generally no, because the alloy has a relatively large resistivity and small additional changes cannot usually be detected. For some thermoelectric measurements there is the possibility of detecting impurities however as illustrated in the paper by Sparks and Powell.

5. Can one measure the purity of iron by the eddy-current decay method? Yes, if measurements are made in high magnetic fields and the results are extrapolated to a calculated zero field value.

#### IV. References

- [1] Weisberg, L. R., *Anal. Chem.* **38**, 31A (1966).
- [2] Weisberg, L. R., in *Trace Analysis—Physical Methods*, G. H. Morrison, ed., Interscience Publ., New York, 1965, pp. 511–543.
- [3] Anderson, J. C., *Dielectrics*, Reinhold, New York, 1964.
- [4] Birks, J. B., and Hart, J., ed., *Progress in Dielectrics*, Academic Press, New York. (Vol. 1, with different authorship, was begun in 1959.)
- [5] de Loor, G. P., *Dielectric Constant of Heterogeneous Mixtures*, thesis, Univ. of Leiden, 1956.
- [6] Meaden, G. T., *Electrical Resistance of Metals*, Plenum Press, New York, 1965.
- [7] MacDonald, D. K. C., *Thermoelectricity*, John Wiley, New York, 1962.

# TRACE CHARACTERIZATION BY ELECTROCHEMICAL METHODS

H. A. LAITINEN

*Department of Chemistry and Chemical Engineering  
University of Illinois, Urbana, Illinois*

In keeping with the theme of this Symposium, this paper will stress the determination of trace constituents rather than the detection or determination of small absolute amounts by micro techniques. Since electrochemical methods in general involve solutions, it will be most meaningful in comparing the sensitivities of various methods to compare detection or determination limits in terms of solution concentrations rather than in terms of absolute quantities.

If a method is selective enough to permit the direct determination of a trace constituent in a solution of the major component, the determination can be made without a prior separation, and the order of magnitude of the percentage of trace constituent bears a simple relationship to the lowest concentration capable of being detected or measured. If we take  $M$  as the upper limit of concentration of the major constituent and if  $C^\circ$  represents the lowest concentration of trace constituent that can be detected or measured, then  $100 C^\circ/M$  represents the lowest mole percentage of trace constituent that can be detected or measured. As a rule,  $M$  is of the order of unity, so a method capable of determining a trace constituent at  $10^{-7} M$  concentration is applicable at  $10^{-5}$  mole %. While not all electrochemical methods are applicable without prior separation, others represent powerful methods of selective concentration, and still others represent sensitive measurement techniques to be coupled with other types of separations.

Electrochemical methods have been classified by Delahay et al. [1].<sup>1</sup> A similar classification, based upon the operational criteria of the processes occurring at the electrodes and the electrical quantities that are controlled and measured, will be used here.

From the historical viewpoint, the development of polarography marked a spectacular advance in electrochemical methodology, because it introduced the element of selectivity through control of electrode potential, an element which was largely lacking in the older electrochemical methods of potentiometry and conductimetry. Several tech-

---

<sup>1</sup> Figures in brackets indicate the literature references at the end of this paper.

niques, such as coulometry, selective electrodeposition, and polarized electrode titrations, which antedated polarography, did not flourish until the theoretical and experimental development of polarography stimulated their resurgence. This discussion, then, will begin with polarography and other methods based upon the net passage of faradaic current. No attempt will be made at an exhaustive survey of the literature, but a selected list of references illustrating notable examples of sensitive determinations will be presented. A critical appraisal of the fundamental limitations of each method, as well as some indications of fruitful and fruitless avenues of investigation in the next few years, will be attempted.

## I. Methods Based on Passage of Faradaic Current

### A. MEASUREMENT OF CURRENT AS RELATED TO CONCENTRATION

#### 1. Classical Polarography

By classical polarography we mean the measurement of time-averaged currents with the dropping mercury electrode under diffusion control. In general, the response is governed by the Ilkovic equation

$$i_d = 605 n C D^{1/2} m^{2/3} \tau^{1/6} \quad (1)$$

where  $i_d$  is the diffusion current (microamperes) averaged over the lifetime of the mercury drop,  $\tau$  (seconds),  $m$  is the mass rate of flow of mercury (mg/sec),  $D$  is the diffusion coefficient of the electroactive species ( $\text{cm}^2/\text{sec}$ ),  $C$  is the concentration in millimole/liter, and  $n$  is the number of electrons involved per molecule of electrode reaction.

For a typical dropping electrode,  $m = 2$  mg/sec,  $\tau = 4$  sec, and taking  $D = 1 \times 10^{-5}$   $\text{cm}^2/\text{sec}$ , the response turns out to be

$$\frac{i_d}{nC} = 3.82 \text{ microamperes/meq/liter.} \quad (2)$$

It is clear from such a trial calculation that classical polarography would be capable of great sensitivity if it were simply a matter of a sufficiently sensitive method of measuring a polarographic diffusion current. Thus, it is simple to measure currents of the order of  $10^{-12}$  A, which would correspond to concentrations of the order of  $10^{-9}$  N.

The practical sensitivity is limited by the fact that even at zero concentration of electroactive material, there is in general a finite current due to the necessity for charging the electrical double layer. This *charging* current imposes a sensitivity limitation which is rather serious, as is shown by the following sample calculation. The charging current  $i_{ch}$  (microamperes) is given by

$$i_{\text{ch}} = \frac{dq}{dt} = \frac{d}{dt} [A C_{\text{dl}} (E - E_{\text{pzc}})] \quad (3)$$

where  $q$  is the charge (microcoulombs) carried by the mercury drop,  $A$  is the instantaneous area ( $\text{cm}^2$ ) of the drop,  $C_{\text{dl}}$  is the differential double layer capacitance (microfarads/ $\text{cm}^2$ ) of the mercury-solution interface, and  $(E - E_{\text{pzc}})$  is the electrode potential with respect to the point of zero charge ( $E_{\text{pzc}}$ ) of the mercury surface.

If as a first approximation it is assumed that  $C_{\text{dl}}$  is independent of potential over the range of potentials involved in the measurement of the polarographic wave height,

$$i_{\text{ch}} = C_{\text{dl}} \frac{dA}{dt} (E - E_{\text{pzc}}) + A C_{\text{dl}} \frac{dE}{dt} \quad (4)$$

In classical polarographic measurements, the rate of change of potential with time is so slow as to make the second term of eq (4) insignificant.

From the first term of eq (4), the slope of the residual current curve is given by

$$\frac{\Delta i_{\text{ch}}}{\Delta E} = C_{\text{dl}} \frac{dA}{dt} \quad (5)$$

where the rate of change of area with time is to be averaged over the drop time  $\tau$ , if the time-averaged charging current is to be measured. If  $\rho$  is the density of mercury ( $13.55 \text{ g/cm}^3$ ), the instantaneous drop area is given by

$$A = \left( \frac{36\pi}{10^6 \rho^2} \right)^{1/3} m^{2/3} t^{2/3} = 8.51 \times 10^{-3} m^{2/3} t^{2/3} \quad (6)$$

and 
$$\frac{dA}{dt} = 5.67 \times 10^{-3} m^{2/3} t^{-1/3} \text{ cm}^2/\text{sec}. \quad (7)$$

The time-average rate of growth of area integrated over the drop life  $\tau$  is

$$\overline{\frac{dA}{dt}} = 8.50 \times 10^{-3} m^{2/3} \tau^{-1/3} \text{ cm}^2/\text{sec} \quad (8)$$

which gives for our typical dropping electrode of  $m = 2 \text{ mg/sec}$  and  $\tau = 4 \text{ sec}$

$$\overline{\frac{dA}{dt}} = 1.07 \times 10^{-2} \text{ cm}^2/\text{sec}. \quad (9)$$

For this electrode, the slope of the residual current curve is estimated from eq (5), taking  $C_{dl}$  to be  $20 \mu\text{F}/\text{cm}^2$ , as

$$\frac{\Delta i_{ch}}{\Delta E} = 20 \times 1.07 \times 10^{-2} = 0.214 \mu\text{A}/\text{V}. \quad (10)$$

Assuming that by graphical or instrumental compensation methods, this current can be eliminated to within 10% of its value, that a ratio of diffusion current to uncompensated charging current of 1:1 represents the limit of useful quantitative measurements, and that a typical polarographic wave measurement involves  $\Delta E = 0.2 \text{ V}$ , we estimate from eq (2) that the limit of quantitative concentration measurement by classical polarography is

$$nC = \frac{i_d}{3.82} = \frac{0.0428}{3.82} \cong 0.01 \text{ meq/liter}$$

or  $10^{-5} N$ , a value in reasonable agreement with polarographic experience.

While some improvement in sensitivity is effected by introducing a linear compensation for residual current, the non-linearity due to variation of  $C_{dl}$  with potential limits the effectiveness of this approach. By introducing a "curve follower" in addition to a linear compensator, to permit subtraction of the residual current run on a blank solution, and by special attention to polarograph design, Kelley and Miller [2] were able to determine  $\text{Pb}^{++}$  in the concentration range of 0.2 to  $2.0 \times 10^{-6} M$ . Since  $\text{Pb}^{++}$  represents a relatively favorable case of a reversible process occurring at a low potential, it would appear that this can be taken as a practical limit for classical polarography even with sophisticated instrumentation. Claims of sensitivities in the range of  $10^{-9}$  to  $10^{-10} M$  appear to be ill-founded [3].

## 2. "Tast" Polarography or Intermittent Polarography

Kronenberger, Strehlow and Elbel [4] devised a polarograph which records the current only during a portion of the drop life, generally selected to be relatively late but not quite at the end of drop duration.

Since the diffusion current increases with time whereas the charging current decreases, it is clear that an improvement in the ratio  $i_d/i_{ch}$  is to be expected by this technique, and that a gain in sensitivity is therefore to be expected. A reasonable estimate would be a gain of about one order of magnitude, to permit quantitative estimates at  $10^{-6} M$  [5].

Other advantages are (1) the violent variations of current near the beginning of drop formation are avoided and hence damping of the oscillations is not required and (2) the variation of drop time with potential does not distort the polarograms as in classical polarography.

## 3. Derivative Polarography

In principle, the measurement of derivatives of polarograms is attractive for high-sensitivity polarography because the measurement of a peak rather than a plateau is inherently more sensitive, particularly when the nonlinearity of the base line and the oscillations with drop formation are considered.

A basic aspect of derivative polarography is that the slope of a polarogram at the half-wave point is at a maximum and is proportional to the concentration provided that the Heyrovsky-Ilkovic equation

$$E = E_{1/2} + \frac{RT}{nF} \ln \frac{i_d - i}{i} \text{ (reversible)} \quad (11)$$

or

$$E = E_{1/2} + \frac{RT}{n_a \alpha F} \ln \frac{i_d - i}{i} \text{ (irreversible)} \quad (12)$$

is obeyed *and* that no uncompensated solution resistance is included in the potential measurements. Clearly, the inclusion of uncompensated  $iR$  drop affects the slope of the polarogram as well as the apparent half-wave potential.

The most elegant experimental solution to the problem of derivative polarography is the apparatus of Kelley, Jones and Fisher [6], in which a three-electrode system using potentiostatic control of the dropping electrode potential is employed. A special RC filter network is used to smooth the curves.

Schaap and McKinney [7] have considered in detail the effects of the residual uncompensated solution resistance in the immediate vicinity of the mercury drop and the residual current on the magnitude of the derivative peak for reversible waves. For the case of most interest here, i.e., negligible solution resistance and appreciable residual current, they write

$$\left( \frac{d\Sigma i}{dt} \right)_{\max} = -(\text{SCAN})(ni_d/4K - S) \quad (13)$$

where  $\Sigma i$  is the total current (faradaic plus residual)

$\text{SCAN} = dE/dt$ , the rate of potential scan

$$K = RT/F$$

$S = di_r/dE$ , the slope of the residual current curve at the half-wave potential.

According to eq (13), the sensitivity of derivative polarography is propor-

tional to the scan rate, and it might appear that this method would be capable of unlimited sensitivity. In practice, the scan rate is limited to *ca.* 40/n mV/min because of time lags introduced by the RC filter networks [7] if undistorted peaks are to be observed. Equation (13) also shows the importance of the slope of the residual current curve, which of course varies with the supporting electrolyte.

Cooke, Kelley, and Fisher [8] showed that the limiting factor to sensitivity in derivative polarography is "electrode noise" or non-reproducible background behavior due to fluctuations in wetting at the electrode orifice. By special design of the electrode tip, they were able in favorable cases to detect metals, e.g. zinc, at  $10^{-7} M$ , a concentration at which the normal polarographic diffusion current would have been only  $2 \times 10^{-10}$  ampere. Derivative polarograms of Cd(II) are shown in Figure 1.

#### 4. Pulse Polarography

Although pulse polarography [9] was developed later than square wave polarography, it is simpler in principle and will therefore be discussed first. Parry and Osteryoung [10] have recently described a solid-state apparatus, to which reference will be made in describing the performance characteristics.

Pulse polarography is applicable in two modes. In the *normal mode*, the initial potential remains constant at the foot of the wave, and as each mercury drop forms it is allowed to grow for a period of time at the initial potential, after which a sudden voltage pulse of 50 msec duration is applied. The current is measured 40 msec after the application of the pulse, to allow time for the spike of charging current to decay. Each succeeding drop is polarized with a somewhat larger pulse, always returning to the initial potential for the beginning of drop formation. The shape of the polarogram thus obtained resembles an ordinary polarogram. The limiting current, however, is larger than in classical polarography, because the concentration gradient at the instant of current measurement is considerably larger. The diffusion limited current in normal pulse polarography is given by the Cottrell equation

$$i_l = nFCA \sqrt{\frac{D}{\pi t}} \quad (14)$$

The ratio of this current to that given by the Ilkovic equation gives a direct comparison of the sensitivities of the two methods. Parry and Osteryoung [10] write

$$\frac{i_l \text{ (normal pulse)}}{i_d \text{ (pol)}} = \frac{t_1^{1/2}}{\sqrt{7/3} t_2^{1/2}} \quad (15)$$

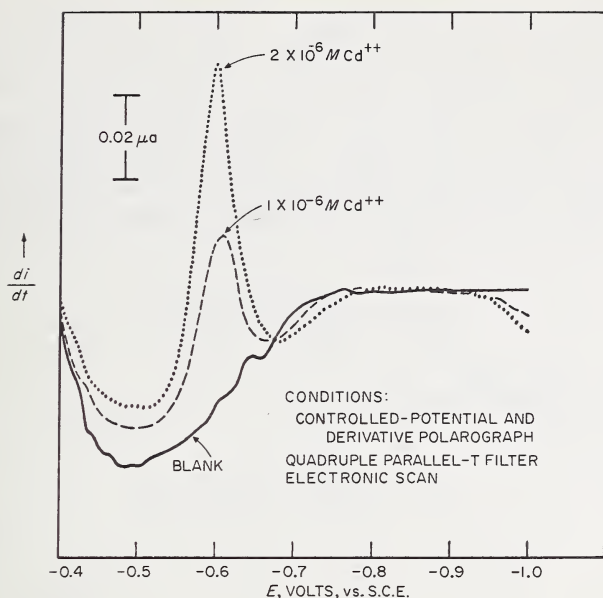


Figure 1. Derivative polarograms of Cd(II) in  $10^{-4} M$   $KNO_3$ . Reproduced with permission from W. D. Cooke, M. T. Kelley, and D. J. Fisher, *Anal. Chem.* **33**, 1209 (1961).

where  $t_1$  is the drop time in classical polarography and  $t_2$  is the time at which the current is measured after application of the pulse. For  $t_1 = 4$  sec and  $t_2 = 40$  msec, the calculated sensitivity ratio is 6.5. A much larger gain in real sensitivity, however, is achieved through the virtual elimination of the charging current.

The charging current presents a different problem in pulse polarography than in classical polarography, because the growth of electrode area during the pulse period is so small, and the voltage change so sudden, that the charging current is determined by the  $RC$  time constant of the circuit. Here  $R$  is mainly the electrolytic resistance of the solution and  $C$  the double layer capacitance of the electrode. For a typical dropping mercury electrode of area  $0.03 \text{ cm}^2$ , taking  $C_{dl} = 20 \mu\text{F}/\text{cm}^2$ ,  $C = 0.6 \mu\text{F}$ . The value of  $R$  is determined by the concentration and nature of the supporting electrolyte, but for typical polarographic conditions may range from  $1000 \Omega$  to a few ohms, depending upon the cell geometry. Taking  $R = 1000 \Omega$ ,  $C = 0.6 \mu\text{F}$ ,  $RC = 6 \times 10^{-4}$  sec. If measurements are made  $4 \times 10^{-2}$  sec after the application of each pulse, 67 time constants are allowed for the decay of the charging current. Since the exponential decay of charging current decreases it 10-fold during each 2.3 time constant, the charging spike would decrease to about  $10^{-29}$  of its initial value. Obviously the charging current would be insignificant except for much higher solution resistances or shorter measurement times.

The other method of application of pulse polarography is in the *derivative mode*. In this method, the voltage pulses are superimposed upon a slowly changing potential ( $\sim 1$  mV/sec) (Fig. 2), and the difference in current between succeeding drops is plotted against the potential. The resulting curve is hump-shaped, approximating the derivative of the classical polarogram for small pulse magnitudes (Fig. 3). Thus for small pulses,  $\Delta E$ , the peak current is given by [9, 10]

$$\Delta i_{\max} = \frac{n^2 F^2}{4RT} AC \Delta E \sqrt{\frac{D}{\pi t}} \quad (16)$$

whereas for large pulses [9], it is given by

$$\Delta i_{\max} = nFAC \sqrt{\frac{D}{\pi t}} \left( \frac{\sigma - 1}{\sigma + 1} \right) \quad (17)$$

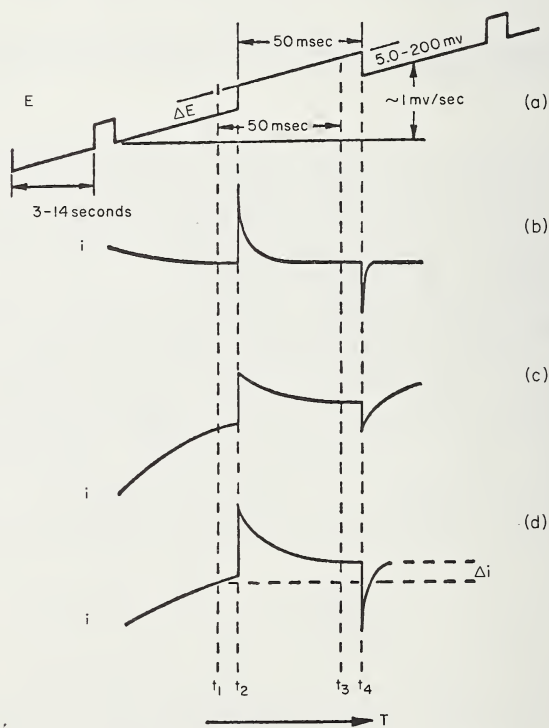


Figure 2. Pulse polarography potential-time and current-time behavior: a. potential-time curve, b. charging current only, c. Faradaic current only, d. both charging and Faradaic current,  $t_1$ ,  $t_3$ —times at which current is measured,  $t_2$ —time at which pulse is applied,  $t_4$ —time at which pulse is removed. Reproduced with permission from E. P. Parry and R. A. Osteryoung, *Anal. Chem.* **37**, 1634 (1965).

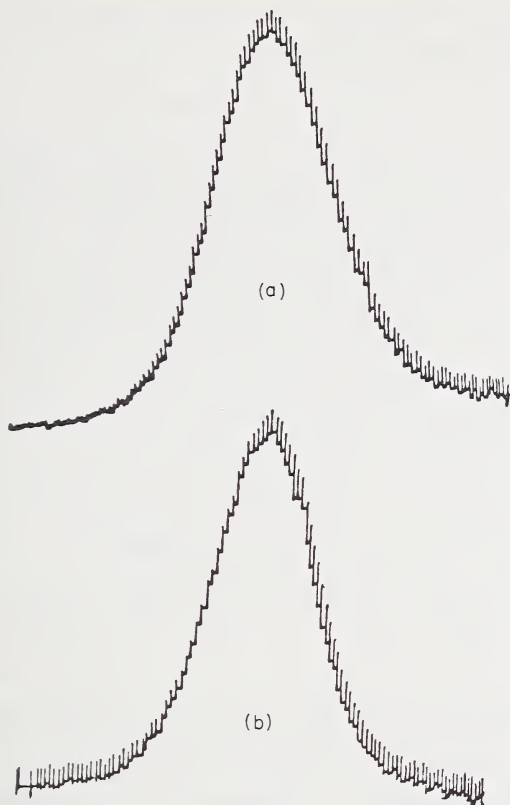


Figure 3. Derivative pulse polarograms of  $2 \times 10^{-5} M$  Cd(II): a. in  $0.001 M$   $KNO_3$ , b. in  $0.01 M$   $KNO_3$ . Reproduced with permission from E. P. Parry and R. A. Osteryoung, *Anal. Chem.* **37**, 1634 (1965).

where

$$\sigma = \exp(\Delta E nF/2RT).$$

In the limit, for  $\Delta E \gg RT/nF$ ,  $(\sigma - 1)/(\sigma + 1)$  approaches unity and  $\Delta i_{\max}$  becomes the limiting current as given by the Cottrell equation (eq 14). Thus, in principle, the derivative mode is less sensitive than the normal mode, but the resolution is better. Calculations show [10] that for reversible waves, a 50 mV pulse amplitude gives a peak height 45, 75, and 90% of the maximum for a very large pulse for a 1-, 2-, or 3-electron process respectively.

Despite this diminution in theoretical sensitivity, the derivative mode in practice is probably more sensitive than the normal mode, because of the hump-shaped response curves. According to Barker and Gardner [9], pulse polarography is capable of detecting  $10^{-8} M$  of a reversible system, or  $5 \times 10^{-8} M$  of an irreversible system. This represents per-

haps a 100-fold increase over classical polarography and a 10-fold increase over derivative polarography.

### 5. Square Wave Polarography

By a square wave polarograph we shall explicitly mean the apparatus developed by Barker [9, 10], since it is available commercially and its characteristics have been fully described [11-13]. After a time delay of *ca.* 2 sec following the beginning of drop formation a small square wave voltage signal of 225 Hz is applied. During each half-cycle of applied square wave signal, the current is measured only during the last 1/12 of the cycle, to allow the charging current to decay to a very small magnitude before the faradaic current is measured. The response curve resembles the pulse method operated in the differential mode.

Considered strictly from the viewpoint of analytical applications at high dilution, the square wave method has disadvantages as compared with pulse polarography. These are brought about through the shorter time scale and the smaller  $\Delta E$  values customarily used. As was pointed out above, the time constant for double layer charging is proportional to solution resistance, and in fact one of the practical limitations of square wave polarography is the need for minimization of solution resistance.

Another important limitation of square wave polarography is that the response for irreversible electrode reactions depends upon the kinetic parameters of the reaction. Von Sturm and Ressel [13] give as approximate limits of concentration for quantitative measurements  $5 \times 10^{-8} M$  for reversible systems and  $5 \times 10^{-6} M$  or higher for irreversible ones. To complicate matters further, the kinetics of electrode reactions are strongly influenced by adsorbed surfactants, and depending upon the reaction rate at a clean surface, the presence of a trace of surfactant may have a greater or lesser effect upon the square wave response. Therefore, pains are taken to avoid the presence of surfactants and in particular the maximum suppressors commonly used in classical polarography are avoided. Fortunately, the response is not sensitive to the presence of polarographic maxima. Nevertheless, it is clearly a disadvantage to have such a sensitivity to the presence of surfactants.

As in high-sensitivity derivative polarography, a problem is that of "electrode noise" resulting from nonreproducible detachment of mercury drops. This difficulty was largely overcome by a technique termed "radiofrequency polarography" [9] in which a high frequency current (100 kHz to 1.6 MHz) is modulated by a square wave signal of 225 Hz. The resulting signal depends upon the symmetry charge transfer coefficient,  $\alpha$ , of the electrode process. For a symmetrical, diffusion-controlled process ( $\alpha=0.5$ ) the output corresponds to the second derivative of the polarograms, and thus has a positive and a negative branch. For unsymmetrical processes ( $\alpha < 0.5$  or  $\alpha > 0.5$ ) or processes

with chemical rate steps, one branch or the other would predominate. The sensitivity of the method is of the order of  $10^{-8} M$  for reversibly reduced metal ions and  $10^{-7} M$  for irreversibly reduced ones. The method has not received wide study, evidently because of its experimental complexity.

### 6. *Alternating Current Polarography*

The AC polarography method of Breyer and his school [14] consists of the application of a sine wave alternating potential of relatively small magnitude and low frequency superimposed upon the slow linear voltage sweep of polarography. The direct component of current is blocked out from the recorder, and the rectified alternating component is displayed as a function of electrode potential. For reversible reactions the response curve, neglecting charging current, is the derivative of the d-c polarogram superimposed upon the residual current proportional to the double layer capacitance at each potential.

An important characteristic of the AC polarographic method is that it responds only to reversible electrode reactions. This, of course, limits its applicability, but in some cases can be advantageous in avoiding interferences.

A fundamental problem is the proper subtraction of the residual current due to double layer charging. The direct numerical subtraction of blank from response is theoretically improper because of the phase relationships between alternating current and potential.

For the charging process the admittance is purely capacitative, and therefore the phase angle between current and potential is  $90^\circ$ .

For the faradaic process, in contrast, the phase angle is  $45^\circ$  for a rapid, diffusion-controlled reaction [15]. For a slow charge-transfer reaction an added resistance (the charge transfer resistance) lowers the phase angle while decreasing the admittance across the double layer. In the limit, for a totally irreversible charge transfer reaction, the faradaic admittance approaches zero and no AC polarographic response is obtained. In general, it is apparent that a direct arithmetic subtraction of the blank is inadequate as a correction for the charging current. Although an empirical procedure involving the use of a working curve will be useful for higher concentrations, the method in general is not successful below about  $5 \times 10^{-5} M$  for reversible processes [14]. The response may be considerably more sensitive for organic substances that are adsorbed at the electrode.

As in square wave polarography, the response decreases with decreasing charge transfer rate, but disappears entirely for a totally irreversible reaction. Thus the effects of surfactants must be taken into consideration.

Another effect of certain surfactants is the appearance of "tensametric peaks" at potentials where adsorption varies strongly with

potential. Such peaks can be of analytical utility for detection of surfactants, but they are relatively non-specific and are applicable only in special cases.

The use of phase-sensitive detectors to reject the charging current component is discussed by Smith and Reinmuth [16] and by Underkoffler and Shain [17] for stationary electrodes. The effect of solution resistance is largely overcome by the use of a three-electrode system with a potentiostat. The difficulties involved in complete elimination of uncompensated resistance are discussed by Schaap and McKinney [6]. The limit of sensitivity is given as  $10^{-8} M$  by Smith and Reinmuth and as  $5 \times 10^{-7} M$  by Underkoffler and Shain. The detection limit is perhaps an order of magnitude more dilute.

Another approach to minimization of the effect of charging current in AC polarography is the second harmonic technique [18]. If the output signal is observed at twice the frequency of the input, the response curve for a reversible reaction and small signal approximates the second derivative of the d-c polarogram, which passes through zero at the half-wave potential. Depending upon whether the absolute or algebraic values are plotted, the response curve has two maxima or a maximum and minimum. To the extent that the double layer behaves as a pure frequency independent capacitance, it yields no second harmonic response. The sensitivity, in principle, should be considerably greater than for conventional AC polarography. Smith and Reinmuth [18] found linear response down to  $5 \times 10^{-5} M$  for the iron(III)-iron(II)-oxalate system, but did not push the method to its limits. The third harmonic would have the advantage of showing a peak output at the half-wave potential. According to Paynter and Reinmuth [19], however, the magnitude of the response falls off roughly with the inverse power of the harmonic, and there appears to be no analytical advantage to the use of harmonics higher than the second.

Still another approach to suppression of the residual current is that recently proposed by Kambara and Hasebe [20] to introduce an inductance into the circuit. An interesting aspect to this approach is that the inductance acts also to decrease the faradaic impedance, which has a capacitive component, and thereby to increase the sensitivity, as well as to decrease the background. Although the effect has been demonstrated to occur, and a response has been observed for  $2 \times 10^{-6} M Pb^{++}$  and  $2 \times 10^{-5} M Zn^{++}$ , it has not yet been studied in detail.

### 7. Radiopolarography

The application of radiochemical detection methods to determine the concentration of a radioisotope deposited as an amalgam appears to have attractive possibilities for trace analysis. The technique, termed radiopolarography by Schaap and Wildman [21], involves the isolation and washing of individual amalgam drops, and plotting the activity

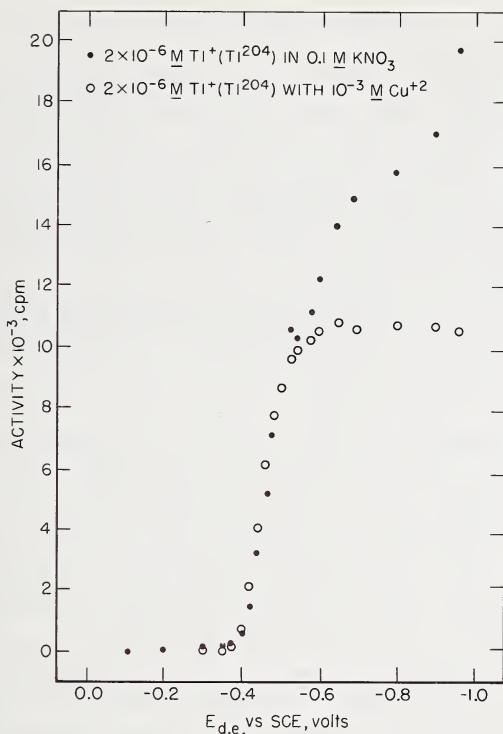


Figure 4. Radiopolarogram of  $2 \times 10^{-6} M$  thallium tracer with  $0.1 M$   $KNO_3$  as supporting electrolyte (solid points) and in presence of  $10^{-3} M$   $Cu^{+2}$  (open circle points). Reproduced with permission from W. B. Schaap and E. Wildman, Proceedings of Sixth Conference on Analytical Chemistry in Nuclear Reactor Technology, Gatlinburg, Tennessee, October 1962.

against electrode potential. An unusual feature of the radiopolarogram at depolarizer concentrations below  $10^{-5} M$  is that the activity continues to rise at potentials where the current reaches the diffusion current plateau (Fig. 4). This effect is due to the further reduction of metal ions by the excess electrostatic charge held by the drops, as they fall through the solution. It is readily eliminated by the addition of a more easily reducible metal ion, e.g.,  $Cu^{+2}$  in the case of thallium.

The potentialities of this technique have not yet been fully investigated. In a recent paper, Katsanos, Tassius, and Zeliotis [22] point out that a radiopolarographic wave is obtained for *inactive* manganese in the presence of radioactive zinc, because of a displacement reaction between manganese amalgam (formed at  $E_{1/2} = -1.51$ ) and zinc ions. The quantitative aspects of such a wave are expected to be ill-defined, however, because such interaction cannot occur until after detachment of the mercury drops.

### 8. *Catalytic Currents in Polarography*

In certain electrode processes a catalytic cycle is so rapid that an electrolysis current many times larger than the diffusion controlled current of the catalyst system is observed. Because the stress in this Symposium is on inorganic determinations, only bare mention will be made of catalytic hydrogen discharge waves for detection of aliphatic amines and alkaloids down to  $10^{-7} M$  [23], and sulfhydryl-containing amino acids and proteins [24].

Platinum (IV) can be detected in concentrations down to  $10^{-7} M$  in the presence of palladium (II) by its catalysis of hydrogen ion discharge from  $2 M HCl$  [25].

Harris and Kolthoff [26] determined U(VI) quantitatively down to  $2 \times 10^{-7} M$  through its catalysis of the reduction of nitrate ion. The reduction path of U(VI) involves U(V) and U(III); the latter is reoxidized rapidly to U(V) at the electrode surface by an excess of nitrate ion.

Kolthoff and Parry [27] detected Mo(VI) at  $10^{-7} M$ , V(V) at  $10^{-8} M$ , and W(VI) at  $10^{-6} M$  through the appearance of catalytic waves of hydrogen peroxide. An intermediate formation of reducible peroxy-compounds is responsible for the catalytic cycle.

### 9. *Adsorption Effects in Polarography*

It has long been noted that traces of certain substances have strong suppressive effects on polarographic maxima. Under certain conditions, notably in dilute supporting electrolytes, maxima can be very pronounced and the suppressive effect can therefore be extremely sensitive. Most surfactants that are exceptionally effective as maximum suppressors are organic in nature. The time-dependent phenomena involved in diffusion of the surfactant to the dropping electrode, its adsorption and suppression of the maximum are extremely complex. The effects therefore will not be described in detail.

Mention should be made, however, of taking advantage of the suppressive effect of adsorbed tetrabutylammonium ion on the reduction of Cd(II) at the hanging mercury drop electrode, as was done by Phillips [28]. By measuring the time necessary for the current to drop to a low steady state value at a fixed potential, he was able to detect tetrabutylammonium ion at concentrations down to  $10^{-7} M$ .

### 10. *Measurements of Current at Electrodes of Constant Area (Voltammetry)*

**a. Steady State Methods.** In principle it should be possible to increase the sensitivity of voltammetric methods enormously by increasing the electrode area and the rate of mass transfer. Within limits, this is true. However, increase of electrode area is accompanied by a corresponding increase in residual currents due to electrolysis of im-

purities, charging current, and oxidation-reduction of the electrode surface itself. Stirring rates cannot indefinitely be increased, for several reasons. Even when pains are taken to maintain laminar flow between electrode and solution, as in the Levich rotating disc electrode [29], turbulence occurs beyond certain limits. With the ordinary rotating wire microelectrode, turbulence is commonly encountered, with the consequence that the mass transport-limited current is not entirely steady, but is accompanied by "noise" or erratic fluctuations. In addition to this hydrodynamic limitation, there is the limitation that the mass transport rate should be the *slowest* step in the electrode process to be rate-determining, and any complications due to slow charge transfer or chemical steps are correspondingly magnified by increasing the mass transport rate.

The simple rotating wire microelectrode [30] is easily capable of detecting oxidants and reductants at the  $10^{-8} M$  level in favorable cases, and the limit can be extended perhaps two orders of magnitude by increasing the electrode area and stirring rate. For highest accuracy at low concentrations, it is best suited as an amperometric indicator electrode in coulometric titrations (*v.i.*). The rotating disc geometry, while superior for absolute measurements, has no particular advantage for such end point indication applications and will not be considered further.

Other types of electrodes that deserve mention because they offer methods of altering the electrode geometry and rate of mass transport are the rotated dropping mercury electrode of Kolthoff and Stricks [31], the convection electrode of Kolthoff and Jordan [32] the streaming electrode of Heyrovsky and Forejt [33] which has been studied in detail by Weaver and Parry [34] and the tubular electrode of Blaedel and co-workers [35]. The latter electrode was demonstrated to be sensitive to  $10^{-8} M$  ferricyanide.

**b. Single Sweep and Cyclic Voltammetry.** The use of stationary electrodes in unstirred solution was enormously advanced by the development of linear voltage sweep voltammetry, in the single sweep [36] or cyclic [37] modes. By restricting electrolysis time from a few seconds to a fraction of a second, extraneous effects such as convection could be eliminated, to allow diffusion theory to be applied to the mass transport process. Nicholson and Shain [38] have presented detailed mathematical studies of the single sweep and cyclic methods for reversible and irreversible processes with and without kinetic complications. For the single sweep method, the peak current is given by the following expressions for reactions without complications due to chemical kinetics [39].

$$i_p = 2.72 \times 10^5 n^{3/2} A C D^{1/2} \nu^{1/2} \text{ (reversible)} \quad (18)$$

$$i_p = 3.01 \times 10^5 n (\alpha n_a)^{1/2} A C D^{1/2} \nu^{1/2} \text{ (irreversible).} \quad (19)$$

Equation (18) and (19) point out the following characteristics of the linear voltage sweep method: (a) the response depends upon the reversibility of the electrode reaction, and (b) the response is proportional to the square root of the scan rate. The latter characteristic constitutes a fundamental limitation to increasing the sensitivity by increasing the sweep rate, because the residual current due to double layer charging increases with the first power of sweep rate (eq 4).

Linear sweep voltammetry has proved to be a powerful method for trace determination when coupled with stripping analysis, to be discussed below. Although much less sensitive than stripping analysis, it is competitive with classical polarography. It can be applied to stationary electrodes as well as to the dropping mercury electrodes, and to reactions for which stripping analysis is inapplicable due to highly irreversible electrode processes or the formation of solution-soluble reaction products.

Ross, DeMars and Shain [40] estimated  $10^{-6} M$  as the limit for quantitative determination and  $5 \times 10^{-8} M$  as the detection limit, for reversibly reduced metal ions. Tyler [41] in the analysis of blood determined down to  $0.1 \mu\text{g}$  of lead in 20 ml solution ( $2.5 \times 10^{-8} M$ ) using the hanging mercury drop electrode.

**c. Voltage Step Chronoamperometry.** If the potential of an electrode is suddenly shifted from a region before a polarographic wave to the potential on the limiting current plateau, the current-time rather than current-potential relationship becomes important. This method has already been considered above, under pulse polarography.

Perone and Mueller [42] observed a barely detectable reduction wave for Cd(II) at  $4 \times 10^{-7} M$ . By plotting the first derivative, they observed a well-defined peak at the same concentration and concluded that the derivative technique increased the sensitivity by at least an order of magnitude.

The technique of staircase voltammetry, originally suggested by Barker [43] to decrease the effect of charging current, has been experimentally studied by Mann [44]. A beneficial effect of the staircase method was noted for mercury electrodes but not for platinum electrodes which show relatively large noncapacitative background currents. Determinations of Cd(II) down to  $10^{-7} M$  were reported. Similar sensitivity limits were reported by Nigmatullin and Vyaselev [45]. Christie and Lingane [46] derived theoretical relationships between the current and potential for reversible reactions and found them to be obeyed satisfactorily.

## B. CHRONOPOTENTIOMETRY

If a constant current is applied under conditions of linear diffusion to a solution of initially uniform concentration, the surface concentration

of diffusing reactant reaches zero at a finite time, the transition time, given by the Sand equation

$$\tau = \frac{\pi n^2 F^2 DC^2}{4 I^2}. \quad (20)$$

Measurement of electrode potential against time allows a measurement of the transition time to be made. A fundamental limitation of the method is the difficulty of making proper correction for the charging current. The difficulty is brought about by the fact that the applied current is distributed between charging the double layer and producing the electrochemical reaction in a variable way. Even after the surface concentration of reactant has reached zero, its *concentration gradient* at the electrode surface is finite, and therefore diffusion continues beyond the transition times.

One or another graphical procedure is generally used in an attempt to subtract out the effect of double layer charging [47]. The method, while a powerful tool for the study of electrode processes and for quantitative work at higher concentrations, is fundamentally limited in its applicability at extreme dilution. The situation has been summarized in a recent review by Reinmuth [48] who states, "As yet the feasibility of trace chronopotentiometry remains unproved."

Coupling of chronopotentiometric measurements with anodic stripping [49] provides a sensitive method for reversibly discharged metals such as Zn, Cd, or Pb, but certainly no more sensitive than the linear voltage sweep method customarily used in stripping analysis.

Thin layer chronopotentiometry [50] is most important when run under conditions of quantitative electrolysis, and therefore is discussed under coulometry.

### C. COULOMETRY

Because of the tremendous "leverage" of the faraday, coulometry, in principle, is a powerful method for trace analysis. Until modern developments in instrumentation, however, its capabilities could not be fully developed.

#### 1. *Coulometry at Constant Potential*

Quantitative electrolysis at controlled potential is a useful technique for performing selective electrochemical reactions, and for determinations at higher concentrations [ $10^{-4}$  M or more] [51], but it has inherent limitations for trace determinations. Generally, the first-order decay of current fails at very low concentrations due to electrolysis of residual impurities or of the supporting electrolyte.

Meites [52] determined chromium in amounts of 5  $\mu$ g at a concentration of  $10^{-6}$  M to an accuracy of  $\pm 1\%$  by reducing Cr(III) to Cr(II)

by controlled potential electrolysis, and performing the coulometric determination upon reoxidation. Booman, Holbrook, and Rein [53] determined 7.5  $\mu\text{g}$  uranium at a concentration of  $6 \times 10^{-6} M$  to an accuracy of  $\pm 2.2\%$  using 5 to 10 min electrolysis.

## 2. Coulometry at Constant Current

For certain special applications, direct coulometry at constant current affords a sensitive, simple, and accurate method of analysis. The coulometric generation of titrant is considered in a separate section.

**a. Coulometry of Surface Layers.** Coulometric methods can be applied to the determination of fractional monolayers of oxides on metal surfaces. A sensitivity of the order of  $10^{-11}$  moles/cm<sup>2</sup> of platinum oxide on platinum surface can readily be achieved [54, 55].

The use of electrochemically deposited films, such as silver halides upon silver, or higher metal oxides upon inert electrodes, will be discussed under *stripping analysis*.

A method called "spot electrolysis," was described by Evans [56]. A drop of solution containing a soluble electro-active constituent is evaporated to form a spot on a gold foil. After adjusting the potential to the desired value with foil contacting the solution but with the sample spot above the solution, the foil was suddenly lowered to bring the supporting electrolyte in contact with the sample spot. The current was measured after a delay of 3 seconds to allow time for decay of charging current. The method is best suited to the analysis of micro samples (down to  $10^{-9}$  moles) but is not exceptionally sensitive for trace concentrations.

**b. Thin Layer Coulometry.** Christensen and Anson [50] showed that if a constant current electrolysis is carried out with a layer of electrolyte of thickness  $\ell$ , applying a current density of such magnitude that the chronopotentiometric transition time would exceed by 100-fold or more the quantity  $\ell^2/3D$ , where  $D$  is the diffusion coefficient of the electroactive species, the electrolysis will proceed to completion. Thus, Faraday's law becomes applicable, and the electrolysis time becomes

$$t = nFC\ell/I \quad (21)$$

where  $I$  is the applied current density.

If  $\ell = 10^{-3}$  cm, and  $D$  is taken to be  $10^{-5}$  cm<sup>2</sup>/sec,  $\ell^2/3D = 0.03$  sec, and electrolysis times of 3 sec or more would lead to quantitative coulometry.

Hubbard and Anson [57] and Reilley and co-workers [58], devised electrodes suitable for thin layer studies. Anderson and Reilly [59] achieved a sensitivity of  $10^{-6} M$  for reasonably accurate determinations measuring the steady state current. Using thin layer geometry, Reilley and co-workers [60] applied a voltage scan coulometric technique to the determination of halides. In general, however, the thin layer method is

not particularly advantageous at extreme dilution, and although the sample volume being examined is very small ( $\sim 10^{-3}$  to  $10^{-4}$  cm<sup>3</sup>) the practical difficulties of introducing new samples into the cell preclude the use of a small total sample volume.

### 3. Coulometric Titration

The coulometric titration, especially with amperometric endpoint indication, has proved to be exceptionally successful at extreme dilution. It is, of course, necessary to have a sufficiently rapid and stoichiometric titration reaction at such extreme concentrations, but the end point can be arranged to correspond to a region slightly removed from the equivalence point to drive the reaction more rapidly.

An excellent example of the potentialities of this method is the determination of submicrogram quantities of manganese (as permanganate) by Cooke, Reilley, and Furman [61]. They generated iron (II) electrolytically, maintaining a slight excess of iron (II) at the end point and during the entire titration for the most dilute solutions ( $10^{-8}$  M) studied. The current between an indicator electrode and a reference platinum electrode set at the desired end point potential was monitored near the end point (Fig. 5). By adjusting the areas of the electrodes and the generating current, a wide range of sensitivities could be achieved. An accuracy of the order of 5% was reached at concentrations down to  $5 \times 10^{-10}$  g Mn/ml ( $10^{-8}$  M). Similar procedures were used for Fe and V [62], with quantitative measurements being made at concentrations down to  $2 \times 10^{-7}$  M and  $3 \times 10^{-6}$  M respectively.

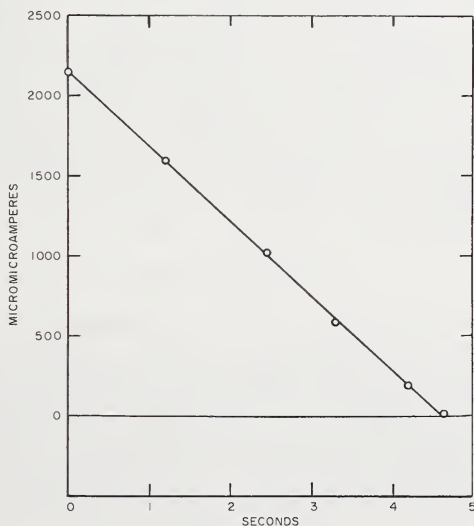


Figure 5. Titration curve for 0.003 microgram Mn [as  $\text{MnO}_4^-$ ] titrated with electrolytically generated Fe(II) using  $5\mu\text{A}$  generating current. Reproduced with permission from W. D. Cooke, C. N. Reilley, and N. H. Furman, *Anal. Chem.* **24**, 205 (1952).

Nikelly and Cooke [63] titrated cadmium and copper at concentrations of  $2 \times 10^{-7} M$ , lead at  $5 \times 10^{-7} M$ , and nickel and zinc at  $10^{-6} M$ , using EDTA as the reagent and a mercury pool indicator electrode.

Swift and co-workers used electrolytically generated bromine [64], chlorine [65], and copper (I) [66] at concentrations of  $10^{-5}$  to  $10^{-6} M$  at relative errors of 1 to 2% using amperometric indication of the end point.

Meites [67] titrated Ce(IV), V(V), Cr(VI), and Mn(VII) with electrolytically generated iron (II) at concentrations down to  $10^{-7} N$  using a potentiometric equivalence point method. There seems to be no reason why an amperometric end point could not have been pushed to  $10^{-8} N$ . Indeed, Christian and Feldman [68] recently determined chromium (VI) at concentration of the order of  $10^{-9} M$  by this method.

Bishop and Dhaneshwar [69] used potentiometry at constant current to detect the end points in the titration of halides using electrolytically generated silver ion. They succeeded in observing a detectable end point even in the titration of  $2 \times 10^{-8} M Cl^-$ , although it is not clear why there is any electrode response at concentration levels so far below the solubility of silver chloride. Bromide gives a response at similarly low concentrations.

An unusual amperometric titration involving only the diffusion layer of a rotating ring-disc electrode was described by Bruckenstein and Johnson [70]. Bromine was electrolytically generated at a rotating disc and detected amperometrically at a closely spaced but electrically insulated ring. Excess bromine over that required to react with arsenic (III) diffusing from the bulk of the solution gave rise to an amperometric current. By plotting the amperometric current at the ring electrode as a function of coulometric generating current and extrapolating to a residual amperometric current, a coulometric current proportional to bulk concentration of arsenic (III) was observed. The method was successful down to  $10^{-7} M$ . A limitation to this method is that the reaction rate must be rapid enough for stoichiometric reaction in the time interval (*ca* 0.01 sec) required for mass transport between the disc and ring electrodes

#### 4. Chronocoulometry

Anson [71] has applied the name "chronocoulometry" to a method in which a voltage step is applied to an electrode, and the electrical charge that flows across the electrode-solution interface is measured as a function of time. If the voltage step is such that no current flows before it, and the maximum diffusion-limited current flows after it, the charge-time behavior is given by the integrated Cottrell equation [72, 73]

$$Q = \frac{2nFAC\sqrt{Dt}}{\sqrt{\pi}} + Q_{dl} \quad (22)$$

where  $Q$  is the amount of charge in coulombs that has passed in time  $t$ .

$Q_{dl}$  is the charge required for the double layer capacitance. If  $Q$  is plotted against  $\sqrt{t}$ , the slope is proportional to concentration and the intercept  $Q_{dl}$  is a measure of the integral capacity of the double layer.

Up to the present time, the main use of the method has been to estimate the quantity of adsorbed reactant, which adds the quantity  $nF\Gamma$  to the amount of charge passed at zero time, where  $\Gamma$  is the quantity of electroactive substance reducible without diffusion, in moles/cm<sup>2</sup> [74]. Its applicability to extremely dilute solutions is limited by the relatively large value of  $Q_{dl}$ .

A double potential-step method, in which the potential is returned to its initial value after a finite time,  $\tau$ , was suggested recently by Anson [71], in an effort to achieve rigorous correction for double layer charging. Here again, the emphasis was upon determining adsorbed reactant, rather than upon achieving maximum sensitivity. Although further work to establish the sensitivity limits is surely warranted, the method does not appear to have inherent advantages over pulse polarography where similar voltage steps can be used, but with direct measurement of electrolysis current.

### 5. Galvanic Analysis

A type of coulometric method in which a galvanic cell is used to generate current has been reviewed by Hersch [75]. The method is a variant of constant potential coulometry in which an internal rather than external source of potential is used. It is especially suited to the monitoring of flowing liquid or gaseous streams. Using a tubular electrode at low flow rates the method approaches 100% current efficiency, and is truly coulometric while at high flow rates the response approaches a voltammetric mass-transport limited current. For example, a cell using a lead anode and silver cathode in 24% KOH, using a polyvinyl chloride diffusion membrane for oxygen, is sensitive to ppm concentrations of hydrogen in the gas phase [76]. Using a porous "filter electrode" or a cell with a long path, the method is useful for monitoring low concentrations of halogen in water and for many indirect determinations based upon halogen. Examples of these and other coulometric techniques are discussed by Bard [77].

### 6. Coulostatic Analysis

A technique involving measurement of the potential of an isolated electrode (usually a hanging mercury drop) following the application of a pulse of charge, and during the dissipation of the charge by an electrochemical reaction of a diffusing reactant, has been independently studied by Reinmuth [78] and Delahay [79], although it had been suggested previously by Barker [80].

If, as a first approximation, the double layer capacitance is taken to be independent of potential, the amount of charge held by the electrode is

proportional to its potential, measured from the point of zero charge. For semi-infinite linear diffusion, the flux at the electrode surface varies linearly with the square root of time. Therefore, as a first approximation, the potential of an isolated electrode under these conditions varies approximately linearly with  $\sqrt{t}$ , the slope of line being proportional to concentration. Delahay and Ide [81] showed that the method is applicable in a concentration range of *ca.*  $10^{-5}$  to  $10^{-7}$  *M*.

Although in principle the method possesses selectivity, the analysis of mixtures is not convenient, and its dependence upon the double layer properties of the electrode makes it responsive to all factors affecting those properties. It appears likely that the method will find only limited application, in especially suitable cases.

A potentiometric method for determination of trace quantities of oxygen in gases is based on a similar principle [82]. In an air-free solution, a dropping mercury electrode at open circuit assumes the potential corresponding to the point of zero charge. If oxygen (or any other strong oxidant) is present in solution, the potential of each mercury drop varies approximately linearly with  $\sqrt{t}$  until the drop falls off. The rate of change of potential during drop life is proportional to concentrations of oxygen. Although the method is sensitive to fractional parts per million, it suffers from a lack of specificity.

#### D. STRIPPING ANALYSIS

The technique known as stripping analysis appears to be one of the most powerful electrochemical approaches to trace analysis. An excellent discussion of the principles and potentialities has been presented by Shain [83].

The procedure consists of two steps, a preelectrolysis step in which the desired component is deposited cathodically or anodically as a solid deposit or amalgam, followed by a reverse electrolysis in which the component is determined. It is clear that many permutations of procedures are possible in principle. The preelectrolysis step may be quantitative or it may be arranged to deposit a reproducible fraction of the component from solution. The reverse electrolysis likewise may be stoichiometric, to yield a coulometric determination, or it may be nonstoichiometric, to give a response proportional to the amount deposited. By controlling the potential during deposition or dissolution, the desired component may be selectively deposited or dissolved. More easily electrolyzed major constituents may be separated out by preelectrolysis.

If a solid electrode is used, the deposition step may be non-stoichiometric or stoichiometric, but the reverse step must be stoichiometric (coulometric). On the other hand, if a mercury electrode is used, the reverse process may also be non-stoichiometric because it can be arranged to be diffusion limited.

At first thought, it would seem obvious that the most sensitive determinations would be achieved by quantitative depositions. A simple calculation, however, demonstrates that by compromising quantitative-ness an enormous saving in time is effected with only a moderate sacrifice in sensitivity. For example, if a preelectrolysis procedure could be arranged to deposit a component quantitatively from 2 ml of solution into a hanging mercury drop electrode delivered from a dropping electrode of  $m=2$  mg/sec,  $\tau=5$  sec to give an electrode of volume  $7.4 \times 10^{-4}$  cm<sup>3</sup> and area  $3.9 \times 10^{-2}$  cm<sup>2</sup>, a concentration increase of 2700-fold would be achieved by quantitative deposition. If the deposition is carried out under reproducible stirring conditions, its rate follows first-order kinetics, with a rate constant given by

$$k = \frac{DA}{V\delta} \quad (23)$$

where  $k$  = fraction deposited per second

$A$  = area of electrode

$V$  = volume of solution

$\delta$  = effective diffusion layer thickness.

Under reasonable stirring conditions von Sturm and Ressel [13] found  $\delta \cong 10^{-3}$  cm, and taking  $D = 10^{-5}$  cm<sup>2</sup>/sec,  $A = 0.039$  cm<sup>2</sup>,  $V = 2$  ml, we calculate from eq (23),  $k = 2 \times 10^{-4}$  sec<sup>-1</sup>. Calculating the enrichment factor from the first order decay law, we find the figures in Table 1. It is evident that a totally impracticable time of preelectrolysis would be required to achieve a quantitative deposition. Using a 500 second

TABLE 1. Dependence of enrichment factor on time.

% Deposition	Time, sec	$C_{\text{amalg}}/C_{\text{solution}}$
0.1	50	2.7
1	500	27
10	4900	270
50	7000	1350
99	23200	2680

preelectrolysis, a concentration increase of 27-fold could be achieved under the assumed conditions. In actual practice, Shain and Lewinson [84] achieved a 500-fold increase in concentration in 5 min of preelectrolysis, evidently because of more efficient stirring.

Theoretically, it would be possible to take advantage of nonuniformity of concentration within the mercury drop during the first instants of preelectrolysis and thus speed up the process without a corresponding loss of sensitivity [85]. However, after a few minutes the amalgam concentration is essentially uniform [84], and sensitivity can be increased by prolonging the preelectrolysis time. Hanging mercury drop electrodes have generally been of two designs, either following Gerischer [86] in catching one or more drops from a dropping electrode and suspending the drop from a platinum wire, or as advocated by Kemula [87] to avoid contamination of the mercury, squeezing out a mercury drop by means of a micrometer screw.

An electrode consisting of a thin film of mercury on a substrate of platinum, silver, nickel, or carbon [88-92] would theoretically be much more sensitive than a hanging drop electrode because of its more favorable geometry. Although early reports indicated poor reproducibility, more recent work by Roe and coworkers [91, 92] has indicated a substantial advantage, both in sensitivity and resolution for thin-film electrodes using nickel or carbon as substrates. For a 1 cm<sup>2</sup> graphite electrode with a thin film of electrodeposited mercury, a half-time for plating of 10 min from 15 ml of solution, and a sensitivity of  $3 \times 10^{-10}$  *M* for quantitative determination of lead was reported. A stripping curve for several metals from a thin film of amalgam on nickel is shown in Figure 6. Van Swaay and Deelder [93] prepared mercury drop electrodes by electrodeposition of mercury onto the flush-ground end of a platinum wire electrode which could be rotated. Evidently the platinum was not completely covered by mercury judging from the cathodic limit of the electrode.

Of the many possible variations in procedure, the most common with mercury electrodes is to use predeposition at a controlled potential under fixed conditions of geometry and stirring for a time of the order of 5 to 10 min, followed by a linear anodic scan for stripping. Using the hanging drop electrode, the peak current during anodic scan is proportional to the square root of scan rate, whereas with thin film electrodes, a direct proportionality is observed [91] because of rapid diffusion in the thin film. Normally, stirring is shut off during the stripping, but with thin film electrodes, the reverse scan can be run with stirring.

The applications of anodic stripping using the hanging mercury drop electrode have largely been confined to a relatively few metals that are reversibly plated as amalgams. The results, however, have been spectacularly successful. DeMars and Shain [94] determined  $10^{-8}$  *M* Cd<sup>++</sup> with a precision of  $\pm 2$  or 3% using 15 min of preelectrolysis and a linear scan rate of 21 mV/sec. By extending the preelectrolysis to 60 min, they were able to extend the sensitivity to  $10^{-9}$  *M*. Monnier et al. [95], determined manganese at concentrations of  $2 \times 10^{-6}$  *M* with precision of 3%, and  $2 \times 10^{-8}$  *M* with precision of 13%. Kemula et al. [96], de-

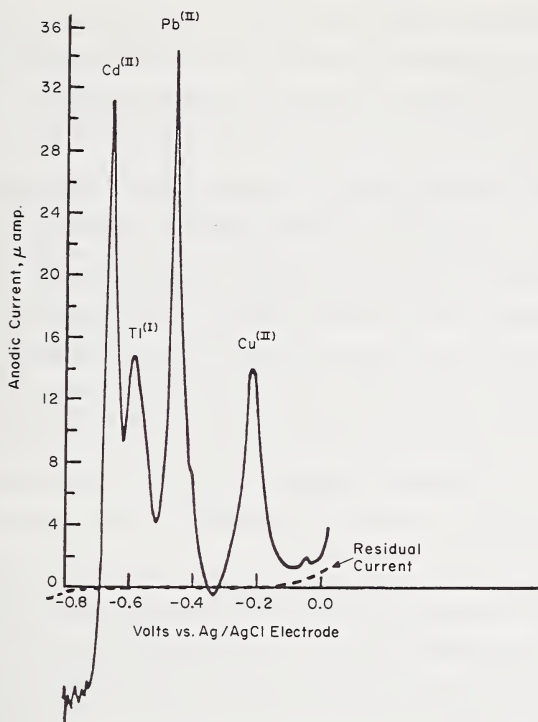


Figure 6. Anodic stripping from thin amalgam film on nickel. Reproduced with permission from D. K. Roe and J. E. A. Toni, *Anal. Chem.* **37**, 1503 (1965).

terminated Pb, Cd, Sb, and In in trace concentrations in high purity zinc, but did not have sufficiently pure zinc samples to test the limit of sensitivity. They reported a detection limit of  $2 \times 10^{-9} M$  for cadmium, and  $10^{-8} M$  for copper, corresponding to  $2 \times 10^{-7}\%$  and  $3 \times 10^{-6}\%$  as weight percentages of the metal in zinc. They could also determine Sn, Bi, and Tl, but could not determine iron. They introduced an important procedure to improve resolution in defining In and Cd. By stopping the anodic scan after the cadmium peak had been passed, they selectively oxidized cadmium from the amalgam, and improved the indium peak upon resuming the scanning. For Sn and Pb, or Bi and Sb, preliminary separations were necessary. Barker and Jenkins [11] using square wave polarography during the anodic sweep, determined traces of impurities in reagent grade chemicals, at concentration levels of  $10^{-7}$  to  $10^{-8} M$ . Von Sturm and Ressel [97] reported limiting concentrations of  $3 \times 10^{-8}$ ,  $1 \times 10^{-7}$ , and  $8 \times 10^{-9} M$  respectively for Pb, Tl, and Cd, using square wave polarography following 2 min electrolysis, and they list relative sensitivities for a series of metals, including Bi, Cu, Sb, Pb, Sn, Tl, Cd, In, Zn, Mn, and Ba. The absolute sensitivities could no doubt be improved by extending the preelectrolysis time.

Kemula [98] has stressed the importance of intermetallic compound formation in lowering the sensitivity of anodic stripping analysis. For example, nickel lowers the peaks for anodic stripping of zinc, particularly at higher Ni:Zn ratios and at higher zinc concentrations for a given ratio.

With solid electrodes using the reverse linear scan method it is not possible to set up diffusion-limited currents, so it is necessary to set up some form of coulometric measurements such as the determination of the area under a current-time curve. Because of disturbances such as undervoltage and overvoltage effects, and the difficulties of making residual current corrections, relatively few applications of inert solid electrodes have been made. Lord, O'Neill, and Rogers [99] determined silver at concentrations as low as  $5 \times 10^{-8} M$ . Nicholson [100] determined nickel in concentrations down to  $10^{-7} M$  by stripping it from platinum into thiocyanate solution. This is an important example, because nickel is so irreversibly oxidized that it cannot be stripped from its amalgams.

Another type of stripping analysis, either anodic or cathodic, consists of forming an insoluble layer at the electrode surface during preelectrolysis, and stripping it off by reverse electrolysis. In principle, it is not possible to carry the deposition to completion because of the limitation imposed by finite solubility of the layer. The stripping process, however, may be stoichiometric or nonstoichiometric. Such a method was used by Ball, Manning, and Menis [101] for determination of chloride using a mercury electrode, and by Shain and Perone [102] for halides using a silver electrode as anode followed by cathodic stripping. Shain and Perone determined iodide at concentrations down to  $10^{-8} M$  and estimated the limit of sensitivity at  $10^{-9} M$ . Brainina and coworkers [103] have compared the sensitivities for cathodic stripping analysis of various anions using mercury electrodes, and have given concentration limits of  $5 \times 10^{-6} M$  for  $\text{Cl}^-$ ,  $1 \times 10^{-6} M$  for  $\text{Br}^-$ ,  $5 \times 10^{-6} M$  for  $\text{I}^-$ ,  $4 \times 10^{-7} M$  for  $\text{WO}_4^{2-}$  and  $1 \times 10^{-6} M$  for  $\text{MoO}_4^{2-}$ . In several other studies, these workers have precipitated hydroxides of metals in higher oxidation states at electrode surfaces, and determined them by cathodic stripping. Examples are Mn(II), Ce(III) [104], Fe(II) [105], and Tl(I) [106]. Chromate was deposited reductively as a  $\text{Cr}(\text{OH})_3$  film on graphite and determined by anodic dissolution [107].

The method of a chemical stripping was introduced by Bruckenstein and Nagai [108] who determined thallium and lead at concentrations as low as  $2 \times 10^{-7} M$  by codepositing the metals with mercury onto platinum and measuring the rate of chemical oxidation by measuring the open-circuit potential as a function of time. A similar method was studied by Bruckenstein and Bixler [109], who determined Ce(IV) at  $10^{-6} M$ ,  $\text{MnO}_4^-$  at  $5 \times 10^{-7} M$  and Fe(III) at  $2 \times 10^{-6} M$  by measuring the time required for chemical oxidation of a known amount of silver de-

posited on a rotating platinum electrode. The main disadvantage of the method is its nonselectiveness for strong oxidants.

### E. ELECTROLYTIC CONCENTRATION

Electrolysis, in principle, is a powerful method of effecting enormous concentration of trace substances. The methods described under stripping analysis, of course, constitute the first step of such concentration methods although they seldom are carried out to completion.

Schmidt and Bricker [110] and Taylor and Smith [111] effected enormous selective concentration operations by electrodeposition into mercury and redissolution into a smaller volume of electrolyte.

Phillips and Shain [112] improved the sensitivity of anodic stripping analysis for tin by shifting from the 1.2 *M* HCl medium in which deposition was carried out to 0.01 *M* HCl for the stripping step, thereby avoiding the interference of residual hydrogen ion discharge. Successful results were obtained on NBS sample 11-g, containing 0.003% Sn. About 10% of the deposited tin was lost during transfer, but reproducible results could be obtained by careful technique.

Ariel, Eisner, and Gottesfeld [113] applied a similar technique, which they called "medium exchange," to anodic stripping analysis. The technique was applied to the determination of copper in the presence of manganese in much higher concentrations in triethanolamine solutions. In the original medium, electrooxidation of Mn(II) to Mn(III) would have occurred upon stripping. The same technique would of course be applicable to electrolytic concentration. Some attention would have to be paid to avoiding appreciable "chemical stripping" during the rinsing and rest periods.

Another technique closely akin to stripping analysis has been recently described by Yarnitsky and Ariel [114]. After a cathodic predeposition with stirring, followed by a brief waiting period without stirring, a short oxidation interval is applied at constant potential. Then a linear cathodic sweep is applied to make the determination. A sensitivity increase is achieved due to the increased concentration in the immediate vicinity of the electrode surface during the oxidation step. The method appears to have promise especially when reoxidation must be carried out at potentials near that of mercury oxidation.

## II. Methods Based on Electrodes at Equilibrium

### A. DIRECT POTENTIOMETRY

#### 1. *Electrodes of the First Class*

Relatively limited analytical application is made of the measurement of electrode potential for the purpose of determining a substance taking part directly in an electrode reaction. A metal-metal ion electrode,

for example, in a cell with liquid junction would respond to the activity of metal ions provided that the problems of elimination of liquid junction potential and single ion activity coefficients could be satisfactorily resolved as is done in pH measurements. Very few electrodes in practice respond rapidly enough at concentrations of analytical interest to make such measurements useful. Moreover, the danger of interferences from other potential-determining systems is frequently present.

In high temperature systems, however, the direct measurement of electrode potential is often analytically useful. In LiCl-KCl eutectic at 400–600°, many metals respond reversibly to their ions, and activity coefficient corrections are unnecessary below mole fractions 0.01 because of the constant ionic environment [115]. As another example, Moebius [116] determined oxygen fugacities down to  $10^{-15}$  to  $10^{-30}$  atm in high temperature gaseous equilibrium mixtures using a concentration cell involving a solid, oxide-ion transporting membrane as the electrolyte.

### 2. Electrodes of Second and Third Classes

Silver electrodes, coated with a layer of halide or sulfide, are available from several commercial sources for the determination of chloride, bromide, or iodide at concentration ranges corresponding to the solubilities of the silver salts. Of course, they cannot be used in the presence of substances forming stable silver complexes, or in the presence of anions forming less soluble silver salts than the one coating the electrode.

An especially interesting electrode for determination of metal ion activity is the mercury-EDTA electrode introduced by Schmidt and Reilly [117]. The potential determining system,  $\text{Hg}|\text{Hg(II)}(\text{EDTA}), \text{EDTA}, \text{M}(\text{EDTA}), \text{M}^{n+}$ , permits mercury to be used as an indicator electrode for various metals that form complexes with EDTA. If equimolar concentrations of the  $\text{Hg(II)}(\text{EDTA})$  and  $\text{M}(\text{EDTA})$  complexes are added to the solution, the electrode potential is given by

$$E = E^0_{\text{Hg(II)}, \text{Hg}} + \frac{RT}{2F} \ln \frac{K_{MY}}{K_{HgY}} + \frac{RT}{2F} \ln a_{M^{n+}} \quad (24)$$

where  $K_{MY}$  and  $K_{HgY}$  are the formation constants of the EDTA complexes of the metal M and mercury(II), respectively.

### 3. Glass Electrodes

Perhaps the most common potentiometric measurement of all, the pH determination, lies outside the scope of this discussion.

Recent developments in special glass electrodes for metal ions, particularly sodium and potassium ions, have been discussed in a thorough review by Eisenman [118]. Addition of  $\text{Al}_2\text{O}_3$  to ordinary pH glass elec-

trodes greatly enhances the "alkaline error" or response to alkali metal ions while decreasing the pH response. By varying the composition of glasses of the systems  $M_2O-Al_2O_3-SiO_2$  where  $M_2O$  is  $Li_2O$ ,  $Na_2O$ ,  $K_2O$ ,  $Rb_2O$ , or  $Cs_2O$ , it is possible to vary the selectivity of response of the glass to each of the alkali metal ions. For example, a selectivity of better than 1000:1 for  $Na^+$  over  $K^+$  at high pH and better than 300:1 in neutral solutions can be achieved with commercially available electrodes.

For  $K^+$ , a selectivity of 10:1 over  $Na^+$  is possible. By making a simultaneous measurement of  $Na^+$ , a correction can be made for its effect. By varying the glass compositions favorable selectivities for  $Li^+$ ,  $Rb^+$ , and  $Cs^+$  can also be achieved. In general, the best glass composition for a given measurement depends upon the nature of the other alkali metal ions present.

Although many attempts have been made to develop glasses sensitive to divalent cations, none is sufficiently selective to be useful in the presence of moderate concentrations of  $Na^+$  or  $K^+$ .

#### 4. Liquid Ion Exchange Membrane Electrode

An important recent development has been the introduction of a technique for using liquid ion exchange materials as a membrane for use as a specific ion electrode. Although the published literature is sparse, there are indications that such electrodes are useful for direct determination of calcium in biological fluids [119]. Errors due to transport of water and to solubility of the ion exchanger have been studied [120]. This field promises to be one of rapid development in the near future.

#### 5. Precipitate-Impregnated Membrane Electrodes

Pungor and coworkers [121, 122] developed a new class of anion selective electrodes involving the incorporation of precipitate particles, e.g., silver halides or barium sulfate, in a matrix of polymerized silicone rubber. The electrodes appear to respond through the selective adsorption of anions upon the precipitate particles. The most selective and sensitive is the silver iodide membrane electrode, shown by Rechnitz and coworkers [122] to respond to iodide concentrations down to  $5 \times 10^{-7} M$  with relatively little interference from common anions.

### B. PRECISION NULL-POINT POTENTIOMETRY

Malmstadt and Winefordner [123] devised a sensitive potentiometric method for species that yield sensitive potentiometric response. Basically a concentration cell method, the procedure involves adjustment of the concentration of electroactive species in the "known" half of a cell until the highly amplified cell response disappears. Liquid junction

effects are eliminated through the use of a high concentration of supporting electrolyte (e.g.,  $\text{H}_2\text{SO}_4$ ) throughout the cell and standard solution. Careful thermostating to eliminate temperature gradients and special attention to electrode preparation to avoid asymmetry effects are necessary to achieve optimum results.

Malmstadt and Winefordner [123] were able to determine chloride, using silver chloride electrodes, with an accuracy and precision of 10% even at  $10^{-6}$  *M*. Using silver iodide electrodes, iodide at 10 ppm ( $10^{-4}$  *M*) levels could be determined within 5% relative error even in the presence of high concentrations of chloride.

Using electrolytic generation of iodine, with precision null-point detection, Malmstadt and Pardue [124] were able to determine oxidants and reductants to within 0.02 ppm of iodine ( $10^{-7}$  *M*  $\text{I}_2$ ), corresponding to a quantitative determination limit of  $10^{-6}$  *M*.

### III. Methods in Which Faradaic Current Is Unimportant

#### A. CONDUCTANCE

Electrolytic conductance is such a nonspecific property that only in special situations is its measurement of practical value in analysis. In these situations, however, it is capable of extreme sensitivity.

A familiar nonspecific determination is the control of quality of distilled or deionized water. The limit of determination would be expected to be of the order of  $10^{-7}$  *M*, the ionic concentration of pure water at room temperature. Ehrenburg and Smit [125] determined  $\text{CO}_2$  at dilutions down to 1:10<sup>9</sup> ( $2 \times 10^{-8}$  *M*) in water or  $10^{-4}\%$  in inert gases by measuring the conductivity of carbonic acid. Determinations of carbon in steel are commonly made by measurement of the decrease in conductivity of  $\text{Ba}(\text{OH})_2$  caused by the  $\text{CO}_2$  produced in vacuum combustion. As an example, Kuo, Bender, and Walker [126] used 0.0065 *M*  $\text{Ba}(\text{OH})_2$  in determining carbon in steels in the 20–400 ppm range and in boron in the 350–1000 ppm range. The sensitivity limit is no doubt imposed by the combustion step.

#### B. HIGH FREQUENCY ADMITTANCE

High frequency measurements permit the determination of changes in conductance or dielectric constant without the introduction of electrodes into direct contact with the solution. Taking advantage of the great sensitivity of measuring small relative changes in oscillator frequencies, Blaedel and Malmstadt [127] were able to carry out conductometric titrations even in the presence of relatively large concentrations of indifferent electrolytes. In general, however, such titrations do not compete in sensitivity with amperometric ones.

Direct measurements of changes in high frequency admittance afford a sensitive and continuous method for monitoring small changes in

dielectric constant. Winefordner and Williams [128] based a detector for gas chromatography on this principle.

### C. DOUBLE LAYER CAPACITANCE MEASUREMENTS

The double layer capacitance of a mercury-solution interface is extraordinarily sensitive to adsorption of surfactants. Since a monolayer of adsorbate may cause a several-fold decrease in capacitance, a fractional monolayer can easily be detected. Assuming 10% coverage of an electrode of  $10^{-2}$  cm<sup>2</sup> area by an adsorbate occupying 20 Å<sup>2</sup> per molecule, a detection limit of  $10^{-11}$  mole is estimated. Aside from testing solutions for the presence of surface active impurities, the method has been of little analytical use because of its lack of specificity. In certain cases it is a convenient method for estimating the fraction of electrode surface covered by surfactant.

In a related method, the "tensammetric" measurement in AC polarography [14], the admittance peaks in regions where adsorption varies strongly with potential are sensitive indications of surfactants. Breyer and coworkers [129] titrated several metal ions at concentrations of  $10^{-5}$  to  $10^{-6}$  M by observing the tensammetric peaks of 8-hydroxyquinoline (oxine).

## IV. Summary

If we define the sensitivity limit of a quantitative method as the lowest concentration at which a determination can be made with a relative precision of 10% in the presence of a large concentration of major constituent, we may compare various electroanalytical methods as in Table II. Such a comparison, however, should be viewed with caution. Most of the methods have been studied with the most favorable examples and some have not yet been pushed to their limits. It is also important to keep in mind that the sensitivity limits of a given method may vary widely with the substance being determined, and that some methods are far more general in applicability than others.

As to the future, one may look with pessimism at some aspects of the field and with optimism at others. It would appear unlikely that spectacular new advances are to be made in the field of trace analysis by varying the types of electrical signal inputs or readouts. For special purposes, such as following rapid changes of concentration with time, or with distance, or measurement of surface concentrations, such approaches still need development. For many applications that are analytical only in the broad sense, such as identification and determination of reaction intermediates, or the pulse generation of reactants we may expect important progress. For the direct observation of solution concentrations at extreme dilution, however, the various permutations of electrochemical signals have been pretty well worked

TABLE 2. *Quantitative sensitivity limits of some electroanalytical methods*

Sensitivity limit, $M$	Methods
$10^{-4} - 10^{-5}$	AC polarography, chronopotentiometry, Thin layer coulometry, Potentiometry with metal-specific glass or membrane electrodes
$10^{-5} - 10^{-6}$	Classical polarography, Coulometry at controlled potential, Chronocoulometry, Tensammetry, Precision null-point potentiometry
$10^{-6} - 10^{-7}$	Fast polarography, Derivative polarography, Square wave polarography, Second harmonic AC polarography, Phase-sensitive AC polarography, Linear sweep voltammetry, Staircase voltammetry, Derivative voltammetry, Coulostatic analysis, Chemical stripping analysis
$10^{-7} - 10^{-8}$	Pulse polarography, RF polarography, Coulometric titrations, Amperometry with rotating electrodes, Conductivity (aqueous)
$10^{-7} - 10^{-9}$	Anodic stripping with hanging mercury drop electrodes
$10^{-9} - 10^{-10}$	Anodic stripping with thin film electrodes or solid electrodes

over. Pulse polarography which is sensitive, selective, and general, offers the greatest immediate promise for extending the enormous scope of polarographic analysis to greater dilution.

The field of stripping analysis deserves special attention, for it offers the selectivity of both the preelectrolysis and analysis steps and also the sensitivity of the final determination. Among the problems appearing to be fruitful for further investigation are the continued study of thin film mercury electrodes, the study of substrates for thin film amal-

gam and direct deposition, the study of media (including nonaqueous solvents) for stripping of irreversibly deposited metals, and the further study of the deposition of insoluble films other than the metals themselves.

Glass electrodes appear to be limited in applicability to the monovalent cations. On the other hand, the area of liquid ion exchange membrane electrodes for specific metal ions seems ripe for rapid progress.

## V. References

- [1] Delahay, P., Charlot, G., and Laitinen, H. A., *Anal. Chem.* **32** [6], 103A (1960).
- [2] Kelley, M. T., and Miller, H. H., *Anal. Chem.* **24**, 1895 (1952).
- [3] Miller, G. W., Long, L. E., and George, G. M., *Anal. Chem.* **36**, 1143 (1964).
- [4] Kronenberger, K., Strehlow, H., and Elbel, A. W., *Leybold Polarog. Ber.* **5**, 62 (1957).
- [5] Kronenberger, K., and Nickels, W., *Z. anal. Chem.* **186**, 79 (1962).
- [6] Kelley, M. T., Fisher, D. J., and Jones, H. C., *Anal. Chem.* **31**, 1475 (1959); **32**, 1262 (1960).
- [7] Schaap, W. B., and McKinney, P. S., *Anal. Chem.* **36**, 29 (1964).
- [8] Cooke, W. D., Kelley, M. T., and Fisher, D. J., *Anal. Chem.* **33**, 1209 (1961).
- [9] Barker, C. C., *Anal. Chim. Acta* **18**, 118 (1958).
- [10] Parry, E. P., and Osteryoung, R. A., *Anal. Chem.* **36**, 1366 (1964); **37**, 1634 (1965).
- [11] Barker, G. C., and Jenkins, J. L., *Analyst* **77**, 685 (1952).
- [12] Ferrett, D. J., Milner, G. W. C., Shalgosky, H. I., and Slee, L. J., *Analyst* **81**, 506 (1956).
- [13] Von Sturm, F., and Ressel, M. *Proc. First Australian Conf. on Electrochemistry* (1963), Pergamon Press, Ltd., 1965, p. 310.
- [14] Breyer, B., and Bauer, N. H., *Alternating Current Polarography and Tensammetry*, Interscience, New York, 1963.
- [15] Grahame, D. C., *J. Electrochem. Soc.* **99**, 370C (1952).
- [16] Smith, D. E., and Reinmuth, W. H., *Anal. Chem.* **32**, 1892 (1960).
- [17] Underkofler, W. L., and Shain, I., *Anal. Chem.* **37**, 218 (1965).
- [18] Smith, D. E., and Reinmuth, W. H., *Anal. Chem.* **33**, 482 (1961).
- [19] Paynter, J., and Reinmuth, W. H., *Anal. Chem.* **34**, 1335 (1962).
- [20] Kambara, T., and Hasebe, K., *Review of Polarography (Japan)* **13**, 132 (1966).
- [21] Schaap, W. B., and Wildman, E., *Proceedings of Sixth Conference on Analytical Chemistry in Nuclear Reactor Technology*, Gatlinburg, Tennessee, October 1962.
- [22] Katsanos, A. A., Tassius, D. P., and Zeliotis, N. D., *J. Electroanal. Chem.* **11**, 36 (1966).
- [23] Pech, J., *Coll. Czech. Chem. Commun.* **6**, 126, 190 (1934).
- [24] Brdicka, J., *Coll. Czech. Chem. Commun.* **5**, 112, 148, 238 (1933).
- [25] Slendyk, I., *Coll. Czech. Chem. Commun.* **4**, 335 (1932).
- [26] Harris, W. E., and Kolthoff, I. M., *J. Am. Chem. Soc.* **67**, 1484 (1945).
- [27] Kolthoff, I. M., and Parry, E. P., *J. Am. Chem. Soc.* **73**, 5315 (1951).
- [28] Phillips, S. L., *Anal. Chem.* **38**, 343 (1966).
- [29] Levich, B., *Acta Physicochim USSR* **17**, 257 (1942).
- [30] Laitinen, H. A., and Kolthoff, I. M., *J. Phys. Chem.* **45**, 1079 (1941).
- [31] Kolthoff, I. M., and Stricks, W., *J. Am. Chem. Soc.* **80**, 2101 (1958).
- [32] Kolthoff, I. M., and Jordan, J., *J. Am. Chem. Soc.* **75**, 4869 (1953).
- [33] Heyrovsky, J., and Forejt, J., *Z. phys. Chem.* **193**, 77 (1943).
- [34] Weaver, J. R., and Parry, R. W., *J. Am. Chem. Soc.* **76**, 6258 (1954); **78**, 3542 (1956).
- [35] Blaedel, W. J., Olson, C. L., and Sharma, L. R., *Anal. Chem.* **35**, 2100 (1963).
- [36] Randles, J. E. B., *Trans. Faraday Soc.* **44**, 322, 327 (1947).
- [37] Sevcik, A., *Coll. Czech. Chem. Commun.* **13**, 349 (1948).

- [38] Nicholson, R. S., and Shain, I., *Anal. Chem.* **36**, 706 (1964).
- [39] Delahay, P., "New Instrumental Methods in Electrochemistry," Interscience Publishers Inc., N.Y., 1954, pp. 119, 126.
- [40] Ross, J. W., DeMars, R. D., and Shain, I., *Anal. Chem.* **28**, 1768 (1956).
- [41] Tyler, J. F. C., *Analyst* **89**, 775 (1964).
- [42] Perone, S. P., and Mueller, T. R., *Anal. Chem.* **37**, 2 (1965).
- [43] Barker, G. C., Proc. 2nd International Congress of Polarography, Cambridge, 1959.
- [44] Mann, C. K., *Anal. Chem.* **33**, 1484 (1961); **37**, 326 (1965).
- [45] Nigmatullin, R. Sh., and Vyaselev, M. R., *J. Anal. Chem. USSR* **19**, 506 (1964).
- [46] Christie, J. H., and Lingane, P. J., *J. Electroanal. Chem.* **10**, 176 (1965).
- [47] Reinmuth, W. H., *Anal. Chem.* **33**, 485 (1961).
- [48] Reinmuth, W. H., *Anal. Chem.* **38**, 270R (1966).
- [49] Vincent, H. A., and Wise, E. N., *J. Electroanal. Chem.* **11**, 54 (1966).
- [50] Christensen, C. R., and Anson, F. C., *Anal. Chem.* **35**, 205 (1963); **36**, 495 (1964).
- [51] Lingane, J. J., ch. 19, *Electroanalytical Chemistry*, 2d ed., Interscience Publishers Inc., N.Y., 1958.
- [52] Meites, L., *Anal. Chim. Acta* **18**, 364 (1958).
- [53] Booman, G. L., Holbrook, W. B., Rein, J. E., *Anal. Chem.* **29**, 219 (1957).
- [54] Laitinen, H. A., and Enke, C. G., *J. Electrochem. Soc.* **107**, 773 (1960).
- [55] Feldberg, S. W., Enke, C. G., and Bricker, C. E., *J. Electrochem. Soc.* **110**, 826 (1963).
- [56] Evans, D. H., *Anal. Chem.* **37**, 1520 (1961).
- [57] Hubbard, A. T., and Anson, F. C., *Anal. Chem.* **36**, 723 (1964).
- [58] Oglesby, D. M., Omang, S. H., Reilley, C. N., *Anal. Chem.* **37**, 1312 (1965).
- [59] Anderson, L. B., Reilley, C. N., *J. Electroanal. Chem.* **10**, 295 (1965).
- [60] Oglesby, D. M., Anderson, L. B., McDuffie, B., and Reilley, C. N., *Anal. Chem.* **37**, 1317 (1965).
- [61] Cooke, W. D., Reilley, C. N., and Furman, N. H., *Anal. Chem.* **24**, 205 (1952).
- [62] Cooke, W. D., Reilley, C. N., and Furman, N. H., *Anal. Chem.* **23**, 1662, 1665 (1951).
- [63] Nikelly, J. G., and Cooke, W. D., *Anal. Chem.* **28**, 243 (1956).
- [64] Sease, J. W., Niemann, C., and Swift, E. H., *Anal. Chem.* **19**, 197 (1947).
- [65] Farrington, P., and Swift, E. H., *Anal. Chem.* **22**, 889 (1950).
- [66] Meier, D. J., Myers, R. J., and Swift, E. H., *J. Am. Chem. Soc.* **71**, 2340 (1949).
- [67] Meites, L., *Anal. Chem.* **24**, 1057 (1952).
- [68] Christian, G. D., and Feldman, F. J., *Anal. Chim. Acta* **34**, 115 (1966).
- [69] Bishop, E., and Dhaneshwar, R. G., *Anal. Chem.* **36**, 726 (1964).
- [70] Bruckenstein, S., and Johnson, D. C., *Anal. Chem.* **36**, 2186 (1964).
- [71] Anson, F. C., *Anal. Chem.* **38**, 54 (1966).
- [72] Christie, J., Lauer, G., and Osteryoung, R. A., *J. Electroanal. Chem.* **7**, 60 (1964).
- [73] Osteryoung, R. A., and Anson, F. C., *Anal. Chem.* **36**, 975 (1964).
- [74] Anson, F. C., *Anal. Chem.* **36**, 932 (1964).
- [75] Hersch, P., Galvanic Analysis, in "Advances in Analytical Chemistry and Instrumentation," C. N. Reilley, ed., Vol. III, Interscience (Wiley), 1964, p. 183.
- [76] Hersch, P., *Anal. Chem.* **32**, 1030 (1960).
- [77] Bard, A. J., *Anal. Chem.* **38**, 88R (1966).
- [78] Reinmuth, W. H., *Anal. Chem.* **34**, 1272 (1962).
- [79] Delahay, P., *Anal. Chem.* **34**, 1267 (1962).
- [80] Barker, G. C., in *Transactions of Symposium on Electrode Processes*, Philadelphia, 1959, E. Yeager, ed., (John Wiley & Sons, N.Y., 1961) p. 325; cf. Delahay, P., and Reinmuth, W. H., *Anal. Chem.* **34**, 1344 (1962).
- [81] Delahay, P., and Ide, Y., *Anal. Chem.* **34**, 1580 (1962).
- [82] Laitinen, H. A., Higuchi, T., and Czuha, M., *J. Am. Chem. Soc.* **70**, 561 (1948).
- [83] Shain, I., Stripping Analysis, in *Treatise on Analytical Chemistry*, I. M. Kolthoff and P. J. Elving, eds., Part I, Vol. 4, ch. 50, Interscience Publishers, 1959.

- [84] Shain, I., and Lewinson, J. *Anal. Chem.* **33**, 187 (1961).
- [85] Mamantov, G., Papoff, P., and Delahay, P., *J. Am. Chem. Soc.* **79**, 4034 (1957).
- [86] Gerischer, H., *Z. physik. Chem. (Leipzig)* **202**, 302 (1953).
- [87] Kemula, W., Kublick, Z., and Galus, Z., *Nature* **184**, 1795 (1959).
- [88] Gardiner, K. W., and Rogers, L. B., *Anal. Chem.* **25**, 1393 (1953).
- [89] Marple and Rogers, L. B., *Anal. Chim. Acta* **11**, 574 (1954).
- [90] Neeb, R., *Z. Anal. Chem.* **180**, 161 (1961).
- [91] Roe, D. K., and Toni, J. E. A., *Anal. Chem.* **37**, 1503 (1965).
- [92] Matson, W. R., Roe, D. K., and Carritt, D. E., *Anal. Chem.* **37**, 1594 (1965).
- [93] van Swaay, M., and Deelder, R. S., *Nature* **191**, 241 (1961).
- [94] DeMars, R. D., and Shain, I., *Anal. Chem.* **29**, 1825 (1957).
- [95] Monnier, D., Martin, E., and Haerdi, W., *Anal. Chim. Acta* **34**, 346 (1966).
- [96] Kemula, W., Kublik, Z., and Glodowski, S., *J. Electroanal. Chem.* **1**, 91 (1959).
- [97] von Sturm, F., and Ressel, M., *Z. anal. Chem.* **186**, 63 (1962).
- [98] Kemula, W., Galus, Z., Kublik, Z., *Bull. Acad. Polon. Sci. Sec. Sci. Chem.* **6**, 661 (1958).
- [99] Lord, S. S., O'Neill, R. C., and Rogers, L. B., *Anal. Chem.* **24**, 209 (1952).
- [100] Nicholson, M. M., *Anal. Chem.* **32**, 1058 (1960).
- [101] Ball, R. G. Manning, D. L., and Menis, O., *Anal. Chem.* **32**, 621 (1960).
- [102] Shain, I., and Perone, S. P., *Anal. Chem.* **33**, 325 (1961).
- [103] Roizenblat, E. M., and Brainina, Kh. Z., *J. Anal. Chem. USSR* **19**, 631 (1964).
- [104] Brainina, Kh. Z., *J. Anal. Chem. USSR* **19**, 753 (1964).
- [105] Brainina, Kh. Z., and Roizenblat, E. M., *J. Anal. Chem. USSR* **18**, 1184 (1963).
- [106] Brainina, Kh. Z., and Kiva, N. K., *Zh. Analit. Khim.* **20**, 1306 (1965).
- [107] Brainina, Kh. Z., *J. Anal. Chem. USSR* **18**, 1010 (1963).
- [108] Bruckenstein, S., and Nagai, T., *Anal. Chem.* **33**, 1201 (1961).
- [109] Bruckenstein, S., and Bixler, J. W., *Anal. Chem.* **37**, 786 (1965).
- [110] Schmidt, W. E., and Bricker, C. E., *J. Electrochem. Soc.* **102**, 623 (1955).
- [111] Taylor, J. K., and Smith, S. W., *J. Res. NBS* **56**, 301 (1956).
- [112] Phillips, S. L., and Shain, I., *Anal. Chem.* **34**, 262 (1962).
- [113] Ariel, M., Eisner, U., and Gottesfeld, S., *J. Electroanal. Chem.* **7**, 307 (1964).
- [114] Yarnitsky, Ch., and Ariel, M., *J. Electroanal. Chem.* **10**, 110 (1965).
- [115] Laitinen, H. A., and Liu, C. H., *J. Am. Chem. Soc.* **80**, 1015 (1958).
- [116] Moebius, H. H., *Z. physik. Chem. (Leipzig)* **230**, 396 (1965).
- [117] Schmid, R. W., and Reilley, C. N., *J. Am. Chem. Soc.* **78**, 2910 (1956).
- [118] Eisenman, G., in *Advances in Analytical Chemistry and Instrumentation*, Vol. 4, C. N. Reilley, ed., Interscience (Wiley), 1965, p. 213.
- [119] Moore, E. W., Ross, J. W., Riseman, J., and Hughes, W. L., Jr., Abstract 1795, 50th Meeting Fed. Am. Soc. for Exptl. Biol., Atlantic City, April 1966.
- [120] Borner, O. D., and Lunney, D. C., Abstract N46, 151st ACS meeting, Pittsburgh, March 1966.
- [121] Pungor, E., Havas, J., and Toth, K., *Acta Chim. Acad. Sci. Hung.* **41**, 239 (1964); *Z. Chem.* **5**, 9 (1965).
- [122] Rechnitz, G. A., Kresz, M. R., and Zamochnick, S. B., *Anal. Chem.* **38**, 973 (1966).
- [123] Malmstadt, H. V., and Winefordner, J. D., *Anal. Chim. Acta* **20**, 283 (1959); **24**, 91 (1961).
- [124] Malmstadt, H. V., and Pardue, H. L., *Anal. Chem.* **32**, 1034 (1960).
- [125] Ehrenburg, J. P., and Smit, G. B., *Anal. Chim. Acta* **29**, 1 (1963).
- [126] Kuo, C. W., Bender, G. T., and Walker, J. M., *Anal. Chem.* **35**, 1505 (1963).
- [127] Blaedel, W. J., and Malmstadt, H. V., *Anal. Chem.* **22**, 1413 (1950).
- [128] Winefordner, J. D., and Williams, H. P., *Anal. Chem.* **37**, 161 (1965).
- [129] Breyer, B., Hayes, J. W., Fujinaga, T., Takagi, C., and Okazaki, S., *Bunseki Kagaku* **14**, 1023 (1965).



# ELECTROCHEMICAL METHODS

## Contributed Papers and Discussion

**R. A. OSTERYOUNG**

*North American Aviation Science Center  
1049 Camino Dos Rios  
Thousand Oaks, California 91360*

### I. Introduction

In his lecture, Professor Laitinen discussed the general nature of a variety of electroanalytical methods. Of particular interest was the indication of factors which affect the ultimate sensitivity of these various methods. It might be worthwhile to comment on the practical application of these electroanalytical techniques and the applicability of the contributed papers to trace characterization. Many of us engaged in electroanalytical or electrochemical work often look at these techniques with selected and favorable examples and samples. (In reference to the electrochemist's tendency to make a "most favored ion" situation, a friend of mine once wanted to know if, in some electrochemical work we were engaged in, we were still doing "cadmiumometry".)

It is my feeling, from an admittedly limited observation point, that, at present, classical polarography, voltammetry, particularly sweep voltammetry, coulometry (in particular, coulometric titrations), and perhaps stripping analysis procedures, are of significant practical importance in trace electroanalytical procedures.

In part, the practical application of a wide host of electroanalytical procedures ultimately seems to depend on the availability of commercial instrumentation. This is not itself sufficient; cost, simplicity of operation, reliability—these factors in part must be taken into account. Some of the techniques discussed by Professor Laitinen—square wave polarography, A.C. polarography, as examples—have had limited commercial instrumentation available for some time, but the instrumentation is quite expensive and their use is complicated. Hence, these techniques—while used for fundamental studies in various laboratories, normally with home-made apparatus—have not been widely applied to practical trace analytical procedures. Our own work in the pulse-polarographic area was triggered by a feeling that for internal practical analytical problems pulse polarography would be a very useful tool. While a commercial unit was available, its cost, about \$20,000, was such

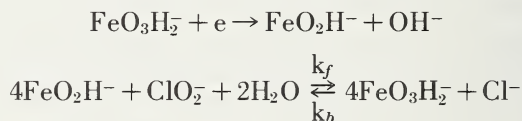
that we constructed a pulse polarograph to meet our own needs. We were fortunate, however, in having facilities and sufficient familiarity with modern electronics to carry this out. The Oak Ridge National Laboratory, as another example, has pioneered in electroanalytical instrumentation as a result of its own internal requirements.

One other factor which I feel limits electroanalytical applications is that much more background and understanding is required for their successful utilization than, say, would be required to carry out spectrophotometric-colorimetric procedures.

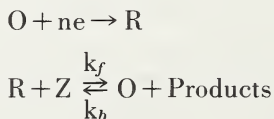
## II. Contributed Papers

I would now like to proceed to a brief discussion of the papers contributed to this Symposium. In so doing, I shall consider them, where possible, as they relate to the electroanalytical methods previously discussed by Professor Laitinen.

Utilizing classical polarography, the papers "Characteristics and Potentialities of the Chlorite Catalytic Wave for Trace Analysis" by L. Gierst, E. Nicolis, L. Vandenberghe, and R. L. Birke from the Free University of Brussels, Brussels, Belgium, and "Application of the Catalytic Behavior of Certain Metal Complex Systems to Trace Analysis" by Harry B. Mark, Jr., of the University of Michigan at Ann Arbor, consider using "catalytic" polarographic waves as a basis for electroanalysis. The first of these papers considers the reaction



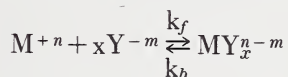
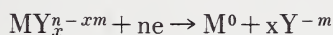
which, carried out in a large excess of chlorite, can be, in principle, utilized for the determination of iron in an alkaline medium. (The general catalytic case



imposes certain restrictions on the material Z. Z must have a high overpotential for reduction on Hg, must be a good oxidant (to react with R), and  $k_f$  must be large.) Over a limited concentration range, the height of the catalytic wave is proportional to the concentration of iron. The reaction itself is very sensitive to pH changes, to ionic strength changes, and to the addition of almost anything which forms an iron complex. From a table of redox potentials, couples which *may* give rise to catalytic

current with chlorite are indicated. Some of these have been found *not* to give rise to the catalytic currents, however.

The second paper dealing with catalytic currents considers catalysis of the type



where the species  $\text{Y}^{-m}$  is determined catalytically in a large excess of  $\text{M}^{+n}$ . For this type of catalytic wave to be observed, the reduction of the complex  $\text{MY}_x^{n-xm}$  must be *easier* (more positive) than the uncomplexed  $\text{M}^{+n}$ , which must be very irreversibly reduced. Again  $k_f$  must be large. The specific example in this work involves the use of nickel ion, which is normally irreversibly reduced, and which, in the presence of pyridine or o-phenylenediamine, shows a catalytic wave. The pyridine determination, carried out in solutions  $10^{-5}$ – $10^{-4}\text{M}$  in pyridine and about  $10^{-2}\text{M}$  in Ni(II), requires a calibration curve as the height of the catalytic current is not linear with respect to the concentration of pyridine. The phenylenediamine system is interesting in that the ortho-isomer gives rise to the catalytic wave, while the meta- and para-isomers do not. Thus, determination of the ortho-content of a mixture may be carried out. A number of other compounds giving rise to catalytic Ni(II) waves are given.

While an understanding of these catalytic waves is interesting and important from an electrochemical point of view, practical analytical utility is limited. The catalytic waves are very sensitive to most solution matrix changes including both kind and amount of supporting electrolyte, pH, temperature (to which they are highly sensitive), and probably any strong complexing agent in solution. In addition, specificity would seem to be low. I would cite the statement of Gierst et al. as the most optimistic point of view—"As can be concluded, the use of catalytic currents does not have extremely wide applicability; however, considering their sensitivity, the effort to broaden their domain of utility is certainly worthwhile." Yet, the sensitivity is *not*, as indicated in the present papers, extremely high—i.e.,  $< 10^{-7}\text{M}$ —and the drastic effects of even small changes in solution composition may result in large changes in the catalytic currents.

The contribution "Adsorption Electroanalysis" by Sidney Phillips of I.B.M. at Poughkeepsie, New York, considers the current-time behavior of a diffusion or mass-transport limited faradaic process which takes place concomitantly with the adsorption of a non-electroactive organic (or inorganic) species at the electrode interface. The electrode is held at a fixed potential where the faradaic reaction takes place, and

the current-time behavior is observed. The adsorbed material interferes with the faradaic process and the *time* required for the elimination or diminution of the faradaic current is related, under certain conditions, to the concentration of the organic material in solution.

To consider analytical use, it must be assumed that the adsorption of the organic material is diffusion limited and that the adsorption coefficient is so large that, up to full coverage of the electrode surface, all the molecules which undergo adsorption are adsorbed as soon as they reach the surface. At the dropping electrode, the time for full coverage required for the faradaic current to drop to zero is then related to the inverse square of the bulk concentration of the adsorbing organic. When the solution is stirred, and one uses a hanging mercury drop, the time for the initially constant faradaic current to decrease to a new, lower steady-state value is determined and is inversely proportional to the concentration of adsorbing material. Data presented indicate that concentrations of tetrabutyl ammonium ion in the  $10^{-6}$ M range can be determined by measuring the time required for the current due to the reduction of millimolar Cd(II) to attain a new steady state value.

However, it appears that the model presented, (which requires that, up to the limit of full coverage, all the molecules adsorb as soon as they reach the surface) cannot represent the situation. Data presented indicate that the current does not decrease to the same final value at each tetrabutyl ammonium concentration, but that the final limiting current values are dependent on the concentration of tetrabutyl-ammonium ion. The theory utilized predicts that the amount of organic adsorbed is the same at all concentrations and should therefore interfere, ultimately, with the electrode reaction to the same extent.

The analytical use of this type of procedure is certainly fraught with difficulty. Every substance must be tested *specifically*, not only to see that there *is* an inhibition process but that the inhibition obeys the derived equations. It is known, for example, that the assumptions of (a) complete inhibition and (b) diffusion-limited adsorption are not always obeyed. It is not, to my knowledge, established that the inhibition of the faradaic process is independent of the concentration of the electroactive species. The complete lack of specificity, if one has mixtures, again indicates problems. While of interest electrochemically and electroanalytically, particularly from the point of view of maxima suppression and perhaps masking, the particular utility again seems limited. One use of this type of analysis scheme is, however, to test for, or determine, the amount of organic adsorbants in a supposedly "pure" solution. However, general utility seems small.

In a paper, "Application of Cathode-Ray Polarography and Anodic Stripping Voltammetry to Trace and Microanalysis", E. June Maienthal and John K. Taylor of the National Bureau of Standards, use a Davis Differential Cathode-Ray Polarotrace to carry out a variety of low-level

determinations via sweep voltammetry, and the Sargent Fast-Scan Polarograph for anodic stripping at a hanging mercury drop. A variety of metals and halides — aluminum, antimony, arsenic, bismuth, cadmium, chromium, copper, indium, iron, lead nickel, tellurium, thallium, titanium, tin, zinc, iodine, and bromine, are included in a list indicating analyses carried out with the Cathode-Ray Polarotrace. Specific results for Te in cartridge brass and in white cast-iron standards are given. The results are in excellent agreement with those found by activation and spectrochemical analysis.

Iodide, as another example, could be determined at the 1 ppm level to a precision of 5 parts per thousand by a comparative technique, in which the sweep voltammetric system involves two electrodes. One of the electrodes is in a solution containing the iodide which has been previously oxidized to iodate; the other electrode is in a solution containing a suitable standard. The difference in the currents is measured on application of sweep. The differential procedure permits greater precision than one would ordinarily expect at this concentration level. It is demonstrated that cadmium, lead and copper can be determined at the 10 ppb level by means of anodic stripping voltammetry.

The NBS work demonstrates that the sweep voltammetric procedure is clearly capable of both selectivity and sensitivity. The use of differential or comparative procedures opens the door to good precision at high sensitivities. Extension to electrode materials other than mercury would permit determination of species, for example, which could be electrochemically oxidized.

The work of R. J. Joyce and C. L. Westcott of Beckman Instruments, Inc., Fullerton, California, investigates a particular form of a mercury electrode for use in stripping analysis procedures. As indicated by Professor Laitinen, deposition—hence concentration—into a small mercury drop, followed by oxidation of the deposited material, can be an extremely sensitive procedure. The use of a thin mercury coating had been suggested initially by K. W. Gardner and L. B. Rogers [1].<sup>1</sup> However, the apparent irreproducibility encountered tended to cause most workers to ignore these electrodes, in spite of certain advantages which have recently been set forth in some detail by D. K. Roe and J. Toni [2].

Joyce and Westcott report some very practical efforts to assess particularly the ease of electrode preparation and stability. Mercury plating was carried out on platinum and nickel wires sealed into a soda-lead, soft glass. Cleaning of the electrodes, particularly nickel, is found to be all important. Although the thickness of the deposited film is constant to only approximately  $\pm 20\%$ , this variation may not appreciably alter the peak current obtained in stripping. This peak current should

---

<sup>1</sup> Figures in brackets indicate the literature references at the end of this paper.

be proportional to both the thickness of film and the concentration of metal plated and, assuming constant plating conditions, the concentration of metal in the film decreases with increasing film thickness. The films do not have the same electrochemical characteristics as a mercury drop; the hydrogen overvoltage is lower. Exposure to air results in rapid deterioration of the film.

It is stated that the reduction of Pb (II) and Cd(II) is less reversible on the plated electrode than on a hanging mercury drop as evidenced from the peak of current-potential curves occurring at more cathodic potentials at the film electrodes. This, however, ignores changes in concentration at the surface of the thin-film which would shift the peak potentials. Peak currents, on anodic stripping of Cd<sup>0</sup>, are not completely linear with the concentration of Cd(II) in solution, which is disturbing. Reproducibility is not too good either. However, if the charge passed on anodic stripping were determined, the linearity of charge versus concentration of species in solution would be considerably better than the peak current-concentration data. Some evidence of interaction between different metals plated into the film is also indicated.

From the present work, it is difficult to assess what advantage, compared to a hanging drop, is offered at present by the plated mercury electrodes. Resolution is claimed by Roe and Toni [2] to be somewhat better than for the hanging-mercury drop, mainly, it would appear, because the "tailing" evident at a hanging drop is absent in what is essentially a "thin-layer" type of stripping and this would be of significant value. However, the difficulty of keeping and preparing the film electrodes, compared to a hanging mercury drop, may well limit their widespread use until stable or easily prepared films can be obtained. Further investigation of these electrodes appears to me to be worthwhile and warranted.

Continuing with the polarographic papers, "Application of Pulse Polarography to Trace and Microanalyses" by E. P. Parry and R. A. Osteryoung of North American Aviation Science Center, Thousand Oaks, California, indicates some use of the pulse polarographic technique previously discussed by Professor Laitinen. Some of the possible trade-offs between sensitivity and resolution which may be obtained by varying pulse amplitude are indicated. The determination of micromolar amounts of a material in the presence of 10,000-fold excess of a more easily reduced species is possible and is a very real advantage of this method, as illustrated by the determination of  $10^{-6}$  to  $10^{-7}$ M Cd(II) in the presence of  $10^{-3}$ M Cu(II). Small sample size is no drawback, and, although sensitivity is highest for reversibly reduced species, manganese, for example, which is irreversibly reduced, is still capable of determination at the  $10^{-6}$ M level. Pulse polarographic procedures are at least as sensitive as the voltammetric sweep methods and are operationally simpler. Since oxidation reactions at solid electrodes can

be carried out, this is an area for future work, particularly since non-metals can be studied by this method. The technique is also useful in stirred or flowing solutions.

The paper of G. A. Rechnitz of the State University of New York at Buffalo, "Ion Specific Electrodes as Tools for Trace Analysis" considers an area which might be introduced by quoting from one of Dr. Rechnitz's earlier publications [3]. "The age-old dream, and nightmare, of analytical chemists has been that someone, someday, will develop a series of probes which, when introduced into a sample, will see and report on a given constituent regardless of the other components present." In essence, the ion-specific electrodes, of which the glass pH electrode is probably the best known type, serves as a means of determining one species in the presence of other species which may otherwise interfere.

The use of a glass electrode, for Ag(I) determination, and a Pungor-type AgI-precipitate-impregnated silicone-rubber membrane electrode for iodide determination are discussed. These electrodes serve as membranes; a solution of fixed activity of the desired constituent is used on one side of the membrane, with the unknown solution on the other side. The membrane potential indicates, in general, the difference in activity of the species on either side. Of major importance is the "selectivity ratio", which in essence indicates the ability of a specific electrode to withstand interference from some other species. For instance, at the 0.1M level the iodide/bromide selectivity ratio at the iodide electrode is about 200, which means that the iodide is two hundred times as effective as bromide as a potential determining entity.

One of the major problems would appear to be the variability of the selectivity ratio with the concentration of the ion in solution. The iodide membrane, in a KI solution, has an essentially theoretical Nernst response to about  $10^{-7}$ M iodide. It is not clear, though, at  $10^{-6}$ M iodide concentration, that the selectivity ratio for bromide is still 200. It appears to me that there would be problems since the electrodes respond to the activity of the ions. Thus measurements involving complexing agents or bulk matrix changes would require calibration in terms of a specific solution at low concentrations.

Recently, calcium sensitive electrodes have come into use (see [4] for a listing of electrodes), while a variety of the Pungor-type electrodes are also commercially available. As indicated by J. M. Friedman [5] the sodium sensitive electrodes appear to be as effective in determining sodium, in the 0.1 molar range, as flame photometry. The use of these electrodes "in vivo" is, of course, of great interest.

It is apparent that this area is one in which a great deal of work will be carried out. While promising in outlook, we are not as yet in the dream world indicated by Dr. Rechnitz, but the area will surely be subjected to a great deal of scrutiny.

The last paper, "Determination of Traces of Protolytic Impurities" by G. Biedermann, L. Newman, and H. Ohtaki, from the Royal Institute of Technology, Stockholm, Sweden, describes, to quote the authors, a ". . . convenient potentiometric method for the estimation of the concentration and of the acidity constant of weak protolytes which have been found to be present at micromolar level in concentrated salt solutions." Constant current coulometry is used to remove added excess acidity and in essence effect a very precise coulometric titration. Measurement of hydrogen-ion concentration is made after each burst of coulometric generation. A "reference acid" is added to the solution of carefully prepared salt solutions, and the reference acid is chosen so that its  $pK_a$  is at least 2 pK units greater than the constant of the sought-for weak protolytes.

The coulometric generation of base (or removal of hydrogen ion) first titrates excess of strong acid, which is initially added to suppress ionization of both the reference and unknown acid, then titrates the weak acids. By consideration of the equilibria involved, the concentration and  $pK_a$  of the unknown weak protolyte are determined from the coulometric titration-hydrogen ion measurements. Most of the trace protolytic materials encountered are found to have  $pK_a$  values of about 5 to 6.5.

This work is an example of a trace procedure developed for a particular purpose and under particular circumstances, namely, for studies of metal ion hydrolysis in high concentration of electrolyte, where it is necessary to assess the acidity present in the electrolyte. The impurity level determined is in the micromolar range and the weak-acid impurities must be taken into account in the metal-ion hydrolysis studies. The method would appear useful, as the authors indicate, in the coulometric standardization of dilute solutions of strong acids, and other situations where a knowledge of trace amounts of acidity may be important.

When I was preparing my remarks, one of the things that I wanted to know was, what is a trace. A rapid scan of the program and of the papers submitted convinced me that an argument might well develop as to what is trace characterization. To quote from a recent book [6], "The connotation of the term trace varies with the background or interests of the reader." At this Symposium we are already in serious difficulty. "To avoid ambiguity, it is herein considered as a constituent making up only a small portion of the sample, the upper limit of the trace or microconstituent being about 100 ppm by weight. There is no necessity for making the boundary a rigid one. Considering the increasing interest in analyses at the parts per billion level, the term ultratrace may be conveniently used to designate the region below a part per million. Any sharp division is, of course, superfluous, and will depend on the nature of the sample to be analyzed, the analytical technique employed and the analyst."

One gram of a solid containing 100 ppm of a substance of molecular weight 100, dissolved in 100 ml of solution yields a  $10^{-5}$ M solution of the sought for constituent. This is clearly in the electroanalytical technique range and under some conditions, identification *and* analysis of mixtures may be carried out. The same 100 ppm, if contained in 1 ml of a solution, corresponds to  $10^{-3}$ M. The factors of sensitivity, selectivity, accuracy, precision, cost (both for analysis and for equipment), time, and applicability to a number of problems on hand are recognized factors which determine the choice of a technique. To this I might also add familiarity with an area or a technique, and just old-fashioned prejudice. Sometimes, of course, the kind of practical problem on hand almost dictates the choice.

Be that as it may, certainly the talk by Professor Laitinen and, I hope, the summaries of the papers and comments given here indicate some of the electroanalyst's tools, problems, capabilities, and current interests.

### III. Discussion

The general discussion at the end of the session was concerned largely with specific-ion electrodes. Dr. Rechnitz pointed out that this technique is still in its infancy. The number of ions for which specific electrodes have been developed is increasing, and improvement in response has been remarkable during the past few years.

The sensitivity and selectivity of these electrodes are interrelated. As an example, electrodes with sodium-over-potassium selectivity ratios of 20,000 are now available. The selectivity ratio varies to some extent with concentration. Multi-valent ions do not generally interfere with sodium ion electrodes but high hydrogen ion concentrations are not readily tolerated.

The relation of electroanalytical techniques to other analytical techniques was discussed briefly. The high sensitivity and selectivity of the former make them very attractive. In some cases, they can offer unique solutions to trace analytical problems. Frequently, they may be used to confirm results obtained by other techniques. The importance of a two-technique approach was emphasized, especially in the case of analysis for certification of standard reference materials.

The selectivity of electroanalytical methods, particularly polarographic measurements, was cited. When the qualitative composition of a sample is known, which is often the case, procedures can ordinarily be selected to minimize interferences. In the absence of such information on any sample submitted for analysis, a spectrographic survey analysis is a valuable preliminary step.

**IV. References**

- [1] Gardiner, K. W., Rogers, L. B., *Anal. Chem.* **25**, 1393 (1953).
- [2] Roe, D. K., Toni, J., *Anal. Chem.* **37**, 1503 (1965).
- [3] Rechnitz, G. A., *Anal. Chem.* **37**, 29A (Jan. 1965).
- [4] *Chem. and Eng. News*, p. 50, May 30, 1966.
- [5] Eisenman, G., Bates, R., Mattock, G., Friedman, J. M., *The Glass Electrode*, Interscience, N.Y. (1965).
- [6] Morrison, G. H., ed. *Trace Analysis*, Interscience, N.Y. (1965).

# OPTICAL AND X-RAY SPECTROSCOPY

N. W. H. ADDINK

*Philips Research Laboratories  
Eindhoven, Netherlands*

## I. Introduction

In any consideration of the pros and cons of a method of analysis and its future possibilities there is some point in reviewing the causes that have led to the results obtained either in one's own experiments or in those of others. In this way it is possible to trace strong and weak points of a method and to compare it with quite different methods of analysis. In that case, of course, also those conditions and those considerations come to the fore which according to the author are of essential significance in the method of analysis under notice. Sometimes these are lost sight of in a publication because of descriptions of details and then one cannot see the forest for the trees.

It is not the purpose of this publication to describe a historical development, for this can be found elsewhere. Nor it is the aim to give an exhaustive summary of present-day working methods. These can all be found in survey articles [1]<sup>1</sup> or periodicals [2] or in publications specialising in short abstracts. In this paper the author desires to review the essential backgrounds of methods of analysis based on excitation in the flame, the arc, and the spark, and on fluorescence produced by means of x-rays.

What then are the standards that must be applied in the appraisal of a method of analysis?

The following criteria are worth considering:

1. Is the method complicated or simple?
2. Is the method of analysis a quick one?
3. Are the results reliable, and how great is the reproducibility?
4. How much sample is required for the analysis?
5. Is the result of the analysis representative of the bulk composition or of the surface composition of the sample?
6. For which concentration regions are certain methods of analysis most suitable; i.e., at what concentration is the reproducibility at its best?
7. What about the possible limits of detection?

---

<sup>1</sup> Figures in brackets indicate the literature references at the end of this paper.

8. It is a well known fact that close to the limit of detection a "poor" reproducibility is found. How can this be influenced favorably? If the processes taking place during atomization, evaporation, dissociation, ionization, excitation at room temperature (x-ray fluorescence analysis) and at high temperatures (flame and arc) and the processes of energy absorption and transfer are known, it becomes possible to start answering the above questions.

Essentially, the author does not wish to become embroiled in discussions of mechanical/technical improvements, in the sense of: the resolving power is determined by the size of the prism used, or by the number of lines or by the blaze of the diffraction grating in question or by the distance between lattice planes and the space group of the analyser crystal; similarly he does not wish to embark on a discussion of the nature of the differences of detection (photographic plate, photoelectric cell, multiplier, counters, etc.) or to describe the use of the slide rule, of the calculating machine or of the computer, though it should here be mentioned that the scientific worker in this field ought by nature to be "lazy"; the less he has to note down himself, the smaller will be the number of "human errors." This applies also, for example, to the preparation of the sample requiring analysis. This point may be illustrated as follows: If it is possible to perform, for example, an alkali determination directly in a solution by means of flame emission or absorption without preliminary chemical separation, then this method of working is preferable to one in which separation or extraction must first be used, for these may give rise not only to human errors but also to unsuspected contaminations, co-precipitations, or absorption processes. On the other hand it should be remembered that with these two latter processes (and also, for example, with electrochemical methods) it is possible to achieve preconcentrations [3] by means of which the limit of detection of an element present in the starting material can be lowered. But these methods of working will here be left out of account. A consideration will now follow of flame, arc and spark excitation and of x-ray fluorescence and electron microprobe analysis.

## II. Flame Emission and Absorption

### A. EXPERIMENTAL TEST OF THEORETICAL CONSIDERATIONS

It will be remembered that in a flame it is possible to distinguish an inner cone, in which the gases supplied undergo combustion proper, and at a small distance above it the outer cone, also known as the measuring volume, in which thermodynamic equilibrium prevails. The substance being analyzed is brought into solution, atomized to form a fine nebula, and then blown through the inner and outer cones. Let us confine ourselves to a description of the state of the outer cone,

where thermal excitation and ionization or the absorption of light of a certain wavelength by ions, atoms, and molecules formed in the inner cone and the intervening space take place. Here we shall pay special attention to

1. ionization of metallic atoms ( $M$ );
2. the equilibrium  $MO \rightleftharpoons M + O$ ;
3. the number of excited atoms.

The object of the test now to be described consists of trying, while restricting ourselves to line emission, to give a quantitative explanation of the results obtained, so that all details are clearly brought to light. Our data can be taken from Table 1.

TABLE 1. Some results of flame photometric measurements.<sup>a</sup>

Aqueous chloride solution	Wavelength emitted	Peak height (above background)
Ba 0.4 $\mu\text{g}$ at/ml	553 $\text{m}\mu$	19.6 mm (arbitrary scale)
Ca 1.38 $\mu\text{g}$ at/ml	422 $\text{m}\mu$	190 mm
Mg 2.26 $\mu\text{g}$ at/ml	285 $\text{m}\mu$	4.5 mm

<sup>a</sup> Flame used: acetylene/air (acetylene in excess).

The energy of the light emitted per unit time (intensity  $I$ ) is proportional to the number of excited atoms  $N_e$  in accordance with

$$I = N_e A h \nu \quad (1)$$

where  $A$  = the transition probability = the reciprocal of the life time of the excited state, which is of the order of  $10^{-8}$  seconds,

$h\nu$  = the energy quantum of the wavelength concerned.

Now how big is the number of excited atoms  $N_e$  in comparison with the total number of atoms  $N$ , that are present? The answer to this is given by the Maxwell-Boltzmann distribution law:

$$N_e = N g \exp(-E_e/kT)/B \quad (2)$$

where  $E_e$  = energy of excitation, expressed in eV,

$k$  = Boltzmann's constant,

$T$  = temperature at which excitation takes place ( $^{\circ}\text{K}$ ),

$g$  = statistical weight factor of the energy level under examination,  $g$  being equal to  $2J + 1$ , where  $J$  is the internal quantum number; for numerical values see [4],

$$B = \text{partition function} = \sum_n g_n \exp(-E_{en}/kT).$$

The ratio  $N_e/N$  is small if  $E_e$  is large or  $T$  is small, and vice versa. On combining eqs (1) and (2) we obtain

$$I = NgAh\nu \exp(-E_e/kT)/B \quad (3)$$

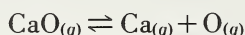
Many people are still under the impression that, in order to give a large signal (large value of  $I$ , corresponding to a low limit of detectability), the temperature must be chosen as high as possible. But it is then forgotten that the degree of ionization, which can be calculated after Saha [5], becomes so great that practically no atoms remain. (If one goes on to measure, for example, resonance lines of the ion one comes up against measurements that are difficult to perform; for instance, the resonance lines of the sodium atom are found at 5890/5896 Å, while those of the sodium ion lie at 370 Å.) Table 2 provides some data indi-

TABLE 2. Fraction of non-ionized atoms of different elements at various temperatures [5].

Element	Ionization energy $V_i$ in eV	Temperature in °K		
		2500 °K	4500 °K	6000 °K
Ba	5.2	0.75	0.50	0.002
Ca	6.1	1	0.9	0.015
Mg	7.6	1	1	0.25
(Zn)	9.3	1	1	1 )
(Al)	6.0	1	0.9	0.015)

cating the factor with which the number of atoms, originating in the amount of salt supplied in the form of a solution, has to be multiplied for calculating the real number ( $N$ ) concerned with this excitation.

Alkemade and collaborators [6] have shown that the molecular bands occurring in an alkaline earth spectrum can be ascribed to the oxides. The conversion to the oxide takes place in the reaction zone (inner cone) of the flame. In the outer cone, the measuring volume, there is an equilibrium, e.g.,  $\text{CaO} \xrightleftharpoons{2500^\circ\text{K}} \text{Ca} + \text{O}$ . It is this equilibrium which determines the intensity of the CaO-bands and that of the discrete Ca-emission. Since we are trying to determine the discrete calcium emission at 422 m $\mu$  we must estimate, if only roughly, this equilibrium. In the gaseous state of the equilibrium



thermodynamics gives us the relation

$$\Delta G = (\Delta H - T\Delta S) = -RT \ln K_p, \quad (4)$$

where  $\Delta G$  = change in standard free energy for this process,

$K_p$  = equilibrium constant.

We can now insert numerical values [7] [8] for the *gaseous* substances:

$$\Delta H_{\text{Ca}} = 46 \text{ kcal/g at.}$$

$$\Delta H_{\text{O}} = 59 \text{ kcal/g at.}$$

$$\Delta H_{\text{CaO}} = (\text{heat of sublimation of CaO} + \text{heat of formation of solid CaO}) \\ = (149.5 - 118) = 31.5 \text{ kcal/mole.}$$

In eq (4)  $\Delta H$  becomes  $46 + 59 - 31.5 = 73.5$  kcal/mole,  $\Delta S = S_{(\text{Ca})} + S_{(\text{O})} - S_{(\text{CaO})} = 37 + 38.5 - 52 = 23.5$  cal/mole.

We therefore find at 2500 °K

$$\Delta G = 73.5 \times 10^3 - 2500 \times 23.5 = 14.8 \times 10^3 \text{ cal/mole, and}$$

$$\log K_p = (-14.8 \times 10^3) / (4.57 \times 2500) = \log 0.05.$$

In a hypothetical experiment let us now, in a closed system (pressure = 1 atmosphere), consider the dissociation equilibrium of CaO, where we have

$$a^2 / (1 - a^2) = 0.05;$$

here we have  $a = p_{\text{Ca}} = p_{\text{O}}$ , and  $a$  then has the numerical value of 0.2. Correspondingly the equilibrium at 4500 °K and at 6000 °K can be calculated; the method is also applicable to other molecules.

Table 3 gives a summary. Tables 2 and 3 now enable us to accomplish the purpose of the experiment, namely to determine the discrete emission of Ca, etc., making use of eq (3). This is shown in Table 4. From this table it will be seen that the calculated ratio of the barium, calcium, and magnesium line intensities is 1:13:0.2, whereas a ratio of 1:10:0.25 has been found by experiment (Table 1), an agreement which may be termed reasonable in view of the fact that so many factors have been taken into account and the rather crude thermodynamic calculations.

## B. THEORETICAL CONSIDERATIONS CONCERNING THE INFLUENCE OF TEMPERATURE

Now it may be asked how great the effect is of a change in temperature, not only on the emission but also on the absorption, apart from

TABLE 3. Shift of the equilibrium  $\text{MO}_{(g)} \rightleftharpoons \text{M}_{(g)} + \text{O}_{(g)}$  calculated at different temperatures for various oxides of metals.

Partial pressure of	2500 °K	4500 °K	6000 °K
Ba atoms	0.008	0.4	0.9
Ca atoms	0.2	1.0	1.0
Mg atoms	0.01	0.7	1.0
(Zn atoms	1.0 (3000 °K)	1.0	1.0)
(Al atoms	~ 0.0001	~ 0.15	~ 0.8)

TABLE 4. Numerical evaluation of equation (3).

$$N \times gAh\nu \times e^{-E_e/kT} \times \frac{1}{B} \times a \times b = I$$

where  $a$  corrects for the sensitivity of the photocell used; and  $b$  corrects for self-absorption in the flame.

	N			$gAh\nu$	$e^{-E_e/kT}$	$\frac{1}{B}$	$a$	$b$	=	$I$
	"correction"									
	Conc.	factors								
	$\mu\text{M/ml}$	Saha <sup>a</sup>	$\text{MO} \rightleftharpoons \text{M} + \text{O}$ <sup>b</sup>							
Ba	0.4	0.75	0.008	$5 \times 10^8$	$2.88 \times 10^{-5}$	$\frac{1}{3}$	72	1	=	$0.83 \times 10^3$
Ca	1.38	1	0.2	$3.3 \times 10^8$	$1.22 \times 10^{-6}$	1	100	1	=	$11 \times 10^3$
Mg	2.26	1	0.01	$45 \times 10^8$	$4.52 \times 10^{-8}$	1	68	0.5	=	$0.16 \times 10^3$

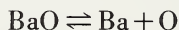
<sup>a</sup> Data from Table 2.

<sup>b</sup> Data from Table 3.

the *method* of excitation. What factors of eq (3) are sensitive to temperature? For the following are subject to change:

1. the ionization (Saha; Table 2), cf. Table 5, column three;
2. the equilibrium  $\text{MO} \rightleftharpoons \text{M} + \text{O}$  (Table 2); cf. Table 5, column four;
3. the proportion of excited atoms ( $N_e/N \sim \exp(-E_e/kT)$ ).

Before considering Table 5 with respect to the *emission* of resonance lines, some remarks should be made. Any mutual influence of both equilibria (of ionization and of dissociation) can be neglected if the correction factors for ionization or dissociation are nearly unity, and if multiplication of both factors is permitted. Otherwise both equilibria have to be taken into account. To take the case of  $\text{Ba}_{4500} \text{ } ^\circ\text{K}$ , for instance, although the two equilibria



are shifted more to the right, the quantity of Ba-atoms available for excitation appears to remain nearly constant.

The following conclusions can be drawn from the results shown in Table 5:

1. For the elements with  $V_i < 7$  eV and of which oxygen compounds exist at 2500 °K a maximum of the emitted energy is found to lie between

TABLE 5. Calculations illustrating the influence of temperature on line intensities (hypothetical conditions).

	$E_e$ (eV)	$V_i$ (eV)	(Saha- correc- tion)	(Dissociation correction)	exp ( $-E_e/kT$ )	Product	Gain against 2500 °K
<i>Ba</i>	2.24	5.2					
2500 °K			0.75	0.008	$2.88 \times 10^{-5}$	$1.73 \times 10^{-7}$	
4500 °K			0.50	0.4	$2.85 \times 10^{-3}$	$0.57 \times 10^{-3}$	$30 \times 10^2$
6000 °K			0.002	0.9	$1.25 \times 10^{-2}$	$2.2 \times 10^{-5}$	$1.3 \times 10^2$
<i>Ca</i>	2.92	6.1					
2500 °K			1.0	0.2	$1.2 \times 10^{-6}$	$2.4 \times 10^{-7}$	
4500 °K			0.9	1.0	$4.7 \times 10^{-4}$	$4.2 \times 10^{-4}$	$20 \times 10^2$
6000 °K			0.015	1.0	$3.2 \times 10^{-3}$	$4.8 \times 10^{-5}$	$2 \times 10^2$
<i>Mg</i>	4.35	7.6					
2500 °K			1.0	0.01	$4.5 \times 10^{-8}$	$4.5 \times 10^{-10}$	
4500 °K			1.0	0.7	$1.16 \times 10^{-5}$	$0.81 \times 10^{-5}$	$180 \times 10^2$
6000 °K			0.25	1.0	$2.0 \times 10^{-4}$	$5.0 \times 10^{-5}$	$1100 \times 10^2$
<i>Zn</i>	5.77	9.35					
3000 °K			1	1	$1.58 \times 10^{-10}$	$1.58 \times 10^{-10}$	
4500 °K			1	1	$2.8 \times 10^{-7}$	$2.8 \times 10^{-7}$	$18 \times 10^2$
6000 °K			1	1	$1.26 \times 10^{-5}$	$1.26 \times 10^{-5}$	$800 \times 10^2$
<i>Al</i>	3.1	6.0					
2500 °K			1	$\sim 0.0001$	$4.5 \times 10^{-7}$	$\sim 4.5 \times 10^{-11}$	
4500 °K			0.9	$\sim 0.15$	$3.0 \times 10^{-4}$	$\sim 4.0 \times 10^{-5}$	$\sim 9 \times 10^5$
6000 °K			0.015	$\sim 0.8$	$2.3 \times 10^{-3}$	$\sim 2.8 \times 10^{-5}$	$\sim 6 \times 10^5$

2500 °K and 6000 °K (this applies also in the case of low overall pressures, with dissociation practically unity, and also incidentally to the corresponding elements having no molecular compounds at high temperatures, e.g. sodium).

2. Elements with  $V_i > 7$  eV do not show such a maximum; for then the gain factor increases with the temperature, this increase being greater if no molecules exist at 2500 °K. The gain calculated in comparison with the intensity of emission at 2500 °K is, however, in part only apparent, for the number of excited atoms at that temperature is extremely small (cf. the column exp  $(-E_e/kT)$ ; a value of  $4.5 \times 10^{-8}$  is still measurable, but only just, if the concentration is in the neighbourhood of 2  $\mu\text{g}$  at/ml. As a rule of thumb it may be said that a temperature of 2500–3000 °K will still just bring about a measurable excitation of 4.5–5 eV, while at a temperature of 4500 °K the excitation reaches about 7 eV and at 6000 °K some 10 eV.

It should be noticed that with aluminum dissociation of the aluminum-oxygen bond greatly prevails over the ionization of the aluminum atom. In this connection it is of special interest to observe the *absorption* (Table 6). For this the same data may be used as those mentioned in Table 5, with the exception of the number of excited atoms  $\exp(-E_e/kT)$ . This number is so small in comparison with the number of non-excited atoms that the total number of absorbing atoms is determined completely by ionization (Saha, third column) and molecule formation (fourth column). From Table 6 a maximum value of the gain of free atoms, with

TABLE 6. Calculations illustrating the influence of temperature on absorption (hypothetical conditions).

	$E_e$ (eV)	$V_i$ (eV)	(Saha- correc- tion)	(Dissocia- tion cor- rection)	Product	Gain against 2500 °K
<i>Ba</i>	2.24	5.2				
2500 °K			0.75	0.008	0.006	
4500 °K			0.50	0.4	0.2	30
6000 °K			0.002	0.9	0.0018	0.3
<i>Ca</i>	2.92	6.1				
2500 °K			1.0	0.2	0.2	
4500 °K			0.9	1.0	0.9	4.5
6000 °K			0.015	1.0	0.015	0.08
<i>Mg</i>	4.35	7.6				
2500 °K			1.0	0.01	0.01	
4500 °K			1.0	0.7	0.7	70
6000 °K			0.25	1.0	0.25	25
<i>Zn</i>	5.77	9.35				
3000 °K			1	1	1	
4500 °K			1	1	1	1
6000 °K			1	1	1	1
<i>Al</i>	3.1	6.0				
2500 °K			1	~ 0.0001	~ 0.0001	
4500 °K			0.9	~ 0.15	~ 0.135	~ 1350
6000 °K			0.015	~ 0.8	~ 0.012	~ 120

respect to a temperature of 2500 °K, is also found to exist at temperatures between 2500 °K and 6000 °K for those elements showing molecular bands in the spectrum. In the case of an element like zinc there is practically no question any more of a maximum.

### C. COMPARISON OF ABSORPTION AND EMISSION

If in Tables 5 and 6 the “products” (the number of available atoms) are considered, then the values given in Table 6 are considerably greater. It should be remembered, however, that for absorption a power of  $e$  also applies:

$$I = I_0 \exp(-kl) \quad (\text{Lambert-Beer})$$

with  $I$  = transmitted energy,

$I_0$  = energy of irradiation,

$k$  = absorption coefficient,

$l$  = thickness of the absorbing medium.

If a comparison is now made of the approximate measuring sensitivities (in ppm) applicable to flame emission and atomic absorption of various elements that can be excited in the flame, this is found to turn out in favour of emission by a factor of between 1 and 15, the mean being 6; see [9]. Nevertheless with a moderate increase of the flame temperature the absorption method permits the determination of a larger number of elements, the reason being a somewhat greater dissociation of the molecules. See [10].

If it were possible to increase the temperature of the outer cone by 500–1000°, this would enable the limit of detection in both absorption and emission to be lowered [11]. The question then arises of whether the absorption method would enable us to determine a larger number of elements. Quite certainly in the case of flame emission a spectrograph of greater resolving power than hitherto used in flame photometry would be required.

### D. ANALYSIS OF MULTICOMPONENT SYSTEMS IN SOLUTION

Let us now briefly consider whether it is always necessary in wet chemical analysis to remove the main components before the trace elements are determined by flame photometry (those cases in which the physicist is interested, for instance the reciprocal influence of the alkali metals, have been worked out). An enormous amount of work could be saved if once and for always such investigations were performed systematically, for example [12] in the case of silver.

### E. FUTURE PROSPECTS

Tables 5 and 6 reveal that at somewhat higher flame temperatures (about 3500–4000 °K) flame emission and absorption can be expected to

bring a larger number of elements within their field of application. At the same time a lower detection limit is to be expected in many cases. For achieving a higher temperature one can think of  $N_2O-C_2H_2$  or cyanogen-oxygen flames, as well as of Langmuir's atomic hydrogen flame. The possibility can also be considered of utilizing a horizontally oriented silver (or copper) arc with water-cooled electrodes (possibly placed in a specific gas atmosphere, e.g.,  $Ar-N_2$ ). The supply of the analysis material, in solution, takes place ultrasonically in the form of a nebula. The above metals (Ag, Cu) have spectra poor in lines, and their arc gas temperature will be about 5000 °K. In the designing of new flames it is important always to consider their energy density, for this must be so great that the temperature equilibrium will not be disturbed by the introduction of the amount of material to be analysed. In this chapter no attention has been paid to excitation in the inner cone. The results of research undertaken on this subject are very encouraging.

### III. Classical Emission Spectral Analysis

#### A. THE ARC

##### 1. *General Considerations*

As already mentioned in the introduction, the best way of testing a method of analysis is to investigate the factors contributing to a complete description of the process that takes place. It will then be found for arc excitation that non-homogeneous selective evaporation, and an excitation volume whose temperature is not homogeneous, strongly affect the accuracy of the analysis results. This will be illustrated with our own data.

Perhaps it is unnecessary to mention that we follow the method of complete evaporation of a certain amount (5 mg) of the substance to be analyzed [13]. The diameter of the graphite electrodes is relatively large (8–10 mm) in order to prevent, after the striking of the arc, a too rapid rise in the temperature of the tip of the anode, where the sample is placed (the maximum temperature of the anode tip is 3500 °C). Furthermore, with such broad electrodes the amount of carbon vapor, which is present during the evaporation of the material, is relatively large. The electrode gap amounts to 9 mm (current strength 10 amps) and the light emitted from the center of the discharge, i.e.,  $4\frac{1}{2}$  mm above the anode, is passed through a diaphragm of 0.5 mm (with the diaphragm slit perpendicular to the electrode axis) and then to the spectrograph by means of a lens which forms the image on the prism or diffraction grating. The temperature of the column amounts to 6100 °K, and that of the mantle to about 4000 °K. (These temperature measurements are relative, depending as they do on the "thermometer element" used. Reference is made to the measurements mentioned in [14]; with the choice of other

“thermometer elements” temperatures in the 10-amp arc of 10000 °K and more have been found. This result is corroborated by the fact that in the same arc there are lines of C II ( $V_i = 21.6$  eV) in the spectrum, and also lines of Zr III ( $V_i$  of Zr III  $\sim 24.7$  eV.)

The temperature of 6100 °K mentioned in this paper must therefore be considered as the mean temperature of the core. With the acetylene-oxygen flame we found, when using the elements lithium and sodium ( $V_i = 5.4$  and  $5.1$  eV), an average temperature of 2500 °K; with the elements cobalt and iron ( $V_i = 7.9$  eV) there was an average temperature of 3000 °K.

Let us now look at the possibility of determining transition probabilities of emitted wavelengths from the large number of analytical data ( $K$ -factors) that have been determined in the course of the years (63 elements, 678 spectral lines). For this, further consideration must be given to the significance of the  $K$ -factors in connection with the rate of evaporation  $S_i$ , so that we can then with the help of eq (5) and Table 8 arrive at final conclusions. By a  $K$ -factor belonging to a certain spectral line of a certain element we mean the ratio of the concentration ( $C$ ) of the element which is present in the analytical sample and the experimentally determined intensity  $I_l$  ( $= I_{l+b} - I_b =$  intensity of line + background minus intensity of background near the line). This may also be put as  $K = C$  for the case of  $I = 1$ . The values of the intensities are standardized on an arbitrary scale.

In contrast to flame photometry, where all the material is introduced as a nebula into the flame, in the arc a partial introduction into the measuring volume takes place: the lower the boiling point of the element to be analyzed, the greater the vapor pressure will be during the rise in temperature of the anode tip, and the greater the sideward losses [15]. In order to determine these losses we have experimentally introduced a “fictitious” rate of evaporation  $S_i$ . In Table 7 a few values of  $S_i$ , in (rel.) cm/s are given. The absolute values of these sideward losses have not

TABLE 7. Relationship of speed of evaporation ( $S_i$ ) and boiling point of some elements.<sup>a</sup>

Element	Boiling point $T$ °C	$S_i$ rel cm/s
Cd	770	400
Te	1390	220
Cu	2300	80
Fe	3000	40
Mo	3700	20
Th (O <sub>2</sub> )	4400	10

<sup>a</sup> The relationship between  $S_i$  and  $T$  can be expressed by  $\log S_i = 2.94 - 0.44 T \times 10^{-3}$ .

been determined, but it is possible to state that the losses with copper ( $S_i = 80$ ) are twice as great as with iron ( $S_i = 40$ ). These sideward losses are thus something quite different from those reported by Corliss and Bozman when under the heading of "persistence of atoms in the arc" they mention sideward losses on account of diffusion into the surrounding atmosphere, which is dependent on the mass of the atom (atomic weight).

If, in order to determine  $A$  (transition probability), we revert to eq (3), then we can rewrite this [16] as

$$A = I \times S / N g h \nu \exp(-E_e / kT). \quad (5)$$

(Reference [16] contains two errors in the calculation: Incorrect application of the formula of Saha, and wrong values of the partition functions.) But we also have to know  $N$  (the number of atoms introduced under standard conditions into the measuring volume) derived from 5 mg of analysis material containing an element of atomic weight  $a$  in a concentration of  $K\%$ . This amounts to  $3K \times 10^{19} / a$ , and after correction for the relative rate of evaporation  $S_i$  it becomes  $3K \times 10^{21} / S_i \times a$ . Now a correction is still required for the sensitivity of the photographic emulsion. By means of  $gA$ -factors of four cadmium lines the instrumental yield was determined, which in our case was  $1/1.5 \times 10^8$ .

In the same way as described in the chapter on flame photometry we can now include the degree of ionization (Saha) and the degree of dissociation of molecules, as well as the temperature of the measuring volume, in our calculation. In this way the reciprocals of transition probabilities of emitted wavelengths were found (Table 8). Agreement with the data of the literature may be termed reasonable and proves that practically all factors having an effect on the spectrochemically determined result have been taken into account.

TABLE 8. Reciprocals of transition probabilities of emitted wavelengths.

	This paper	Allen [17]	Corliss and Bozman [18]
Au 2427 I	$1.8 \times 10^{-8} \text{ s.}$	—	$2.2 \times 10^{-8} \text{ s.}$
Ba 3071 I	$1.3 \times 10^{-8} \text{ s.}$	—	$1.7 \times 10^{-8} \text{ s.}$
Cd 3261 I	$170 \times 10^{-8} \text{ s.}$	$220 \times 10^{-8} \text{ s.}$	$330 \times 10^{-8} \text{ s.}$
Co 3453 I	$1.0 \times 10^{-8} \text{ s.}$	$0.8 \times 10^{-8} \text{ s.}$	$0.5 \times 10^{-8} \text{ s.}$
Fe 3719 I	$5 \times 10^{-8} \text{ s.}$	$20 \times 10^{-8} \text{ s.}$	$5 \times 10^{-8} \text{ s.}$
Na 3302 I	$18 \times 10^{-8} \text{ s.}$	$35 \times 10^{-8} \text{ s.}$	$6 \times 10^{-8} \text{ s.}$
Ti 3349 II	$0.2 \times 10^{-8} \text{ s.}$	$0.8 \times 10^{-8} \text{ s.}$	$0.3 \times 10^{-8} \text{ s.}$
V 3185 I	$0.1 \times 10^{-8} \text{ s.}$	$0.9 \times 10^{-8} \text{ s.}$	$0.5 \times 10^{-8} \text{ s.}$
Zn 3076 I	$200 \times 10^{-8} \text{ s.}$	—	$230 \times 10^{-8} \text{ s.}$

Here it is of importance to observe that in the choice of spectral lines for spectrochemical purposes attention must be paid to the transition probabilities: a relatively small  $A$ -value produces the chance that energy that has been taken up will be given off again, not by the relevant discrete emission but by energy transfer to a second component that may be present in the sample (collisions of the second kind). Spectral lines of this type are the resonance intercombination lines of atoms and ions, as well as those originating from two electron transitions.

## *2. The Significance of the Rate of Evaporation, Sideward Losses and the Temperature of Column and Mantle*

If this method of complete evaporation is going to be used for series analysis, where standard samples resembling the specimens in composition are used, no attention need be paid to  $S_i$  or to the temperature  $T$  of column or mantle. This is generally the case with all the variations of this technique that there are. If, however, one is dealing with a large measure of difference of the samples to be analysed, the above method is still the best to use, in spite of the objection that the properties, such as melting point, boiling point, vapor pressure, reactivity with carbon, of the elements, compounds, or mixtures occurring in the specimens are not always known. In the case of volatile salts (halides) it is always advisable to convert these, with nitric acid, to nitrates which at higher temperatures easily decompose into oxides; in many cases these are reduced by carbon to the metals, which then vaporize with their specific rate of evaporation. Sulfates are in many cases reduced to sulfides and metal. The tendency of a number of metals to combine with oxygen is sometimes so great that they vaporize as oxides in the carbon arc (aluminum, for example). Other metals, for example tungsten, form carbides of such a high boiling point that they cannot be vaporized. As the principal component of a specimen they cannot then be determined quantitatively other than by subtraction of the sum of the impurities from 100%.

The elements on the left of the periodic table with their low ionization potentials reduce the temperature of the column. For example, during the evaporation of sodium ( $V_i = 5.1$  eV) from a glass the temperature of the column, with our method of analysis, falls from 6100 °K to 5600 °K. Elements (or compounds) evaporating simultaneously (for example zinc;  $V_i = 9.4$  eV) are then excited much less. For such cases correction curves are naturally available. During the evaporation of calcium ( $V_i = 6.1$  eV) from a glass a temperature fall of 300° is measured. This relatively slight reduction in temperature is achieved by the specimen's rather slow evaporation rate, caused by the relatively large diameter of the electrodes (already mentioned above). Narrow electrodes are the cause of greater sideward losses [19], a larger measure of simultaneous vaporization, and a greater concentration of the vapor of the specimen,

with accordingly greater changes in temperature. By way of orientation it is recommended to examine moving plate spectra.

Quite generally it may be stated that elements which are excited in the column ( $V_{i \text{ atom}} > 7 \text{ eV}$ , and also ionic lines of elements with  $V_i < 7 \text{ eV}$ ) exhibit more reproducible results than elements excited in the mantle ( $V_i < 7 \text{ eV}$ ). The latter, after all, is much more susceptible to temperature fluctuations on account of direct exchange of heat with the surroundings. For an accurate determination of these elements the flame photometer will therefore have to be used.

### 3. Additions Before Arcing

Alterations in the temperature of the column, brought about by the kind of specimen being analysed (components with a low value of  $V_i$ ), can be suppressed to advantage by addition of an excess of, for example, a lithium compound [20] in which case it is only necessary to ensure that lithium is present from the beginning of the exposure to the end. Then the effect is a virtual increase of the mantle at the expense of the column. This reveals an endeavor to "homogenize" the temperature of the arc.

In the selection of an internal standard, either one of the components of the specimen being analyzed or an additive, it is important to ensure simultaneous vaporization of the internal standard and of the element (or compound) to be determined as well as excitation at the same place in the column or mantle of the arc.

In the analysis of refractory materials fruitful use has been made of additives which, on account of their high boiling point and in accordance with the principle of carrier distillation, carry along all impurities that would otherwise have remained behind in the specimen (classical example of Scribner and Mullin and many others).

### 4. Limits of Detection

With the d-c arc, described in section III.1.a. and indicated for short as the *K*-arc, it is possible to reach limits of detection equal to about  $\frac{1}{3} \times K$ -factor, corresponding on average to 0.001%. The factor  $\frac{1}{3}$  is based on the practical experience that with low background a line blackening of 0.03 can still be observed significantly, both visually and instrumentally. A modification of this *K*-arc permits the limit of detection to be lowered even further: electrode gap 2 mm (= sum of cathode and anode layer); 10 mg instead of 5 mg analytical material; the same current of 10 amps (mean temperature of the arc 6700 °K); all the light is transmitted to the spectrograph. This arc discharge will be termed the *Q*-arc [21]. The vaporization of the analytical material takes place in a shorter time, and sideward losses and temperature change to a greater extent than in the *K*-arc. Where the precision of the results

( $2 \times \text{c.o.v.}^2$ ) with the  $K$ -arc varies between 10 and 2% rel. in the concentration range of 0.1 to 100%, with the  $Q$ -arc in the range of 0.001 to 0.0001% it amounts to 25% or more. (Obviously this percentage can be reduced if the number of exposures is multiplied.)

For the determination of concentrations in the ppm range it will be necessary to examine resonance lines and single lines whose upper levels lie somewhat higher in the term scheme. It has been shown by experiments that for those elements excited in the column ( $V_i > 7.5 \text{ eV}$ ) the relation  $\log (K\text{-factor}/Q\text{-factor}) = 0.24 V_i - 0.64$  applies, while for those excited in the mantle ( $V_i < 7 \text{ eV}$ ) the relation is  $\log (K\text{-factor}/Q\text{-factor}) = 0.04 V_i + 0.86$ . In the case of sodium, for example, the limit of detection is reduced by a factor of 12 if instead of the  $K$ -arc the  $Q$ -arc is used. This is quite definitely not a consequence of the higher temperature of the  $Q$ -arc but mainly because *all* the light of the  $Q$ -arc is transmitted to the spectrograph. It should be remembered, however, that with the imaging of the light source on the prism, as described above, the latter is not completely illuminated [22]. Complete illumination can be achieved if the light source is imaged on the slit of the spectrograph, so that, in our case with a Hilger large quartz spectrograph, an increase of signal and noise by a factor of 14 is obtained. The enhancement factor of 14 can be raised to 30 if one starts not with 10 mg but with 25 mg of analytical material. Furthermore it is sometimes possible to superimpose spectra, by which means a hundredfold amplification of signal and background is obtainable in accordance with

$$I_{l+b} - I_b = I_l$$

$$100(I_{l+b} - I_b) = 100I_l.$$

This method of analysis will be indicated by s.p.s.: superimposed spectra; light source projected on slit. This does not mean, however, that a decrease of the limit of detection by a factor of 100 will be found. If a significant value is to be given, it is necessary to take into account the variability of the background and that of the line. The above considerations can also be described in a somewhat different way: in the spectrum of the  $Q$ -arc a resonance line of an element may not be observed because of the fact that the line lies submerged in the background; even though the photographic plate does not record it, the relationship  $I_l = I_{l+b} - I_b$  holds, but both densities lie in the lower (horizontal) region of the characteristic curve. However, if the signals  $I_{l+b}$  and  $I_b$  are amplified a hundredfold, for example, then they give rise to densities lying on the straight part of the characteristic curve. The spread of the two densi-

<sup>2</sup> c.o.v. = coefficient of variation.

ties must be known, and the presence of a line can be determined significantly if the difference with  $n$ -fold amplification complies with

$$nI_{l+b} - nI_b > 2\sigma_b\sqrt{2}.$$

For a general discussion of the determination of the limit of detection reference should be made to paper [23]. From a paper on the further working out of the above principle the following may be quoted [22]: with hundredfold amplification the real gain factor was 45, reduced by interference with molecular bands to 12 or by impurities present in the graphite electrodes to 25. In Table 9 the limits of detection ( $1/3$   $Q$ -factor and s.p.s.) of a number of elements are given. The latter values are corrected for the increase in the background above 3100 Å.

### 5. Impurities Present in Graphite Electrodes

When an arc burns between unloaded electrodes the evaporation of the carbon impurities takes place in such a way that a relatively large fraction does not reach the zone of excitation but is lost sideways in the stream of air ascending along the electrodes. This means that the investigation of spectroscopic graphite must not be carried out by having an arc burn between two clean electrodes. The material to be analyzed has a collecting action, and the effect of collection can be defined as the ratio of the intensities of spectral lines found with and without a material not containing the element in question. In practice we use extremely pure germanium dioxide. It is understandable that the time in which the material (the specimen of  $\text{GeO}_2$  being analyzed) is evaporating will determine the collecting action. This effect, described for the first time in [24], and at greater length later in [22], will be described in detail in a future publication (Witmer and Addink) after routine experience during three years.

### 6. Other Methods of Evaporation and Excitation

At the C.S.I. XII (Exeter 1965), the most recent one to be held, various methods have been described which essentially boil down to a different way of tackling the problem of atomization, viz, the uncoupling of the sampling of the analytical material from the physical state in the measuring volume, something that has long been standard practice in flame photometry. Reference should be made to the papers by Margoshes and those of the school of Kaiser.

Of the application of the laser, which reminded the present author of the exploding wire technique, long since abandoned, beautiful examples were given by Mme Vilnat.

## B. THE SPARK

The spark, which is used so often and which may be considered with its small measuring volume to attack practically always a fresh part

TABLE 9. Limits of detection of various elements in the D.C. arc, expressed in ppm ( $\mu\text{g/g}$ ).

Element	Wavelength $\text{\AA}$	Limit of detection	
		Q-method <sup>a</sup>	s.p.s.-method <sup>a</sup>
Ag	3280	0.1	0.01
Al	3092	1.	0.1 - 1.
As	2350	30.	
	2780	50.	1.
Au	2675	2.	0.05
B	2497	2.	~ 0.05
Be	3130	0.1	0.1
Bi	3067	1.	.05
Cd	3261	10.	1.
Co	2521	3.	.01
Cr	2835	10.	.02
Cu	3247	0.2	~ 0.02
Fe	3020	2.	~ 0.1
Ga	2943	1.	0.02
Ge	2651	1.	0.02
Hg	2536	3.	0.07
In	3256	2.	0.2
Ir	3220	10.	1.
	2849	10.	0.2
Mg	2852	0.2	0.01 - 0.1
Mn	2576	1.	0.02
Mo	3132	10.	1.
Ni	3002	3.	0.06
Os	2909	10.	0.2
P	2535	30.	0.6
Pb	2833	1.	0.02
Pt	3064	2.	0.05
Rh	3434	10.	1.
Sb	2598	7.	0.2
Se	2413		300.
Si	2516	1.	0.05 - 0.5
Sn	2840	3.	0.07
Te	2385	70.	10.
Ti	3242	10.	1.
Tl	2767	20.	0.5
V	3185	10.	1.
Zn	3076	20.	1.
Zr	3391	10.	1.

<sup>a</sup> See Section III.A.4.

of the surface, shows a great measure of reproducibility. In our laboratory for a number of years the main constituents of magnetic steel have been determined accurately:  $2 \times \text{c.o.v.} = 0.5\% \text{ rel.}$  On account of greater sideward losses, smaller amounts of vaporized material, and more ionization it will be difficult to achieve extremely low limits of detection. Yet it was found possible, by projection of the spark on the slit of the Hilger large quartz spectrograph and by extension of the exposure time by a factor of 3 ( $1\frac{1}{2} \text{ min} \rightarrow 4\frac{1}{2} \text{ min}$ ), to achieve amplification by a factor of 60 and a real lowering of the limit of detection by a factor of 35 [25].

One more aspect should be pointed out particularly: also with the spark, on account of the high temperature of the sparked spot, there is selective evaporation (and diffusion in the solid towards the sparked spot). To avoid such effects and possibly the influence of the previous history of the material being analyzed it might be better to cool the electrodes with, for example, liquid nitrogen. In this way the effect of sputtering would be simulated, in other words the composition of the vapor would be completely identical with that of the solid [26].

Another point worth mentioning is the shortening of the exposure time in automatic spectrum analysis by increasing the frequency of the spark. The amount of material converted into the vapor phase will be correspondingly greater, so that the exposure time can be reduced.

A further point to be mentioned is the examination of the composition at the surface of conducting materials (Fig. 1). In this figure the depth of penetration is plotted against the spark time, and thus spectra can be obtained in which the thickness of the layer being analyzed is established unambiguously.

### C. FUTURE PROSPECTS

The d-c graphite arc, though not exhibiting such a large measure of reproducibility on account of the evaporation of analytical material, which is coupled to the kind of excitation volume, has its own special merits as a general method of analysis, especially with its extremely low limits of detection (Table 9). In consequence of the relatively large amount of analytical material that can be examined (10–100 mg) the effect of heterogeneity of the sample can be circumvented, in contrast with the spark source mass spectrometer which has the same or even lower limits of detection but in which the consumption of material is less.

The endeavors to uncouple vaporization and excitation deserve every attention. Raising of the excitation temperature, so far from being significant, is probably even harmful. "Homogenization" of the temperature of the excitation volume (with greater energy density) as well as exact temperature measurements are aspects to which attention should be paid, and so is the use of selected gas atmospheres for arc and spark.

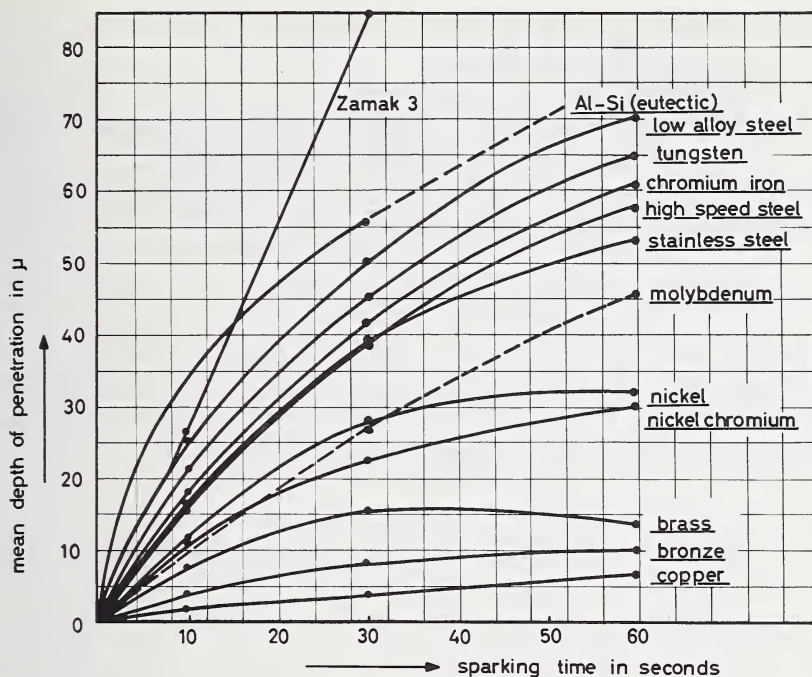


Figure 1. Mean depth of penetration, in  $\mu$ , for various metals and alloys as a function of the sparking time (in seconds). Point-to-plane technique; silver counter electrode (angle  $120^\circ$ ); gap width 2 mm; 15000 V; 0.005  $\mu$ F (Hilger Power Supply).

## IV. X-Ray Fluorescence and Microprobe Analysis

### A. X-RAY FLUORESCENCE

#### 1. General Considerations

While in flame photometry and classical spectral emission analysis the material to be examined is introduced in vapor form, whereafter excitation of atoms takes place by collisions with each other or with electrons, the analytical material in the case of x-ray fluorescence analysis remains unchanged in phase. It is irradiated by a source of almost completely constant energy, and it is possible in advance to predict a large measure of reproducibility of the results of analysis. All the same, unless a comparison is made with a standard which is identical as far as composition is concerned, the systematic error may be large, being caused by changing *absorption of primary and fluorescent energy* on account of changes in the chemical composition of the analytical material. In general, the following relation holds:

$$I_{\text{trans}} = I_{\text{prim}} \exp(\mu_m \times m) \quad (6)$$

where  $I_{\text{prim}}$  = intensity of the primary radiation,

$I_{\text{trans}}$  = transmitted intensity,

$\mu_m$  = mass absorption coefficient,

$m$  = mass of irradiated material, given by its surface ( $1 \text{ cm}^2$ )  
and the depth of penetration (expressed in cm).

If the material consists of the elements  $A, B, \dots$ , we can say, with  $C_A$  as the concentration of element  $A$ , etc.:

$$\mu_m = \mu_{mA} \times C_A + \mu_{mB} \times C_B + \dots \quad (7)$$

Now, following Liebhafsky et al. [27], let us consider the contribution of an element  $A$  to the fluorescent yield ( $dI_A$ ) of a small element  $dm$ , situated in such a way that a mass  $m$  lies between  $dm$  and the surface. From eqs (6) and (7) we find, with  $k$  as a proportionality constant,

$$dI_A = k \times I_{\text{prim}} \exp - [(\mu_{mA} \times C_A + \mu_{mB} \times C_B)_{\text{prim}} \times m] \\ \times \exp - [(\mu_{mA} \times C_A + \mu_{mB} \times C_B)_{\text{fluor}} \times m] \times dm \times C_A. \quad (8)$$

Equation (8) can be rewritten as

$$dI_A = k \times I_{\text{prim}} \exp - [(\mu_{m \text{ prim}} + \mu_{m \text{ fluor}}) \times m] \times dm \times C_A \\ = k \times I_{\text{prim}} \exp (-Qm) \times dm \times C_A. \quad (9)$$

For the sake of simplicity the angles of incidence and reflection have here been left out of account.

On integration over a total mass  $M$ , which may be considered infinitely thick, eq (9) becomes:

$$\int_0^{I_A} dI_A = k \times I_{\text{prim}} \times C_A \int_0^M \exp (-Qm) \times dm$$

or

$$I_A = k \times I_{\text{prim}} \times C_A \times [1 - \exp (-Qm)]/Q.$$

In the case of infinite thickness, we have  $e^{-Qm} = 0$ , so that we find:

$$I_A = k \times I_{\text{prim}} \times C_A/Q. \quad (10)$$

From the above eqs (9) and (10) it is possible to draw two conclusions: Conclusion 1, derived from eq (10): if  $Q$  remains constant for various concentrations of the elements  $A, B$ , etc.,  $I_A$  and  $C_A$  are linearly proportional.

Conclusion 2, from eq (9): if  $e^{-Qm}$  is unity, which means that  $Qm$  is approximately zero, there is a linear relationship of  $I_A$  to  $C_A$ , with no attention having to be paid to interelement effects and the like.

## 2. *Non-Linear Working Curves (First Conclusion; See also [28])*

In many cases the concentration range chosen is so small that, above all with interpolation, the systematic error is very small. It may happen, however, that really extreme cases are involved:

*I.* The determination of a heavy element present in a light matrix; in this case the analytical curve is concave to the concentration axis and may in fact be practically parallel to it, so that there can be no question any more of an analysis. Such a case is encountered in the determination of lead in a lead glass; lead concentrations in excess of 20% can in practice no longer be determined. To overcome this difficulty the relevant sample, in powder form, can be mixed with a heavy element or its compound in powder form (similar particle size!). The value of  $Q$  in eq (10) is then increased by a large amount, depending on the quantity added, so that  $Q$  becomes practically constant. Analysis results:  $2 \times \text{c.o.v.} = 1\% \text{ rel.}$

In the above case it was always the Pb  $L_{\alpha}$ -line that was measured. If the Pb  $M_{\beta}$ -line is measured, the absorption coefficients come to lie closer to each other: the result is as if a light element in a light matrix were determined: the objection of strongly bent analytical curves is cancelled [29].

*II.* In the case of a light element present in a heavy matrix we did not encounter analytical curves strongly bent in such a way that at low concentrations the curves would tend to run parallel to the concentration axis. In such an extreme case the addition of a light element (or compound) might be favorable, but where the absorption by the heavy element is, let us say, infinitely large the contemplated object is not achieved. This is important for trace analysis of light elements.

## 3. *Thin Layers (Second Conclusion)*

An extensive description and discussion of the method followed will be found in [30]. A few details will here be given: mean layer thickness about  $0.1 \mu$ ; weight of the material to be analysed about 0.5 mg. The layer is obtained by homogeneous distribution of a small quantity of the powdered sample on "Mylar" foil; the holder of the foil, with sample, is turned upside down and tapped gently; the layer is hardly visible; other methods of applying such layers have been described [31], and there are analogous methods in which a diluted solution is applied to filter paper which is afterwards dried.

According to eq (9) we find under standard conditions of excitation  $C = K \times I$ , where  $C$  = concentration of the element to be analysed,  $I$  = intensity of the line in question, and  $K$  = a proportionality factor, which is equal to the concentration if  $I$  is unity. We can call them micro- $K$ -factors. Their values are given in Figure 2. Although the c.o.v. is relatively high ( $2 \times \text{c.o.v.}$  in the case of nickel is 3%) it is certain

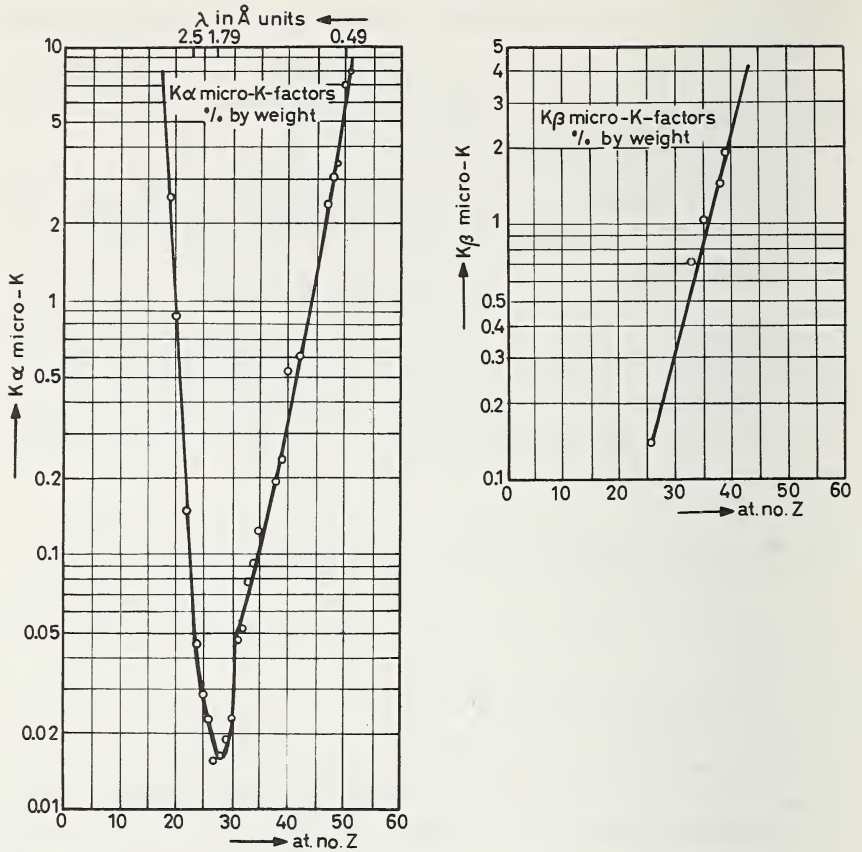


Figure 2. "X-Flu" micro-K factors ( $K_\alpha$ ,  $L_\alpha$ ) as a function of the atomic number  $Z$ .

that, if the application of thin layers is improved, a fruitful method of analysis can be obtained.

#### 4. Factors Bearing on Fluorescence Energies

In [30] results are shown of the calculated ratio of the intensities of the three elements chromium, nickel, and antimony ( $Z$  respectively 24, 28, and 51) and these results are compared with the experimentally determined micro- $K$ -factors. For this purpose the following factors have been taken into account, which may in general be considered to apply:

- I. the intensity of the primary radiation of continuum and characteristic emission;
- II. the constant  $K$  (eq (9)), made up of the fraction of the irradiated energy absorbed by the layer and the fraction of the absorbed energy available for the excitation, the fluorescence yield, and the transition probability;
- III. the counting efficiency;

IV. the length of the analyzer crystal.

The reflection coefficient of the analyzer crystal (mosaic structure) and the absorption by beryllium, air and "Mylar" foil were neglected, and then found

$$I_{Cr} : I_{Ni} : I_{Sb} = 0.23 : 1 : 0.005:$$

determined experimentally

$$1/K_{Cr} : 1/K_{Ni} : 1/K_{Sb} = 0.35 : 1 : 0.002.$$

The agreement may be considered reasonable.

Without change in items I-IV above it is only possible to lower the limit of detection if the number of counts is increased. Experimentally it has been shown that if the counting time is increased by a factor of 100, which means a decrease in the c.o.v. by a factor of  $\sqrt{100} = 10$ , a decrease by a factor of 6 has actually been found [32].

### B. MICROPROBE ANALYSIS

While with the above "micro-K" method an amount of material of on average 0.5 mg was sufficient for an analysis, the smallest amount of analytical material for the microprobe amounts to  $10^{-8}$  mg. Essential for this method is that a volume of  $1 \mu^3$  can be investigated apart from neighboring volumes. Since the object acts directly as the anticathode it is not necessary to take absorption by beryllium and other substances into account. By the use of polymolecular soap crystals ( $2d \approx 100 \text{ \AA}$ ) it has been found possible to demonstrate, for example, 0.1% of carbon in iron. The difficulty encountered in the calculation of the concentrations lies in the lack of the values of the mass absorption coefficients at these relatively long wavelengths [33]. Data for the depths of penetration of accelerated electrons can be taken from the literature [34]. Incidentally the concentration calculation is analogous to that used in x-ray fluorescence analysis.

### C. FUTURE PROSPECTS

Many aspects have been omitted from our considerations: absorption analysis, discussions concerning accuracy [35] and many more [36]. As far as the analysis of lighter elements is concerned, the following quotation of Pomey [37] is apposite: "In order to achieve the determination of still lighter elements it is necessary to make a breakthrough more in the field of equipment than in the methods used." This is a challenge for the instrument makers but it falls outside the scope of this paper.

## V. Final Conclusions

At the end of this paper it is desirable, with the points mentioned in the introduction in mind, to give a brief summary, understanding by "flame" the analysis by flame absorption and emission, by "arc," including "s.p.s. arc," and "spark" classical emission spectroscopy, and by "X-Flu," including micro "X-Flu," x-ray fluorescence analysis, also of thin layers, while "microprobe" refers to x-ray emission electron microprobe analysis.

1. Is the method complicated or simple?

Answer: Except for "microprobe" the methods are simple. Dissolving is necessary for "flame," sometimes desirable for "X-Flu" (reduction of interelement effects and preparation of synthetic standards).

2. Is the method of analysis a quick one?

Answer: Yes, in all cases except "microprobe."

3. Are the results reliable (systematic errors), and how great is the reproducibility (c.o.v.)?

Answer: *Systematic errors* are caused by

a. interelement effects ("flame" and "arc": shift of ionization and dissociation equilibria, "arc": change of evaporation rate and of the magnitude of the measuring volume);

b. history of the analytical material ("spark");

c. unknown absorption coefficients ("X-Flu" and "microprobe").

The *reproducibility* is determined mainly by the constancy of the exciting light source. Arranged in ascending order of c.o.v. we find: "X-Flu," "flame," "spark," and "arc."

5. Is the result of the analysis representative of the bulk composition or of the surface composition of the sample?

Answer: With appropriate sampling, the methods here described, except for "microprobe," can be used for the determination of the bulk composition. With "X-Flu" and "spark" it is *possible* to perform very good surface analyses (chemical surface treatment here being left out of account).

6. For which concentration regions are certain methods of analysis most suitable, i.e. at what concentration is the reproducibility at its best?

Answer: As a rule of thumb, it may be said, at a concentration of at least 3 to 5 times the limit of detection. In this marginal region the value of  $2 \times \text{c.o.v.}$  amounts to 20% rel. [22] for the least reproducible method of analysis (our s.p.s. arc method). For the methods with the best reproducibility ("X-Flu" and "spark") values of  $2 \times \text{c.o.v.}$  of 0.5% rel. apply at relatively high concentrations.

4. and 7. How much sample is required for the analysis?

What about the possible limits of detection? .

Answer: For the former question it is possible to distinguish between

the amount of examined material that is involved in excitation, and the amount of material that can be handled. Of an amount of, for example,  $10^{-8}$  mg examined with "microprobe" it is no longer possible to say that it can be handled, though it does merit this epithet if it is contained in a bigger mass. An amount of 0.2 to 0.5 mg ("micro X-Flu" and "arc" [38]) can already be handled quite easily, but the relative limits of detection here lie considerably higher than the ppm range. With "flame," where the work is always performed with amounts in solution that can be handled, it is difficult to indicate the amount of material by numerical examples, because of uncertainties connected with the concentration of the relevant element in the solution and the equipment used.

In Table 10 a few data have been collected which indicate *by way of orientation* the limits of detection in ppm and  $\mu\text{g}$ , as well as the amount of analytical material required.

8. It is a well known fact that close to the limit of detection a "poor" reproducibility is found. How can this be influenced favorably?

Answer: With chemical methods of preconcentration left aside, the reproducibility of "X-Flu" can be improved if the number of pulses is increased and, particularly with the light elements, if pulse discrimina-

TABLE 10. Limits of detection of various methods of analysis.

Method	Mean limit of detection		Required amount for carrying out analyses
	ppm	$\mu\text{g}$	
"Arc"	7(0.01-30)	0.15(0.0002-0.6)	20 mg (duplicate analysis)
"Arc s.p.s."	0.3(0.01-1)	0.1(0.003-0.3)	300 mg (analysis in 6-fold)
"X-Flu"	8(2-15)	0.4(0.1-0.8)	50 mg (single analysis)
"Micro X-Flu"	2000(200-50000)	6(0.6-150)	3 mg (analysis in 6-fold)

#### Remarks.

a. Values in parentheses indicate the lower and upper limits, depending on the element.

b. "Arc" and "arc s.p.s." figures, taken from Table 9, refer to a *general method of analysis*.

c. "X-Flu" figures [25] refer to a number of impurities present in steel.

d. "Micro X-Flu" figures, taken from figure 2, refer, though with more restrictions than those of "arc", to a *general method of analysis*.

tion is applied; that of "arc" and of "spark" can be improved if the number of exposures is increased and if measures are taken to reduce the background (controlled gas atmosphere, selective evaporation, and the like); that of "flame" can be improved by the selection of a somewhat higher flame temperature (increase of signal), in which case attention should be paid particularly to the elimination of molecular bands (low noise). But here it should be remembered that the intensities of bands of  $N_2$ , CN, and NO, excited in the column of an arc at 6000 °K, are decreased strongly if the temperature is brought down to about 5500 °K, whilst molecular bands of OH and  $O_2$  show lower excitation energies; they are excited at a temperature of 4000 °K [25]. These data are mentioned here in connection with the choice of the vaporizing gas to be used.

### VI. Future Prospects (General)

Apart from the remarks made at the end of each section, "flame" (emission and absorption) and "arc" can be considered to be approaching each other ever more closely, with the desire for a homogeneous, adjustable temperature and a great energy density of the measuring volume playing an important role. The supply of the analytical material need not take place exclusively via an aqueous solution but can perhaps also take place in powder form (the work described in [39] is pointing in this direction). Furthermore the aim in view should be a *general*, uncomplicated method of analysis, which, as proved by experience (our *K* and *Q* methods) can quickly solve most problems.

### VII. Acknowledgments

In his esteemed letter of invitation of 22 March 1966, Dr. W. Wayne Meinke wrote to me, among other things: "I am convinced that you will feel a definite sense of satisfaction in broadening your own horizons." It is just in this respect that I am so grateful to him, particularly since in our laboratory in Eindhoven facilities are available to perform trace analyses with "flame," "arc," and "spark" (automatic and non-automatic), "X-Flu" and mass spectrometry, as well as with the help of modern wet methods of chemical analysis (including micro gas analysis and gas chromatography), electron microprobe and radioactivation analysis and where "a rather parochial point of view," to quote Dr. Meinke, must always be overcome in order to find the best answer to the required analysis.

I am very grateful to Mr. A. Witmer, Dr. C. van de Stolpe, Dr. H. Vink, Mr. H. Wallace, and Dr. M. Margoshes for the many discussions I have had with them, and to Dr. M. Klerk for data given to me on electron microprobe analysis, Mr. F. de Boer for his careful measurements carried out in the field of flame photometry, and Dr. A. Bril for the determination of the sensitivity of the photoelectric cell of the flame photometer.

## VIII. References

It should be noted that C.S.I. is the abbreviation of Colloquium Spectroscopicum Internationale.

- [1] Margoshes, M., Proceedings of the XII C.S.I. (Exeter 1965) Hilger & Watts, London (1966) pp. 26-42.
- [2] Alimarin, J. P., Pure Appl. Chem. **7**, 455-472 (1963).
- [3] Oldfield, J. H., and Mack, E. L., Analyst **87**, 778-785 (1962).
- [4] Moore, Ch. E., An Ultraviolet Multiplet Table. NBS Circular 488.
- [5] Boumans, P. W. J. M., Theory of Spectrochemical Excitation. Hilger & Watts, London (1966).
- [6] Kalf, P. J., Hollander, T., and Alkemade, C. T. J., J. Chem. Phys. **43**, 2299-2307 (1965).
- [7] Kubaschewski, O., and Evans, E. L. L., Metallurgical Thermochemistry. Pergamon Press, London (1965).
- [8] Geiseler, G., Z. Physik. Chem. **202**, 424-437 (1954).
- [9] Mavrodineanu, R., and Boiteux, H., Flame Spectroscopy. Wiley, New York (1965), p. 207.
- [10] Walsh, A., Proceedings of the XII C.S.I. (Exeter 1965) Hilger & Watts, London (1966), pp. 43-65.
- [11] Pinta, M., Recherche et dosage des elements traces. Dunod, Paris (1962), Chapter XIII
- [12] Dean, J. A., and Stubblefield, C. B., Anal. Chem. **33**, 382-386 (1964).
- [13] Addink, N. W. H., c.s., Appl. Spectry. **10**, 128-137 (1956).
- [14] Thiel, B., and Krempl, H., Z. Angew. Phys. **14**, 341-347 (1962).
- [15] Addink, N. W. H., J. Iron Steel Inst. (London) **194**, 199-211 (1960).
- [16] Addink, N. W. H., Spectrochim. Acta **15**, 349-359 (1959).
- [17] Allen, C. W., Astrophysical Quantities. The Athlone Press. London (1955), pp. 63-78.
- [18] Corliss, C. H., and Bozman, W. R., Experimental Transition Probabilities for Spectral Lines of Seventy Elements. NBS Monograph 53 (1962).
- [19] Eichhoff, H. J., and Addink, N. W. H., Proceedings of the VIII C.S.I. (Lucerne 1959) Verlag, H. R. Sauerlander & Co., Aarau, Switzerland (1960), pp. 89-92.
- [20] Kroonen, J., and Vader, D., Line Interference in Emission Spectrographic Analysis. Elsevier, Amsterdam (1963).
- [21] Addink, N. W. H., Proceedings of the C.S.I. VI (Amsterdam 1956) Spectrochim. Acta **11**, 168-178 (1957).
- [22] Addink, N. W. H., and Witmer, A. W., Proceedings of the C.S.I. IX (Lyon 1961), Groupement pour l'Avancement des Methodes Spectrographiques, Paris (1962), Vol. 2, pp. 340-354.
- [23] Kaiser, H., and Specker, H., Z. Anal. Chem. **149**, 46-66 (1956).
- [24] Webb, D. A., Nature **139**, 258 (1937).
- [25] Addink, N. W. H., Limitations of Detection in Spectrochemical Analysis. Hilger & Watts, London (1964), pp. 96-118.
- [26] Addink, N. W. H., Werner, H. W., and Witmer, A. W., Proceedings of the XII C.S.I. (Exeter 1965), Hilger & Watts, London (1966), p. 653.
- [27] Liebhafsky, H. A., et al., X-Ray Absorption and Emission in Analytical Chemistry. Wiley, New York (1960), p. 154.
- [28] Addink, N. W. H., Kraay, H., and Witmer, A. W., Proceedings of the C.S.I. IX (Lyon 1961), Groupement pour l'Avancement des Methodes Spectrographiques, Paris (1962), Vol. 3, pp. 368-384.
- [29] Groot, T., et al., Nature, in press.
- [30] Witmer, A. W., and Addink, N. W. H., Science and Industry **12**, 1-6 (1965).
- [31] Eichhoff, H. J., and Bech, K., Publ. GAMS 1962, pp. 339-354.

- [32] See [25], p. 100.
- [33] Klerk, M., and Roeder, E., *Chemie-Ingenieur-Technik*, in press.
- [34] v. Ardenne, M., *Tabellen der Elektronenphysik, Ionenphysik und Übermikroskopie*, VEB Verlag Berlin (1956), Vol. 1, pp. 151-152.
- [35] Mack, M., and Spielberg, N., *Spectrochim. Acta* **12**, 169-178 (1958).
- [36] de Vries, J. L., *Proceedings of the XII C.S.I. (Exeter 1965)*, Hilger & Watts, London (1966), pp. 81-98.
- [37] Pomey, G., *Proceedings of the C.S.I. IX (Lyon 1961)*, Groupement pour l'Avancement des Methodes Spectrographiques, Paris (1962), Vol. 1, pp. 460-462.
- [38] Addink, N. W. H., *Mikrochim. Acta* (1956), pp. 299-303.
- [39] Czakow, J., *Proceedings of the C.S.I. VIII (Lucerne 1959)*, Verlag H. R. Sauerlander & Co., Aarau, Switzerland (1960), pp. 114-118.

# OPTICAL AND X-RAY SPECTROSCOPY

## Contributed Papers and Discussion

H. KAISER

*Institut für Spektrochemie und Angewandte Spektroskopie  
Dortmund, Germany*

### 1. Introduction

There were 15 papers submitted for this session, covering a large variety of subjects. Most of these dealt with special analytical problems of microanalysis or trace determination, giving many details of working procedures, suggestions for technical improvements, and numbers for precision, limits of detection, and sometimes accuracy of calibration. Four papers dealt with questions of primary importance. These were by Adams and North, Fassel and Golightly, Hobbs and Rees, and Winefordner. The first one contained general considerations about terminology and the other three were concerned with the theory and practice of the limit of detection.

But the question of how the limit of detection of an analytical procedure should be defined and what limits of detection actually had been achieved occurred in nearly all of the papers, and so the chairman of the session and the rapporteur decided that these principal questions should have greater attention than details of analytical procedures during the rather short period of the discussion session, itself. This report then tries to summarize remarks and considerations which were brought forward during the discussion session, and also many points which were raised in connection with other topics of the symposium and in the many small group discussions which took place.

### II. Contributed Papers

To give a more complete survey of the contributed papers, it may be said that three papers dealt with new methods, which seemed to be promising, but for which the field of analytical problems where they may be used has not yet been thoroughly explored. There were two papers dealing with atomic fluorescence. One, by Winefordner, considers atomic fluorescence when a flame is used to evaporate the sample and to produce the neutral atoms which may absorb and reemit radiant energy brought to them at the wavelengths of the resonance lines. Limits of detection are reported for different elements and shown

to be in the range of 0.0001 ppm to several ppm. The other paper, by Svoboda describes the use of a heated graphite crucible to evaporate the sample into an argon atmosphere.

The paper by Walters et al., described a method which may be used in the analysis of rare earths to determine traces of other rare earths by the characteristic fluorescence line spectra of these elements, the fluorescence being excited by x-rays. The effects of the matrix composition and of particle size distribution on the measured intensities are discussed as are calibration problems. As an example, detection limits in  $Y_2O_3$  are reported for seven other rare earth elements and shown to lie in the range from 0.02 to 10 ppm.

Two papers dealt with problems of local microanalysis. One, by Chaplenko and Landon, revives the nearly forgotten technique of a microspark; the other, by Cunningham and Ryan, uses a laser microprobe to evaporate the material and to excite the radiation with an auxiliary electric discharge. With both methods the area of the sample which is analyzed is of the same order of magnitude (several  $10^3$ 's of microns diameter) and the amount of sample may be several nanograms. Since these two very different methods were used to solve different analytical problems no immediate comparison of their relative merits is possible from these papers.

Several papers, particularly those by Adams et al., Adler, Campbell et al., and Elfers, consider combination methods for trace determination, different procedures of preconcentration and separation being discussed; in particular, ion exchange chromatography in the paper by Elfers on cesium determination.  $^{137}Cs$  is used as a tracer to control the preconcentration and separation reactions.

In nearly all of the contributed papers, as in the invited lecture given by Dr. Addink, the same principal problems raised their dragon's head and revealed that even such well established methods as atomic emission spectroscopy and x-ray fluorescence are not thoroughbred if the field of their normal applications has to be extended to microanalysis and trace determination. There actually is much hidden embarrassment about basic concepts and about the possibility of comparing the different methods not just arbitrarily but in a meaningful and universal way.

Many of these open problems are arranged around the central question of the limit of detection. One such problem is calibrating the analysis function for the determination of traces. It is not only the preparation of standards but also the extrapolation of the analysis function from the range of decent high concentrations down to the dark region of low concentrations. This brings up the most important task—how to measure correctly the background intensity under the analysis line and how to make a background correction in practical, routine analytical work.

In the discussion, E. B. Owens, MIT Lincoln Laboratory, pointed out that the poor limits of detection which were arrived at by direct

reading spectrometers in the analysis of metals were mainly due to the fact that no individual background corrections are made and that, in many cases, no provisions to make such measurements and corrections may be given. One method to overcome the drawbacks of insufficient instrumentation—in this case by scanning the spectrum and by the use of signal discrimination—was mentioned but did not receive much attention and further discussion. The question remains open whether this technique may be only a substitute for continuous observation of background and of line intensity by means of a high resolving spectrometer or if there are inherent advantages beyond that possibility.

Closely related to the problem of calibration is that of reliable standards of known composition and another one, how to produce samples which may be regarded as representative for a bulk sample. These questions are raised in different ways in papers by Adams et al., Adler, Rigdon, and Walters et al. Influences of matrix composition on the analytical functions and interelement effects are considered in the papers by Adams et al., Campbell et al., Chaplenko and Landon, and Walters et al.

There are two other problems which lead immediately to the central problem of this report, which is the limit of detection. One is the control of reagents for impurities, which may actually determine the practical limit of detection which one may get, in spite of the fact that the very core of the analytical procedure, itself, may yield much lower limits of detection if only pure substances would be available. The second is the choice of the best optical instrumentation for a distinct analytical problem.

Going through the contributed papers, the invited papers, and the topics of this symposium, the reader will detect considerable uncertainty about this point. Some rather fuzzy statements about instrumentation may be found in many of the papers, indicating that the problem, itself, has been realized but no solution could be given. Just one quotation may be useful: "The monochromator must be capable of minimizing spectral interference, whether line or background, without loss of sensitivity." A general approach to how instrumentation could be optimized is offered in the second paper by Winefordner, but so far only the formal mathematical treatment has been given. It is urgently wanted to give not only the approach but concrete solutions for many different spectrochemical procedures.

The present embarrassment is the result of a transient period in the further development of atomic spectrochemistry and in the winning of new fields of applications or of a wider range of concentrations. Many private terminologies and private definitions are abundant, which may not facilitate communication among the workers in different fields. There is a general tendency to hide difficulties in understanding and the lack of knowledge about the complicated procedures occurring in the

light sources behind a protecting wall of words or theoretical considerations without practical consequences. One main and general result of the discussions during the colloquium was to make this intellectual situation obvious and to start efforts of common meditation. The very important theories of modern physics on the production of radiation are highly important. They may offer valuable *guidance to a deeper understanding* of the most complicated processes which are going on in spectrochemical light sources, but they should not be misused to replace a more pragmatic and direct approach to a problem.

### III. Nomenclature

In this situation, agreement on nomenclature and symbols is necessary. In the paper by Adams and North, some general considerations on nomenclature are given, some questions raised, and some proposals made. Adams was given an opportunity to add remarks during the discussion session. The results of the discussion may be summarized as follows: An agreement on nomenclature cannot be gained by public discussions alone or by balloting. A systematic approach can only be made by relatively small and competent committees which have to consider all the proposals and opinions which may have come up in public discussions.

At present, the ASTM Committee E-2 is especially interested in questions of nomenclature and there are committees within the Analytical Division of the International Union of Pure and Applied Chemistry (IUPAC) which are working on such topics. The IUPAC Committee V.4 on "Spectrochemical and Other Optical Methods of Analysis" is preparing a document on nomenclature and symbols and since B. F. Scribner, NBS, V. A. Fassel, Iowa State University, and L. S. Birks, Naval Research Laboratory, are members of this committee there should be a good and constant communication with ASTM Committee E-2.

The general idea about nomenclature seems to be that there are two classes of terms. Those of the first class have a very precise meaning. These terms should preferably be defined by a mathematical equation or by an experimental procedure and not in words. Concepts belonging to this class are "limit of detection" (see below), "sensitivity," "concentration," etc. These terms are by nature connected with numerical values. There is a second class of terms which are used in colloquial scientific language. They don't require a very rigid definition. Their exact meaning will become clear by the context or by some additional explanations as the case may be. Some guidance may be useful to avoid misuse, but too narrow regulations will produce a very clumsy language. Examples for such terms are: "trace," "ultratrace," "major or minor constituent," etc. For instance, if the meaning of "trace" shouldn't be clear from the context, the best thing would be to give the

range of concentrations (e.g., 1 to 10 ppm) and not to rely on any foregoing statement which may long be forgotten.

There is special confusion about the term "sensitivity." This term in analytical chemistry is sometimes used to describe that quality of an analytical procedure which leads to a low limit of detection. However, in most other branches of science and engineering, "sensitivity" is a differential quotient giving the slope of the characteristic curve for the measured quantity. In analytical chemistry this might be the slope of the analytical function relating the measured quantity to concentration values. Therefore, it is advisable to use the word "sensitivity" only in this latter and more general sense. An analytical method which yields a low limit of detection may be said to have a high "power of detection." Such an expression would match well with terms like "resolving power," etc.

#### IV. Limit of Detection

As to the limit of detection, itself, it has become the general opinion that only a statistical definition will hold and will give an objective number for a limit which is *independent of any personal judgment*. The idea is to give a generally applicable criterion when the measured quantity can be detected with a sufficiently high level of confidence among the unavoidable statistical fluctuations which every measuring device will show [1].<sup>1</sup> Only values which fulfill this criterion will be accepted as being real; smaller ones are to be rejected. This idea is probably more than 50 years old. It has been used in spectrochemical analysis for more than 20 years and nowadays it is often referred to as the concept of "signal-to-noise ratio." This terminology was created by electronic engineers and it is certainly a good description of their actual experience, since in electronic communication systems the noise is heard and it is always the question whether the useful signal, for instance the words and phrases in a telephone conversation, can be detected clearly enough among the "noise."

But it must be said, *the use of this term "signal to noise ratio" in analytical work should be discouraged*. The term "analytical signal," perhaps, may be a good one and could be retained but it is certainly hard to call the possible fluctuations in the contamination in any reagent a "noise." The use of "signal to noise ratio" may be misleading, since in many analytical processes electronic devices are used for the amplification and readout systems. But it would be a bad mistake to think of their electronic noise as the decisive fluctuation which determines the limit of detection of an analytical procedure. This may be so in some cases, but in chemical analysis there may be a level of statistical disturbances an order of magnitude above the electronic noise. This has

---

<sup>1</sup> Figures in brackets indicate the literature references at the end of this paper.

been pointed out in many of the contributed papers, for instance, by Campbell et al., and by Winefordner. To illustrate this point further, some of the causes of statistical disturbances are listed below:

1. Counting of single events, Poisson distribution ( $\sigma = \sqrt{N}$ ) (photons, atoms, electrons . . .).
2. Receiver (shot noise, dark current, thermal noise of amplifier, grain of photographic plate).
3. Light source (background, bands, line intensity, temperature, volatilization, chemical processes).
4. Inhomogeneity of sample.
5. Contamination of sample and reagents.
6. Measuring process, errors and deviations (e.g., balance, recorder, photometer, etc.).

A *general definition* of the limit of detection which is applicable to any analytical procedure is given by the following triplet of equations:

$$\underline{x} = \bar{x}_{bl} + k \cdot \sigma_{bl}^* \quad (1a)$$

$$\underline{c} = f(\underline{x}) \quad (1b)$$

$$\underline{g} = \underline{c} \cdot M \quad (1c)$$

In equation (1a) "x" is any measured quantity. For instance, voltage, transmittance or a weight. The bar underneath indicates the limit. The suffix "bl" points to "blank" analysis. Therefore,  $\bar{x}_{bl}$  is the average value measured in blank analysis.  $\sigma_{bl}^*$  denotes the standard deviation of the blank measurements and the star is a "caution mark" to remind one of the necessity to investigate very carefully to what extent the standard deviation computed from conventional type blank analysis actually represents this quantity for the whole procedure in question. For instance, in spectrochemical analysis when blank values are taken for the background alone, in the actual analysis two intensity measurements of this type have to be combined to correct for background and, therefore, the essential standard deviation

$$\sigma_{bl}^* = \sqrt{2} \sigma_U$$

where  $\sigma_U$  is the standard deviation for intensity measurements at background level.

It should be clearly seen that Formula (1a) gives a pragmatic approach. For any given analytical procedure it is possible to determine experimentally the value of " $\sigma_{bl}^*$ " if the procedure is critically considered.

It is not necessary to develop a theory of this standard deviation. Sometimes, however, in particular for electronic noise, a theory can be developed and may be used but the determination of the essential standard deviation  $\sigma_{bl}^*$  is by no means dependent on a theory.

Equation (1b) is used to symbolize the analytical function correlating the measured quantity "x" and the concentration "c"; hence,  $\underline{c}$  symbolizes the concentration value at this limit of detection, determined by  $\underline{x}$ . Equation (1c) is added for the case where the limit of detection is required in absolute quantities  $\underline{g}$ , for instance in grams, micrograms, etc.,  $M$  (for magnitude) is a symbol for the quantity of the sample to be expressed in the same units as for  $\underline{g}$ . It is useful to realize that the splitting of the problem by the two equations, (1a) and (1b), avoids the appearance of ghostly negative concentrations in the computation of the limit of detection. Actually, the measured quantity "x" is the analytical signal which has to be detected among the statistical fluctuations and by no means the concentration,  $c$ , itself.

There is still some disagreement about the value of the factor "k" which gives the level of statistical confidence. This, it may be hoped, can be settled by convention. At present some authors, for instance Winefordner, Fassel, and Addink, prefer  $k=2$  while others, for instance Kaiser and Specker, prefer  $k=3$ . During the discussion it was mentioned that the theoretical high limit of confidence given by the factor of 3 may not be justified but in many practical cases only a limited number of the tedious blank analyses may be performed and for this reason some additional statistical insurance may be packed into the factor "k". However, the general opinion seems to be that the factor  $k=1$  gives too low a level of confidence to be significant at all. Therefore, as long as no international convention has been arrived at, the value of "k" which has been used in the calculations should be given.

The splitting up of the problem as indicated by (1a) and (1b) is a most powerful means to optimize the parameters of an analytical procedure. This may be pointed out by the diagram given in Figure 1. This diagram is very schematic. The abscissa corresponds to the measured quantity,  $x$ , the ordinate to the concentration,  $c$ , the straight line symbolizes the analytical function, and it is assumed that this analytical function has been determined by standard samples reading I, II, and III in a range of higher concentrations. The double arrow indicates the process of critical extrapolation to lower concentrations. So this part of the diagram corresponds to Equation (1b). By Equation (1a) the lower limit of "x" is given and the region  $x < \underline{x}$  where the signal can no longer be detected is the lined section in the diagram. The point where the analytical function enters this forbidden zone corresponds to the concentration value,  $\underline{c}$ , at the limit of detection.

Now it can be clearly seen that this value depends on two things: the position of the analytical function in the diagram and the position of

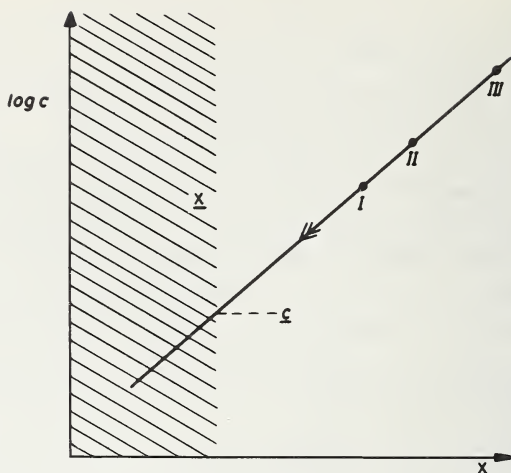


FIGURE 1. Diagram illustrating relation between analytical function, signal, level of statistical fluctuations (noise?), and the limit of detection.

the border of the forbidden zone. These two may change quite independently of each other. The parameters of the light source and of the optical instruments may act in quite different ways on these two decisive positions. The reason why many theoretical investigations about the limit of detection in spectrochemical emission analysis have become so complicated and so few successful is that the position of the analytical function and that of the forbidden zone have not been treated separately. This point will be taken up later in this report.

It must be clearly realized that this rigid statistical definition of the limit of detection by its nature can only be used for definite "complete analytical methods" and not for general "analytical principles." For instance, nobody can give general limits of detection for polarographic analysis, for emission spectroscopic analysis, or for atomic absorption analysis. The concept of a complete analytical method comprises the statement of the analytical problem. The nature of the sample and the elements to be determined must be given. Furthermore, the analytical procedure must be described in all detail together with the instruments used. Finally, the evaluation of the measurements must be prescribed. For instance, whether the outcome of single measurements are used to give the analytical result or whether the average of several measurements is taken will cause a considerable change in the limit of detection.

Many misunderstandings have occurred because the strict correlation between numerical values for the limits of detection and the distinct "complete method of analysis" has not been seen. This was made clear during the symposium by the discussion of the paper by Hobbs and Rees which has the provocative title, "Confident Analysis Above and *Below* the Limit of Spectrographic Detection." The obvious con-

tradition occurs since the "limit of detection" in the title refers to a method when only a single analysis is considered; the claim, however, to detect the element in question below this limit refers to another type of analysis where many repeated determinations on the same sample are brought together by a special evaluation procedure.

Hobbs and Rees give a rather rough but most useful procedure to get some kind of an average of many repeated runs just by counting the number of "detected" and "not detected" analyses (yes or no). This can be particularly useful at very low concentrations when only "purity" of the sample has to be judged. It might be helpful to translate the notion used by the authors into the more conventional notion so that the correlation of these ideas might become more obvious.

A good example where by averaging the results of 10 analyses the limit of detection is reduced by a factor of  $\sqrt{10}$ , is given by Figure 2 for the case of the photometric determination of iron in a solution with o-phenanthroline. The solution contained 0.02 mg/ml. In the left half of the diagram the results of single measurements have been plotted. The blanks (open circles) and the results from the sample (crosses) are partly mixed up. The statistical limit of detection was computed to be 0.04 mg/ml. Therefore, a concentration of 0.02 mg/ml cannot safely be detected. The right half gives the average values for 10 single measurements, and now the values for all measured samples are clearly distinguished from the values for the blanks. This illustrates that this change in evaluation, averaging 10 single measurements, *constitutes a new analytical method* and *therefore* a lower limit of detection is arrived at.

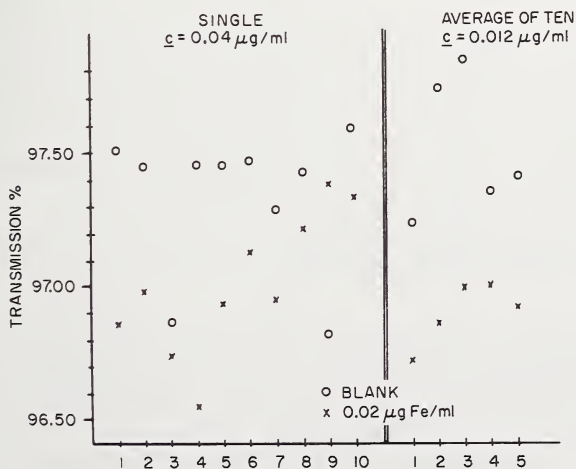


Figure 2. Improvement of detection limit by replicate measurements, for the determination of iron with o-phenanthroline.

Figure 3 demonstrates, for the photometric determination of nitrate, that the "sensitivity" of an analytical method and the "limit of detection" may be quite independent quantities. It is well known that the "sensitivity" of a photometric method is proportional to the length of the absorption cell. Thus, the sensitivity for the analysis in the right half of the diagram was 5 times as high as for that in the left part. Also, the average level of absorbance for the blanks was different in both cases but the statistically calculated limit of detection practically did not change. The diagram shows that the statistical fluctuations grew with the length of the absorption cell [7].

This diagram also demonstrates that the statistical fluctuations which are described by the essential standard deviation,  $\sigma_{bl}^*$ , by no means should be confused with the average value of the blank measurements. For instance, in emission spectrochemical analysis a constant background can always be corrected for. What prevents the analytical signal (the analysis line) from being detected is not the size of the background itself, but the unpredictable fluctuations around the average level of the background. Therefore, the statement which is found in some papers in the literature that the limit of detection for spectrochemical emission analysis be given by the ratio of line intensity over background intensity is decisively wrong. The cause for this mistake may be found in the uncritical acceptance of the concept of signal to noise. "Noise" is not simply "background" and — referring to the corresponding

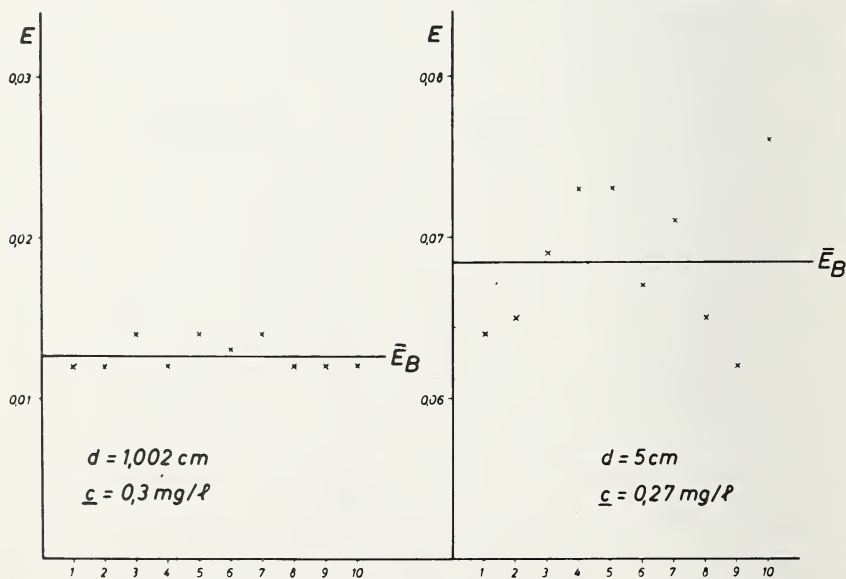


Figure 3. Effect of cell path length on detection limit for the photometric determination of nitrate.

fact in electronics—it must be said that the electronic noise also does not contain the constant dc component.

In connection with this well-defined and widely-accepted concept of the limit of detection there is one problem which only recently has found some attention among analytical chemists. This is the problem of what it means when the search for an element in a sample was in vain and the report about this analysis says “not detected.” It may be surprising that this question must not be answered by a statement that obviously the concentration of this “not detected” element must be lower than the limit of detection. The lower limit of concentration which can be given as a guarantee for the purity of the sample is always higher than the limit of detection for the analytical method. This is so because one must take into account that, in the case of the actual analysis, by some statistical haphazard, the expected analytical signal may be very low.

Further explanation may be helpful. With any homogeneous sample, analyzed by an accurate method in repeated runs, half of the results will lie below the actual concentration and half above: the average will be about right. For a sample having the concentration  $c$ , corresponding to the limit of detection, this will—by definition—have a peculiar consequence: The half of the determinations below the average will have an analytical signal  $< x$ , so that they cannot be recognized among the statistical fluctuations. Therefore, this half will be recorded as “not detected” [3]. This difference is the inevitable consequence of the fact that these concepts are based on statistics; no sophistication can bridge this gap. This will be even worse if the sample is locally inhomogeneous. *Therefore, the limit of guarantee for purity is always higher than the limit of detection.* The former limit is the result of sample and analytical method together, while the limit of detection is a quality of the analytical method alone.

It was said before that the question of how the limit of detection of a distinct analytical method may depend on the experimental parameters is split up in two parts by the symbolic equations (1a) and (1b). The usefulness of the old Roman motto “divide et impera” in this case was demonstrated by an investigation of how the limit of detection of an emission spectrochemical method depends on the slit width and the resolving power of the spectrometer or spectrograph used, all other parts of the procedure, e.g., kind of sample, light source, radiation detector, being kept constant.

It has been known for quite a while that the position of the analytical curve within the field of the diagram, Figure 1, depends on the resolving power of the spectrograph. K. Laqua [2] seems to have first realized that this analytical function becomes independent of the optical parameters of the spectrograph as soon as the resolving power of the instrument becomes much higher than that which is required to show the profile of the analysis line as it is produced by the light source. Now, in the

range of low concentrations the half width of the line profile remains practically constant, as long as no self-absorption or self-reversal is observed. Therefore, this half width  $\Delta\lambda_L$  may be taken as a characteristic property of the light source and the element in question.

A resolving power,  $R_L = \lambda/\Delta\lambda_L$  corresponding to this half width can be defined. It may be called here the "line profile resolving power." Let  $R_0$  be the resolving power of the spectrometer, then  $\hat{R} = R_0/R_L$  can be used as a measure for what the spectrometer can show of the line profile. Now, when the slit width of the spectrometer "s" is measured in units of the "critical slit width," " $s_0$ ", which describes the half width of the diffraction image, hence  $\hat{s} = s/s_0$ , then the calibration function for any emission spectrochemical method in the range of low concentrations can be set up as:

$$c = c_{V\infty} \frac{I_L}{I_U} \frac{\sqrt{1 + \hat{s}^2 + \hat{R}^2}}{\hat{R}} \quad (2)$$

In this equation  $c_{V\infty}$  is a calibration constant which depends only on the light source, the sample and the line of the element.

As can be seen, it is that concentration for which line and background have the same intensity where a spectrometer of infinitely high resolving power is used. The intensity ratio of line to background,  $I_L/I_U$ , is the *actual* value of this quantity as it is measured in a *given* spectrometer. It must be said that the intensity of the line must have been corrected for background. The last term contains all that enters this relationship from the side of the spectrometer. Only the reduced slit width,  $\hat{s}$ , and the reduced resolving power,  $\hat{R}$ , are of importance in this respect.

This equation has been derived elsewhere [4] and also its general validity has been discussed; for the moment it may be accepted without further discussion. Only one assumption may be mentioned to prevent mistakes. For this equation it is presupposed that the spectrometer is completely and correctly illuminated and that the resolving power is not restricted by aberrations, bad adjustment, or by the graininess of the photographic plate. A generalization of this equation considering these influences, too, can easily be made.

The third factor in this equation gives the interrelationship of analytical functions which are measured with different spectrometers or spectrographs; it is shown in the diagram of Figure 4. The variable parameter of the different curves is the reduced slit width. All the curves approach unity at a sufficiently high resolving power. By this function it is possible to translate the calibration constants from one spectrometer to another. Furthermore, by measuring the values  $c_{V\infty}$  with a spectrometer of very large resolving power or by computing them from measurements with smaller instruments using equation (2), it is possible

to get calibration factors characterizing mainly the light source in respect to the special analytical problem. These constants are truly universal and they, therefore, should be given in publications, not the ones which are dependent on the instrumentation which was more or less accidentally at hand.

The curves of Figure 4 also show how the limits of detection depend on the optical parameters, presupposing that the essential standard deviation  $\sigma_{bl}^*$  is constant and does not depend on the optical parameters. Then it can be seen that the lowest limit of detection is arrived at with a spectral apparatus having a resolving power much higher than that characterizing the width of the line. But, of course, this is only one side of the problem, for the optical parameters may have considerable influence on the value of  $\sigma_{bl}^*$ . In a complete theory, allowing for optimization of the method, these influences must be investigated for the different radiation detectors. For photographic intensity meas-

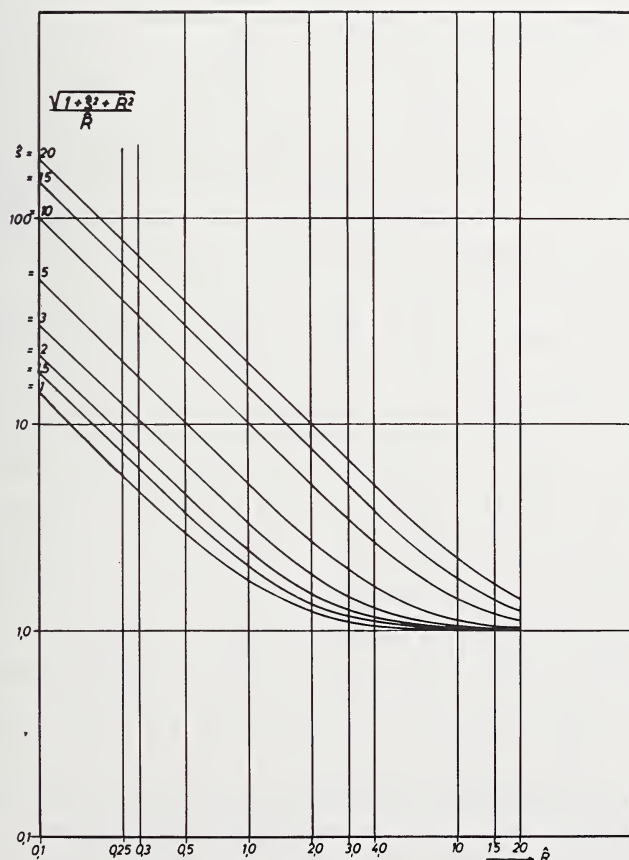


Figure 4. Dependence of the analytical function (and, for  $\sigma^* = \text{const.}$  limits of detection) on the reduced resolving power,  $R$ , and the reduced slit width,  $s$ .

urements, it can be shown that a further decrease of the limit of detection is possible by using a spectrograph not only of higher resolving power but also of high linear dispersion, since the image of the line then covers a greater area on the plate, thus reducing the standard deviation caused by the graininess of the emulsion.

Yet, there is a remarkable difference whether the quantity of the sample consumed in such an analysis is restricted or not. If it is restricted sometimes the blackening of the photographic plate which is necessary to give high precision in photometry may not be arrived at ( $\geq 0.2$ ). Then it may be better to use a smaller instrument, which may yield higher blackening.

Most of the commercial large grating spectrographs are not large enough in resolving power and/or linear dispersion to yield the lowest possible detection limits. What can be done with a spectrograph having a resolving power of more than one million is shown in Table 1 for different elements in a dc graphite arc. The amount of sample actually consumed in this analysis was so chosen that a blackening of 0.2 for the background was produced. These values may be compared with those given in the paper of Dr. Addink for a more conventional spectrograph. (These tables were first shown by K. Laqua at the Conference on Chemical Analysis at Lindau, April 1966 [5].) It may be mentioned here that the line-profile-resolving power in conventional light sources for most elements lies in the range 50 000 to 100 000. Therefore, a spectrograph might well have a resolving power of 500 000 to reduce the limit of detection by optical means.

Such general considerations open the door to gathering data, in particular for the coefficients in analytical functions which are independent of the instrument which was used in the actual measurement. This would allow us to compare more reliably the different light sources and other steps or devices in the analytical procedure. In their paper, Fassel and Golightly have given a very comprehensive collection of data referring to flame emission and flame absorption spectrochemical analysis. These tables allow us to compare the two methods and to decide which one may be the best for a distinct analytical problem. But these values are bound to the present state of the art and the usual instrumentation. The last step is missing. It would be important to have such values which are independent of the instrumentation, characterizing only the very heart of the procedure, so that it may become possible to realize which principal possibilities for further development are given.

During this symposium sometimes the question arose how the different methods for trace determination might be compared as to the limits of detection which have been attained or may be attained. There is no doubt that even for such old techniques as emission spectrochemical analysis considerable progress may be ahead of us. Beyond

TABLE 1. Relative and absolute detection limits in graphite matrix

Element, $\lambda$	Direct-current arc				Spark		
	%	ng	mg <sub>sample</sub>	atm	%	ng	mg <sub>sample</sub>
Ag I 3280	$9.0 \times 10^{-8}$	0.75	837	Air	$1.1 \times 10^{-6}$	41.3	3755
Al II 3962	$1.5 \times 10^{-6}$	25	1630	CO <sub>2</sub>			
As I 2780	$1.8 \times 10^{-4}$	1610	897	CO <sub>2</sub>	$8.3 \times 10^{-6}$	920	11100
B I 2498	$1.0 \times 10^{-6}$	7	659	Air			
Ba II 4554	$1.3 \times 10^{-7}$	2.0	1540	CO <sub>2</sub>			
Be II 3130	$1.2 \times 10^{-7}$	0.13	107	CO <sub>2</sub>	$4.0 \times 10^{-7}$	5.9	1470
Bi I 3068	$2.8 \times 10^{-6}$	13.5	483	Air	$1.4 \times 10^{-5}$	724	5170
Ca II 3934	$1.0 \times 10^{-8}$	0.18	1825	CO <sub>2</sub>			
Cd I 3261	$6.8 \times 10^{-6}$	78	1140	Air	$6.8 \times 10^{-5}$	2690	3960
Ce II 4187	$1.3 \times 10^{-5}$	277	2130	CO <sub>2</sub>			
Co I 3453	$2.6 \times 10^{-6}$	4.9	260	KCl	$1.4 \times 10^{-5}$	137	3960
Cr I 3579	$3.2 \times 10^{-6}$	8.3	260	CO <sub>2</sub>			
Cu I 3247	$5.0 \times 10^{-8}$	0.2	426	Air	$1.7 \times 10^{-6}$	28	1648
Fe I 3720	$3.2 \times 10^{-6}$	117	3650	CO <sub>2</sub>			
Ga I 4172	$1.7 \times 10^{-6}$	37	2160	CO <sub>2</sub>			
Ge I 3039	$2.4 \times 10^{-6}$	16.7	696	Air	$1.8 \times 10^{-5}$	675	3750
Hg I 2537	$1.2 \times 10^{-4}$	1730	1440	CO <sub>2</sub>			
In I 4511	$5.2 \times 10^{-6}$	67	1282	CO <sub>2</sub>			
Li I 6708	$8.3 \times 10^{-6}$	7.6	93	Air			
Mg I 2852	$7.2 \times 10^{-8}$	0.13	221	Air	$4.3 \times 10^{-7}$	56.5	13140
Mn I 2794	$7.9 \times 10^{-7}$	12.4	1568	Air	$2.0 \times 10^{-6}$	218	10900
Mo I 3798	$1.7 \times 10^{-6}$	148	8700	CO <sub>2</sub>			
Na I 5890	$4.9 \times 10^{-6}$	118	2400	CO <sub>2</sub>			
Nb II 3094	$7.9 \times 10^{-6}$	14.2	180	Air	$4.0 \times 10^{-5}$	253	634
Ni I 3414	$1.7 \times 10^{-6}$	11.4	674	KCl	$1.4 \times 10^{-5}$	252	1805
Pb I 4058	$2.9 \times 10^{-6}$	119	4110	CO <sub>2</sub>			
Rb I 4202	$1.1 \times 10^{-4}$	2740	2490	CO <sub>2</sub>			
Sb I 2598	$9.7 \times 10^{-6}$	93.5	963	Air			
Si I 2882	$4.3 \times 10^{-7}$	6.6	1540	Air			
Sn I 2840	$1.5 \times 10^{-6}$	30.4	2025	KCl	$8.3 \times 10^{-6}$	914	1100
Sr II 4078	$5.5 \times 10^{-7}$	5.7	1017	CO <sub>2</sub>			
Ta I 2653	$9.7 \times 10^{-5}$	2730	2820	KCl			
Th II 2837	$1.3 \times 10^{-5}$	115	882	CO <sub>2</sub>			
Ti II 3349	$9.7 \times 10^{-7}$	1.3	136	CO <sub>2</sub>	$1.2 \times 10^{-6}$	40	3330
Tl I 5350	$3.2 \times 10^{-5}$	197	614	CO <sub>2</sub>			
U I 3670	$1.4 \times 10^{-5}$	1130	8080	CO <sub>2</sub>			
V I 3185	$5.0 \times 10^{-7}$	6.4	1280	KCl			
W I 4009	$7.3 \times 10^{-6}$	244	3340	CO <sub>2</sub>			
Zn I 3345	$2.2 \times 10^{-5}$	58	264	CO <sub>2</sub>	$2.2 \times 10^{-4}$	3610	1640
Zr II 3392	$1.3 \times 10^{-6}$	4.6	358	CO <sub>2</sub>			

the question of optical instrumentation lies the still open problem of how the spectrochemical light source can be improved. One point is how to keep the atoms for a long time within the zone where they can be excited and observed. What can be done in this respect using absorption spectrometry may be demonstrated by Figure 5 which was shown at the Exeter Colloquium, 1965, by H. Massmann [6]. This

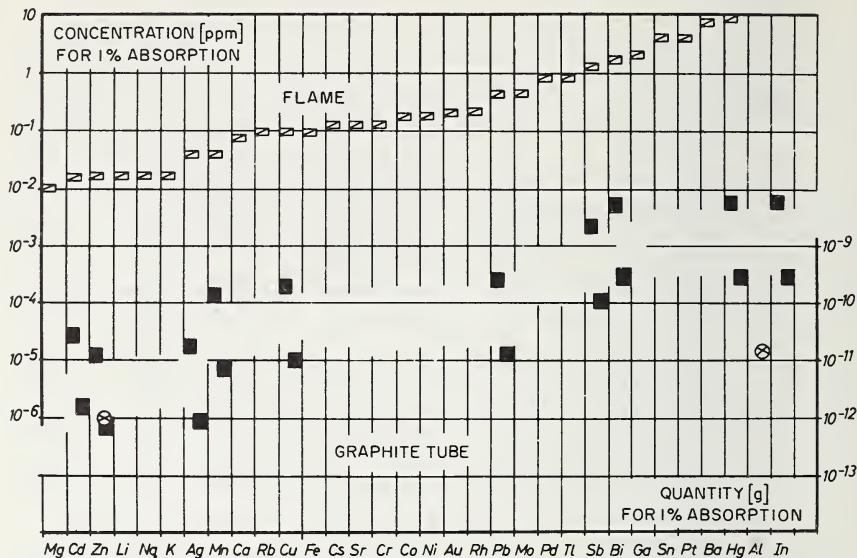


Figure 5. Limits of detection by atomic absorption with the flame and with a graphite tube absorption cell. Length of cell = 5.5 cm.; sample volume = 0.04 ml.; most sensitive resonance lines measured.

diagram gives a comparison of the limits arrived at for 1% absorption using as the absorption cell a flame or a heated graphite tube as first developed by L'vov in which the atoms stay for a long time after volatilization.

During the symposium there was some kind of competition between different possible principles of analysis. For instance, solid state mass spectrometry or neutron activation may yield very low limits of detection, but it must be said that the nearly classical methods of emission spectrochemical analysis are by no means exhausted. There are quite a number of new ideas and experimental possibilities for further development, in particular to provide a high power of detection. But from all the discussions in the symposium it became quite clear that there may be no other principle of analysis which has the same universality and such an enormous information capacity as is incorporated in emission spectrochemical analysis as a principle.

## V. References

- [1] Morrison, G. H., and Skogerboe, R. K., in *Trace Analysis—Physical Methods*, G. H. Morrison, ed., Interscience, New York, 1965, pp. 1–23.
- [2] Laqua, K., Hagenah, W. D., and Waechter, H., presented at XI Colloquium Spectroscopicum Internationale, Belgrade, Sept. 30–Oct. 4, 1963, Paper No. B–8.
- [3] Kaiser, H., *Z. Anal. Chem.* **216**, 80 (1966).
- [4] Laqua, K., Hagenah, W. D., and Waechter, H., *Z. Anal. Chem.*, in press.
- [5] Laqua, K., *Z. Anal. Chem.* **221**, 44 (1966).
- [6] Massmann, H., *Proc. XII Colloquium Spectroscopicum Internationale*, Exeter, Hilger, and Watts, London, 1965, pp. 275–278.
- [7] Specker, H., *Z. Erzbergbau u. Metallhüttenwes.* **17**, 132 (1964).

# EFFECTS OF TRACE IMPURITIES ON X-RAY DIFFRACTION

**J. CHIKAWA**

*Research Associate*

*On leave from NHK Research Laboratories, Tokyo, Japan*

and

**J. B. NEWKIRK**

*B. F. Phillipson, Professor*

*University of Denver, Denver, Colorado*

## I. Introduction

Modern techniques of crystal growth have produced various kinds of large and highly perfect crystals. To observe imperfections in these crystals, numerous x-ray diffraction techniques, collectively called x-ray topographical methods, have been developed [1].<sup>1</sup> Although these experimental methods are capable of giving a picture of the actual extended imperfections present, the effects of point defects on x-ray diffraction have received relatively little attention, probably because the magnitude of their contributions is usually too small to permit accurate measurement. The diffraction effects of homogeneously distributed trace impurities are also expected to be extremely small. However, there are some experimental approaches to the detection of these small effects which appear to be successful, but which depend upon minimizing the contributions from other imperfections through the use of highly perfect crystals.

For understanding diffraction from highly perfect crystals, one must use the so-called dynamical theories of diffraction, in which multiple reflections inside the crystals are taken into account. These theories have been developed for ideally perfect crystals and date from the time immediately after the discovery of x-ray diffraction (Darwin [2], 1914; Ewald [3-5], 1917, 1920, 1924; Bethe [6], 1928; von Laue [7], 1931). In recent years, these theories have been extended to include distorted crystals, and have been of great help in the understanding of the diffraction images of lattice defects. The theories, however, are complex and are still in the process of development both in their fundamental

---

<sup>1</sup> Figures in brackets indicate the literature references at the end of this paper.

aspects and in their applications. The relatively small effects of trace impurities on x-ray diffraction are understandable only by exact theoretical treatments. Such treatments, however, must be based on the dynamical theories and have not yet been formulated.

Inhomogeneous distribution of impurities results in fairly large variations of diffracted intensity and in some systems can readily be observed by x-ray topography. This effect is caused by lattice distortion or lattice parameter variation due to the impurities, and can be explained by the theories which have been developed for understanding extended lattice imperfections such as dislocations. Some observations and explanations for this effect are described in Sec. II. Section III is devoted to diffraction effects due to impurities which are uniformly distributed. These latter effects are observed in the integrated diffracted intensities as deviations from the theoretical intensities for the ideally perfect crystal. The distribution of electrons in crystals is also expected to be changed by the presence of impurities. This change results in very small variations of the crystal structure factor. A precision method for the detection of small changes in the structure factor is discussed in Sec. IV. Finally, in Sec. V, other effects of impurities on material properties which are somewhat distantly related to x-ray diffraction are described by two examples.

## II. X-Ray Diffraction Topography

X-ray diffraction topography is concerned with point-to-point variations in the directions and/or the intensities of x-rays that have been diffracted by crystals. From those variations, certain features of the defect structure of a crystal may be displayed and examined in the form of an unmagnified, photographically recorded image of the crystal specimen.

Methods that mainly measure the local variations of the *direction* of the diffracted beam are useful for the detection of gross misorientations such as grains or subgrains but they are not sensitive to impurity variations. (Methods of Guinier and Tennevin [8], Schulz [9], Weissmann [10]). *Intensity* mapping methods, on the other hand, are chiefly useful for revealing individual defects such as dislocations, stacking faults, and local variations in impurity content.

Since topographic methods can detect only variations of intensity and direction within a broad diffracted beam, a perfectly uniform distribution of impurity gives no detectable effects on topography. Actually, however, impurities in most crystals have non-uniform distribution due to slight variations of the crystal growth conditions or to other imperfections such as dislocations which may or may not have interacted with impurities. The intensity mapping methods give a topographical image of the specimen and are quite sensitive to such non-uniform distribution.

First, the intensity mapping methods for both the Laue case (diffracted beam leaves the crystal by a *different* surface than the one entered by the incident beam) and the Bragg case (diffracted beam leaves the crystal from the *same* surface that was struck by the incident beam) will be reviewed and then the causes for contrast will be discussed. Next in this Section, we shall describe the effects of impurities on other imperfections such as dislocations and imperfections produced from impurities, i.e., precipitates and segregation. Finally, the topographic detection of very small variations of lattice parameters due to impurities will be discussed.

### A. EXPERIMENTAL METHODS

Intensity mapping methods have been developed by several workers independently. Among these have been Newkirk [13], Bonse and Kappler [14], Lang [15-17] and Borrmann, Hartwig and Irmeler [18]. Newkirk used a refinement of the Berg-Barrett technique in which characteristic x-rays are diffracted from the surface of a single crystal specimen. A reflection method using single crystals was also used by Bonse and Kappler, but with a double crystal spectrometer for collimating and monochromatizing the beam. Lang developed a method for using diffracted x-rays that have been transmitted through the specimen. Borrmann et al., employed an anomalous transmission method using relatively thick crystals. These methods will be briefly described here. Other techniques for diffraction topography are known but, on the whole, are variations of those we shall discuss [19-21].

#### 1. Berg-Barrett [11, 12]

In this method the crystal is set to diffract the characteristic radiation from a line focus x-ray source (Fig. 1). By placing the plate close to the crystal, geometric resolutions of  $\sim 1 \mu$  are realized. Across the diffracted beam local variations of the reflecting power occur, due to the imperfections in the crystal. Newkirk showed that single dislocations could be detected by this technique and their Burgers vector can be experimentally determined. Topographs taken by this method are shown in Figure 2.

The corresponding transmission arrangement has been developed by Barth and Hosemann. [19]



Figure 1. The Berg-Barrett arrangement.

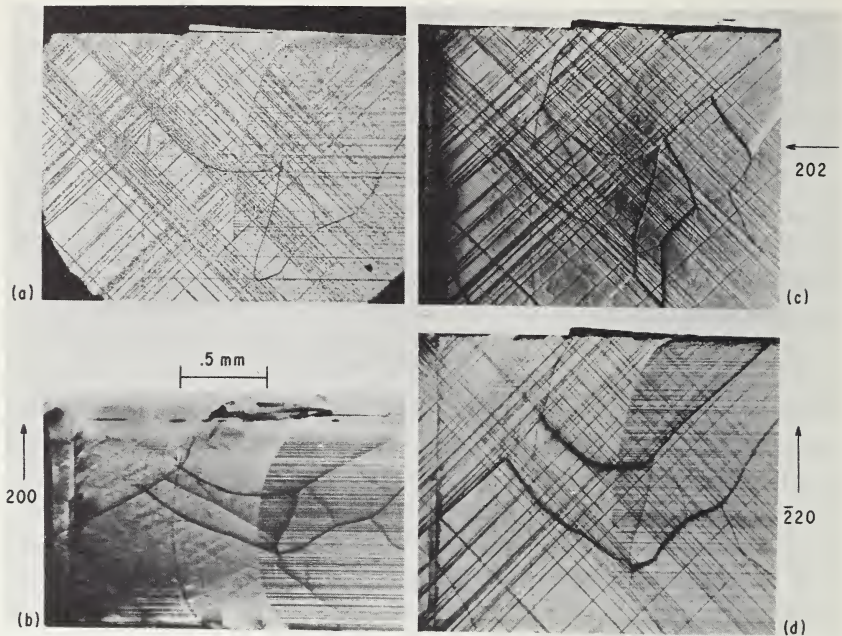


Figure 2. (a) Light micrograph and (b-d) diffraction micrographs single crystal of LiF. Berg-Barrett method (b) 200, (c) 202 and (d) 220 reflections. Some grain boundaries and dislocations (diagonal straight lines) can be seen. From the contrast variation of the dislocations with the various  $hkl$  reflections, the directions of the Burgers vectors can be determined to be  $\langle 110 \rangle$ . In the present paper, all the photographs of diffraction topographs are positives of the x-ray photographic plates, i.e., blacker regions correspond to higher diffracted intensities [13].

## 2. Double Crystal [14]

X-rays from a line focus are reflected from a perfect reference crystal, then from the specimen surface, and finally are recorded on a fine grained film (Fig. 3). In this method the reference crystal and the specimen are usually made of the same kind of material so that exactly the same  $d$ -spacing of the diffracting planes can be used in both crystals. As a result of this arrangement, the shape of the rocking curve is nearly independent of the spectral distribution of the radiation used (dispersion is eliminated) and becomes 10–100 times narrower than any spectral line [22]. This makes the method very suitable for measuring small local tilts in the specimen lattice. When the specimen is slightly mis-set from the exact parallel position, i.e., on one wing of the rocking curve, tilts of only  $\approx 0.1$  sec of arc result in detectable changes of diffracted intensity. This much tilt corresponds to a normal strain of about  $\Delta d/d = 10^{-7}$ , where  $d$  is the interplanar spacing. Strains of this magnitude occur at distances of 50 to 100  $\mu$  from the cores of single dislocations, depending upon the material examined. Kohra [24] and

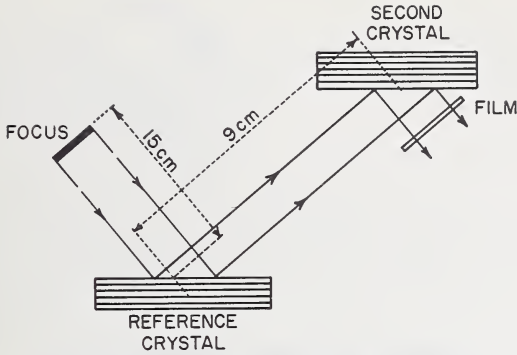


Figure 3. The double-crystal geometry.

Renninger [25] have used a first crystal (of the double crystal arrangement) with greatly different spacing of the diffracting planes than those in the specimen crystal, thereby allowing greater dispersion of the beam than when the  $d$ -spacings are identical. This combination results in appreciable loss of contrast sensitivity. Recently Deslattes [25a] has shown that if only a slightly different  $d$ -spacing is used, the small amount of increased dispersion that results does not seriously reduce the contrast sensitivity of the method. His results have made it unnecessary to find two identical crystals when using the double crystal method. The double crystal arrangement may also be used with the specimen set for transmission [23].

### 3. Scanning Transmission [16-17]

In this method, a ribbon x-ray beam is collimated to such a small angular divergence that only one characteristic wavelength is diffracted by the single crystal specimen (Fig. 4). A stationary opaque screen containing a slit allows only the diffracted beam to reach the photographic plate. A diffraction photograph, made with the diffracted beam passing through a narrow region of the specimen as shown is called a "section topograph." On the other hand, a large area/volume of the crystal can be surveyed by scanning both the crystal and photographic plate in synchronism past the incident beam. In a transmission method developed by Barth and Hosemann [19] a line x-ray source is used which achieves much the same result as the Lang method, viz, a horizontally extended field of view in the image. The drawback of Lang's more complicated traverse apparatus, however, is compensated by the lower background associated with the Lang technique, less trouble with simultaneous reflections (because a strongly collimated beam is used), and a higher resolution, since the photographic plate may be placed closer to the specimen.

Many different types of lattice defects have been observed by the Lang technique. An example is the topograph in Figure 5(a) showing dis-

## TRACE CHARACTERIZATION

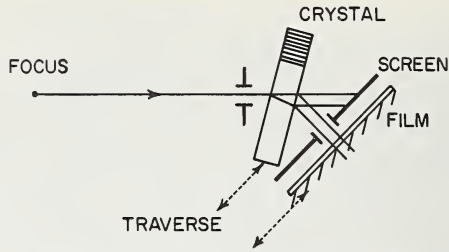


Figure 4. The Lang scanning method.

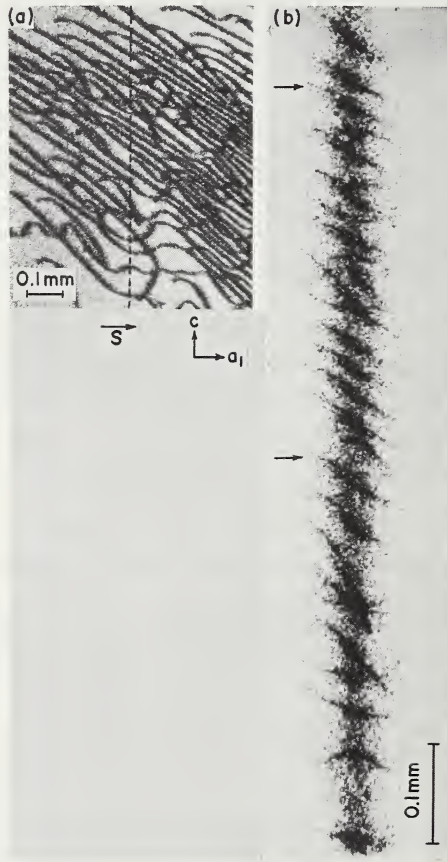


Figure 5. Diffraction topographs of dislocations with  $\frac{1}{3} \bar{2}110$  Burgers vectors in a CdS platelet. (a) Scanning transmission method, (b) Section topograph by a divergent beam from a point focus. The topograph was taken in such a position that the axis of the beam satisfied the Bragg condition on the dotted line drawn in (a). In (b), each dislocation image consists of two lines. From this contrast the signs of the Burgers vectors can be determined. Crystal thickness:  $70\mu$ ,  $\mu_{01} = 0.86$ ,  $MoK\alpha_1$ , 2110 reflection.

locations in CdS. Such topographs are called "traverse topographs" or "Lang topographs." Although the traverse topographs are convenient for surveying large areas, section topographs sometimes are more informative as will be described later.

#### 4. Anomalous Transmission [18]

Inside a perfect crystal, the incident and diffracted waves are dynamically coupled. At the Bragg angle  $\theta_B$ , their interaction produces a standing wave pattern fitting onto the set of diffracting planes. Depending on the positions of the antinodes of this standing wave, the energy transport of the wave field occurs with anomalously high (antinodes coincident with planes) or anomalously low (antinodes between the planes, Borrmann effect) absorption. (See Fig. 6.) Therefore, a perfect crystal set at the precise Bragg angle is capable of transmitting interfering x-rays at crystal thicknesses which would absorb almost all the energy of a non-interfering x-ray beam. It is apparent from this argument that any source of imperfection which moves atoms away from the geometric planes reduces the transmitted intensity. An example of this effect is the intensity decrease due to thermal vibrations of the atoms [26]. Borrmann et al. [18], using this principle to examine relatively thick crystals, observed dislocations as lines of low intensity on a gray background (Fig. 7).

#### B. CAUSES OF CONTRAST [12]

It has been mentioned that when the Bragg condition exists in a perfect crystal the primary wave  $K_0$  and the diffracted wave  $K_h$  form the entity of the x-ray wavefield inside the crystal [27]. Depending on the devia-

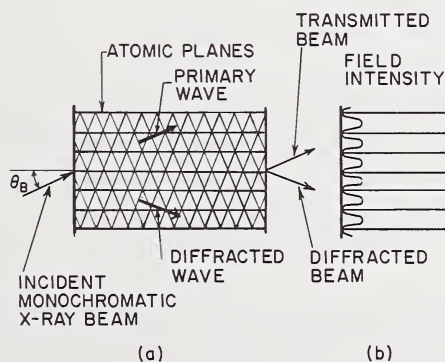


Figure 6. X-ray wave paths inside a crystal. (a) Interaction of two waves in the primary and diffracted beam directions when the Bragg condition is satisfied. (b) The distribution of intensity as a function of position between the atomic planes resulting from the superposition of the two waves in (a). The phases have been chosen to produce nodes at the lattice planes.

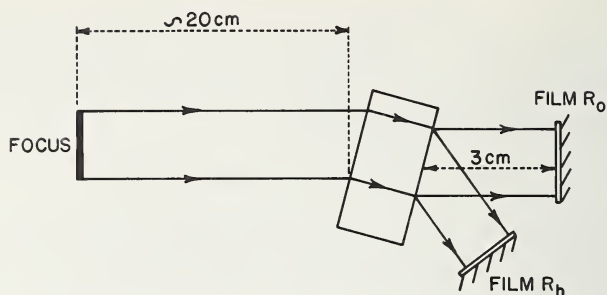


Figure 7. The Borrmann arrangement for anomalous transmission topography.

tion of the incident beam from the Bragg condition, the direction of energy flow of the dynamic wave field varies between the incident and diffracted directions [28, 29]. Since the angle between the incident and diffracted beams is relatively large, variations in the direction of the energy flow due to lattice distortions, as well as variations in local intensity, contribute to the image contrast. According to the kind of distortions that are involved, one can consider the following three causes of contrast.

### 1. Homogeneous Dilator and Tilt Contrast

If the energy flow of the x-ray wave field produced in each part of a crystal does not encounter any appreciable variations in  $d_{hkl}$  or tilt of the lattice, one can treat the contrast by regarding each part of the crystal as a perfect crystal. The cause for the contrast is that each part may simply be more or less mis-set from the diffraction peak given by the Bragg equation  $\lambda = 2d \sin \theta_B$ . The mis-setting can be due to either a change of orientation  $\theta_B$  or of  $d_{hkl}$ , or of both simultaneously. How large a mis-setting has to be before it causes a detectable intensity change depends on the "precision" of the diffraction condition, i.e., the width of the rocking curve (double crystal arrangement) or of the  $\lambda$ -spread (Berg-Barrett, etc.). In any case, the contrast should be proportional to

$$\frac{1}{W} \left[ \left( \frac{\Delta d}{d} \tan \theta_B \right) \pm \Delta \theta \right],$$

( $W$  = width of rocking curve or  $\lambda$ -spread respectively). This is the most straightforward cause of contrast in the double crystal method, where the image is formed by diffraction from the thin surface region. Owing to the extreme narrowness of the double crystal rocking curve and the steepness of its slope, this mis-setting is very sensitive in the double crystal technique. Notice that the sign of the contrast depends on the sign of the deformation as well as the direction of the mis-setting [30, 31].

## 2. Direct Image

This image is due to strongly distorted regions. The beam deviated from the Bragg condition for perfect regions of the crystal enters the distorted region, passing through the perfect region. Then, in the distorted region, if the beam satisfies the Bragg condition it is diffracted. The diffracted beam then passes through the perfect region of the crystal between the distorted region and the exit surface of crystal. If the incident beam has a far larger divergency than the angular width of the rocking curve, the diffracted beam from the distorted region superimposes upon the diffracted beam from the perfect region. Therefore, the images are always observed as intensity enhancements. If the distorted region has a mosaic structure, the intensity enhancement is expected to be proportional to the total volume that is distorted.

As can be seen from the above argument, the signs of the deformation can be determined by contrast variation with the sign of the deviation of the beam from the Bragg condition [32–35]. Figure (5b) is a section topograph which was taken with the crystal in such a position that the Bragg condition was satisfied on the dotted line drawn in (5a). In (b) the dislocation images can be seen crossing the vertical black band. The Bragg condition was satisfied exactly on the center of the black band, and, since the incident beam diverged from a point focus, on the right side of the center  $\theta < \theta_B$  and on the left side  $\theta > \theta_B$ , where  $\theta$  is the actual glancing angle of incident beam on the reflecting plane and  $\theta_B$  is the Bragg angle. Each dislocation image in (5b) consists of two lines which are considered to be located on opposite sides of the dislocation core. Therefore, the two-line images show that almost all the dislocations have screw components of the right-handed screw type.

## 3. Dynamical Images

We shall now consider weakly strained regions which still behave locally like perfect crystals, although, taken over longer distances, a continuous change of orientation and spacing of reflecting planes occurs. The wave field can adapt itself to these changes by a continuous variation of the direction of its energy flow and correspondingly of the ratio  $I_h/I_0$  of the intensities of its components  $K_h$  and  $K_0$  [36] in the transmitted and diffracted beams respectively.

In transmission methods, both the bending of the energy flow and the shift of energy between  $K_0$  and  $K_h$  are responsible for considerable contrast effects in the  $K_0$  and  $K_h$  waves when they leave the crystal at its exit surface [37–44]. Moreover, the Borrmann contrast may also be counted in this category [43], since it is due to the breaking up or at least the continuous modification of wave field beams with anomalously low absorption into highly absorbed wave fields or single waves.

In reflection techniques, wave field beams can be bent back to the entrance surface where they add to the beam which is reflected at the surface itself [45, 46], thereby causing density variations in a topographical image. In the Berg-Barrett method a major cause of the dynamical image contrast is due to a local change in primary extinction. This type of intensity extinction is due to the rediffraction of a once-diffracted ray back into the crystal in the same direction as the entering or incident beam. Because of a phase lag of  $90^\circ$  at each diffraction, the twice diffracted ray is just  $180^\circ$  out of phase with the incident beam and therefore interferes destructively with it [13].

In the case where the distorted region is fairly strongly strained, i.e., intermediary between the case of the slightly distorted region and that of the strongly distorted region responsible for the direct image, the waves from the intermediate case form a new wave field between the distorted region and the exit surface [35]. The new wave field and the original wave field show very complicated features of interference, and will not be discussed here.

---

Actually all the above causes may be responsible for contrast simultaneously. For example, the two line images arrowed in Figure 5(b) have asymmetric contrast. Notice that the right line in each of these two line images is darker than the left one. This asymmetric contrast depends on the dislocation depth from the crystal surface and is explained as a dynamical effect. That is, some part of the contrast is due to the dynamical image, although a large part of the contrast may be due to the direct image. However, depending on the kind of crystals, crystal thickness, the  $hkl$  reflection, etc., one of the above causes usually is dominant. In the Berg-Barrett technique and in transmission techniques, for  $\mu_0 t \approx 1$ , the direct image predominates. In the range where  $1 < \mu_0 t < 10$  both direct and dynamical images are visible. With  $\mu_0 t > 10$  practically only Borrmann contrast is observed.

In the double crystal arrangement contrast is mainly due to homogeneous dilations and tilts, and, sometimes, to wave field beams which have been bent back to the surface.

The general condition for the visibility of a defect is that it produce a sufficiently large disturbance of the set of diffracting planes used. From this it follows that, for isotropic materials, dislocations can in principle completely vanish only if  $\mathbf{g} \cdot \mathbf{b} = 0$  and  $\mathbf{g} \cdot \mathbf{n} = 0$  ( $\mathbf{g}$ : diffraction vector,  $\mathbf{b}$ : Burgers vector,  $\mathbf{n}$ : vector normal to the slip plane). This is referred to as the "visibility rule" in the present paper. Since, for dislocations containing both screw and edge components, both equations cannot be satisfied simultaneously, mixed dislocations can never totally vanish. In the anisotropic case, dislocations can vanish only if their direction is normal to a mirror plane of elastic symmetry.

Table I summarizes the features which characterize the various x-ray diffraction topography methods that have been discussed.

### C. THE EFFECTS OF IMPURITY ON DISLOCATION IMAGES

The direction of the Burgers vector of a dislocation can be determined by applying the above visibility rule to topographs made with various reflections, all of which contain the dislocation to be studied. However, if the crystal contains some impurity, the dislocations may be altered by the segregation of the impurity atoms upon them. The impurity atmosphere may so modify the strain-field about the dislocation as to make the visibility rule inoperable. Such dislocations are referred to as "decorated dislocations." Therefore an excellent means is provided for detecting minute traces of impurities. This impurity effect has been seen in BeO [47], quartz [48], diamond [49], and Si [50] crystals.

Certain dislocation groups are visible in the Lang topographs of Figure 8(a) but are not visible in Figure 8(b) where  $\mathbf{g}$  and  $\mathbf{b}$  are perpendicular. The dislocation group seen in Figure 8(a) was generated by plastic deformation; therefore, one can assume that these dislocations are relatively free of impurities. The micrograph shown in Figure 8(c) shows the x-ray image of the same wafer after copper was allowed to diffuse into the wafer at 900 °C for ten minutes. The x-ray image of Figure 8(b) is identical with that of Figure 8(c), except that it was taken before copper diffusion. The dislocation group and several other dislocations not seen in Figure 8(b) are clearly visible in Figure 8(c) because

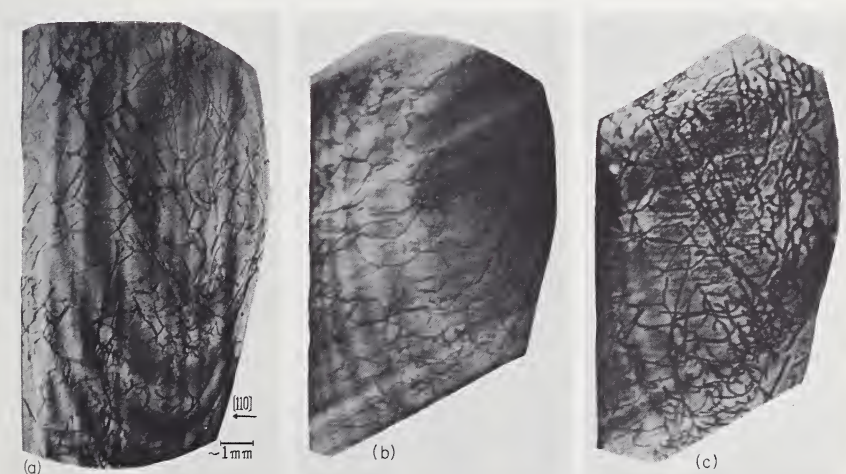


Figure 8. X-ray topographs of a silicon wafer containing a dislocation group generated by plastic deformation. Scanning transmission method. (a) 110 reflection. (b) Same wafer as shown in (a). 101 reflection. The dislocation group seen in (a) is not visible here because  $\mathbf{b} \perp \mathbf{g}$ . (c) Same wafer as shown in (a) and (b) after copper diffusion. The picture was obtained by using the same reflection as in (b). These topographs were made by G. H. Schwuttke.

TABLE I. Summary of x-ray diffraction topography techniques

Technique	Berg-Barrett	Double crystal	Wide beam transmission		Scanning transmission (Lang)
			Borrmann	Hosemann	
Apparatus	Simple	Complicated	$\mu_{ot} > 10$ Simple	$\mu_{ot} < 1$ Simple	$\mu_{ot} < 1$ Complicated
Exposure time	Short ( $\sim 1$ hr)	Short ( $\sim 1$ hr)	Long ( $\sim 10$ hr)	Short ( $\sim 1$ hr)	2-10 hr
Defect for which technique is most suited with kind of contrast <sup>a</sup>	Subgrains (1) Dislocations (2)	Subgrains (1) Dislocations (1) Stacking faults	Dislocations (3)	Subgrains (1) Dislocations (2) Stacking faults	Subgrains (1) Dislocations (2) Stacking faults
Best geometric resolution.	$1\mu$	$1\mu$	$1\mu$	$1\mu$	$1\mu$
Sensitivity to deformations.	Low	High	High	Low	Low

	Subgrains: Yes	Yes	Yes	No	Yes	Yes	Yes
Sensitive to the sense of deformations?	Disloc.: No	Yes (Difference)	Yes (Gradient)	Yes (Gradient)	Yes (Gradient)	Yes (Gradient)	Yes
Sensitive to impurities	Yes (Gradient)	Yes (Difference)	Yes (Gradient)	Yes (Gradient)	Yes (Gradient)	Yes (Gradient)	Yes (Gradient)
Thickness $t$ of specimen contributing to topography <sup>b</sup>	$\leq 5\mu$	$\leq 5\mu$ (back refl.) $\leq 300\mu$ (transm.)	$1 \rightarrow 5$ mm	$0 \rightarrow 2$ mm	$0 \cdot 1 \rightarrow 5$ mm.	$0 \rightarrow 2$ mm	$0 \rightarrow 2$ mm
Dislocation image width <sup>c</sup>	$1 \rightarrow 5\mu$	Up to $150\mu$	$\geq 50\mu$	$\sim 5\mu$	Up to $150\mu$	Up to $150\mu$	$1 \rightarrow 10\mu$
Upper limit of dislocation density [lines/cm <sup>2</sup> ].	$5 \times 10^6$	$10^5$	$5 \times 10^3$	$5 \times 10^6$	$5 \times 10^3$	$5 \times 10^6$	$5 \times 10^4$

<sup>a</sup> (1) homogeneous dilation and tilt contrast, (2) extinction contrast, (3) dynamical contrast.

<sup>b</sup> This is determined, in the Bragg case by the extinction depth and, in the Laue case, by the value of  $\mu_0$  (the absorption coefficient) for the materials and the value of  $t$  imposed by the technique.

<sup>c</sup> Based on the assumption that this is determined by normal image overlap.

of the copper precipitation along the dislocation lines. An infrared micrograph [51] of the wafer used for Figure 8(c) showed the presence of fine needles at all dislocations. These were presumably precipitated copper. From the size and spacing of the copper needles, the number of copper atoms along a 1-cm dislocation line has been estimated to be not more than  $10^{15}$  atoms [50]. This concentration of decoration is apparently enough to enable all the dislocations to ignore the visibility rule, thereby allowing them all to appear in topograph (c). The fine copper needles on the dislocations are not resolved in these topographs. Under some conditions individual precipitate particles can be seen in diffraction topographs. This is discussed in Part D-1 of this Section.

Undecorated dislocations are defined as those whose visibility in x-ray topographs conforms with the visibility rules, i.e., their visibility is not modified by strains introduced through the presence of impurities. However, it cannot be concluded that any dislocation which follows the visibility rule is entirely free from impurity on an atomic scale; it is unlikely to be so clean. The Burgers vectors of dislocations in some impurity-doped crystals can be determined by their visibility variation with the angle between  $\mathbf{b}$  and  $\mathbf{g}$ . Furthermore, the contrast sensitivity seems to depend on the kind of impurity but little further is known about this effect.

It is known that a straight screw dislocation can become a helix [52-54] by the absorption or generation of point defects at the dislocation when the point defects are in excess or shortage of the equilibrium concentration. By the copper decoration method, Dash [55] observed right-handed helices in Si containing Au in a concentration of  $10^{15} \text{ cm}^{-3}$  or less. These right-handed helices were formed from left-handed screw dislocations that had been introduced into the crystal by controlled twist deformation. In this case, the sign of the screw dislocations was determined from the sign of the deformation. From this observation, he inferred that, owing to the low energy of combination of vacancies and Au atoms, the Au atoms occupy the vacancy sites and, consequently, cause a vacancy deficiency which is responsible for the helix formation. Such observations also can be made by stereo x-ray topography [13] without the need for decoration, and thus the sign of the screw dislocations can be determined directly [32-35]. The topographs in Figure 9 show a helical dislocation  $\mathbf{b}=1/3 [2\bar{1}\bar{1}0]$  in a CdS crystal. Figures 9(a) and (b) are a stereo pair made by the Lang method. They were made using  $\bar{2}110$  and  $2\bar{1}\bar{1}0$  reflections as illustrated in Figures 9(d) and (e), respectively. The stereo pair shows that the helix is left-handed. Figure 9(c) is a section topograph which was taken in such a position that the Bragg condition was satisfied on the dotted line drawn in (a). A two-line image in Figure 9(c) can be seen. As in the case described for Figure 5(b), it can be concluded from this two-line image that the helix was formed from a right-handed screw dislocation. Since

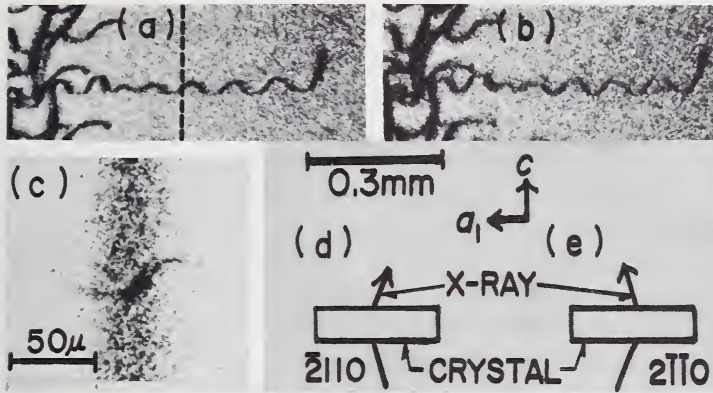


Figure 9. A helical dislocation with a  $\frac{1}{3} [2\bar{1}10]$  Burgers vector in a CdS crystal. (a) and (b) are the left-eye and right-eye views of a stereo pair as seen in (d) and (e). The topographs were made with  $\bar{2}110$  and  $2\bar{1}10$  reflections, respectively, using the scanning transmission method. They show that the helix is left-handed. (c) Section topograph taken at the position of the dotted line drawn in (a). The observation shows that the left-handed helix was formed from a right-handed screw dislocation. Crystal thickness:  $70\mu$ ;  $\mu_{0t} = 0.86$ ;  $MoK\alpha_1$ .

the left-handed helix was formed from the right-handed screw dislocation, the helix could not have formed by the accretion of vacancies onto the dislocation. Instead, the presence of some impurity, as in the case of gold in silicon [55], must have been responsible for the formation of the helices. A relatively small total number of impurity atoms could produce this effect.

In some materials stacking faults can also be observed by x-ray topography [56–60]. It is well known that the presence of impurities can lower the energy of a stacking fault, though the local strain field may be increased. Therefore, it is likely that stacking faults can be more readily observed in crystals containing trace impurities. If this is so, the observation of stacking faults in a diffraction topograph may be an indication of trace impurities. For example, in CdS crystals, stacking faults have been observed only for impurity-doped crystals [60–62].

#### D. IMPERFECTIONS PRODUCED FROM TRACE IMPURITIES

Precipitated impurity particles, systematic variations in impurity distribution, and even randomly distributed impurity atoms have a large effect on x-ray diffracted intensity. Each type of aggregation can be seen by x-ray topography; precipitates especially have been observed by many investigators.

1. *Precipitates*

There is a tendency for large precipitate particles to be formed from even trace amounts of impurities in some highly perfect crystals. This is probably because highly perfect crystals, containing few, if any, dislocations or other crystallographic defects, offer few sites for preferred nucleation of a precipitating phase. Therefore, only a few stable nuclei appear and the dissolved impurity atoms have only a few sites on which to deposit. Using the Lang method, Schwuttke observed individual precipitated particles of copper in dislocation-free Si crystals containing copper in a concentration of less than  $10^{17}$  atoms  $\text{cm}^{-3}$  [63-64]. Such precipitates usually give a double crescent shape of diffraction image [65], i.e., the images have a contrast-free region between the two crescents, as can be seen in Figure 10. The long direction of this contrast-free region always appears parallel to the reflecting plane that is used to make the topograph. The images are formed by the strain field around the precipitate particles as shown schematically in Figure 11. The contrast-free part of the image can be explained by the visibility rule which provides that no contrast is produced when the displacement of atoms is parallel to the reflecting plane. The atom displacements within a spherical coherent precipitate particle are, to a first approximation, radial with respect to the particle. Any diffracting plane passing through the center of the particle contains atoms which have no component of displacement normal to the diffracting plane. According to the rule of visibility therefore, no enhanced intensity will occur from any diffracting plane passing through the center of the precipitate particle. By the same argument, one would predict

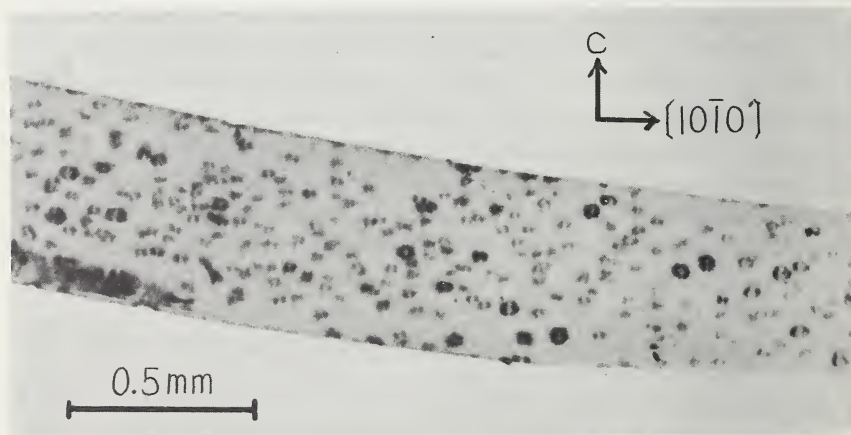


Figure 10. X-ray topographs of impurity-doped CdS ( $\text{GaCl}_3$ ). Scanning transmission method  $10\bar{1}0$  reflection. Circular images due to precipitate particles can be seen. See text for proposed explanation of double crescent shaped images.

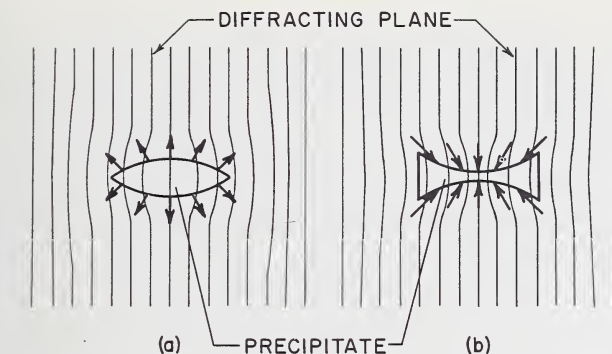


Figure 11. Schematic cross-section of the strains around convex-lens and concave-lens shaped precipitates. The choice of form apparently depends on whether the interplanar spacing of the precipitate particles is larger or smaller than that of the matrix. The arrows indicate the directions of displacements of the atoms, and the lines illustrate the curved atomic planes.

increased diffracted intensity from planes which are in the close vicinity of the precipitate particle, but which are enough removed from its center so that the atom displacements have a large component normal to the diffracting plane. The above discussion leads logically to the prediction of the double crescent figures which are commonly seen. The sign of the strain around precipitate particles can be determined [66] in the manner described for Figure 5.

Notice that the exact sizes of the precipitates cannot be obtained from the image sizes because the diffraction images are determined by the strain field around precipitates rather than by the precipitate itself. However, rough estimation of precipitate size may be possible from the very faint images of the precipitate particles which are sometimes obtained by adjusting the orientation of the specimen so as to maximize the difference in diffraction direction of the beams from the matrix and the precipitate particles. Under this condition, the images lie between the crescent pairs because they are formed by the highly distorted regions close to the precipitates. The sizes and the population density of the precipitates may be used for estimation of impurity concentration as has been done by Furusho [67].

As seen from the image formation mechanism, identification of the precipitates or the impurity is impossible at present. However, it may sometimes be possible to obtain a diffraction pattern from precipitates by a micro-diffraction technique. Furusho [67] has observed topographic images of disc-shaped precipitates in Si crystals containing  $10^8$  atoms  $\text{cm}^{-3}$  of oxygen. He also obtained a diffraction pattern from a single precipitate particle by means of a very narrow x-ray beam which was directed upon the particle. The pattern thus obtained was a diffuse Debye-Scherrer ring that indicated crystalline  $\text{SiO}_2$  [68]. No diffrac-

tion ring was obtained for a perfect region of the silicon crystal. For such a small impurity concentration, diffraction patterns of precipitates cannot be obtained by usual diffraction techniques using an x-ray beam with larger cross section.

If one can make a diffraction pattern of precipitates by a micro-diffraction technique and, in addition, if the average size and population density of the precipitates can be seen by topography, the identity of the impurity and a rough idea of its concentration may be estimated.

Elistratov and Kamadzhiev [69-70] made an x-ray diffraction study of precipitates from supersaturated solid solutions of Cu and Ge (concentration:  $\sim 10^{16}$  atoms  $\text{cm}^{-3}$ ) and of Ni in Ge ( $\sim 5 \times 10^{15}$  atoms  $\text{cm}^{-3}$ ). They found that, in spite of the very low concentrations of Cu and Ni in Ge, extra diffraction spots appeared near the main diffraction spot of the Ge matrix crystals. These extra-spots could not be explained by scattering from Guinier-Preston zones or from nucleation centers of the precipitate, because of the very small concentration of Cu and Ni. They proposed that the anomalous effect may be due to large deformation at micro-cracks of the matrix Ge crystal caused by the precipitate.

Diffraction anomalies such as "spikes" and "satellites" due to high impurity concentrations have also been studied using topographic methods [49, 71, 72]. These effects are very interesting but are somewhat out of the category of trace impurity studies.

## *2. Impurity Segregation: Non-Uniform Impurity Distribution*

Non-uniform distribution of impurities produces strong contrast in x-ray topographs. A typical example of this effect is the oxygen banding which has been seen in Si crystals by Ishii et al. [73], by Schwuttke [50, 63, 74], and Kohra et al. [75], and others. The oxygen segregation bands appear to be perpendicular to the growth direction in Si crystals which were made in a quartz crucible by the Czochralski method. Figure 12 is a topograph of the banded pattern which was obtained using reflecting planes that are perpendicular to the growth direction. Corresponding oxygen segregation bands [76] have also been observed by the  $9\mu$  infrared absorption method [51]. Variations of oxygen concentration, computed from the absorption coefficient for the infrared, of as little as  $10^{16}$  atoms  $\text{cm}^{-3}$  have been recorded by this x-ray technique [74]. Kohra et al [75], found that topographs of certain silicon wafers, using the 111 reflection perpendicular to the [111] growth direction, show an array of alternating weak and strong striations, whereas, for the  $\bar{1}\bar{1}\bar{1}$  reflection, the positions of weak and strong striations are reversed, as can be seen in Figure 13. Such local failure of Friedel's law was explained using the theory by Penning and Polder [36] as follows [77]: We assume variation of oxygen concentration along the growth direction, as shown schematically in Figure 14(a). Since interplaner spacings vary with impurity concentration, the interplaner spacing also

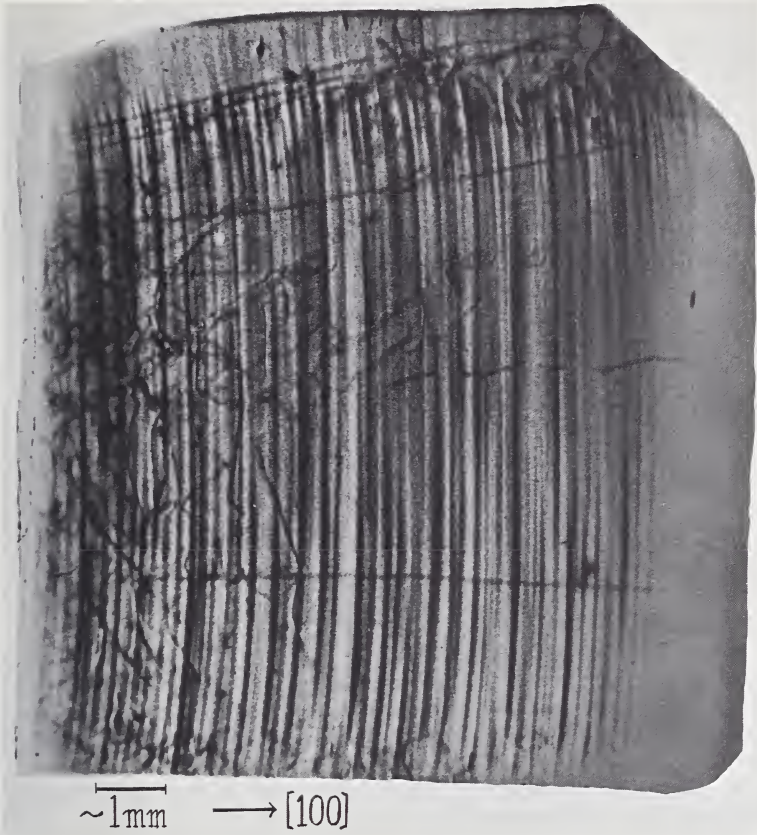


Figure 12. X-ray topograph of a silicon wafer showing oxygen segregation bands. Scanning transmission method, 100 reflection. The crystal growth axis is perpendicular to the reflecting plane. After Schwutke.

varies along the growth direction with the same period. A divergent beam is used for making the Lang topograph. The energy of x-rays which satisfy exactly the Bragg condition flows along the reflecting plane. Incident x-rays which are slightly off the Bragg angle flow mainly along the incident direction. Consequently, the latter x-ray waves encounter the variations of the interplanar spacing during their transmission. If the waves encounter an increase of the interplanar spacing, the paths of the waves that are excited on the farther branch of the dispersion surface [27] from the origin of the reciprocal lattice are bent around into the diffracted beam direction and, at the crystal exit surface, they split. Therefore, most of their energy travels in the diffracted beam direction, with little in the direct beam direction. This results in a diffracted intensity increase. Similarly, if the waves encounter a decrease of interplanar spacing, the waves that are excited on the other branch of the dispersion surface contribute to the diffracted intensity increase. In

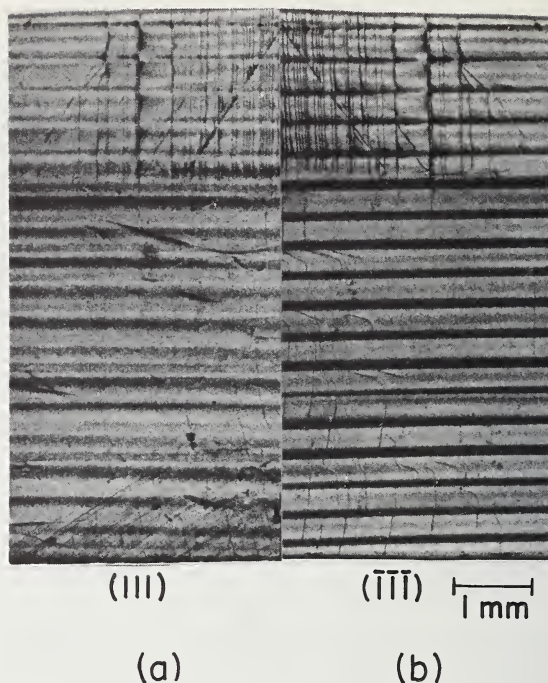


Figure 13. Local failure of Friedel's law seen in oxygen segregation bands of a Si crystal. (a)  $111$  reflection, (b)  $\bar{1}\bar{1}\bar{1}$  reflection. Scanning transmission method. The strong lines in the striation pattern of (a) appear at the positions of the weak lines in (b) and vice versa. The crystal growth axis is perpendicular to the  $(111)$  diffracting plane. After Kohra, Nakano, and Yoshimatsu [75].

the region where the gradient of impurity concentration is small, the intensity contribution of the x-rays which are initially off the Bragg condition is expected to be small. Therefore, at the places with the largest *gradients* of impurity concentration, the *maxima* of diffracted intensity appear, as shown schematically in Figure 14(b). Since the waves that are excited on the farther branch of the dispersion surface are more strongly transmitted than those on the nearer branch, higher intensities are obtained in the regions where the interplanar spacing increases along the paths of the waves. Thus, the weak and strong striations appear alternately as in Figure 13a and as illustrated schematically in Figure 14(b).

Similar striation contrast due to non-uniform impurity distribution has been observed in BeO crystals [47]. These striations were also perpendicular to the growth direction (see Fig. 15) and are believed to be the manifestation of variations of impurity concentration, probably Li, Mo, or Pt. The crystals were flux grown under non-steady thermal conditions. Therefore, varying degrees of BeO supersaturation with time was not unexpected. Crystals which showed a definite banded structure in

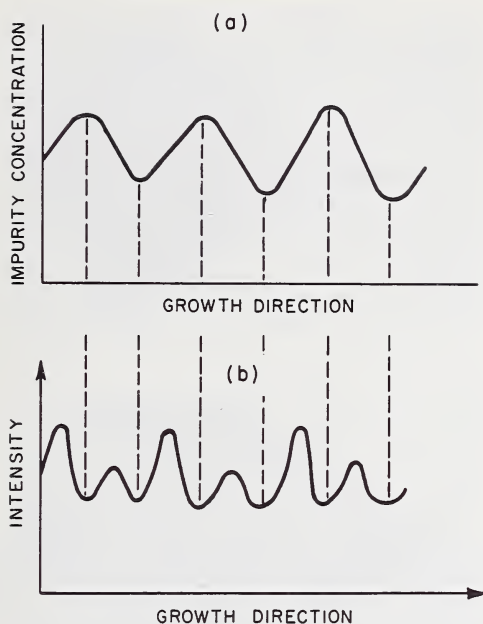


Figure 14. Schematic drawing of variations in image contrast of a striation pattern observed by the scanning transmission method (b), and corresponding impurity concentration in the crystal specimen (a). The contrast variation in (b) is expected to arise from the concentration in (a) as described in the text.

the topograph were sectioned and examined by D. K. Smith, using an electron microprobe and using proton and neutron radio-activation, followed by autoradiography [78]. The lower limits of detectability for these methods varies with the impurity for each method. According to Smith, activation analysis can detect as little as 100 ppm in a bulk sample and perhaps less under favorable conditions. To locate the source of the radiation, film methods are used which have a resolution limit around 10 microns. Within a 10 micron volume, a concentration of about 1% would be detected. Also, the depth into the matrix will modify the sensitivity and the resolution. The electron microprobe is said to be able to detect as little as 10 ppm of a heavy element in a light matrix like  $\text{BeO}$ , in a surface area of the order of 5 microns in diameter. The microprobe identifies and gives the location of the impurity directly but is limited to material within a few microns of the surface. None of these tests by Smith led to a banded image corresponding to that seen in the x-ray topograph. Apparently, it can be concluded that the negative results for the three methods just mentioned indicate that the absolute level of impurity concentration in the striations seen in the  $\text{BeO}$  topographs is probably below 10 ppm.

It is evident from the above explanation that the striation patterns are dynamical images. Lang [79] observed the similar local failure of

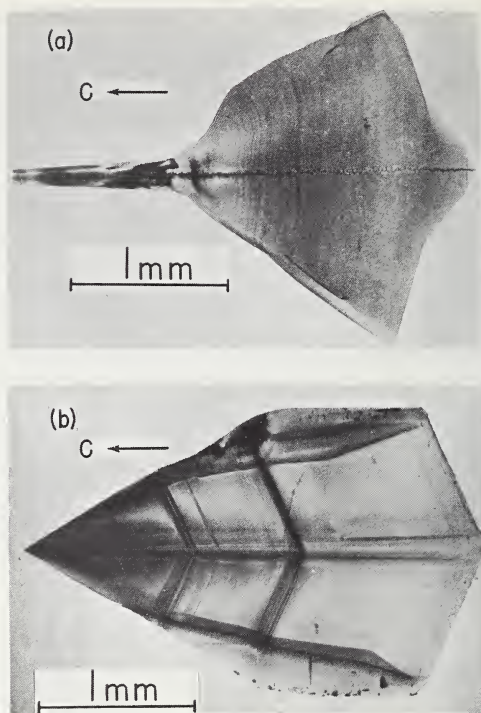


Figure 15. X-ray topographs of BeO crystals. Scanning transmission method. (a) 0002 reflection, (b) 1010 reflection. Striations appear perpendicular to the growth directions and seem to be due to variations in impurity concentration. The fringes parallel to the crystal edge in (a) are due to the thickness variation near the edge. (Pendellösung fringes.)

Friedel's [80] law on the dynamical images of edge dislocations in the case where their slip planes are parallel to the reflecting planes. The present explanation for the contrast seen in the segregation bands is, in principle, the same as that for the dislocation images. Non-uniform distribution of impurity can also be observed by the double crystal method as will be described in the next section. However, the causes of contrast are quite different in the Lang method than they are in the double crystal method.

#### E. LATTICE PARAMETER VARIATIONS DUE TO IMPURITIES

It is well known that impurities cause changes of lattice parameters. However, this effect is very small for trace amounts of impurities. Minute variations of cell size, due to trace impurities, can be detected by precise measurement of lattice parameters using such methods as the powder method [81], and the Kossel technique [82]. Variations of  $|\Delta d/d| \gtrsim 10^{-6}$  can be detected using the powder and divergent beam (Kossel) method, whereas, for the double crystal [14, 25, 30, 31] and the

Moiré methods [83-85] distortions as small as  $|\Delta d/d| \gtrsim 10^{-8}$  can be measured. In this paper the two topographical methods are described with examples. The other methods (non-topographical) are adequately described in the references so they will not be included here.

### 1. Double Crystal Method

We have shown in section II-A-2 that the double crystal method is very sensitive to tilts of lattice planes and to gradients of interplaner spacings. Variations of  $|\Delta d/d| \sim 10^{-8}$  can now be detected as contrast variation. Bonse [86] studied striations which were first seen by Deslattes [25b] in double crystal diffraction topographs of natural quartz crystals. Figure 16 shows typical striation patterns of opposite surfaces of a quartz crystal using double crystal topographs (see Fig. 3). Since the striations on opposite faces of the crystal match precisely, it was

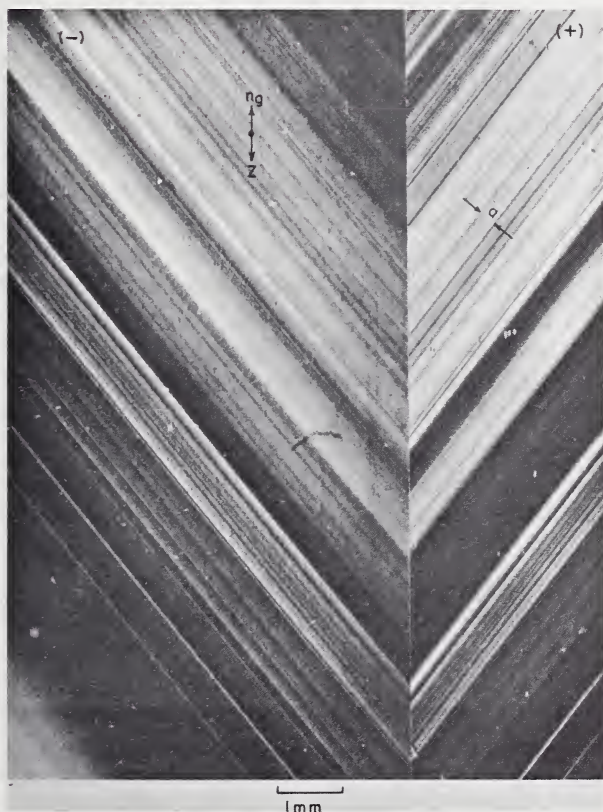


Figure 16. Striation patterns in a quartz crystal observed by the double crystal method. The left picture is the topograph of the  $(2\bar{1}10)$  surface of the crystal as visualized by a  $43\bar{1}0$  reflection and the right shows the reverse side by  $4310$  reflection. Note the matching of the patterns in the left and right topographs. After Bonse.

concluded that the striation lines are traces of layers extending through the thickness of the crystal. From the similarity of these striations to the impurity bands in Si and BeO (II-D-2), it is inferred that they originated in the crystal growth process by deposition of layers having different impurity concentrations. It is known that natural quartz usually contains Al, Na, and Li as impurities [87-88].

For the double crystal method the change in diffracted intensity,  $\Delta I$ , which produces image contrast has been shown to be

$$\Delta I = K(\Delta d/d) \tan \theta_B + \mathbf{n}_g \cdot \mathbf{n}_t \Delta \theta \quad (1)$$

where  $K$  is a constant that is proportional in magnitude to the steepness (with sign) of the slope of the rocking curve.  $\mathbf{n}_g$  is a unit vector normal to the plane that is defined by the incident and the diffracted beams.  $\mathbf{n}_t$  is a unit vector parallel to the axis of the lattice tilt. Pure dilation  $\Delta d/d$  can be obtained from two topographs taken with  $+\mathbf{n}_g$  and  $-\mathbf{n}_g$ , since the contribution from tilt  $\Delta \theta$  simply changes sign. If both topographs give identical contrast, then  $\mathbf{n}_t$  must be normal to  $\mathbf{n}_g$ . If identical contrast is obtained using two sets of diffracting planes with different orientations, then the direction of  $\mathbf{n}_t$  has been determined. In principle the amount of lattice tilt  $\Delta \theta$  can be obtained from any two topographs with  $+\mathbf{n}_g$  and  $-\mathbf{n}_g$  by subtraction, provided  $\mathbf{n}_g$  has not been chosen normal to  $\mathbf{n}_t$ .

In this way, it was found that the striation patterns in the quartz topographs are due to the structure near the surface as illustrated in Figure 17. Bulk stresses, which are caused by variations of impurity concentrations, relax at the crystal surface. The smaller the shear modulus, the larger will be the depth from the surface at which the relaxation dies out. These stresses may be of opposite sign in adjoining layers and cause tilts in the transition regions between these layers. From the magnitude of the contrast, the tilts and the dilations between different layers were found to lie in the range of 0.25 sec of arc and  $\Delta d/d = 10^{-6}$  respectively.

These crystals were colorless before this striation pattern was observed. However, after irradiation with x-rays (46 hr 20 kV and 40 mA), a non-uniform coloration began to become visible. The coloration had the same lamellar structure as in the x-ray topograph. Comparison of these results with studies on color centers of smoky quartz [87-92] led to the conclusion that all lamellae contain Al as a main impurity but with different concentrations and perhaps also in a different structural arrangement. It was also concluded that the striation patterns observed by the double crystal method are associated mainly with variations of Al concentration rather than vacancy concentration. Evidence for this is in Bonse's finding that the x-irradiation caused a slight expansion of the lattice ( $\Delta d/d \sim +5 \times 10^{-7}$ ) in all the lamellae. This expansion saturated

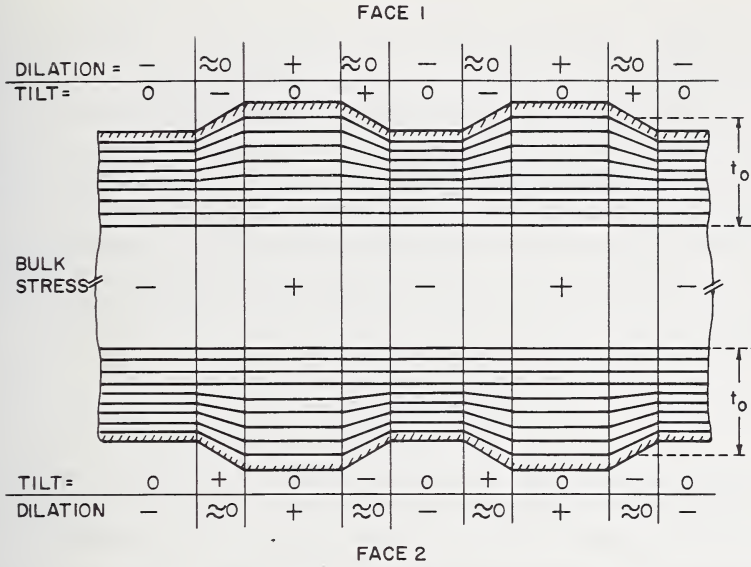


Figure 17. Model for surface relaxation of bulk stresses of the layers with different impurity concentrations. After Bonse.

at higher radiation doses. If the cause of the expansion were the formation of point defects such as vacancies, then it would be difficult to understand why saturation occurs at such small dilations. Therefore it is believed that the expansion is due to an electronic process occurring at defects (impurity atoms) which are already present before the irradiation and whose number does not increase during irradiation. If this is true, the saturation (maximum) value of radiation-induced expansion would be proportional to the grown-in defect concentration. To date this suggestion has not been tested.

It should be noticed that the principle of image formation in the double crystal method is quite different from that of the Lang method described in Section II-D-2. In the Lang method, the striation contrast is formed only by strain gradients and, therefore, no contrast is obtained for such regions where the impurity concentration is maximum or minimum (see Fig. 14). It may be impossible in a Lang topograph to distinguish between two regions with even a larger difference in impurity concentration if the two regions are separated so far that the gradient in the transition region between them is too small. On the other hand, in the double crystal method, regions with uniform but different impurity concentrations can be distinguished by diffracted intensity differences.

## 2. Moiré Patterns

In the experiments with quartz, the layers with different impurity concentrations are inclined to the crystal surface. In the case where

such layers are parallel to the crystal surface, Moiré patterns can be observed by the Lang method. The topographs in Figure 18 show parallel Moiré patterns of a CdS crystal which consist of two layers with different impurity concentrations [85]. In figures 18(b) and (c), Pendellösung fringes [93-95] appear due to the wedge shape of the crystal illustrated in figure 18(a). The Moiré fringes with spacings of about  $100\mu$  are seen parallel to the reflecting planes used. The fringe spacing of a Moiré pattern is determined by a difference in orientation and/or lattice spacing between two superposed crystals through which the radiation passes successively. For a parallel Moiré, the spacing  $S$  is given by [96]

$$S = d_A d_B / |d_A - d_B| \quad (2)$$

where  $d_A$  and  $d_B$  are the interplaner spacings of two superposed crystals  $A$  and  $B$ . Using eq (2), it was found from the observed fringe spacing that the differences in the lattice parameters,  $a_0$  and  $c_0$  between the two superposed CdS crystals are 3.6 ppm and 3.4 ppm, respectively. Since these two values are nearly equal, one can conclude that an isotropic lattice variation is caused by the impurity. The equidistant fringes indicate a uniform impurity distribution in directions parallel to the layer.

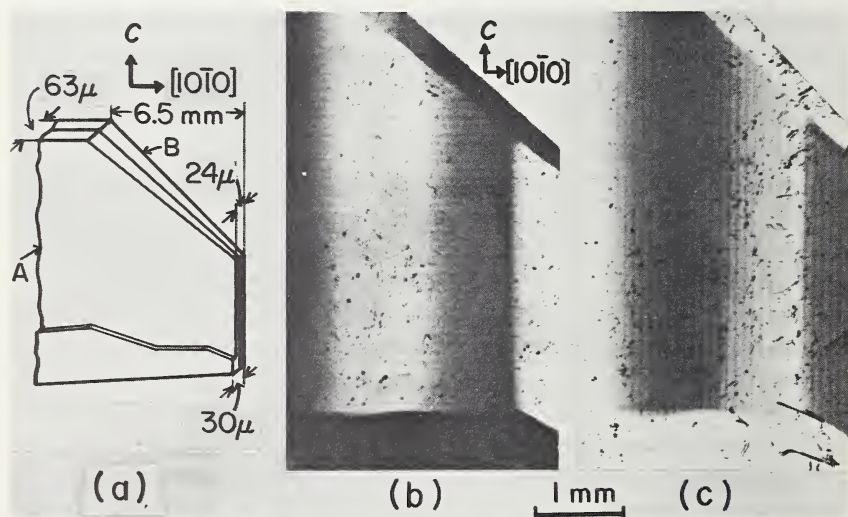


Figure 18. Parallel Moiré patterns of two superposed wedge-shaped CdS (CuS) crystals as shown by scanning transmission topographs. (a) Shows the wedge shape of the crystal which consists of two layers A and B. (b) 0002 reflection. (c)  $10\bar{1}0$  reflection. The topographs show the tip region of the crystal. Pendellösung fringes are visible which are parallel to the  $c$ -axis. These are due to the wedge shape shown in (a).

Such crystals were grown in vapor flow from heated CdS powder which was mixed with CuS to introduce Cu into the crystals. In the initial stage of the crystal growth, platelets were rapidly formed by the dislocation mechanism [62] and then epitaxial growth occurred on one of the platelet surfaces that faced the direction of vapor flow. Since the mixed impurity evaporates very rapidly, the platelet grown in the initial stage and the thin layer grown epitaxially on it may have different impurity concentrations. Red luminescent emission of the crystal was observed under ultraviolet irradiation. The emission of the substrate platelet was stronger than that of the epitaxially grown layer, an observation which also indicates that the layers have different impurity concentrations. Nearly straight fringes such as are seen in Figure 18, were seldom obtained. Instead, almost all crystals gave irregular fringes, indicating that the crystals are easily distorted.

In Moiré interference, smaller lattice variations result in larger fringe spacings. Therefore, if large crystals are available, small lattice variations ( $\sim \Delta d/d \lesssim 10^{-8}$ ) can be detected by this method. For crystals that have no layer structures, it is necessary to superpose artificially the doped crystal and a perfect crystal of standard high purity. However, the superposition may be technically difficult.

### III. Effect of Impurities on Integrated Intensity of X-ray Diffraction

The effects of isolated point defects on the intensity of an x-ray reflection has been treated kinematically by several investigators [97-101]. They concluded that strains due to point defects influence diffraction in a manner similar to thermal motion, i.e., the intensity of a Bragg reflection is decreased and a diffuse scattering builds up in the vicinity of the peak, while the peak itself is not broadened. However, the effects of trace impurities seem to be so small that they are overwhelmed by the effects of any other lattice imperfections. Therefore, it is considered that the kinematic effects of trace impurities can be detected only for nearly perfect crystals. However, for nearly perfect crystals, it appears that the destruction of the dynamical interaction of x-ray beams within crystals become dominant. To our knowledge the effects of point strains on dynamical x-ray interaction has not yet been treated theoretically. On the other hand, the impurity effects on the intensity of reflection have been detected experimentally by Batterman [102]. Also Efimov and Elistratov [103, 104] and Patel and Batterman [105] observed the effect of impurities on the anomalous transmission intensity. This is discussed in greater detail (in Sec. III-B). In both cases, crystals with low dislocation density were used, and it was confirmed that the intensity effects due to dislocations were small enough so as not to overwhelm the impurity effect.

## A. INTEGRATED DIFFRACTED INTENSITY IN REFLECTION

Batterman [102] measured the absolute values of x-ray integrated intensities from Ge single crystals using a double crystal spectrometer (Fig. 3), and compared these values to those that were calculated for ideally perfect [2, 106, 107] and ideally mosaic or imperfect crystals [108]. He found that, for germanium and  $\text{CuK}\alpha$  radiation, variations in dislocation density below  $10^5 \text{ cm}^{-2}$  did not significantly affect the integrated intensities and that the measured intensities agree quite well with theoretical values which were calculated for a perfect crystal by the Darwin-Prins theory [106, 107].<sup>1</sup> He also observed for Ge crystals with a low dislocation density ( $5 \times 10^3 \text{ cm}^{-2}$ ) that additions of about one part in  $10^4$  of substitutional indium or precipitated lithium atoms significantly increased integrated intensities. Figure 19 shows the 333 rocking curve for Ge before the addition of lithium and after lithium has precipitated. The average half-width increased by only 3 sec of arc. However, the increase in total diffracted intensity is evident from the superposition of the two curves. The curve for the precipitated crystal has higher and longer tails, showing the presence of diffuse scattering. The increase of 24% in integrated diffracted intensity, due to only 0.01% lithium, presumably shows the high sensitivity of this parameter to lattice strains. For the In-doped crystal, the integrated intensities varied with position of the x-ray beam across the face of the crystal. The intensities for the most intense region are approximately 4, 11, and 33% greater than is predicted theory for the 111, 333, and 444 reflections, respectively. The variation over the crystal face is consistent with the fact that the impurity densities were known to fluctuate.

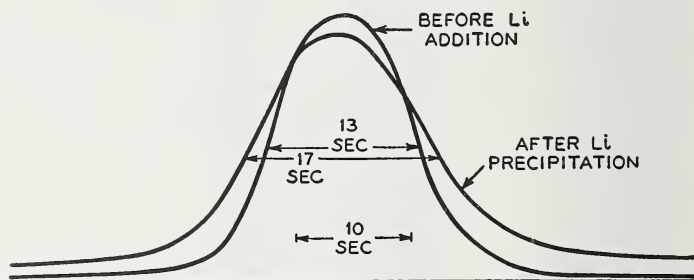


Figure 19. Effect of lithium precipitation on rocking curve for a 333 reflection from germanium. After Batterman.

<sup>1</sup> As Batterman indicated, it should not be assumed that dislocation density less than  $10^5 \text{ cm}^{-2}$  will not affect integrated intensities for all crystals and wavelengths. The sensitivity will depend upon the sharpness of the Bragg peak for the perfect crystal which is determined by the scattering factor of the atoms of the crystals and the wavelength used: the sensitivity is higher for higher order reflections. As can be also expected, less penetrating radiation is less sensitive to low dislocation density. See also J. R. Patel, R. S. Wagner, and S. Moss, *Acta Met.* **10**, 759 (1962).

Since the impurity concentration by itself is too small to contribute to the x-ray scattering factor, the increase in the integrated intensity is probably due to a decrease in primary extinction caused by distortion of the lattice due to the impurity atoms. The observed increase of the intensity with order is consistent with this explanation. In the case of lithium, it is most probable that the precipitate particles themselves produce the strain. For the In-doped crystal, however, it appears that the regions of large fluctuations in dissolved indium concentration are responsible for the intensity increase, as in the case of the oxygen bands in Si crystals. These observations show that the total intensity of reflection in a nearly perfect crystal can be a sensitive measure of low impurity content, especially if they induce much lattice distortion due to segregation or precipitation.

### B. IMPURITY EFFECT ON ANOMALOUS TRANSMISSION

From the theory of the anomalous transmission (I-A-4), one can expect an intensity decrease due to local strain caused by impurity atoms. Patel and Batterman [105] observed this effect, using the experimental arrangement shown in figure 20. The first crystal serves merely as an x-ray monochromator. These authors studied dislocation-free Si crystals ( $\mu_0 t \approx 15$ ). Their result is as follows: Heat treatment at 1000 °C results in impurity clustering, i.e., the formation of strained regions, which results in a decrease of transmitted and diffracted x-ray intensity of over two orders of magnitude. Upon heating at 1350 °C, the clusters dissolved and the original perfection of the crystal was restored. From the kinetics of the impurity clustering, the impurity was concluded to be oxygen. The changes in the x-ray intensity occur before there is any detectable change in the infrared absorption band for oxygen, a standard measure of the dissolved oxygen content. Anomalous x-ray transmis-

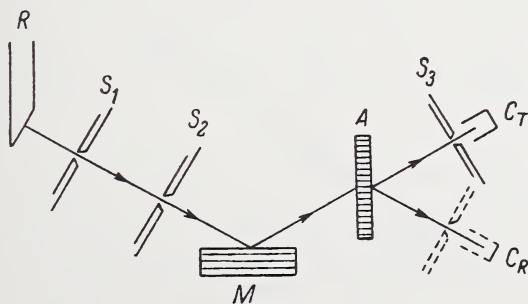


Figure 20. Experimental arrangement for the intensity measurement of the transmitted and diffracted beams. R) X-ray tube;  $S_1$ ,  $S_2$ ,  $S_3$ ) slits; M) crystal monochromator; A) crystal analyzer;  $C_T$ ) photomultiplier in position to record the transmitted beam;  $C_R$ ) photomultiplier in position to record the Laue reflection. The lines drawn across the crystal show the orientation of the (220) reflecting planes.

sion, therefore, appears to be very sensitive to changes in the early stages of impurity clustering and should, therefore, be an important tool for the investigation of precipitation phenomena occurring in crystals of high initial perfection. However, these results indicate that, in the dissolved state, the impurity atoms have only a small effect on the intensity of anomalous transmission.

Efimov and Elistratov [103] observed a small effect of dissolved impurities in the dissolved state on anomalous transmissions, using very thick Ge crystals. Using the arrangement in Figure 20 they [109] found experimentally and then verified theoretically that for thick perfect crystals ( $\mu_0 t > 30$ ), the anomalously transmitted and diffracted beams,  $T_i$  and  $R_i$ , have equal integrated intensity, i.e.,  $T_i = R_i = i$ , and there is a linear relation between  $\ln i$  and the thickness  $t$ , viz,  $\ln i = -\mu_i t + y_i$ . The interference absorption coefficient  $\mu_i$  is equal to the slope of the line which is obtained by plotting the logarithm of the observed integrated intensities against thickness. The value of  $y_i$  is the intercept found by extrapolating the line to the  $\ln i$  axis. They [110] concluded that a dislocation density less than  $10^2 \text{ cm}^{-2}$  does not affect  $\mu_i$  and  $y_i$  appreciably. Using germanium crystals with low dislocation density ( $\sim 10^2 \text{ cm}^{-2}$ ), they [103] studied the effects of diffused impurities on  $\mu_i$  and  $y_i$ . An example is shown in Figure 21. From the slopes of the two lines for the pure (curve 2) and the hydrogen-diffused crystals (curve 1), the change in  $\mu_i$  can be seen. Using this method, they observed the change of integrated intensities due to the impurities  $\text{H}_2$ , Cu, and Ni in the dissolved state and obtained the following results:

1. Small concentrations of hydrogen ( $\sim 10^{14} \text{ cm}^{-3}$ ), copper ( $\sim 10^{16} \text{ cm}^{-3}$ ) and nickel ( $5.5 \cdot 10^{15} \text{ cm}^{-3}$ ) cause a considerable decrease in the integrated anomalous transmitted intensity in nonequilibrium solid

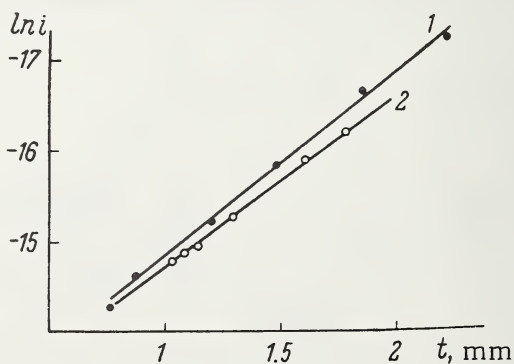


Figure 21. Dependence of  $\ln i$  on  $t$  ( $i$  = integrated intensity of the diffracted or transmitted beam,  $t$  = crystal thickness). The lines (1) and (2) were obtained for the specimens from the same single crystal which was grown in a stream of hydrogen. (1) As-grown specimen, dislocation density  $N = 1 \cdot 10^2 \text{ cm}^{-2}$ . (2) Specimen annealed in vacuum for 2 hr at  $700^\circ \text{C}$ ,  $N = 3 \cdot 10^2 \text{ cm}^{-2}$ . After Efimov and Elistratov [103].

solutions in germanium. This effect is especially pronounced for large thicknesses ( $\mu_0 t \sim 70$ ) and leads to intensity variations of some tens of percents. The value of  $\mu_i$  increases regularly with increase in the impurity concentration. No noticeable effect on  $y_i$  was observed.

2. The observation indicates that distortion of the crystal lattice caused by the impurity is greater for impurities with low solubility.

They [104] also studied the effects of impurity precipitates (Ni and Cu) on  $\mu_i$  and  $y_i$ , and found that the precipitation from the solid solution gives greater change in the integrated intensity as compared with the initial solid solutions. A very thin ( $\sim 35\mu$ ) heavily distorted surface layer is formed by the precipitation. Owing to this distorted layer, the values of  $\ln T_i$  and  $\ln R_i$  fall sharply from the straight lines relating the logarithm of the intensity to the thickness. After removing the surface layer, the linear relationship is preserved for the main body of the crystals, but  $\mu_i$  is greater than that for the solid solution. The decrease of integrated intensity for the main body is also attributed to the distortion due to the precipitation.

As can be seen from the above experiments, anomalous x-ray transmission is very sensitive to impurities, especially to precipitated impurities. However, the change in intensity is not due to the impurity itself, but is caused by a lattice strain introduced by the impurity atoms. Therefore, it appears that impurities are detectable by diffracted x-ray intensities only in highly perfect crystals, and that it is impossible thus far to identify the *kinds* of impurities by measuring the changes in transmitted intensity. This method appears to be suitable for studying the distribution of deliberately added impurities, as in doping operations.

#### IV. Impurity Effect on Electron Density Distribution

The impurity effects on x-ray diffraction described in the above sections appear through lattice distortion caused by impurities. However, it is well-known that the presence of impurities can also cause changes in various other properties of crystals. For instance we can expect impurities to change the electron distribution in crystals. We may ask the question: Are impurity effects on structure factors too small to detect?

##### A. ELECTRON DENSITY MAP—DIFFERENCE METHOD

Mohanty and Azaroff [111] showed experimentally that if impurity atoms are interstitially dissolved, and, if enough of them occupy the same types of sites in a crystal structure, then their total contribution to the diffracted intensities can be detected. They studied zinc oxide crystals, pure and doped with excess zinc. ZnO has a hexagonal structure, which, when projected along the  $c$  axis, contains pairs of superimposed zinc and oxygen atoms in one unit cell. If the origin of the unit cell is placed at the projected position of the octahedrally coordinated void in

this structure, then a small maximum should be seen at the origin of the cell in the electron density projection of an artificially Zn-doped crystal. To exaggerate this effect, they used pairs of crystals, one as pure as could be grown by normal procedures and one deliberately doped to saturation in zinc vapor. A "difference" electron density map was next calculated by subtracting the electron density of the pure crystal from that of the doped crystal at each point  $(x, y)$  in the unit cell, according to the relation:

$$\Delta\rho = \rho_D - \rho_P = (1/A) \sum_h \sum_k (F_D - F_P)_{hk0} \cos 2\pi(hx + ky), \quad (3)$$

where  $A$  is the area of the projected unit cell and the subscripts  $D$  and  $P$  refer to the doped and pure crystals, respectively. Such a difference map not only has the advantage of showing any real differences between the electron densities of the two crystals, but it also does not suffer from series termination errors, since the terms omitted in each series can be expected to cancel in the subtraction. It is important to realize that the above Fourier series is unlike the usual difference synthesis used in crystal structure analysis in which the coefficients are differences between observed and calculated structure factors. Also, since the differences between two measured values are used in this work, any systematic errors due to scaling, instrumentation, etc., should be the same for both terms. Such errors, therefore, may introduce small uncertainties regarding the peak height of the final synthesis but do not affect its main features.

Their difference map is shown in Figure 22. The small maximum is clearly visible at the origin of the projected cell. From this map, it is possible to calculate the number of interstitial zinc atoms present, on the average, in one unit cell. The volume of the origin peak corresponds to  $6 \times 10^{+20}$  atoms  $\text{cm}^{-3}$  in the interstitial site, or approximately one interstitial atom per one thousand unit cells at room temperature.

They also carried out an identical study with CdS crystals, but did not observe any maxima whose magnitude exceed possible effects caused by errors inherent in the measurement of diffraction intensities [112]. Thus it appears that this method for studying point defects in crystals is effective only when they are present in fairly large amounts. Conversely, more precise measurements of structure factors should serve to increase the sensitivity of this method.

## B. PRECISE DETERMINATION OF STRUCTURE FACTORS BY MEANS OF PENDELLÖSUNG FRINGES

The main error in the experimental determination of the structure factor by intensity measurements arises from the uncertain corrections for extinction. Actually we can formulate an exact treatment for dif-

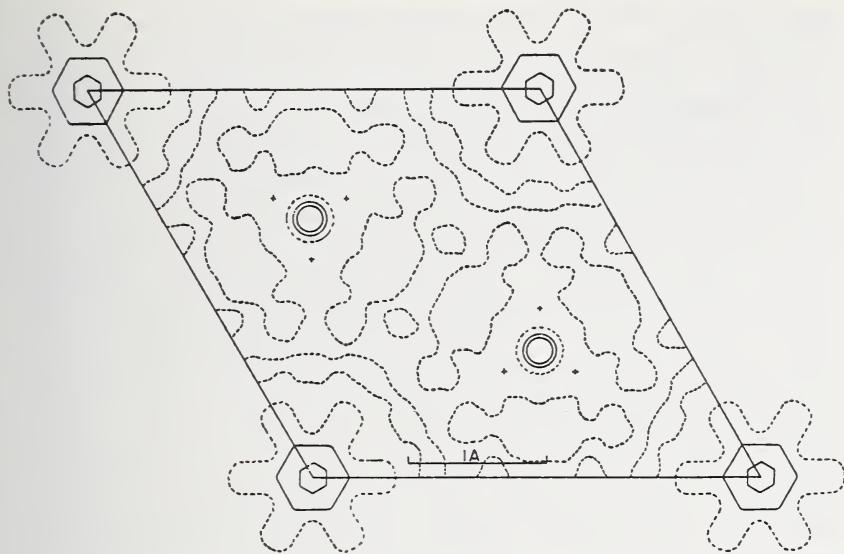


Figure 22. Difference map of the *c*-axis projection of ZnO obtained by subtracting the electron density of a "pure" crystal from that of a doped one. The zero contour is shown dashed. The solid contours are in equal steps of  $1e/\text{Å}^2$ . After Mohanty & Azaroff [111].

fraction only for the cases of the "ideally imperfect" and "ideally perfect" crystals. In general, however, real crystals have a texture between both of these extremes. Therefore structure analyses of real structures contain some inherent ambiguity. However, recent technique has produced highly perfect crystals and it has been possible to treat them as "ideally perfect crystals". There have been attempts to measure structure factors using highly perfect crystals and the phenomenon of Pendellösung fringes which were predicted and described by Ewald [113] early in 1916. The determination of structure factors from Pendellösung fringe data observed by electron microscopy has been reported by several authors [114]. Kato and Lang [93] first observed the Pendellösung fringes in the x-ray case using topography, but Hattori, et al. [115], were the first to report structure factors which had been determined by means of x-ray Pendellösung fringes. According to the theory [94, 95], the fringe distance  $\Lambda$  observed when the Bragg condition is satisfied is given approximately by

$$1/\Lambda = (1/2) (1 + \cos 2\theta_B) |\psi_g| / (\lambda \cos \theta_B) \quad (4)$$

where  $|\psi_g|$  is related to the structure factor  $F_g$  by the well-known formula

$$|\psi_g| = \frac{\lambda^2}{\pi V} \frac{e^2}{mc^2} |F_g|$$

where  $V$  is the volume of the unit cell, and  $e$ ,  $m$ , and  $c$  have the usual meanings. This approximation is fairly accurate except for the initial few fringes. Hattori et al. [115], observed Pendellösung fringes with section topographs of wedge-shaped perfect Si crystals and determined the structure factors from the observed fringe distances by using eq (4). The absolute value of the structure factor obtained in this way is accurate to within a few percent. The main errors are caused by the uncertainties in the geometrical measurements such as the wedge angle and the crystal orientation. It appears that measurement of structure factors with high accuracy may be possible by improving the geometrical measurements. Therefore it is possible that the effects of small impurity concentrations on structure factors can be detected if the crystals containing the impurity are still perfect enough. Because the spacings of Pendellösung fringes are contracted by lattice distortion [41, 116, 117] it may be possible by this means to detect traces of even the highly soluble impurities, where the lattice distortion is relatively small for a given amount of impurity, as has been described in Section III-B.

## V. Other Effects of Impurities

Small amounts of impurities may produce other effects on material behavior which are admittedly only distantly related to x-ray diffraction. Since effects of the type discussed below are apparently not included elsewhere in this Symposium they are given brief recognition here by the mention of two examples.

### A. INFLUENCE OF IMPURITIES ON PHASE STABILITY

Stadelmaier [118] has studied the impurity stabilization of ternary phases of certain transition metals (Mn, Fe, Co, Ni, Pd, Pt), of the B-metals (Mg, Zn, Cd, Hg, Al, Ga, Ge, In, Sn, Pb), and the metalloids (B, C, N). He found that the Cu, Au-type structure could be stabilized by the presence of carbon and nitrogen and proposed that the metalloid partly fills the octahedral hole of the  $L_{12}$  structure, yielding the perovskite-type structures in extreme cases. Von Phillipsborn and Laves [119] found that the presence of small amounts ( $\sim 1\%$ ) of oxygen, nitrogen or carbon stabilized the  $\text{Cu}_3\text{Au}(L_{12})$  structure of  $\text{Ti}_3\text{Au}$  and  $\text{V}_3\text{Au}$  in place of the Cr Si(A15) structure which normally forms in the respective high purity binary alloys [120]. They observed that for the  $(L_{12})$  structure of  $\text{Ti}_3\text{Au}$ , the radius of the octahedral hole equals  $0.60\text{\AA}$ , which agrees well with the radius of the oxygen atom ( $0.60\text{\AA}$ ) found for solutions of oxygen in metallic titanium (Ehrlick) [121]. Detailed x-ray diffracted intensity observations also support their idea that the influence of oxygen in stabilizing the  $\text{Cu}_3\text{Au}$ -type structure is a result of filling the central octahedral hole in that structure.

## B. INFLUENCE OF IMPURITIES ON SOLID STATE REACTION KINETICS

There is evidence that certain types of impurities can have a strong influence on reaction rates, especially those which are diffusion limited. An example of this effect is found in the work of Hendricks, et al. [122], who studied the influence of small additions of  $\text{Ca}^{++}$  to the rate of precipitation of  $\text{AgCl}$  in  $\text{NaCl}$ , as observed by small-angle x-ray scattering. They found that additions of about 150 ppm of  $\text{Ca}^{++}$  caused the  $\text{AgCl}$  to precipitate about ten times faster than in binary mixtures of  $\text{NaCl}$ - $\text{AgCl}$  without the added aliovalent impurity. It was assumed that to maintain electrical neutrality in the crystal, the divalent cation impurity introduced an equivalent number of extrinsic cation vacancies. The extra cation vacancies were then presumed to promote the diffusion movement of the silver ions, thereby accelerating the rate of the precipitation reaction. In a sense, therefore, a small amount of an added aliovalent impurity appears to act as a reaction catalyst, since it does not take any part in the reaction except to accelerate it. Many other examples of the influence of minor amounts of impurities or vacancies to promote or inhibit reaction rates can be found.

## VI. Summary

The presence of impurity traces in crystalline materials can cause small changes in lattice parameters and large changes (usually an increase) in the intensity of x-rays diffracted by that material. If the identity of a uniformly dissolved impurity is known, a meaningful estimate of its *concentration* can be made from precise measurements of crystallographic lattice parameters or the structure factor  $F$  of its host. X-ray diffraction topography, on the other hand, is an effective method for observing the *distribution* of trace impurities in relatively large crystals if those crystals are otherwise highly perfect. However, at its present state of development, diffraction topography cannot identify the impurity nor measure quantitatively its concentration level. Further development of x-ray diffraction techniques toward these ends is conceivable in principle and is currently in progress.

## VII. Acknowledgements

We are grateful to Drs. G. H. Schwuttke and M. Yoshimatsu for supplying original photographs and slides illustrating their studies. Also we are indebted to Professors P. A. Beck and L. V. Azaroff; to Drs. K. Schubert, T. B. Massalski, and W. B. Pearson for their helpful comments during the preparation of the manuscript.

## VIII. References

- [1] See, for example, *Direct Observation in Crystals*, J. B. Newkirk and J. H. Wernick, eds., Interscience Publishers, New York, 1962.

- [2] Darwin, C. G., *Phil. Mag.* **27**, 315, 675 (1914).
- [3] Ewald, P. P., *Ann. Phys. Lpz.*, **54**, 519 (1917).
- [4] Ewald, P. P., *Z. Phys.* **2**, 332 (1920).
- [5] Ewald, P. P., *Z. Phys.* **30**, 1 (1924).
- [6] Bethe, H. A., *Ann. Phys., Lpz.* **37**, 55 (1928).
- [7] Laue, M. von, *Ergeb. exact. Naturw.* **10**, 133 (1931).
- [8] Guinier, A., and Tennevin, J., *Acta Cryst.* **2**, 133 (1949).
- [9] Schulz, L. G., *J. Metals*, **200**, 1082 (1954).
- [10] Weissmann, S., *J. Appl. Phys.*, **27**, 389 (1956).
- [11] General Reviews, J. B. Newkirk, *J. Metals*, **14** (1962) 661 ff; also A. R. Lang, *The Encyclopedia of X-Rays and Gamma Rays*, Ed. G. L. Clark (Reinhold Pub. 1963) pp. 1053-1063.
- [12] Bonse, U., Hart, M., and Newkirk, J. B., *Encyclopaedic Dictionary of Physics, General Review*, Pergamon Press, pp. 391-394.
- [13] Newkirk, J. B., *Phys. Rev.* **110**, 1465 (1958); also *AIME Trans.* **215**, 483 (1959).
- [14] Bonse, U., and Kappler, E., *Z. Naturforsch.* **13a**, 348 (1958).
- [15] Lang, A. R., *J. Appl. Phys.* **29**, 597 (1958).
- [16] Lang, A. R., *J. Appl. Phys.* **30**, 1748 (1959).
- [17] Lang, A. R., *Acta Cryst.* **12**, 249 (1959).
- [18] Borrmann, G., Hartwich, W., and Irmeler, H., *Z. Naturforsch.* **13A**, 423 (1958).
- [19] Barth, H., and Hosemann, R., *Z. Naturforsch.* **13a**, 792 (1958).
- [20] Webb, W. W., *J. Appl. Phys.* **31**, 194 (1960); Yoshimatsu, M., and Kohra, K., *J. Phys. Soc., Japan* **15**, 2367 (1960).
- [21] Schwuttke, G. H., *J. Appl. Phys.* **36**, 2712 (1965).
- [22] James, R. W., *The Optical Principles of the Diffraction of X-Rays*, G. Bell & Sons, London, 1950.
- [23] Renninger, M., *Z. Naturforschung* **19A**, 783 (1964).
- [24] Kohra, K., Yoshimatsu, M., and Shimizu, I., *Direct Observation of Imperfections in Crystals*, eds. J. B. Newkirk and J. H. Wernick (1962), pp. 461-470.
- [25] Renninger, M., *Angew. Phys.* **19**, 20, 34 (1965).
- [25a] Deslattes, R. D., "Advances in X-ray Analysis", Vol. 10, Plenum Press, and *J. Appl. Phys.* **37**, 541 (1966); also Deslattes, R. D., and Paretzkin, B., this symposium.
- [25b] Private Communication, Deslattes, R. D., National Bureau of Standards, Washington, D.C., 1963.
- [26] Batterman, B. W., *Phys. Rev.* **126**, 1461 (1962).
- [27] See, for example, Batterman, B. W., and Cole, H., *Rev. Mod. Phys.* **36**, 681 (1964).
- [28] Ewald, P. P., *Acta Cryst.* **11**, 887 (1958).
- [29] Kato, N., *Acta Cryst.* **11**, 885 (1958).
- [30] Bonse, U., *Z. Phys.* **153**, 287 (1958).
- [31] Bonse, U., *Direct observation of Imperfections in Crystals*, New York Interscience (1962), pp. 431-457.
- [32] Chikawa, J., *Appl. Phys. Letters* **4**, 159, **5**, 31 (1964).
- [33] Chikawa, J., *J. Appl. Phys.* **36**, 3496 (1965).
- [34] Lang, A. R., *Z. Naturforsch.* **20a**, 636 (1965).
- [35] Authier, A., *Proceedings of the 15th Annual Conference on Applications of X-ray Analysis*, eds. J. B. Newkirk and G. Mallett, to be published.
- [36] Penning, P., and Polder, D., *Philips Res. Repts.* **16**, 419 (1961).
- [37] Bonse, U., *Z. Physik* **177**, 385 (1964).
- [38] Kato, N., *Acta Cryst.* **16**, 276, 282 (1963).
- [39] Kato, N., *J. Phys. Soc. Japan* **18**, 1785 (1963).
- [40] Kato, N., *J. Phys. Soc. Japan* **19**, 67 (1964).
- [41] Kato, N., *J. Phys. Soc. Japan* **19**, 971 (1964).
- [42] Takagi, S., *Acta Cryst.* **15**, 1311 (1962).
- [43] Kambe, K., *Z. Naturforsch.* **18a**, 1010 (1963).

- [44] Kambe, K., *Z. Naturforsch.* **20a**, 770 (1965).
- [45] Bonse, U., *Z. Physik* **177**, 529 (1963).
- [46] Bonse, U., *Z. Physik* **177**, 543 (1964).
- [47] Austerman, S. B., Newkirk, J. B., and Smith, D. K., *J. Appl. Phys.* **36**, 3815 (1965).
- [48] Schlössin and Lang, A. R., *Phil. Mag.* **12**, 283 (1965).
- [49] Takagi, M., and Lang, A. R., *Proc. Roy. Soc.* **A281**, 301 (1964).
- [50] Schwuttke, G. H., *Ultrapurification of Semiconductor Materials*, eds. M. S. Brooks and J. K. Kennedy (The Macmillan Comp. 1962) pp. 434-453.
- [51] Kaiser, W., and Keck, P. H., *J. Appl. Phys.* **28**, 882 (1957).
- [52] Bontinck, W. and Amelinckx, S., *Phil. Mag.* **2**, 94 (1957).
- [53] Amelinckx, S., Bontinck, W., Dekeyser, W., and Seitz F., *Phil. Mag.* **2**, 355 (1957).
- [54] Weertman, J., *Phys. Rev.* **107**, 1259 (1957).
- [55] Dash, W. C., *J. Appl. Phys.* **31**, 2275 (1960).
- [56] Fourdeux, A., Bergehan, A., and W. W. Webb, *J. Appl. Phys.* **31**, 918 (1960).
- [57] Kohra, K. and Yoshimatsu, M., *J. Phys. Soc. Japan* **17**, 1041 (1962).
- [58] Yoshimatsu, M., *Japan J. Appl. Phys.* **3**, 99 (1964).
- [59] Schwuttke, G. H., and Sils, V., *J. Appl. Phys.* **34**, 3127 (1963).
- [60] Chikawa, J., *J. Phys. Soc. Japan* **18**, 148 (1963).
- [61] Chikawa, J., *Japan J. Appl. Phys.* **3**, 229 (1964).
- [62] Chikawa, J. and Nakayama T., **35**, 2493 (1964).
- [63] Schwuttke, G. H., *Direct Observation of Imperfections in Crystals*, eds. J. B. Newkirk and J. H. Wernick (Interscience Pub. New York, 1962), pp. 497-508.
- [64] Furusho, K., *Japan J. Appl. Phys.* **2**, 585 (1963).
- [65] Chikawa, J., *Appl. Phys. Letters* **4**, 25 (1964).
- [66] Chikawa, J., *Proceedings of the 15th Annual Conference on Applications of X-Ray Analysis*, eds. J. B. Newkirk and G. Mallett, to be published.
- [67] Furusho, K., *Japanese J. Appl. Phys.* **3**, 203 (1964).
- [68] Furusho, K., private communication. This result was left unpublished because of his death.
- [69] Elistratov, A. M., and Kamadzhiev, P. R., *DAN SSSR*, **125**, 538 (1959) (*Soviet Physics Doklady* **4**, 427).
- [70] Elistratov, A. M., and Kamadzhiev, P. R., *Fizika Tverdogo Tela*, **4**, 3492 (1962) [*Soviet Physics-Solid State* **4**, 2557 (1963)].
- [71] Lang, A. R., *Proc. Phys. Soc.* **84**, 871 (1964).
- [72] Kamiya, Y., and Lang, A. R., *J. Appl. Phys.* **36**, 579 (1965).
- [73] Ishii, S., Fūruqa, T., Sasaki, Y., and Kohra K., *J. Phys. Soc. Japan* **15**, 206 (1960).
- [74] Schwuttke, G. H., *J. Electrochem. Soc.* **108**, 163 (1961) and **109**, 27 (1962) *J. Appl. Phys.* **33**, 2760 (1962).
- [75] Kohra, K., Nakano, S., and Yoshimatsu, M., *J. Phys. Soc. Japan*, **18**, Supplement II, 341 (1963).
- [76] Dash, W. C., *Phys. Rev.* **98**, 1536 (1955).
- [77] Takagi, M., Read to Japanese Physical Society (1965).
- [78] Smith, D. K., Private communication; Lawrence Radiation Lab., Livermore, Calif.
- [79] Lang, A. R., *An Investigation of Crystal Imperfections by X-Ray Diffraction* (Rept. for Contract AF61(052)-449) p. 115.
- [80] Kato, N., *Acta Cryst.* **16**, 276, 282 (1963).
- [81] See, for example, International Union of Crystallography, Conference in Stockholm "The Precision Determination of Lattice Parameters," *Acta Cryst.* **13**, 818 (1960).
- [82] Ellis, T., Nanni, L. F., Shrier, A., Weissmann, S., Padawer, G. E., and Hosokwawa, N., *J. Appl. Phys.* **35**, 3364 (1964); Gillen, P., Yakowaitz, H., Ganow, D., and Ogilvie, R. E., *J. Appl. Phys.* **36**, 773 (1965).
- [83] Bonse, U., and Hart, M., *Appl. Phys. Letters* **6**, 155 (1965); *Z. Physik* **190**, 455 (1966).
- [84] Lang, A. R., and Miuscov, V. F., *Appl. Phys. Letters* **7**, 214 (1965). *Proceedings of*

- the 15th Annual Conference on Applications of X-Ray Analysis, eds. J. B. Newkirk and G. Mallett, to be published.
- [85] Chikawa, J., *Appl. Phys. Letters* **7**, 193 (1965); *Proceedings of International Conference of Crystal Growth*, to be published.
- [86] Bonse, U., *Z. Physik*, **184**, 71 (1965).
- [87] Griffiths, J. H. E., Owen, J., and Wend, I. M., *Defects in Crystalline Solids: Report of Bristol Conference*. London: Physical Society 1954.
- [88] Bambauer, H. U., G. O. Brunner and F. Laves: *Z. Kristallographie* **116**, 173 (1961).
- [89] O'Brien, M. C. M., and Pryce, M. H. L., *Defects in Crystalline Solids; Report of Bristol Conference*. London: Physical Society (1954).
- [90] O'Brien, M. C. M., *Proc. Roy. Soc. Ser. A* **231**, 404 (1955).
- [91] Lietz, J., and Hanisch, M. R., *Naturwissensch.* **46**, 67 (1959)
- [92] Lietz, J., and Hanisch, M. R., *Fortschr. der Mineralogie* **39**, 38 (1961).
- [93] Kato, N., and Lang, A. R., *Acta Cryst.* **12**, 787 (1959).
- [94] Kato, N., *Z. Naturforsch.* **15a**, 369 (1960).
- [95] Kato, N., *Acta Cryst.* **14**, 520, 627 (1961).
- [96] See, for example, Hashimoto, H., Mannami, M., and Naiki, T., *Phil. Trans. Roy. Soc.*, London **253**, 490 (1961).
- [97] Zachariassen, W. H., *Theory of X-Ray Diffraction in Crystals*, 1945.
- [98] Matsubara, T., *J. Phys. Soc. Japan*, **7**, 270 (1952).
- [99] Huang, K., *Proc. Roy. Soc. (London)* **A190**, 102 (1947).
- [100] Borie, B. S., *Acta Cryst.* **10**, 89 (1957).
- [101] Ekstein, H., *Phys. Rev.* **68**, 120 (1945).
- [102] Batterman, B. W., *J. Appl. Phys.* **30**, 508 (1959).
- [103] Efimov, O. N. and Elistratov, A. M., *Fizika Tverdogo Tela*, **5**, 1869 (1963) [*Soviet Physics-Solid State*, **5**, 1364 (1964)].
- [104] Efimov, O. N., and Elistratov, A. M., *Fizika Tverdogo Tela*, **5**, 2116 (1963) [*Soviet Physics-Solid State*, **5**, 1543 (1964)].
- [105] Patel, J. R., and Batterman, B. W., *J. Appl. Phys.* **34**, 2716 (1963).
- [106] Prins, J. A., *Z. Physik* **63**, 477 (1930).
- [107] Miller, F., *Phys. Rev.* **47**, 209 (1935).
- [108] See, for example, James, R. W., *The Optical Principles of the Diffraction of X-rays*, G. Bell & Sons, London, 1950, Chap. II.
- [109] Elistratov, A. M., and Efimov, O. F., *Fizika Tverdogo Tela*, **4**, 2397 (1962) [*Soviet Physics-Solid State*, **4**, 1757 (1963)].
- [110] Efimov, O. N., and Elistratov, A. M., *Fizika Tverdogo Tela*, **4**, 2908 (1962) [*Soviet Physics-Solid State*, **4**, 2131 (1963)]. See also Efimov, O. N., *Fizika Tverdogo Tela*, **5**, 1466 (1963) [*Soviet Physics-Solid State*, **5**, 1066 (1963)].
- [111] Mohanty, G. P., and Azaroff, L. V., *J. Chem. Phys.*, **35**, 1268 (1961).
- [112] Mohanty, G. P., and Azaroff, L. V., *Phys. Rev.* **120**, 1224 (1960).
- [113] Ewald, P. P., *Ann. Phys.* **49**, 117 (1916).
- [114] See, for example, J. M. Cowley, *Fourier Methods in Structure Analysis by Electron Diffraction*, *Reports on Progress in Physics*, **XXI**, 165 (1958).
- [115] Hattori, H., Kuriyama, H., Katagawa, T., and Kato, N., *J. Phys. Soc. Japan* **20**, 988 (1965).
- [116] Kato, N., and Ando, Y., **21**, 964 (1966).
- [117] Hart, M., *Appl. Phys. Letters* **7**, 96 (1965).
- [118] Stadelmaier, H. H., *Z. Metallk.* **52**, 758 (1961).
- [119] Philipsborn, H. von, and Laves, F., *Acta Cryst.* **17**, 213 (1964).
- [120] Greenfield, P., and Beck, P. A., *Trans. Amer. Inst. Min. (Metall.) Engrs.* **206**, 265 (1956).
- [121] Ehrlick, P., *Z. Anorg. Chem.* **247**, 53 (1941).
- [122] Hendricks, R. W., Baro, R., and Newkirk, J. B., *Trans. AIME* **230**, 930 (1964).

# X-RAY DIFFRACTION

## Contributed Papers and Discussion

H. S. PEISER

*NBS Institute for Materials Research  
Washington, D.C. 20234*

### I. Introduction

In his opening remarks the author, as the session rapporteur, raised the question of how relevant and how important were the x-ray diffraction techniques to trace characterization. Were we overoptimistic in our assessment of results obtainable by x-ray diffraction techniques? It is the very insensitivity of many conventional x-ray measurements to the presence of impurities which over and over again has enabled the crystallographer by rather simple methods to interpret measurements in terms of idealized features of crystal structures. In fact only when we either have exceptionally perfect crystals or use refined and sophisticated x-ray techniques, do we stand a fair chance of answering some real trace problems. In their paper J. B. Newkirk and J. Chikawa have shown that these techniques have in fact progressed quite far. The rapporteur challenged the audience to test the prophetic capabilities of these authors to make forecasts on the general applicabilities in trace characterizations of the Pendellösung and Moiré fringe techniques which Dr. Chikawa especially had recently developed.

Dr. Meinke also had convinced us that we were not on the platform under false pretenses. He had pointed out that this Symposium was intended to stress the state of the art with all its present limitations and that no strict definitions of "trace" in terms of ppm or ppb were intended. Indeed let us go back to percent if that is the best we can do.

The highly perfect crystal is the most promising kind of material for reproducibility and with the most varied properties of possible utility. That the x-ray techniques discussed by Drs. Newkirk and Chikawa were mostly limited to such crystals may ultimately not be a serious limitation. Moreover, it is well known how some traces can affect the properties critically. So the determination of these traces is a central aim in the control of properties and reproducibility.

Before introducing the first contributed paper, Peiser made a general comment intended as a guiding thread running through evaluations in this subject area. The chemical analyst's task in the past had been to evaluate quantitatively the composition of materials. He has had, as

others at this Symposium had emphasized, to answer the chemical questions "what" and "how much." The characterization of modern materials requires—and the evidence that leads to this philosophy is compelling—that the additional question be asked: "where in the crystal structure lies the culprit" or, often more appropriately, "where is the crux of the matter?" Closely linked with the "where" is the topic of non-chemical impurities. The host atoms can be replaced by vacancies or they can slip into interstices and thus act like a trace of foreign atoms.

Moreover, everyone appreciated how phase changes may affect properties when in fact there is no change in stoichiometry whatever, and x-ray diffraction can give useful information in this respect. In this audience everyone could tell a tale or two on how a good quantitative analysis had lost its significance through bulk contamination of the specimen surface. However, the discussion should concern traces within crystals. Sizeable three-dimensional inclusions is one possible location for trace elements. Peiser proposed that one should for the sake of this discussion assume that such contaminations can be satisfactorily dealt with by preconcentration treatments, the subject of later sessions.

Other traces within crystals themselves fall into three simple classes: those on two-dimensional crystal planes, one dimensional rows, and those that are of zero-dimensional extent. We know very little about two-dimensional defects—that is, traces concentrated on crystal fault planes, i.e., typically stacking faults. What little could be said concerns chiefly stoichiometry rather than trace contamination.

One-dimensional dislocations are much more accessible to study and permit a few predictions. Quite good crystals have  $10^5$  dislocations per square centimeter. This is not many, yet in such a  $1 \text{ cm}^3$  crystal there are 3 km of fault lines. The crystal stability is undoubtedly increased when these 3 km long atomic-scale passage ways are filled with trace elements of the right size and shape. Up to  $10^{14}$  atoms can hide without introducing much strain. This is only in the part per billion range and the dislocations will be little selective to specific kinds of atoms. It is not difficult to see, however, why crystals will show remarkable resistance to purification at levels below the requirements for reasonable stabilization of dislocations. Conversely, as was properly emphasized in Dr. Newkirk's talk, dislocations lend themselves to decoration, that is they form rows of contamination with diameters of more than one atom. Grain-boundaries and subgrain boundaries can be regarded as regions of very high dislocation densities. Concentration of trace elements at grain boundaries is a well-known phenomenon.

The most challenging type of trace contamination occurs inside the otherwise perfect lattice array by atomic substitution, or in structural interstices. Even here the properties are profoundly affected by the type of geometric relationship at what we call the point defect, the zero-

dimensional defect. It is the crystal chemistry of point defects which undoubtedly will become progressively of greater importance as knowledge of trace characterization advances.

There is a general rule that the better the crystal-chemical fit of a kind of foreign atom in a structure the more evenly distributed these atoms will be. Such atoms will be subject to the classical order-disorder phenomena, in itself a wide-ranging subject not covered in this Symposium. It is these kinds of point defects that are least easily measured by most of the x-ray diffraction procedures discussed. On the other hand, the poorer the crystal-chemical fit the greater the tendency to segregation, constituting a completely different kind of "order," and the more likely are compositional fluctuations and lattice strains that will be detectable by x-ray diffraction methods.

## II. Contributed Papers

The meeting then dealt, all too briefly, with the contributed papers. The one by R. L. Prickett and F. W. Wahldick was entitled, "A High Temperature Single Crystal X-Ray Camera." That work [1]<sup>1</sup> takes the art of x-ray diffraction studies to high temperatures at which precise x-ray diffraction measurements on single crystals have hitherto been virtually unobtainable. The fine instrumental work that has gone into this development was highly praised. Yet, Peiser warned that for most trace characterization work the word "trace" in connection with this paper should be interpreted as parts per hundred. This limitation applies even to vacancy concentration determinations unless the measurements can be combined with good dimensional data. Prickett pointed out the important and unique potentialities of the camera for high-temperature diffusion studies.

Next the rapporteur introduced the paper by T. Inouye and H. Nagami, both originally from the Central Research Laboratory of Tokyo Shibaura Electric Co., well known for a fine research outlook. Dr. Inouye is now working at MIT. The authors asked the rapporteur to speak for them. They have developed a new method of Fourier analysis of observed x-ray powder diffraction line profiles interpreted in terms of stress distribution. The rapporteur put their fine work into perspective in relation to the subject matter of this Symposium. They are describing work on polycrystalline materials. As Dr. Newkirk explained, this severely limits applications to trace characterization. Line shape, moreover, is so complex a subject and so sensitively dependent on a score of other parameters that the interpretation of obtainable results is full of pitfalls, which these authors fully recognized. Nevertheless, Mr. Peiser expressed the view, not challenged by the Symposium members, that the Inouye-Nagami method had two attractive features: first, it enabled internal strain caused by traces to be directly compared

<sup>1</sup> Figures in brackets indicate the literature references at the end of this paper.

with that caused by externally applied mechanical stresses; secondly, Fourier analysis of a line profile was in itself a mathematically justifiable procedure for deriving more usable information contained in a composite resonance, relaxation or other response curve than is often obtained by more direct tests and definitions of resolution.

R. D. Deslattes and B. Paretzkin had carried out microstrain measurements on highly perfect single crystals. The rapporteur's usual warning to listeners in this instance was based on the remarks in Newkirk's and Chikawa's paper that their method does not measure the trace atoms themselves but only the strain effects they produce. Yet these secondary effects give the opportunity to use powerful and sensitive procedures which may become of great value. It must be remembered, however, that some trace elements may, in some crystal-chemical sites, introduce no measurable strain.

Dr. Deslattes, himself, showed some beautiful x-ray topographs of quartz, silicon, and ruby crystals of high perfection taken by their new generally usable method of two-crystal topography [2]. In this method the reference crystal, known to be free of dislocations and observable microstrain, is chosen so that it is slightly mismatched in  $d$ -value with respect to the crystal under observation. This procedure leads to a small decrease in sensitivity compared with the corresponding one using precisely matched crystals. However, such a matched crystal method would need very precise beam collimation and an almost infinite set of reference crystals. For their method the authors had developed a set of six silicon reference crystals cut for external Bragg reflection from chosen sets of atomic planes so that virtually any "unknown" crystal of high perfection could be topographically examined. Deslattes answered questions on the techniques the authors had developed for the cutting, sectioning and strain-free polishing of the silicon crystals.

In view of the critical shortage of time and the perceptive treatment of accurate x-ray intensity measurements for trace characterization in Newkirk's and Chikawa's paper, G. Burley's paper was taken as read, although his analysis follows a different and perhaps even slightly more conservative line than that of Azaroff et al. presented by Dr. Newkirk. Dr. Burley and some other authors in this country and in Japan have obtained x-ray atomic scattering factors of high accuracy from Debye-Scherrer lines. Dr. Burley had pointed out that with these values it has become possible to compare x-ray intensities of crystal powders for the quantitative measurement of point-defect content. He has applied the theory of propagation of errors to individual x-ray lattice reflections. No doubt a similar treatment might be given to the observation of forbidden reflections. The present state of the art for point defect detection sensitivities by x-ray intensity measurements lies in the region of parts per thousand although detailed predictions vary with atomic weights concerned. The rapporteur emphasized, however,

that these results are obtainable especially for foreign atoms that give the best crystal-chemical fit, i.e., for atoms which will form solid solutions with least fluctuations of composition and lattice strain. If the Pendel-lösung fringe technique became effective the sensitivity of detection of point defects by x-ray scattering amplitudes might well jump by several orders of magnitude.

In introducing the last contributed paper by W. van Gool, the rapporteur expressed pleasure that van Gool had come to participate in the Symposium. On our question of where in the crystal structure did the defects lie, his message to us was: we had better develop a good formal language in describing the relevant locations. In science, a precise language often precedes understanding.

Dr. van Gool, himself, presented to the Symposium some of the basic concepts from his recent book, "Chemical Principles of Defect Chemistry of Crystalline Solids" [3]. Accepting that the progress in experimental techniques provides the possibility to determine impurities in host materials in ever decreasing concentrations, the question of the significance of such determinations becomes more important. Two aspects are essential in answering that question. First, the function of trace analysis in materials research is to obtain information helpful in the understanding and control of trace-sensitive properties. Secondly, native defects (vacancies, misplaced atoms, etc.) may be just as important as impurities for those properties.

The first aspect illustrates why information about certain impurities may be more valuable than knowledge of some other impurities. The influence of the different groups of impurities upon the physical properties may differ considerably. Therefore, the experimental possibility of determining certain impurities in very low concentrations does not guarantee that the essential impurities have been detected. The second aspect shows that even a complete determination of all impurities by atomic absorption, emission spectroscopy, activation analysis, etc., still does not guarantee that the essential information has been obtained.

The problem then is to find methods revealing the actual situation: first the predominant species and then the defects present in lower concentrations. Recently some progress in this problem has been made for inorganic crystalline materials by introducing a generalized description of the defect chemistry. This description permits the interpretation of measurements of densities, lattice parameters, solubility of impurities, and deviation from stoichiometry, without assuming special models. The description is not detailed, but it characterizes the predominant species of all defect situations reconcilable with the observed data. It is encouraging that in some situations this generalized description fulfills already the purpose of the trace determination, viz, the description and the means for control of the trace-sensitive material properties.

### III. Discussion

Dr. van Gool has given the example of density-sensitive defect properties. This is a topic which leads us right into the subject of the highest attainable accuracy in density determinations, a subject clearly of direct concern to the NBS Metrology Division. At the invitation of the rapporteur H. A. Bowman of that Division presented the state of the art in density comparisons, although Dr. H. Kaiser's comment applies—this is a single-number characterization—yet a very useful one. Although the precision of modern density experiments referred to water is better than one part in 10 million, such measurements are uncertain by several parts in one million due to the uncertainty in the density of a particular sample of water. Recently, Cook [4] has measured the density of mercury directly to about one part in a million, but difficulties in transferring the accuracy inherent in this density value to other materials have prevented full utilization of this measurement as a reference in other density work.

NBS is currently developing a family of solid objects which will collectively serve as a reference density in comparison work [5] and it is expected that densities derived experimentally from this reference will be uncertain by significantly less than one part in a million. The Bureau's Cartesian Diver system [6] is a primary tool in this work because it can detect differences of apparent mass in water of objects weighing 10 grams reproducibly to better than  $10^{-7}$  grams. When specimen wetting is a problem, a very small addition of a wetting agent can be used without introducing a significant error.

The rapporteur pointed out that Mr. Bowman had also made significant simplifications in technique for density determinations to 1 part in  $10^5$ , so that such measurements can be carried out simply with standard laboratory equipment. Mr. Peiser expressed hope this technique will shortly be published, as it might prove very useful at least for the empirical comparison of crystals of differing trace content.

Dr. Newkirk in further discussion emphasized the potentiality of the Pendellösung method by which an x-ray intensity could be effectively measured by an angle and a length measurement. This is a very unusual physical situation which should be exploited because generally in metrology lengths and angles can be measured far more readily than a radiation flux.

Dr. Chikawa commented further on his Moiré fringe measurement by which lattice spacings could be compared between very similar crystals differing only in trace element content causing lattice expansions or contractions of the order of 1 in  $10^8$ . The method is akin to a vernier formed by the lattices compared and is not limited by the sharpness of an x-ray emission line, as are other methods in current use.

Peiser in thanking the authors of contributed papers summarized his view that x-ray diffraction techniques had an established and important

place in the characterization of materials. For the time being, however, the trace analyst should not build too much confidence in existing x-ray diffraction procedures. Nevertheless, crystal strain measurable by such methods was an important parameter additional to the trace composition of materials. Furthermore, the most recent developments in x-ray diffraction methods left the substantive hope that by their use direct data on trace composition will soon be obtainable.

#### IV. References

- [1] Prickett, R. L., and Wahldick, F. W., A High Temperature Single Crystal X-Ray Camera, Proceedings of the 13th Annual Conference on Application of X-Ray Analysis, Denver **8**, 86 (1965).
- [2] Deslattes, R. D., Torgesen, J. L., Paretzkin, B., and Horton, A. T., Observations of Dislocations in Ammonium Dihydrogen Phosphate: Production of Dislocation-Free Crystals, *J. Appl. Phys.* **37**, 541 (1965).
- [3] Van Gool, W., *Chemical Principles of Defect Chemistry of Crystalline Solids*, Academic Press, New York (1966).
- [4] Cook, A. H., Precise Measurements of the Density of Mercury at 20 °C, *Phil. Trans. Roy. Soc.* **254**, 125-154 (1961).
- [5] Bowman, H. A., The Development of a Working Density Standard, 14.8-4-65, Proc. I.S.A. Conference, Los Angeles (1965).
- [6] Bowman, H. A., and Schoonover, M. R., The Cartesian Diver as a Density Comparator, *J. Res. NBS* **69C**, 217-223 (1965).



# PHYSICAL OPTICAL METHODS

## Contributed Papers and Discussion

H. P. R. FREDERIKSE

*National Bureau of Standards, Washington, D. C. 20234*

### I. Introduction

The purpose of this session was to focus attention on optical phenomena investigated as physical effects but hitherto little used as a method for chemical trace characterization. While in a spectrochemical analysis the sample is evaporated and the observed optical spectra are associated with the free atoms or ions, the physical effects presently under discussion are due to atoms, ions, and defects, surrounded by the host lattice. Hence one could call the latter kind of characterization non-destructive as opposed to the destructive method of spectrochemistry.

The wealth of optical phenomena that lend themselves to exploitation as a method for chemical analysis is enormous. As in every area of characterization, one will need a catalogue of measured and calculated spectra and intensities before these effects will be ready for everyday use by the scientist interested in the purity of his sample. Although a fair amount of such data can be found in the literature, very little effort has been made to put the results systematically in the handbooks. Only in the limited area of semiconductors and color centers does one find some systematic listings of absorption and luminescence data.

The need for characterization *in situ* has become more apparent during the last 10-15 years. Many important solid state effects and electronic devices depend not only on the nature of the foreign element or defect, but also on its location and its environment in the lattice. The development of magnetic materials (e.g., ferrites) requires a knowledge of the position of the magnetic ion. The question of "random-distribution-or-clusters" is important in semiconductors and insulators. The maser and laser provide examples where the crystalline environment of the "trace-impurity" is essential to the functioning of the device. Electron-, neutron- and other high-energy radiation produces desired or undesired defects whose nature and location have to be known.

In nearly all cases the important physical effects are caused by foreign elements or defects present in amount of  $10^{-4}$  to  $10^4$  ppm. Concentration changes of one or two orders of magnitude often radically alter the observed effects.

The optical phenomena fall into three categories:

(a) electronic excitation (or de-excitation) to higher (lower) states of the "impurity" or defect itself [1].<sup>1</sup>

Examples: optical absorption and luminescence of  $\text{Cr}^{3+}$  in  $\text{Al}_2\text{O}_3$  or Mn in CdS; F-center absorption, bleaching, luminescence, photoemission, etc. [2].

(b) electronic excitation from "impurities" to energy bands of the host lattice [3],

Examples: optical absorption and photoconductivity of B in Si or Cu in InSb.

(c) local vibrations or perturbations of the Reststrahlen spectrum (lattice vibrational or phonon states) due to foreign elements of different mass.

Examples:  $\text{OH}^-$  in many host lattices (e.g., KCl,  $\text{TiO}_2$ ); Ne in solid Ar.

A great number of optical effects can be observed especially if one counts also those variations caused by external fields. An incomplete listing includes: optical absorption, reflectivity, luminescence (also electro, tribo, thermo, and cathode luminescence), photoconductivity, photoemission, Zeeman effect, Stark effect, piezo-optical effects and stimulated emission.

## II. Invited and Contributed Papers

Eugene Wong's (UCLA) introductory discussion was concerned with some of the phenomena mentioned under (a) above. He focused attention particularly on the spectra of transition metal ions and rare earth ions in simple host lattices. These spectra can be understood—at least qualitatively—in terms of the free ion states, the crystalline field surrounding the ion, the spin-orbit splitting, and other minor effects affecting the position and strength of the absorption lines [1].

In the first contributed talk J. A. Baker (Dow Corning Corp.) made a strong plea to exploit infrared spectroscopy for the detection of trace impurities in semiconductors. He illustrated his point by discussing five major impurities in silicon: carbon, oxygen, arsenic, boron and phosphorus. The first two give rise to vibrational bands at  $16 \mu$  [4] and  $9 \mu$  [5], respectively. These bands are obscured by the intrinsic absorption bands of the host lattice. However, by employing a difference technique, using a slice of pure silicon as the reference material in a double beam spectrophotometer, it is possible to measure the carbon or oxygen bands accurately. The limit of detection for these two elements is 0.2 ppm.

At low temperatures the elements arsenic, boron, and phosphorus produce absorption bands at  $26 \mu$ ,  $32 \mu$ , and  $32 \mu$ , respectively. These

---

<sup>1</sup> Figures in brackets indicate the literature references at the end of this paper.

bands are caused by electronic ionization of the ions. Because silicon is reasonably transparent beyond  $16 \mu$ , no difference technique is required. From comparison with resistivity measurements (on silicon samples containing only one of these elements as major impurity) one can conclude that the limit of detection is 0.5 ppb.

The method is appropriate for determining the concentration of single doping elements in silicon and germanium [3], III-V compounds, and several other semiconductors. The lowest amount that can be detected and identified depends on the maximum purity attainable for the host lattice.

The contributed paper by Lorimor and Spitzer (University of Southern California) and Willardson and Allred (Bell and Howell) dealt with a similar infrared detection method. These authors discussed local modes due to associated pairs of foreign elements. For instance, by diffusing lithium into boron-doped silicon (p-type) one produces Li-B pairs [6]. The pairs (as well as the single lithium and boron-atoms) give rise to local vibrational modes in the  $14\text{--}20 \mu$  spectral region. Substitutional impurities lighter than the atoms they replace will increase the frequencies of the host-lattice modes. An example is the peak at  $362 \text{ cm}^{-1}$ , resulting from aluminum in GaAs. Table I summarizes the lower limit of detectability for several of the impurities considered in this study.

TABLE I. Lower limits of detectability for several impurities.

Semiconductor	Impurity	Lower limit of detectability	
		ppm	atoms/cc
Si	B(-Li)	40	$2 \times 10^{18}$
GaAs	P	1	$4 \times 10^{16}$
GaAs	Al	1	$4 \times 10^{16}$
GaAs	Te (-Li)	20	$1 \times 10^{18}$
GaAs	Zn (-Li)	20	$1 \times 10^{18}$
GaAs	Mn (-Li)	20	$< 1 \times 10^{18}$
GaAs	Cd (-Li)	20	$\sim 1 \times 10^{18}$
GaAs	Si and Si-Li	2	$1 \times 10^{17}$

T. Chang (NBS) presented a contributed paper advertising the potentialities of electron spin resonance absorption as an analytical tool. The spectrum results from transitions between electronic levels split by an external magnetic field and is observed in the microwave region. A commonly used frequency is 9000 Mc (corresponding to  $\lambda = 3 \text{ cm}$ , X-band) and the applied field is of the order of 3000 oersted.

Any ion or defect with an unpaired electron can be detected; often low temperatures are required to observe the spectrum. A vast amount of theoretical and experimental knowledge is available in the literature [7]. Some of the best known examples are: ions of the transition elements

(e.g.,  $\text{Cr}^{3+}$  in  $\text{Al}_2\text{O}_3$ ), color centers (F-center in  $\text{KCl}$ ), "impurities" in semiconductors ( $\text{Sb}^{5+}$  in  $\text{Ge}$ ), free radicals ( $\text{I}^-$  in  $\text{CH}_3\text{I}$ ).

The method is extremely sensitive; in some cases as few as  $10^{10}$  spins can be detected. More generally, concentrations of  $10^{-1}$  to  $10^{-3}$  ppm in a sample of one gram are easily observable. Often the e.s.r. method is able to identify the trace impurity (e.g., from the hyperfine structure); also, it can provide information about the location of the center (substitutional or interstitial).

In this paper the example of transition metal ions in  $\text{TiO}_2$  was discussed, including  $\text{Ti}^{3+}$ ,  $\text{Cr}^{3+}$ ,  $\text{Mn}^{4+}$ ,  $\text{Mn}^{3+}$ ,  $\text{Fe}^{3+}$ ,  $\text{Ni}^{3+}$ ,  $\text{Co}^{2+}$ ,  $\text{Ni}^{2+}$ ,  $\text{Cu}^{2+}$ ,  $\text{Nb}^{4+}$ ,  $\text{Ta}^{4+}$ ,  $\text{Ce}^{3+}$ , and  $\text{Gd}^{3+}$  [8].

## II. References

- [1] Ballhausen, C. J., *Ligand Field Theory*, McGraw-Hill Book Company, New York, 1962.
- [2] Schulman, J. H., and Compton, W. D., *Color Centers in Solids*, The Macmillan Company, New York, 1962.
- [3] Geballe, T. H., in *Semiconductors*, N. B. Hannay, ed., Reinhold Publishing Corporation, New York, 1959, Chap. 8.
- [4] Newman, R. C., and Willis, J. B., *J. Phys. Chem. Solids* **26**, 373 (1965).
- [5] Kaiser, W., and Keck, P. H., *J. Appl. Phys.* **28**, 882 (1957).
- [6] E.g., Balkanski, M., and Nazarewicz, W. A., *J. Phys. Chem. Solids* **27**, 671 (1966).
- [7] E.g., Low, W., *Solid State Physics*, Suppl. 2, F. Seitz and D. Turnbull, ed., Academic Press Inc., New York, 1960.
- [8] Gerritsen, H. J., *Paramagnetic Resonance*, Proceedings of the First International Conference, Jerusalem, 1962, Academic Press Inc., New York, 1963, p. 3.

# CHEMICAL SPECTROPHOTOMETRY IN TRACE CHARACTERISATION

T. S. WEST

*Department of Chemistry, Imperial College of Science and Technology,  
University of London, London S.W. 7, U.K.*

## I. Introduction

The principal concern of this contribution is to review the current status of analytical potentiality within the area of chemical spectrophotometry. This is an extensive area and, for present purposes, it will be defined as being associated with the absorption of radiation in the range *ca.* 2000–8000 Å, *i.e.*, the spectral range of a conventional u.v./visible spectrophotometer. In times gone by the word spectrophotometry has been associated almost exclusively with the mechanised or instrumented aspects of colorimetry in solution. But, recent developments within the past few years have made it patently obvious that there are uses for spectrophotometers other than the measurement of absorption of radiation by molecules in solution or in the solid state. It has also become apparent that some of these developments offer very attractive possibilities for trace characterisation and determination which were hitherto scarcely thought to be possible.

The absorption of radiation by molecular species has long been used by analytical chemists, and the basic requirements and characteristics of the technique are well recognized. However, although the majority of molecular species absorb radiation of a characteristic waveband, thus exhibiting a 'colour' corresponding to the sum of the unabsorbed parts of the visible range of the electromagnetic spectrum, there are many which not only absorb (primary) radiation, but subsequently re-emit (secondary) radiation, usually of a longer wavelength. These are fluorescent or phosphorescent compounds. Based on these phenomena we have the twin techniques of spectrofluorimetry and spectrophosphorimetry which offer some unique advantages not possessed by absorption spectrophotometry. These techniques have been grossly neglected by analytical chemists for reasons which are not easy to define. It is obvious that this neglect is not likely to persist in view of the remarkable analytical sensitivity and versatility which they offer.

In many philosophical arguments of recent years there has been much discussion of the areas of responsibility of the chemist and the physicist and the general conclusion appears to be that, broadly speaking, chemists

should be concerned with molecules and physicists with atoms. However, sharp lines of demarkation are nonscientific in this context and there has recently been a trend shown in the naming of the departments of some new universities and government research institutions whereby, instead of departments of chemistry or physics, we find departments of 'molecular studies' or of 'atomic studies' which cut across the older and perhaps more rigid ways of compartmentalised thinking. In the U.K. the Atomic Energy Research Establishment at Harwell has recently re-designated its former Division of Analytical Chemistry as the Division of Analytical Sciences, and similar events have probably occurred in many other places. It may yet prove to be the case that the new designations of university departments will be more rigid and inflexible than the older, now rather elastic ones but, be that as it may, it is certainly appropriate that those of us who, in the past, have thought of ourselves as analytical chemists should now consider ourselves as *analytical scientists* and cease to worry too much about Liebafsky's now classic comment that the chemistry is going out of analytical chemistry [1].<sup>1</sup> This trend towards analytical *science* rather than *chemistry* is certainly very obvious in the programme of this 1st Symposium of the National Bureau of Standards on Trace Characterisation and it appears to the writer that these wider horizons are very much to be welcomed.

It is against this background of thought that the words 'chemical spectrophotometry' in the title of this contribution will, therefore, be interpreted broadly to include the absorption of u.v./visible range radiation by atoms as well as by molecules. The concepts and techniques of atomic-absorption spectrophotometry (AAS) are indeed more familiar to 'physicists' than to 'chemists,' but the analyst or analytical scientist must not, and indeed cannot, allow any artificial conceptual barrier to hinder or proscribe the development of his researches. The analytical implications of the absorption of radiation by free atomic species are very impressive indeed. The sensitivity of the technique is uniformly high and in all known instances it can be regarded as specific for individual elements.

Most atoms will absorb radiation in the u.v./visible range of the spectrum, as will most molecules, so that the coverage of atomic-absorption spectrophotometry as presently practised extends over a wide area of the periodic table. But, whereas a relatively small number of molecules exhibit fluorescence, it appears from our present state of knowledge that the new technique of atomic-fluorescence spectrophotometry (AFS) will have a much wider coverage than molecular-fluorescence spectrophotometry.' The author and his colleagues have as yet not failed to find atomic fluorescence wherever they have looked for it within the limits of their present experimental capability. Moreover, the technique

---

<sup>1</sup> Figures in brackets indicate the literature references at the end of this paper.

offers unique sensitivity as well as specificity of determination and there appears to be every reason to forecast a very considerable impact for it within the next decade.

These then are the phenomena and techniques which will be principally discussed in this contribution:

1. the absorption of radiation by (dissolved) molecules, Molecular-Absorption Spectrophotometry;
2. the absorption/re-emission of radiation by (dissolved) molecules, Molecular-Fluorescence Spectrophotometry;
3. the absorption of radiation by (free) atoms, Atomic-Absorption Spectrophotometry;
4. the absorption/re-emission of radiation by (free) atoms, Atomic-Fluorescence Spectrophotometry.

Within this framework it is the author's intention to discuss briefly and non-mathematically the basic principles of these techniques and to review some recent progress, though in most instances this is particularly well done in the biennial reports of these areas published in "*Analytical Chemistry*" and need scarcely be added to here. It will be an important consideration to assess the present day capabilities of these techniques and to try and forecast probable developments in the near future. It is not, however, at all intended that this should be an exhaustive review of the current status of these techniques, but rather that it should show the scene as viewed through the eyes of one person engaged in these particular areas of analytical research.

## II. Molecular-Absorption Spectrophotometry

(The absorption of radiation by molecules in solution)

Although there is probably a considerable future for the development of solid-state absorption spectrophotometry in thin films and for techniques allied to diffuse-reflectance spectrophotometry, particularly in view of the increasing attention which is being paid to direct solid-state analytical techniques, this discussion will be limited entirely to the absorption spectrophotometry of solutions since this is undoubtedly one of the backbone techniques of modern trace analysis.

The principles and techniques of molecular absorption spectrophotometry are, of course, very well known and little need be said about fundamental aspects except in as much as it is necessary for the purpose of discussion.

### A. SELECTIVITY OF REACTION

A molecule may be regarded as possessing two different kinds of energy, kinetic and potential, whereas a beam of radiation may be regarded as an electromagnetic waveform disturbance or photon (particle) of energy propagated at the speed of light. Before the molecule

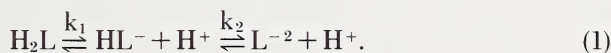
can absorb radiation it must interact with it and this interaction must occur within the period of oscillation of the light wave, *ca.*  $10^{-15}$  sec, *i.e.*, the period during which the photon and the molecule are in contact. There is no possibility of direct interaction between the translational energy of the molecule and a light beam since a charge separation *must* be involved. Consequently, exchange can only occur by interaction with the potential energy component of the molecule's total energy *via* movement of electrons. The energy of photons in the u.v./visible range of the spectrum corresponds to *ca.* 50–150 kcal/mole so that we are concerned here with electronic transitions rather than with vibrational or rotational transitions, though these may also be involved and impart superimposed fine structure on the electronic absorption bands. Furthermore, the electronic levels inside molecules are quantized so that the absorption bands can occur only at definite values corresponding to the energies required to promote electrons from one level to another. As a result of this the absorption spectrum of a molecule should correspond to sharply defined absorption bands, but the effect of the multiplicity of different vibrational and rotational levels in molecules and of solvent molecules associated with the solute molecules is to smooth out these bands so that broad, rather featureless absorption spectra are usually exhibited by almost all molecules in solution. This at once places a physical restriction on the selectivity of molecular-absorption spectrophotometry, for obviously in a given expanse of wavelength scale as presented by the resolution of a spectrophotometer one can only obtain a very limited number of absorption bands without very considerable overlap. Consequently, even where spectra are well separated, it is only possible to resolve a mixture of a very few absorbing species without recourse to complicated mathematical analysis in the process.

Although very many organic compounds absorb quite strongly, only a limited number of inorganic ions do, and it is the normal *modus operandi* of inorganic absorption spectrophotometry to add a molecule or reagent species to the solution of the inorganic ion which will react with it and, in the process, bring about a marked change in the spectral absorption characteristics of the reagent. It is necessary that, along the wavelength axis, the absorption spectrum of the reagent-ion adduct should be well separated in at least one place from the absorption spectrum of the reagent itself, though it generally matters little if it is separated from that of the ion because the intensity of the absorption band due to the latter is low. In any event, it is common practice to add a fairly large excess of the reagent so that virtually all of the ionic species are caused to react with the reagent. It is also desirable, though not strictly essential, that the separation between the two spectra should be good with respect to the absorbance axis so that the maximal sensitivity of reaction may be forthcoming.

1. *Mechanism of Colour Production*

As a generalisation, it can be said that most of the organic molecules which are used as reagents in inorganic absorption spectrophotometry constitute the chromophore of the absorbing species which is formed and that the spectral response which is produced can be ascribed to structural changes which are brought about in the reagent molecule following reaction with the inorganic ion. Usually, a complex formation reaction between the ion and the organic molecule acting as a multi-dentate ligand is involved. Now, complex formation may be defined as the union of a ligand, in which a donor atom furnishes a lone pair of electrons, and a cation, which acts as an acceptor and incorporates these electrons into empty levels in its own orbitals. G. N. Lewis defined a base as an electron-pair donor and an acid as an electron-pair acceptor. It is, therefore, apparent that there is no essential difference between acid-base and complex formation phenomena. The implications of this for absorption spectrophotometry are clear.

Most organic chelating agents are themselves protic acids and dissociate according to a well defined pattern, e.g.,



Obviously there will be serious competition between hydrogen and metal ions for the ligand molecules. Metal ions which form weakly bound chelates will only be able to react efficiently with the reagent in solutions of high pH, whereas metal ions which react more strongly will form complexes in solutions of much lower pH. Thus pH control can provide some means of interelement analytical selectivity for those metals which react in more acidic media than most others. Another more important implication for selectivity of reaction may also be drawn, however. Consider the reaction between a metal ion,  $\text{M}^{+2}$ , and a ligand species,  $\text{HL}^-$ , to form a chelate complex,  $\text{ML}_2^{-2}$



The net effect of the reaction is that each ligand molecule has one proton removed in the process. It is not surprising, therefore, to find that in most instances the colour reaction developed as a result of complex formation closely resembles that which is produced by the addition of the same amount of alkali to the reagent solution to remove the same number of protons per ligand molecule. Although the Lewis theory signifies that there is not any *essential* difference between the proton and the metal ion,  $\text{M}^{+2}$ , there is, of course, an enormous physical difference between the two, particularly with respect to size and electronic structure, so that it is not possible to argue that there should be no change of

colour as a result of complex formation since each proton is replaced by one equivalent of another cation. The hydrogen ion constitutes a 'bare' proton, whereas the nucleus of other cations is heavily screened by their associated electrons. Consequently, the addition or removal of a proton to a ligand molecule has a marked effect upon the electronic structure of a chromophore, whereas the addition or removal of other cations, unless they themselves are deformable or undergo charge-transfers, is usually of little effect. This point is well illustrated by an examination of the absorption spectra of some of the 1:1 complexes formed between various metal ions and the dicarboxymethylaminomethyl substituted 1,2-dihydroxyanthraquinone reagent, Alizarin Complexan, *cf.* Figure 1. Apparently, any metal ion of suitable co-ordination geometry and affinity for the donor atoms in a ligand, can be expected to react with the formation of similarly coloured complexes all of which approximate to that of one of the more highly ionised (i.e., deprotonated) forms of the ligand molecule. Some divergence of the absorption spectra can only be expected to occur where there is some degree of covalency in the bonding between ligand and cation. The more covalent the bond the greater the interaction between the electrons of the ligand's molecular orbitals and those of the cation and the greater the divergence of the absorption spectrum of the chelate away from that of the appropriately deprotonated metal-free ligand.

## 2. Identity of Liganding Atom

The implication of this is that one cannot expect to achieve any simple or easily won degree of analytical selectivity by moving from one reagent to another relying on the conventional oxygen and nitrogen donor atoms

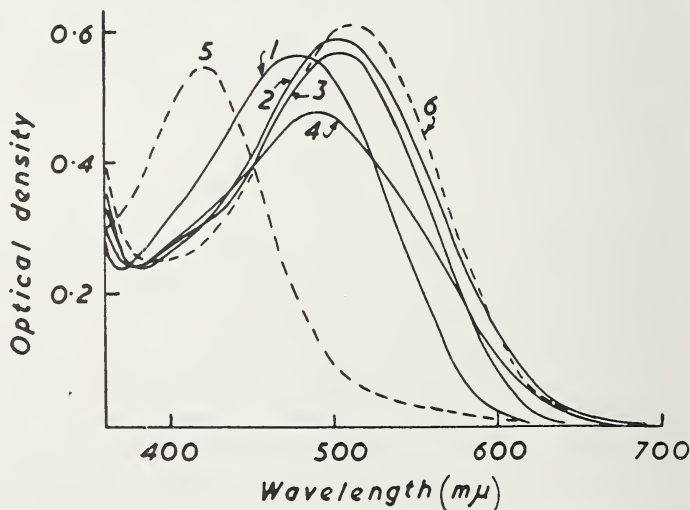


Figure 1. Absorption spectra of metal chelates of Alizarin Complexan at pH 4.3. (1) Pb; (2) Th; (3) Ni; (4) Ce(III); (5) Free reagent; (6) Free reagent at pH 7.

that are used almost exclusively in most organic reagents. However, it is apparent that the introduction of some other donors such as sulphur, selenium, arsenic and phosphorus should achieve some selectivity of response. Some work has already been done in this area and it is probable that some measure of success will be achieved with this type of reagent in the future. For example, it is interesting to study the reactivity of 8-mercaptoquinoline, the sulphur analogue of 8-hydroxyquinoline. Bankovskii and his co-workers [2] have shown that this reagent has high selectivity for metals with a high affinity for sulphur. Thus rhenium [3] may be determined very selectively at 438  $m\mu$  in a chloroform extract from 11.5M hydrochloric acid without interference from molybdenum and tungsten. Similarly, [4] palladium may be determined at 485  $m\mu$  following extraction from 50% hydrochloric acid in the presence of some thiourea to mask copper, gold, mercury (II), osmium, platinum, ruthenium and silver which would also extract. The only interference appears to be due to molybdenum (VI) and this can easily be back-washed from the organic phase by 8M hydrochloric acid. It is out of the scope of a brief review such as this to cite other instances, but a survey of the biennial reviews in *Analytical Chemistry* will reveal other examples of selectivity gained in this direction by the substitution in organic reagents of donor atoms other than nitrogen or oxygen. It is also apparent that permutations of the available donor atoms may lead to some rather interesting gains in selectivity of reaction, and that this is an avenue of approach which is worthy of further exploration.

### 3. Steric Hindrance in Organic Reagents

In the past, however, more attention has been paid to steric hindrance as a means of increasing selectivity of reaction. This has not been singularly successful, except in one or two rare instances, however. It is, of course, a rather negative approach in that one is trying to suppress the activity of a reagent towards certain ions and consequently there is danger that all reactivity may be suppressed or that rather weak complexes may be produced for those cations which still react. Some of the outstanding successes in this area have led to some curious errors in the literature. For example, remaining with the 8-hydroxyquinoline model, we have the now classic work of Merritt and Walker [5] who made the exciting discovery in 1944 that the 2-methyl substituted reagent was selectively unreactive towards the precipitation of aluminium, whilst it still precipitated most other ions in an exactly similar manner to 8-hydroxyquinoline. They ascribed this, not unreasonably, to steric hindrance. Now it is true that 2-methyl-8-hydroxyquinoline shows no visible signs of reaction with aluminium and it may have been this that led Hynek and Wrangell [6] to describe an ingeniously specific spectrophotometric method for aluminium. First of all, other extractable metals were removed by a chloroform extraction with the 2-methyl-8-

hydroxyquinoline reagent and then the aluminium was extracted similarly with 8-hydroxyquinoline and determined in the usual way. However, this method is based on a fallacy, because appreciable amounts of aluminium are extracted by 2-methyl-8-hydroxyquinoline even at pH 4.5. The author and his co-workers [7] recently showed that a fluorescent complex (370/480  $m\mu$ ) is extracted from aqueous solution. Earlier work by Ohnesorge and Burlingame [8] had demonstrated the existence of a 1:1 complex in an entirely non-aqueous solution. The 'selectivity of steric hindrance' must, therefore, be interpreted rather carefully within prescribed conditions.

The reagent 2,9-dimethyl-1,10-phenanthroline or neo-cuproine furnishes another example of a similar nature. Because of the steric hindrance of the methyl groups this reagent does not form a coloured product with iron (II) and it is, therefore, virtually specific for copper (I) [9] though it offers a rather low sensitivity. However, this has led to a suggestion that the reagent may be used as a specific extractant for copper [10], whereas several other metals, e.g. cadmium, cobalt, nickel, silver and zinc can be quantitatively extracted by it [11] so that it is once again demonstrated that it is dangerous to extrapolate the meaning of the words "selectivity" or "specificity" from one context to another.

Once again, these are only two examples of the use of steric hindrance to gain selectivity of reaction.

#### 4. Chelate-Cage Reagent Molecules

The phenomenon of the clathrate type of compound is well recognized. This idea can be extended to the realm of absorption spectrophotometry using chelating agents *via* the principle of devising chelate "cages" into which only ions of the requisite size may fit. Close and West [12], for example, devised the reagent *cyclo*-tris-7-(1-azo-8-hydroxynaphthalene-3,6-disulphonic acid) now known as Calcichrome, which functions on this principle. The reagent, Figure 2, is constituted of three self condensed diazotized H-acid units which have formed a cyclic trimer involving a three ortho-hydroxyazo bond system in a tight cage in the centre of the molecule. At pH 12 this reagent reacts only with calcium ions (ionic radius 0.99 Å) to form a colour body. Strontium (1.12 Å) and barium (1.34 Å) are too big to fit into the cage and other ions which might be expected to fit are either precipitated at the pH of operation or are present as anionic complexes (e.g., zincate, etc.) and are not capable of reacting with the anionic ligand. The reagent has been used for the spectrophotometric determination of calcium in the presence of several thousand-fold amounts of barium or strontium [13] thus forming an interesting, though not particularly sensitive [ $\epsilon_{615m\mu} = 7600$ ] spectrophotometric method for calcium. It must be reported, however, that Russian workers have challenged the cyclic nature of the molecule and

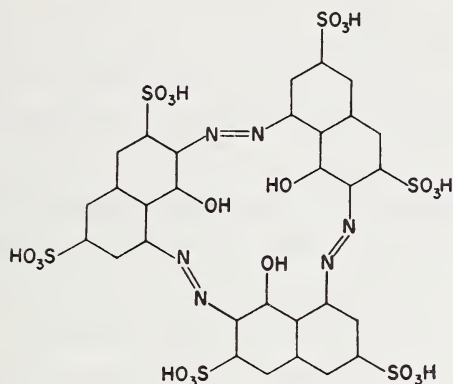


Figure 2. Calcichrome [(Cyclotris-7-(1-azo-8-hydroxynaphthalene-3,6-disulphonic acid)].

have proposed [14] an alternative open-chain structure in which one of the amino groups is replaced by a hydroxyl group, thus terminating the possibility of ring closure as originally proposed by Close and West.

More recently another 'chelate cage' molecule has been proposed as a spectrofluorimetric reagent for magnesium. The reagent is *N,N'*-bis-salicylidene-2,3-diaminobenzofuran, (BSAF), Figure 3, which provides a fairly rigid square planar cavity between the azomethine nitrogen atoms and the phenolic oxygens suitable for accommodation of ions having an ionic radius of ca. 1 Å [15]. It was found that most of the ions examined which had ionic radii between 0.5 and 0.8 Å reacted, whilst none with radii greater than 1 Å showed any reaction whatsoever. Structurally similar reagents such as *N,N'*-bis-salicylideneethylenediamine and *N,N'*-bis-salicylidene-1,2-diaminobenzene have been examined also [16] [17] but these form complexes with a wider range of ions, many of them having ionic radii larger than 1 Å and, in addition, they form fluorescent complexes with ions such as aluminium, beryllium, gallium, indium and zinc, whereas BSAF forms strongly fluorescent complexes only with

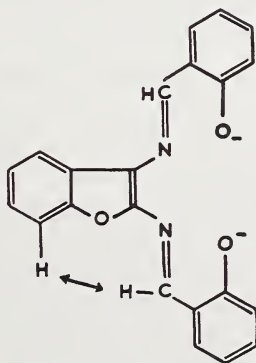


Figure 3. *N,N'*-Bis-salicylidene-2,3-diaminobenzofuran.

magnesium (0.66 Å) at pH 10.5 (475/545 m $\mu$ ) and gallium (0.60 Å) at pH 5 (475/545 m $\mu$ ). The BSAF reagent furnishes an elegant and sensitive spectrofluorimetric method for the determination of submicrogram amounts of magnesium in the presence of preponderant amounts of calcium [18].

The 'chelate cage' principle has been little exploited as yet, but it would appear to offer many interesting possibilities for further investigation and it will very probably become a much more thoroughly explored avenue of research in future years.

### 5. Formation of Ternary Complexes

Most of the complex or chelate systems which are used in inorganic absorption spectrophotometry are binary complexes (mono- or polynuclear as the case may be) in which the test ion 'M' reacts with one species of ligand, 'L' to form absorbing species of the nature ML, ML<sub>2</sub>, ML<sub>3</sub>, etc. It has already been pointed out that the chances of other metal ions 'M'', 'M"', etc. duplicating the reactions of 'M' are excellent and that the absorption spectra of these other complexes may very well closely resemble those of each other and of a more fully deprotonated form of the ligand molecule. It is interesting, therefore, to speculate that if one were to devise complexes in which two ligands 'L' and 'R' react simultaneously with a metal ion 'M' to form a 'mixed' or 'ternary' complex, e.g., MLR, ML<sub>2</sub>R; or some such body, then the possibilities of duplication of such ternary complex formation should be considerably less. As a result, such ternary complexes should probably be analytically more selective than conventional binary complexes. Very little work has been done in this area, but that which has been done has yielded some significant results and may perhaps be illustrated by two differing reagent systems investigated by the author and his co-workers.

**a. Methods of Ternary Complex Formation.** There are two principal ways in which a ternary complex may be put together. In one of them one can consider that the ion forms a co-ordination unsaturated complex or chelate with the first ligand so that not all the positions on the co-ordination sphere of the ion are taken up by the first ligand. These positions may then be taken up by the second ligand if the geometry is suitable to form a ternary complex. A glance at the co-ordination numbers and principal valences of various ions shows us that for many ions there is a 2:1 relationship between these two numbers. Thus we have Ag $\bar{n}=2$ , Cu $\bar{n}=4$ , Al $\bar{n}=6$ , Th $\bar{n}=8$  and so on. These ions will obviously tend to react with typical bifunctional analytical reagents such as oxine, Ox $\bar{n}=2$ , to form co-ordination-saturated zero-charge complexes, so that the possibilities of ternary complex formation are low. However, other ions such as Mg $\bar{n}=6$ , Ca $\bar{n}=6$ , Be $\bar{n}=6$  will obviously tend to form co-ordination-unsaturated complexes with typical bidentate ligands, so that ter-

nary complex formation with these ions is possible according to the first scheme.

In the second mode of formation, ternary complexes may arise where the first ligand forms purely co-ordinate bonds with the metal ion or when it has a 'surplus' of ionogenic or purely dative groups so that although the first ligand does form a co-ordination-saturated complex it does so with the formation of a positively or negatively charged primary complex which may then ion-associate with an anionic or cationic dyestuff or other body to form a ternary complex.

**b. The Alizarin Complexan-Lanthanone System for Fluoride Ion.** The first type of (ternary complex) formation system may be illustrated by the Alizarin Complexan reagent system for fluoride which yielded the first 'positive' colour reaction to be described for this ion [19]. All previous colour reactions depended on the bleaching of a coloured metal complex, *e.g.* ferric thiocyanate by fluoride ion or on the liberation of a free dyestuff from the metal lake compound of a metal such as zirconium or aluminium which forms a strong complex with aluminium. Alizarin Complexan (3-dicarboxymethylaminomethyl-1,2-dihydroxy-anthraquinone) [20] ionises according to the pattern shown in Figure 4 and reacts in its yellow form at pH 4.3 to form red-coloured metal complexes, the absorption spectra of which closely resemble that of the metal-free reagent *ca.* pH 7, *i.e.*, the next higher ionisation stage of the chromophore, *cf.* Figure 1. All these metals except thorium react to form 1:1 complexes with the reagent, and the lanthanides in particular form very stable complexes. When any of the Alizarin Complexan chelates of one of the first six members of the lanthanide series, *viz.*, elements of atomic numbers 57 to 62, is treated with a substoichiometric amount of fluoride ion a new blue colour body exhibiting a 1:1:1 reagent:lanthanide:fluoride stoichiometry is formed. The reaction is particularly intense with lanthanum and cerium (III). The colour formation is unique in that it is the only known positive colour reaction of the fluoride ion. Furthermore, it is a sensitive reaction, ( $\epsilon \approx 30,000$ ), and it also appears to be specific for the fluoride ion. This unusual reaction may be ex-

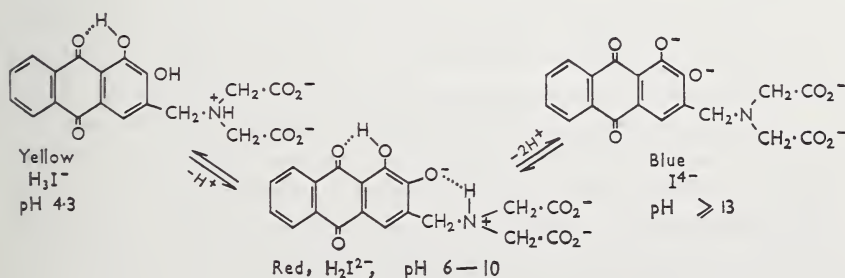


Figure 4. Dissociation pattern of Alizarin Complexan.

plained [21] very simply in terms of classical resonance theory by accepting Pauling's postulate that a partial double bond characteristic may be ascribed to metal-oxygen bonds. Before the entry of the fluoride ion into the binary complex the latter may be depicted as in Figure 5. The ligand has formed a co-ordination-unsaturated complex with the lanthanide ion 'M'. Entry of the strongly electrophyllic fluoride ion into the co-ordination sphere of the lanthanide leads to a general withdrawal of electrons from the Alizarin Complexan molecule along the conjugated bond system presented between the lanthanide atom and the remaining undissociated phenolic group of the molecule, Figure 6.

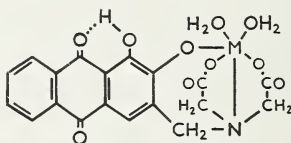


Figure 5. Structure of typical metal chelate of Alizarin Complexan, e.g., M=Ce(III).

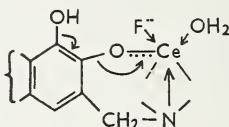


Figure 6. Induction pattern of 1:1:1 ternary fluoride complex.

As a result, the proton-oxygen bond is weakened and the proton dissociates even at pH 4.3, although it does not normally do so till *ca.* pH 12-13. This is borne out by an examination of the close similarity of the spectra of the ternary complex and that of the Alizarin Complexan reagent alone at pH 12.4, *cf.* Figure 7. It has already been mentioned that this reaction is given only by the reagent chelates of the first six members of the lanthanide series, *i.e.* those metals where the entry of the first '5d' electron in lanthanum triggers off subsequent filling of the '4f' shell so producing the inner transition series of the lanthanons. These are the elements which readily form fluorides when their oxides are heated with chlorine trifluoride. The intermediate lanthanons (63-68) form fluorides less readily and the higher ones not at all. There is every reason to suppose that this reaction could possibly be reversed to form very selective spectrophotometric procedures for these particular lanthanons in the presence of the others, though the sensitivity would most probably only be good for lanthanum and cerium (III). The danger implicit in trying to reverse the procedure is, however, that the reaction is essentially a substoichiometric one as far as fluoride ion is concerned. If the ratio of fluoride ion to lanthanon greatly exceeds unity not only will

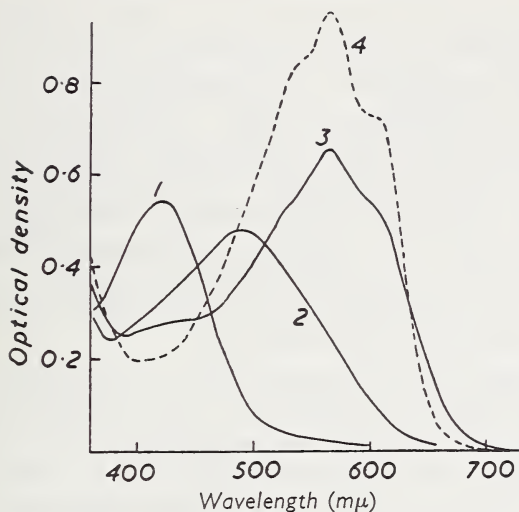


Figure 7. Absorption spectra of ternary fluoride complex. (1) Alizarin Complexan at pH 4.3. (2) Cerium(III) chelate at pH 4.3. (3) Ternary complex with fluoride at pH 4.3. (4) Alizarin Complexan at pH 12.4.

the (blue) ternary complex not be formed, but the (red) lanthanon-reagent complex will be bleached, liberating the metal-free (yellow) reagent in the process. This danger may indeed arise when attempts are made to determine larger amounts of fluoride [22] though the analysis may easily be done when due precautions are observed [23].

**c. The *Bis* [diphenanthroline-silver (I)] BPR Ternary System, etc.** The second (ternary complex) formation system is well illustrated by some recent work on the spectrophotometric determination of silver [24] and more recently still on cadmium, cobalt (II), copper (I) and (II), gold, manganese (II), nickel, lead, zinc, etc. [25]. These other metals form firmly bound 'primary' complexes with tertiary amines such as 1,10-phenanthroline in which the metal is bound to the liganding atoms by purely dative bonds so that the complex species thus formed still retains the same formal charge as the original cation. These coordination-saturated complex cations can ion-associate with anionic dyestuff molecules to form very intensely absorbing bodies. This principle is not, of course, a new one. Many methods are known, *e.g.*, for boron [26], gallium [27] etc., where colourless complex ions may be associated with solvent-inextractable basic, *i.e.*, cationic, dyes to form neutral (uncharged) ion-associated species which extract well. The work of several Russian authors in this area [28] is particularly interesting. These dyestuffs have high molar absorptivities and the absorption spectrum of the extracted species is, of course, identical to that of the dyestuff in aqueous solution apart perhaps from some small solvation effects.

However, the systems discussed here are different in that we have the unusual phenomenon of a colour change upon ion-association of the complex cation and the anionic dye. For example, silver ion reacts with the polyphenolic triarylmethane dyestuff, Bromopyrogallol Red, BPR, Figure 8, to form slowly a rather nondescript brown compound in which the silver ion is apparently present as Ag(II) and is united to one ligand molecule across the vicinal phenolic groups. The process of complex formation is slow and is very dependent on experimental conditions such as the volume of the medium in which formation occurs. The course of the reaction can be followed potentiometrically by the release of hydrogen ions from the ligand in the usual way.

However, when the two reactants, *viz.* Ag<sup>+</sup> and BPR are brought together in the presence of an excess of 1,10-phenanthroline an entirely new colour-body which is bright turquoise blue is formed instantaneously [24]. Furthermore, this compound formation occurs *without* the release of hydrogen ion and the stoichiometry of the compound formation corresponds to [Ag-Phen<sub>2</sub>]<sub>2</sub>BPR. It is, therefore, apparent that the silver ion is datively bonded to two 1,10-phenanthroline molecules and that two of the monopositive di-phenanthroline silver (I) ions thus formed ion-associate with a BPR molecule to form a neutral body. The compound thus formed is not very soluble and can only be formed successfully in very dilute solution. It yields a molar absorptivity value of 51,000 which is *ca.* twice that of the very temperamental dithizone procedure, and in the presence of EDTA, fluoride and peroxide only gold (III) yields cationic interference. The complex can also be extracted [29] into nitrobenzene away from anionic interferences. Whilst all of this unites to provide a method which is both more sensitive and selective than any previous absorptiometric method for silver ion it still leaves unexplained the unique fact that a very profound colour change is obtained, *cf.* Figure 9, upon ion-association of the primary complex and the BPR molecule. Work is still in progress on the mechanism of the colour reaction, but the three principal theories around which current investigation revolves are that it may possibly be explained (1) as has the action of adsorption indicators in the past, to distortion of dyestuff

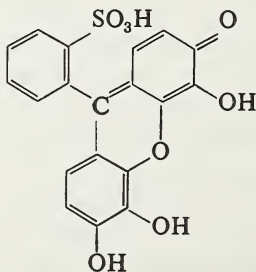


Figure 8. Bromopyrogallol Red.

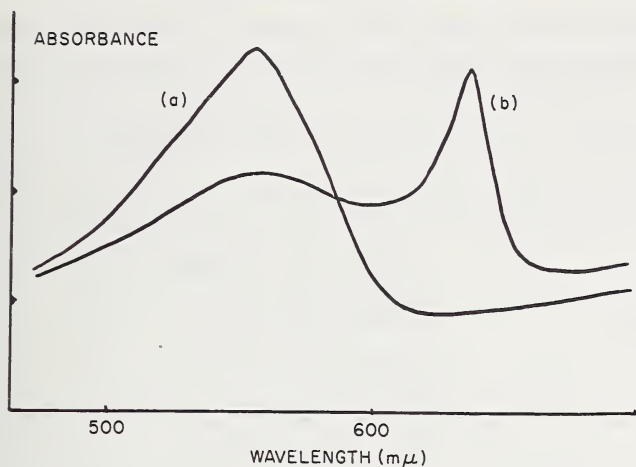


Figure 9. Absorption spectra of silver-bromopyrogallol red-phenanthroline complex. (a) Bromopyrogallol Red. (b) Ternary silver complex.

molecules following physical adsorption on a colloidal  $\text{Ag}(\text{Phen})_2$  body, or (2) to a charge-transfer mechanism in a definite *bis* [di-phenanthroline silver (I)] BPR compound or (3) to a sandwich layer type of mechanism in which BPR molecules are bonded between two layers of silver-phenanthroline molecules. The first explanation does not explain the firm stoichiometry of the compound and the second is difficult to explain in a completely satisfactory manner at present, though further work may clarify matters. The third possibility is, in some ways, a combination of the others and may be a closer approximation to the true state of affairs.

More recent work [25] allied systems using 1,10-phenanthroline as the ligand and tetrachloro(P)tetraiodo(R)fluorescein [trivial name Rose Bengal Extra, (RBE)] as the counter anion has yielded yet higher sensitivities, *cf.* Table 1. In these latter systems the complexes have been extracted into various solvents to provide increased selectivity of determination. Iron (II), which is well known for its reaction with 1,10-phenanthroline, does not undergo ternary complex formation. This is probably due to orbital stabilisation which makes the formation constant for the *tris*-phenanthroline iron (II) complex from the *bis*-phenanthroline iron (II) greater than the first or second. Only a limited number of ions are capable of undergoing ternary complex formation, principally those mentioned in Table 1, but even amongst these it is possible to arrange for interelement selectivity. Thus, copper may be determined specifically amongst 56 cations and in the presence of most anions by extraction of the neo-cuproine complex of Cu(I) from an EDTA medium [25]. Conversion to the  $[\text{Cu}(\text{phen})_2]$  RBE system is made by simple addition of reagents, thus providing a molar absorptivity of 62,500 and permitting solutions containing only 0.002 ppm

TABLE I. Tentative sensitivities of ternary ion-association systems.

Ion determined	Mol. absorptivity coefficient (solvent)	M.A.C. (Dithizone)
Cd	92,000 (ethyl acetate)	85,000
Co	92,000 (ethyl acetate)	59,000
Cu(II)	78,000 (ethyl acetate)	45,000
Mn	65,000 (ethyl acetate)	32,000
Ni	50,000 (CHCl <sub>3</sub> )	34,000
Pb	70,000 (nitrobenzene)	72,000
Zn	95,000 (ethyl acetate)	94,000

to be readily analysed for copper. The colour system is stable for several days. This again offers a very attractive alternative reagent system to the well established dithizone procedure. The sensitivities of several of these ternary systems under the conditions established to be maximal for copper are shown in Table 1, and are compared there with the recorded data for dithizone, which was certainly one of the most sensitive reagents hitherto available for the absorptiometric determination of inorganic cations. It is probable that these figures for the elements other than copper are capable of improvement following routine optimisation of experimental variables.

It is apparent that these selective ternary complex systems hold out worthwhile possibilities for future development in molecular absorption spectrophotometry as an inorganic trace technique. The judicious use of masking agents, particularly 'mass-masking agents' such as EDTA which is 'selectively unreactive' towards certain ions, *e.g.*, silver, beryllium, copper (I), thallium (I), or of cyanide which is 'selectively unreactive' towards the alkaline earths, aluminium, beryllium, lead, bismuth, etc., will obviously go a long way to avoiding the tedious separations which were formerly required and which made trace analysis a very difficult area.

#### B. SENSITIVITY OF REACTION

The problem of obtaining selectivity of reaction has obviously become a major preoccupation amongst analytical chemists and this aspect of absorption spectrophotometry has been featured almost exclusively in these paragraphs up to this point. However, it is also necessary to take into account the sensitivity of molecular absorption-spectrophotometry as a trace technique because the limits of detection and determination are being pushed to ever lower levels by legislation and

manufacturing know-how. There is little doubt that, whereas the situation seldom arose in years gone by, the analyst must now frequently wonder if absorption spectrophotometry is sensitive enough for the analysis which he must perform.

The basic law of absorption spectrophotometry relates the absorbance ' $A$ ' to the concentration of the absorbing species ' $C$ ' linearly through the length of the absorbing layer of solution ' $\ell$ ' and the molar absorptivity of the absorbing species,  $\epsilon$

$$\text{i.e. } A = \epsilon \cdot \ell \cdot C \quad (3)$$

Obviously the analytical signal can be increased for a given concentration of the reacting ion ' $C$ ' by increasing the pathlength ' $\ell$ ' or by using a compound which has a greater molar absorptivity,  $\epsilon$ . At first sight it might appear to be simple to increase the sensitivity of any given determination by a factor of 100-fold by replacing the conventional 1 cm cell by one measuring 1 metre. This might work reasonably well if the reagent, which is always added in considerable excess, had no absorbance whatsoever at the wavelength of analytical measurement. But this is rarely the case, and the most efficient reagents usually exhibit considerable spectral overlap between reagent and complex. Consequently such solutions would be optically so dense as to become useless for analytical purposes. Indeed, even if the reagent does not absorb appreciably, success can only be achieved where the absorbing species itself has a low absorptivity, and is therefore *very* insensitive. Yet again, in dealing with long path cells there are even more serious difficulties from light scattering, internal reflections, stray light and so on.

### 1. *The Sensitivity Barrier*

The best hope of increasing sensitivity of determination would, therefore, appear to be to use reagents which yield high molar absorptivities. This approach has been used extensively. An absorbing molecule can be considered as a mesh of electrons which is spread in the path of the beam of incoming photons. Each absorbing molecular species may be regarded as having a photon-capture cross section and anything which can be done to increase this cross-section will obviously increase the sensitivity of determination. Now the analogy of the photon-capture cross-section, taken in conjunction with the realization that the absorption spectrum of a complex will closely resemble that of a higher ionisation state of the metal-free reagent reveals that the simple addition of one, two or even three identical ligand species to a metal ion will not cause much increase in selectivity after addition of the first ligand, whereas the addition of two differing species simultaneously to a metal ion may cause a substantial increase in photon-capture cross section. A crude analogy may be obtained by studying the shadow patterns

obtained by placing two rigidly aligned sieves in front of a light-source. If identical sieves are used there will be no deepening in the pattern if one uses two sieves rather than one. If the sieves are of different design, however, a considerable increase in shadow will be obtained by using the two sieves simultaneously. A better analogy still may be obtained by consideration of the effects of impurities on the neutron-capture cross-sections of atomic reactor materials. This, in effect, is what is being done in putting together ternary complexes where two different ligand species are involved in reaction with one cation.

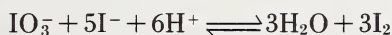
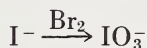
Another approach to increase of sensitivity using a single ligand species is, of course, to build up the molecule's electron orbitals so that it presents a more effective cross-section. This, however, is not an easy route to sensitivity and it has not always been a very successful one because complex molecules frequently react only unwillingly with cations and the tendency for spectral broadening to occur may swamp the effect produced by chelation with the reacting cation.

However, it is interesting to speculate about just how far the photon-capture cross-section of an organic molecule can be increased. This has already been done by Braude [30] who calculated that the maximal value of the molar absorptivity would be of the order of 100,000. Now, common values for the effective molar absorptivity of determination for most inorganic analyses lie in the range 10,000–40,000, though some of the newer methods described above tend to yield values as high as 90,000, *i.e.*, virtually theoretical values. Some simple arithmetic on this sensitivity barrier reveals that for a 1 cm cell and a value of 0.002 absorbance unit the minimum *detectable* concentration would be  $2 \times 10^{-8}M$ . For the purposes of *determination* a minimum value of 0.01 absorbance unit is more realistic and for most systems a molar absorptivity of 50,000 is perhaps better than can be expected. This would produce a limit of  $2 \times 10^{-7}M$ . If now one remembers that reagents such as buffers, masking agents, the reagent itself, etc., must be added to the test solution, we find that the most dilute solution we could normally expect to analyse by absorption spectrophotometry would be *ca.*  $10^{-6}M$  or even  $10^{-5}M$ . Consequently, there is a very definite limit to the sensitivity of molecular absorption spectrophotometry as a trace technique in inorganic analysis, though it is comforting to turn up the textbooks and find that in terms of molar absorptivities we can still go a long way to improve on existing methods.

## 2. Surmounting the Sensitivity Barrier

The idea of amplification reactions is not unfamiliar in analytical chemistry. Perhaps the best known is the Leipter method for the determination of iodide ion. The latter is oxidised by bromine to give iodate ion and the iodate is subsequently reduced by an excess of iodide ion

to yield six equivalents of iodine for each iodide ion originally oxidised to iodate, *i.e.*



In this reaction there is a six-fold amplification and it may be considered to be a direct one. There are numerous other such reactions, most of which are of an indirect nature, but these cannot be discussed here. Obviously, this is one potential way of surmounting the sensitivity barrier and though an example of this will be given for absorption spectrophotometry in subsequent paragraphs it is true to say that it is a device which has not yet been used to any great extent.

Another obvious way of overcoming the limiting sensitivity of  $\epsilon \approx 100,000$  is to persuade the test ion to act as a type of catalyst to promote the kinetics of another reacting system. This again is a device which is theoretically capable of yielding very high *effective* molar absorptivities for ions which require to be determined with very high sensitivity. There are perhaps more numerous examples of this in the literature, but it is true to say that little or no systematic work has been done on this approach. The author has suggested the term *kinetochromic spectrophotometry* for this type of determination [31] and this too will be illustrated by some recent work in the ensuing paragraphs.

**a. Evolution of Amplification Reaction.** Almost simultaneously, Umland and Wünsch [32] and Djurkin, Kirkbright and West [33] devised extremely sensitive indirect amplification reactions for the phosphate ion. The procedure devised by the latter authors is marginally more sensitive and is probably less subject to interference by other ions because of the extractive procedures employed.

In this procedure [34] the phosphate solution is treated in the usual way with an excess of molybdate ion to form the conventional,  $12 \text{MoO}_3 \cdot \text{PO}_4^{-3}$ , phosphomolybdate ion. The phosphomolybdic acid thus formed is extracted away from the excess of molybdate ion in the aqueous solution into a butanol-chloroform solvent. The phosphomolybdic acid extract is then well washed free of excess molybdate ion and is equilibrated with an ammonia solution. The latter breaks down the complex phosphomolybdate ion into the original phosphate ion and twelve associated molybdate ions. The latter can then be determined by means of Kirkbright and Yoe's reagent, 2-amino-4-chlorobenzenethiol [35] so that twelve molybdenum chelate molecules are extracted into chloroform from the aqueous ammonia extract. The method involves a considerable amount of manipulation, but by virtue of the sensitivity of the reagent used ( $\epsilon_{710} \text{ m}\mu \approx 36,000$ ) a very sensitive determination is possible. The *effective* molar absorptivity

for phosphate by this amplification procedure is  $\epsilon_{710 \text{ m}\mu} = 359,000$  which compares favourably with that obtained by the usual heteropoly blue methods and which readily allows the determination of nanogram amounts of phosphate using a simple spectrophotometer with 1 cm cuvettes. By virtue of Wadelin and Mellon's extractive procedure which is used in extracting the phosphomolybdic acid [36], there is no interference from hundred-fold concentrations of other heteropoly acid formers such as silicon, germanium, antimony and arsenic and up to thirty-fold excesses of tungsten (VI) can be tolerated in the presence of 1,2-dihydroxyazobenzene-3,5-disulphonic acid as a masking agent. Work is now afoot to arrange conditions so that a sequential determination of several of these heteropoly acid formers, *e.g.*, silicate, phosphate and arsenate, may be effected by this amplification reaction, and it is very much apparent that much of the manipulative work may be eliminated by substituting atomic-absorption spectrophotometry for molecular-absorption spectrophotometry as the means of analytical measurement.

Umland and Wünsch's procedure is essentially similar, except that thiocyanate is used as reagent in place of 2-amino-4-chlorobenzene thiol as absorptiometric reagent and the colour system is developed in the aqueous extract.

**b. Evolution of Kinetochromic Spectrophotometry.** In aqueous solutions of intermediate acidity, zirconium in the form of zirconyl ions,  $\text{ZrO}^{+2}$ , tends to polymerise to produce rather inactive species. Thus a freshly prepared solution of zirconyl oxychloride reacts very rapidly with the reagent Xylenol Orange, Figure 10, to produce a fairly intense red chelate compound. The speed of this reaction varies inversely with the age of the solution, however, so that after the solution has aged overnight very little colour develops within a conventional development time, *e.g.*, 60 minutes. We [37] have found, however, that in the presence of fluoride ion the red colour due to the 2:1 zirconium: Xylenol Orange complex is formed very much more quickly in such aged solutions provided that the amount of fluoride ion is considerably less than that of the added zirconium. In addition, there is a linear relationship between the absorbance due to the complex and the

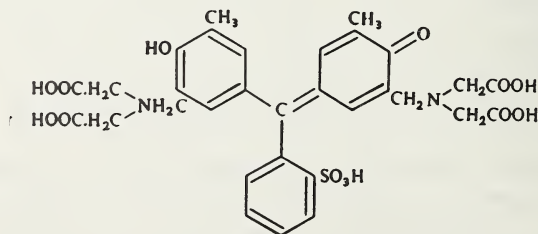


Figure 10. Xylenol Orange.

amount of added fluoride over a given interval of time, *i.e.*, the fluoride ion exhibits a limited catalytic effect on the kinetics of production of the complex. If the colour reaction is allowed to proceed for a limited period of time only, during which the 'blank' reaction between the zirconium and the Xylenol Orange scarcely proceeds, it is found that there is a firm stoichiometry for the reaction between the three components. This corresponds to a ratio of X.O.:Zr:F = 4:8:1, *i.e.*, each fluoride ion appears to be responsible for the rapid production of four zirconium:Xylenol Orange chelate molecules. It must be stressed, of course, that if the reaction is allowed to proceed long enough, the presence of the fluoride ion will have practically no effect because it merely speeds up a reaction that is otherwise very slow. In addition, if the amount of fluoride is more than substoichiometric in relation to the zirconyl ion the reaction will be retarded or completely inhibited because of the formation of polyfluoro zirconium species.

Because of the acidity of the reaction, no other cations interfere by forming coloured complexes with the Xylenol Orange and only aluminium exhibits a negative cationic interference by forming a stable complex with fluoride ion at 100-fold concentration. None of the common anions interferes, but some other anions which exhibit a strong complexing action on zirconium, *e.g.*, phosphate, arsenate and sulphate (and also some complexing organic anions, *e.g.*, oxalate and citrate) exhibit an effect similar to that of fluoride ion.

The practical implications of these *kinetochromic* reactions are very considerable. The *kinetochromic extinction coefficients* or *effective molar absorptivities* for these reactions are as follows

fluoride	$\epsilon_k \approx 200,000$
arsenate	$\epsilon_k \approx 340,000$
phosphate	$\epsilon_k \approx 400,000$
sulphate	$\epsilon_k \approx 22,000$

For fluoride, arsenate and phosphate these methods of kinetochromic spectrophotometry offer sensitivities *ca.* one order of magnitude greater than existing spectrophotometric methods. In the case of sulphate the sensitivity is conventional at *ca.* 22,000, but it is, to the best of the author's knowledge, the only 'positive' colour method so far proposed for the sulphate ion. Furthermore, the system for phosphate, apart from its high sensitivity is unique in that it does not depend on the formation of a heteropoly acid of any kind. Yet again, in relation to fluoride ion the above system constitutes a considerable advance on the Alizarin Complexan method [19-23] and is subject to considerably less cationic interference.

Although work is still in progress on the elucidation of the mechanism of these unusual reactions, it is perhaps permissible to speculate briefly

here on their possible course. The reacting ratios for the other ions appears to be as follows



The zirconyl oxychloride solution can only be used after it has aged for twenty four hours and its effective life is *ca.* five days. The extent of the catalytic reaction is also temperature dependent. The reacting ratio between the zirconium and the Xylenol Orange remains constant throughout at 2 : 1 which corresponds to that which would be expected between zirconium and Xylenol Orange in pure solution. It appears, therefore, that in all instances the colour body is the zirconium: Xylenol Orange 2 : 1 complex and this is confirmed by the coincidence of all the absorption spectra. It may be concluded, therefore, that the fluoride, arsenate, phosphate or sulphate ions *activate* the polymerised slow-reacting zirconyl species present in aged solutions by rendering them *labile* towards reaction with Xylenol Orange. The aqueous chemistry of zirconium solutions is, unfortunately, a very obscure area and consequently any theories developed to explain the above reactions can, in our present state of knowledge, only be highly speculative. It is tempting, however, to wonder if the reaction can be explained on the basis that several zirconyl ions (or zirconium ions) may be coordinated around one central anion such as fluoride, phosphate, etc. The possible existence of such a *labile* species, *e.g.*,  $[\text{F}(\text{ZrO})_n]^{+(2n-1)}$  or  $[\text{F}(\text{Zr})_n]^{+(4n-1)}$  tempts one to suggest further that in the above instance  $n = 8$  since this would explain the apparent X.O. : Zr : F = 4 : 8 : 1 stoichiometry of the reaction. It is certain that the existence of a labile unpolymerised species such as this would allow more rapid formation of the  $\text{Zr}_2$  : X.O. complex. These matters must, of course, remain a matter of pure speculation at the present time since the apparently firm stoichiometry of these reactions may be coincidental on a combination of the many variables involved. What is certain, however, is that these so called [31] kinetochromic reactions present a very valuable and unique technique for the analysis of these ions. The intercombination of different cations, anions and reagents presents fascinating possibilities for further exploration.

It must be recognized that there is a very great need for more attention to be paid to the analytical absorption spectrophotometry of anions. Even though the principle of these kinetochromic reactions is only imperfectly understood at present it should be capable of extension to many other reacting systems and it may well be that this will prove the most fruitful area yet for the development of sensitive absorptiometric techniques for the determination of trace non-metals in solution.

### C. MOLECULAR ABSORPTION SPECTROPHOTOMETRY IN THE FUTURE

Several possibilities for future development have already been suggested in the previous paragraphs, but these have largely been of a fairly specific nature, although their general implications are apparent. The use of differential spectrophotometry should allow much more precise determinations to be made on solutions of high absorbance so that the upper limit of the technique may be extended into the domain of macro-analysis. This is inherently important because absorption spectrophotometry is a technique which is easily automated. At the other extreme, the intelligent use of scale expansion should allow much smaller amounts of material to be determined with greater precision than is possible by means of conventional spectrophotometers. Another interesting possibility for the improvement of sensitivity would be to endeavour to persuade molecules to abandon their random orientation in solution and to align in the optimal position for light-capture. Obviously this may be no easy task for some molecules, but possibilities for such ordered arrangements do exist and the principle appears to be worthy of investigation.

Means of increasing selectivity of reaction are perhaps more elusive, but much of the need for this has been removed by advances which have been made in the use of masking agents, particularly in the realm of compleximetric titration. Some considerable need exists here for systematic examination of the reactions of masking agents, because most of our knowledge in this area has arisen empirically and largely by chance observation. It is possibly also true to say, however, that little is likely to be gained in terms of increased selectivity by modification of reagent structure, apart from introducing liganding atoms other than nitrogen and oxygen. Perhaps the most promising approach appears to be an increased use of catalytic action since this is most frequently of a highly selective nature.

Lastly, it can be said that despite the introduction of many new spectroscopic trace techniques there is as yet no reason to suppose that this well-tried and much used technique may become obsolescent within the next decade.

### III. Molecular Fluorescence Spectrophotometry (Spectrofluorimetry)

In the instance of the compounds and reactions which have been discussed above in connection with molecular absorption spectrophotometry we have not been concerned with the fate of the photons which have been absorbed by interaction with the compounds. It has been sufficient to know that the absorption of energy has been a proportional process. However, the molecules which have absorbed the energy have undergone electronic transitions and since they are,

therefore, in an excited state, they must be considered as unstable until they lose their acquired energy and return to the ground state. Now some molecules which are very highly coloured are well known for their photochemical instability and in these instances we can clearly consider that the energy which is acquired upon exposure to light is an activation energy for chemical reaction. The coincidence of high tinctorial power and lack of "fastness to light" is all too well known to the dyestuff chemist. However, the great majority of coloured compounds are reasonably stable to normal (daylight) radiation and in these instances the excess energy is largely spent by transfer into increased vibrational energy and thermal activity of the molecules which result in non-reactive intermolecular collisions so that we can say that the energy is lost by dissipation of heat. The whole process is generally referred to under the most misleading title of loss of energy by "radiationless transfer." This unfortunate designation presumably arises out of the third category of energy shedding by excited-state molecules which is the visible (or u.v.) re-radiation of light. There are very many compounds which exhibit light emission in this way and those constitute the general category of luminescent compounds. Although it is very germane to the consideration of analytical potentiality, particularly in terms of selectivity of reaction, the author is not concerned, for the purpose of this discussion, with chemiluminescence phenomena whereby molecules emit energy which they have acquired as a result of *chemical* reaction. These compounds and reactions will therefore be excluded from all further discussion in this context. Fluorescence and phosphorescence constitute the other two categories of luminescence and of these, fluorescence is the more common and will be chiefly considered. Outwardly it is difficult to distinguish between fluorescence and phosphorescence since the latter appears to be merely a case of delayed incidence of the former, but there is a fundamental difference which will be explained briefly in due course. The essential difference between compounds which absorb light and those which absorb and subsequently re-radiate light is that the latter have unusually stable excited states so that these molecules can retain acquired energy in a definite energy level for a finite time before they dissipate it and return to the ground state. Only those compounds which have stable excited state configurations will therefore exhibit the phenomenon. Resonance re-radiation, *i.e.*, re-emission of photons of the same energy as those originally absorbed is, to the best of the author's knowledge, completely unknown in solution. Invariably less energetic photons are re-emitted by the luminescent compound so that the fluoresced light has a longer wavelength or lower frequency than the absorbed light. The fluorescence is also characteristic of the compound in the sense that the emission spectrum is always the same irrespective of the wavelength of the incident light which promotes the fluorescence. It is perhaps

best to outline the reasons for these and other phenomena before discussing the analytical implications of spectrofluorescence and comparing its merits and demerits with respect to other trace techniques, particularly molecular absorption spectrophotometry.

### A. ABSORPTION RE-EMISSION PROCESSES

Figure 11 depicts the electronic energy levels in a molecule, ignoring all the vibrational and rotational levels for the sake of simplicity. Excitation occurs by absorption of energy and translation of an electron from the ground state,  $E_0$  along path AB to the first excited state,  $E_1$ , although excitation may also occur to higher excitation states,  $E_2$  and  $E_3$ , etc., along paths AU and AV. Fluorescence emission occurs when the electrons follows path CD in falling from the first excited state to the ground state. The excited state,  $E_1$  has a finite life-time of  $10^{-7}$  to  $10^{-8}$  sec which may be equated to BC on the diagram. Phosphorescence emission may occur when the molecule has a triplet excited state,  $T_1$ , lying below the first (singlet) excited state,  $E_1$ . The electron may pass over into the triplet state, by path EF shown on the diagram, and phosphorescence is emitted when the electron falls back to the ground state along path XY. Now the triplet state is a 'forbidden' one and this has two main consequences. These are, (1) that direct promotion of the electron into  $T_1$  from  $E_0$  is virtually unknown because it demands

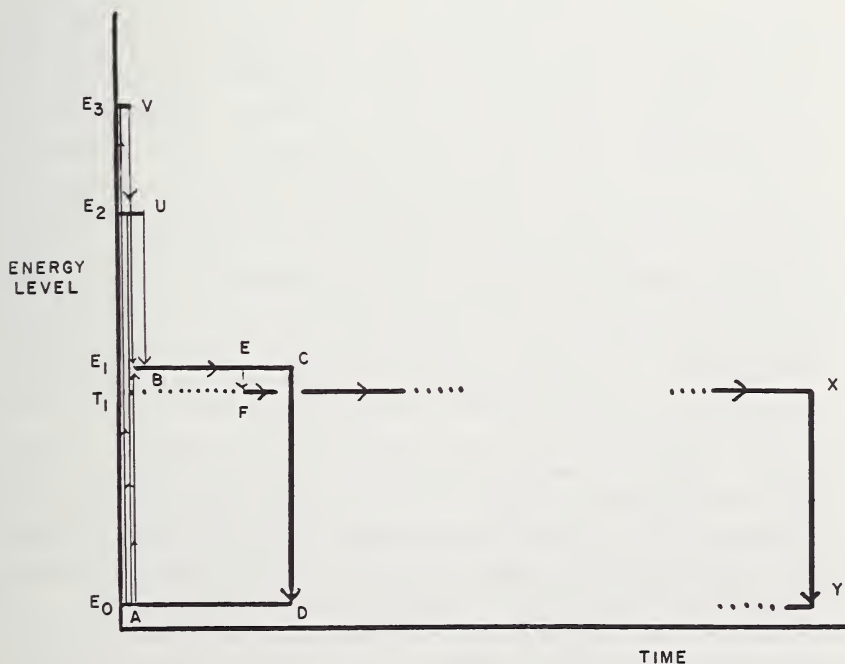


Figure 11. Energy levels in molecular fluorescence and phosphorescence.

simultaneous spin-decoupling so that no singlet $\rightarrow$ triplet absorption band will be observed and (2) once indirect occupation of the  $T_1$  level has been achieved along path ABEF, re-radiation along path XY will be difficult since spin reversal must once more occur so that the lifetime of the triplet excited state will be relatively long (*ca.*  $10^{-4}$ – $10$  sec). The essential difference between fluorescence and phosphorescence is, therefore, that the former involves a singlet $\rightarrow$ singlet electronic transition, whereas the latter involves a triplet $\rightarrow$ singlet transition. As a consequence of this difference, fluorescence *appears* to be an instantaneous process (emission within  $10^{-8}$ – $10^{-7}$  sec after absorption) whereas phosphorescence can be seen to be time-dependent (emission within  $10^{-4}$ – $10$  sec). Another important consequence of the life-time of the excited state arises, however. This is that whilst some deactivation of excited state molecules may occur as a result of collisions with solvent molecules before the energy is re-emitted as fluorescence, this effect becomes preponderantly important in phosphorescence where the phenomenon is virtually unknown for dissolved molecules and can only be observed on any scale when the solutions are frozen into glasses at low temperatures so that collisional deactivation is prevented or at least severely restricted.

Consideration of the potential energy diagram, Figure 12, serves to show some more useful explanations of some of the phenomena of fluorescence and phosphorescence. A simple binary molecule AB is considered as having end A clamped so that all vibration along the bond axis may be considered as motions of B. In the  $E_0$  ground state B will have a vibrational motion XY along the axis with the mean position of B corresponding to the mid-point of XY. If energy is imparted to the molecule gradually and progressively the amplitude of XY will increase to levels 1, 2, 3, 4, etc., and the extremities of X and Y will trace out the potential energy curve for the ground state of electronic energy,  $E_0$ . The maximum distances apart  $AY_1$ ,  $AY_2$ ,  $AY_3$ , etc., will increase steadily but the minimum distances apart  $AX_1$ ,  $AX_2$ ,  $AX_3$ , will not decrease proportionally because of interatomic repulsions between A and B, *i.e.*, the compression arm of the diagram will have a much steeper angle than the stretching arm. It would appear that eventually a position  $AY_n$  will be reached when any further addition of energy will cause B to recede to an infinite distance from A so that the AB bond is completely broken. However, before this happens the molecule will normally adjust to the increased absorption of energy by undergoing an electronic transition to the first excited state,  $E_1$  on the diagram or to a still higher electronic energy level, *cf.*  $E_2$ ,  $E_3$  on Figure 11. In the first (singlet) excited state,  $E_1$ , the mean distance apart of A and B will be greater than in  $E_0$ , consequently the trough of the  $E_1$  potential energy curve must lie to the right of that of  $E_0$  in the figure. Under normal conditions the molecule AB may be considered to exist almost entirely in the lowest vibrational

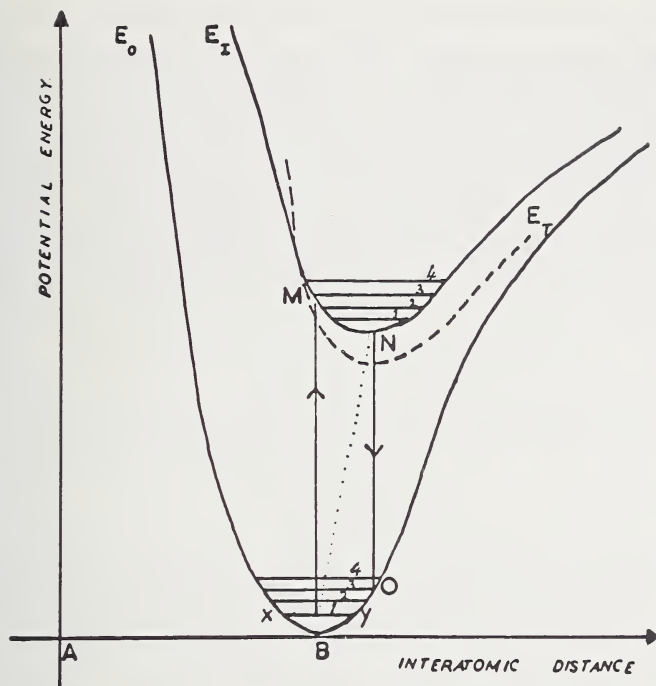


Figure 12. Potential energy curves in molecular fluorescence and phosphorescence.

level of its ground state of electronic energy,  $E_0$ . Excitation from  $E_0$  to  $E_1$  must occur during the 'life-time' of a photon (*i.e.*, period of vibration of a light wave) which is  $10^{-15}$  sec. Vibrational frequency in a molecule, on the other hand, is *ca.*  $10^{-12}$  sec so that to all intents and purposes the geometry of a molecule may be considered to be "frozen" during the transition from  $E_0$  to  $E_1$ , *i.e.*, the distance between A and B will remain virtually constant during the life-time of the transition which is so rapid that it can be depicted as a vertical line in Figure 12. Thus the excitational transition does not occur to the lowest vibrational level of  $E_1$ , but rather to a higher vibrational level, *e.g.*, level 4 of  $E_1$ . This means that the excitation places the electrons on the compression side of the potential energy trough so that the molecule is set vibrating like a spring by virtue of excitation. The period of these vibrations is *ca.*  $10^{-12}$  sec, whereas the lifetime of the excited state is *ca.*  $10^{-8}$  sec. Consequently, during the latter the molecule will have reached the lowest vibrational level of the first electronic excited state. It is, therefore, from this position that the molecule re-emits fluorescence radiation along path NO. Invariably, therefore, the absorbed photon, corresponding to BM in this diagram, is more energetic than the emitted photon NO, *i.e.*, the fluorescence emission band has a longer wavelength than the excitation (absorption) band. Fine structure might

arise if the molecule fell back from the ground vibrational level of the first excited state to various vibrational levels of the ground state  $E_0$  just as fine structure might be similarly expected in the excitation (absorption) band. However, in the majority of instances in solution at low temperature vibrational energy is lost in less than the period of a single vibration so that fine structure is almost totally absent. The main reason why broadband spectra are obtained rather than the line spectra suggested by Figure 12 has been explained in connection with absorption spectrophotometry and will not, therefore, be discussed further here.

### 1. Phosphorescence and the Triplet State

Electrons in atomic and molecular orbitals are spin coupled and the singlet states corresponding to these are typified by the  $E_0$  and  $E_1$  states shown in Figure 12. However, reversal of the spin of an electron may occur and by the Pauli exclusion principle a new orbital must be created to accommodate the uncoupled electron. The molecule may now be regarded as a diradical and because of the interaction of spins and orbitals this shows up spectroscopically as a three-band or triplet system. According to Hund's rule, spin multiplicity favours the ground state and as a result the triplet excited state,  $E_r$ , is less energetic than the  $E_1$  state from which it was formed. The energy difference is not great, however, and consequently there is considerable overlap of energy levels in the singlet and triplet excited states so that intersystem crossing is readily possible. Thus one electron can readily be passed over into the relatively long lived triplet state during the life-time of the  $E_1$  state. Higher energy levels  $E_2$ ,  $E_3$ , etc., were shown in Figure 11 and transition up to these levels is quite common. These AU and AV transitions in Figure 11 correspond to higher energies than AB of course, and show up as shorter wavelength bands in the absorption or excitation spectra. However, the fluorescence emission band is almost invariably the mirror image of the longest wavelength absorption band, when plotted on a linear energy scale, and these higher energy bands have no counterpart in the emission spectrum. This arises because almost invariably the higher states  $E_1$ ,  $E_2$ ,  $E_3$  are more closely spaced than the  $E_0$  and  $E_1$  states. Thus considerable overlap of energy levels can occur and internal conversion or intersystem crossing leads to complete dissipation of excess energy down to the lowest vibrational level of the first excited state,  $E_1$  within the life-time of the latter. As a result, almost without exception, fluorescence (or phosphorescence) occurs by emission from the lowest vibrational level of the first excited state (or its associated triplet state). Consequently, fluorescence emission spectra in solution are usually less complex than absorption spectra and occur at a wavelength longer than that of the longest wavelength absorption band.

## B. EXTINCTION OF FLUORESCENCE

It is now relevant to discuss some of the phenomena which have a deleterious effect on the efficiency of fluorescence of molecular species. It will have been recognized that because of internal degradation of energy the photon or quantum of energy which is emitted has less energy than that which was absorbed. The quantum efficiency,  $\Phi$ , of fluorescence relates the *number* of quanta emitted to the number absorbed. Ideally, this should have a value of unity and under favourable circumstances some authors [38] have reported very high quantum efficiencies, *e.g.*, 0.97 for Rhodamine B in ethanol and 0.92 for fluorescein in 0.1 M NaOH. Factors which reduce the fluorescence may be classified as quenching effects, *i.e.*, those which reduce the quantum efficiency itself, or as inner-filter effects, *i.e.*, those which interfere mechanically without having any effect on the value of  $\Phi$ .

1. *Quenching Processes*

**a. Chemical Reaction.** One very important quenching effect is the chemical reactivity of excited state molecules and this, of course, is well recognized in many quarters where u.v. irradiation is used to promote reaction. However, under the conditions of analytical spectrofluorimetry as it is practised at present, the irradiation dose is usually small since only relatively weak sources and brief exposures are employed. Furthermore, unstable reagent systems will tend to be discarded in favour of those which are stable. For these reasons this type of quenching action will not be discussed further.

**b. Intermolecular Collision and Temperature Effect.** Collisional deactivation of excited state molecules with others, particularly the solvent molecules, has a very big role to play in the quenching of fluorescence. Generally it is found that an increase in temperature causes a very marked decrease in the fluorescence as a result of increased collisional frequency, so that negative temperature coefficients of 1–2 percent per degree centigrade at room temperatures are very common. At first sight this might appear to be a serious practical restriction on the analytical applications of the technique, but it must be remembered that spectrofluorimetry is usually practised as a technique in the submicrogram range where an error of up to 5% represents an insignificant physical difference in the amount of material being reported. For this reason it seems to be common practice not to go to any great length to thermostat the apparatus used to measure analytical fluorescence though this may arise out of the common analytical trace practice of simultaneous standard analysis along with unknowns rather than from disregard of the temperature effect. It is also interesting to note in passing, however, that Bowen and his co-workers [39, 40] have drawn some conclusions from the magnitude of the temperature

coefficient. With aromatic systems a low temperature coefficient is taken to indicate deactivation by intersystem crossing to the triplet state which is a process largely independent of temperature, whereas a high coefficient is indicative of external conversion which is an extremely temperature sensitive process. Because of the longer life-time of the excited state the effect of temperature is obviously much more critical in phosphorescence than in fluorescence.

**c. Viscosity of Medium.** Obviously an increase of the viscosity of the medium will have the opposite effect to an increase of temperature since it will minimise intermolecular collisions. The viscosity effect is particularly marked where the quenching efficiency is low.

**d. Nature of Solvent Medium.** The nature of the solvent molecule has a profound effect in the same way as temperature. For example, solvents which are capable of operating strong van der Waal's binding forces with the excited state molecule will prolong the life-time of a collisional encounter and will, therefore, favour de-activation. Similarly solvents which possess molecular substituents such as bromo-, iodo-, nitro or azo groups, etc., are undesirable because the strong magnetic fields which surround their bulky atomic cores promote spin de-coupling of electrons and triplet state formation. Consequently these solvents have a marked quenching effect on fluorescence though they may show promotion of phosphorescence. The mechanism whereby those exchanges occur is the subject of some discussion. Kasha [41] assumed that an energetic collision between the excited molecule and the quenching solvent molecule was involved whilst McGlynn and his co-workers proposed a weak charge-transfer system [42].

Solvent molecules which are strongly polar generally have an adverse effect on fluorescence relative to nonpolar systems as far as metal chelate systems are concerned due to their solvation of the complex, but with purely aromatic systems the situation may be reversed. Thus Van Dauren [43] has reported the relative fluorescence intensities of quinoline in benzene, ethanol and water as 1, 30 and 1000.

**e. Charge-transfer Processes.** Charge-transfer systems are also probably responsible for the quenching which is observed from certain anions in solution. For example, the fluorescence of fluorescein, quinine, Rhodamine B, etc., is greatly reduced by the presence of bromide, iodide, thiocyanate and thiosulphate which readily act as electron donors. It is probable that a complex of the type  $Q^* \cdot Br^-$ , is formed in which the charge on the anion is rapidly transferred,  $Q^{*-} \cdot Br$  backwards and forwards between the pair during close proximity. As a result, the entry of the  $\pi^*$  electron into its vacant orbital in the ground state may be prevented by the presence there of a donated electron. The fluorescence of naphthol and of anthranilic acid may be quenched by the reverse process because of charge-transfer with electrophillic anions

such as iodate, nitrate, etc., so that excited electrons which would normally be free to fall back to their  $\pi$  orbital are transferred to the anion and are not, therefore, available for fluorescence.

Leonhardt and Weller [44] suggest an interesting mechanism for charge-transfer quenching whereby an excited fluorescent molecule  $E^*$  forms a charge-transfer complex with the quencher  $X$ , giving an ion pair  $E^- \cdot X^+$  which may dissociate to the ground state entities  $E$  and  $X$ , dissipating the energy of the former excited state thermally in the process, or to give a triplet state of  $E$  and the ground state quenching molecule with similar dissipation of excess energy.

**f. Dissolved Cations and Ionic Strength.** Dissolved cations also have a profound effect, particularly when the fluorescent molecule is a chelate former for the cations concerned. Generally only those cations which are diamagnetic when co-ordinated and are non-reducible will form fluorescent complexes. Generally the transition metals with unfilled outer 'd' orbitals will quench fluorescence completely. On the other hand, whereas paramagnetic species quench fluorescence they strongly promote intersystem crossing so that at low temperatures those cations will be observed to promote phosphorescence.

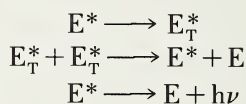
Fluorescence may also be markedly influenced by variations of the ionic strength of the medium when the fluorescent species or the quenching agent or both exist as charged species. This arises because ionic strength has a marked effect on the activity of the ions whilst it may not affect their analytical concentration in any way.

**g. Effect of Dissolved Oxygen.** The presence of dissolved oxygen has a pronounced quenching action on many organic systems though it does not appear to have very much effect on very many inorganic-organic chelate systems. In many instances the quenching may perhaps be due to photooxidation, but in others there appears to be no marked decomposition. Bowen and Wokes [45] in their excellent monograph on fluorescence, note that the ground state of the oxygen molecule is, in fact, a triplet state and that formation of its singlet excited level requires the energisation of only 24–40 kcal/mole. Quenching may, therefore, occur by collision or by long range dipole-dipole transfer of a singlet excited molecule with the triplet ground state oxygen molecule producing a singlet excited  $O_2$  molecule and a triplet state form of the other. This supposition is certainly a very convincing one in explaining the extremely efficient quenching action of oxygen on many organic systems since the dissipation of anything like the necessary 40–100 kcal/mole is difficult to explain by simple collisional quenching.

**h. Radiative Quenching and Delayed Fluorescence.** There are several other quenching mechanisms which could profitably be discussed here, but considerations of space dictate that these cannot be considered in detail. For example, the long range dipole-dipole transfer of energy has been mentioned as a typical nonradiative quenching mechanism,

but there are also some very interesting long range (up to 100 Å) non-collisional processes which are radiative. The energy of an excited state,  $E^*$ , is transferred to the ground state of another species which becomes excited,  $H^*$ , in the process, and subsequently radiates its own characteristic fluorescence. In this process fluorescence of  $E^*$  is prevented so that  $H$  acts as a radiative quenching agent for  $E^*$ . The possession of a common vibrational frequency to allow coupling of energy appears to be essential and also the presence in  $H^*$  of a lower vibrational level than in  $E^*$  so that internal degradation in  $H'^*$  dequantizes the reaction for  $E$ . The first recorded instance of such a reaction [46] is that between 1-chloroanthracene and perylene. This process must clearly be distinguished from that whereby fluorescence *emission* by  $E^*$  is absorbed by  $H$  to give  $H^*$ , etc.

Another quenching mechanism which has recently been engaging attention is the phenomenon of delayed fluorescence. Outwardly this appears to be akin to phosphorescence, but it involves a singlet-singlet transition and the wavelength of its fluorescence is identical to that of 'normal' fluorescence, whereas phosphorescence invariably has a longer wavelength. The mechanism is thought to involve decay of a singlet excited state  $E^*$  to the triplet  $E_T^*$  followed by interaction between two triplet molecules to give back a radiative singlet excited state and a ground state,  $E$ , molecule [47] according to the mechanism:



## 2. Non-Quenching Extinction Processes

Many substances interfere with the evolution of fluorescence without acting upon the quantum efficiency,  $\Phi$ , in any way. The most common mode of extinction in this way is the inner-filter effect, whereby excitation radiation which would otherwise reach the fluorescent molecule is cut off by the presence of another absorbing molecule which is usually non-fluorescent. Alternatively the inner-filter compound may act as the screen for the emitted fluorescence, thus preventing some of the radiation from reaching the detector. The fluorescent molecule can, of course, act as its own inner-filter. This effect is only marked in fairly concentrated solutions, however. Typical behaviour is shown in Figure 13A and B. In A the excitation radiation,  $I_0$ , is largely absorbed at the front face of the cuvette so that little radiation is transmitted,  $I_t$ , and so that the fluorescence signal,  $F$ , observed in the sector  $XY$  is not proportional either to the intensity of the excitation radiation or to the concentration of the fluorescing solute. In B, where the concentration of the solute is much lower,  $I_t \approx I_0$  and absorption and emission is uniform

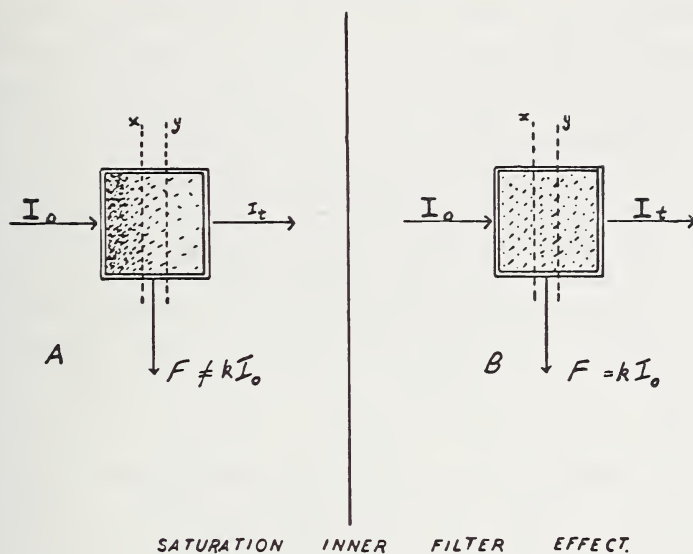


Figure 13. Effect of concentration on fluorescence emission. (a) Strong solution. (b) Dilute solution.

throughout the cuvette. This self-absorption can obviously be eliminated by appropriate dilution of the solution and in general this device is useful for minimising all inner-filter effects.

Substances which react chemically with the fluorescent molecule by oxidation, neutralisation, complexation, precipitation, etc., may also be very effective in extinction of fluorescence, but these again cannot be considered as quenching actions and they are common hazards in all solution techniques of trace analysis involving the use of organic reagents.

### C. INSTRUMENTATION

The apparatus which is used for the analytical application of fluorescence and phosphorescence phenomena is fairly well known and little need be said of it. The essential parts are:

1. A detector to sense the level of the emitted radiation, usually with an amplifier to enhance the analytical signal;
2. A monochromator or filter system to disperse the fluorescent radiation before it reaches the detector;
3. A cell or cuvette to hold the solution;
4. A monochromator or filter system to disperse the excitation radiation and
5. A source of radiation of suitable intensity and emission characteristics.

For phosphorimetry a device is also necessary to permit examination of emitted radiation during the interval when the excitation radiation is shut off from the sample. Instrumentation of spectrofluorimetry and

phosphorimetry has been discussed extensively by many authors in recent years and their papers [48-52] should be consulted for a detailed assessment of various items and of the merits of some commercially available apparatus. Fluorescence is usually observed at right angles to the incident beam of light to eliminate 'contamination' of the fluorescence signal by radiation of the excitation wavelength, but the use of efficient monochromators is fairly effective unless there is considerable overlap of the excitation and fluorescence spectra. Special care must, however, be taken in this mode that the detector does not "see" the walls of the cuvette which may otherwise cause serious interference by self-fluorescence or by scatter and internal reflection. The right angle arrangement is most used because it is advantageous for dilute solution (i.e. trace) work. Frontal analysis is most useful for the examination of solutions of fairly high concentration, *cf.* Figure 13A, or for the examination of solid specimens. The straight-through system is most used in phosphorimetry, but Parker and Rees [48, 49] have indicated that in fluorescence it sometimes has advantages not possessed by the other methods.

The analytical signal which is obtained is, of course, the amplified output from a photomultiplier tube or other suitable transducer and as such it has no physical significance unless it is calibrated carefully and the output is converted to quanta of radiation. However, it must also be noted that the response of a photomultiplier tube varies with the wavelength of the incident radiation as does the output of the source with selected wavelength. These factors will also be modified by monochromator transmission characteristics, *cf.* Figure 14. Thus the apparent spectra which are obtained require to be corrected for these characteristics of the apparatus before they can be correlated with other results. Instrumental correction is also possible by devices in which part of the light from the monochromated source is led onto a thermocouple which generates a signal corresponding to the *energy* reaching it irrespective of its wavelength. This signal operates a slit-servo-mechanism so that constant energy is fed into the irradiation cell. A second servomechanism similarly operates on the fluorescence side of the instrument. Commercial equipment is now available for this purpose and has been described recently by Slavin *et al.* [53], and by Turner [54].

### 1. Choice of Instrument

However, such refined instrumentation is more suited to physico-chemical studies of a fundamental nature rather than to the needs of trace analysis except in certain circumstances where much developmental work is involved. The main choice of instrumentation which faces the prospective user of analytical fluorimetry is whether to work with an instrument with monochromators in both the excitation and the

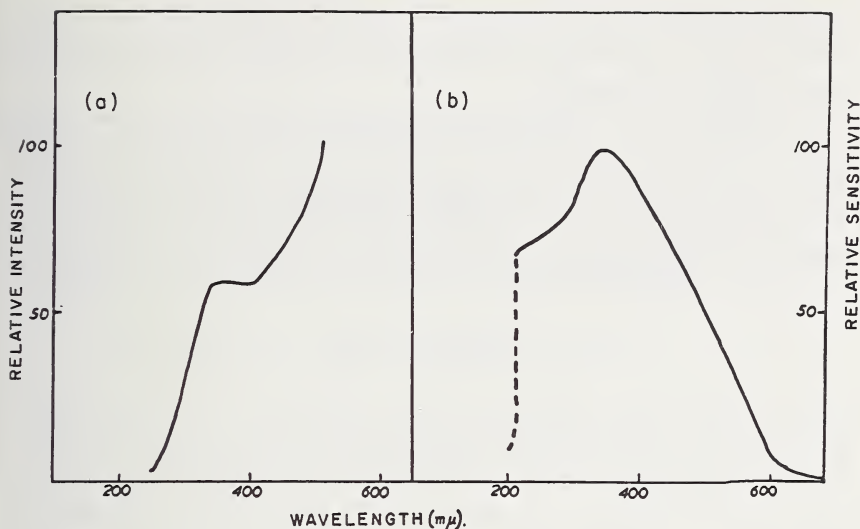


Figure 14. Spectral response characteristics. (a) Output of 150 W Xenon arc lamp. (b) Response of IP 28 photomultiplier.

fluorescence beams or with a monochromator in one and a filter in the other or with filters in both. Briefly, a double monochromating instrument is attractive, particularly in the exploration of a relatively unknown system and indeed such instruments have been used extensively, if rather laboriously, for basic studies in the past. However, for analytical work the use of an instrument with a filter in the excitation arm is very attractive because it allows much more intensity of irradiation and a wider spectrum of irradiation whilst the monochromator in the emission side allows more precise resolution of the fluorescence radiation. Light losses inside most monochromating devices are usually rather great. As a result, when sensitivity of detection or determination is the desideratum a filter instrument is best suited, but when resolution and precision is required, a spectrofluorimeter with twin monochromators should be used. The signals which are received from filter instruments frequently include spurious signals from Raman emission, light-scatter, etc., which cannot be detected separately and measured readily by such instruments. Consequently, such apparatus can only be used satisfactorily on a purely empirical basis when the excitation/fluorescence characteristics of the system are known.

#### D. PHYSICAL LAWS GOVERNING FLUORESCENCE EMISSION

Fluorescence emission is necessarily preceded by the absorption of radiation of the wavelength of excitation. Consequently, the laws which

govern the relationship between the activity of a fluorescent species in solution and the intensity of fluorescence arise out of, and depend on, those relating to absorption.

If radiation of the wavelength necessary to excite fluorescence falls upon a solution of the fluorescent substance in a suitable cuvette of absorbing cross-section  $A$ , *cf.* Figure 15, it will be absorbed according to the Lambert-Beer law. Suppose that the intensity of the incident light is  $I_0$  and that of the transmitted light is  $I_t$ , both measured in quanta per sq cm. This gives us

$$I_t = AI_0 \exp^{-\epsilon \ell a}$$

where  $\epsilon$  is the molar absorptivity of the substance at the given wavelength of absorption,  $\ell$  is the pathlength in cm and  $a$  is the activity of the absorbing species. The amount of energy absorbed is, of course, given by  $AI_0(1 - \exp^{-\epsilon \ell a})$  and it is this energy which will promote fluorescence. Let the quanta of fluorescence generated be  $F$ . If we consider a small layer of absorbing solution of thickness  $dx$  situated at a distance  $X$  from the front face of the cuvette, the fluorescence generated in this layer will be proportional to the amount of energy absorbed,  $dI$ , according to the quantum efficiency,  $\Phi$ , of generation of fluorescence.

$$\text{i.e. } dF = \Phi dI$$

The light intensity which falls on the layer  $dx$  at a distance of  $X$  cm from the front is  $AI_0 \exp^{-\epsilon X a}$  whilst the transmitted intensity is  $AI_0 \exp^{-\epsilon(X+dx)a}$ . Therefore  $dI = AI_0[\exp^{-\epsilon X a} - \exp^{-\epsilon(X+dx)a}] = AI_0 \exp^{-\epsilon X a}[1 - \exp^{-\epsilon dx a}]$ . If we assume that we are dealing with a dilute solution and a very thin incremental layer,  $dx$ , therefore

$$dI = AI_0 \epsilon a \exp^{-\epsilon X a} dx$$

As a result we can now write

$$dF = \Phi AI_0 \epsilon a \exp^{-\epsilon X a} dx$$

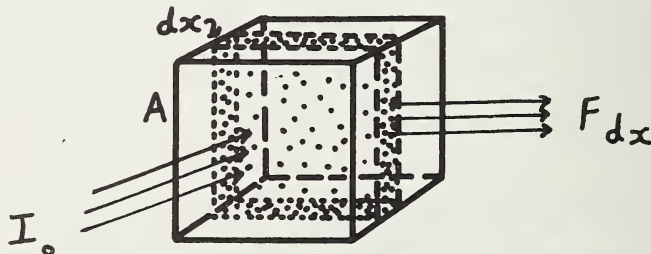


Figure 15. Production of fluorescence in solution.

The total fluorescence is obtained by integrating over the entire path-length of the absorbing/fluorescing solution

$$\begin{aligned}
 \text{i.e.,} \quad F &= A\Phi I_0 \epsilon a \int_0^{\ell} \exp^{-\epsilon x a} dx \\
 &= A\Phi I_0 [1 - \exp^{-\epsilon \ell a}]
 \end{aligned}$$

Expansion of the bracketed term gives the factorial function

$$\begin{aligned}
 F &= A\Phi I_0 \left[ \epsilon \ell a - \frac{(\epsilon \ell a)^2}{2!} + \frac{(\epsilon \ell a)^3}{3!} - \frac{(\epsilon \ell a)^4}{4!} + \dots \right] \\
 &= A\Phi I_0 \epsilon \ell a \left[ 1 - \frac{\epsilon \ell a}{2} + \frac{(\epsilon \ell a)^2}{6} - \frac{(\epsilon \ell a)^3}{24} + \dots \right]
 \end{aligned}$$

If  $\epsilon \ell a$  is less than or equal to 0.05,  $\frac{\epsilon \ell a}{2} \leq 0.025$ ,  $\frac{(\epsilon \ell a)^2}{6} \leq 0.0004$ , and so on, so that virtually all terms save the very first one may be neglected. It is easily possible to arrange that  $\epsilon \ell a$  should have a small value by using a very low concentration,  $c$ , of the fluorescing solute so that the activity  $a \approx c$ , the analytical concentration, and by using a fairly short path-length. This is achieved in effect by arranging that less than 5% of the incident light is absorbed by the compound. Under these conditions  $I_t \approx I_0$  and so the distribution of fluorescence throughout the solution is almost entirely uniform and the situation depicted in Figure 13B results. The fluorescence equation, therefore, simplifies per sq cm to

$$F = \Phi I_0 \epsilon \ell c$$

However, it is more common to work on a logarithmic (base 10) scale and to view only a fraction of the total fluorescence generated by surveying a small segment of solution in a direction at right angles to the incident light beam. If, therefore, we convert our equation to the base 10 and introduce a fractional factor "p" we arrive at a final equation

$$F = 2.303 \Phi I_0 \epsilon \ell c p$$

It should be remarked at this stage, however, that the true fluorescence yield  $F$  is rarely measured in quanta, but is generally replaced for analytical purposes by the signal response of a photomultiplier tube which is sensitive to the fluorescence radiation.

The alternate parameters  $I_0$ ,  $\ell$  and  $p$  are instrumental factors. It is apparent, therefore, that the analytical signal for a given chemical sys-

tem will vary directly with the intensity of the radiant signal  $I_0$  provided by the source, with the path-length  $\ell$  of the cuvette and with the fraction of the total fluorescence fed to the detector. The remaining parameters in the equation,  $\Phi$  and  $\epsilon$  are functions of the efficiency of the fluorescent reagent system which we chose to use for the analysis of the trace constituent of concentration  $c$ . Obviously a reagent having a high quantum efficiency should be selected and also one having a high value for its molar absorptivity, though the latter factor can cause some difficulties.

#### E. BASIC DIFFERENCES BETWEEN FLUORIMETRY AND ABSORBANCE

The linear equation which has been derived illustrates two very important differences between absorption spectrophotometry and spectrofluorimetry. In the former the basic equation is

$$A \text{ (absorbance)} = \text{Log } I_0/I_t = \epsilon \cdot \ell \cdot c$$

Any increase in  $I_0$  will be matched by a corresponding increase in  $I_t$  with no net gain in the analytical signal  $A$ . With fluorescence, however, any increase in  $I_0$  the intensity of the source, is matched by a corresponding increase in  $F$ . Thus it is possible to 'improve' the analytical signal in fluorescence. Yet again, any increase in amplifier gain in absorption spectrophotometry will amplify  $I_0$  and  $I_t$  correspondingly whereas in fluorescence the analytical signal  $F$  will once more be enhanced. For these two reasons the analytical sensitivity of molecular fluorescence spectrophotometry is inherently greater than that of molecular absorption spectrophotometry and as a generalisation it may be said to be more sensitive by 2 to 4 orders of magnitude so that it is easily possible by many fluorescence procedures to determine subnanogram/ml. concentrations of traces. This aspect will be discussed further in the subsequent section dealing with the merits and demerits of the technique as an analytical tool.

These same factors do, however, make it difficult to compare the relative sensitivities of fluorimetric procedures or, even with a given method, to compare the results obtained on one instrument with those obtained by another. This is no problem in absorptiometry since differences in source intensity and detector response are automatically cancelled out by the  $I_0/I_t$  signal ratio that corresponds to absorbance. Comparison is, however, only made more troublesome because it can easily be done by correcting for source and detector characteristics and relation to the performance of a standard substance such as quinine bisulphate (see reference 72).

#### F. REAGENTS FOR SPECTROFLUORIMETRIC ANALYSIS

It is a fact that molecular fluorescence spectrophotometry has not been used to a very great extent in inorganic trace analysis and this, in

view of the rather high selectivity and sensitivity, is rather surprising at first sight. But it is only recently that instrumentation of a really suitable nature has become available and it must be confessed that except for a few elements there is a dearth of the fluorogenic reagents which are necessary since very few simple inorganic species are capable of yielding any significant fluorescence in aqueous or non-aqueous solutions. It is also true that whereas the development of reagents for absorption spectrophotometry took place gradually over a fair number of years, based largely on empirical rules and observation, the evolution of inorganic spectrofluorimetry as a trace technique has been a more sudden process. Although we have now a better understanding of molecular structure and function, it is still unfortunately usually a more rapid and successful process to screen large numbers of compounds for reactivity by experiment than to predict and produce a reagent, if indeed this has ever been done.

### 1. *Character of Reacting Cation*

However, there are certain guidelines and facts that are extremely useful for those who wish to pioneer in this area. First of all there are certain metals for which there appears to be no lack of fluorimetric reagents of quite widely ranging characteristics, *e.g.*, aluminum, beryllium, the rare earths, zinc, indium, gallium, calcium. These are chiefly the metals which largely form 'colourless' complexes. The only fluorimetric methods available for metals such as iron, copper, nickel, chromium and other metals which readily form 'coloured' salts and complexes are usually based on the extinction of fluorescence of a fluorescent molecule with which they react. This can clearly be seen with many fluorogenic reagents, *e.g.*, 8-hydroxyquinoline, which forms fluorescent complexes with aluminium, beryllium, etc., and non-fluorescent complexes with iron, copper, etc. One of the features which we clearly must consider here is that in the 'coloured' ions the energy levels for electron transition must lie close together since the absorption occurs in the relatively unenergetic visible range of the spectrum whilst the 'colourless' ions must have relatively wide spaced electronic levels since any absorption which occurs is found in the u.v. region. Close spacing of excitation levels is conducive to the processes of non-radiative loss of energy. Consequently, the presence of such 'low-level' ions in an otherwise fluorescent molecule may lead to an electron-sink action which will completely extinguish fluorescence. Yet again, ions which are paramagnetic promote triplet state formation in a ligand's  $\pi$  orbitals and cannot offer good possibility for the production of a fluorescent complex upon reaction with a molecule which is itself non-fluorescent, though they may well be determined by fluorescence extinction with a self-fluorescent reagent. Generally speaking, in any given periodic group the heavier atoms of the series will be found to produce weaker

fluorescence than the lighter elements due to the disturbance produced by the electric fields of their bulkier atomic cores. On the other hand, this process tends to favour the production of phosphorescence though this will not be seen in solution at *ordinary* temperatures. For example, no fluorescent copper complexes are known, but several are phosphorescent [55]. In many instances there appears to be a type of pendulum balance between fluorescence and phosphorescence emission so that where one is lost the other is found.

## G. NATURE OF FLUOROGENIC REAGENTS

### 1. *Aliphatic Compounds*

It is a matter of considerable comfort to find that generally, whereas synthesis has produced ever more complex molecules for absorption spectrophotometry, it is the simpler molecules which are most suited to fluorescence spectrophotometry. Aliphatic compounds rarely show efficient fluorescence because they show only feeble absorption in the near u.v. or visible range, and consequently cannot be expected to fluoresce strongly anywhere. Moreover they rarely contain sufficient delocalised  $\pi$  electrons which are necessary. Most aliphatic compounds which do absorb strongly do so in the *far* u.v. ( $< 2000 \text{ \AA}$ ) where the energy involved is so great that decomposition is produced rather than fluorescence, or even the curious process of predissociation [56] which again precludes fluorescence emission.

### 2. *Aromatic Compounds*

Aromatic compounds, on the other hand possessing good  $\pi$  bonding systems are commonly fluorescent and it is interesting to note that replacement of one of the methyl groups of acetylacetone, which forms no fluorescent metal complexes, by a benzene ring to form benzoylacetone (or both methyl groups in dibenzoylmethane) results in many fluorescent metal chelate compounds. Most simple aromatic hydrocarbons fluoresce strongly with their fluorescence moving inevitably ahead of their absorption spectra into the longer wavelengths with increasing complexity, *e.g.*, benzene and naphthalene in the u.v., anthracene, green; pentacene, red [57]. It is, therefore, generally found that fluorescence reagents for inorganic trace analysis can best be built by substitution of chelating groups on an aromatic skeleton. As a general rule one would only look for fluorescence from molecules possessing a good delocalisation of electrons. Electron donating groups generally favour fluorescence, whilst electrophilic groups diminish it. Thus alkyl groups, hydroxyl groups, amino groups are favourable, whereas the presence of nitro groups, halogens, etc., should be avoided. Inside the halogen group progressive substitution of fluorine by chlorine, bromine and iodine in monohalogenated naphthalene progressively

decreases the intensity of fluorescence emission and increases the phosphorescence yield due to the effect of their nuclear field in promoting excited singlet-triplet transitions. The introduction of any heavy atom into the fluorophore, either as a cation at the chelation centre or as a substituent in the aromatic ring system, generally diminishes fluorescence and favours phosphorescence. Nitro groups are particularly effective in this respect so that their presence is particularly effective in suppressing fluorescence (usually completely). Many aromatic carbonyl compounds undergo  $n/\pi^*$  rather than the usual  $\pi/\pi^*$  transitions, *i.e.*, non-bonding electrons rather than  $\pi$  electrons are promoted. These bands are usually less intense and the excited state has a longer life-time than in a  $\pi/\pi^*$  transition so that fluorescence is most frequently not observed. On the other hand, the difference in energy between the excited state and the associated triplet state is usually much smaller for such systems so that phosphorescence is frequently common. It now becomes doubly interesting to find that substitution of a hydroxyl or an amino group in a position vicinal to a carbonyl group on the aromatic skeleton frequently produces a fluorescent molecule because this combination of groups in such close proximity is of importance in producing metal-chelate compounds of importance to inorganic trace analysis. It is probable that the hydroxyl or amino hydrogen atoms lock up the non-bonding lone pair electrons on the carbonyl oxygen through hydrogen bonding thus preventing the  $n/\pi^*$  transition and favouring  $\pi/\pi^*$  excitation. Carboxylic acids behave similarly. Thus benzoic acid is non-fluorescent, though benzene is, but salicylic and anthranilic acids are both quite strongly fluorescent. The  $n/\pi^*$  system is also largely responsible for the non-fluorescence of many aromatic compounds containing heterocyclic nitrogen atoms. These heterocyclic compounds can, however, function like the carbonyl and carboxylic acids mentioned above and like the former they are susceptible to the effect of solvent molecules and so on. For example, quinoline is non-fluorescent in aqueous solution, but fluoresces strongly in an acid medium due to locking up of the lone pair electrons upon protonation. Similarly, many aldehydes and ketones [58] and heterocyclic nitrogen bases [59, 60] which do not fluoresce in non-polar solvents do so in hydrogen bonding and strongly polar solvents. This must, however, be contrasted with the behaviour of some metal chelate compounds which fluoresce more strongly in non-polar solvents [61].

### 3. Molecular Configuration

The configuration of the molecule is, also very significant. Generally a fairly rigid structure is necessary and preferably a planar one since molecular vibrations which might otherwise dissipate energy are minimised and coplanarity ensures good delocalisation of  $\pi$  electrons.

Fluorescein, for example, differs only from the entirely non-fluorescent phenolphthalein in possessing an oxygen bridge across the two phenol rings. The absence of the bridge enables free rotation of the phenol rings about their bonds with the central carbon atom in the latter molecule and ready dissipation of energy, whereas no such dissipation is possible in the rigid planar fluorescein molecule. The presence of flexible side chains which are free to rotate and dissipate energy should be avoided in fluorimetric reagents wherever possible, although there are instances when this can be turned to good advantage. For example, the presence of an aminomethyl-dicarboxymethyl group in a position adjacent to the hydroxyl group in the reagent Calcein Blue, *cf.* Figure 16, is of interest [62, 63]. When this side chain is not completely ionised, *e.g.*, *ca.* pH 7–10, it is fluorescent and has its fluorescence quenched by many ions, *e.g.*, mercury, copper, etc. In strongly alkaline solution, however, it is non-fluorescent, presumably due to the removal of the hydrogen bonding between the amino nitrogen and the phenolic oxygen and free rotation of the dicarboxyamino group. At pH 12, however, the alkaline earths produce fluorescence once more when they react with the reagent since they will now function as a bridge in place of the former hydrogen bond which allowed fluorescence at the lower pH values. This reaction is very selective for the alkaline earths because other metals are incapable of reacting at such a high pH.

#### 4. Steric Effects

Molecules which possess any appreciable degree of steric hindrance are usually not efficient fluorescers since the close proximity of groups favours dissipation of absorbed energy which might otherwise be shed by fluorescence and this effect has been well studied in the case of the cyanine dyes [60]. It has also been noted that in some compounds which exist as *cis-trans* isomers that the *trans* form is more intensely fluorescent than the *cis*. This has been attributed, for example, to steric interaction of hydrogen atoms in *cis* stilbene which is non-fluorescent, whereas *trans* stilbene fluoresces strongly [64]. A similar, but less marked observation, has been made in the instance of 2-vinylanthracene which exhibits fluorescence in both forms, but with a marked difference between the two sets of spectra [65]. This *cis-trans* effect may have very considerable implications for trace analysis because a considerable number of compounds which are of value as fluorimetric reagents are

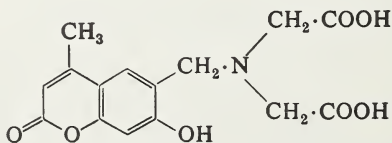


Figure 16. Calcein Blue.

based on stilbene and Schiff's base condensation products. Indeed, it might be said that the latter bear the same useful relationship to fluorimetry as hydroxyazo dyes do to absorptiometry where they constitute a good starting off point for those in search of a new general purpose reagent. Not a few azo dyes exhibit useful fluorimetric activity also, but the electron excitation levels lie rather closely spaced in azo dyes so that the longest wavelength absorption band falls well into the visible range with the result that the fluorescence emission band is pushed over to yet longer wavelengths where detectors are not particularly satisfactory with respect to sensitivity. 0,0'-dihydroxyazobenzene has been used with success for the fluorimetric determination of magnesium [66] and in terms of the aromatic structure about the azo bond, Pontachrome Blue Black R which is used as an aluminium reagent is probably the most complex molecule to have been used in this connection (it exhibits red emission).

#### H. PRINCIPAL TYPES OF FLUROGENIC REAGENT

Analytically speaking it is significant to note that some of the most successful *types* of fluorimetric reagent are based on aromatic ring systems which are bridged by simple conjugated bond systems or systems which have partial double bond characteristics (by keto-enol tautomerisation for example), *cf.* Figure 17. For the purposes of trace metal analysis it is, of course, necessary that there should be a suitable disposition of donor atoms attached to the bridge or the *ortho* position in the aromatic skeleton. Generally, in these reagent types the introduction of a metal ion of suitable electronic character, *qv*, most probably induces fluorescence in the appropriate ionisation form of the ligand by the localisation of the non-bonding lone pair electrons on the donor atoms, thus pre-

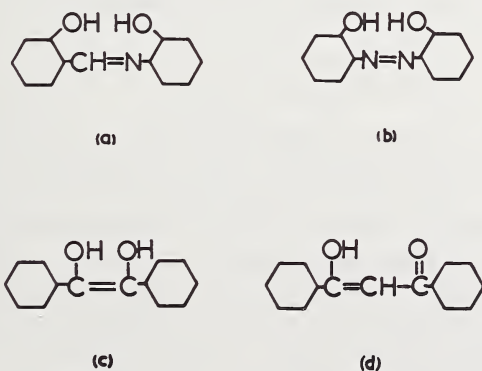


Figure 17. Types of metallofluorescence reagent. (a) Salicylidene-o-aminophenol (Schiff's Base Link). (b) 0,0' Dihydroxyazobenzene (Azo Link). (c) Benzoin (Ethine Link). (d) Dibenzoylmethane ( $\beta$  Diketone Link).

venting the energetically favoured  $n/\pi^*$  transition process and permitting the necessary fluorogenic  $\pi/\pi^*$  transition.

It will be seen, therefore, from the foregoing discussion that although the approach to the development of a fluorimetric reagent is still largely an empirical process there are well recognized pathways to the production of fluorimetric ligands and a wealth of necessary associated empirical knowledge from the older technique of absorption spectrophotometry on the selective functionality of co-ordinative groupings towards reaction with certain ions.

### I. FLUORESCENCE ENERGY TRANSFER SYSTEMS

Before leaving the area concerning the structure of fluorimetric reagents it is important to note that whereas all the examples already discussed have had the ligand acting as the fluorophore with the cation serving merely as a necessary partner in the process, there are some instances where the metal ion has a direct role to play in the primary absorption/emission process. In these, the chelate absorbs energy characteristic of the ligand species, but re-emits energy which is characteristic of the metal. This situation arises where the metal possesses an excited  $f$  (or  $d$ ) level lying just below the first triplet excited state of the liganding species. Thus  $\pi/\pi^*$  excitation and  $f^*/f$  emission is found in the chelates of many of the rare earths, *e.g.*, those with benzoylacetone and dibenzoylmethane [67] and even  $d^*/d$  emission following  $\pi/\pi^*$  excitation in some of the 'non-fluorescent' transition metals which possess partly filled  $d$  orbitals [68]. These systems are obviously of unique analytical importance, particularly in view of the narrow atomic line-spectra which are emitted in place of the usual molecular band emissions. The reverse process in which the metal undergoes a  $f/f^*$  excitation and the chelate emits a  $\pi^*/\pi$  fluorescence is also not unknown [69], and probably presents an occasion when it is better, analytically, to use the excitation rather than the (more usual) emission spectrum for analytical measurement.

### J. FLUOROMETRIC REAGENTS IN PRACTICE

An excellent coverage of spectrofluorimetric procedures and other matters pertaining to fluorimetric analysis has been given for many years in the biennial reviews of C. E. White [70] and more recently in conjunction with A. Weissler [71]. Since these are comprehensive and readily available only a tabular unreferenced summary of *selected* methods is given here, *cf.* Table 2. In connection with this table, it must regretfully be pointed out that the values quoted for sensitivity must not be strictly interpreted because they depend on the sensitivity of the detector/amplifier system, the intensity of the source, the geometry of the excitation/emission system, etc. These factors have recently been discussed briefly by the author [72] and will not, therefore, be reported here. In

many cases improvement of the sensitivity should be possible with use of recent equipment. Naturally, the information on interferences varies from paper to paper and this column must also be interpreted accordingly.

#### K. ASSESSMENT OF MOLECULAR FLUORESCENCE SPECTROPHOTOMETRY AS AN ANALYTICAL TECHNIQUE

Molecular fluorescence spectrophotometry possesses two unique advantages as a trace technique for inorganic analysis. Firstly, it is very highly sensitive and may be applied to the analysis of solutions 100 to 10,000 times more dilute than corresponding absorptiometric techniques. The reasons for this have been discussed already in connection with the derivation of the fluorescence equation. The same equation also revealed in its derivation that because of non-linearity fluorimetry must remain essentially a trace or ultratrace technique. An even more cogent reason is, of course, depicted in Figure 13A, although the same figure clearly reveals that a frontal examination of the evolved fluorescence could be used for 'strong' solutions with some measure of success. Secondly, molecular fluorescence spectrophotometry possesses an even more desirable property as a trace technique—selectivity of determination. It has already been mentioned that only certain ions are capable of producing fluorescence. Even with an unselective reagent such as 8-hydroxyquinoline only a few ions produce fluorescence, whereas over 30 produce absorption spectra. Even amongst those metals which are themselves fluorescent, however, interelement selectivity is possible because measurement may be made on the excitation or the fluorescence emission spectrum and, of course, it is possible to control the incidence of fluorescence by selecting the wavelength of excitation so that one metal fluoresces only weakly or not at all, while the other fluoresces strongly. Collat and Rogers [73] have shown, for example, that both gallium and aluminium 8-hydroxyquinoline complexes may be extracted into chloroform and yield virtually coincident emission spectra. However, there is a difference of nearly three-fold in the relative ease of excitation of the spectra so that they were able to carry out a sequential determination of the two metals by excitation at 366 m $\mu$  and then at 436 m $\mu$  using a mercury lamp source. In common with absorptiometry, spectrofluorimetric methods may be used in conjunction with pH control to achieve selectivity of reaction and, of course, with masking agents and simple batch extraction. In this respect, because of its own 'built in' selectivity of reaction, molecular fluorescence spectrophotometry is a good deal more selective than molecular absorption spectrophotometry. For example, Dagnall, Smith, and West [74] have recently shown in this way that aluminium may be determined fluorimetrically in aqueous solution with salicylidene-*o*-aminophenol as reagent in the presence of 46 cations with interference only from chromium (III),

TABLE 2(a). Spectrofluorimetric methods for inorganic ions

Determination	Reagent	Conditions	Maxima			Sensitivity	Interferences
			Absorption m $\mu$	Fluorescence m $\mu$			
Al	Alizarin Garnet R (CI 168)	pH 4.6	470	500	0.007 $\mu$ g/ml	Be, Co, Cr, Cu, F <sup>-</sup> , Fe, NO <sub>3</sub> <sup>-</sup> , Ni, PO <sub>4</sub> <sup>3-</sup> , Th, Zr	
	Morin	pH 3.3	430	500	0.05 $\mu$ g/ml	Ag, AsO <sub>4</sub> <sup>3-</sup> , Be Cr, F <sup>-</sup> , Fe, Ga, In, PO <sub>4</sub> <sup>3-</sup> , R. Earths	
	2,3-hydroxynaphthoic acid	pH 5.8	370	460	0.002 $\mu$ g/ml	Be, Sc, B <sub>4</sub> O <sub>7</sub> <sup>2-</sup> , PO <sub>4</sub> <sup>3-</sup> , F <sup>-</sup> , MoO <sub>4</sub> <sup>2-</sup> , WO <sub>4</sub> <sup>2-</sup>	
	8-hydroxyquinoline	(CHCl <sub>3</sub> ) pH 5.7	365	520	0.1 $\mu$ g/ml	Ga, etc.	
	Salicylidene-o-aminophenol	pH 5.6	410	520	0.0002 $\mu$ g/ml	Only Cr(III), Sc, Th	

$B_4O_7^{2-}$	1-amino-4-hydroxy- anthraquinone	Conc. $H_2SO_4$	546	Red	—	—
	Benzoin	(EtOH) pH 12.8	370	480	0.04 $\mu g/ml$	Be, Sb
	Morin	Dil. $HCl-H_2Ox^-$	365	460-540	1 $\mu g$	
Be	1-amino-4-hydroxy- anthraquinone	0.02 M NaOH	540	620	0.2 $\mu g/ml$	$CrO_4^{2-}$ , Li
	2,3-hydroxynaph- thoic acid	pH 7.5	380	460	0.0002 $\mu g/ml$	Sc, Cr(III), Bi(III), Ce, Sn(IV), Ti(IV), Th(IV), Fe
	8-hydroxyquinoline	( $CHCl_3$ ) pH 8.0	—	—	0.001 $\mu g/ml$	Al, Bi, Cd, Cr, Cu, Fe, In, Sn, Ti, Zn

TABLE 2(b). Spectrofluorimetric methods for inorganic ions

Determination	Reagent	Conditions	Maxima		Sensitivity	Interferences
			Absorption m $\mu$	Fluorescence m $\mu$		
Cd	2-( <i>o</i> -hydroxyphenyl)benzoxazole	pptd., dissolved in HOAc	365	Blue	2 $\mu$ g/ml	NH <sub>3</sub>
Cu(II)	Tetrachlorotetraiodo-fluorescein <i>o</i> -phenanthroline	pH $\approx$ 7	560	570	0.001 $\mu$ g/ml	Cyanide
F <sup>-</sup>	Al complex of alizarin garnet R or Eriochrome red B	pH 4.6 (quenched reaction)	470	590	0.001 $\mu$ g/ml	Be, Co, Cr, Cu, Fe, Ni, PO <sub>4</sub> <sup>3-</sup> , Th, Zr

Ga	8-hydroxyquinoline	(CHCl <sub>3</sub> ) pH 3.9	—	492	0.02 μg/ml	Cu, Citrate
	8-hydroxyquinoline	(CHCl <sub>3</sub> ) pH 2.8-5.7	436	470-610	0.05 μg	Al, Cu, F <sup>-</sup> , Fe, In, Mo, Se, V, Citrate
	Salicylidene-o-aminophenol	pH 4.0	420	520	0.007 μg/ml	—
Ge	Benzoin	alk. EtOH	365	Yellow-green	2 μg/ml	AsO <sub>4</sub> <sup>-3</sup> , B, Be, CrO <sub>4</sub> <sup>-2</sup> , NO <sub>2</sub> , SiO <sub>3</sub>
In	8-hydroxyquinoline	(C <sub>6</sub> H <sub>6</sub> ) pH 7.5	—	—	0.2 μg/ml	Be, Cu, Fe, Ga, Zn,
	8-hydroxyquinoline	(CHCl <sub>3</sub> ) pH 5.1	—	—	0.04 μg/ml	Al, Be, Cu, Fe, Zr
Mg	Disalicylidene diamino benzofuran	pH 10.5	475	545	0.002 μg/ml	Mn
Mo	Carminic acid	pH 5.2	560	590	0.1 μg/ml	

TABLE 2(c). Spectrofluorimetric methods for inorganic ions

Determination	Reagent	Conditions	Maxima			Sensitivity	Interferences
			Absorption m $\mu$	Fluorescence m $\mu$			
Sc	Salicylaldehyde semicarbazone	pH 6	370	455	0.002 $\mu$ g/ml	—	
Se	Diaminobenzidine	(Toluene) pH 7.4	420	550-600	0.002 $\mu$ g/ml	—	
Sn(IV)	Flavanol	0.1M H <sub>2</sub> SO <sub>4</sub>	400	470	0.1 $\mu$ g/ml	F <sup>-</sup> , PO <sub>4</sub> <sup>3-</sup> , Zr	
Tl(III)	Rhodamine B	(C <sub>6</sub> H <sub>6</sub> ) 2M HCl	360	580	0.1 $\mu$ g/ml	Au, Fe, Ga, Hg, Sb	
Tl(I)	HCl/KCl	3.3M HCl/ 0.8 M KCl	250	430	0.01 $\mu$ g/ml	Au, Bi, Pt, Sb	
W(VI)	Carminic acid	pH 4.6	515	585	0.04 $\mu$ g/ml		

scandium and thorium. As little as 27 ng (or  $2.7 \times 10^{-4}$  ppm) were determined by the method.

It is sometimes held against molecular fluorescence spectrophotometry as an analytical technique that it is applicable only to dilute solutions. This may well be a limitation for some analyses, but certainly not for trace work. It is also sometimes said that fluorimetric reagents are pH sensitive, but in this respect they do not differ from absorptiometric reagents. Another objection which is sometimes raised is that fluorescence is subject to quenching effects, and oxygen is mentioned as the chief source of difficulty. This may well be true for certain organic compounds, particularly those of bio-chemical interest, but it is the author's experience with metal chelate compounds that quenching is rarely met from oxygen or any other common substance likely to be present. Temperature coefficients constitute yet another factor which is raised as a detraction. But, absorptiometric methods are also subject to temperature coefficients and in any instance the normal convention of running two standards with every series of unknowns will overcome any difficulty likely to arise if it is not convenient to thermostat the cell compartment. Photodecomposition of the sample under irradiation is negligible under the conditions of analytical measurement because of the small dose rate involved.

Perhaps the most telling criticism that may be made of the technique at present is that as far as inorganic trace analysis is concerned there is, in comparison to absorptiometry, a dearth of reagents. This, in itself, is perhaps inherent in the chemical selectivity of reaction of such reagents, but it also arises from the fact that it is only recently that serious attention has been paid to the technique and the availability of reagents should increase rapidly. Most metals can, of course, be determined by fluorescence extinction but direct (positive emission) methods are now being found for even the transition metals *via* the fluorescence energy exchange reactions mentioned above and by indirect (positive emission) methods such as that described recently by Bailey, Dagnall, and West [75] for copper (II) in which the ternary ion-association complex between copper (II), 1,10-phenanthroline and Rose Bengal is caused to dissociate and fluoresce by addition of ammoniacal acetone to its extract. These authors found no interference from 56 cations or any common anion and even with the IP 28 photomultiplier, which is not very responsive at the wavelength of emission (570 m $\mu$ ), they were able to work at levels down to  $1 \times 10^{-3}$  ppm.

The cost of equipment required for analytical measurements based on molecular fluorescence spectrophotometry is comparable to that for absorption spectrophotometry, though that required for double monochromating instruments is somewhat (though not greatly) more expensive. Quartz optics and cuvettes must generally be used at least on the excitation side of the apparatus and quartz cuvettes are almost invariably

necessary. Maintenance and running costs constitute no great problem and are indeed much less expensive than those for most other trace methods, *e.g.*, X-ray fluorescence, spectrography, mass-spectrometry, etc. Manipulatively, the technique generally presents fewer problems than many others with the proviso that the cleanliness of handling requisite to all trace methods is observed here also.

#### L. PROSPECTS FOR THE FUTURE

There is little doubt that molecular fluorescence spectrophotometry has a considerable future and will undergo considerable development as an inorganic trace technique over the next few years. There can be few laboratories that will be able to neglect such an elegantly selective, sensitive and inexpensive technique. Like absorptiometry it is easily automated and consequently should play a big part in this rapidly expanding area because of its selectivity and sensitivity. Much of the modern equipment which has now become available commercially is extremely satisfactory and the real surge forward will probably arise from a systematic development of a range of reagents such as that which is now available for absorption spectrophotometry. Solid state fluorescence will probably develop fairly extensively, particularly in conjunction with the development of thin-layer chromatography, but a technique of pulsed short duration high intensity irradiation from sources other than Xenon arcs and mercury lamps may well prove to become significant. The polarisation effects which are associated with fluorescence have not been mentioned in this survey, but they are undoubtedly significant. At the lowest level of information the polarisation spectrum of the fluorescing solution provides additional information of diagnostic value, but much more useful analytical work may be centred around the phenomenon in future developments.

Lastly, phosphorescence has been mentioned only in passing. It is, of course, slightly more complex to practise spectrophosphorimetry because of the need to operate at low temperatures and to 'chop' the incident and emission beams out of phase, but it is inherently a more selective technique than spectrofluorimetry and may be applicable to a wider range of analyses though present indications are that its sensitivity may be considerably lower. The flexibility of being able to observe one phosphorescent species in the presence of others by variation of irradiation/observation times appears to be an attractive proposition which may well outweigh the factor of the lower sensitivity. There is as yet, however, a shortage of suitable equipment available from manufacturers for the analytical exploration of spectrophosphorimetry.

#### IV. Atomic Absorption Spectrophotometry

Atoms are capable of absorbing light in exactly the same way as molecules by interacting with a photon of the energy requisite to promote

an electronic transition from the ground state to one of the excited states of the atom. Consequently, a technique of atomic-absorption spectrophotometry closely similar to molecular absorption spectrophotometry should be possible, but for a long time many problems stood in the way until in 1955 A. Walsh of the Australian C.S.I.R.O. [76] successfully overcame them and evolved the analytical technique of atomic-absorption spectrophotometry which has proved to be so successful for inorganic trace analysis. The physical laws which govern the relationship between the amount of light absorbed and the 'concentration' of the absorbing atoms closely resemble those of molecular absorption spectrophotometry and the principle of analytical measurement and the experimental arrangement of the apparatus are also closely similar in the two techniques, though there are, of course, several points of difference. Much of the discussion given for molecular absorption is applicable to atomic-absorption of radiation and consequently the author is chiefly concerned with the differences between the two in the following paragraphs.

#### A. PRESENTATION OF ATOMS FOR ANALYSIS

Analytical molecular absorption spectrophotometry is always presented in dilute solution where the absorbing species are dispersed uniformly and do not undergo complicating interactions with each other. Free molecules are, of course, easily obtained by dispersing the absorbing solute in a suitable solvent medium, but free atoms cannot be presented for analysis in this way and it is here that the first essential difference between the experimental arrangements for the two techniques becomes apparent, *cf.* Figure 18. Free atoms can only be obtained in a gas phase and consequently gasification of the sample is one of the first requisites of atomic-absorption spectroscopy.

##### 1. The Atom Furnace Reservoir

Most inorganic compounds can be gasified by the application of sufficient heat to pass the solid material through a liquid phase into the

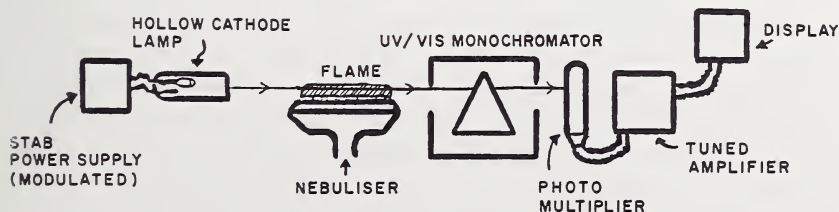


Figure 18. Apparatus for atomic absorption spectrophotometry.

gas phase or directly so by sublimation. At first sight, therefore, it would appear to be simplest to place the sample in a box having two optically transparent sides and to heat it to sufficient temperature, probably under vacuum or at least in the absence of a reactive gas such as oxygen which forms molecular (oxide) species with most metals which are only dissociated to free atoms at very high temperatures. The nearest approach to this type of atom reservoir has been described by Vidale [77] who was able to analyse  $10^{-4}$   $\mu\text{g}$  amounts with this type of reservoir. Essentially the solid specimen was placed in a quartz tube which was heated in another evacuated tube inside a split furnace at *ca.* 1400 °K. This idea of the atom furnace reservoir has also been used, in a more sophisticated form than that described above, by L'vov [78] with a fair degree of success down to  $10^{-5}$   $\mu\text{g}$  but it is difficult manipulatively, particularly for routine analyses and consequently it does not appear to have been used to any great extent. It would appear reasonable, however, to prepare the sample for analysis by chemically converting the trace ion into a volatile species before submitting it to such an atomisation process. There are known to be very many volatile metal chelate compounds (*e.g.*, many with acetylacetonone and other  $\beta\beta$  diketones) which could conveniently be passed into such a 'box' either as discrete samples or continuously in a flowing gas stream with a suitable carrier gas. The knowledge gained from recent activity in studying the gas phase chromatography of metal chelate compounds [79] should be most helpful in such a development.

## 2. Flame Reservoirs

However, the technique which was favoured by Walsh and which is used almost exclusively in present day practise is to generate free atoms from molecular species within the plasma of a flame rather than to use the latter as an external source of heat to produce dissociation in some other milieu. In making this choice Walsh was no doubt influenced by the information and experience gained in the well established technique of flame photometry (thermal emission spectrophotometry) and the choice is both logical and extremely convenient for many elements.

**a. Processes in Flames.** By various means which will be discussed subsequently, a dilute solution of the test ion, either as a salt or other compound, in a suitable solvent, is introduced to the reacting gases of the flame, in the form of a fine mist. The small droplets evaporate very quickly in the flame to leave behind even smaller solid particles (clotlets [80]) composed of the solutes. Depending on their nature, the solid particles sublime directly into the gas phase or fuse and subsequently evaporate into the gas phase as free atoms. The chain of events for a salt MX then becomes



reaches of the flame. Yet again, it must be realized that not all of the molecular species containing the test ion will pass through the reactive hot regions, for a definite fraction of them must necessarily pass through the cooler (sheath) outer regions where atomisation may scarcely be accomplished in many instances. The latter consideration is probably most important where premixed flame gases are used.

Despite these complications, however, it is found with a great number of elements that atomic absorption bands can be observed with a fair degree of intensity in a great number of flames just above the primary reaction zone of the flame gases so that it is apparent that all the reactions proceed with a good measure of efficiency. It will also be apparent from the foregoing discussion that the position in the flame where measurements are made will vary quite considerably from elements which are easily atomised to those which are not and from those which react easily with constituents of the flame to those which do not. Some flames, e.g., simple  $H_2/O_2$ ,  $CO/O_2$  flames show a fairly continuous build-up of temperature up to the tip of the flame due to (slow) three body collision propagation processes, whereas hydrocarbon/oxygen flames exhibit their highest temperatures just above the primary zone since they are propagated by (fast) two body collisions. This can also affect the region of the flame best suited to absorption measurements. Free radicals are also much more common in the upper reaches of non-hydrocarbon flames than they are in hydrocarbon ones.

**b. Nebulisation of Solutions.** The nebulisation process whereby the solution enters into the flame must also be considered, *i.e.*, the equilibrium on the left hand side of the dotted line in the equation. This process is, unfortunately, very frequently referred to as atomisation as a result of loose terminology borrowed from other areas, whereas it is the process whereby atoms are produced in the flame or the *complete* process from the bulk test solution through to the atomic species that should be so called. There are two main types of nebuliser in common use. In one of these the solution is drawn bodily up into the inner regions of the flame and the entire solution is nebulised there. This will be referred to as *total consumption nebulisation*. In the second type the solution is nebulised in one of the reacting gases, usually the oxidant and only the small droplets are carried through into the flame while the larger droplets are spun off by cyclone action as, for example, in the *Unicam* nebuliser, or are allowed to fall to the bottom of an expansion chamber, as for example in the *Hilger* nebuliser. In the highly successful *Eyans Electro Selenium* (EEL) nebuliser the solution loaded gas stream is allowed to impinge on a rotating vane which further aids the process. This type of nebulisation will be referred to as *aspiration nebulisation*. It is easily possible to gauge the efficiency of nebulisation for the latter type of device and for aqueous solutions it is usually of the order of 10–20%.

Consequently, it will be seen that the complete process of nebulisation and atomisation in flames appears to be a rather inefficient and haphazard process. In practice, however, it is found to be very reproducible and the chief detraction is that many elements, *e.g.*, aluminium, niobium, molybdenum, etc., form refractory oxides in the flame which do not readily break down whilst others cannot be measured easily (*e.g.*, the non-metals such as S, etc.) because the flame plasma also absorbs in the same region of the spectrum. However, the flexibility of choice of flame which is available is an attractive feature of flame-based methods.

### 3. Other Atom Reservoirs

Many other devices have been utilized for presenting or maintaining a dispersion (population) of atoms for analytical measurement and some of these, *e.g.*, the previously mentioned L'vov atom furnace are much more efficient in their atomisation than flames, but it is doubtful at present if any yet devised offers a serious challenge to the present supremacy of the flame reservoir despite their individual merits.

**a. Hollow Cathode Sputtering.** The chief challenge most probably arises from the hollow cathode sputtering device of Gatehouse and Walsh [81]. The work was concerned with metallic specimens. A suitably prepared sample of the metal or alloy was made into an open-ended cylindrical hollow cathode and a discharge of *ca.* 500 V was struck across from it with an anode in a vessel purged with argon and evacuated to *ca.* 1 mm pressure. A cloud of atomic vapour arose in the cathode cavity and absorption measurements were made by directing the light beam through the cloud of vapour in the cavity. The technique is eminently suitable for the analysis of alloys of constant matrix composition with regard to major constituents, but is otherwise difficult to use on a quantitative basis. It must also be remembered that only the surface layer of the cathode is sampled in the process and consequently errors may arise from alloy segregation, surface contamination, boundary effects, etc. However, this could be turned to good effect for the study of these specific problems, though it is doubtful if it could offer a serious challenge to electron-probe microanalysis. There is good reason to suppose that the technique has not yet found its major potential and future developments may well favour a much more extensive application. Solutions should be capable of being handled by deposition of solute from a layer of solvent evaporated on a suitable demountable hollow cathode of a compatible material [82] and there is every reason to expect that this technique has very much to offer, particularly for the analysis of discrete minute samples as in forensic work, etc.

**b. Electric Discharge and Plasma Jets.** Electric discharges between two metal or graphite electrodes has long been used in ac and dc spectrography and Robinson has made attempts [83] to adapt this to atomic-absorption spectrophotometry, but with no great degree of

success. The energy available between the electrodes is such that considerable ionisation may take place so that ionic as well as atomic emission are obtained with consequent depletion of the ground state population. The stability of such a source is generally inferior to that of a flame and the 'windows' in the discharge may be inadequate. Recent use of the plasma jet in emission work [84] suggest possible applications of these as flame reservoirs for difficult elements such as aluminium, molybdenum, niobium, titanium, zirconium, etc. They may, of course, be open to the same detractions as the dc and ac sources, but they appear to have greater potentialities.

Other devices used as atom reservoirs include flash-heating tubes [85] and shock tubes [86].

### B. ATOMIC SPECTRA AND THE HOLLOW CATHODE LAMP

Atomic spectra differ chiefly from those obtained for dissolved molecules in having very narrow profiles so that the lines are only *ca.* 0.02 Å wide. This at once introduces another difference between the two analytical techniques. The band passed by a monochromating device from a continuous source such as a tungsten or deuterium lamp, *cf.* Figure 19A, may be monochromatic with respect to the absorption band of a dissolved molecule, but when it is superimposed upon the absorption line due to an atom in a flame, *cf.* Figure 19B, it will be seen that it is not possible to obtain any measure of the decrease in signal because of the 'width' of the signal of the incident light. Walsh [76] calculated that it would not be possible to use light from a monochromated continuous light source since a monochromator with a resolution of 500,000 would be necessary in order to be able to make measurement at the centre of the absorption line. For this reason he resorted to the use of hollow cathode lamps. The principal lines emitted from the cathode 'glow' in these lamps are due to emission from the atomic vapour which is excited in the cavity of the cathode by the electric discharge struck across to the anode. Consequently, the lines emitted by the lamp correspond to those which will be absorbed by an unexcited population

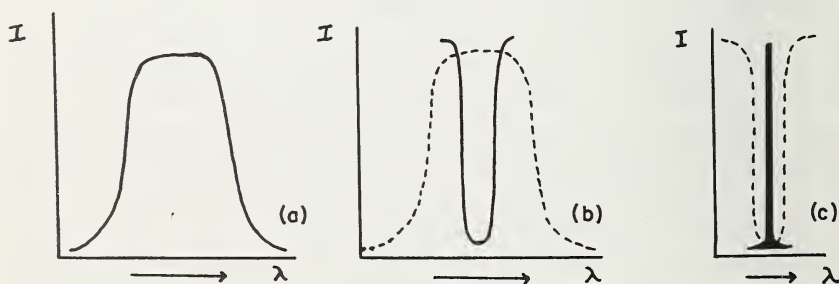


Figure 19. Spectral profiles. (a) Monochromator transmission band. (b) Absorption line. (c) Hollow cathode emission line.

of atoms of the cathode metal when those are present in a flame. Because of the relatively small incidence of broadening effects (Doppler, Stark, Pressure) in the cathode cavity it is found that the lines emitted by such a lamp are much narrower than those absorbed in the flame. Consequently, when a beam of such radiation is shone through a flame-dispersion of ground-state atoms of the same metal, absorption takes place at the centre of the atomic absorption line in the flame, *cf.* Figure 19C. Consequently, the continuous source and monochromator which is used in molecular absorption spectrophotometry is replaced by a hollow cathode lamp for the element being determined.

### 1. *Necessity for Monochromator*

The lamp, however, emits numerous atomic lines for each element and, of course, a continuum from the inert carrier gas which is necessary to provide sputtering in the cathode cavity. If all this light fell upon the detector the decrease in signal due to the selected transition line would be swamped out by the signal from unabsorbed lines and those which are only poorly absorbed. Consequently, it is necessary to place a monochromator in the system to disperse the unwanted lines so that these latter do not fall on the detector. For most purposes a monochromator similar to that used in a conventional u.v./visible spectrophotometer is sufficient, though there may be occasions, *e.g.*, in dealing with line rich spectra such as that of iron, when a monochromator with a greater than normal resolving power may be advantageous. When the continuum from the carrier gas of the hollow cathode lamp shows strong emission over the same spectral region as the absorption line this device will not, of course, be successful, but the problem rarely arises when commercial hollow cathode lamps are used. Generally the situation obtaining in molecular absorption spectrophotometry where the monochromator is situated between the source and the absorbing cuvette is reversed because it is experimentally more convenient for reasons which need not be discussed here.

### 2. *Multi-element Lamps*

The fact that a hollow cathode lamp is required for each element is sometimes seen as a disadvantage of atomic-absorption spectrophotometry, but in fact these lamps with their narrow band emissions provide virtually complete specificity for each element and in comparison to molecular absorption spectrophotometry the manipulative and chemical prehandling is much less. However, a considerable amount of activity has recently gone into the development of multielement hollow cathode lamps [87, 88] in which the cathode is made up of sections or rings of the different metals or alternatively from an alloy containing the elements blended in the proportions best suited to obtaining emission bands of approximately equal intensity from each. These lamps, unfortunately,

leave much to be desired because the intensity obtained from individual lines is usually weakened and it is said that the more volatile metals sputter in preference to others so that a film of this metal gradually deposits on the entire cathode surface, thus strengthening the emission for that element and diminishing those of others.

### 3. *Monochromated Continuum Sources*

Recently, Walsh's supposition that monochromated sources could not be used because of poor resolution, and because insufficient energy would be available in such a narrow band from a continuum, has been challenged by Gibson, Grossman and Cooke [89] who used a monochromator with a 30,000 line/inch grating and a focal length of 50 cm to obtain a band-pass of 0.16 Å from a tungsten lamp. Whilst this is approximately ten times the absorption line width in the flame, they were able to obtain approximately half-strength absorption signals for sodium (in comparison to those obtained with a sodium discharge lamp as the source) and the detection limit was equally good. This significant contribution was unfortunately only published in abstract form, but subsequently Fassel, Mossotti, Grossman and Kniseley took up the work [90] and, accepting the previous suggestion of scale expansion, they were able to obtain very excellent sensitivities for atomic absorption signals for thirty two elements which were either comparable to, or in some instances (barium, indium, lithium, vanadium, and the rare earths) better than those obtained using hollow cathode sources. Objectors to the hollow cathode lamp may well see this as one of the most significant developments yet to have taken place in this area, and it is undoubtedly a very fine contribution indeed. Ivanov and Kozireva [91] appear to have made a similar, though somewhat less extensive examination in the USSR.

### 4. *Spectral Discharge Lamps*

Spectral discharge lamps have long been used as sources of monochromatic radiation for several purposes and those for the alkali metals, alkaline earths, and more volatile elements such as thallium, cadmium and zinc are useful alternatives to the hollow cathode lamp, particularly when they are run at currents lower than those recommended by the manufacturers. This has the effect of reducing the temperature in the discharge chamber of the lamp and thus reducing the self-reversal which is rather a prominent feature of this emission [92] and also, of course, pressure and Doppler broadening, etc., though these are less serious. Generally speaking it is found that the stability of these lamps is not as good as that of hollow cathode lamps and it is frequently advisable to use an attenuating device with them to prevent radiative damage to the light sensitive cathode of the detector since their radiation intensity is very much greater than that of a hollow cathode lamp or a monochromated continuous source.

5. *Microwave-powered Sources, etc.*

In their excellent monograph 'Atomic Absorption Spectrophotometry' Elwell and Gidley [93] comment on the possible use of Geissler tubes and of high frequency electrodeless discharge tubes, but these appear to have found little application as yet. We have found [94] that much better results may be obtained with an attenuated signal obtained from a microwave powered iron-containing tube operated at 2450 Mcps and *ca.* 10 watts than with a conventional iron hollow cathode lamp. We presume that this is due to the considerably higher energy fed into the resonance line and the higher resolution that may be obtained by narrowing the slits of the monochromator. We have also found a similar improvement for other elements, *e.g.*, Ag and particularly for those which have resonance lines bordering on the vacuum u.v. region, *e.g.*, Se [95].

Walsh [96] considered the use of an emitting flame saturated with the necessary atomic species to be unsuitable because of self-reversal and line broadening, but the continuous source work discussed above [90] may lead to a re-assessment. It is probable, however, that the stability of a flame source would be inadequate without double beam operation. Strasheim and Butler [97] have recently investigated the use of the time-resolved spark source and have shown that it has merits worthy of further consideration.

## C. TYPES OF BURNER

Two types of flame have been used chiefly in the study of atomic absorption phenomena. The first of these is the (pre-mixed gases) laminar-flow flame obtained from a slotted burner used in conjunction with an external aspirator-nebuliser and the second is the turbulent-flow flame from a (unmixed gases) total consumption burner. Both types of burner are well described in the literature of flame photometry and they will not be discussed here. The long thin laminar flame is best suited to analytical absorption measurements because it presents the maximum number of absorbing atoms to the light beam from the source. It is, however, advisable to ensure that no light from the source by-passes the flame and enters the monochromator. It must also be considered, however, that if the flame is too long and thin, excessive cooling of its outer regions may occur and consequently it is sometimes found that there is an optimal length of between 5 and 10 cm for many hot flames. The shape of the flame is also relevant because the number of absorbing atoms is inversely proportional to the cross section of the flame. Consequently for a given length of flame the highest concentration of absorbing atoms will be obtained by the narrowest flame which is not adversely affected by cooling.

The small droplets introduced to the flame from the aspirator nebuliser are also more uniform and are free from large droplets which may cause a loss of signal by reflection, scatter and even diffraction. In contrast,

the (integral nebuliser) total consumption burner presents only a short pathway for the absorption of light and concentrates all the self-emissive features of the flame in front of the monochromator slit. The droplets which are introduced have a wide range of sizes and many of them are too big to be useful. In addition, much insidious incrustation of the burner tip may occur with solutions of moderate electrolyte concentration and cause non-reproducible results with no visible sign of deficiencies in nebulisation. A side issue is that total consumption burners are rather noisy in use in comparison to laminar-flow burners.

### 1. *Long Flames*

The absorption of the atoms in the flame is within limits directly proportional to the length of the absorption path for a uniform population. The path-length of a total consumption burner is of the order of 1 cm or less, unless a multiple passage of the light beam is made through the same part of the flame, whereas 10–15 cm flames are common for some laminar-flow flames with no appreciable increase in volume. However, adaptations of the turbulent total-consumption flame have been described which cause similar and much greater extension of absorption path and these may prove useful in future work. Fuwa and Vallee [98] led the gases from a total consumption burner into a long horizontal tube with the tip of the burner just outside the rim and below the central axis. The beam of light from the hollow cathode lamp was passed down the tube from the other end and the absorption measured by a monochromator/detector situated opposite the burner end. A Vycor, Alundum, or Zirconia tube of diameter 1–2 cm and 20–90 cm long was used and best results were obtained with tubes 70–90 cm long and 1 cm diameter. Koirtgochann and Feldman [99] have described a similar device with a slightly different disposition of apparatus. The results achieved indicate a very considerable increase in sensitivity with oxy-hydrogen flames, but difficulties are experienced when organic solvents or acetylene are used. High background signals are obtained and whilst the reasons for these are not apparent, it is probable that the unusual absorption signal is due to molecular species generated or accumulating appreciably in the tube which would otherwise not be formed in an unconfined flame. It has also been observed that the oxygen/hydrogen ratio has a very marked effect on the absorption due to spraying a constant solution of metal ions and that this appears to coincide with the visible length of the flame in the tube [100]. It is probable that the highest signals are obtained over the narrow range of conditions of gas pressures which successfully produce a long laminar flow flame in the tube. The life-time of free atoms in the cool regions of the flame or outside the body of the flame can only be of limited duration and it is probable that the device is successful chiefly because it produces a long flame rather than an

accumulation of free atoms in the combusted gases within its confines. In their paper Fuwa and Vallee demonstrated increases in sensitivity with increase in pressure of the absorption cell and they suggest that the efficiency of the Vycor tube relative to the others is due to internal reflection and multiple traverse of the tube. Earlier work by Robinson [83] demonstrated a simpler T piece adaptor which was placed over a turbulent flow flame. Measurement of absorption was made across the ends of the horizontal arm. No constructional details were given, but presumably the device gave a path-length comparable to those for laminar flow flames. The device does not, however, permit absorption measurements to be made low down in the flame which may account for some of the poor sensitivities obtained for certain metals.

An understanding of the mechanism of the flame production and propagation in devices such as those mentioned above may yet provide a significant advance to the practice of atomic-absorption spectrophotometry.

## 2. Types of Flame Medium

**a. Conventional Flames.** Many different flame gases have been used in flame photometry [101] and most of them have been examined for atomic absorption measurements also. Much of the early work was done on the relatively cool air-propane and air-hydrogen flames. These have the merit of low emissive backgrounds so that simple defocussing systems could be used to allow the monochromator/detector to respond only to the light beam from the hollow cathode which is focussed on the entrance slit to the monochromator. Walsh [76], however, used a modulation system to overcome radiative effects in the flame. The beam from the hollow cathode lamp was interrupted at regular intervals by a rotating sector and the amplifier of the detector system was tuned to the interrupting frequency so that only the pulsed signal was amplified. This arrangement has now been modified in most instruments by modulation of the supply to the hollow cathode lamp. The temperature of such flames is, however, rather low and whilst at first sight it would appear that the flames used for atomic absorption need not be so hot as those used for flame photometry since excitation is not required, the latter process is largely accomplished by mechanisms other than the application of thermal energy to the free atom. Atomisation, *i.e.*, the production of atoms *within* the flame, is the least efficient process in atomic absorption (*ca.* 1.5% only for magnesium in an oxy-acetylene flame at approximately 2400 °K [102]) and consequently some very high temperature flames have been used, *e.g.*, oxy-cyanogen (*ca.* 4600 °K) [103]. The use of the plasma jet has also been mentioned, for which temperatures of *ca.* 15,000 °K have been claimed [104]. However, very high temperatures will produce serious depletion of ground state populations for easily excited elements and these flames invariably produce

higher background noise. In any event it is true that one of the decisive factors governing the population of atoms is their limited life times ( $10^{-6}$ – $10^{-8}$  sec) so that it may well be true that increase of flame temperature beyond a certain level appropriate to good dissociation of the clotlet species may have little further effect.

**b. The Nitrous Oxide-Acetylene Flame.** The use of fuel-rich luminous flames, *e.g.* oxy-acetylene, is particularly effective in providing absorption signals from atoms which form refractory oxides, *e.g.*, aluminium, molybdenum, etc. [105]. These flames do, however, place a rather heavy radiative load on the photomultiplier. Recently, the use of the nitrous oxide-acetylene flame by Willis [106] and by Amos and Willis [107] has provided a significant advance. Good signals were received for many difficult elements, *e.g.*, Be, Ti, Zr, Hf, V, Nb, Ta, W, U, Re, and the rare earths and moderately improved signals for Mo, Sn, and the alkaline earths. We, ourselves, have found the nitrous oxide-acetylene flame easy to handle and have obtained good signals for molybdenum, sufficiently sensitive to permit its determination in steels [108] and in trace amounts in metallic niobium and tantalum [109].

Most elements appear to be best determined in or very near to the characteristic red-feather zone of the flame which appears close to the primary reaction zone. There is every reason to suppose that the low intensity emission from this zone is due to the CN band and it may well be that this flame amounts or closely approximates to a sheathed oxygen-cyanogen flame (which was used originally by Robinson [103]) with the burning gases sheathing a zone where free cyanogen is being produced and combusted. This flame appears to offer distinct advantages over fuel-rich acetylene flames and to constitute a distinct advance in extending the range and sensitivity of atomic-absorption spectrophotometry.

Species which are easily ionised in a 'hot' flame may frequently be brought back to the absorbing groundstate by addition of the salt of a more easily ionised metal since this (*e.g.*, potassium) will be excited in preference in the flame and diminish the ionising capacity of the flame without reduction in temperature.

#### D. TYPES OF HOLLOW CATHODE LAMP

Hollow cathode lamps are available for most elements, some using cathodes of another suitable metal coated with a volatile salt of the required element where the element itself is too easily fused. A range of multi-element lamps is also available in which several elements compose the cathode or in which alloys are used. Lamps containing individual cathodes which can be separately connected to the source of potential difference, and de-mountable flow-through lamps have all been used with varying degrees of success.

### 1. *High Intensity Hollow Cathode Lamps*

The only significant advance to have been made in lamp technology is the evolution of the high intensity hollow cathode lamp. In these a secondary discharge is struck across the atomic vapour at the mouth of the cathode cavity. Normal lamps must be run at rather low currents to prevent broadening, self-reversal and even self-absorption by the larger cloud of cool vapour which is generated around the cathode by higher currents. In the high intensity lamp, Jones and Walsh [110] used the secondary electrodes coated with alkali metal salts to pass a cloud of low energy electrons through the 'cool' ground state vapour in front of the cathode cavity. The energy of the electrons is insufficient to excite ionic spectra, but causes good atomic emission. These lamps then permit much more energy to be passed into the cloud of atomic vapour in a flame and thus allow narrower slits to be used where resolution is a particular problem and permit lower amplifier gains to be used so that the background noise of the electronic circuitry does not cause serious problems. The length of the linear zones of calibration curves are usually significantly increased as a matter of course with these lamps.

It should be noted, however, that the radiant energy from these lamps is lower than that from microwave-powered sources.

### E. ANALYTICAL RELATIONSHIPS IN ATOMIC-ABSORPTION SPECTROPHOTOMETRY

The laws which govern the relationship between the amount of light absorbed by atoms in a flame and their concentration are subject to the same rules as those for molecules in solution and may be expressed as

$$A = \text{Log } I_0/I_t = \epsilon_A \cdot \ell \cdot c$$

where  $A$  denotes absorbance,  $I_0$  and  $I_t$  the incident and transmitted signals,  $\epsilon_A$  the atomic absorptivity,  $\ell$  the path-length and  $c$  the concentration of the atoms in the supporting medium. In point of fact, however, we are never in a position to know the concentration of the atoms in a flame because of the many variables in the atomisation process, the dynamic nature of the system, the life-time of free atoms, parasitic side reactions, etc. Nevertheless, the law may be used empirically by calibration curve principles. As a result it is possible to work in exactly the same way as in molecular absorption spectrophotometry.

### F. CHOICE OF WAVELENGTH

Most of the absorption lines used in atomic-absorption spectrophotometry lie in the u.v. region of the spectrum, except for those elements which are easily excited and consequently absorb in the less energetic visible region. The choice of the most sensitive band for

analytical measurement in molecular absorption is usually fairly obvious because there are very few bands, but for most atomic species there is a considerable number from which a choice must be made. The electron transitions corresponding to most atomic lines are well recognized, however, and in many instances this knowledge is helpful. For the majority of elements in virtually all flames the bulk of the atomic population exists in the ground state so that only those transitions from the ground state to one of the excited levels need seriously be considered. In many instances the most sensitive line used in the technique of flame photometry proves to be the best also for atomic absorption measurements, but it must be stressed that for most atomic species there is a choice of lines which will yield various sensitivities according to their oscillator strength. The most sensitive line is not always the same, however, and may alter according to flame conditions. It is generally now well recognized which lines are most favourable, but where this knowledge is not available it is a simple matter to screen the sensitivities of the stronger lines. Allen [111] devised a photographic method for complex spectra which indicates the absorbing lines and yields the most sensitive line by microphotometry, but it is not usually necessary to resort to such a procedure.

#### G. ASSESSMENT OF ATOMIC-ABSORPTION SPECTROPHOTOMETRY AS AN ANALYTICAL TRACE TECHNIQUE

As an analytical technique, atomic-absorption spectrophotometry has one unique advantage over the two other trace techniques discussed above and indeed over most other trace techniques. It may be expressed in one word—specificity. The method available for each element is virtually specific for it. This arises because of the narrow spectral profile of atomic absorption lines in flames and the even narrower source emission lines used to measure their mid-point absorption. In terms of inherent specificity there is no comparison to be made in favour of molecular absorption spectrophotometry or even molecular fluorescence spectrophotometry. Except in a few instances where unpleasant matrix components are present it is not necessary to resort to separations and even then it is sometimes possible to account for the matrix at very high levels by adding approximately the same amount of matrix component to the standard solutions. Matrices which cause difficulty in this way are largely those which form refractory compounds in the flame, *e.g.*, aluminium, niobium, zirconium, etc., and which lock-up the sought element in clots which do not fuse and break down sufficiently in the flame. In some instances difficultly fusible or involatile compounds may be formed in the absence of a matrix of the above nature. Calcium in the presence of phosphate shows this behaviour [112]. The addition of a liganding species EDTA may be helpful here, because it sequesters the calcium away from the phosphate ion so that even

though the phosphate is present in the clotlet it is either volatilised away before the complex dissociates or additionally has insufficient time to bond with it before the exothermal decomposition of the chelate releases the calcium. Sodium chloride and sucrose [113] exhibit effects similar to EDTA and this has led Baker and Garton to cast doubts upon the validity of chelation action. However, it must be recognized that anything which dissolves or fuses or explodes a refractory clotlet will have a beneficial effect in increasing the vapour pressure of the sought element.

There are very few interelement effects shown in atomic-absorption spectrophotometry which is in marked contrast to the behaviour of flame photometry. It is also noticeable that whereas the sensitivity of flame photometry is critically dependent on the temperature of the flame this is not so in atomic absorption. Yet again, with few exceptions a fairly uniform high sensitivity is apparent for most elements by atomic absorption, whereas sensitivities vary greatly in the older technique. The reasons for these three important differences can be seen at a glance from Walsh's equation [76] relating the number of atoms,  $N_0$ , in the ground state to that  $N_j$  in an excited state of energy  $E_j$  through the absolute temperature  $T$

$$N_0/N_j = P_0/P_j \cdot \exp \frac{E_j}{kT}$$

and  $P_0$  and  $P_j$  the statistical weights for the ground and  $E_j$  state respectively. Walsh calculated the ratios shown in Table 3 for the number of atoms in the excited state to those in the ground state. Even for cesium, 99.99% of the atomic species exist in the ground state at 3000 °K. Temperature has little effect on the number of atoms in the ground state but causes an exponential variation of the number in the excited state. Consequently it would appear that variations in flame temperature will scarcely affect atomic absorption, but will greatly alter the signal for flame photometry. Again, it will be seen that if all

TABLE 3. Calculated ratio of atoms in excited state to atoms in ground state.

Resonance line	T = 2000 °K	T = 3000 °K	T = 4000 °K	T = 5000 °K
Cs 8521 Å	$4.4 \times 10^{-4}$	$7.2 \times 10^{-3}$	$3 \times 10^{-2}$	$6.8 \times 10^{-2}$
Na 5890 Å	$9.8 \times 10^{-6}$	$5.9 \times 10^{-4}$	$4.4 \times 10^{-3}$	$1.5 \times 10^{-2}$
Ca 4227 Å	$1.2 \times 10^{-7}$	$3.7 \times 10^{-5}$	$6.0 \times 10^{-4}$	$3.3 \times 10^{-3}$
Zn 2139 Å	$7.3 \times 10^{-15}$	$5.6 \times 10^{-10}$	$1.5 \times 10^{-7}$	$4.3 \times 10^{-6}$



down to  $1 \times 10^{-2}$  ppm even without recourse to the hotter flames of most modern instruments or the availability of scale-expansion, both of which would probably have yielded analyses down to  $10^{-3}$  to  $10^{-4}$  ppm.

Organic solvents cause difficulty in flame photometry because they appreciably alter the flame temperatures, but this effect of solvents is insufficient to cause any perturbation of absorbance signals. In most instances an increase of atomiser efficiency up to 60% is easily possible with organic solvents, though there are occasions when some solvents may not be used. For example, Kirkbright, Peters, and West [109] found it impossible to use chloroform as a solvent for molybdenum in nitrous oxide-acetylene flames though butanol was entirely satisfactory.

Because of the minimization of handling, atomic-absorption spectrophotometry is a rather rapid procedure, particularly for routine analysis of single elements, and it can easily be manipulated by relatively unskilled staff following development of a method. It is also a process that is easily automated and in terms of some of the most popular trace techniques, *e.g.*, x-ray fluorescence, mass spectrometry, its cost of installation and maintenance is very fractional indeed. Current instruments cost from *ca.* \$1700 to \$8000 according to their complexity. As it is presently practised the technique has not been applied to solid specimens, unlike x-ray fluorescence, mass spectrometry, etc., but there appears to be no reason why finely pulverised particulate material should not be examined by adaptation of the technique.

Atomic absorption measurements may generally be made with an accuracy of  $\pm 1-2\%$  which compares favourably with that of most other trace techniques. Perhaps the chief restriction for atomic-absorption spectrophotometry at present is that, unlike some others, it yet remains to be developed as a method for the simultaneous determination of several elements, but it must be recognized that it is as yet relatively new to the scene. In general its specificity, sensitivity, ease of application and analytical range make it one of the most attractive and elegant techniques available for the characterisation of traces.

#### H. FUTURE DEVELOPMENTS IN ATOMIC-ABSORPTION SPECTROPHOTOMETRY

It is difficult to forecast the future direction of development of such a rapidly expanding technique, but it is probable that since good analytical methods are now available for most metallic elements and some non-metals, that more workers will turn their attention to the development or improvement of sources, atom-reservoirs and handling methods.

Apart from the hollow cathode the two most promising sources appear to the author to be the monochromated xenon arc type of source—preferably used in conjunction with scale expansion and integration and the microwave powered source. Paradoxically considerable progress could be made by dispensing with the flame as atom-reservoir but until

such a development occurs the evolution of the nitrous oxide-acetylene flame and the long-tube flame are probably most significant. The restrictions imposed by the necessity to use a flame also include the need for dissolution of samples and it is hypothetical if much progress may be made in dealing with solid specimens unless the flame is dispensed with. However, in reading the literature of atomic-absorption spectrophotometry it is startling to find how often an observation that 'such and such' cannot be done (or is impossible) is disproved within periods as short as twelve months.

*Footnote:* After this manuscript had been prepared two very fine monographs on atomic-absorption spectrophotometry have been published by W. T. Elwell and J. A. F. Gidley ('Atomic-Absorption Spectrophotometry', Pergamon, Oxford, 1966) and by J. W. Robinson ('Atomic-Absorption Spectroscopy', Marcel Dekker, Inc., New York, 1966). These both give first class accounts of the theory and practical applications of the technique.

### V. Atomic Fluorescence Spectrophotometry

In proceeding from molecular absorption to molecular fluorescence spectrophotometry we observed that there was a very considerable gain in the sensitivity of determination and an improvement in selectivity. It is logical, therefore, to expect a similar improvement in passing from a technique of atomic-absorption to one of atomic-fluorescence spectrophotometry. No increase in selectivity can be expected, however, since the technique just discussed is already virtually specific for each element. It has long been recognized that atoms can emit fluorescence in a manner similar to molecules when they are irradiated with light of sufficient energy to promote an electron transition, but the first description of atomic fluorescence in flames appears to be that of Nichols and Howes [116] who reported weak fluorescence signals for lithium, sodium and the alkaline earths. Robinson [117] detected a weak fluorescence of magnesium in an oxy-hydrogen flame using a magnesium hollow cathode lamp as the source of irradiation, but found no signals for sodium and nickel over and above their thermal emission in the flame. This, however, is not surprising in view of the extremely low emission of hollow cathode lamps and the absence of modulation. However, the latter author was not attempting to develop an analytical technique and the first serious and successful attempts to do this were described by Winefordner and his co-workers in a series of four papers [118-121] published in 1964-65 and in the latter year by Dagnall, West, and Young [33, 122].

In atomic-absorption spectrophotometry the eventual fate of the energy absorbed by the atoms was of little concern since it had no effect on subsequent studies. Most of the energy is lost by collisions with other atomic and molecular species in the flame plasma. However, the energy which is imparted to an atom creates an unstable situation

since a charge separation has occurred and the electron will be pulled back into its equilibrium orbit with the energy released as a photon characteristic of the difference between the excited state and the ground state, *i.e.*, characteristic of the atomic species. In molecular fluorescence spectrophotometry no matter which of the higher electronic states was excited, vibrational dissipation and intersystem crossing ensured that within the lifetime of the excited species the lowest vibrational level of the *first* excited state was always attained so that irrespective of excitation, fluorescence re-emission was always at the same wavelength with the fluoresced band mirroring the image of the longest wavelength absorption band.

Such a situation cannot arise in atomic excitation-emission since there are no vibrational motions of electrons within chemical bonds to permit such a process. Instead, the energy can only be shed by collisional deactivation with other atoms or molecules (which may subsequently emit their own characteristic fluorescence) or by the emission of a photon of energy, *i.e.*, by atomic fluorescence. Because of the simplicity of the system, resonance fluorescence predominates, *i.e.*, the excited atoms emit energy of the same wavelength as that which caused their excitation.

At this stage it might be asked why this resonance radiation does not cause serious problems in atomic absorption measurements since the atoms can emit light of the same wavelength as that which they absorb. The principal reason is that the intensity of the sources which are used in absorption work is very low. As in molecular fluorescence the intensity of the atomic fluorescence signal is proportional to the intensity of the source and consequently the emitted signal must necessarily be very low indeed. Secondly, in absorption, a long thin flame is used so that the weak fluorescence is emitted in all directions and that which passes towards the entrance slit of the monochromator must traverse a long path through a population of atoms which is largely in the absorbing ground state. Although they are relatively weak still, it is probable that fluorescence emission may cause complications in absorption measurements with the relatively new high intensity hollow cathode lamps and that appreciable fluorescence signals could be detected at the end of the flame nearest the lamp when a strong solution of the metal is being sprayed and the flame is examined at right angles to its axis. It is doubtful, however, whether this will cause serious difficulties under normal circumstances.

Although it has yet to be demonstrated widely it should be possible to excite atomic fluorescence at very many wavelengths for each element because of the multiplicity of discrete atomic absorption lines which are associated with most elements. Moreover, it should be found that the radiation which is emitted as fluorescence should principally have the same wavelength as the excitation radiation. Consequently, it is

theoretically possible to control the spectral range in which incidence of fluorescence occurs in a manner which is not possible in molecular fluorescence. Yet again, it is true to say that whilst there are many absorbing lines which may be used in atomic-absorption spectrophotometry, their sensitivity is dictated entirely by the oscillator strength of the atomic line. On occasion, in atomic absorption it may be desirable to use a line other than the principal one because of flame characteristics or the presence of elements or compounds with continua in the region, but it may not always be possible to use it because of poor intensity. With atomic fluorescence it is, however, possible to 'turn up' the sensitivity of such a line by increasing the intensity of irradiation or, of course, by increasing the amplification within the limits of the combined electrical noise of the detector, source and flame. Atomic fluorescence is in this respect much more flexible than atomic-absorption spectrophotometry.

#### A. TYPES OF ATOMIC FLUORESCENCE LINES

Winefordner and Vickers [118] designate three modes of atomic fluorescence other than resonance re-radiation from an excited state  $E_x$  to the ground state  $E_0$ . These are *direct-line fluorescence* produced by transitions from higher states to lower states other than the ground state and *stepwise fluorescence* in which resonance radiation is emitted following excitation by light of a wavelength which promotes excitation to a level higher than the first excited state, but in which non-radiative deactivation has resulted in population of the first excited state. In *sensitised fluorescence* one atomic species is excited by absorption of light of the requisite wavelength and transfers the energy to another atomic species which subsequently fluoresces its own characteristic quanta. Examples of this behaviour cited by Winefordner and Vickers are:

- (a) *direct-line fluorescence*: Tl 5350 Å fluorescence following excitation at 3776 Å;
- (b) *stepwise fluorescence*: Na 5890 Å fluorescence following excitation at 3303 Å;
- (c) *sensitised fluorescence*: Tl 5350/3776 Å emissions from a flame containing a much denser population of mercury atoms and irradiated by the 2537 Å Hg line [123].

However, though all these forms of fluorescence may be observed, resonance fluorescence, at the present limited stage of development, is the most useful and certainly the most sensitive.

Much of what has been said in the previous section relating to atomic-absorption spectrophotometry is directly applicable to atomic-fluorescence spectrophotometry, particularly in relation to the means of producing populations of ground-state atoms in flames.

B. ANALYTICAL RELATIONSHIPS IN ATOMIC-FLUORESCENCE  
SPECTROPHOTOMETRY

The relationship between the concentration of the fluorescing species in the flame and fluorescence signal has been fully discussed by Winefordner and Vickers [118] and their derivation of an analytical equation should be consulted for full details of all the factors involved. However, the exercise is largely of academic interest only, as in the case of atomic-absorption spectrophotometry, since usually the actual concentration of atoms present in a flame at any given instant is unknown. There is, however, a very close similarity between the relationship established for molecular-fluorescence spectrophotometry and that for atomic fluorescence.

The equation may, therefore, be framed in the same terms, *viz.*

$$F = 2.303 \Phi . I_0 . \epsilon_A . \ell . c . p .$$

for dilute solutions of atoms in flames.  $F$  denotes the resonance fluorescence signals,  $I_0$  the intensity of the excitation light,  $\epsilon_A$  the atomic absorptivity at the wavelength of irradiation,  $\ell$  the pathlength in the flame,  $c$  the concentration of absorbing atomic species and  $p$  a proportionality factor relating to the fraction of the total fluorescence observed by the detector. In this instance the same quanta of energy are emitted as are absorbed, but not all the atoms which undergo excitation exhibit resonance fluorescence. Consequently, a factor relating to the quantum efficiency,  $\Phi$ , of the fluorescence process must be incorporated into the equation.  $\Phi$  may be defined as the ratio of the number of atoms which fluoresce from the excited state to the number of atoms which underwent excitation to the same excited state from the ground state in unit time.

The concentration of preatomic species in the solution phase may be related to the concentration of free atoms in the flame by multiplying the former by a nebuliser efficiency factor "n" ( $< 1$ ), which may easily be established, and by an atomisation efficiency factor,  $a$ , *i.e.*,

$$C = C_s . n . a$$

Unfortunately, we are not in a position to know the number or concentration of free atoms produced from a known concentration of preatomic species drawn into the flame because of the uncertain efficiency of the conversion process, the limited lifetime of free atoms, parasitic side reactions, etc. Consequently, the equation which may be written in the form

$$F = 2.303 \Phi . I_0 . \epsilon_A . \ell . C_s . p . n . a$$

is instructive, but has little significance. For a given nebuliser and instrumental set of conditions the analytical relationship becomes

$$F = K \cdot \Phi \cdot I_0 \cdot C_s$$

where  $K$  is a constant, *i.e.*, the fluorescence signal is proportional to the intensity of irradiation and to the concentration of the preatomic species in the solution. It is also apparent that the intensity will vary from from one fluorescence line to another by variation of  $\Phi$ . Both  $\Phi$  and  $a$  may be altered by alteration of the flame matrix and an optimum value probably may be found for the two processes with a compromise struck between increase of the number of free atoms (before ionisation becomes serious) and an increase in collisional deactivation and quenching process as temperatures are raised. The length of the absorption path may only be used within limits where self absorption and total frontal absorption *cf.* parallel in Figure 13A, does not become a serious problem. The nebuliser efficiency may be increased considerably by the use of organic solvents and possibly by preheating the vapour and even introducing ultrasonic frequencies into the fog chamber whilst the 'p' factor may be increased by light-collection, *via* lenses, etc., or by use of an ellipsoid mirror and off axis mounting of the flame as indicated in Figure 21.

Although many of the factors in the equation may not easily be determined, its validity is easily demonstrated by the empirical process of drawing up calibration curves in exactly the same way as in virtually all spectroscopic processes. It must be remembered that in the conventional right-angled mode of operation, atomic-fluorescence spectrophotometry is only applicable to trace amounts of material, but there appears to be no reason why a frontal mode using an acute angle between incident and emergent beams should not be reasonably successful as in the molecular technique.

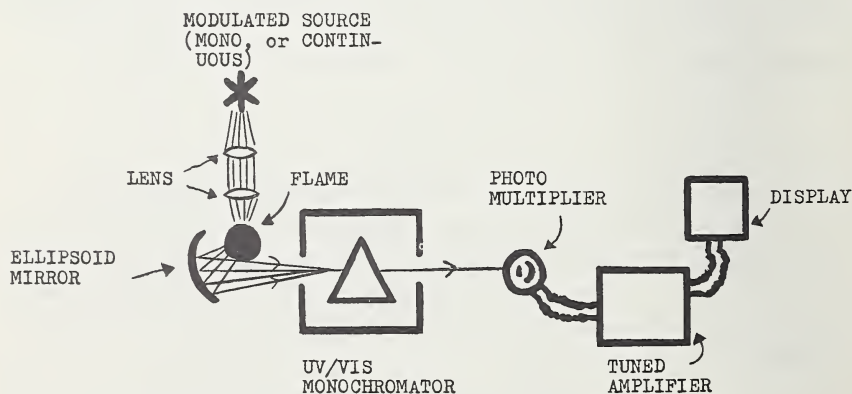


Figure 21. Apparatus for atomic fluorescence spectrophotometry.

## C. INSTRUMENTATION

It must be stressed that in the following paragraphs the work that is being referred to relates only to published work from the University of Florida and from the writer's laboratory at the Imperial College of Science and Technology of London University. Other groups are no doubt very active in the area, but no further information is available at the time of writing.

1. *General Arrangement*

A schematic set-up is shown in Figure 21 [124]. Light from a suitable source is focussed on the population of atoms in the flame and the fluorescence, which is, of course, emitted in all directions, is examined in the same plane at right angles to the direction of the incident light. The light from the flame is then passed through a monochromator to disperse unwanted radiation and the signal is passed to a photomultiplier, etc. In our experiments we have simply made use of a conventional Beckman DU flame photometer or the SP 900A Unicam flame emission/absorption spectrophotometer, principally the latter, with a suitable source of irradiation placed near the flame and subtending a right angle with the entrance slit of the monochromator at the centre of the flame. Winefordner *et al.* [119, 125], have built special apparatus which does not, however, differ substantially from that used by ourselves.

2. *Types of Burner*

In most respects flame photometry bears a closer relationship to atomic-fluorescence spectrophotometry than does atomic-absorption spectrophotometry. Ideally both require the same shape of flame which should be small and capable of being viewed over as much of its area as possible by the monochromator so that the maximum possible part of the analytical signal can enter the monochromator and fall on the detector. In all his studies to date Winefordner and his colleagues have used turbulent flames from total consumption burners. We have preferred to use laminar flames from a Meker type of circular burner head, as used on the Unicam SP 900 flame spectrophotometer, with a separate aspirator nebuliser. The near homogeneous dispersion of uniform droplets which enters such a flame produces much finer uniform particles or clotlets than can be obtained by use of an integral nebuliser-burner. This aspect is very important because light-scatter is a much more critical phenomenon than it is in either atomic absorption or flame photometry and a powerful source can produce an appreciable scatter signal. In our experiments we have observed considerably less scatter than that recorded by Winefordner and his co-workers probably because of the difference in nebulisers and burners.

### 3. Fuel Gases

Winefordner *et al.* have worked largely with oxy-acetylene and oxy-hydrogen flames and have more recently [125] described the use of what they call an argon-hydrogen flame but which in fact contains sufficient entrained air to support combustion of the fuel gas with the argon acting chiefly as a diluent.

We have made a study of air-based laminar-flow flames burning on a cylindrical burner head perforated by a series of concentric holes with hydrogen, propane and acetylene as the fuel gases [126]. To study the background emission of the flames we have used the SP 900A in its emission mode so that the light from the flame entering the monochromator is chopped at 100 cps in phase with the amplifier. We have also used an EMI 9601B photomultiplier because of its good response in the u.v. region. These measurements were made with distilled water aspirating through the flame, since this cools it and reduces the background by *ca.* 15%. We found that in the air-propane and air-hydrogen flames background emission could be virtually eliminated by working high up in the flame but a distance *ca.* 3 cm above the primary reaction zone was consistent with maximum stability. Background emission with the air-acetylene flame was much higher and although our early work [122] was done on this flame, we subsequently preferred to use air-propane or air-hydrogen. Both these flames exhibit an increase in background with increase of fuel pressure, but although the air-hydrogen flame exhibits a lower background emission than air-propane at all wavelengths except between 2810 and 2850 Å and over the OH band (3060–3200 Å) the air-propane system is attractive because of its low burning velocity and is very convenient in use. We have found that, in general, doubling the slit width quadrupled the background, but produces a linear response in fluorescence signal, *i.e.*, the signal to background ratio decreases with increasing slit width.

In measuring the fluorescence signal the SP 900A is held in its absorption mode whereby the light entering the monochromator is not chopped, but the source was modulated to match the a.c. amplifier. In comparing the suitability of the three flames for metallofluorescence, the air-acetylene one was discarded, although modulation eliminates its effect, because of its higher background and because it produces greater scattering under irradiation. We also observed that with air-acetylene we could only observe cadmium resonance fluorescence at 2288 Å [122] but with the other two flames signals could additionally be observed at 3261 Å. With our equipment we also obtained a more stable flame with air-propane than with air-hydrogen. In addition, it was found, both with zinc and with cadmium at 2139 and 2288 Å respectively, that the fluorescence signal in an air-hydrogen flame was adversely affected by an increase in hydrogen pressure whilst variation of the propane pressure had no effect.

With oxy-acetylene Mansefield, Windfordner and Veillon [121] found that the signal for thallium fell away rapidly beyond the luminous tip of the flame whilst in the lower regions thermal emission was greater than the intensity of fluorescence; best results were obtained at 3776 Å with a hydrogen-rich flame. A height about 1 cm above the luminous tip of the flame was used for both thallium and mercury whilst other metals, zinc and cadmium, were measured about 1 cm above the reaction zone in the turbulent flame.

#### 4. *Excitation Sources for Atomic Fluorescence Spectrophotometry*

In atomic-absorption spectrophotometry a hollow cathode lamp has to be used for each element or a multi-element cathode for a restricted group of metals. This arises because it is essential to have a source which has an emission line much narrower than the absorption line (although recent work has shown that an extremely well monochromated continuous source may in fact be used [90]). In atomic fluorescence, on the other hand, it is not necessary to have such a 'narrow line' source. It is sufficient if the emission brackets the absorption line of the atoms in the flame, although there are obvious occasions when it may be advantageous to use a narrow line source when dealing with a system that exhibits many lines in very close proximity to that of analytical interest.

##### **a. Spectral Discharge Lamps and Microwave-powered Sources.**

Both Winefordner *et al.*, and ourselves have made use of the readily available spectral discharge lamps which have a nominal rating of 18–20 watts and have used these to study the fluorescence of cadmium, zinc, mercury and thallium and have additionally used microwave-powered discharge tubes for many other elements, *e.g.*, mercury, indium, gallium [121] selenium, tellurium [127] and for several other elements, *e.g.*, antimony, arsenic, cadmium, nickel, silver, tin, thallium, etc. [128]. We used an Electromedical Supplies 'Microtron 200' unit operating at  $2450 \pm 25$  megacycles/sec with a small cavity operating approximately 1 metre from the magnetron at the end of a coaxial cable. Our source tubes are of quartz and operate under  $< 1$  mm pressure of argon. We have found these very easy to prepare. In most instances we used a small amount of the metallic element sealed in the tube plus a crystal of iodine to run the tube in. Winefordner *et al.*, used commercially available discharge tubes and a similar 2450 megacycle microwave unit rated at 100 watts. Both sets of workers operated their tubes at less than full power but whereas we used  $< 10$  watts output (plus loss due to reflected power) the other group operated their equipment in the range 40–60 watts and report some problems due to self reversal of the source. We have noted a considerable stabilisation of output by blowing a stream of air over the tube in the tuned cavity. We have used several of these tubes, *e.g.*, those for nickel, iron, silver, selenium, tellurium, etc., for atomic absorption as well as atomic fluorescence measurements and

have found them to be possessed of a stability equal to that of hollow cathode lamps.

**b. Continuum Sources.** Both groups have also made use of continuum sources thus demonstrating the source tolerance of the newer technique. Veillon, Mansfield, Parsons and Winefordner [125] used a dc 150 watt xenon arc lamp and chopped the excitation beam leading the fluorescence through a monochromator/detector (I.P. 28) into a tuned amplifier. We [126] used an ac 150 watt xenon arc lamp operating at mains frequency. Under these circumstances continuum radiation from the flame over the waveband transmitted by the monochromator is not recognized, though it produces an increase in electronic noise. The results shown in Table 4 summarise some of the data obtained by both groups using such a source.

In contrast to the others who reported signals for Ag, Au, Ba, Bi, Ca, Cd, Cu, Ga, Mg, Ni, Pb, Tl, and Zn, we found no signals for Ga or Ni and none for Pb at 4058 Å though a good signal was obtained at 2833 Å which is the resonance line used for atomic absorption work, whereas the 4058 Å line is usually used for flame photometry. It is possible that our failure to find the Ga and Ni signals is due to the cooler flame used and the lack of protection afforded by the argon sheathed flame used by the other workers. It is certainly noticeable that the sensitivities they reported for Ga and Ni are much lower than the others and these elements are prone to form molecular oxide species in the flame. As expected, we found no fluorescence at any of the bands we examined for Al, Be, Hg(II), Pd(II), Sn(IV) and Zr in the air-propane and air-hydrogen flames and with the continuous source. We did not examine Au, Ba, Bi and Ca which yielded good spectra in the other study [125] but obtained good spectra for Co, Fe, and Mn. The wavelengths shown in Table 4 correspond to the strongest fluorescences observed under our conditions. It must be stressed, however, that alteration of the radiative characteristics of the source may well alter the relative strengths of the fluorescent lines since emission is a function of the intensity of the source emission lines as well as the oscillator strengths of the absorbing atoms.

It is also noticeable from the table that those elements which are more difficult to atomise in cool flames (air-propane) gave lower sensitivities than in the hotter oxy-hydrogen flame, *e.g.*, Mg, Ag, Cu, whilst those which are easily atomised, *e.g.*, Zn, Tl, gave similar signals. Thus one arrives at the fairly obvious fact that, as in atomic absorption spectrophotometry, the flame must be hot enough to produce a good population of free atoms.

#### D. SENSITIVITY AND SELECTIVITY OF ATOMIC FLUORESCENCE SPECTROPHOTOMETRY

It must also be stressed, however, that Table 4 apparently shows that on the whole atomic fluorescence is less sensitive than atomic-absorption

TABLE 4. Atomic-fluorescence with a 150 watt xenon arc-lamp.

Element	Wavelength (Å)	Slit-Width (mm)	Detection Limit (ppm)		Detection Limit (ppm) <sup>a</sup> A.F.S. <sup>c</sup> oxy-hydrogen	Detection Limit (ppm) <sup>b</sup> using air-acetylene
			air-propane A.F.S. <sup>c</sup>	air-hydrogen A.F.S. <sup>c</sup>		
Zn	2139	2.0	0.6	0.6		
Cd	2288	2.0	0.25	0.25	0.6	0.04
Co	2407	1.0	1.5	1.0	0.08	0.05
Fe	2483	0.8	5.0	5.0		0.5
Mn	2794	0.25	0.3	0.15		0.5
Pb	2833	0.3	20	10		0.2
Mg	2852	0.2	2.0	2.0	0.2	1.0
Cu	3248	0.2	1.0	0.4	0.35	0.02
Ag	3281	0.4	0.35	0.15	0.08	0.15
	3383	0.4	0.2	0.10		0.1
Tl	3776	0.1	1.0	0.5	0.55	5.0

<sup>a</sup> Data from Winefordner et al.<sup>b</sup> Data from operating manual for SP 900A (Unicam Instruments Ltd., Cambridge, England).<sup>c</sup> A.F.S. denotes atomic-fluorescence spectrophotometry.<sup>d</sup> F.E. denotes flame-emission.<sup>e</sup> A.A.S. denotes atomic-absorption.

spectrophotometry. In fact, the reverse is the case, but the table refers to the use of a 150 watt source which emits energy over the whole of the spectrum from 2000 Å into the infra-red range. The intensity of radiation available from the lamp in any one waveband must be quite small and it is surprising to find such sensitivity as these show. Using spectral discharge lamps we have found sensitivities of  $2 \times 10^{-10}$  g for cadmium and similarly for zinc, corresponding to a signal : noise ratio of 1 : 1. Good rectilinear calibration curves were obtained for cadmium with  $10^{-7}$ M solutions [122] and with zinc using  $5 \times 10^{-8}$ M solutions [126]. In the range  $10^{-5}$ M a percentage standard deviation of 0.7 was found and with  $<10^{-6}$ M solutions *ca.* 3.0. With cadmium and zinc we found it easily possible to prepare linear calibration curves over the area  $10^{-5}$ – $10^{-7}$ M. Forty-one cations and eighteen anions were examined for interference at hundred-fold concentrations relative to the test ion in both instances and none was found. The ions were  $\text{NH}_4^+$ , Ag, Al, As, Au, Ba, Be, Bi, Ca, [Cd], Ce, Co, Cr, Cu, Fe(II) and (III), Ga, Hg, In, K, Li, Mg, Mn, Mo, Na, Ni, Pb, Sb, Sc, Se, Sn, Sr, Te, Th, Tl, Ti, U, V, W, Y, [Zn], Zr, acetate, borate, bromide, carbonate, chloride, citrate, perchlorate, cyanide, fluoride, iodide, nitrate, oxalate, phosphate, thiocyanate, silicate, sulphite, sulphate, and tartrate. Hydrolysis was prevented where necessary by the addition of sufficient acid to maintain a clear solution. Mansefield, Winefordner, and Veillon similarly report near linear curves for zinc over the range  $1 \times 10^{-4}$  to 10 ppm,  $2 \times 10^{-4}$  to 10 ppm for cadmium, 0.1 to 1000 ppm for mercury and  $4 \times 10^{-2}$  to 1000 ppm for thallium using spectral discharge lamps.

#### E. DETERMINATION OF SELENIUM AND TELLURIUM

More recently, [127] we have employed microwave-powered sources for selenium and tellurium and have compared their determination by both absorption and fluorescence on the same equipment, *viz.* the Unicam SP 900A.

The  $^3\text{P}_2$  ground state in selenium and tellurium is part of a triplet  $^3\text{P}_2$ ,  $^3\text{P}_1$ ,  $^3\text{P}_0$ . For selenium the  $^3\text{P}_2 \rightarrow ^3\text{S}_1^\circ$ ,  $^3\text{P}_1 \rightarrow ^3\text{S}_1^\circ$  and  $^3\text{P}_0 \rightarrow ^3\text{S}_1^\circ$  transitions show up as lines at 1961, 2040 and 2063 Å whilst for tellurium the same transitions resulted in lines at 2143, 2386 and 2383 Å. Intercombination lines at 1900, 2075 and 2558 Å correspond to  $^3\text{P}_2 \rightarrow ^5\text{S}_2^\circ$  transitions whilst those at 1915, 2164, 2531 and 5746 Å correspond to  $^3\text{P}_1 \rightarrow ^5\text{S}_2^\circ$ . Fluorescence was observed for all three lines for selenium and tellurium but only very slightly for the intercombination bands. Since the ground state line absorbs ten to five times more strongly than the metastable  $^3\text{P}_1$  and  $^3\text{P}_0$  states there is little doubt that the 2040 and 2063 lines for selenium and the 2386 and 2383 lines for tellurium arise from direct-line fluorescence.

Difficulties were encountered with the 9601B photomultiplier, which has a Corning uv. end-window, and the 1961 Å selenium line, but the

photomultiplier gave a satisfactory response with the direct line at 2040 Å. Using a selenium tube under an argon pressure of < 0.1 mm at 40 watts we were able to obtain good calibration curves between 0.25 and 125 ppm (higher limit not explored) with a (signal:noise = 1:1) detection limit of 0.15 ppm. With tellurium the 2143 Å line was used, with a tellurium (iodine) tube at *ca.* 0.1 mm argon and operating at 30 watts as source, to obtain calibration curves in the range 0.06 to 125 ppm (upper limit not sought) with a detection limit of 0.05 ppm. We anticipate that use of the directly interchangeable EMI 9526B photomultiplier would increase the sensitivity by a factor of between 10 and 100 fold, particularly for selenium. As before, no interferences were observed. Using the same equipment for atomic absorption measurements we obtained a detection limit of 1 ppm for each element. The 2143 Å resonance line was used for tellurium and (despite the insensitivity of the photomultiplier) the 1961 Å line for selenium.

The fact that the better sensitivity of the photomultiplier could be used with advantage by the fluorescence technique, whilst it could not by absorption, is a good example of the flexibility of the former technique. The signal obtained in fluorescence was found to be largely independent of the flame composition and height of measurement in the flame, but a slightly fuel-rich air-propane flame was used with measurement about 3 cm above the burner head.

Veillon, Mansfield, Parsons, and Winefordner have observed some very broad scattering bands in the argon (air)-hydrogen flame due to molecular aggregates in the flame, particularly with the total consumption burner, but we have not detected these using more conventional flame gases and the laminar-flow flame. As in atomic absorption we have generally found that the analytical signal can be enhanced by a factor of four or five times when the element concerned is extracted into an equal volume of a non-miscible organic solvent. Similar results have been observed by Winefordner *et al.* In our work we have been able to show that the enhancement appears to bear a direct relationship to the increased nebuliser efficiency using organic solvents.

#### F. ASSESSMENT OF ATOMIC FLUORESCENCE SPECTROPHOTOMETRY AS AN ANALYTICAL TECHNIQUE

In his recent monograph on absorption spectrophotometry Edisbury [129] has remarked that atomic-absorption spectroscopy promises to become a major technique because it involves 'the World's most selective possible absorption of light'. This is certainly true also of atomic fluorescence and, with it, the newer technique promises to bring along a flexibility of operation and sensitivity that considerably exceeds those of atomic absorption. The range of elements which have as yet been determined is limited still by the newness of the technique, but it is, *cf.* Figure 22, nevertheless very promising indeed. There is every reason



However, at present the microwave powered source appears to be one of the best available. Not only can it be used to provide narrow 'line' sources consisting of individual quartz 'lamps' which can be made at a cost of *ca.* \$0.5 each within a matter of a few minutes [127] but multielement lamps may also be prepared by suitable blending of the desired constituents *and* a continuous xenon, argon, neon, etc., source as well, simply by ampouling the necessary gas under a suitably reduced pressure.

Every technique has its limitations, and at the present for atomic fluorescence these are inherently the largely unknown possibilities of interference by quenching and by light scatter. However, in the few experiments that have as yet been described, they do not appear to constitute a very serious limitation. It will be freely admitted that lack of commercial equipment may cause some delays in adoption of the technique, but anyone who has experience of flame spectrophotometry or atomic absorption and some knowledge of fluorescence phenomena will not be deterred from exploring such an enticing new area by such a triviality.

#### G. FUTURE DEVELOPMENTS IN ATOMIC-FLUORESCENCE SPECTROPHOTOMETRY

Speculation on the future of atomic fluorescence spectrophotometry is perhaps pointless and foolish at such an early state of its development, but it is fairly safe to predict that it is a technique which will attract widespread attention and be much used in the near future. Commercial equipment will no doubt rapidly become available as manufacturers realise its potential but the adaptation of a flame spectrophotometer is so simple that it need not hold the enthusiast back at all. The xenon arc lamp and power supply are readily available in many laboratories and suitable microwave units are in common use in many hospitals for therapeutic purposes. They cost only *ca.* \$800 and a simple vacuum line can be devised [127] in a very short space of time to blow 'lamps' by the dozen.

The inexpensive and simple nature of the fluorescence equipment necessary to do subnanogram analyses with absolute specificity should be a serious consideration in all laboratories currently considering the purchase of items such as x-ray fluorescence, etc.

As in atomic absorption, the flame is a non-ideal atom reservoir for reasons which have already been discussed. No doubt many more flame media deserve exploration, but the use of demountable hollow cathode lamps, plasma jets, atom furnaces, etc., demand very close attention, particularly in view of the possibility of working at last on the non-metals such as sulphur and the halogens. It is not too much,

I think, to suppose that the sensitivity and specificity of this new technique will yet make it one of the most widely used and revolutionary techniques of our time.

## VI. References

- [1] Liebhafsky, H. A., Pfeiffer, H. G., Winslow, E. H. and Zemnay, P. D., 'X-ray Absorption and Emission in Analytical Chemistry,' J. Wiley and Sons, New York, 1960.
- [2] Bankovskii, Y. A., and Lobanova, E. F., *Zhur. Analit. Chem.* **14**, 523 (1959).
- [3] Bankovskii, Y. A., Ievinsh, A. F., and Luksha, E. A., *ibid.* **14**, 714 (1959).
- [4] Bankovskii, Y. A., and Ievinsh, A. F., *ibid.* **13**, 507 (1958).
- [5] Merritt, L. L., and Walker, J. K., *Ind. Eng. Chem. Anal. Ed.* **16**, 387 (1944).
- [6] Hynek, R. J., and Wrangell, L. J., *Anal. Chem.* **28**, 1520 (1956).
- [7] Dagnall, R. M., West, T. S., and Young, P., *Analyst* **90**, 1066 (1965).
- [8] Ohnesorge, W. E., and Burlingame, A. L., *Anal. Chem.* **34**, 1086 (1962).
- [9] Smith, G. F., and McCurdy, W. H., *Anal. Chem.* **24**, 371 (1952).
- [10] Morrison, G. H., and Freiser, H., 'Solvent Extraction in Analytical Chemistry,' J. Wiley and Sons, New York, 1957, p. 155.
- [11] Bailey, B. W., Dagnall, R. M., and West, T. S. *Talanta* **13**, 753 (1966).
- [12] Close, R. W., and West, T. S., *ibid.* **5**, 221 (1960).
- [13] Herrero-Lancina, M., and West, T. S., *Anal. Chem.* **35**, 2131 (1963); Palkans, P., and Florence, T. M., *Anal. Chim. Acta* **30**, 353 (1964).
- [14] Lukin, A. M., Smirnova, K. A., and Zavarikhina, G. B., *Zhur. Anal. Khim.* **18**, 444 (1963).
- [15] Dagnall, R. M., Smith, R., and West, T. S., *J. Chem. Soc.* 1595 (1966).
- [16] Freeman, D. C., and White, C. E., *J. Amer. Chem. Soc.* **78**, 2678 (1956).
- [17] White, C. E., and Cuttitta, F., *Anal. Chem.* **31**, 2083 (1959).
- [18] Dagnall, R. M., Smith, R., and West, T. S., *Analyst* **92**, 20 (1967).
  
- [19] Belcher, R., Leonard, M. A., and West, T. S., *Talanta* **2**, 92 (1959).
- [20] *Idem.* *J. Chem. Soc.*, 2390 (1958).
- [21] Leonard, M. A., and West, T. S., *ibid.*, 4477 (1960).
- [22] Bartkiewicz, S. A., and Robinson, J. W., *Anal. Chim. Acta* **22**, 427 (1960).
- [23] Belcher, R., and West, T. S., *Talanta* **8**, 853 and 863 (1961).
- [24] Dagnall, R. M., and West, T. S., *ibid.* **11**, 1533 (1964).
- [25] Bailey, B. W., Dagnall, R. M., and West, T. S., *ibid.* **13**, 753 (1966).
- [26] Ducret, L., and Seguin, P., *Anal. Chim. Acta*, **17**, 207 (1957); also Pasztor, L., Bode, J. D. and Fernando, Q., *Anal. Chem.* **32**, 277 (1960).
- [27] Jankovsky, J., *Talanta* **2**, 29 (1959).
- [28] Belcher, R., Wilson, C. L., and West, T. S., *New Methods of Analytical Chemistry*, 2d Edition, Chapman and Hall, Ltd., London, 1964, pp. 264-267.
- [29] Dagnall, R. M., and West, T. S., *Talanta* **11**, 1627 (1964).
- [30] Braude, E. A., in *Determination of Organic Structures by Physical Methods*, Volume I, E. A. Braude and F. C. Nachod, editors, Academic Press, New York, 1955, p. 131 et seq.
- [31] West, T. S., *Chemistry and Industry*, 1005 (1966).
- [32] Umland, F., and Wunsch, G., *Z. Anal. Chem.* **213**, 186 (1965).
- [33] West, T. S., lecture to Society for Analytical Chemistry, Burlington House, London, 6th October 1965, *cf.* *Analyst* **91**, 69 (1966).
- [34] Djurkin, V., Kirkbright, G. F., and West, T. S., *Analyst* **91**, 89 (1966).
- [35] Kirkbright, G. F., and Yoe, J. H., *Talanta* **11**, 415 (1964).
- [36] Wadelin, C., and Mellon, M. G., *Analyt. Chem.* **25**, 1668 (1953).
- [37] Cabello-Tomas, M. L., and West, T. S., unpublished studies, *cf.* Ref. 31.

- [38] Weber, G., and Teale, F. W. J., *Trans. Faraday Soc.* **53**, 646 (1957).
- [39] Bowen, E. J., and West, K., *J. Chem. Soc.* 4394 (1955).
- [40] Bowen, E. J., and Sahu, J., *J. Phys. Chem.* **63**, 4 (1959).
- [41] Kasha, M., *J. Chem. Phys.* **20**, 71 (1952).
- [42] McGlynn, S. P., Reynolds, M. J., Daigre, G. W., and Christodouleas, N.D., *J. Phys. Chem.* **66**, 2499 (1962).
- [43] Van Duuren, B. L., *Chem. Rev.* **63**, 325 (1963).
- [44] Leonhardt, H., and Weller, A., *Z. Physik. Chem.* **29**, 277 (1961).
- [45] Bowen, E. J., and Wokes, F., *Fluorescence of Solutions*, Longmans Green and Co., London, 1953.
- [46] Bowen, E. J., and Brockelhurst, B., *Trans. Faraday Soc.* **51**, 774 (1955).
- [47] Parker, C. A., and Hatchard, C. G., *Proc. Chem. Soc.* 147 (1962).
- [48] Parker, C. A., and Rees, W. T., *Analyst* **85**, 587 (1960).
- [49] *Idem. ibid* **87**, 83 (1962).
- [50] Lott, P. F., *J. Chem. Education* **41**, A 327 (1964).
- [51] Cheng, K. L., in *Trace Analysis: Physical Methods*, G. H. Morrison, editor, Interscience Publishers, New York, 1965, pp. 161-192.
- [52] Ellis, D. W., in *Fluorescence and Phosphorescence Analysis*, D. M. Hercules, editor, Interscience Publishers, New York, 1966, pp. 41-79.
- [53] Slavin, W., Mooney, R. W., and Palumbo, D. T., *J. Opt. Soc. Am.* **51**, 93 (1961).
- [54] Turner, G. K., *Science (No. 3641)* **146**, 183 (1964).
- [55] Allison, J. B., and Becker, R. S., *J. Chem. Phys.* **32**, 1410 (1960).
- [56] Kauzmann, W., *Quantum Chemistry*, Academic Press, New York, 1957, pp. 542-544.
- [57] West, W., *Chemical Applications of Spectroscopy*, Interscience Publishers, New York, 1956.
- [58] Brederick, K., Förster, T., and Oesterlin, H. G., in *Luminescence of Organic and Inorganic Materials*, H. Kallmann and G. M. Spruch, editors, J. Wiley & Sons, New York, 1962, p. 161.
- [59] Kasha, M., and El-Sayed, M. A., *Spectrochim. Acta* **15**, 758 (1959).
- [60] Kasha, M., *Radiation Res. Suppl.* **2**, 243 (1960).
- [61] Popovych, O., and Rogers, L. B., *Spectrochim. Acta* **16**, 49 (1960).
- [62] Eggers, J. H., *Talanta* **4**, 38 (1960).
- [63] Wilkins, D. H., *ibid.* **4**, 182 (1960).
- [64] Lewis, G. N., Magel, T. T., and Lipkin, D., *J. Am. Chem. Soc.* **62**, 2973 (1940).
- [65] Cherkosov, A. S., *Dokl. Akad. Nauk. SSSR* **146**, 716 (1962).
- [66] Diehl, H., Olsen, R., Spielholtz, G. I., and Jensen, R., *Anal. Chem.* **35**, 1144 (1963).
- [67] Crosby, G. A., Whan, R. E., and Alire, R. M., *J. Chem. Phys.* **34**, 743 (1961).
- [68] De Armand, K., and Forster, L. S., *Spectrochim. Acta* **19**, 1393, 1403, 1687 (1963).
- [69] Tomaschek, R., Reichesber, Physik (Beihefte Physik Z.) **1**, 139 (1944); cf. C. Abstr. 6815g (1947).
- [70] White, C. E., *Anal. Chem.* **21**, 104 (1949); **22**, 69 (1950); **24**, 85 (1952); **26**, 129 (1954); **28**, 621 (1956); **30**, 729 (1958); **32**, 47R (1960).
- [71] White, C. E., and Weissler, A., *ibid.* **34**, 81R (1962); **36**, 116R (1964); **38**, 155R (1966).
- [72] West, T. S., *Lab. Practice*, 1030 (1965).
- [73] Collat, J. W., and Rogers, L. B., *Anal. Chem.* **27**, 961 (1956).
- [74] Dagnall, R. M., Smith, R., and West, T. S., *Talanta* **13**, 609 (1966).
- [75] Bailey, B. W., Dagnall, R. M., and West, T. S., *Talanta* **13**, 1661 (1966).
- [76] Walsh, A., *Spectrochim. Acta* **7**, 108 (1955).
- [77] Vidale, G. L., GEC (USA) TIS Rep., R 60 SD 330 (1960).
- [78] L'vov, B. V., *Spectrochim. Acta* **17**, 761 (1961).
- [79] Moshier, R. W., and Sievers, R. E., *Gas Chromatography of Metal Chelates*, Pergamon Press, Oxford, 1966.

- [80] Menzies, A. C., in *Atomic-Absorption Spectrophotometry*, W. T. Elwell, and J. A. F. Gidley, Pergamon Press, Oxford, 1961, p. 28.
- [81] Gatehouse, B. M., and Walsh, A., *Spectrochim. Acta* **16**, 602 (1960).
- [82] Goleb, J. A., and Brody, J. K., *Anal. Chim. Acta* **28**, 457 (1963).
- [83] Robinson, J. W., *ibid.* **27**, 465 (1962).
- [84] Greenfield, S., Jones, I. L. L., and Berry, C. T., *Analyst* **89**, 713 (1964); Mavrodineanu, R., and Hughes, R. C., *Spectrochim. Acta* **19**, 1309 (1963); West, C. D., and Hume, D. N., *Anal. Chem.* **36**, 412 (1964).
- [85] Nelson, L. S., and Keubler, N. A., *Spectrochim. Acta* **19**, 781 (1963).
- [86] Parkinson, W. H., *Proc. Phys. Soc.* **78**, 705 (1961).
- [87] Massman, H., *Z. Instrumentenk* **71**, 225 (1963).
- [88] Sebens, C., Vollmer, J., and Slavin, W., *Perkin Elmer Atomic Absorption Newsletter* **3**, 165 (1964).
- [89] Gibson, J. H., Grossman, W. E. L., and Cooke, W. D., in *Analytical Chemistry 1962*, edited by P. W. West, A. M. G. Macdonald and T. S. West, Elsevier (1963), pp. 288-290.
- [90] Fassel, V. A., Mossotti, V. G., Grossman, W. E. L., and Kniseley, R. N., *Spectrochim. Acta* **22**, 347 (1966).
- [91] Ivanov, N. P., and Kozireva, N. A., *Zhur. Anal. Khim.* **19**, 1266 (1964).
- [92] Russel, B. J., Shelton, J. P., and Walsh, A., *Spectrochim. Acta* **8**, 317 (1947).
- [93] Elwell, W. T., and Gidley, J. A. F., *Atomic-Absorption Spectrophotometry*, Pergamon Press, Oxford, 1st edition, 1961, pp. 9 and 12.
- [94] Marshall, G. B., and West, T. S., *Talanta*, submitted for publication.
- [95] Dagnall, R. M., Thompson, K. C., and West, T. S., unpublished work.
- [96] Walsh, A., in *Analytical Chemistry 1962*, edited by P. W. West, A. M. G. Macdonald, and T. S. West, Elsevier, 1963, p. 286.
- [97] Strasheim, A., and Butler, L. R. P., *Appl. Spectry.* **16**, 109 (1962).
- [98] Fuwa, K., and Vallee, B. L., *Anal. Chem.* **35**, 942 (1963).
- [99] Koirtiyohann, S. R., and Feldman, C., *Develop. Appl. Spectry.* **3**, 180 (1963).
- [100] Goodfellow, G. I., and Turner, C., private communication.
- [101] Dean, J. A., *Flame Photometry*, McGraw-Hill, New York, 1960.
- [102] Huldt, L., and Lagerquist, A., *Arkiv. Fysik.* **2**, 333 (1950).
- [103] Robinson, J. W., *Anal. Chem.* **33**, 1067 (1961).
- [104] Margoshes, M., and Scribner, B. F., *Spectrochim. Acta* **15**, 138 (1959).
- [105] David, D. J., *Analyst* **86**, 730 (1961).
- [106] Willis, J. B., *Nature* **207**, 715 (1965).
- [107] Amos, M. D., and Willis, J. B., *Spectrochim. Acta* **22**, 1325 (1966).
- [108] Kirkbright, G. F., Smith, A., and West, T. S., *Analyst* **91**, 700 (1966).
- [109] Kirkbright, G. F., Peters, M. K., and West, T. S., *ibid.* **91**, 705 (1966).
- [110] Jones, W. G., and Walsh, A., *Spectrochim. Acta* **16**, 249 (1960).
- [111] Allan, J. E., *ibid.* **15**, 800 (1959).
- [112] Willis, J. B., *Spectrochim. Acta* **16**, 259 (1960).
- [113] Baker, C. A., and Garton, F. W. J., *UKAEA Rept. AERE R. 3490* (1961).
- [114] Clinton, O. E., *Spectrochim. Acta* **16**, 985 (1960).
- [115] Belcher, R., Dagnall, R. M., and West, T. S., *Talanta* **11**, 1257 (1964).
- [116] Nichols, E. L., and Howes, H. L., *Phys. Rev.* **23**, 472 (1924).
- [117] Robinson, J. W., *Anal. Chim. Acta* **24**, 254 (1961).
- [118] Winefordner, J. D., and Vickers, T. J., *Anal. Chem.* **36**, 161 (1964).
- [119] Winefordner, J. D., and Staab, R. A. *ibid.* **36**, 165 (1964).
- [120] *Idem.* *ibid.* **36**, 1369 (1964).
- [121] Mansfield, J. M., Winefordner, J. D., and Veillon, C., *ibid.* **37**, 1051 (1965).
- [122] Dagnall, R. M., West, T. S., and Young, P., *Talanta* **13**, 803 (1966).
- [123] Mitchell, A. C. G., Zemansky, M. W., *Resonance Radiation and Excited Atoms*, Cambridge University Press, Cambridge, 1961.

- [124] West, T. S., Inaugural Lecture at Imperial College, 25th January, 1966, cf. *Chemistry and Industry*, 1014 (1966).
- [125] Veillon, C., Mansfield, J. M., Parsons, M. L., and Winefordner, J. D., *Anal. Chem.* **38**, 205 (1966).
- [126] Dagnall, R. M., Thompson, K. C., and West, T. S., *Anal. Chim. Acta* **36**, 269 (1966).
- [127] Idem, *Talanta*, submitted for publication.
- [128] Idem, unpublished work.
- [129] Edisbury, J. R., *Practical Hints on Absorption Spectrophotometry*, Hilger and Watts, Ltd., London, 1966, p. 171.



# CHEMICAL SPECTROPHOTOMETRY

## Contributed Papers and Discussion

### OSCAR MENIS

*NBS Institute for Materials Research, Washington, D. C. 20234*

#### I. Introduction

At the conclusion of Dr. West's lecture the chairman of the session reported on the highlights of the contributed papers. Because of the limited time, only one of these papers was presented by the author. Coincidentally, the six papers which were summarized were representative of the several areas covered by the lecture. They included atomic absorption, fluorescence, spectrophotometry utilizing an organic chelate with a high molar absorptivity index, ternary complex reactions, and chelate extractions. In addition, the contributions included studies of problems associated with the recovery of trace elements from sample dissolution processes.

#### II. Contributed Papers

The paper on trace elements in marine waters by atomic absorption spectrophotometry, by D. C. Burrell, evaluated the application of atomic absorption methods to the determination of ten elements which included alkaline earth and transition elements. Some of the aspects of interest were: (1) The assessment of the advantages of the laminar flow, premixed gas burner over the turbulent flow burner; (2) the presence of spectral interference of the CaO band in the determination of barium; (3) the use of standard addition technique to overcome the interference of "light scatter" from the sample background; and (4) the use of a two-step preconcentration technique in which the transition elements were adsorbed on ferric hydroxide and then separated by solvent extraction.

The paper on spectrophotometric determination of microgram and submicrogram amounts of silver with Thio-Michler's ketone by K. L. Cheng described the use of 4,4'-bis(dimethylamino)thiobenzophenone, Thio-Michler's ketone, for the determination of silver. This reagent forms a complex with silver ion at pH 3 in a water-ethanol solution or, alternately, it can be extracted into isoamyl alcohol. The complex has an absorptivity index of 94,000, thus approaching closely the theoretical value of 100,000 discussed by Dr. West in his lecture. In the presence of EDTA and citric acid, it is very specific and only noble metals interfere.

In the paper on some problems in the assessment of trace impurities in highly refractory electronic materials, with particular reference to single crystal ruby and sapphire for maser and laser use by E. M. Dodson, the problem of dissolving small samples (10 mg) of ruby crystals was discussed. A study with tracer iron-59 revealed losses due to the platinum crucibles used in the alkaline fusion. The mechanism of these losses was described. It was shown that by the use of zirconium crucibles and a potassium hydroxide fusion, these losses could be avoided.

In the paper on dual atmospheric tracers utilizing the fluorescence of fluorescein and calcium acetylsalicylate by J. D. Ludwick, a procedure was developed for the sensitive detection of certain fluorescent materials in a study of their possible use as atmospheric tracers. Instrumentation was used which allowed differentiation of excitation and emission spectra. This permitted independent analysis of the fluorescent materials, fluorescein and the calcium salt of aspirin, simultaneously collected from the atmosphere in diffusion studies. Cross-tracer interference was reduced to a minimum and as little as  $5 \times 10^{-11}$  g of fluorescein and  $3 \times 10^{-9}$  g of Ca-aspirin were measured.

Excitation and fluorescence spectra were presented for these compounds. After consideration of these spectra it is apparent that excitation of fluorescein at  $490 \text{ m}\mu$  will not induce fluorescence in Ca-aspirin, and the excitation of Ca-aspirin at  $300 \text{ m}\mu$  will influence fluorescein fluorescence to only a small extent.

In the paper on spectrophotometric determination of vanadium in steel by C. L. Luke, a rapid method for determination of trace quantities of vanadium in steel was described. It is based on the extraction of vanadium with  $\alpha'$ -benzoinoxime in chloroform and adding 8-quinolinol for the formation of the colored complex of vanadium. The interferences which accompany vanadium can be removed with a dilute hydrochloric acid wash. The control of acidity prior to extraction and oxidation of vanadium by permanganate are the critical steps in the procedure.

In the paper concerning evaluation of absorptiometric methods for the determination of nanogram quantities of elements in high-purity materials by O. Menis, R. W. Burke, and T. C. Rains, the analysis of high-purity material, defined as "6-nines" of major component, presented an analytical challenge. As readily recognized, instrumental methods require calibration in order to assure reasonable accuracy. Since this represents a major difficulty with high-purity materials, analytical results based on independent methods must be relied upon to minimize systematic errors.

By atomic absorption and spectrophotometric procedures 40 ppb of copper was found in "6-nines" purity zinc. In the atomic absorption a TTA-hexone solvent extraction method was used to isolate the copper. In the spectrophotometric procedure the displacement of zinc from

dibenzylthiocarbamate chelate provided a means of measuring the absorbance of the copper chelate at  $435\text{ m}\mu$ . This appears to be a remarkable process since it occurred in the presence of a millionfold excess of zinc. The estimation of antimony and (gold + thallium) at less than 0.05 and 0.1 ppm respectively was also achieved by means of the Brilliant Green dye reaction [1].<sup>1</sup>

The final paper on precision photometric analysis using a  $\beta$ -excited isotopic light source by H. H. Ross, was discussed by the author. Early in 1966, the Analytical Chemistry Division of Oak Ridge National Laboratory introduced a new technique for making high precision photometric measurements [2]. This new method utilizes the unusual spectral properties of a  $\beta$ -excited light source combined with pulse-height measuring equipment. The advantages of the technique include high stability, controlled sensitivity, simplicity, small power requirements, direct digital output, and straightforward error analysis.

### III. Discussion

In the general discussion, H. Kaiser (Dortmund), presented information on a furnace-type excitation cell for atomic absorption. This idea was originated by a Russian scientist and developed by H. Massman at Kaiser's Institute in Dortmund. With the aid of a slide, Figure 1, he described the cell. It consists of a carbon tube 5 cm long, inner diameter of 8 mm and with a wall thickness of 1 mm. In the center of the cylinder there is a small hole through which as little as 0.04 microliters of test solution or a solid sample can be introduced.

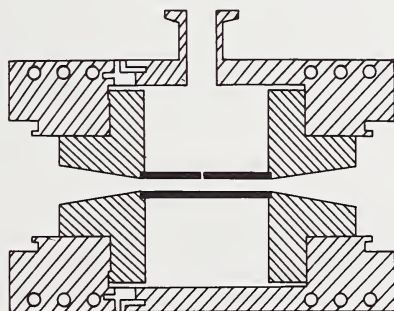


Figure 1. Furnace excitation cell for atomic absorption.

The carbon tube is supported in a copper block. This block is then heated electrically by means of a low voltage transformer supplying a current of 400 amps. A temperature of up to  $2800\text{ }^{\circ}\text{C}$  can be obtained. The entire chamber is enclosed in an argon atmosphere to prevent the

<sup>1</sup> Figures in brackets indicate the literature references at the end of this paper.

introduction of impurities from inside of the tube by oxidation processes. Furthermore, the movement of argon gas is kept at a minimum in order to retain the excited atoms within the absorption path inside the carbon cylinder. In a second slide some detection limits for 1% absorption were shown for cadmium, zinc, and mercury, indicating sensitivity at the  $10^{-10}$  g level. Dr. Kaiser felt that this technique when fully developed should be competitive with spark source mass spectrometry.

To a question from the audience as to the memory effect of the carbon tube Dr. Kaiser replied that these carbon cylinders are relatively inexpensive and should be changed after each test.

T. S. West remarked that as far as ultimate sensitivity, atomic fluorescence offered the best approach for increasing detection limits. Using relatively simple equipment one can determine  $10^{-9}$  and  $10^{-10}$  molar solutions with good precision. In his laboratory this has been demonstrated with zinc, cadmium, selenium, tellurium in the presence of over 40 cations and 18 anions.

H. Kaiser remarked that in atomic fluorescence an increase in sensitivity by a factor of ten could be attained by changing the optical arrangement.

Kaiser also added another comment on the subject of high precision atomic absorption measurement. He proposed a multi-component monitoring system to provide automatic corrections for the several variables. First, he would measure the output from the hollow cathode lamp of a nonresonance line after it passes through the flame source to correct for background radiation and fluctuation of the hollow cathode output. Secondly, he would monitor another element as an internal standard to correct for the variation of solution aspiration and flame variations. Finally, he would monitor the output from the hollow cathode outside the flame path. These corrections could then be electronically compensated and the final measurement would be free from these systematic errors.

#### IV. References

- [1] Burke, R. W., Menis, O., *Anal. Chem.* **38**, 1719 (1966).
- [2] Ross, H. H., *Anal. Chem.* **38**, 414 (1966).

# RADIOACTIVITY TECHNIQUES IN TRACE CHARACTERISATION

A. A. SMALES

*Atomic Energy Research Establishment, Harwell, Great Britain*

## I. Introduction

The authors of the chapters in this book were asked to summarise the “state-of-the-art” in their particular speciality. This is difficult enough for a specialist to do in the area of nuclear techniques even with mass spectroscopy – a nuclear technique of the very greatest importance in the field of trace elements – detached for treatment elsewhere. But for one who is really no longer a specialist, or at any rate tries hard *not* to be, it might be thought to be even more difficult! However, in the context of this Conference, where this presentation is merely to serve the dual purpose of (a) acquainting the non-specialist with a reasoned appreciation of the present possibilities and future potential and (b) being a preliminary to a discussion amongst all the most active specialists in the area, it may be that there is some value in having the appreciation made by someone who has experience of a wider range of competent areas of trace element characterisation, for he may be more sympathetic to the problems of the non specialist, leaving the real specialists to point out any omissions or underestimates of their particular line of enthusiasm.

At any rate, this paper cannot be perfect, least of all to its author trying to distil into a few pages what has taken several conferences and books, many reviews and a few thousand research papers to describe.

The area can be divided broadly into two sections, (a) *activation* techniques where a sample is irradiated to *produce* radioactive or excited states of elements in the sample and (b) the use of radioactive materials as *tracers* for an element or a compound. There are of course many subdivisions of each section – perhaps some enthusiastic proponents of particular subsections may be hurt in that their speciality is not given full sectional status!

## II. Activation Analysis

### A. GENERAL PRINCIPLES

The general principles have not altered since they were set out with some clarity in a few key papers in the late 1940's and early 1950's,

though of course it should be remembered that the approach had been used first by Hevesy and Levi in the mid 1930's.

The basic equation for activation is:—

$$A = \sigma f \frac{W\phi}{M} (1 - e^{-\lambda t}) \times 6.02 \times 10^{23}$$

where  $A$  = induced activity in disintegrations/sec at the end of irradiation.

$f$  = flux of "particles" used in the irradiation, in number/cm<sup>2</sup>/sec.

$\sigma$  = the activation cross section for the nuclear reaction concerned, in cm<sup>2</sup>.

$W$  = weight of element irradiated, in grams.

$\phi$  = fractional abundance of the particular isotope of the element concerned.

$M$  = atomic weight of that element.

$\lambda$  = the decay constant of the induced radionuclide, in sec<sup>-1</sup>.

$t$  = irradiation time, in seconds.

After the irradiation, the induced activity will of course decay with a characteristic half life, falling by a factor two in each half life period.

It follows from this equation that there is a limit to the activity that can be induced under given conditions, i.e. when the term  $(1 - e^{-\lambda t})$  reaches a value of 1, for practical purposes after an irradiation time of about ten half lives of the radioactive species induced. It is possible to get an indication of the potential sensitivity of the method for any element or indeed any isotope of an element (and it is worth pointing out that this method involves a *nuclear* reaction and therefore cannot give any assistance on identifying the *chemical form* of that element), given the necessary information on the values for the different components of the equation. Such sensitivities will be discussed later for each type of irradiation discussed.

In applying activation analysis the generally accepted approach is not to rely on absolute values of the components of the above equation but rather to irradiate a sample and a known mass of a standard under identical conditions so that a simple comparison of the induced activity gives the mass of element to be determined in the sample.

The above equation is quite general, but is normally used where species concerned have values of half life comparable with or longer than the time needed to measure the induced activity *after* irradiation is completed, though there is one development which is worth pointing

out at this stage and in which there is growing interest. This involves counting, *during* the irradiation, what is arbitrarily called “prompt” radiation. This latter refers to the radiation emitted from species, usually denoted as “excited states” with very short half lives, perhaps at the level of nanoseconds or less. A similar dependence of induced activity on cross section and flux occurs, but a counter observing such “prompt” radiation will yield a count-rate  $C$  which is proportional to the rate of reaction, i.e.,  $C = Kf\sigma W$  where  $f$ ,  $\sigma$ , and  $W$  have the same definition as earlier, and  $K$  is a constant which depends on the efficiency and geometry of the detector and the proportion of the decay emitting the radiation to be determined. Such “prompt” counts can be accumulated for an extended period of irradiation when the total counts registered in time ‘ $t$ ’ will be

$$C_{(t)} = Kf\sigma W t$$

This apparently gives the possibility of infinite sensitivity (note the difference from the earlier case, where it was assumed that counting was done *after* the irradiation) but in practice a lower useful limit will be imposed because of the measurement of activity from other sources which interfere with the determination. Nevertheless the approach has some advantage in saving of time and mention will be made subsequently of examples that have appeared.

In what might be considered as an intermediate state between the “prompt” approach and the longer established “removed radioactivity” situations, some work has been done using pulsed irradiations with induced activities of intermediate half life values comparable to the pulse time, counting during the interval between pulses.

By far the most commonly used approach to activation analysis, remains however the “removed radioactivity” method where measurement of the radioactivity follows the completed irradiation. Such measurement can sometimes be made directly on the irradiated sample using gamma ray spectrometers or even in a few cases simple beta counting, but it still remains generally true to say that for the utmost sensitivity and selectivity to be attained radiochemical separations are necessary before counting.

For those still not familiar with what is involved in practice, the experimental steps in a typical activation analysis may be re-stated.

1. Irradiate weighed quantities of the sample and standard in suitable containers for a sufficient time to give adequate radioactivity in the element to be determined.
2. After irradiation, dissolve the samples and standards and add a known weight of the element being determined as carrier for the small quantity that has been irradiated.

3. Treat the solution in such a way that the carrier and the element in the sample are in the same chemical form.

4. Carry out chemical separations to isolate the element (or a suitable compound) free from all other radionuclides: i.e., until it is radiochemically pure.

5. Determine the chemical "yield" by any conventional method. The fact that this step is included makes it unnecessary for the chemical separation in step 4 to be quantitative, since the final measured activity will be corrected for losses, using the chemical yield figure.

6. Compare the radioactivity of sample and standard under identical counting conditions, making correction if necessary for self-absorption, dead-time losses, decay, etc.

7. Check the radiochemical purity of the isolated active compound by measuring (a) the rate of decay, from which the half-life may be obtained, (b) the activity through different thicknesses of aluminium, from which an estimate of the energy of the rays or particles emitted may be made, and (c) the gamma energy, using, for example, a scintillation or solid state gamma spectrometer.

In certain favourable cases, steps 2 to 5 may be omitted.

Then the mass of  $X$ , the constituent to be determined, is obtained as follows:

$$\frac{\text{Mass of } X \text{ in unknown}}{\text{Mass of } X \text{ in standard}} = \frac{\text{Total activity from element } X \text{ in unknown}}{\text{Total activity from element } X \text{ in standard}}$$

## B. ACTIVATING AGENTS AND IRRADIATION FACILITIES

### 1. *Slow Neutrons*

There is no doubt that the most generally useful and available activating source for *high sensitivity* in the determination of trace elements remains the nuclear reactor with its abundant flux of *slow* neutrons, and because of the relative simplicity with which irradiations can be carried out. The particular advantage of slow neutrons is that usually only one nuclear reaction occurs (the  $n, \gamma$  reaction, illustrated by  $^{75}\text{As}(n, \gamma)^{76}\text{As}$ ) and that the cross section for this type of reaction is often quite high.

Many tables have been published giving theoretical sensitivities attainable, each author making his own set of assumptions about irradiation time, time for chemical processing and/or counting, type of counter used etc. Perhaps the most generally useful reference to give here is the book of R. C. Koch [1]<sup>1</sup> where are listed sensitivities for all elements using several types of activating agent. For slow neutrons Koch defines sensitivity as the mass in micrograms of the trace element which yields 1000 disintegrations/minute of activation product after irradiation in a flux of  $10^{14}$  neutrons/cm<sup>2</sup>/sec to saturation or for a maximum period of

<sup>1</sup> Figures in brackets indicate the literature references at the end of this paper.

thirty days. The sensitivity for each element quoted by Koch for each nuclear reaction available with thermal neutrons is assembled as Table 1. Individual users of the information can readily adjust the figures given to fit in with reactor fluxes available to them. Perhaps the most serious limitation of the sensitivities quoted in this table apply to those nuclear reactions producing short lived nuclides. Again the individual user must make his own allowance for the decay of such a nuclide during operations following the irradiation such as transport, radiochemistry and counting.

TABLE 1. *Sensitivity for thermal neutron reactions*

Element	Nuclear reaction	Sensitivity in micrograms
Hydrogen	$^2\text{H}(n,\gamma)^3\text{H}$	$2 \times 10^3$
Lithium	$^6\text{Li}(n,\alpha)^3\text{H}$	$6 \times 10^{-6}$
Beryllium	$^9\text{Be}(n,\gamma)^{10}\text{Be}$	$1 \times 10^4$
Carbon	$^{13}\text{C}(n,\gamma)^{14}\text{C}$	$4 \times 10^4$
Sodium	$^{23}\text{Na}(n,\gamma)^{24}\text{Na}$	$2 \times 10^{-5}$
Magnesium	$^{26}\text{Mg}(n,\gamma)^{27}\text{Mg}$	$2 \times 10^{-3}$
Aluminium	$^{27}\text{Al}(n,\gamma)^{28}\text{Al}$	$4 \times 10^{-5}$
Silicon	$^{30}\text{Si}(n,\gamma)^{31}\text{Si}$	$2 \times 10^{-3}$
Phosphorus	$^{31}\text{P}(n,\gamma)^{32}\text{P}$	$6 \times 10^{-5}$
Sulfur	$^{34}\text{S}(n,\gamma)^{35}\text{S}$	$4 \times 10^{-3}$
	$^{36}\text{S}(n,\gamma)^{37}\text{S}$	$4 \times 10^{-1}$
Chlorine	$^{37}\text{Cl}(n,\gamma)^{38}\text{Cl}$	$7 \times 10^{-5}$
Argon	$^{36}\text{Ar}(n,\gamma)^{37}\text{Ar}$	$1 \times 10^{-3}$
	$^{40}\text{Ar}(n,\gamma)^{41}\text{Ar}$	$2 \times 10^{-5}$
Potassium	$^{41}\text{K}(n,\gamma)^{42}\text{K}$	$2 \times 10^{-4}$
Calcium	$^{44}\text{Ca}(n,\gamma)^{45}\text{Ca}$	$7 \times 10^{-3}$
	$^{48}\text{Ca}(n,\gamma)^{49}\text{Ca}$	$7 \times 10^{-3}$
	$^{48}\text{Ca}(n,\gamma)^{49}\text{Ca} \xrightarrow{\beta^-} ^{49}\text{Sc}$	$7 \times 10^{-3}$
Scandium	$^{45}\text{Sc}(n,\gamma)^{46 + 46m}$	$3 \times 10^{-6}$
Titanium	$^{50}\text{Ti}(n,\gamma)^{51}\text{Ti}$	$2 \times 10^{-3}$
Vanadium	$^{51}\text{V}(n,\gamma)^{52}\text{V}$	$3 \times 10^{-6}$
Chromium	$^{50}\text{Cr}(n,\gamma)^{51}\text{Cr}$	$5 \times 10^{-5}$
	$^{54}\text{Cr}(n,\gamma)^{55}\text{Cr}$	$2 \times 10^{-3}$
Manganese	$^{55}\text{Mn}(n,\gamma)^{56}\text{Mn}$	$1 \times 10^{-6}$
Iron	$^{58}\text{Fe}(n,\gamma)^{59}\text{Fe}$	$1 \times 10^{-2}$
Cobalt	$^{59}\text{Co}(n,\gamma)^{60m}\text{Co}$	$1 \times 10^{-6}$
	$^{59}\text{Co}(n,\gamma)^{60 + 60m}\text{Co}$	$4 \times 10^{-5}$
Nickel	$^{64}\text{Ni}(n,\gamma)^{65}\text{Ni}$	$9 \times 10^{-4}$
Copper	$^{63}\text{Cu}(n,\gamma)^{64}\text{Cu}$	$6 \times 10^{-6}$
	$^{65}\text{Cu}(n,\gamma)^{66}\text{Cu}$	$3 \times 10^{-5}$

TABLE 1. *Sensitivity for thermal neutron reactions—Continued*

Element	Nuclear reaction	Sensitivity in micrograms
Zinc	$^{64}\text{Zn}(n,\gamma)^{65}\text{Zn}$	$1 \times 10^{-3}$
	$^{68}\text{Zn}(n,\gamma)^{69\text{m}}\text{Zn}$	$1 \times 10^{-3}$
	$^{68}\text{Zn}(n,\gamma)^{69}\text{Zn}$	$1 \times 10^{-4}$
Gallium	$^{69}\text{Ga}(n,\gamma)^{70}\text{Ga}$	$2 \times 10^{-5}$
	$^{71}\text{Ga}(n,\gamma)^{72}\text{Ga}$	$1 \times 10^{-5}$
Germanium	$^{70}\text{Ge}(n,\gamma)^{71}\text{Ge}$	$3 \times 10^{-5}$
	$^{74}\text{Ge}(n,\gamma)^{75} + ^{75\text{m}}\text{Ge}$	$2 \times 10^{-4}$
	$^{76}\text{Ge}(n,\gamma)^{77} + ^{77\text{m}}\text{Ge}$	$2 \times 10^{-3}$
Arsenic	$^{75}\text{As}(n,\gamma)^{76}\text{As}$	$4 \times 10^{-6}$
Selenium	$^{74}\text{Se}(n,\gamma)^{75}\text{Se}$	$6 \times 10^{-4}$
	$^{80}\text{Se}(n,\gamma)^{81}\text{Se}$	$9 \times 10^{-5}$
	$^{80}\text{Se}(n,\gamma)^{81\text{m}}\text{Se}$	$1 \times 10^{-3}$
	$^{82}\text{Se}(n,\gamma)^{83}\text{Se}$	$6 \times 10^{-2}$
	$^{82}\text{Se}(n,\gamma)^{83}, ^{83\text{m}}\text{Se} \xrightarrow{\beta^-} ^{83}\text{Br}$	$4 \times 10^{-3}$
Bromine	$^{79}\text{Br}(n,\gamma)^{80\text{m}}\text{Br}$	$1 \times 10^{-5}$
	$^{79}\text{Br}(n,\gamma)^{80}\text{Br}$	$5 \times 10^{-6}$
	$^{81}\text{Br}(n,\gamma)^{82}\text{Br}$	$1 \times 10^{-5}$
Krypton	$^{82}\text{Kr}(n,\gamma)^{83\text{m}}\text{Kr}$	$5 \times 10^{-6}$
	$^{84}\text{Kr}(n,\gamma)^{85\text{m}}\text{Kr}$	$4 \times 10^{-4}$
	$^{86}\text{Kr}(n,\gamma)^{87}\text{Kr}$	$2 \times 10^{-3}$
Rubidium	$^{85}\text{Rb}(n,\gamma)^{86}\text{Rb}$	$6 \times 10^{-5}$
	$^{87}\text{Rb}(n,\gamma)^{88}\text{Rb}$	$7 \times 10^{-4}$
Strontium	$^{84}\text{Sr}(n,\gamma)^{85}\text{Sr}$	$2 \times 10^{-2}$
	$^{86}\text{Sr}(n,\gamma)^{87\text{m}}\text{Sr}$	$2 \times 10^{-4}$
	$^{88}\text{Sr}(n,\gamma)^{89}\text{Sr}$	$2 \times 10^{-2}$
Yttrium	$^{89}\text{Y}(n,\gamma)^{90}\text{Y}$	$2 \times 10^{-5}$
Zirconium	$^{94}\text{Zr}(n,\gamma)^{95}\text{Zr}$	$6 \times 10^{-3}$
	$^{96}\text{Zr}(n,\gamma)^{97}\text{Zr}$	$9 \times 10^{-3}$
Niobium	$^{93}\text{Nb}(n,\gamma)^{94\text{m}}\text{Nb}$	$3 \times 10^{-5}$
Molybdenum	$^{98}\text{Mo}(n,\gamma)^{99}\text{Mo}$	$3 \times 10^{-4}$
	$^{100}\text{Mo}(n,\gamma)^{101}\text{Mo}$	$1 \times 10^{-3}$
	$^{96}\text{Ru}(n,\gamma)^{97}\text{Ru}$	$2 \times 10^{-3}$
Ruthenium	$^{102}\text{Ru}(n,\gamma)^{103}\text{Ru}$	$2 \times 10^{-4}$
	$^{104}\text{Ru}(n,\gamma)^{105}\text{Ru}$	$2 \times 10^{-4}$
	$^{103}\text{Rh}(n,\gamma)^{104\text{m}}\text{Rh}$	$2 \times 10^{-6}$
Rhodium	$^{103}\text{Rh}(n,\gamma)^{104\text{m}}\text{Rh}$	$2 \times 10^{-6}$
	$^{108}\text{Pd}(n,\gamma)^{109}\text{Pd}$	$1 \times 10^{-5}$
	$^{110}\text{Pd}(n,\gamma)^{111}\text{Pd}$	$8 \times 10^{-4}$
Palladium	$^{110}\text{Pd}(n,\gamma)^{111}, ^{111\text{m}}\text{Pd} \xrightarrow{\beta^-} ^{111}\text{Ag}$	$7 \times 10^{-4}$
	$^{107}\text{Ag}(n,\gamma)^{108}\text{Ag}$	$1 \times 10^{-6}$
Silver	$^{107}\text{Ag}(n,\gamma)^{108}\text{Ag}$	$1 \times 10^{-6}$
	$^{109}\text{Ag}(n,\gamma)^{110\text{m}}\text{Ag}$	$2 \times 10^{-4}$

TABLE 1. Sensitivity for thermal neutron reactions—Continued

Element	Nuclear reaction	Sensitivity in micrograms
Cadmium	$^{114}\text{Cd}(n,\gamma)^{115\text{m}}\text{Cd}$	$2 \times 10^{-3}$
	$^{114}\text{Cd}(n,\gamma)^{115}\text{Cd}$	$1 \times 10^{-4}$
	$^{116}\text{Cd}(n,\gamma)^{117\text{m}}\text{Cd}$	$3 \times 10^{-4}$
Indium	$^{113}\text{In}(n,\gamma)^{114\text{m}}\text{In}$	$4 \times 10^{-5}$
	$^{113}\text{In}(n,\gamma)^{114}\text{In}$	$4 \times 10^{-4}$
	$^{115}\text{In}(n,\gamma)^{116\text{m}}\text{In}$	$2 \times 10^{-7}$
Tin	$^{120}\text{Sn}(n,\gamma)^{121}\text{Sn}$	$7 \times 10^{-4}$
	$^{122}\text{Sn}(n,\gamma)^{123}\text{Sn}$	$4 \times 10^{-3}$
	$^{124}\text{Sn}(n,\gamma)^{125\text{m}}\text{Sn}$	$3 \times 10^{-3}$
Antimony	$^{121}\text{Sb}(n,\gamma)^{122}\text{Sb}$	$9 \times 10^{-6}$
	$^{123}\text{Sb}(n,\gamma)^{124}\text{Sb}$	$1 \times 10^{-4}$
Tellurium	$^{126}\text{Te}(n,\gamma)^{127}\text{Te}$	$2 \times 10^{-4}$
	$^{128}\text{Te}(n,\gamma)^{129}\text{Te}$	$9 \times 10^{-4}$
	$^{130}\text{Te}(n,\gamma)^{131}\text{Te}$	$5 \times 10^{-4}$
	$^{130}\text{Te}(n,\gamma)^{131}\text{Te} \xrightarrow{\beta^-} ^{131}\text{I}$	$5 \times 10^{-4}$
Iodine	$^{127}\text{I}(n,\gamma)^{128}\text{I}$	$6 \times 10^{-6}$
Xenon	$^{132}\text{Xe}(n,\gamma)^{133}\text{Xe}$	$7 \times 10^{-4}$
	$^{134}\text{Xe}(n,\gamma)^{135}\text{Xe}$	$2 \times 10^{-3}$
Cesium	$^{133}\text{Cs}(n,\gamma)^{134\text{m}}\text{Cs}$	$2 \times 10^{-3}$
	$^{133}\text{Cs}(n,\gamma)^{134}\text{Cs}$	$5 \times 10^{-5}$
Barium	$^{130}\text{Ba}(n,\gamma)^{131}\text{Ba}$	$4 \times 10^{-3}$
	$^{136}\text{Ba}(n,\gamma)^{137\text{m}}\text{Ba}$	$2 \times 10^{-3}$
	$^{138}\text{Ba}(n,\gamma)^{139}\text{Ba}$	$1 \times 10^{-4}$
Lanthanum	$^{139}\text{La}(n,\gamma)^{140}\text{La}$	$5 \times 10^{-6}$
Cerium	$^{140}\text{Ce}(n,\gamma)^{141}\text{Ce}$	$3 \times 10^{-4}$
	$^{142}\text{Ce}(n,\gamma)^{143}\text{Ce}$	$4 \times 10^{-4}$
Praseodymium	$^{141}\text{Pr}(n,\gamma)^{142}\text{Pr}$	$4 \times 10^{-6}$
Neodymium	$^{146}\text{Nd}(n,\gamma)^{147}\text{Nd}$	$2 \times 10^{-4}$
	$^{148}\text{Nd}(n,\gamma)^{149}\text{Nd}$	$2 \times 10^{-4}$
	$^{150}\text{Nd}(n,\gamma)^{151}\text{Nd} \xrightarrow{\beta^-} ^{151}\text{Pm}$	$2 \times 10^{-4}$
Samarium	$^{152}\text{Sm}(n,\gamma)^{153}\text{Sm}$	$1 \times 10^{-6}$
	$^{154}\text{Sm}(n,\gamma)^{155}\text{Sm}$	$3 \times 10^{-5}$
Europium	$^{151}\text{Eu}(n,\gamma)^{152\text{m}}\text{Eu}$	$6 \times 10^{-8}$
	$^{153}\text{Eu}(n,\gamma)^{154}\text{Eu}$	$5 \times 10^{-5}$
Gadolinium	$^{158}\text{Gd}(n,\gamma)^{159}\text{Gd}$	$4 \times 10^{-5}$
	$^{160}\text{Gd}(n,\gamma)^{161}\text{Gd}$	$2 \times 10^{-4}$
	$^{160}\text{Gd}(n,\gamma)^{161}\text{Gd} \xrightarrow{\beta^-} ^{161}\text{Tb}$	$2 \times 10^{-4}$
Terbium	$^{159}\text{Tb}(n,\gamma)^{160}\text{Tb}$	$4 \times 10^{-6}$
Dysprosium	$^{164}\text{Dy}(n,\gamma)^{165\text{m}}\text{Dy}$	$3 \times 10^{-7}$
	$^{164}\text{Dy}(n,\gamma)^{165}\text{Dy}$	$8 \times 10^{-8}$

TABLE 1. Sensitivity for thermal neutron reactions—Continued

Element	Nuclear reaction	Sensitivity in micrograms
Holmium	$^{165}\text{Ho}(n,\gamma)^{166}\text{Ho}$	$7 \times 10^{-7}$
Erbium	$^{168}\text{Er}(n,\gamma)^{169}\text{Er}$	$1 \times 10^{-4}$
	$^{170}\text{Er}(n,\gamma)^{171}\text{Er}$	$3 \times 10^{-5}$
Thulium	$^{169}\text{Tm}(n,\gamma)^{170}\text{Tm}$	$2 \times 10^{-6}$
Ytterbium	$^{168}\text{Yb}(n,\gamma)^{169}\text{Yb}$	$6 \times 10^{-6}$
	$^{174}\text{Yb}(n,\gamma)^{175}\text{Yb}$	$2 \times 10^{-6}$
	$^{176}\text{Yb}(n,\gamma)^{177}\text{Yb}$	$7 \times 10^{-5}$
	$^{176}\text{Yb}(n,\gamma)^{177}\text{Yb} \xrightarrow{\beta^-} ^{177}\text{Lu}$	$7 \times 10^{-5}$
Lutecium	$^{175}\text{Lu}(n,\gamma)^{176\text{m}}\text{Lu}$	$1 \times 10^{-6}$
	$^{176}\text{Lu}(n,\gamma)^{177}\text{Lu}$	$5 \times 10^{-7}$
Hafnium	$^{174}\text{Hf}(n,\gamma)^{175}\text{Hf}$	$8 \times 10^{-5}$
	$^{180}\text{Hf}(n,\gamma)^{181}\text{Hf}$	$4 \times 10^{-5}$
Tantalum	$^{181}\text{Ta}(n,\gamma)^{182\text{m}}\text{Ta}$	$2 \times 10^{-3}$
	$^{181}\text{Ta}(n,\gamma)^{182}\text{Ta}$	$2 \times 10^{-5}$
Tungsten	$^{184}\text{W}(n,\gamma)^{185}\text{W}$	$3 \times 10^{-4}$
	$^{186}\text{W}(n,\gamma)^{187}\text{W}$	$5 \times 10^{-6}$
Rhenium	$^{185}\text{Re}(n,\gamma)^{186}\text{Re}$	$1 \times 10^{-6}$
	$^{187}\text{Re}(n,\gamma)^{188}\text{Re}$	$1 \times 10^{-6}$
Osmium	$^{190}\text{Os}(n,\gamma)^{191}, ^{191\text{m}}\text{Os}$	$3 \times 10^{-5}$
	$^{192}\text{Os}(n,\gamma)^{193}\text{Os}$	$8 \times 10^{-5}$
Iridium	$^{191}\text{Ir}(n,\gamma)^{192\text{m}}\text{Ir}$	$5 \times 10^{-7}$
	$^{191}\text{Ir}(n,\gamma)^{192}\text{Ir}$	$8 \times 10^{-7}$
	$^{193}\text{Ir}(n,\gamma)^{194}\text{Ir}$	$7 \times 10^{-7}$
Platinum	$^{196}\text{Pt}(n,\gamma)^{197}\text{Pt}$	$3 \times 10^{-4}$
	$^{198}\text{Pt}(n,\gamma)^{199}\text{Pt}$	$2 \times 10^{-4}$
	$^{198}\text{Pt}(n,\gamma)^{199}\text{Pt} \xrightarrow{\beta^-} ^{199}\text{Au}$	$2 \times 10^{-4}$
Gold	$^{197}\text{Au}(n,\gamma)^{198}\text{Au}$	$5 \times 10^{-7}$
Mercury	$^{196}\text{Hg}(n,\gamma)^{197}, ^{197\text{m}}\text{Hg}$	$2 \times 10^{-5}$
	$^{202}\text{Hg}(n,\gamma)^{203}\text{Hg}$	$1 \times 10^{-4}$
	$^{204}\text{Hg}(n,\gamma)^{205}\text{Hg}$	$2 \times 10^{-3}$
Thallium	$^{203}\text{Tl}(n,\gamma)^{204}\text{Tl}$	$1 \times 10^{-3}$
	$^{205}\text{Tl}(n,\gamma)^{206}\text{Tl}$	$8 \times 10^{-4}$
Lead	$^{208}\text{Pb}(n,\gamma)^{209}\text{Pb}$	0.2
Bismuth	$^{209}\text{Bi}(n,\gamma)^{210\text{m}}\text{Bi}$	$3 \times 10^{-3}$
Thorium	$^{232}\text{Th}(n,\gamma)^{233}\text{Th}$	$9 \times 10^{-6}$
	$^{232}\text{Th}(n,\gamma)^{233}\text{Th} \xrightarrow{\beta^-} ^{233}\text{Pa}$	$5 \times 10^{-6}$
Uranium	$^{238}\text{U}(n,\gamma)^{239}\text{U}$	$2 \times 10^{-5}$
	$^{238}\text{U}(n,\gamma)^{239}\text{U} \xrightarrow{\beta^-} ^{239}\text{Np}$	$2 \times 10^{-5}$

Now it may be asked why the Koch tables have been chosen to illustrate the sensitivities attainable by slow neutron activation rather than the more modest lists available in some other papers or books. The reason is that it is important in a conference of this kind that the *potential* of a method is made clear, provided that the *limitations* are too. A very great deal of the work published up to the present has been done using fluxes of  $10^{12}$  n cm<sup>-2</sup> sec<sup>-1</sup> i.e., where the attainable sensitivity for each element is lower by a factor of 100 than is given in Table 1. Broadly speaking, apart from a few special cases, such irradiations have been found extremely easy, indeed almost routine. Precautions needed to deal with the total radioactivity of a batch of samples have been minimal and it has been possible to irradiate most sample materials without trouble. So, generally, it can be said that Koch's sensitivities, reduced by a factor of 100, are currently regularly achieved or achievable except in special cases which include that involving very short lived nuclides (say half lives of less than a few minutes). There have been some successful examples of work in fluxes of  $10^{13}$  and  $10^{14}$  but it must be realised that with these higher fluxes there may be severe problems of handling the increased total activity of the irradiated sample, necessitating quite a different order of laboratory facility, at any rate for the preliminary stages following the irradiation. There will be problems too in the type of sample material and container which can be irradiated, but broadly speaking, there seems to be no reason why the sensitivities quoted by Koch should not be attainable except in those cases where short half lives are the limitation, where "self shielding" is significant (see for example Høghahl [2] and Kenna [3]) or where nuclear reactions interfere. These latter two possibilities have been clearly pointed out on many occasions. In particular any attempt to achieve high sensitivity by activation analysis for a trace impurity in a sample containing significant amounts of elements with atomic numbers very near to that of the trace impurity element (or containing fissile elements in the case of interfering fission radionuclides) *must* recognise the difficulty and make sure either that interference is insignificant or that steps are taken to overcome it. Where the interference is due to nuclear reactions induced by the fast neutron component then a knowledge of the variation of flux with neutron energy in the reactor, and of the cross sections involved, is necessary to make the calculation of the extent of interference (see for example Durham [4] and Roy and Hawton [5]). If such information is not available then measurement of the extent of interference may be made by irradiation of the sample shielded with cadmium. Often, such interference can be avoided by choice of irradiation position in the reactor, but this usually involves a lower available flux and hence lower sensitivity. In the case of secondary reactions such as  $^{74}\text{Ge}(n,\gamma)^{75}\text{Ge} \xrightarrow{\beta^-} ^{75}\text{As}$  leading to the production, from the matrix element, of the impurity element being determined,

then there is little if anything that can be done, other than accepting a lower sensitivity, except to make the best use of irradiation time. Ricci and Dyer [6] have provided graphs showing calculations of this kind of interference for a range of cases. Pre-irradiation concentration of the impurity is of course possible to avoid such difficulties and it may be that in the future this will be done on an increasing scale in these relatively few special cases, but it must be realised that this involves the forfeiture of *the* major advantage that activation analysis has over almost all other analytical techniques i.e., the avoidance of the "reagent blank".

With some types of reactor e.g., the TRIGA, it is possible to use *pulses* of about 30 milliseconds per pulse which give bursts of slow neutrons with peak flux of  $5 \times 10^{16}$ . Lukens, Yule and Guinn [7] have shown that this can be used to give increased sensitivity, in those cases where direct identification by gamma spectrometry is possible, for radionuclides of half life of less than about 1 minute.

At the other end of the scale laboratory neutron generators are now available with thermal neutron fluxes of  $10^8$  or maybe  $10^9$ . They may be of some value for *thermal* neutron activation in the trace field though sensitivity is clearly limited by the low flux. Nevertheless the combination of thermal neutron *and* fast neutron activation for the modest capital involved is very attractive and it would be very surprising if over the next few years most reasonably sized analytical departments did not consider installation of such a generator to be essential.

## 2. Fast Neutrons

Consideration was given earlier to the possible interferences in reactor thermal neutron activation analysis due to the fast neutron component. Clearly from this it can be seen that there is the possibility of utilising these fast neutrons in some cases for worthwhile purposes. Yule, Lukens, and Guinn [8] have investigated this possibility by determining the sensitivity of 35 elements with reactor fast neutrons. They conclude that for 6 elements (O, Si, P, Fe, Y, Pb) the sensitivity is greater using fast than thermal neutrons, and for 15 others it is only slightly less and may well therefore be superior in certain matrices.

The main interest in fast neutrons however stems from the original work of Coleman [9]. In particular the possibility of the non destructive determination of oxygen has led to a boom in the development and sale of commercial 14 MeV neutron generators. It may be argued that those generators at present available have usable fluxes too low to put this technique really into the "trace characterisation" category. Strain [10] gives a list of nuclear reactions and realistic lower limits of detection for short ( $\leq 10$  min) irradiations in a  $10^8$  flux of 14 MeV neutrons. Generally the sensitivity, defined as "based on spectral measurement at a level of twice background" is from a few tens to a few hundreds

of micrograms for the elements N, O, F, Al, Si, P, Cr, Mn, Cu, Y, Mo, and Nb. Nevertheless the use of samples of several grams puts the detection limits at a few to a few tens of ppm for the favourable elements and because the list includes several of the lighter elements which are difficult or impossible to determine using thermal neutrons, and give some difficulty with methods other than activation analysis, there has been tremendous interest in this area. There are available now several thorough compilations of gamma spectra, reactions involved and sensitivities achieved using neutron generators, one for example being that of Cuypers [11]. The fact that some of the nuclides produced, especially that from oxygen, have half lives of a few seconds only, has spurred designers to make available fast sample transport and rapid identification, measurement and read out of results for industrial use. Indeed some first class work has arisen on automatic computer coupled activation analysis, both for reactor and neutron generator irradiations at a number of laboratories particularly but not exclusively in the United States.

Further improvements in commercial neutron generators seem possible; the recent development of sealed tubes has given prospects of constant neutron flux over many hours and future developments in higher flux availability seem encouraging—all this well within the range of modern analytical instrument costs.

There has been relatively little work on choosing the energy of neutrons for irradiations aimed at improved selectivity, but in some cases this can be worthwhile. Steele [12] has shown some of the possibilities recently. It seems clear that while this approach is likely only to be used in a few cases, it is worth consideration where particular combinations of impurity element and matrix warrant it.

### 3. *Gamma Photons*

The pioneer work [13] and the continued eminence of the French workers in this field must be mentioned. Not too many establishments have available a betatron or linear accelerator giving, via bremsstrahlung, a high flux of high energy photons. Even fewer can have access to such machines for analytical purposes, but where this is possible then there is a rich reward in the availability of sensitive determinations especially of some light elements.

In general the threshold energy for the initiation of  $\gamma, n$  reactions, those used for much the largest part of work in this area, lies in the region 10–20 MeV for light nuclei falling steadily to 7–10 MeV for the heavier elements. Similarly the maximum cross sections occur for gamma energies falling from 20–25 MeV for light elements to about 15 MeV for others, with values ranging from a few millibarns to a few hundreds of millibarns [1, 14], so, with electron currents of up to 50  $\mu\text{A}$  available in some linear accelerators, it is possible to obtain sensitivities

for some elements well below the microgram level. Schweikert and Albert [15] and Baker [16] give sensitivity calculations and Table 2 is taken from Baker's paper. Again these sensitivities have been calculated for ideal systems free from interferences but are realistic when using a large linear accelerator under the following conditions:

Accelerator parameters	5 $\mu$ A, 30 MeV electron beam 1 mm tungsten radiator. Sample position 10 cm. behind radiator.
Irradiation time	One half life of induced nuclide or one hr., whichever is shorter.
Counting time	Immediately following irradiation, for one half life or one hour, whichever is shorter.
Counter	Well-type NaI crystal with discriminator set at 100 keV.
Limit of detection	Defined as that weight of an element which will give a count equal to twice the standard deviation on the background count, the latter being taken as 120 c/m.

If chemical separation is required before counting then of course the sensitivity must be halved for each half life delay. (Half lives of under 10 minutes are *underlined*.)

Albert [17] and Engelmann [18] have given details of much of their work which was concerned mainly with the determination of light element impurities in beryllium and other metals non-destructively i.e., using decay measurements only (the products of  $\gamma$ , n reactions decay mainly by positron emission). Carbon was however separated by combustion in oxygen followed by trapping out the carbon dioxide formed, for counting. Although Albert [17] mentions a chemical separation of nitrogen as ammonia, following gamma irradiation, Engelmann [19] in a later paper says for nitrogen "no separation with a good and reproducible yield has been found". Baker [16] at Harwell has used rapid radio-chemical separations for both carbon and oxygen. For carbon in metals, e.g., in molybdenum and in steels, a combustion and trapping method was used giving figures for steels in good agreement with published values down to 10 ppm and he quotes a limit of detection of better than 0.1  $\mu$ g. For carbon in ceramic materials such as MgO and CaO, a borax flux was used at 1250 °C in a stream of oxygen to evolve the carbon as dioxide. In this case however, due to the high oxygen content, there is interference from the reaction  $^{16}\text{O}(\gamma, n\alpha)^{11}\text{C}$  which can be eliminated by reducing the energy of the gamma photons used in the irradiation below the threshold value of 25.8 MeV, resulting in a rather poorer sensitivity but still better than 1  $\mu$ g. Baker has determined oxygen in matrices such as Fe and Mo which themselves give rise to short lived activities making it difficult to differentiate  $^{15}\text{O}$  by simple decay measurements. He used a separation based on vacuum fusion in an iron bath

TABLE 2. Sensitivity for gamma activation

Nuclide	Half life of $\gamma, n$ product	Limit of detection $\mu\text{g}$	Limit reported in literature
$^{12}\text{C}$	20.3m	0.01	0.01 $\mu\text{g}$ in Be 0.1 $\mu\text{g}$ chemical sep'n
$^{14}\text{N}$	10.05m	0.01	1 ppm in pure Be
$^{16}\text{O}$	2.1m	0.04	1 ppm in pure Be 1 $\mu\text{g}$ chemical sep'n
$^{19}\text{F}$	1.87h	0.05	
$^{20}\text{Ne}$	18s	0.3	
$^{23}\text{Na}$	2.6y	200	
$^{24}\text{Mg}$	12s	0.3	
$^{27}\text{Al}$	6.5s	0.2	
$^{28}\text{Si}$	4.2s	0.2	
$^{31}\text{P}$	2.6m	0.05	
$^{32}\text{S}$	2.6s	0.3	
$^{35}\text{Cl}$	32.4m	0.08	
$^{39}\text{K}$	7.7m	2.0	
$^{40}\text{Ca}$	0.9s	1.0	
$^{46}\text{Ti}$	3.1h	0.1	
$^{50}\text{Cr}$	42m	0.1	
$^{55}\text{Mn}$	278d	20	
$^{54}\text{Fe}$	8.4m	0.2	
$^{59}\text{Co}$	9h	0.02	
$^{58}\text{Ni}$	37h	0.2	
$^{63}\text{Cu}$	9.8m	0.001	
$^{64}\text{Zn}$	38m	0.01	
$^{75}\text{As}$	18d	2	
$^{79}\text{Br}$	6.4m	0.1	
$^{87}\text{Rb}$	18.7d	3	
$^{86}\text{Sr}$	70m	0.03	
$^{89}\text{Y}$	105d	7	
$^{90}\text{Zr}$	4.4m	0.01	0.1 $\mu\text{g}$ in Hf
$^{93}\text{Nb}$	10.2d	0.02	
$^{92}\text{Mo}$	15.5m	0.2	
$^{103}\text{Rh}$	210d	10	
$^{107}\text{Ag}$	24m	0.02	0.1 $\mu\text{g}$ in Bi
$^{113}\text{In}$	14.5m	2	
$^{123}\text{Sb}$	3.5m	0.02	
$^{127}\text{I}$	13d	0.4	1 $\mu\text{g}$
$^{181}\text{Ta}$	8.1h	0.01	
$^{197}\text{Au}$	9.5h	0.02	

in graphite at 2000 °C and subsequent purification of oxygen activity by passing the gas evolved through two copper oxide furnaces, one at 600 °C to oxidise CO to CO<sub>2</sub> without loss of radioactive oxygen, the second at 1100 °C retaining > 99% of the <sup>15</sup>O without contamination by <sup>14</sup>C or other activities. This separation can be carried out in 4 minutes with a limit of detection better than 1 μg.

There is no doubt that gamma photon activation is a very powerful complementary technique to reactor thermal neutron activation. While not having sensitivity quite as high for some elements it competes in several cases and excels in some vital ones such as carbon, oxygen, nitrogen and fluorine. While it has the disadvantage of producing mainly positron emitting nuclides, so that gamma spectrometry cannot be as useful as it is for neutron activation, there is, to offset this, the elimination of self shielding problems so that it becomes possible to measure impurities in high neutron absorption cross section matrices such as boron, tungsten, cadmium, hafnium, etc.

Perhaps the only other variety of gamma photon activation worth present mention in the context of trace characterisation is that instead of measuring induced radioactivity, the neutron product itself may be measured. This has usually only been done for the two  $\gamma, n$  reactions whose threshold energies are so low that the reactions can be effected by  $\gamma$  photons from radionuclides. Thus the  ${}^9\text{Be}(\gamma, n){}^8\text{Be}$  reaction with a threshold energy requirement of only 1.67 MeV has been made the basis for measuring quite small quantities of Be using <sup>124</sup>Sb or <sup>88</sup>Y as  $\gamma$  sources, and deuterium has similarly been determined using <sup>228</sup>Th or <sup>24</sup>Na as  $\gamma$  sources.

The use of the Mössbauer effect to give information on chemical structure, bonding, etc., might be classified under this general heading of gamma irradiation and absorption, but at this juncture it seems best to regard this as a promising technique for future development.

#### 4. Charged Particles

Historically, charged particles were second only to thermal neutrons in being used for activation analysis. The reason they appear as fourth in the order in this paper is because they have a major limitation and yet perhaps a benefit. This reason is that charged particles can penetrate only relatively short distances into matter. Activation therefore takes place only very near the surface of an irradiated sample. The benefit of this can be seen as an ability to analyse surfaces and if such layers can be removed mechanically or chemically, then that ability extends to the analysis of layers *through* a sample. The possibility of irradiating very small areas of a surface by a beam of charged particles also exists so that *location* of a trace element is in principle available. However, the high heat dissipation occurring if large beam currents are used may be a limitation.

Nevertheless a variety of charged particle methods has been developed, especially for light elements that cannot conveniently be determined by thermal neutrons. If low energy charged particles are used then the nuclear reactions occur mainly with the light elements, but as particle energies are increased the problems of nuclear interference become more acute. Standardisation is also complicated by variations in stopping power as the matrix composition alters.

Particle energies of 1 MeV or less can be obtained conveniently with a Cockcroft-Walton voltage multiplier; Van de Graaff generators provide higher energies (6 MeV for a single stage machine), while yet higher energies require multiple stage Van de Graaffs, cyclotrons or linear accelerators.

Until recently there has been little development of charged particle machines solely for analytical purposes, but Markowitz and Mahoney [20] have proposed a small cyclotron for  $^3\text{He}$  particles of 8 MeV, because they suggest that by using such particles very sensitive methods are available for a number of light elements. It has also been pointed out by Ricci [21] that if a 100  $\mu\text{A}$  beam of 10 MeV  $^3\text{He}$  ions impinges on a thick lithium, beryllium or boron target there would be available a neutron yield of from 2 to  $4 \times 10^{11}$  n/sec, comparable with that obtained from an ordinary neutron generator; and although the neutrons would not be monoenergetic, choice of target material could give some control over neutron energy and hence to some extent over the nuclear reactions with different elements involving those neutrons. Ricci makes the following conclusions about  $^3\text{He}$  activation: its advantage is that the detection limits for low atomic number elements, using a 100  $\mu\text{A}$  beam of up to 10 MeV  $^3\text{He}$  ions, lie in the range from parts per million to parts per thousand million; its disadvantage is that  $^3\text{He}$  reactions with several elements and with comparable sensitivities lead often to the same nuclide and thus interferences may be important in matrices containing two or more low atomic number elements.

Results of work on other charged particles are somewhat difficult to classify succinctly because of the variety of particles and energies involved but the same disadvantages noted for  $^3\text{He}$  are apparent. Engelmann in two papers [18, 22] gives a useful summary of the situation for light elements:

(1) Using a 10  $\mu\text{A}/\text{cm}^2$  beam of 44 MeV alpha particles the estimated sensitivities for *carbon* and *oxygen* are  $10^{-2}$  ppm and  $10^{-3}$  ppm with chemical separation of the  $^{11}\text{C}$  and  $^{18}\text{F}$  respectively.

(2)  $10^{-3}$  ppm of *nitrogen* or *boron* can be detected in any material after irradiation with protons in the 6–15 MeV range by separating  $^{11}\text{C}$ . *But* as  $^{11}\text{C}$  is the product of such an irradiation from both elements the method is non-specific and recourse must be made to using the different energy dependence of the two nuclear reactions involved. By reducing the proton energy to less than 5 MeV the process becomes

more selective for boron, which can be determined in materials containing  $N/B \leq 100$  but sensitivity is reduced by a factor 100, and of course penetration depth is reduced too. By increasing the energy to 20 MeV, nitrogen gives 3 times as much  $^{11}\text{C}$  as does an equal mass of boron.

(3) Non destructive determination of nitrogen and boron is possible in beryllium, silicon and tantalum, with sensitivity of 0.1–1 ppm for a 10  $\mu\text{A}$  beam (presumably with the same limitations as in (2) above).

Koch [1] lists values for sensitivity and the nuclear reactions involved for many elements but in view of the competing reactions mentioned above it hardly seems worthwhile quoting each one here.

Charged particles emitted as a result of reactor neutron irradiation can occasionally be used, for example the sequence  $^6\text{Li}(n,\alpha)^3\text{T}$ ,  $^{16}\text{O}(T,n)^{18}\text{F}$  has been used with moderate sensitivity for determination of oxygen by irradiation of the powdered sample mixed with a lithium compound. Other reactions are available [23] such as  $^{18}\text{O}(p,n)^{18}\text{F}$  for determination of  $^{18}\text{O}$  using recoil protons from hydrogen containing matrices or  $^{12}\text{C}(d,n)^{13}\text{N}$  for determination of deuterium in deuterated organic compounds.

In summary then the position on charged particle activation analysis is that high sensitivity, especially for light elements, is available, that the technique is especially useful for surfaces or thin layers (this may of course be a restriction, too) but that great care is needed to ensure specificity. For the future it seems that small cyclotrons may become available especially for  $^3\text{He}$  work, that variable energy cyclotrons with their high beam current and selective energy choice may play an increasingly important part, and that prospects of scanning by use of collimated beams are hopeful, especially in cases where prompt counting is possible.

### C. "PROMPT" RADIATION TECHNIQUES

There have been only sporadic attempts to measure the "prompt" radiation emitted with the sample in its irradiation position. Although this approach to activation analysis has the disadvantage that there is no opportunity for chemical separation before counting, nor even the possibility of etching to remove surface contaminants once the sample is in position, and requires a counting method of high specificity, nevertheless there are some potential advantages which make consideration of the general approach desirable.

Prompt techniques permit the radiation emitted during decay of very short lived excited nuclear states to be counted rather than of the radioactive nuclides of "finite" half life used in conventional activation analysis. As an example, if  $^{16}\text{O}$  (stable) is irradiated with low energy deuterons a d, p reaction forms  $^{17}\text{O}$ , also stable. But the  $^{17}\text{O}$  is formed

in an excited state which reaches the ground state by rapid emission of a 0.87 MeV gamma photon. These gamma photons, the so called "prompt radiation" can thus be counted during the irradiation and used as a measure of the  $^{16}\text{O}$  present in the irradiated sample. In principle the method is therefore faster than conventional activation analysis because the counting is done during the irradiation rather than after it. Again, the irradiation can be carried on as long as necessary to give a statistically useful count, saturation activity being reached almost immediately after the irradiation is started.

Using low energy charged particles with all their disadvantages (listed earlier) rather than penetrating radiations such as neutrons, in order to simplify the radiation measurement, Pierce [24, 25] has shown some of the possibilities for determining carbon, oxygen and boron using Van de Graaff and Cockcroft-Walton machines. For *carbon* he used (1) 1.5 MeV deuterons for the reaction  $^{12}\text{C}(\text{d}, \text{p})^{13}\text{C}$  measuring the 3.09 MeV gamma photons from the excited state of  $^{13}\text{C}$ , (2) 0.8 MeV protons for the reaction  $^{12}\text{C}(\text{p}, \gamma)^{13}\text{N}$  measuring the 2.3 MeV first excited-ground state gamma ray from  $^{13}\text{N}$  (and *not* using the radioactivity from decay of the 10 min half life  $^{13}\text{N} \xrightarrow{\beta^+} ^{13}\text{C}$ ) (3)  $^3\text{He}$  ions for the reaction  $^{12}\text{C}(^3\text{He}, \text{p})^{14}\text{N}$  measuring the 1.64 MeV gamma ray from excited  $^{14}\text{N}$ . All three approaches showed that determination of carbon in steel down to a few hundred ppm was feasible within a few minutes, the most convenient being the deuteron irradiation. Similar conclusions were reached for oxygen and boron and although the levels reached in any of these examples hardly qualify the technique to be included yet in the "trace characterisation" class, the future possibility exists of rapid, on stream measurement and, with modern high current accelerators, of improved sensitivity. In addition the possibility of scanning, mentioned earlier can now clearly be seen.

Prompt or 'capture' gammas have also been used from neutron irradiation and Greenwood and Read [26] Lussie and Brownlee [27] and Isenhour and Morrison [28] have discussed possibilities, the latter using a modulation technique with a fast chopper in a thermal neutron beam from a reactor. They also make sensitivity calculations for thermal neutrons, their conclusion being that while sensitivity by measuring prompt gammas is inherently better if the same neutron flux is used for each, where neutron beams are used with a consequent large drop in available flux then of course the prompt technique loses in proportion. Even here however, with a drop in flux of a factor of  $10^6$ , sensitivity for ten elements is as good as or better than that by delayed gamma ray activation analysis (B, Be, C, Cd, Fe, Gd, H, P, Nb, Ti).

#### D. RADIOCHEMICAL SEPARATIONS

In spite of the impression that is often given in some quarters that anyone now using radiochemical separations in activation analysis is

rather out of date, it remains a fact that in the majority of high sensitivity applications, such separations are still essential. Indeed as far ahead as can reasonably be predicted they will be needed, perhaps on a decreasing scale as improvements in resolution of detectors are developed.

Separation schemes can be very simple involving perhaps only the removal of much of the major activity component; alternatively, the separations can be made groupwise, and both such approaches are usually followed by gamma spectrometry to obtain final specific measurement of each individual nuclide. Occasionally and especially where the highest possible sensitivity is aimed for, or where nuclides concerned are pure beta emitters, really thorough radiochemical purity of each element is sought so that beta counting with its very low background, can be used. It is worth restating, in an era of heavy spending on instrumentation, that any analytical chemist wishing to get started in activation analysis can do so with an expenditure of only a few hundred pounds sterling, provided he is willing to do a little chemistry after his sample is irradiated.

Broadly speaking, it is now possible to devise a radiochemical procedure to separate any single element from any combination of others given adequate time. The series of monographs on the radiochemistry of the elements, issued by the U.S. National Academy of Sciences Sub-committee on Radiochemistry, is an excellent reference set for which all who use it are grateful to its various authors and especially to Wayne Meinke as chairman of the originating sub-committee. It would be quite impossible to condense usefully the wide range of available separation schemes, but there is still scope for ingenuity especially in finding rapid methods for use with short lived radionuclides. Separation of nuclides with half lives of a minute or two is fairly commonplace now, and perhaps the stumbling block to further advance is in the process of dissolution, especially of refractory materials; we are still searching for the universal solvent—and its container! Direct fluorination with subsequent gas phase separations may prove helpful, certainly there will have to be a move from the conventional methods of attack on materials; high temperatures and pressures with containment of vigorous reactions may be an approach. One recalls in the present surroundings the still very useful but unconventional procedure of Wichers, Schlecht and Gordon [29] for dissolution of refractory platinumiferous materials.

Automatic separation methods are now becoming available and it needs but little imagination to visualise the extension of automatic transfer, activation and counting, at present used nondestructively, to include a further step of automatic radiochemical separation provided the sample material can be dissolved fairly simply. Girardi [30] and Samsahl

[31] and others have already introduced automation into radiochemical separations elegantly and effectively.

### E. INSTRUMENTATION

This is but a brief picture of the position on detectors, analysers, computers, etc., used in the final stage of an analysis by activation, though mention might be made briefly of the use of computers to calculate optimum conditions for irradiation of a given sample too [32].

The most widely used detector in activation analysis is the sodium iodide crystal, on which is based gamma ray scintillation spectrometry with multichannel pulse height analysers, and there are available several compilations of spectra enabling identification of unknowns [e.g., 33]. The problem of identifying the components of a complex spectrum has led to the use of computers to make the best use of the data available and there are many reports on how this is best done [e.g., 34]. Suffice it to say that it has been the growth in these spectrometric techniques which over the past 10 years or so has led to the intensive use of nondestructive activation analysis, with very rapid turnover of samples for which the approach was feasible. So here again can be seen one of the advantages of activation analysis in some cases—that of *speed* of availability of results.

Over the last year or two there has arisen the possibility of very much improved *resolution* of individual peaks in the spectrum due to the replacement of the sodium iodide detector by the lithium drifted germanium detector. Whereas the former might have a resolution (defined as peak width at half maximum height divided by centre-peak energy) of say 7% for the 660 KeV gamma ray of  $^{137}\text{Cs}$  the recent developments in germanium detectors give possibilities of resolutions as good as 0.1%. This is having a dramatic effect in the field of activation analysis as might be expected and already examples of applications are appearing [35]. There seems to be no doubt that a great leap forward will occur in activation analysis exploiting the possibilities of these detectors comparable to that generated say 10–15 years ago in the move from simple  $\beta$  counting to sodium iodide scintillation spectrometry. But the present limitations of semi-conductor detectors must be recognised: (a) the detectors must be operated at liquid nitrogen temperature, (b) the volume of the detectors is rather limited and hence the efficiency of counting gamma rays is significantly less than with sodium iodide, particularly at higher energies (for example a 5 cm<sup>3</sup> detector had 1/100 the efficiency of a 3" × 3" NaI crystal at 200 KeV, 1/200th at 1 MeV and 1/500th at 5 MeV [35]), (c) distinctly improved electronics are needed for full utilisation. Higher sensitive volumes are however becoming increasingly available, for example 50 cm<sup>3</sup> detectors are now being used [36] with very much improved efficiencies, so that there is no doubt the new detectors will be extremely important.

The increased resolution leads to the desire to have a far greater number of channels available in the pulse-height analyser in order to make full use of all the information available. There seems in fact to be a trend away from pulse-height analysers to small computers with their greater versatility and decreasing comparative cost, the bigger computers then being used for complex programmes (as at present) using the information then obtained.

Coincidence techniques using sodium iodide counters continue to be of value in specific cases [37] and this of course will also apply to the semi-conductor detectors though there are several practical difficulties with the latter, not only that of low efficiency.

#### F. ACCURACY AND PRECISION

The main errors which can arise in activation analysis are those due to self shielding, unequal flux at sample and standard position, inaccurate counting procedures (e.g., differences in self scattering, self absorption, geometry between sample and standard), and of course counting statistics. Any experienced devotee of activation analysis knows that errors from these sources can be reduced to levels that are unimportant in most instances. Rather few papers are published however which demonstrate this fact; occasionally some papers demonstrate the reverse, upon which the experienced devotee usually considers he knows why. One reason for the paucity is the virtual absence of homogeneous "standard samples" in which the impurities occur at the desired low level and whose trace element content is known accurately. A generalisation might be attempted that where no special difficulties of competing nuclear reactions or self shielding occur, and where enough activity is finally available to make counting statistics reasonable, then in most cases the accuracy and the precision could be much better than  $\pm 10\%$ .

#### G. POSITION OF ACTIVATION ANALYSIS RELATIVE TO OTHER "TRACE CHARACTERISATION" METHODS

It is either brave or foolhardy to make comparisons of this kind on a general basis. So much depends on the type of material to be analysed, the individual elements to be determined etc. But if a large programme were to be postulated requiring the determination of forty or fifty trace impurities at levels of 10 ppm or less, each in a matrix say of some ceramic containing six major elements, what part would activation analysis play, assuming the analytical laboratory concerned had all available resources?

It would be very surprising if activation did not play some part. Almost certainly it would be used to *supplement* results on given elements from other techniques in an aim to provide a few samples whose impurity levels could really be said to be known. For a few elements

at *very* low levels activation and mass spectrometric isotope dilution might be the only two approaches with adequate sensitivity. But once good standards were available it might be thought that spark source mass spectrometry (or its successor) would take over the bulk of the determinations for routine use, leaving perhaps only a few which, perhaps because they were at levels too low for that technique, would be tackled regularly by activation analysis.

This opinion may cause surprise, but the conditions leading to it must be remembered. There will certainly be specific examples of materials and trace impurity requirements where automatic activation analysis of one kind or another will be the choice, but the method has competitors and this Conference is designed to make each one of us learn that that applies to every technique discussed.

### III. Analysis Using Radioactive Tracers

#### A. INTRODUCTION

The adoption of radioactive tracers to avoid the necessity for quantitative separations in conventional methods of analysis has been surprisingly slow. It seems inconceivable to the experienced radiochemist that someone trying, for example, to separate microgram quantities of elements such as molybdenum, niobium, tantalum, and tungsten prior to their determination by spectrophotometry or polarography, should not check on the efficiency of the separations involved by the very simple technique of adding a measured volume of a tracer to his starting solution and counting a measured volume of his final solution. The equipment needed costs very little, the tracer solutions are no more expensive than reagents and the laboratory facilities needed are no more complex than are required for such a conventional determination anyway. And for such a small investment, the return is complete insurance against losses of the particular element at all stages subsequent to the addition of the tracer.

Perhaps inorganic chemistry is too quantitative and every separation can be guaranteed. Even if that is so then the experience gained in using the general technique and equipment would surely be of value as a basis for further adventures into the use of radioactive tracers for *determining* elements or even for activation analysis.

It is all too common to find analytical laboratories pleading that they cannot use activation analysis because they have no reactor in the locality. Even though that excuse is becoming more difficult to use with the spread of reactors, very often it turns out that the same laboratories will not use radioactive tracers either, when such tracers are as readily available as normal reagents.

Methods using tracers for *determining* elements can be broadly divided into two types. One type uses a radioactive tracer of the element

to be determined (isotopic labelling), the other a tracer of a different element from that being determined (non isotopic labelling). Although many fancy names have been given to slight variations in each technique (perhaps the use of such fancy names has been one of the reasons for their relatively little use?), the broad principle is clear in each case. In isotopic labelling methods the principle is that if a fraction of the element to be determined can be isolated (that fraction being determined by measurement of radioactivity) and if the mass of the element in that fraction can then be determined either by some conventional measurement technique or by reacting with an equivalent amount of a reagent, then the original mass of the element can be calculated. (This is a complicated way of saying that a radioactive tracer is used to correct for an inefficient separation in a conventional determination!) There are some extensions of this broad approach designed to avoid the conventional measurement step and they will be dealt with later.

In non-isotopic labelling methods the principle is, simply, that provided the element to be determined can react in some quantitative manner with a known excess of a second material, the latter being labelled, and provided the fraction of the second material thus released can be measured via its radioactivity, then the original mass of the element can be calculated.

In addition to the two broad types just outlined there is a third approach which incorporates points from both types. This third approach is usually called "radiometric titration" and involves following the course of a titration either with a labelled titrand, a labelled titrant or a labelled indicator element. The measurement of the change of radioactivity within the system involves a phase separation.

McMillan [38] has recently written a very clear review of all these techniques, especially from the viewpoint of trace element determinations and his classification has been used in the remainder of this section.

## B. ISOTOPIC METHODS

All the methods in this class depend on the fact that the specific radioactivity of a given element is, by definition, inversely proportional to the concentration of the inactive element, and the various methods differ only in the manner of using that proportionality.

### 1. *Single Isotope Dilution*

The principle here is the simple one already mentioned in section A above and it seems a pity to complicate matters by explaining the principles mathematically.

On mixing a radioactive tracer element with its inactive isotopes, clearly the overall specific activity is reduced.

If the specific activity of the tracer is  $S_0$  and by definition

$$S_0 = \frac{A_0}{W_0} \quad (1)$$

where  $A_0$  is the radioactivity of a weight  $W_0$  of the tracer element, then if activity  $A_0$  is added to a sample material containing a weight  $W_x$  of that inactive element, the new specific activity will become

$$S_x = \frac{A_0}{W_0 + W_x} \quad (2)$$

Now  $S_x$  can be measured by recovering (and measuring) a pure fraction  $W_2$  of  $(W_0 + W_x)$  and measuring its activity  $A_2$

Then 
$$W_x = W_0 \left( \frac{S_0}{S_x} - 1 \right) \quad (3)$$

If  $W_0$  is small compared to  $W_x$

then 
$$W_x = W_2 \cdot \frac{A_0}{A_2} \quad (4)$$

In trace element analysis the main difficulty in applying this method is that of measuring  $W_2$ , (and as  $W_2$  is always smaller than  $W_x$ , one might ask in fact, is it not easier to measure  $W_x$  directly and cut out all this radioactivity nonsense? The answer is that one imagines that this method will only be used where *quantitative separations* are not readily possible).

It was to overcome this problem of measuring  $W_2$  at very low levels that the method known as Substoichiometric Radioactive Isotope Dilution Analysis was introduced.

## 2. Substoichiometric Isotope Dilution

In this method equal partial amounts of the element being determined are removed both from the tracer solution and from the tracer + sample solution. The radioactivity in each,  $A_0$  and  $A_x$  respectively, will be directly proportional to the respective specific activities, so that equation (3) may be rewritten

$$W_x = W_0 \left( \frac{A_0}{A_x} - 1 \right).$$

The problem then becomes one of removing exactly equal amounts of the element from two solutions of different composition, and possibly different volume and containing different amounts of the element. Ru-

zicka and Sary, in a series of papers, mainly in the journal *Talanta*, have used the principle of substoichiometry to solve that problem, i.e., they add equal *substoichiometric* quantities of a suitable reagent to each solution, that reagent then reacts stoichiometrically and the product of the reaction is separated from the unreacted element in each case. Ruzicka and Sary [39] concluded that only two types of reagent are suitable for this technique at the submicrogram level, the first type comprising those organic reagents forming complexes with high extraction constants and therefore easily separable from the unreacted element by solvent extraction, e.g. dithizone and cupferron; the second, those reagents forming complexes with high stability constants that are readily separable from unreacted elements by ion exchange, e.g., ethylene diamine tetraacetic acid.

Several elements including Cu, Hg, Ag, Zn, Fe, In, have been determined by methods such as these, usually in model experiments, some at levels as low as  $10^{-9}$  and  $10^{-10}$  g. With practical materials the question of interferences arises and selectivity must be obtained, e.g., by masking or preseparation.

Of course a major limitation in these methods is the reagent blank, a factor common to all analytical methods requiring the use of chemical reagents, except activation analysis. For example a recent paper on the use of substoichiometric isotope dilution to determine zinc in germanium dioxide mentions a reagent blank of 1  $\mu$ g zinc. But this difficulty though it must be recognised must not be allowed to obscure the possibilities of this quite promising method.

There have been additional variants on this substoichiometry theme, for example DeVoe and his colleagues [40, 41] have suggested "double radioactive isotope dilution" and "double substoichiometric isotope dilution" but for a discussion of these either the original papers or the review by McMillan [38] should be consulted. The same workers have suggested the use of differential controlled-potential coulometry in isotope dilution. Clearly the problems and possibilities are being given the broadest consideration by those workers and already some ingenious approaches are being studied.

### 3. Isotopic Exchange

Reactions of the following type are used in this method



and



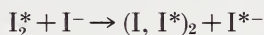
$MX$  and  $MY$  must be easily separable for example by solvent extraction, and the most strongly complexing ligand must be associated stoichiometrically with one portion of  $M$  prior to exchange.

If the amount of  $M$  associated with  $Y$ ,  $[M]_y$  is unknown and that with  $X$ ,  $[M]_x$  is known, then

$$[M]_y = \frac{[M]_x}{(D_{m^*})_s}$$

where  $(D_{m^*})_s$  is the distribution of  $M^*$  between the organic solvent and the aqueous phase assuming  $MX$  is the extractable species.

To illustrate the method the example of the determination of iodine in natural waters may be quoted [42]. Iodine tracer is added to the water and after conversion of all forms of iodine to elemental iodine, an extraction into benzene is made. (The fact that up to this stage recovery need not be quantitative as any loss can be corrected for by determining the tracer yield at this point is incidental). The iodine in the benzene is then allowed to exchange with a known amount of iodide in aqueous solution:—



The quantity of iodine originally present in the water sample can then be evaluated from the distribution of the tracer together with the weight of iodide used. At least 1  $\mu\text{g}$  iodine/litre of water can be determined by this method. Perhaps it is worth saying at this point that iodine is a tricky element for isotopic methods because of its rather complex chemistry, and it must be clearly understood that in these methods, for determining elements, before any separations are made, *all* the element including that in the tracer must be in the same chemical form.

The remarks made earlier in section 2 about sensitivity attainable and reagent blank limitations apply equally to this method.

### C. NON-ISOTOPIC METHODS

These methods depend on the fact that the mass of an element is related to the activity derived on its reaction with a labeled reagent. In fact the group of methods is sometimes called "Radioreagent Techniques".

#### 1. *Isotope Derivative and Derivative Dilution*

Here, the element to be determined is made to react quantitatively with a labelled reagent of known specific activity to form a compound which can be separated and counted. If the recovery is quantitative then the amount of the element being determined,

$$W_x = \frac{A_x}{S_r} \cdot E \cdot$$

where  $A_x$  = activity of compound formed

$S_r$  = specific activity of labelled reagent

and  $E$  = ratio of equivalent weights of the element and the reagent.

For this method to be successful there are two requirements; first to ensure that the reaction is quantitative by choosing the proper reagent and conditions; second to recover the radioactive compound in a known yield. This latter may be done in any of three ways,

- (1) by making the separation completely quantitative
- (2) by adding carrier quantities of inactive product and correcting for loss on the basis of chemical yield
- (3) by adding a quantity of product labelled with a *different* tracer and correcting for losses radiometrically.

The distinction between "isotope derivative" and "derivative dilution" methods is that the former uses only (1) above while the latter, which has been used exclusively in organic analysis so far, uses (1), (2), and (3).

Some quite sensitive applications of the isotope derivative method have been reported, especially in combination with paper chromatography. Welford [43] has briefly reported separation and determination of less than 0.01  $\mu\text{g}$  of Pb, Ca, Sr, and Ba using S-35 labelled sulphate as a spraying reagent, and less than 0.001  $\mu\text{g}$  Be and Zr using  $^{32}\text{P}$ -labelled phosphate. Location of the individual elements on the chromatogram before spraying with labelled reagent was done very neatly by using two separate sample aliquots to one of which radioactive tracers for each element had been added and then running the two chromatograms side by side. Welford makes the statement that all elements which can be isolated chromatographically can be determined at these low sensitivity levels, so the potential is clear. Though still subject to reagent blank problems the technique has such simplicity that it seems possible these may be reasonably controlled.

### 2. Isotope Displacement

This technique uses the differences in stability constants of the complexes of a series of different elements with an organic reagent. Thus an unknown amount of an element forming a complex of high stability with a particular reagent will release a proportionate amount of activity from a labelled complex of that reagent of lower stability. Provided that the released activity can be separated from that remaining as the complex, then the amount of either can be used as a measure of the mass of the displacing element.

An example is the determination of as little as 0.1  $\mu\text{g}$  of mercury by displacement of silver-110m from its di-*n*-butyl phosphorothioate complex [44]. The same paper also describes the use of an isotopic exchange method for mercury, using the same reagent, this time labelled with Hg-203 and makes some interesting observations in a comparison of the two methods, each having its advantages and disadvantages.

### 3. Radiorelease

Methods based on this technique depend on the release of a radioactive species from a labelled material when this reacts chemically with the

trace element and may or may not be isotopic with the material carrying the label. The trace element may react directly or indirectly to release the radioactivity. Of course the reaction which does occur must be highly selective and sensitivity is achieved by using a high specific activity tracer.

The technique has been used mainly for trace elements in water and in gases.

Examples in the water field are the determination of added inactive vanadate or dichromate in water tracing work, but could be applied generally to the elements vanadium or chromium. Silver labelled with  $^{110\text{m}}\text{Ag}$  reacts in acid solution with vanadate [45] or dichromate [46] to release silver ions, the reaction is stoichiometric and the released activity is readily measured. Clearly the reaction is not specific, although for these water tracing purposes, masking of naturally occurring interferences such as chloride and iron was possible. Sensitivities of  $0.1 \mu\text{g/ml}$  and  $0.01 \mu\text{g/ml}$  for vanadate and dichromate respectively were reached.

A similar example though to a direct problem, is the measurement of dissolved oxygen in water by reaction with labelled thallium where very high sensitivity is potentially available.

The gas analysis methods usually rely on the release of krypton-85 from a clathrate compound, or from the surface of a material such as copper which has had krypton-85 implanted or diffused into it.

These methods are all highly sensitive but not usually specific. However in simple cases they are very useful and have the advantage that they can readily be adapted to automatic operation.

#### D. RADIOMETRIC TITRATION

This method, as explained earlier, spans both the isotopic and non-isotopic methods and depends on using changes in radioactivity within the system to follow the course of a titration. A labelled titrand, titrant or indicator may be used; in fact more than one species may be titrated and more than one titrant used, with, perhaps, different tracers being employed for the different stages. Measurement of the activity requires a phase separation such as precipitation or solvent extraction, though the former is hardly applicable to trace element analysis. Using chelate extraction, cobalt and zinc have been determined at  $0.1 \mu\text{g}$  levels but in general the method has not played a very important role.

#### E. ASSESSMENT OF RADIOACTIVE TRACER METHODS

It seems inevitable in trying to assess the "state of the art" in tracer methods that there should be comparison with activation analysis. The freedom from reagent blanks makes the very high theoretical sensitivity of activation analysis readily attainable on a practical basis in straight-

forward cases, and it would usually be the preferred method assuming availability of irradiation facilities.

Nevertheless there are perhaps two broad reasons for the continued interest in tracer methods. One is that tracer methods offer a real alternative in cases where activation analysis runs into difficulty. For example activation analysis may be unsuitable where sensitivity is very low either because the cross section involved is low or the induced activity is of very short or very long half life; or where the bulk material of the sample has such a high cross section that severe self shielding would occur; where the overall radioactivity of the irradiated sample is too high for the facilities available; or where interfering nuclear reactions prove limiting. The other reason is that tracer methods are very simple in practice, and require only low cost equipment usually. In fact this has led to the applications in automatic instrumentation as mentioned earlier. So it could be predicted that most analytical laboratories should take up these tracer methods if only as an introduction to radioactivity. Once confidence had been gained then the laboratory personnel would be able to make a balanced judgement as to when to proceed to the further investment needed for activation analysis.

#### F. AVOIDANCE OF ANALYSIS BY MEANS OF TRACERS

Many requests for analysis arise from research in other departments involving processing operations, for example purification of a commercial starting material to produce a high quality product. Usually the starting material and the product are submitted to the analytical department for analysis for the trace impurity elements of interest, in order to measure the extent of the success of the purification. Analysis of the impure starting material is usually fairly easy because of the relatively high level of the impurities, whereas the product analysis may be much more difficult. If radioactive tracers had been added to the starting material then with a knowledge of the impurity levels in that material, some very simple radiochemistry or even direct gamma spectrometry could make very easy the measurement of the remaining fraction of each tracer and hence of the fraction of each remaining individual impurity.

Far too little use is made of this approach to trace element problems. While "avoidance of analysis" may be too strong a term, certainly "simplification of analysis" is justified in such cases. Of course, not all trace element analysis can be dealt with in this manner, and there is still need for development of any technique of high sensitivity analysis. But surely the analytical laboratory should lead the way in using these tracer techniques and prove to their colleagues in other parts of the research department that collaboration *before* the request for analysis would be mutually beneficial.

#### IV. Concluding Remarks

This paper does not claim to be comprehensive. There are recognised omissions, for example no mention is made of scattering techniques nor of the use of radioactive nuclides for X-ray fluorescence spectrometry. There may well be unrecognised omissions, if so then perhaps these will be pointed out during the subsequent discussion. But at least it may be said by one with a third of a century's experience in analytical chemistry including a quarter of a century's experience in radioactivity, that nuclear methods are right in the forefront in solving problems of trace characterisation. There seems no reason to doubt that they will continue to be so, as far ahead as can be predicted. There are exciting possibilities—the analytical chemist must be among the leaders in exploiting them.

#### V. Acknowledgments

The author acknowledges with humility and gratitude the contributions made by his colleagues. He has had the benefit of seeing a recent review of parts of the field by R. F. Coleman and T. B. Pierce [47] as well as those by C. A. Baker and by J. W. McMillan already referred to. He has benefited much by discussions with D. Mapper, T. B. Pierce, R. K. Webster, C. A. Baker, and others.

#### VI. References

- [1] Koch, R. C., *Activation Analysis Handbook*, Academic Press, New York and London, 1960.
- [2] Høgdahl, O. T., *Radiochemical Methods of Analysis*; I.A.E.A. Vienna, 1965. Vol. 1, p. 23.
- [3] Kenna, B. T., and Van Domelen, B. H., *Inter. J. App. Rad. & Isot.* **17**, 47, (1965).
- [4] Durham, R. W., Navalkar, M. P., and Ricci, E., *Proc. Int. Conf. Modern Trends in Activation Analysis*, A. & M. College of Texas, College Station, 1961, p. 67.
- [5] Roy, J. C., and Hawton, J. J., *Atomic Energy of Canada Ltd.*, Report AECL-1181. Dec. 1960.
- [6] Ricci, E., and Dyer, F. F., *Nucleonics* **15**, 447 (1964).
- [7] Lukens, H. R., Yule, H. P., and Guinn, V. P., *Nucl. Inst. & Methods* **33**, 273 (1965).
- [8] Yule, H. P., Lukens, H. R., and Guinn, V. P., *Nucl. Inst. & Methods* **33**, 277 (1965).
- [9] Coleman, R. F., *Analyst* **86**, 39 (1961); **87**, 590 (1962).
- [10] Strain, J. E., in *Guide to Activation Analysis*, W. S. Lyon, Jr., Ed. D. Van Nostrand Co. Inc., New York, 1964, p. 43.
- [11] Cuypers, M., and Cuypers, J., *Gamma-Ray Spectra and Sensitivities for 14 MeV Neutron Activation Analysis*, Texas A & M University, College Station, April 12, 1966.
- [12] Steele, E. L., *Proc. Int. Conf. Modern Trends in Activation Analysis*, Texas A & M University, College Station, 1965, p. 102.
- [13] Basile, R., Hure, J., Leveque, P., and Schuhl, A., *Compt. Rend.* **239**, 422 (1954).
- [14] Strauch, K., *Ann. Rev. Nucl. Sci.* **2**, 105 (1953).
- [15] Schweikert, E., and Albert, P., *Radiochemical Methods of Analysis*, I.A.E.A., Vienna 1965, **1**, 323.
- [16] Baker, C. A., *A.E.R.E. Report R 5265*, 1966.

- [17] Albert, P., Proc. Int. Conf. Modern Trends in Activation Analysis, A & M College of Texas, College Station, 1961, p. 78.
- [18] Engelmann, C., Proceedings Salzburg Conference 1964, I.A.E.A., p. 341.
- [19] Engelmann, C., Cabane, G., Proc. Int. Conf. Modern Trends in Activation Analysis, Texas A & M University, College Station, 1965, p. 331.
- [20] Markowitz, S. S., and Mahoney, J. D., Anal. Chem. **34**, 329 (1962).
- [21] Ricci, E., Proc. Int. Conf. Modern Trends in Activation Analysis, Texas A & M University, College Station, 1965, p. 200.
- [22] Engelmann, C., Radiochemical Methods of Analysis, I.A.E.A. Vienna, 1965, **1**, 405.
- [23] Aumann, D. C., and Born, H. J., Inter. J. App. Rad. Isotopes **16**, 727 (1965).
- [24] Pierce, T. B., and Peck, P. F., Proc. S.A.C. Conference, Nottingham, 1965, p. 159. W. Heffer & Sons Ltd., Cambridge, England.
- [25] Pierce, T. B., 1st Int. Meeting on Practical Aspects of Activation Analysis with Charged Particles, Grenoble, June 1965.
- [26] Greenwood, R. C., and Reed, J., Proc. Int. Conf. Modern Trends in Activation Analysis, A & M College of Texas, College Station, 1961, p. 166.
- [27] Lussie, W. G., and Brownlee, J. L., Jr., Proc. Int. Conf. Modern Trends in Activation Analysis, Texas A & M University, College Station, 1965, p. 194.
- [28] Morrison, G. H., and Isenhour, T. L., Anal. Chem. **38**, 164, 167 (1966).
- [29] Wichers, E., Schlecht, W. G., and Gordon, C. L., J. Res. Nat. Bur. Std., **33**, 363, 451, 457 (1944).
- [30] Girardi, F., Proc. Int. Conf. Modern Trends in Activation Analysis, Texas A & M University, College Station, 1965, p. 337.
- [31] Samsahl, K., Aktiebolaget Atomenergi Reports AE 159 (1964), AE 215 (1966).
- [32] Isenhour, T. L., Evans, C. A., and Morrison, G. H., Proc. Int. Conf. Modern Trends in Activation Analysis, Texas A & M University, College Station, 1965, p. 123.
- [33] Heath, R. L., Gamma-Ray Spectrum Catalogue 2d Ed., IDO 16880-1; U.S.A.E.C., 1964.
- [34] O'Kelley, G. D. (Ed.) Applications of Computers to Nuclear and Radiochemistry, NAS-NS 3107, U.S.A.E.C., 1962.
- [35] Prussin, S. G., Harris, J. A., and Hollander, J. M., Proc. Int. Conf. Modern Trends in Activation Analysis, Texas A & M University, College Station, 1965, p. 357.
- [36] Glos, M. B., Nucleonics **24**, (5), 44, 1966.
- [37] Reed, W. P., and DeVoe, J. R., N.B.S. Tech. Note 276, p. 52 (1966).
- [38] McMillan, J. W., A.E.R.E. Report R. 5266 (1966).
- [39] Ruzicka, J., and Sary, J., Atomic Energy Review, **2**, (4), 3 (1964).
- [40] Landgrebe, A. R., McClendon, L. T., and DeVoe, J. R., N.B.S. Tech. Note 248, p. 10, 1964.
- [41] Landgrebe, A. R., McClendon, L. T., and DeVoe, J. R., N.B.S. Tech. Note 276, p. 124, 1966.
- [42] Richter, H. G., Anal. Chem. **38**, 772, 1966.
- [43] Welford, G. A., Chiotis, E. L., and Morse, R. S., Anal. Chem. **36**, 2350, 1964.
- [44] Handley, T. H., Anal. Chem. **36**, 153, 1964.
- [45] Gillespie, A. S., and Richter, H. G., Anal. Chem. **36**, 2473, 1964.
- [46] Richter, H. G., and Gillespie, A. S., Anal. Chem. **37**, 1146, 1965.
- [47] Coleman, R. F., and Pierce, T. B., The Analyst, in press.

# NUCLEAR METHODS

## Contributed Papers and Discussion

VINCENT P. GUINN

*General Atomic Division, General Dynamics Corporation  
San Diego, California 92112*

Although nuclear methods of trace analysis other than activation analysis methods are also included in the scope of this program on nuclear methods—and are represented by a number of interesting contributed papers—this discussion will be largely limited to the subject of activation analysis methods. This narrowness of presentation is not due to the author's lack of interest in, or lack of appreciation of, the other nuclear methods—nor entirely to his ignorance of such methods—but rather is due to the fact that the activation analysis methods are much broader in their range of applicability.

The general theory and nature of activation analysis have been admirably treated by A. A. Smales—in his “state-of-the-art” paper at this Symposium—so need little further discussion by the present author. Instead, this author will present some additional remarks to fill in small gaps, reemphasize certain especially important points, and make a few comments concerning some of the contributed papers on activation analysis. He will also draw upon some developments in this field reported in the recent literature, and upon some of the recent work of his colleagues in the activation analysis group at the laboratories of General Atomic.

### 1. Neutron Activation Analysis

#### A. THERMAL-NEUTRON

Thermal-neutron activation analysis is the most fully developed and most widely applicable form of the activation analysis method. For most elements, it is the most sensitive form. The great bulk of the published literature in the field is concerned with this form of the method. Smales has pointed out above the tremendous sensitivity attainable for some 75 elements of the periodic system, if a very high ( $10^{14}$  n/cm<sup>2</sup>-sec) thermal-neutron flux is used, and if very long (30-day) irradiations are employed—for the longer-lived induced activities. Under such rather extreme conditions, he indicates defined limits of interference-free detection ranging from as low as  $6 \times 10^{-8}$   $\mu$ g (Eu)

to as high as  $0.2 \mu\text{g}$  (excluding the very insensitive elements, hydrogen, beryllium, and carbon). The median limit of detection for these  $\sim 75$  elements is approximately  $10^{-5} \mu\text{g}$ . This is obviously an ultra-sensitive method of elemental analysis, under these conditions, but these are indeed heroic conditions!

What about the limits of detection that are more usually attainable—in many laboratories around the world—employing a nuclear-reactor thermal-neutron flux of  $10^{13} \text{ n/cm}^2\text{-sec}$  and more reasonable irradiation periods (one or a few hours maximum, rather than 30 days)? As shown in Table 1, even with a flux of  $10^{13}$  and a maximum irradiation period of one hour, excellent sensitivities are still attainable: ranging from about  $10^{-7} \mu\text{g}$  (Dy) up to about  $10 \mu\text{g}$  (Fe), with a median limit of detection of about  $10^{-3} \mu\text{g}$  (these limits are defined in a way slightly different from those of Smales—namely, they are those defined by Buchanan [1].<sup>1</sup> Thus, even with more common and practical conditions of irradiation, excellent sensitivities are still attainable for most elements—and without some of the complications that set in when very high fluxes and very long irradiations are employed (such as extensive sample radiolysis and decomposition, appreciable recoil effects, container problems, excessive sample heating, etc.). In the author's laboratory three reactors are used for neutron activation analysis (NAA) work at thermal-neutron fluxes of from  $2 \times 10^{12}$  to  $2 \times 10^{13} \text{ n/cm}^2\text{-sec}$ .

A wide range of sample sizes can be accommodated by this method, namely, from micrograms to tens of grams. The use of large samples, if available, is very helpful in improving the concentration limits of detection and also in improving the representativeness of sampling—if the sample material is quite heterogeneous. The limits of detection cited in Table 1 can be achieved for many of the elements shown purely instrumentally (nondestructively)—if the matrix is fairly simple, from the neutron activation analysis standpoint (i.e., matrices such as water, organic compounds, Be, C, etc.), or if the major induced activities, because of their half lives or radiation energies, do not interfere with the gamma-ray detection of the trace-element activity of interest. Even where mild or severe interfering activities are encountered, they can be removed by radiochemical separations with carriers and hold-back carriers—thus still enabling one to attain the limits of detection shown. Normally, one employs the purely-instrumental method, based upon multichannel gamma-ray spectrometry, for the simple reason that it requires less of a chemist's time than the more tedious radiochemical-separation procedure. However, if the one technique will not work satisfactorily, the other almost certainly will. In neither form of the method (instrumental or radiochemical) is there any blank correction—the bane of many other methods for micro-level or micro-concentration analysis.

<sup>1</sup> Figures in brackets indicate the literature references at the end of this paper.

TABLE 1. Interference-free limits of detection for 75 elements by neutron activation analysis at a thermal-neutron flux of  $10^{13}$  n/cm<sup>2</sup>-sec (for 1 hour maximum).

Median sensitivity = 0.001  $\mu$ g

Limit of Detection, Micrograms	Elements
$1-3 \times 10^{-7}$	Dy
$4-9 \times 10^{-7}$	Eu
$1-3 \times 10^{-6}$	
$4-9 \times 10^{-6}$	Mn, In, Lu
$1-3 \times 10^{-5}$	Co, Rh, Ir
$4-9 \times 10^{-5}$	Br, Sm, Ho, Re, Au
$1-3 \times 10^{-4}$	Ar, V, Cu, Ga, As, Pd, Ag, I, Pr, W
$4-9 \times 10^{-4}$	Na, Ge, Sr, Nb, Sb, Cs, La, Er, Yb, U
$1-3 \times 10^{-3}$	Al, Cl, K, Sc, Se, Kr, Y, Ru, Gd, Tm, Hg
$4-9 \times 10^{-3}$	Si, Ni, Rb, Cd, Te, Ba, Tb, Hf, Ta, Os, Pt, Th
$1-3 \times 10^{-2}$	P, Ti, Zn, Mo, Sn, Xe, Ce, Nd
$4-9 \times 10^{-2}$	Mg, Ca, Tl, Bi
$1-3 \times 10^{-1}$	F, Cr, Zr
$4-9 \times 10^{-1}$	Ne
1-3	S, Pb
4-9	Fe

Many of the potential sources of error in thermal-neutron activation analysis are discussed very clearly by G. W. Smith, D. A. Becker, G. J. Lutz, L. A. Currie, and J. R. DeVoe (all of the National Bureau of Standards), in their Symposium paper on the determination of trace elements in standard reference materials by NAA. These possible sources of error are well known, and can all be minimized to essentially negligible levels, but they certainly must be recognized by the analyst who is endeavoring to carry out NAA to obtain absolute accuracies of the order of  $\pm 1\%$  of the value.

The paper at this Symposium by J. Blouri, T. Chaudron, and P. Albert (of the Centre d'Etudes de Chimie Métallurgique, Vitry, France), on the NAA determination of traces of sulfur and several metals (especially Fe, Na, Mn, and Zn) in zone-refined carbazole, is an excellent example of a combined attack on a difficult problem—employing both the instrumental and the radiochemical-separation forms of the NAA method.

Smales has referred to the reactor-pulsing NAA studies carried out at General Atomic. Earlier studies [2] showed that the sensitivity enhancement attainable in a 1,000-megawatt pulse, compared to saturation irradiation at the usual 250-kilowatt level of operation of the TRIGA Mark I research reactor (shown in Figure 1) is equal to  $70/T$ , where  $T$  is the half life of the induced activity (thermal-neutron or fast-neutron),



Figure 1. View of the core of a modern research-type nuclear reactor. TRIGA Mark I Reactor, General Atomic, San Diego.

in seconds. Thus, sensitivity improvements of 700-fold, 70-fold, and 7-fold should be attainable for elements with induced activities having half lives of, respectively, 0.1 second, 1 second, and 10 seconds. A new pneumatic tube, with a transit time, from reactor core to counter, of 0.1 second, has now been installed and is in use. Several quite practical applications of this sensitivity enhancement via reactor pulses have now been developed in the author's laboratory, particularly by H. R. Lukens.

#### B. FAST-NEUTRON

As mentioned already by Smales and others, some elements can be more sensitively detected, or more conveniently detected, by activation with fast neutrons than with thermal neutrons. Some common elements that fall into this category, for example, are the elements nitrogen, oxygen, silicon, phosphorus, chromium, and iron. In particular, oxygen is now determined in many laboratories by activation with 14-MeV neutrons, to form 7.35-sec  $^{16}\text{N}$  via the  $^{16}\text{O}(n, p)^{16}\text{N}$  reaction. The gamma radiation emitted by  $^{16}\text{N}$  is exceptionally high in energy (mostly 6.13 MeV, with a little at 7.13 MeV), so there are essentially no interferences (if, however, fluorine is present to an appreciable extent, a correction must be applied—since it also forms  $^{16}\text{N}$ , via the  $^{19}\text{F}(n, \alpha)^{16}\text{N}$  reaction).

It has been shown [3], that the large fast-neutron (fission-spectrum) flux that is present in the core of a nuclear reactor can be used to advantage in fast-neutron activation analysis. The principal difficulty, however, is that the activation of other elements in the sample by the very high thermal-neutron flux also present may greatly complicate the detection of fast-neutron products, especially instrumentally. Shielding the sample with cadmium or boron during the irradiation, as is well known, reduces the extent of  $(n, \gamma)$  activation by the thermal and epithermal neutrons (while not affecting the fast-neutron activation), but often not sufficiently. Thus, at least in many instances, one prefers to use an accelerator as a pure source of fast neutrons for such work.

The usual small accelerator source is a 100–200 keV Cockcroft-Walton deuteron accelerator. Using a water-cooled metallic tritium target (1–10 curies) and a  $D^+$  beam current of 1–2 milliamperes, a fresh target will isotropically produce  $\sim 2 \times 10^{11}$  neutrons per second. These neutrons are formed by the highly exoergic  $^3\text{H}(d, n)^4\text{He}$  reaction, and have energies of about 14 MeV. Thus, a tiny sample placed very close to the target can be exposed for a short time to a 14 MeV neutron flux of about  $10^{10}$  n/cm<sup>2</sup>-sec; larger samples to an average flux of about  $10^9$  n/cm<sup>2</sup>-sec. Thus, the limits of detection published by Strain (and referred to by Smales) may be overly conservative, since they are only for a flux of  $10^8$  n/cm<sup>2</sup>-sec. His 10-minute maximum irradiation period is certainly reasonable, in view of the rapid decline in neutron output of the tritium targets at high deuteron beam currents.

In the General Atomic Laboratory, three high-output 14-MeV neutron generators are used for fast-neutron activation analysis work. One is set up as an automated system for routine high-sensitivity oxygen determinations. It employs an automatic sample input loading rack, dual pneumatic tubes (for sample and standard), a spinning device (to spin sample and standard during irradiation), a pair of 5-inch  $\times$  5-inch NaI(Tl) detectors for the activated sample, and a single 3-inch  $\times$  3-inch NaI(Tl) detector for the activated standard—cross-calibrated with the sample detector system. Total analysis time on this system, for oxygen, is less than one minute. The limit of detection for oxygen, with a fresh target, is about 10  $\mu\text{g}$ , i.e., 10 ppm in a 1 g sample, or 1 ppm in a 10 g sample. At levels well above the limit of detection, precisions and absolute accuracies of about  $\pm 1$ –2% of the value are attained. On this system, many thousands of samples (many kinds of metals, organic materials, etc.) are analyzed per year for oxygen.

The paper by K. Perry, G. Aude, and J. Laverlochere (of the Centre d'Etudes Nucléaires, Grenoble, France) at this Symposium represents an interesting assessment of the capabilities of a 14-MeV neutron generator that is not so familiar to U.S. workers, namely, that of a French accelerator that can accelerate deuterons up to energies of 400 keV,

at beam currents up to 2 milliamperes. Their neutron-output measurements at deuteron energies of 150, 250, and 350 keV show relative outputs of about 1, 3, and 7—showing the advantage of having a somewhat higher-energy machine to work with. Of course, there is the disadvantage that, in general, the higher the energy of the accelerator, the more it costs. They report measurements on the determination, with this accelerator, of oxygen, fluorine, and boron with various detector systems (boron via the  $^{11}\text{B}(n, p)^{11}\text{Be}$  reaction). Beryllium-11 has a half life of 13.6 seconds.

## II. Photonuclear Activation Analysis

This type of activation analysis, involving activation by bombardment with high-energy photons, has also been well described by Smales. It is also the subject of two of the contributed papers at this Symposium.

Photonuclear activation analysis has one advantage also possessed by NAA—namely, the high degree of penetration of the bombarding particles (high-energy photons in this case, instead of thermal or fast neutrons) in most matrices. With typical electron linear accelerator sources of bremsstrahlung photons, samples can be exposed to photon fluxes (above the threshold of the reaction in question) in the range of  $10^{12}$ – $10^{13}$   $\gamma/\text{cm}^2\text{-sec}$ . Since, for most elements, the  $(\gamma, n)$  reaction cross sections are one or two orders of magnitude smaller than the thermal-neutron  $(n, \gamma)$  cross sections, photonuclear activation analysis, although still fairly sensitive, is less sensitive than high-flux thermal NAA. However, there are a number of important exceptions to this generalization—especially the low atomic number elements carbon, nitrogen, and oxygen. For these elements, far better sensitivities are attainable by photonuclear activation analysis than by either thermal or fast NAA.

The pioneering work in this field has been carried out by Engelmann and his co-workers at Saclay (Centre d'Etudes Nucleaires de Saclay, France), and his paper at this Symposium mentions some of their most recent work in this field. As in the work of the author's group, Engelmann determines carbon, nitrogen, and oxygen via their  $(\gamma, n)$  products: 20.4-minute  $^{11}\text{C}$ , 10.0-minute  $^{13}\text{N}$ , and 2.07-minute  $^{15}\text{O}$ . Since all of these are pure positron emitters, their gamma-ray spectra are exactly the same. One must therefore either (1) resolve the 0.511 MeV  $\beta^+$  annihilation photopeak in the sample spectrum into its radioisotopic components—by mathematical analysis of its decline with increasing decay time, or (2) radiochemically separate the species of interest ( $^{11}\text{C}$ ,  $^{13}\text{N}$ , or  $^{15}\text{O}$ ) from the other species present. Both the author's group and Engelmann's group have found that the purely-instrumental procedure is sufficient in some instances, but that the radiochemical-separation procedure must be used in more complicated cases. The multiscaler mode of operation, and a computer least-squares procedure, are nor-

mally employed if the instrumental method is used (some additional pure  $\beta^+$  emitters sometimes present to a significant degree are 1.87-hour  $^{18}\text{F}$ , 9.73-minute  $^{62}\text{Cu}$ , and 7.7-minute  $^{38}\text{K}$ ).

In his Symposium paper, Engelmann has described excellent rapid means for the radiochemical separation of  $^{11}\text{C}$  (combustion, then absorption of  $\text{CO}_2$  on Ascarite),  $^{13}\text{N}$  (reductive fusion, then absorption of  $\text{N}_2$  on molecular sieve at low temperature and  $^{15}\text{O}$  (reductive fusion in graphite, oxidation of  $\text{CO}$  to  $\text{CO}_2$ , the absorption of  $\text{CO}_2$  on Ascarite). At a  $100\ \mu\text{A}$  beam current of 30 MeV electrons, his limits of detection for C, N, and O are  $2 \times 10^{-8}$  g,  $4 \times 10^{-8}$  g, and  $5 \times 10^{-8}$  g, respectively. He also discusses the interferences in the carbon determination resulting from the  $^{14}\text{N}(\gamma, t)^{11}\text{C}$  and  $^{16}\text{O}(\gamma, \alpha n)^{11}\text{C}$  reactions; in the nitrogen determination from the  $^{16}\text{O}(\gamma, t)^{13}\text{N}$  reaction; and in the oxygen determination from the  $^{19}\text{F}(\gamma, tn)^{15}\text{O}$  reaction.

It is worth remarking that the  $(\gamma, n)$  method of determining oxygen can be quite useful in distinguishing between oxygen distributed throughout a metal sample (bulk oxygen) and oxygen present just in the surface oxide layers of the sample (surface oxygen). The sample may be simply activated and counted, to obtain a measure of the total oxygen present—then it can be activated again, but this time etched for 30–60 seconds before counting. The etching removes all of the oxide film, so the resulting value gives a good measure of the bulk oxygen content. This technique has been used to advantage at General Atomic, by G. H. Andersen, to determine the bulk oxygen content of low-oxygen beryllium samples. In some such samples, it was shown that specimens with a total oxygen content of about 30 ppm actually had a bulk oxygen content of about 8 ppm (incidentally, giving excellent agreement with the metallurgical properties)—the rest of the oxygen being present as surface oxide. Such work is carried out with two high-current ( $500\ \mu\text{A}$ ) electron linear accelerators—os maximum energies of 17 MeV and 45 MeV, respectively.

Some of the photonuclear activation analysis studies at the Los Alamos laboratories are described in a Symposium paper by D. M. Holm and W. M. Sanders. This particular study is one in which they succeeded in greatly minimizing the interferences from 2.60-year  $^{22}\text{Na}$  and 7.7-minute  $^{38}\text{K}$  in the photonuclear determination of low levels of oxygen in samples of metallic sodium (which typically contain 100–200 ppm K impurity). They utilize coincidence counting techniques to distinguish between the pure positron emitter,  $^{15}\text{O}$ , and the positron/coincident gamma-ray emitters,  $^{22}\text{Na}$  and  $^{38}\text{K}$ . They cite several counting arrangements studied, in which the  $^{22}\text{Na}$  and  $^{38}\text{K}$  interferences were reduced by anywhere from 20% to 90%.

To date, studies in photonuclear activation analysis have been limited to just a handful of laboratories that possess the necessary, quite expensive, linear accelerators. Perhaps, as more and more useful applica-

tions of this technique are developed, there may be enough incentive for some group to develop and market a suitable but less expensive accelerator, perhaps costing around \$200,000.

### III. Charged-Particle Activation Analysis

This form of the activation analysis method, although by no means new, is still only slightly developed—except for a few low atomic number elements in a few matrices. The method has some inherent complications which tend to limit its applicability. Its chief complications are related to the rather small penetration of accelerated charged particles (protons, deuterons, helium-3 ions, and alpha particles—at energies in the range of 1–30 MeV) in typical sample matrices. The penetration depths are only in the range of perhaps ten to a few hundred microns, depending upon the particle used, its energy, and the stopping power of the matrix. Thus, such analyses really only give a measure of the surface composition of the sample. Sometimes this can be shown to be identical with the bulk composition—but often it is not. Of course, if one is especially interested in the surface composition (oxide layers, corrosion layers, etc.), this is an advantage.

P. Albert has employed a technique of activation with charged particles, followed by a controlled etching to a desired depth before counting, to eliminate the effect of a different surface composition, thus allowing him to measure bulk composition. Allowance must be made for the fact that the reaction cross sections change markedly with particle energy (the particle, of course, is continually slowing down as it penetrates into the sample). One also encounters severe sample heating and often many interfering nuclear reactions in charged-particle work. Because of Coulomb repulsion barriers, the method is generally much more sensitive for low  $Z$  elements than it is for high  $Z$  ones.

In their Symposium paper, M. Deyris, G. Revel, and P. Albert (of the Centre d'Etudes de Chimie Metallurgique, Vitry, France) give an excellent and detailed account of their utilization of various charged particles (protons, helium-3 ions, and alpha particles) for the determination of trace levels of oxygen in high-purity aluminum. Careful consideration is given to the effects of various possible interfering reactions—and their energy dependences. Whereas, under their conditions, practical limits of detection of about 1 ppm oxygen in aluminum were found—using either protons or alpha particles—a practical limit of about 0.02 ppm was attainable with  $^3\text{He}$  ions. The product detected is 1.87-hour  $^{18}\text{F}$ , formed by the  $^{16}\text{O}(^3\text{He},\text{p})^{18}\text{F}$  and  $^{16}\text{O}(^3\text{He},\text{n})^{18}\text{Ne} \xrightarrow{\beta^+} ^{18}\text{F}$  reactions. Results obtained nondestructively with  $\text{He}^3$  agreed well with results obtained by proton bombardment—followed by radiochemical separation of the  $\text{F}^{18}$  formed by the  $^{18}\text{O}(\text{p},\text{n})^{18}\text{F}$  reaction. The  $\sim 40 \text{ \AA}$  thick oxide film was etched off, after activation, in each case, so as to determine the bulk oxygen content of the aluminum.

In his Symposium paper, Engelmann discusses not only photonuclear activation analysis (mentioned earlier), but also some determinations of boron and nitrogen employing activation with deuterons (at a beam current of  $10 \mu\text{A}$ , in the energy range of 5–20 MeV): via the  $^{10}\text{B}(\text{d},\text{n})^{11}\text{C}$  and  $^{14}\text{N}(\text{d},\alpha\text{n})^{11}\text{C}$  reactions. In this energy range, limits of detection for boron of from  $10^{-9}$  to  $10^{-10}$  grams, and for nitrogen of from  $10^{-8}$  to  $10^{-10}$  grams, are attainable.

During the past few years, interest in the use of charged-particle activation *analysis*—especially using  $^3\text{He}$  ions and especially for the determination of trace levels of low Z elements in medium or high Z metals—has increased considerably. The recent commercial availability in the United States of medium-cost ( $\sim \$200,000$ ) small cyclotrons, suitable for such work, should stimulate further development of the method. Two companies now produce such cyclotrons.

#### IV. Other Activation Analysis Topics

Time does not permit an in-depth discussion of some of the other important developments in the field of activation analysis: the use of lithium-drifted germanium semiconductor detectors for high-resolution x-ray and gamma-ray spectrometry; the use of coincidence and anti-coincidence techniques; the use of various computer programs for data processing; new areas of application; and prompt gamma-ray techniques.

Brief reference has been made at this Symposium to the advantages, in certain cases, of the use of Li-Ge detectors—namely, in the papers by T. B. Pierce, of the Atomic Energy Research Establishment, Didcot, England (the paper being mainly concerned with analysis via prompt gamma rays emitted during charged-particle activation), and by D. E. Fisher, L. Rancitelli, J. F. Lawrence, R. L. Currie, and E. Berkey, of Cornell University (paper mainly devoted to the instrumental NAA of meteorites). In their Symposium paper, K. K. S. Pillay and W. W. Miller, of the Pennsylvania State University, describe the detection of electron-capture and internal-conversion characteristic x-rays in NAA work, using gas proportional counters at the lower energies and thin NaI(Tl) scintillation crystals at the higher energies. In such work, Li-drifted Si or Ge detectors should also be very useful.

Coincidence and anti-coincidence techniques are described by D. M. Holm and W. M. Sanders in their Symposium paper (already referred to), and by D. E. Robertson and R. W. Perkins, of the Battelle Northwest Laboratory, in their Symposium paper (mainly concerned with the instrumental NAA detection of various trace elements in sea water).

The only Symposium paper devoted to computer techniques in activation Analysis work is that by H. P. Yule, presently at Texas A & M University. This paper describes a very useful computer method for obtaining firm ( $3\sigma$ ) upper limits for concentration for as many as seventy-two elements from instrumental NAA data.

In the areas of applications of NAA techniques, there are several interesting Symposium papers: those by (1) G. W. Leddicotte, of the University of Missouri, on trace-element studies in the biomedical field, (2) N. E. Erickson, S. S. Krishnan, and A. K. Perkons, of the Attorney General's Laboratory, Toronto, Canada—on applications in the field of scientific crime investigation (a subject of great interest to this author also), (3) H. H. Kramer, W. J. Hampton, V. I. Molinski, and W. H. Wahl, of the Union Carbide Nuclear laboratories, on the geographical characterization of chromium ores via their trace elements, (4) D. E. Fisher et al., mentioned earlier, on meteorite analyses, and (5) D. E. Robertson and R. W. Perkins, also mentioned earlier, on oceanographic applications.

### V. Other Nuclear Methods

Time only permits a brief mention of the several interesting papers contributed to this Symposium on nuclear methods of analysis other than activation analysis methods. These are papers on (1) thickness measurements, by J. Krugers (Hewlett-Packard Company), (2) substoichiometric radioisotopic dilution applications, by A. R. Landgrebe, P. A. Pella, L. T. McClendon, and J. R. DeVoe (National Bureau of Standards), (3) fission track etching, by H. S. Rosenbaum and J. S. Armigo (General Electric Company, Vallecitos Laboratory), (4) radio-gaschromatography, by R. M. Statnick and F. Schmidt-Bleek (Purdue University), and (5) ion-exchange membrane radiochelometric titrations, by J. Tölgyessy, J. Konecny, and T. Braun (Slovak Technical University, Bratislava, Czechoslovakia and L. Eötvös University, Budapest, Hungary).

### VI. References

- [1] Buchanan, J. D., Proceedings of the 1961 Int'l. Conf. on Modern Trends in Activation Analysis (Texas A & M University, College Station, Texas), pp. 72-77.
- [2] Lukens, H. R., Yule, H. P. and Guinn, V. P., Nucl. Instr. & Methods **33**, 273 (1965).
- [3] Yule, H. P., Lukens, H. R., and Guinn, V. P., Nucl. Instr. & Methods **33**, 277 (1965).

# SPARK SOURCE MASS SPECTROMETRIC ANALYSIS OF SOLIDS

A. J. AHEARN

*Bell Telephone Laboratories, Incorporated  
Murray Hill, New Jersey 07971*

## I. Introduction

Solid state physics, chemistry, and technology have grown rapidly in the past two decades. This in turn stimulated the development of new analytical techniques [1]<sup>1</sup> for determining the chemical composition of materials—particularly the detection and measurement of trace quantities of impurities in solids.

The demands of our semiconductor technology stimulated the initial development of one of these new methods of analysis. As an example, the electrical properties of germanium and silicon are markedly changed by the introduction of as little as 10 ppba (parts per billion atomic) of copper [2] into the former or 2 ppba of gold [3] into the latter.

But there are many other properties of materials that are appreciably influenced by the presence or absence of selected impurities in the low ppm region. Ordinary tungsten [4] is quite brittle but when it is purified to a level below 10 ppm it becomes readily machinable. At 15 °K the thermoelectric power of gold [5] is increased by a factor of 100 when the cobalt content is reduced from 200 ppm to 20 ppm. The ductility of beryllium [6] increases by a factor of 40 when impurities therein are reduced to a few ppm.

The superconducting transition temperature of molybdenum [7] is degraded from 0.9 °K to 0.3 °K by introducing 100 ppm of iron. With titanium [8] containing less than 5 ppm manganese and less than 2 ppm iron the transition temperature is 0.42 °K, whereas with 30 ppm manganese and 20 ppm iron it is depressed to 0.17 °K, and with 100 ppm manganese, it is below 0.06 °K. In the recrystallization of lead [9], the grain boundary velocity is reduced by a factor of 1000 by a few ppm of silver. The efficiency of graphite [10] in a nuclear reactor is markedly reduced by the presence therein of only 2 ppm of boron.

The magnetic permeability of iron [11] is increased from a few thousand to a few hundred thousand when its carbon, sulfur, nitrogen and oxygen content are reduced from a few hundred ppm to a few dozen ppm.

---

<sup>1</sup> Figures in brackets indicate the literature references at the end of this paper.

Reviewed elsewhere [12] are many more examples of solid state properties that are appreciably affected by trace impurities in the ppm to ppb region. This is the region in which one of the new analytical techniques—spark source mass spectrometry [13]—can effectively contribute by identifying the trace impurity and by determining its approximate concentration.

## II. Mass Spectrometry With Spark Source

This spark source technique is not the first instance in which mass spectrometry has been used for solids analysis. Semiconductors and metals have been analyzed using an electron bombardment type source of positive ions [14]. Very high detection sensitivities for certain elements have been obtained by isotopic dilution [15] techniques. Ions sputtered from a solid under ion bombardment have been employed to study solid surfaces [16].

Professor A. J. Dempster [17] was the first to do mass spectrometric analyses with positive ions from a spark source. As the spark source [18] is usually employed, a radio frequency voltage of several tens of kilovolts is applied between two electrodes of the material under investigation. When the gap between these electrodes is  $\leq 100$  microns, the electric field is high enough to produce a field current—an emission of electrons from the cathode. These field currents appear when the average applied field is substantially lower than that predicted by theory. Consequently the electrons probably come from surface irregularities such as whiskers or other sharp projections where the field is enhanced. Some heating and vaporization of the cathode material occurs at these projections. In turn the anode is locally heated and vaporized by these electron beams. Electron bombardment ionization of cathode and anode atoms occurs in the interelectrode gap. Under positive ion bombardment, cathode material is sputtered some as neutral atoms and some as positive ions. These vaporization and ionization processes yield ion currents that, to a first approximation, represent the electrode material [13]. The degree of this approximation will be discussed later.

Spark source mass spectrometry as a technique for the analysis of solids has grown in use enormously in the past decade or so because of two inherent advantages. First, its detection sensitivity is high whether defined in terms of the low concentration of an impurity that can be detected [19] in a matrix or in terms of the total amount of sample [20] needed to detect impurities.

The second outstanding advantage of the spark source as an analytical tool is its nonselectivity—its mass spectrum reveals all elements in the sample with approximately the same detection sensitivity [13]. This presents a great advantage over a thermal ion source for example where elemental sensitivities vary by several decades. This nonselectivity makes the spark source the preferred ion source for general analytical

work on solids primarily because the demands of modern physics and chemistry of solids cover most if not all of the elements in the periodic table.

The spark source is used widely in spite of a number of disadvantages [13] from which it suffers. It is an erratic ion source—it requires almost constant adjustment to keep it running and in spite of this nearly continuous monitoring, the ion current fluctuates widely with time. Consequently, in nearly all work with the spark source an integrating detector is used. The spark source being a high voltage device, the positive ions therefrom are not monoenergetic. Experiments show that they have a spread in energy of two to three kilovolts [21]. In addition to the usual requirement of direction focusing whereby ions within some small solid angle are focused, this ion energy spread imposes the additional requirement of velocity focusing [13] in the mass spectrometer used with the spark source. Such double focusing mass analyzers add considerably to the complexity and cost of these instruments. Moreover this velocity focusing can be achieved only over an energy band of a few hundred electron volts. Consequently, much of the ion current must be discarded leaving a relatively small useable ion current of about  $10^{-10}$  amperes.

The erratic nature of the spark source would require that an electrical detector measure the ratio of a mass resolved beam to that of the total beam entering the mass analyzer. The small magnitude of this latter beam makes this ratio measurement so difficult [13] that in practice an integrating detector in the form of a photographic plate is usually used.

The requirement of photographic detection added to the need that the entire periodic table be encompassed in the recorded mass spectrum has resulted in the widespread choice of a particular geometry—the Mattauch-Herzog geometry [22] of double focusing. Every commercial make of spark source mass spectrograph [18] uses this geometry.

This geometry is sketched in Figure 1. Ions from the radio frequency spark source after acceleration are limited to an appropriately small solid angle by apertures in electrodes  $S_1$  and  $S_2$ . They next enter the electrostatic analyzer where velocity dispersion occurs. The aperture in the electrode  $S_3$  passes an appropriately narrow energy band of ions to the magnetic sector where mass analysis occurs.

Consider the two ion trajectories that delineate the angular divergence of the beam. Those of mass  $m_1$  and  $m_2$  and energy  $E_1$  and  $E_2$  are sketched in Figure 1. Two nondivergent beams emerge from the electrostatic analyzer. In the magnetic sector where mass separation occurs the various ion paths of each mass are brought to a focus at a plane beyond the exit of this analyzer.

This focusing of all masses on a given plane is a necessary and sufficient requirement for photographic detection for general analytical work where a wide range of elements needs to be simultaneously registered on the photographic plate.

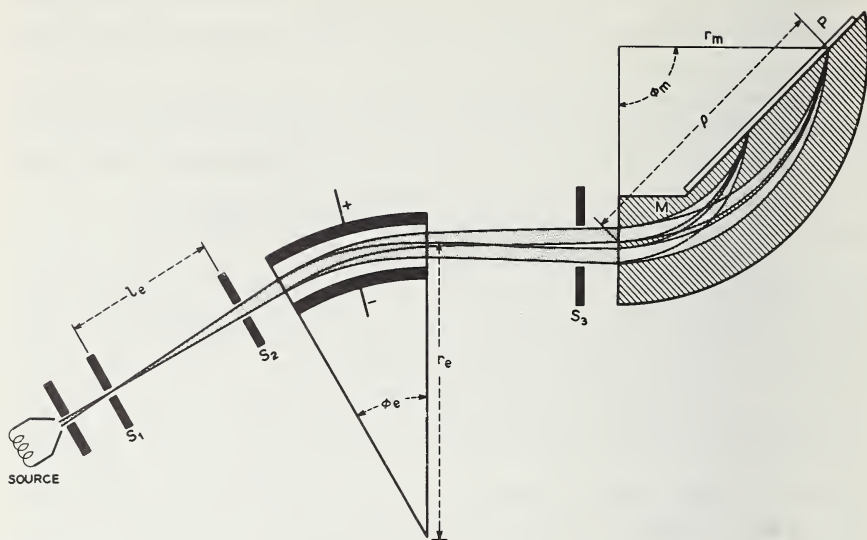


Figure 1. Double focusing in a Mattauch and Herzog type spark source mass spectrograph. After Hannay, N. B., *Science* **134**, 1220 (1961).

### III. Analytical Capabilities of Spark Source Technique

The radio frequency spark can be used to analyze many different kinds of materials. With electrical conductors and semiconductors, the spark can be formed directly between electrodes of the sample. Moreover, techniques have been developed whereby an electrical insulator [23] contributes to a spark thereby enabling its analysis to be obtained.

Samples of metals, semiconductors and insulators in powder form are sometimes presented for analysis. Techniques [24] have been developed for sintering powders or for mixing with suitable binders, or conductors which after compacting into rod form are suitable for sampling with the spark source.

The preparation, cleaning, and handling of samples [24a] is critical since less than a monatomic layer of surface contamination [25] is readily detected. With liquid samples a clean surface of a suitable material is deliberately contaminated [25] by the liquid, or a wet sludge [26], with a suitable powder, is compacted into a dried electrode.

When there is plenty of sample and it can easily be machined, the sample should be in the form of rods about 20 mm long and 2 or 3 mm in diameter.

On the other hand, samples from solid state devices or crystal growing set-ups frequently are small enough to be termed microsamples [27]. There are techniques for sparking and analyzing such small samples. This spark source technique is usually employed to detect trace impuri-

ties but in the case of microsamples where the total amount of material available is too small to examine by other analytical methods, it is frequently used to determine major components.

The high detection sensitivity is one of the two distinguishing features of spark source mass spectrometry. With a few exceptions, all elements can be detected under favorable conditions when the trace element in the ion samples presented to the detector is in the neighborhood of a part per billion [19] atomic (ppba) fraction of the major component.

In general, the ion sample presented to the detector does not accurately represent the solid sample comprising the electrodes of the spark source. However, for most elements the concentration of a trace element in the ion sample usually differs from that in the solid sample by less than a factor of ten [13]. This small selectivity is a most important feature of spark source mass spectrometry for analytical work because it makes the technique so widely applicable.

The detection sensitivity of a few ppb, quoted for this spark source technique, was carefully qualified as applying to "nearly all elements" and "under favorable conditions." What are these "favorable conditions" and how poorly are they realized in practice? How serious are the corresponding losses in detection sensitivity? What can be done to retrieve these losses? To what extent, as a general analytical method is this spark source technique limited by less than "favorable conditions."

The second feature of the spark source technique is its nonselectivity but again this characterization was carefully qualified—"for most elements the concentration of a trace element in the ion sample usually differs from that in the solid sample by less than a factor of 10." If this misrepresentation or selectivity is neglected, the spark source technique concentrations could be in error by a factor of 10. How serious is this? In general is it not sufficient to know trace concentrations to within a factor of 10 particularly in the ppm to ppb region? What are the important factors determining accuracy and precision with this analytical technique? How can the latter be improved?

These are the questions and considerations treated in the forthcoming sections of this paper.

## IV. Factors Limiting Detection Sensitivity

### A. DIFFUSE BACKGROUND

What are the favorable conditions under which it is possible to detect a trace element in the ion sample presented to the photographic detector when this trace element is present at about 1 ppba? The weakest mass line that can be detected visually or instrumentally on the photographic plate determines the detection sensitivity under a given set of conditions. This is a signal-to-noise problem, where the noise is the diffuse background in the emulsion in the presence of which the mass line must be

detected. As the exposure is increased, elements with progressively lower concentration will appear but the background increases also. Consequently there is an optimum exposure beyond which still lower concentrations are not uncovered. With modern commercial spark source instruments this optimum exposure is about one microcoulomb [28].

In addition to the intrinsic background of the emulsion, two other factors contribute background. Some ions in transit are scattered from the beam by collisions with residual gas molecules. Those scattered in the magnetic analyzer may reach the emulsion. Ions that undergo a charge transfer in a collision with a residual gas molecule by picking up one or more electrons are frequently revealed by rather sharply terminated bands of diffuse background [13]. The end points of the band correspond to charge transfers at the emulsion and between the electrostatic analyzer and the magnetic analyzer.

In modern commercial instruments, high vacuum techniques [28] such as metal gasket seals, high speed pumping and baking are employed to minimize this ion scattering and background. The minimal scattering thus achieved permits the detection of elements in the ppba range provided these elements are substantially greater or smaller in mass than the major component ions of the sample.

For those elements near the major component, particularly for those on its high mass side, the diffuse background is substantially greater [29]. Ions in a spark source mass spectrograph on striking the photographic emulsion, produce a mass line spectrum plus one or more of the following secondary products: x-rays, luminescence, negative ions, secondary electrons, reflected and/or sputtered positive ions all of which would fog the emulsion. The magnetic field would return the negatively charged particles to the low mass side of the incident ion, and the positively charged ones to the high mass side. The fogging generated by the x-rays and luminescence would probably not be thus directionally limited.

This fogging is appreciable when the integrated ion charge is sufficient to detect an element in the ppba region. This limitation in detection sensitivity has been partially circumvented in different ways. In our own laboratory, the photographic plate and plate holder were modified as shown in Figure 2. The plate was split at the mass position of the major component ions. At this position rectangular shaped apertures were cut in the backing plate and the plate holder. By this simple device, the major component ion beam (d) passes right through the assembly without striking the photographic plate at all. With the MS7 being used, this ion beam thus enters a cavernous space in which the dimensions are large compared with the rectangular opening thereto. Consequently, it should serve as an efficient Faraday collector to trap not only the incident positive ions of the major component but also their secondary products.

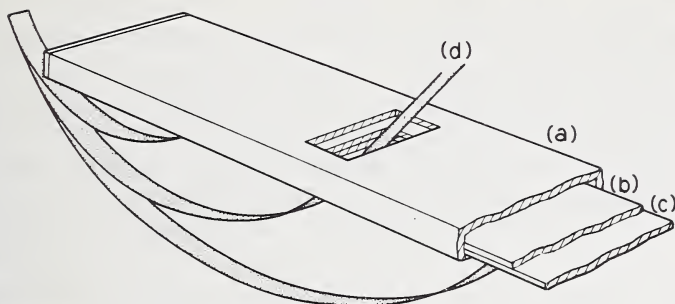


Figure 2. Modifications of standard photographic plate holder for MS-7 mass spectrograph to bypass the major component of the sample. a. Plate holder. b. Backing plate. c. Photographic plate. d. Major component ions. After Ahearn, A. J., and Malm, D. L., *Appl. Spectr.* **20**, 411 (1966).

The suppression of fogging by the modifications of Figure 2 is indicated by curve B in Figure 3. Here the sample was gallium arsenide and, to accommodate the arsenic singly charged ion and the two singly charged ions of the gallium isotopes, the widths of the rectangular apertures in the backing plate and plate holder were made 11 and 13 mm respectively. The optical transmission of the plate is plotted on the vertical axis. In this measurement the microphotometer was set at 100 percent transmission at a place where the emulsion was removed from the glass. To simplify the presentation in Figure 3 the spikes corresponding to the various mass lines have been omitted and only the diffuse background is presented in curve B. Mass number is plotted on the horizontal axis.

For comparison, curve A in Figure 3 gives the corresponding diffuse background when the standard plate (not split) and standard plate holder were used.

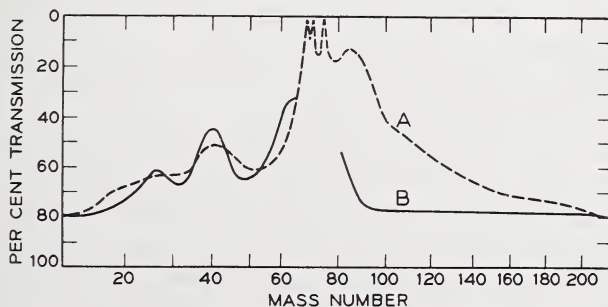


Figure 3. Diffuse background in mass spectrum of gallium arsenide. A. Standard photographic plate and plate holder. B. Modified unit to suppress fogging by trapping major component ions. After Ahearn, A. J., and Malm, D. L., *Appl. Spectr.* **20**, 411 (1966).

Curve B shows that with this split plate modification of Figure 2, the low transmission of 80 percent at the high mass end of the plate is maintained down to about mass 90. Consequently there is little or no loss in sensitivity from the high mass end of the spectrum to about mass 90. On the other hand, with the standard plate as shown in curve A, the background rises to about 20% transmission at mass 90. These correspond to detection sensitivity losses, by factors as high as 30, that are retrievable by this split plate technique. The abrupt rise in background below mass 90 on curve B is not understood. It may be caused by secondary products of major component ions escaping back through the wide (10 to 12 mass units) aperture system to fog the plate. It may be due to major component ion scattering. One with a charge transfer from +5 to +2 would introduce background that would bunch near and terminate approximately at mass 90.

The background on the low mass side of the major components is approximately the same for A and B in Figure 3. Doubtless it could be reduced on the high mass side of the doubly charged major components by splitting the plate there and introducing a second set of apertures to capture these ions and their secondary products.

In curve A and B of Figure 3, the measured monitor exposure was  $1 \times 10^{-6}$  coulombs requiring about 2 hours in each case with an object slit width of .006 inches. The spark source was run at a repetition rate of 300 cps and a pulse length of 25 microseconds. In each case the analyzer and source pressure were the same—about  $1 \times 10^{-8}$  torr with the spark not running.

The background shown in curve A is not an extreme case. Substantially lower transmission values have sometimes been recorded at this exposure— $1 \times 10^{-6}$  coulombs. The degree of fogging depends to some extent on the magnitude of the ion current to the photographic plate, being larger for large currents. This could mean that the secondary products depend in part on the amount of electrostatic charging of the emulsion or that they vary nonlinearly with current such as would occur if the mechanisms involved two or more steps.

H. Mai [30] employed a split plate technique similar to that of Figure 2 with similar diminution of plate fogging.

This method of trapping major component ions suppresses the fogging produced by their secondary products more completely than did our 1954 technique [13] in which a grounded metal mask was placed on the emulsion at the position of incidence of the major component ions. This simpler technique recently has been adapted and modified by painting a strip of graphite paint [30a] on the emulsion at the position of the major component ions, the strip being grounded. Some diminution of fogging is reported.

An entirely different approach to the suppression of this fogging, produced by these 15 to 20 keV ions incident on the photographic emul-

sion, has recently been made by Kennicott [31]. The assumption was made that the secondary products would be lower in energy than the incident ions. This suggested that the latent image produced by the secondary products would be closer to the surface of the silver bromide crystals of the emulsion than the latent image of the incident ions themselves. A developing procedure was devised wherein a latent image on or near the surface of the AgBr crystal was bleached out after which the internal image produced by the 15 to 20 keV incident ions was developed.

A substantial reduction in fogging as compared with D19 developing is reported. The improved signal-to-noise ratio enables one to slightly extend the detection limit of this mass spectrometric technique in spite of a loss in absolute sensitivity of the emulsion.

In a broad program to improve on the properties of the conventional emulsion of silver bromide crystals in a gelatin matrix, Honig, Woolston and Kramer [32] reported on a gelatin-free photographic detector consisting of a thin film of silver bromide crystals deposited on a glass plate. Among other advantages indicated by experiments in progress, the fogging with this gelatin-free detector is substantially smaller than with the Ilford Q2 gelatin emulsion. This suggests that the secondary products of ion bombardment come in part from the gelatin in the Q2 emulsion.

The split plate technique is cumbersome particularly with a sample like gallium phosphide where two splits are needed to bypass the major component ions. Perhaps the split plate or its equivalent in the form of a miniature but near perfect ion collector [33] at the proper position on the plate and supplemented by internal image development is the best alternative for the present. Perhaps a high electrical conductivity glass with a gelatin-free photographic detector is an alternative.

## B. LINE BACKGROUND

Traces of hydrocarbons [19] are not uncommon in high vacuum systems of the character of commercial spark source mass spectrographs. In this high voltage ion source, such hydrocarbons are fragmented in part. As a consequence, mass lines due to hydrocarbons or fragments thereof sometimes appear. Fortunately, the resolving power available in these spectrographs is usually adequate to separate these ions from elemental ions of the same nominal mass. Consequently, line background from such hydrocarbons can usually be circumvented.

One of the advantages of this mass spectrographic technique derives from the simple spectrum that is obtained—simple by comparison with that of the spectrochemical technique. Nevertheless with this high voltage spark ion source which produces many multiply charged ions, many elements have mass lines (mass/charge values) of the same nominal value as other elements and masking occurs unless the resolving power is adequate. Singly charged molecular species consisting of 2 or more

major component atoms are also produced in the spark. With some elements, molecular species consisting of as many as 30 atoms [34] have been recorded. In addition to oxides, hydrides, hydroxides, and carbides of the major component that may appear, complex molecular ions [35] like  $\text{GaP}_2$  and  $\text{Ga}_2\text{P}$  have been recorded. The isotopes of these molecular ions and multiply charged ions occupy a not negligible portion of the mass spectrum. The resolving power needed to separate them from the elements of the same nominal mass is not always available.

The limitations imposed on this spark source mass spectrometric technique for solids analysis by available resolving power can be considered in the following context. What resolving power would be needed to detect almost any element in almost any simple matrix? The mass differences that need to be resolved for this purpose have been compiled from the Sandia Corporation Monograph "Table of Atomic Masses." This table compiled with the spark source in mind includes ion masses of most but not all isotopes up to 6 electronic charges and includes the singly-charged ions of most but not all isotopic polymers up to mass 210.

Figure 4 [36] shows the percentage of the elements resolved from their nearest neighbor as a function of the resolving power  $M/\Delta M$  needed for this separation. Figure 4 shows that with a resolving power  $R=1000$  only 10 percent of the elements are resolved from their nearest neighbors, but with  $R=2000$ , 35 percent of the elements are resolved. Now with today's modern spectrographs, resolving powers in the 2000 to 3000 range are available. It is evident that the separation of additional elements requires large increases in resolving power. For instance,

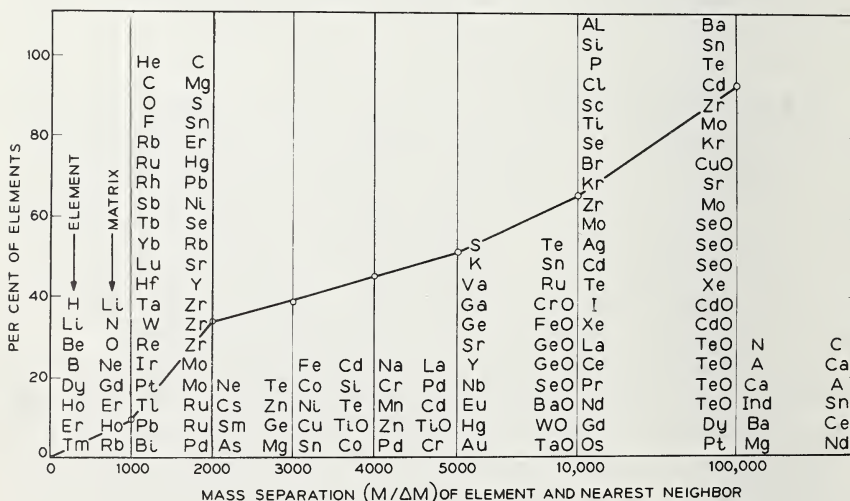


Figure 4. Resolving power needed to separate singly charged ions of elements from the nearest  $m/e$  matrix ions in spark source mass spectrometry.

with a resolution of 5000, only 52 percent of the elements would be separated from their nearest neighbor.

In Figure 4 the elements and their nearest neighbors are listed in columns according to their mass difference  $M/\Delta M$ . For example, with  $R=1000$ , only hydrogen, lithium, beryllium, boron, dysprosium, erbium, holmium, and thulium are resolved from the matrices that are the nearest neighbors. Many of the cases calling for high resolving powers correspond to nearest neighbors in the form of oxides. One might argue that their inclusion is not realistic, but since we are frequently concerned, in this technique, with ppb concentrations, this presumes either a very low oxide concentration or a very high degree of dissociation in the spark. Moreover, the situation is not markedly improved if these oxides are excluded from consideration.

In compiling the data of Figure 4 the most abundant isotope of the element in question was not necessarily used. An arbitrary decision was made to sacrifice abundance by a factor of  $\leq 3$  if by so doing a less abundant isotope of the element has a more remote nearest neighbor, i.e., if thereby a lower resolving power sufficed for mass separation.

This decision to sacrifice some abundance and therefore some detection sensitivity where necessary although arbitrary is not unrealistic. Even this sacrifice in sensitivity by a factor of 3 is not an available alternative for the 27 percent of the elements that are monoisotopic.

It should be emphasized that what is plotted on the horizontal axis in Figure 4 is the limit of resolution—where the valley between the two mass lines in question just disappears. Doublets near this limit of resolution could be identified as doublets only if they were substantially above the limit of detection but below the point of line broadening characteristic of the approach to saturation. Moreover, at this extreme, the doublets could be detected as such only if the two lines had nearly the same intensity. Furthermore, quantitative measurements of optical transmission and line width would be worth little with a valley between the doublet lines of less than 50 percent.

The limitations portrayed in Figure 4 can be circumvented in some elements by resorting to a low abundance isotope of the element but this is necessarily at a corresponding sacrifice in detection sensitivity. For monoisotopic elements, this circumvention can only be achieved by resorting to a multiply charged ion of the element. But since the intensity of a doubly charged ion may be less than 10 percent of that for the singly charged ion, this also entails an appreciable loss in detection sensitivity.

In Section III, it was indicated that even under the favorable conditions specified earlier in the present section, there were exceptions among the elements to the generally high detection sensitivity of a few ppba. These principal exceptions are hydrogen, carbon, nitrogen, oxygen and their products. Carbon and oxygen are of particular interest. The

minimum apparent concentration observed for carbon and oxygen is usually not below a few ppma [37]. This concentration is labeled "apparent" because these elements coming from the solid sample are not readily distinguished from instrument background due to dissociation of carbon monoxide, water vapor and/or hydrocarbons.

However, recently Socha and Willardson [38] reported experiments on mass spectrographic measurements of apparent concentrations of gases in solid samples as a function of pumping speed and of the partial pressure of the gases in the source chamber. Table 1 summarizes their determinations of the contribution of source chamber gases oxygen, nitrogen, carbon monoxide and water vapor to the mass spectrum of gallium arsenide when the partial pressure of each gas was  $1 \times 10^{-9}$  torr. This indicates that oxygen in samples at much less than 2 ppma would be lost in the noise of the instrument background, but that nitrogen and particularly hydrogen and carbon in a sample can be detected at substantially lower values.

TABLE 1. Contribution of source gases to the mass spectrum at a partial pressure of  $1 \times 10^{-9}$  torr.

<i>Source gas</i>	<i>Ion</i>	<i>Contribution in PPMA</i>
O	$16_{\text{O}^+}$	2
N	$14_{\text{N}^+}$	0.3
CO	$12_{\text{C}^+}$	0.01 <sup>a</sup>
CO	$28_{\text{CO}^+}$	0.02
H <sub>2</sub> O	$1_{\text{H}^+}$	0.02 <sup>b</sup>
H <sub>2</sub> O	$18_{\text{H}_2\text{O}^+}$	0.01

<sup>a</sup> Estimated.

<sup>b</sup> Includes contribution from H<sub>2</sub>.

(Socha, A. J., and Willardson, R. K., presented at the 14th Annual Conference on Mass Spectrometry and Allied Topics, Dallas, 1966.)

### V. Factors Limiting Accuracy of Analysis

Spark source mass spectrometric analyses of solids are normally made as follows. A graded series of exposures is made covering the range  $10^{-13}$  to a maximum of  $10^{-6}$  coulombs measured by a monitoring electrode located at S<sub>3</sub> of Figure 1. At the lowest exposures ideally some of the isotopes of the major components are recorded in the linear portion of the response curve of the photographic emulsion. As the exposures are progressively increased, impurities of progressively lower concentration appear in the mass spectra. The concentration of an impurity in its matrix is then derived from the inverse ratio of exposures [39] of impurity and major component that produce the same response on the emulsion. In deriving sample composition from these spectra the following factors are important.

## A. TRANSMISSION STABILITY OF INSTRUMENT

The electric charge delivered to the emulsion is assumed to be directly proportional to the charge measured by the monitor, i.e., the monitor aperture passes a fixed fraction of the charge incident on the monitor. Data [13, 20] indicate that this assumption is justified.

## B. RECIPROCITY FULFILLMENT

The assumption is made that when the response of the emulsion produced by an isotope of one element equals that for an isotope of a second element, then the charge producing each mass line is the same. This is true only if the response is first corrected for its dependence on ion mass [39] and ion energy [39], and if the reciprocity relation is satisfied.

This requires that in the relation  $R = It^x$  for the response  $R$ , the ion current  $I$  and the exposure time  $t$ , the power  $x$  be equal to unity, i.e., that the photographic response is determined by the total charge regardless of the rate of arrival of the charge. Franzen and Hebeda [40] used 30 keV singly charged ions of argon, neon, and krypton in which the exposure time on Ilford Q2 emulsions was varied from 0.07 to 240 seconds—a range of 3300. Their ion currents varied from  $1.4 \times 10^{-12}$  to  $4 \times 10^{-16}$  amperes. Over this range of time and current they found that the  $x$  was greater than unity by less than 1 percent. Less accurate measurements on 19 keV singly charged ions of boron [13] and antimony over a current range of about  $10^3$  and with gold [20] ions over a range of  $10^5$  did not indicate any departure from reciprocity. Although the current ranges in these reciprocity tests are smaller than the  $10^7$  range used in analyses by this spark source technique, the assumption that the reciprocity relation is satisfied is probably justified.

## C. EMULSION SENSITIVITY—DEPENDENCE ON ELEMENT

The sensitivity of Ilford Q2 plates to ions in the neighborhood of 20 keV energy is assumed to vary as  $M^{-x}$ . Experiments confirm this relation [41] and suggest an  $x$  value between 0.5 and 0.8 which may depend on mass.

When a mass spectrum is recorded on an emulsion, in addition to the latent image that is produced in the silver bromide crystals at each of the mass line positions, these crystals are doped by ion implantation with the particular element responsible for that mass line. Some of these dopants will be electrically more active than others in the AgBr crystals. One would expect that the active elements would not fall on the simple  $M^{-x}$  curve for sensitivity as a function of mass  $M$ . Only about 16 elements [41] have been so tested of which only 7 are above mass 40. Consequently there are wide gaps in the region above mass 40 which need filling before the simple  $M^{-x}$  relation should be accepted.

## D. CALIBRATION OF EMULSION

The next assumption made is that the photographic emulsion can be adequately calibrated to express ion intensity as a function of the darkening of the emulsion as revealed by optical transmission measurements. Sometimes this is done by making a graded series of exposures in which the ion intensity is given by electrical measurements at the monitoring electrode [39] at  $S_3$  in Figure 1. The precision in such electrical measurements is usually poor.

Another method uses a single mass spectrum of an element with a number of isotopes that vary considerably in abundance [39]. The relative ion intensity of the various isotopes is given by their relative abundance. Electrical measurements of ion intensities are not necessary. For this purpose tin is the most satisfactory element to use; its ten isotopes are adequately spaced in abundance to cover the range of the Ilford Q2 emulsion.

In the Churchill two line method [39], graded values of optical transmission are obtained from many pairs of mass lines corresponding to a specific pair of isotopes of a given element. The corresponding ion intensities are derived from the relative abundance of the two isotopes in question. Electrical measurements are not needed.

A modification of this Churchill technique is reported [42] which employs a single pair of mass lines of the selected isotopes of a given element. Here the graded series of optical transmissions are read directly from corresponding points along the optical transmission profiles of the two mass lines. Electrical measurements are unnecessary.

## E. SPARK SOURCE IONIZATION PATTERN

Usually trace concentrations are derived by comparing the singly charged ion intensities of impurity and major component. This assumes that the ionization pattern—the relative abundance of the ions of different electronic charge—is the same for impurity and major component. This assumption is not justified since the singly charged ions of one element may be 95 percent of the total ionization of that element and that of another element may be as low as 60 percent.

This difficulty is easily circumvented by determining the total ionization in each case. An adequate measure of this is usually given by the sum of the singly and doubly charged ions.

Sometimes the doubly charged ions of impurity and major component are compared. This is obviously a very dangerous practice.

## F. INTEGRATION OF ION INTENSITY PROFILE

The optical transmission profile of a mass line on an emulsion can be converted to an ion intensity profile [43] by means of an emulsion calibration. The ion charge recorded on the emulsion is obtained by integrating

[44] this intensity profile. This integration is time consuming. However a reasonably adequate measure of the ion charge is given by the product of the ion intensity corresponding to the peak optical transmission and the half width—the mass line width at half of the peak ion intensity [39].

The peak ion intensity alone is an adequate measure of the ion charge only provided the line widths for lines being compared are the same. This assumption is not justified. Under controlled conditions this line width varies linearly with the square root of the ion mass. However, in an analysis where a trace element is being compared with a major component this line width relation may not hold and line width measurements are therefore preferable.

A promising alternative to the integration of the ion intensity profile is the integration of the optical transmission profile [44a].

### G. THE RELATIVE SENSITIVITY PROBLEM

The preceding assumptions have been concerned with the analysis of the ion sample, but, as pointed out in Section III, the composition of the ion sample in general does not accurately represent the composition of the solid sample. Presumably, the factors contributing to this lack of fidelity in the ion sample are selective evaporation and ionization in the spark source and selective transmission by the double focusing mass spectrograph.

Woolston and Honig [45] made measurements on the ion energy distribution at the position of  $S_3$  in Figure 1, for a number of solids. Typical results are shown in Figure 5. Considerable variation is shown

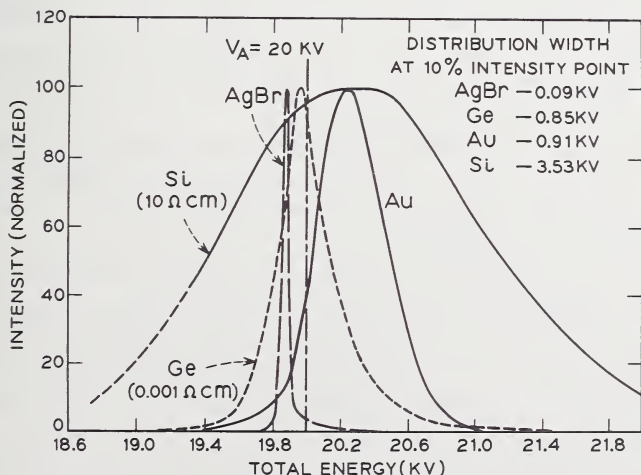


Figure 5. Energy distribution of ions in spark source mass spectrometry. After Woolston, J. R., and Honig, R. E., *Rev. Sci. Instr.* **35**, 69 (1964).

in the width of the energy distribution curves for different materials and also in their position on the energy scale.

The double focusing capabilities of the Mattauk and Herzog geometry [22] are limited to an ion energy band of a few hundred electron volts energy. In some cases the ions have an energy spread of a few keV as shown in Figure 5. In those cases only a fraction of these ions are passed by  $S_3$  of Figure 1. Moreover for any given element the fraction passed depends on this distribution shape and on its location relative to the pass band. The energy band passed by  $S_3$  may misrepresent the total ion sample presented to  $S_3$  by an appreciable factor, thereby contributing to the overall misrepresentation of the solid sample, by the ion sample presented to the detector.

This lack of fidelity in the ion sample can best be determined experimentally by measurements on standard samples. This problem is treated in the following section.

## VI. Ion Samples vs. Standard Solid Samples

Gorman, Jones, and Hipple [46] at the National Bureau of Standards first analyzed standard samples with a spark source double focusing instrument. Since high concentration (one percent or more) components in a stainless steel sample were studied, electrical measurements could be made. The concentrations derived from these measurements were significantly different from the certified values of the standard sample.

They interpreted this to be a lack of fidelity in the ion sample and calculated an empirical correction factor now called the Relative Sensitivity Coefficient (RSC)—the ratio of the concentration of an element to that of its certified value. Measurements on a second standard sample containing the same components as the first but with different concentrations were then made. The calculated concentrations, corrected by the above RSC, were in excellent agreement with the certified values of this second standard sample.

The importance of this RSC is directly proportional to the amount by which it differs from unity. The author compiled available data [47] in 1963 showing RSC values ranging from 0.21 to 6.5—about half of the values falling in the range 1.0 to 1.5.

Table 2 lists similar data available since 1963. Some of these deal with well established iron and copper standard samples. Much of it is based on concentrations determined by other methods thought to be reliable. Examples of these are spectrophotometric measurements of dopants in GaP and radiochemical, electrical, and spectrochemical measurements in silicon and GaAs.

The data of Table 2 are summarized in Figure 6. Here the fraction of the values within a given interval is plotted as a function of the RSC value irrespective of the element or matrix involved. About 70 percent

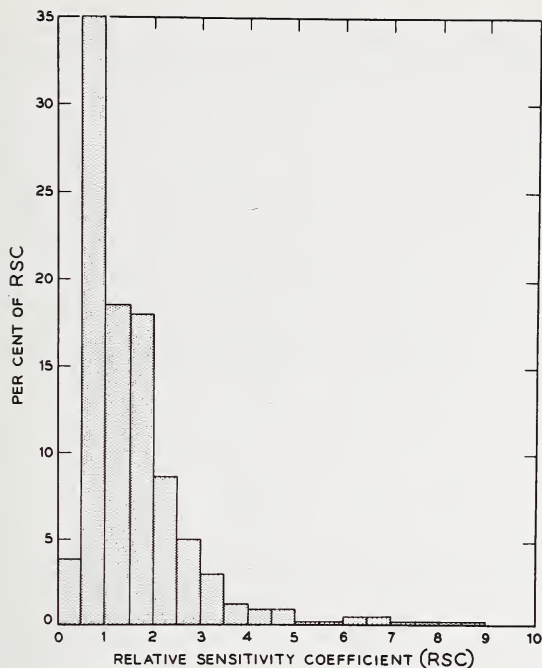


Figure 6. Distribution of relative sensitivity coefficient values in Table 2.

of the values are in the range 0.5 to 2.0. Most of the remainder are greater than 2.0.

Dejardins [50] found that the RSC values for a given element in several different matrices were grouped around an average with a standard deviation of about 25 percent. This degree of independence of an element from its matrix was observed for a number of elements, particularly cobalt and manganese.

Copellen, Conzemius and Svec [49] measured 12 impurities electrically and photographically in 8 National Bureau of Standards iron standards. The photographic data for most of the elements gave average values with average deviations clustered near 20 percent.

Other measurements indicate that Relative Sensitivity Coefficients determined from standard samples have standard deviations that usually are not below 30 percent and may be above 50 percent.

A number of theoretical calculations [18] of Relative Sensitivity Coefficients have been made but the uncertainty in the present experimental values makes comparisons difficult.

The certified values, for the components in a standard sample, are average values for the volume sampled by the particular technique employed in establishing this standard, and these values tell nothing about the distribution of components within this volume. The use of any standard sample in any analysis is based on the assumption that the





components are homogeneously distributed on the scale appropriate to the technique employed, i.e., that the volume of the standard that is sampled accurately represents the standard sample.

But many of the standard samples that have been employed in spark source mass spectrometry have been standardized by techniques requiring substantially larger volumes than that sampled by the spark source.

Measurements supporting or refuting the above assumption of homogeneity are important. This problem has been treated by Halliday [20] and his collaborators. The homogeneity requirement becomes more stringent for samples of higher impurity concentration since a smaller sample is consumed by the spark. For impurities in the 10 to 100 ppma range, the linear dimensions of the sample volume consumed are in the range 15 to 300 microns [18].

This homogeneity requirement can be circumvented in two quite different ways. Samples in the form of solid cylinders are rotated about their respective axis by appropriate arrangements [56]. In this way, the spark samples an area large enough so that the volume consumed is representative of the gross sample. This technique is of course only applicable to samples that are available in cylindrical form. In the second technique the sample consumed is increased by continuous running of the spark but turning the ion beam on only intermittently [57]. This is a deliberate debasement of the sensitivity in terms of the amount of sample needed for an analysis. For sufficiently small samples this practice can only be employed at the expense of detection sensitivity. Because these techniques for circumventing sample inhomogeneities have limited applicability, the problem of homogeneity of standards and unknown samples remains one of considerable importance.

## VII. Precision Capabilities of Spark Source Technique

The generally large scatter particularly in inter-laboratory comparisons of samples has led to questions about the precision with which ion beams can be measured with spark source double focusing mass spectrographs. The author undertook measurements with an MS7 Mattauch and Herzog geometry instrument using Ilford Q2 photographic plates. As pointed out earlier, the ions of the various components of a sample do not always accurately represent the solid sample. Moreover, this misrepresentation may fluctuate in an uncontrolled way. Furthermore minor components may not be homogeneously distributed in a sample. In order to circumvent these uncertainties, the measurements were made on the major component mass lines of reasonably pure elements. In this way, a fixed fraction of the major component ions that are electrically measured at the monitor electrode ( $S_3$  in Fig. 1) are simultaneously recorded on the photographic plate.

Samples of platinum, tantalum, and tin were tested principally because they have isotopes whose relative abundances were appropriate

for these tests. Using dual sample holders, 12 platinum and 12 tantalum or tin replicate exposures were recorded on a given photographic plate under specified conditions.

From the optical transmission profile the ion peak intensity and the half width (width at half peak intensity) were obtained with the aid of a calibration curve. The product of these was taken as the photographic measure of the ion charge of a specific mass line of a particular isotope. Since multiply charged atomic ions and molecular ions are formed, their contribution must be considered. In practice the sum of the singly and doubly charged ions was assumed to be adequate since this sum comprised about 95 percent of the total ionization.

The 12 replicate spectra from each of the 2 elements on a given plate yield an average value and standard deviation for the number of ions of the particular isotope in question. These data are summarized in Table 3 giving the plate number, the corresponding isotopes of the platinum-tantalum comparison or the platinum-tin case as well as the quantity  $E$  for the monitor measure of the exposure in coulombs. The quantity  $R$  is the photographic measure of the number of ions for the given isotope where  $I$  and  $W$  represent the peak ion intensity and half width as discussed earlier. The next 3 columns for platinum, tantalum, and tin respectively give the values of  $R/EF$  where  $F$  is the fractional abundance of the isotope in question.  $R/EF$  is a measure of the plate sensitivity for the particular element. The listed standard deviation described the fluctuations of  $(I^+{}^1W_1 + I^+{}^2W_2)$  about  $R$  since the exposure was terminated automatically when  $E$  reached its preset value. The last 3 columns give the contribution of the singly charged ion in terms of the total ionization as measured in these tests.

With the spark source, the ionization pattern—the distribution of the ions according to their charge—may fluctuate even though controllable parameters are kept constant. These data indicate that for tin the standard deviation in  $R/EF$  when  $R$  includes only the contribution of the singly charged ions might be almost as small as when the doubly charged ions are included in  $R$ , but in the case of tantalum the standard deviation probably would be larger.

The standard deviation values for the tin data range from 10 to 20 percent while that for the tantalum averages below 5 percent. Some of the platinum data gives standard deviations that average below 5 percent and the rest is in the 10 to 12 percent range. Inspection quickly reveals that it is the value of  $E$  that determines whether the standard deviation is high or low. When  $E = 1$  or  $2 \times 10^{-9}$ , it is below 5 percent not only for tantalum but also for platinum. On the other hand, when  $E = 3 \times 10^{-11}$  it is largely in the 10 to 20 percent range for platinum as well as for tin.

Among the factors that contribute to the fluctuations summarized in Table 3 are the following: (1) the precision with which the integrating circuit measures monitor charge, (2) the precision with which the ratio

TABLE 3. Quantitative analysis of solids from MS-7 photographs of mass spectra.

Plate	Isotope measured	Monitor exposure in coulombs	$I^{+1}W_1 + I^{+2}W_2$	Pt		Ta		Sn		S.D. %	S.D. %	Pt	Ta	Sn	
				R/EF	S.D. %	R/EF	S.D. %	R/EF	S.D. %						$\frac{I^{+1}W_1}{I^{+1}W_1 + I^{+2}W_2}$
332	Pt 190	$1 \times 10^{-9}$	195.5	1.55	3.2	1.55	3.2	1.55	3.2						
332	Ta 180	$1 \times 10^{-9}$	146.8			1.19	3.1						.65		
333	Pt 190	$1 \times 10^{-9}$	227.5	1.79	5.6	1.79	5.6	1.79	5.6				.83		
333	Ta 180	$1 \times 10^{-9}$	147.5			1.20	4.3						.71		
346	Pt 192	$3 \times 10^{-11}$	418.2	1.79	10.0	1.79	10.0	1.79	10.0				.84		
346	Sn 114	$3 \times 10^{-11}$	580.0					2.98	17.8					17.8	.96
346	Sn 115	$3 \times 10^{-11}$	315.7					3.10	19.8					19.8	.96
347	Pt 192	$3 \times 10^{-11}$	(1842.0)					12.4					.88		
347	Sn 114	$3 \times 10^{-11}$	607.5					3.12	10.5					10.5	.97
347	Sn 115	$3 \times 10^{-11}$	318.0					3.11	12.0					12.0	.97

369	Pt 190	$2 \times 10^{-9}$	539.0	2.12	3.7						.85
370	Pt 190	$2 \times 10^{-9}$	562.7	2.22	4.6						.91
370	Ta 180	$2 \times 10^{-9}$	347.1			1.41	5.2				.62
374	Pt 190	$1 \times 10^{-9}$	193.5	1.52	3.0						.88
374	Ta 180	$1 \times 10^{-9}$	124.7			1.01	5.2				.66
376	Pt 192	$3 \times 10^{-11}$	362.2	1.55	4.0						.88
376	Sn 115	$3 \times 10^{-11}$	185.4					1.82	11.6		.97
377	Pt 192	$3 \times 10^{-11}$	467.6	2.00	11.4						.94
377	Sn 115	$3 \times 10^{-11}$	205.8					2.02	12.2		.96
Average Values of R/EF											
				1.8	15	1.2	14	2.7	14		

of charge passed by the monitor to that intercepted by the monitor is maintained, (3) the variation in sensitivity of the photographic plate. These three factors are independent ones and therefore the fluctuations that each introduces must be within that given by the standard deviations of Table 3 which in many cases are below 5 percent. However, for monitor exposures of  $3 \times 10^{-11}$  coulombs and presumably for still smaller values, the fluctuations in  $R$  arise principally from those in  $E$ , i.e., the precision with which the integrating circuit measures monitor charge is degraded to a standard deviation of 10 to 20 percent.

Because it was somewhat unexpected, it is of special interest that the fluctuations in sensitivity along the 2 inch width of the Ilford Q2 plates are within the 5 percent standard deviation of Table 3. This uniformity within a given plate is accompanied by comparably small fluctuations in sensitivity from plate to plate<sup>2</sup> as shown by the  $R/EF$  values for any 1 of the 3 elements tested. As shown at the bottom of Table 3, the average  $R/EF$  value for such data carries a standard deviation of about 14 percent.

Every plate containing platinum and tantalum spectra consistently gives higher  $R/EF$  values for the platinum. This is contrary to the  $M^{-x}$  mass dependence discussed in Section V.C. and lends credibility to the suggestion there that some elements may not conform to this simple mass dependence. On the other hand, the platinum-tin plates consistently give higher  $R/EF$  values for tin in qualitative agreement with the simple mass dependence  $M^{-x}$ . In summary, these measurements indicate that under optimum conditions the MS7 spark source double focusing mass spectrograph with Ilford Q2 plates can measure ion beams with a precision of less than 5 percent standard deviation. In addition, the evidence that the uniformity of these photographic plates was within this precision was reassuring.

Many studies have demonstrated that even better precision can be obtained in photographic measurements of isotopic abundance ratios. However for such cases a small scale plate uniformity is sufficient. Therefore such tests do not establish the large scale (2 inch) plate uniformity indicated by Table 3.

### VIII. The Homogeneity Problem

Having established the precision with which ion beams could be measured by this technique, the measurements were extended to elemental dopants in Johnson, Matthey copper standard samples CA2 and CA4. In these tests a platinum probe electrode was sparked to the copper electrode which was electrically tied to the dc accelerating voltage. After each exposure of a replicate series similar to those sum-

---

<sup>2</sup> The  $R/EF$  value for platinum in plate 347 is not given as the  $R$  value is obviously high. Probably the monitor exposure was inadvertently made greater than the indicated value by a factor of 4 or 5.

marized in Table 3, the copper electrode was moved about 0.5 mm so that a fresh spot on the copper was sampled by the platinum probe.

Preliminary experiments demonstrated that the platinum ions contributed not more than 5 percent of the ion sample to the detector. That this nearly negligible contribution by the platinum ions persisted was verified by interspersing 4 appropriately short exposures among the replicate exposures on each plate.

Preliminary measurements indicate that the replicate exposures yield average values for the dopants with standard deviations between 5 and 12 percent in the case of the CA2 standard. For the CA4 sample, the corresponding standard deviations were in the 10 to 20 percent range. However on one plate, the CA4 chromium dopant gave a standard deviation of 45 percent.

In addition to the three factors itemized in Section VII, others that could contribute to the fluctuations, characterized by the above standard deviations, are the following: (1) The dopants may not be homogeneously distributed in the copper. (2) Any misrepresentation in the ion sample, due to selectivity in the vaporization and/or ionization of the dopants in the copper, may fluctuate in an uncontrolled way. All of these five factors are independent and therefore the fluctuations that each introduces on a statistical basis must be within that given by the above standard deviation values.

The measurements in progress on these copper standards suggest that the standard deviation for some of the dopants in CA2 may not be significantly higher than the upper limit of 5 percent indicated in Table 3 for major components and that the sample homogeneity is within this limit. For the other dopants, the sample homogeneity is within the 12 percent limit. The CA4 measurements suggest that in this standard, the dopant inhomogeneities may be as high as 20 percent and in the specific case of chromium it may be as high as 45 percent. Evidence for comparable inhomogeneities was observed by J. R. Woolston [57a] in similar replicate tests on another rod of this copper CA4 standard.

It should be remembered that in tests of this sort, the spark source mass spectrograph determines the degree of homogeneity of a sample on exactly the scale desired for spark source mass spectrographic work.

### IX. Standard Sample Needs and Possibilities

A wide array of standard samples with components not only in the ppm range but also well below this are seriously needed for spark source mass spectrometry. Furthermore the degree of homogeneity must be appropriate to this spark source technique.

Standards in the ppb range are needed to supplement and confirm detection sensitivities derived by other methods [58]. For these purposes samples consisting of dilute solutions of selected elements in appropriate matrices should be useful. The selected elements should

be polyisotopic ones with a spread in relative abundances and those with an isotope of very low abundance would be particularly useful. The doping level could be high enough to determine the absolute value of the concentration by established techniques with good accuracy, while the low abundance isotopes reach into the low ppm and even into the ppb region. Such a standard sample consisting of a dilute solution of platinum in gold [36] has been used by the author. Elements like sulfur, osmium, barium, tellurium, tantalum and calcium have equally attractive distributions in relative abundance.

Perhaps the more urgent need for standard samples is for the accurate determination of Relative Sensitivity Coefficient (RSC) values. For these purposes two classes of standard samples are needed. The first would be an array of non-interfering elements in a matrix. These elements need not be simultaneously in a given matrix since this may not be feasible in many cases. The second would be an array of the same elements in a number of different matrices which again may have either simultaneous or individual element doping.

Such an array of standards, with dopants and matrices composed of elements with properties covering a range of values, should help to answer the following questions. Is the RSC of element  $x$  the same in many or all matrices? Could empirical relations be established to predict the RSC of element  $x$  in matrix  $y$ ? It would be of considerable importance, if, from known properties of dopant and matrix or from empirical relations, it were possible to calculate the RSC of element  $x$  in matrix  $y$  without the aid or need of a standard sample.

## X. Summary

1. Plate fogging from secondary products generated when the ion sample strikes the photographic emulsion results in a serious loss in detection sensitivity—a factor of 30 or more. Plate splitting although helpful is cumbersome at best. Efficient miniature ion collectors and/or emulsions insensitive to secondary products are needed.

2. The resolving power available in commercial instruments precludes the study of many elements in many matrices. The fraction of these excluded combinations would be diminished only slowly even with substantial increases in resolving power.

3. Heretofore, instrument line background of carbon, oxygen, hydrogen, nitrogen, etc., limited the detection of these elements in samples to a few ppma. Recent studies indicate that with partial pressures of about  $1 \times 10^{-9}$  torr, nitrogen, hydrogen and carbon can be detected at substantially lower values.

4. There may be appreciable departures from the simple  $(\text{Mass})^{-x}$  relation for the variation of emulsion sensitivity among the elements. This could introduce serious errors in determining the concentration of an element in a matrix.

5. Since the ionization pattern for a dopant and its matrix may be significantly different, the ratio of singly charged ions of dopant and matrix may give an erroneous measure of the dopant concentration.

6. In general, the composition of the ion sample presented to the detector does not accurately represent the composition of the solid sample. Accurate values of Relative Sensitivity Coefficients (RSC) to correct for this misrepresentation are needed.

7. The scatter in RSC values, obtained by comparing spark source mass spectrographic analyses with the certified values of the standard sample, is serious.

8. In general the standards used were based on analytical techniques requiring samples that were substantially larger than the spark source technique consumes. Information on the homogeneity of such standards on the spark source technique scale is needed.

9. Under optimum conditions with this spark source technique, an ion beam can be photographically measured with a precision of less than 5 percent standard deviation.

10. Replicate measurements indicate that the variation in sensitivity of Ilford Q2 plates is within a standard deviation of 5 percent.

11. Items 9 and 10 indicate that the homogeneity of a sample on the scale needed by the spark source technique can be established by replicate measurements with the spark source technique itself.

12. Replicate measurements in which a platinum probe sampled different areas of a copper standard indicate that the minor components were not all homogeneously distributed.

13. A wide range of standard samples is needed. The homogeneity of these needs to be appropriate to the spark source technique. Dopant concentrations should be in the ppma to ppba range. Dilute solutions of selected polyisotopic elements in compatible matrices are suggested for some standards.

14. The accuracy and precision of the spark source technique at present is not adequate to characterize the role of trace impurities in the physics and chemistry of solids. Two examples of the latter given at the beginning of this paper illustrate this inadequacy. A tenfold change in the concentration of cobalt in gold produces a 100 fold change in its thermoelectric power. A tenfold change in the concentration of manganese and iron in titanium changes its superconductivity transition temperature by a factor of 2.5.

## XI. Conclusion

The background problem remains a serious one. Probably plate fogging by secondary products can be adequately circumvented. Ion scattering by residual gases might be appreciably reduced by faster pumping and/or the introduction of a helium cold finger in the magnetic sector. These two pumping aids also near the spark source might sub-

stantially reduce the instrument background lines of carbon, oxygen, and nitrogen.

It might be possible to increase the transmission of these double focusing mass spectrographs in two ways. It might be done by ion focusing techniques since it is unlikely that the present simple geometry of the spark source yields the optimum current. Another possibility would be to introduce ion energy bunching techniques.

A substantial increase in transmission could be very useful. Times required for exposures would be correspondingly reduced. This would be important for long exposures and for microsamples. An alternative use of the increased transmission would be to reduce  $S_2$  and  $S_3$  of Figure 1. The smaller solid angle and the smaller energy band involved in the double focusing might yield an increase in resolving power. This could be very useful in selected cases in spite of an undesirable selectivity that might be introduced by the narrower energy band passed by  $S_3$ .

The variation in emulsion sensitivity among the elements needs further investigation in view of the wide gaps in the experimental data and the possible consequences of the ion implantation suggested in Section V.C. Because the contribution of multiply charged ions to the total ionization is not generally negligible, the dependence of emulsion sensitivity on ion energy is important particularly in view of the discontinuities in this relation reported by Woolston, Honig and Botnick [59].

The spark source mass spectrographic technique is capable of measuring the ions of a given mass/charge in an ion sample with a precision of 5 percent standard deviation. With a standard sample that is homogeneous on the spark source scale, the degree by which the ion sample misrepresents this standard sample, should be measurable with corresponding precision and accuracy. The present accuracy and precision may or may not be improved when these conditions are fulfilled. If they are not improved, must one then conclude that there are uncontrollable parameters in spark source mass spectrometry that limit the accuracy and precision of solids analysis to the present unsatisfactory values?

## XII. References

- [1] Morrison, G. H., Trace Analysis—Physical Methods, Interscience Publishers, New York, 1965.
- [2] Slichter, W. P., and Kolb, E. D., Phys. Rev. **87**, 527 (1952).
- [3] Bemski, G., and Struthers, J. D., J. Electrochem. Soc. **105**, 588 (1958).
- [4] Ultra High Purity Metals, American Society for Metals, Metals Park, Ohio (1962).
- [5] Pearson, W. B., Reference 4.
- [6] Schaub, B., and Cabane, G., Compt. Rend. 444 (1963).
- [7] Matthias, B. T., Geballe, T. H., Corenzwit, E., and Hull, G. W., Jr., Phys. Rev. **129**, 1025 (1963).
- [8] Falge, R. L., Jr., Phys. Rev. Letters **11**, 248 (1963).
- [9] Rutter, J. W., and Aust, K. T., Trans. Met. Soc., A.I.M.E. **218**, 682 (1960).

- [10] Hausner, H. H., and Roboff, S. B., *Materials for Nuclear Reactors*, Reinhold Publishers, New York, 1955.
- [11] Schumacher, E. E., *Trans. A.I.M.E.* **188**, 1097 (1950).
- [12] Hannay, N. B., in Reference 1—Pfann, W. G., *Zone Melting*, Wiley Publishers, New York, 1965.
- [13] Hannay, N. B., *Rev. Sci. Instr.* **25**, 644 (1954).  
Hannay, N. B., and Ahearn, A. J., *Anal. Chem.* **26**, 1056 (1954).
- [14] Hickam, W. M., *Phys. Rev.* **74**, 1222A (1948); *ASTM Bull.* **149**, 17 (1953); Honig, R. E., *Anal. Chem.* **25**, 1530 (1953); *J. Chem. Phys.* **22**, 1610 (1954).
- [15] Inghram, M. G., *ASTM Bull.* **149**, 1 (1953).  
Inghram, M. G., *J. Phys. Chem.* **57**, 809 (1953).
- [16] Honig, R. E., *J. Appl. Phys.* **29**, 549 (1958); also Reference 18.
- [17] Dempster, A. J., *Proc. Phil. Soc.* **75**, 755 (1935); *Rev. Sci. Instr.* **7**, 46 (1936).
- [18] Honig, R. E., in *Mass Spectrometric Analysis of Solids*, Ahearn, A. J., ed., Elsevier Publishers, Amsterdam, 1966.
- [19] Hannay, N. B., *Science* **134**, 1220 (1961).
- [20] Halliday, J. S., Swift, P., and Wolstenholme, W. A., in *Advances in Mass Spectrometry*, Vol. III, Mead, W. L., Editor, Institute of Petroleum Publishers, London, 1966.
- [21] Woolston, J. R., and Honig, R. E., *Rev. Sci. Instr.* **35**, 69 (1964).
- [22] Herzog, R., *Z. Physik* **89**, 447 (1934); Mattauch, J., and Herzog, R., *Z. Physik* **89**, 786 (1934); Mattauch, J., *Phys. Rev.* **50**, 617 (1936).
- [23] Guthrie, J. W., in Reference 18.
- [24] Guthrie, J. W., in Reference 18.
- [24a] Brown, R. A., Craig, R. D., James, J. A., and Wilson, C. M., *Conference on Ultra Purification on Semiconductor Materials*, Brooks, M. S., and Kennedy, J. F., Editors, MacMillan Publishers, New York, 1962, Duke, J. F., *ibid.*
- [25] Guthrie, J. W., in Reference 18.
- [26] Guthrie, J. W., in Reference 18.
- [27] Hickam, W. M., and Sweeney, G. G., in Reference 18.  
Guthrie, J. W., in Reference 18.
- [28] Elliott, R. M., Craig, R. D., and Errock, G. A., *Instruments and Measurements*, von Koch, H., and Lyungberg, G., Editors, Academic Press Publishers, New York, 1961.
- [29] Ahearn, A. J., and Malm, D. L., *Applied Spectroscopy* **20**, 411 (1966).
- [30] Mai, H., in *Advances in Mass Spectrometry*, Vol. III. Mead, W. L., Editor, Institute of Petroleum Publisher, London, 1966.
- [30a] Witmer, A. W., *Proceedings of the Sixth Annual MS7 Users Conference*, Manchester, England, March 28, 1966.
- [31] Kennicott, P. R., *Anal. Chem.* **38**, 633 (1966).
- [32] Honig, R. E., Woolston, J. R., and Kramer, D. A., presented at the 14th Annual Conference on Mass Spectrometry and Allied Topics, Dallas, March 1966.
- [33] Blosser, E. R., Battelle Memorial Institute, Columbus, Ohio, private communication.
- [34] Dornenburg, E., and Hintenberger, H., *Z. Naturforsch.* **14a**, 767 (1959).
- [35] Ahearn, A. J., and Thurmond, C. D., *J. Phys. Chem.* **66**, 575 (1962).
- [36] Ahearn, A. J., presented at the 11th Annual Conference on Mass Spectrometry and Allied Topics, San Francisco, 1963.
- [37] Consensus of American MS7 Users Conferences.
- [38] Socha, A. J., and Willardson, R. K., presented at the 14th Annual Conference on Mass Spectrometry and Allied Topics, Dallas, March 1966.
- [39] Owens, E. B., in Reference 18.
- [40] Franzen, J., and Hebeda, E., *Z. Naturforsch.* **17a**, 476 (1962).
- [41] Burlefinger, E., and Ewald, H., *Z. Naturforsch.* **16a**, 430 (1961).  
Owens, E. B., and Giardino, N. A., *Anal. Chem.* **35**, 1172 (1963).

- Wagner, H., *Ann. Physik* **7**, 189 (1964).
- Werner, H. W., *Philips Res. Repts.* **21**, 63 (1966).
- [42] Dejardins, M., private communication.
- [43] Hull, C. W., presented at the 10th Annual Conference on Mass Spectrometry and Allied Topics, New Orleans, 1962.
- [44] Paulson, P. J., and Branch, P. E., 14th Annual Conference on Mass Spectrometry and Allied Topics, Dallas, 1966.
- Kennicott, P. R., *ibid.*
- [44a] Kennicott, P. R., private communication. Skogerboe, R. K., Harrington, W. L., and Morrison, G. H., *Anal. Chem.* **38**, 1408 (1966).
- [45] Woolston, J. R., Honig, R. E., Reference 21.
- [46] Gorman, J. G., Jones, E. J., and Hipple, J. A., *Anal. Chem.* **23**, 438 (1951).
- [47] Ahearn, A. J., presented at the 11th Annual Conference on Mass Spectrometry and Allied Topics, San Francisco, 1963.
- [48] Harrington, W. L., Skogerboe, R. K., and Morrison, G. H., *Anal. Chem.* **37**, 1481 (1965).
- [49] Capellen, J., Conzemius, R. J., and Svec, H. J., presented at the 13th Annual Conference on Mass Spectrometry and Allied Topics, St. Louis, 1965.
- [50] Dejardins, M., Corning Glass Works, Corning, N.Y., private communication.
- [51] Goshgarian, B. B., and Jensen, A. V., presented at the 12th Annual Conference on Mass Spectrometry and Allied Topics, Montreal, 1964.
- [52] Aulinger, F., private communication to Honig, R. E., *Advances in Mass Spectrometry*, Vol. III, Mead, W. L., Editor, Institute of Petroleum Publishers, London, 1966.
- [53] Chupekhin, M. S., and Glavin, G. G., *Zh. Anal. Khim* **18**, 618 (1963) (translated by Assoc. Tech. Services, East Orange, N.J.).
- [54] Klein, H. M., and Larrabee, G. B., Pittsburgh Conference on Analytical Chemistry and Applied Spectroscopy, Feb. 21-25, 1966.
- [55] Ahearn, A. J., Trumbore, F. A., Frosch, C. J., Luke, C. L., and Malm, D. L., presented at the 14th Annual Conference on Mass Spectrometry and Allied Topics, Dallas, 1966.
- [56] Blosser, E. R., Battelle Memorial Institute, Columbus, Ohio, private communication.
- Franzen, J., Max Planck Institute f. chemie, Mainz, Germany, private communication.
- Aulinger, F., Proceedings of the Sixth Annual MS7 Users Conference, Manchester, England, March 28, 1966.
- [57] Franzen, J., Schuy, K. D., and Hintenberger, H., presented at the 12th Annual Meeting on Mass Spectrometry and Allied Topics, Montreal, 1964.
- [57a] Woolston, J. R., private communication.
- [58] Hull, C. W., and Blanchard, C. G., presented at the 13th Annual Conference on Mass Spectrometry, St. Louis, 1965.
- Elliott, R. M., and Swift, P., presented at the 13th Annual Conference on Mass Spectrometry, St. Louis, 1965.
- [59] Woolston, J. R., Honig, R. E., and Botnick, E. M., presented at the 14th Annual Conference on Mass Spectrometry and Allied Topics, Dallas, 1966.

# MASS SPECTROSCOPY

## Contributed Papers and Discussion

E. B. OWENS

*Lincoln Laboratory,\* Massachusetts Institute of Technology  
Lexington, Massachusetts 02173*

### I. Introduction

We have six contributed papers to discuss. Four of the papers deal with analytical applications, and we will discuss these four first. Each paper has features which we might profitably consider, and some of these points of discussion are found in more than one paper. In order to give due credit to each contributor, I propose to present very briefly the major contribution of his paper. Then I will discuss the other ideas contained in these papers in a general fashion. The two remaining papers will then be discussed.

At the close of my remarks, each contributing author will have the opportunity to make additional comments if he feels that my presentation has not done justice to his paper. After these additions to the presentation, I will bring up one by one points from these papers for general discussion.

### II. Analytical Applications

The analysis of trace impurities in beryllium and uranium by spark source mass spectrometry is described in the paper by Bourguillot, Cavard, Cornu, and Stefani. They used the usual system of sparking solid, self electrodes and, with minor modifications, rather generally accepted methods of densitometry and data handling which incorporate most of the corrections discussed by Dr. Ahearn. They report very good results for the analysis of uranium for aluminum, silicon, manganese, chromium, iron, nickel, and copper. These results were obtained using sensitivity coefficients derived from the analysis of known samples of uranium. The average error given is 19% compared to the value obtained from chemical analysis. For the beryllium analysis, they evidently did not have known samples from which they could obtain sensitivity coefficients. This may explain the large errors of their reported results. The average error in this case was 37%. This paper is an excellent example of the work that can be done when standards are available.

---

\*Operated with support from the U.S. Air Force.

In his paper entitled "Trace Impurity Analysis by Spark Source Mass Spectrometry" Desjardin discusses some rather novel ways of handling samples of various forms. A graphite film may be evaporated onto the nonconducting film which is to be analyzed or the graphite film may be put down as a mesh instead of a solid film. Special systems are shown to shorten the distance between the supporting conductor and the spot of sparking, thereby allowing the use of insulators as self electrodes. This paper uses the same methods of densitometry and data handling as did the previous paper except that a computer is used in the calculations. The paper reports values for the sensitivity coefficients of a number of elements in various matrices. These will be discussed later. The paper is a good illustration of the efforts that have been made to increase the versatility of the spark source method.

In a paper on trace analysis in oxidic matrices by solids mass spectroscopy Oblas, Bracco, and Yee discuss a method using pressed electrodes made from mixtures of powdered oxide samples, graphite, and an internal standard. Sensitivity coefficients were obtained from the analysis of synthetic standards. The densitometry and data handling methods conform to accepted practices and include corrections for line width and the mass effect on photoplate sensitivity. The paper reports a relative deviation of 20% of the true values on the analysis of other synthetic samples, but the data of one of their tables showed that much larger errors were sometimes encountered. The techniques used for powdering samples are well illustrated in this paper.

The paper by Strock and Oblas on the spark source mass spectrometric analysis of refractory metals gives preliminary results on the analysis of tungsten wire sparked as the metal, and as the oxide mixed with graphite and pressed to form electrodes. Sensitivity coefficients are reported for seven elements, apparently from the analysis of known samples; but no comparative analytical results are given from which the accuracy of the analysis could be evaluated. The preliminary results on the carbon, oxygen, nitrogen, and hydrogen content indicated correlation with certain physical properties. This paper is a good reminder of the fact common to most trace analysis methods, namely, that even preliminary analytical results often are found to have useful correlations with some other properties of the material investigated.

### III. The State of The Art—Improving Accuracy

Before I begin to discuss the other ideas these papers present, I would like to make a few comments not limited to the papers of this symposium but including all current publications in spark source mass spectroscopy. The work in analytical applications can be classified as either semi-quantitative or quantitative. The semi-quantitative work assumes and accepts large errors. Many papers give data to indicate the size of the errors for a given matrix. Others correlate the analytical data with

other properties of the materials. Both types of paper are valuable despite the large errors.

Much of the work in the field today is aimed at reducing the large analytical errors, i.e., at making spark source mass spectroscopy truly quantitative. In this endeavor people are investigating the relative ion yields in the spark discharge, the uniformity of transmission of all ions through the instrument, the properties of the photoplate as an ion detector, and methods of interpreting the data on a photoplate. The present state of the art has moved away from the large error factors of semi-quantitative analysis and is moving encouragingly along the path to quantitative analysis. I make these general remarks now to place the following discussions in proper perspective. Much of what we will discuss will be these efforts to reduce the analytical error.

#### A. SENSITIVITY COEFFICIENTS

Several of the papers that we had considered use the term "sensitivity coefficient". In Dr. Ahearn's review this sensitivity coefficient is defined as the ratio of the concentration of an element as determined by mass spectroscopy to the true concentration. An element for which the method consistently gives high answers has a sensitivity coefficient greater than one. The method has high sensitivity for that element.

This high sensitivity can be due to one or more of a number of factors. The spark discharge may produce a disproportionately large amount of ions for an element. Addink [1]<sup>1</sup> has suggested that the high ion yield may be a function of the relative volatility and diffusion coefficients of the elements. He has had some success in calculating sensitivity coefficients from these properties. Oblas, Bracco, and Yee feel that their data show good agreement between the sensitivity coefficients and the boiling points. The paper of Bourguillot and coworkers state that a number of parameters were carefully chosen to avoid a selective effect. It would be of great value if during the discussion they would tell us which variables had the greatest effect on selectivity and what tests they made to evaluate such effects.

Dr. Ahearn has pointed out that selective transmission of ions through the mass spectrograph may also contribute to high or low sensitivity coefficients. Franzen and Hintenberger [2], and Woolston and Honig [3] have shown that the ions of the various elements do not all have the same energy when they leave the spark discharge area. Consequently, different energy spectra are formed for the various elements as the ions pass through the electrostatic analyzer. Since the energy slit permits only a small portion of the energy spectrum to pass into the magnet field, the elemental composition of the ion beam passing into the magnetic field is likely to be quite different from the composition of the ion beam which passed through the electrostatic field. The transmission through

<sup>1</sup> Figures in brackets indicate the literature references at the end of this paper.

the electrostatic field and energy slit is higher for some elements than for others. The ratio of these transmissions will stay constant only if the energy spectrum relationships stay constant. However, the high degree of reproducibility achieved by a few workers shows that the relative instrumental transmission and the relative ion yield can be held constant when the sparking parameters are carefully controlled.

We have seen so far that relative sensitivity coefficients are produced by relative ionization factors and relative instrument transmission factors. We must add to this list the relative response characteristics of the photoplate. Fortunately, the response characteristics of the photoplate can and have been evaluated. We know how to calibrate the photoplate, how to correct for line width and background, and how to correct for the effects of ion mass and energy on the photoplate response [4]. However, some workers use none or only a few of these corrections. This, of course, affects their accuracy and, adds appreciably to the large differences seen in the comparisons of relative sensitivity coefficients.

In terms of quantitative analysis, a relative sensitivity coefficient value is unique for a given element in a given sample, for a given set of sparking parameters, for the transmission characteristics for a given instrument, and for a given method of photoplate evaluation. Change any one of these factors and you change the sensitivity coefficient value. The values are not interchangeable between laboratories. There are some who think they are interchangeable and that changing the matrix has no effect. But they are talking about semi-quantitative analysis. Desjardin states in his paper that most of the elements for which he presents data possess a sensitivity coefficient which appears to be independent of matrix. But a look at the data in one of his tables shows the semi-quantitative nature of his observation. We have seen from Bourguillot's paper that a quantitative accuracy of 19% can be achieved with sensitivity coefficients obtained from the analysis of known samples of the same matrix as the unknown.

## B. PHOTOPATE EVALUATION

As was mentioned previously, there is disagreement among the many laboratories on the number of corrections used in evaluating photographic data. We see some of this disagreement in the papers in this symposium. In one paper the authors correct for the width of some but not all lines. And in evaluating lines due to polycharged ions they omit corrections for the fact that the photoplate response increases linearly with ion energy. Other authors omit corrections for the effect of mass on photoplate response. It has been shown that these corrections are large [5] and they must be considered even in semi-quantitative work if the total errors are to be kept within factors of 2 or 3.

### C. ION CHARGE DISTRIBUTION

Bourguillot and co-workers and Strock and Oblas point out that poly-charged ions may constitute a significant portion of the total ion beam. It is possible that for one element the singly charged ions may be 80% of the ion yield while for another they may be only 50%. Errors that might result from this ion charge distribution are avoided by measuring the lines of singly, doubly, and maybe even the triply charged ions and summing to get the ion yield for each element.

### IV. Computer Use in Calculations

In their paper Paulsen and Branch describe an electronic analog computer for measuring intensity areas on mass spectrographic plates. Similar computers have appeared in the past few years with at least two companies producing them commercially. They differ in the number of corrections that we have discussed that the computer will make on the photographic data. The computer described in this paper corrects for the background, the non-linearity of the photoplate response, and the line width or more exactly the line profile.

### V. Molecules Found in Spark Spectra

The paper by Doan discusses the existence of metal carbide molecules in the vapor state. While this paper does not deal with trace characterization in the sense of trace impurity analysis, some comments on the theory presented on the spark discharge might be worthwhile at this time. Doan suggests that a quasi-steady state vaporization exists in the spark, that a reasonably constant temperature for the specimen can be maintained, and that the specimen continues to vaporize between each spark.

These hypotheses are difficult to reconcile with the results of the time resolved studies reported by Franzen [4]. It was shown that the more volatile elements were ionized during the early part of each discharge half cycle, and the less volatile elements were ionized later in the same half cycle. This cycle of ionization was repeated for each discharge half cycle indicating a repetitive, wide excursion of temperature. In other studies [6] light detectors put at the window of the mass spectrograph source chamber indicate the emitted light completely disappears between each half cycle of the discharge. These results do not seem consistent with the long term type of equilibrium Doan suggests.

However, some studies [7, 8, 9] can be interpreted as indicating the existence of very short periods of quasi-equilibrium in the vapor phase within each half cycle of the rf spark under certain conditions of operation. It seems very unlikely that at any time during the half cycle there exists equilibrium between the solid and the vapor phases. I would suggest that some attempt be made to reconcile these apparently contradictory theories.

## VI. Quantitative Mass Spectrography

I would like to discuss now some areas of development which I feel are most encouraging in the effort toward quantitative mass spectrography.

We have come to realize that the rf-spark ion source is both tedious to operate and difficult to control to the degree that good reproducibility can be obtained. A pulsed dc arc discharge has been investigated as an ion source by Honig [10] and by Franzen [11]. They report that with this new source good reproducibility is more easily and more consistently achieved. I would not be surprised to see this source replace the rf spark, but today I know of only one instrument manufacturer that offers it commercially.

Some investigators [12, 13] have reported considerable improvement in precision when they rotate the electrodes continuously during the sparking. A good part of this improvement could be due to the elimination of inhomogeneity effects by this constant introduction of new surface into the spark gap. This is a technique used for years by emission spectroscopists.

Another area of development has to do with the problem of standards. It appears inescapable that for quantitative accuracy we must have standards that match our samples in chemical composition and in physical form. The very small volume of the sample consumed in the ionizing discharge imposes stringent requirements on the homogeneity of both samples and standards. Therefore, it is understandable that it may be some time before our hosts, the National Bureau of Standards, can supply us with standards having the homogeneity required. But I suggest that it is not necessary that we wait.

Dr. Nicholls of the University of Manchester [14] has shown that by grinding and decomposition in a flux, he can prepare very homogeneous samples from inhomogeneous mineralogical specimens. And by this same technique he can prepare matching standards from reagent grade chemicals. In this manner Dr. Nicholls has achieved relative standard deviations of about 5% of the true value.

It seems to me that we should apply this technique to all of our samples, be they metals, semiconductors, or insulators. Those of us who have done trace determinations by emission spectroscopy will remember that some of the best quantitative results were obtained by applying this same approach to the preparation of samples and standards. It will require more work, and some sensitivity may be lost. But in this way, we should be able to overcome inhomogeneity and standardization problems and move further along that road toward real quantitative mass spectroscopy.

## VII. Comments from the Authors and Discussion from the Floor

Desjardin made some comments on the sensitivity coefficients found in his paper and in the paper by Bourguillot et al. He stated that the

32% reproducibility of the sensitivity coefficients found for manganese in a number of matrices constituted, in his opinion, quantitative results. Later experiments using more corrections on the photographic data produced very similar values for these coefficients. He stated that the additional corrections reduced the scatter but did not change the value itself. Desjardin said he was very optimistic about the method and predicted that by this method absolute analysis would some day be possible.

Bourguillot said that because of the language difficulties he could not reply immediately to the questions raised about his paper by the rapporteur. He asked those interested to consult his publications.

R. E. Michaelis (NBS) called attention to the NBS Miscellaneous Publication 260 series containing reports of investigations of homogeneity on certain NBS standard materials. He said that the NBS Steel Standard Material No. 461 had been found to be sufficiently homogeneous to be used for any current analytical technique. Other materials have also been investigated and the results reported in the 260 series. He then called attention to the NBS OSRM Bulletin No. 6 dealing with the needs for standard reference materials in spark source mass spectroscopy and invited comments from the participants.

Strock called attention to the very high results for potassium reported in his paper. These results varied between 2 and 15 times the true concentration depending perhaps on the heat treatment the sample had experienced. R. E. Honig (RCA) commented that he thought that these high values were the results of thermal ionization. The boiling off of elements of low ionization potential from a material of high work function (such as tungsten) could cause the results Strock reported.

R. J. Conzemius of Iowa State University called attention to the advantages of using electrical detectors in place of the photographic plate. They have achieved a precision of 1% in the analysis of the NBS 461 steel standard with electrical detection.

W. Reuter (IBM) stated that he gets results that agree well with the true values for a variety of materials. He asks then how can the variations of sensitivity suggested by Dr. Ahearn and the rapporteur be reconciled with his consistently good results.

Concerning the variability of sensitivity coefficients, Desjardin reported that he obtained different values for the same samples on two different instruments. He felt that an instrument factor must be used with a general sensitivity coefficient.

H. Kaiser (Dortmund) remarked that the problems we are discussing today closely parallel the problems that confronted emission spectroscopists some years ago. He stated that, because of the complexity of the problem and in particular the rf spark, he doubted that absolute analysis would be possible.

P. R. Kennecott (G.E.) stated that absolute values are not always needed if the precision is good. Relative values are useful.

Smales (AERE) expressed some disappointment that only spark discharges were discussed as ion sources and gave an example of some excellent quantitative results achieved by an isotope dilution method using a thermal ion source. The rapporteur replied that perhaps the reason for the emphasis on spark source was due to its relatively uniform sensitivity for all elements. Kaiser stated that he too had gotten good results with thermal ion sources. He then pointed out that the method of standard additions is one way to get around the standards problem.

Doan stated that some of the questions about his paper might be explained by the fact that he operated the spark so as to get his electrodes very hot, instead of the usual mode of operation.

W. W. Meinke (NBS) remarked that as Michaelis has said, the NBS has a program to develop standards for spark source mass spectroscopy. But the NBS must know the needs of the people in this field in order to choose the most important material first. The rapporteur replied that the answer to the Bureau's questions depended greatly on the answer to the question of interchangeability of sensitivity coefficients. If any grouping of elements or matrices is possible, the task of standardization is simplified somewhat. However, he believed that we do not have today sufficient knowledge to answer this question.

### VIII. References

- [1] Addink, N. W. H., *Z. Anal. Chem.* **206**, 81 (1964).
- [2] Franzen, J., and Hintenberger, H., *Z. Naturforsch.* **18a**, 397 (1963).
- [3] Woolston, J. R., and Honig, R. E., presented at the 11th Annual Conference on Mass Spectrometry and Allied Topics, San Francisco, May 1963.
- [4] Franzen, J., *Z. Naturforsch.* **18a**, 410 (1963).
- [5] Owens, E. B., in *Mass Spectroscopy of Solids*, Ahearn, A. J., ed., Elsevier, Amsterdam, 1966, pp. 56-110.
- [6] Owens, E. B., and Giardino, N. A., *Anal. Chem.* **35**, 1172 (1963).
- [7] Franzen, J., Schuy, K. D., and Hintenberger, H., presented at the 12th Annual Conference on Mass Spectrometry and Allied Topics, Montreal, June 1964.
- [8] Franzen, J., and Hintenberger, H., *Z. Naturforsch.* **16a**, 535 (1961).
- [9] Chupakhin, M. S., *Sovrem. Metody Analiza, Metody Issled. Khim. Sostava i Stroeniya Veshchestv*, Akad. Nauk SSSR, Inst. Geokhim. i Analit. Khim (1965), 33.
- [10] Honig, R. E., Glass, S. S., Woolston, J. R., *Proceedings 6th International Conference on Ionization Phenomena in Gases*, Paris, 1963. Vol. 2, pp. 209-216.
- [11] Franzen, J., and Schuy, K. D., *Z. Naturforsch.* **20a**, 176 (1965).
- [12] Franzen, J., Max Planck Institute für Chemie, Mainz, Germany, private communication
- [13] Habfast, K., Atlas Mess-und Analysen Technik. GMBH, Bremen, Germany, private communication.
- [14] Nicholls, G. D., *Analysis of Geological Materials by Spark Source Mass Spectroscopy*, presented at Fourth National Meeting, Soc. Appl. Spectroscopy, Denver, Colo., Sept. 2, 1965.

# PRECONCENTRATION IN TRACE ANALYSIS

JERZY MINCZEWSKI

*Technical University of Warsaw,  
Institute of Nuclear Research, Warsaw, Poland*

## I. Introduction

Methods currently at our disposal in modern analytical chemistry for the determination of trace impurities do not always ensure, unfortunately, direct determination of these impurities in all high purity materials. Influence of the main component of the sample, mutual effects of the trace components involved, limited sensitivity of methods, and sometimes difficult access to costly apparatus are all in part responsible for trace impurities in high purity materials still being very widely determined indirectly after the traces have been isolated from the sample by concentration and eventual separation.

The problem of the determination of trace components is not related exclusively to that of high-purity materials. The former has been used first of all in agrochemical, biochemical, biological, agrotechnical, and oceanographic studies, where the idea of microcomponents has been known for quite a long time, and where methods for their determination have been developed even before the so-called high purity materials became important.

Yoe and Koch [1]<sup>1</sup> have presented a remarkable report on this question with respect mainly to the requirement of natural sciences, the report being published with the materials of a symposium on trace analysis (New York, 1955).

Methods of measurement of trace constituents have been discussed in other papers. Problems to be considered here, in general, are presented in Table 1. In the middle column all analytical operations are listed to which the material tested is subjected and from which an average laboratory sample is withdrawn, and the most important chemical processes resulting in isolation, concentration, and separation of the trace components to be determined.

In the left column are presented the agents which may directly or indirectly influence the particular steps of the process discussed, the composition of the withdrawn sample and the successive steps of its chemical processing, causing concentration changes in the micro-

---

<sup>1</sup> Figures in brackets indicate the literature references at the end of this paper.

TABLE 1. General scheme of the analysis of high purity materials.

Agents influencing	Analytical operations	Methods of determination
Homogeneity → Storage → tools atmosphere } → reagents } → changes in } composition }	MATERIAL to be tested → ↓ ↓ ↓ { sampling grinding mixing surface cleaning	nondestructive methods
containers } → reagents } → atmosphere } → volatility }	↓ { laboratory sample → ↓ sample solution → ↓ ↘ separation of matrix    separation of traces ↘ ↙ concentration ↓ solution of traces → ↓ separation ↙ ↓ ↘ individual trace components →	direct methods (solids) direct methods (solutions) simultaneous determinations of many components determination of individual components

components to be determined and leading consequently to an erroneous chemical characterization of the analyzed material.

In the right column are indicated the analytical methods which can be applied in the individual steps of the process.

Chemical problems of the processing of samples of high purity materials in order to isolate, concentrate, and separate trace impurities were the subject both of the plenary reports at the conferences of the IUPAC in Lisbon [2], London [3], and Moscow [4], and of many reviews [5-12].

## II. Preparation of Sample

### A. THE ANALYZED MATERIALS AND SAMPLING

The high-purity materials that will be discussed later in this report can be divided into three groups, using the type of sample as the criterion: solids, powdered materials, and liquids. Included in the first group are mainly metals of high purity and materials used in production and processing of metals of high purity. To the second and third groups belong in principle chemicals of high purity used as starting materials for obtaining metals, auxiliary production materials, and reagents used in trace analysis.

The most difficult to analyze undoubtedly are solid materials because of their considerable lack of homogeneity. The segregation of components, known from metallurgical analysis, also appear in the case of high purity metals, qualified as 5 *N*, 6 *N*, and higher. Figures 1 and 2 present autoradiograms of aluminum-copper (Al-Cu 4) and aluminum-nickel (Al-Ni 0.3) ingots [13]. The observed unequal distribution of the admixture is very indicative of errors which can be brought about by withdrawing for analysis a random part of the material portion. As a proof of these inhomogeneities, application of the zone melting method for concentration of traces can be mentioned.

Metallurgical methods can be applied to prepare a homogeneous sample from a block. Repeated melting, mixing, and rapid crystallization may possibly produce a fine-crystalline structure without segregation. This procedure has the inherent danger, however, of introducing impurities in the process of melting and, in addition, is not easily carried



Figure 1. Autoradiogram of Al-Cu 4; ingot;  $\times 3$ .



Figure 2. Autoradiogram of Al-Ni 0.3; ingot;  $\times 8$ .

out in an ordinary analytical laboratory. More suitable to the average laboratory conditions is a fine shaving of the material or powdering of brittle materials, mixing, eventually etching and washing. Samples, carefully withdrawn from such a material, do not show inhomogeneity.

In Table 2, are listed the variances of the spectrochemical results from an analysis of four aluminum samples (3 g each) prepared in the way outlined above from a block (200 g). The comparison of the calculated Fisher's factor with the value taken from the table indicates satisfactory homogeneity [14].

The inhomogeneous distribution of admixtures in metals are evidently related to the solubility of the trace component in the matrix metal. The determination, for example, of lead in aluminum (insoluble component) has shown (table 2) an appreciably larger dispersion than the determination of manganese (soluble component—larger probability of equal distribution).

Obviously, it should be remembered that the analysis of an averaged sample results in a mean content of impurities, but it gives no picture of the degree of homogeneity.

Shaving of metals even as soft as aluminum always introduces contamination of metals from a turning tool. Figure 3 presents the autoradiograms of an aluminum piece cut with an ordinary steel turning tool (Fig. 3a) and with a turning tool made from tungsten carbide (Fig. 3b).

Both the mechanical treatment of solid materials and the etching with acids to wash the secondary admixtures may change the structure

TABLE 2. Comparison of normalized variances of trace determinations in standard aluminum sample ( $V_{st}$ ) and in a sample homogenized in laboratory ( $V_h$ ).

F = Fisher test value taken from the table for given freedom degrees number [14].

Element	$V_h$	$V_{st}$	Fisher test value	
			calculated $F = \frac{V_h}{V_{st}}$	table value
Fe	6.80	4.04	1.68	2.60
Si	6.92	11.71	0.59	2.60
Mg	2.76	5.12	0.54	2.60
Mn	2.51	1.76	1.43	2.60
Pb	8.99	4.64	1.94	2.60

and composition of the metal involved. In particular etching of fine-grained samples may cause appreciable washing of the individual components from the sample. For this reason crushing cannot be carried too far.

In summary it may be said that the problem of sampling metals of high-purity is difficult to solve in a universal and satisfactory way. Insufficient correlation between the physical properties of high purity metals and the chemical composition determined analytically probably lies in the problem of sampling. An interesting discussion of a similar problem, i.e., with homogeneity of semiconductor materials and their



Figure 3. Autoradiograms of aluminum block cut using: a) ordinary steel turning tool; b) turning tool made from tungsten carbide.

surface and structure investigations has recently been reported by Kane [15].

It is much easier to take representative samples of powdered materials, but such powders can readily be contaminated in the course of eventual grinding before dissolution.

It seems that in the case of hard materials, mortars from a corundum monocrystal, tungsten carbide [16], or pure molybdenum [17] would be preferable. Since grinding always is accompanied by contamination of the sample, such mortars introduce to the latter only one definite component to be neglected in the determination.

No difficulties are encountered in withdrawing representative samples of liquid materials. A serious problem is presented, however, by their storage.

## B. THE TECHNIQUE OF WORK

Burriel-Marti [2] has rightly stated that all operations concerning the determination of trace components require the preservation of "chemically aseptic" conditions of the work. Indeed, already the determination of  $10^{-4}\%$  quantities of universally dispersed elements such as sodium, potassium, calcium, magnesium, silicon, boron, and zinc presents difficulties in any ordinary unconditioned laboratory. By going to the determination of  $10^{-7}\%$  quantities and lower, analogous difficulties arise with a number of other elements such as iron, copper, lead, aluminum, and titanium.

Factors directly influencing the final results of trace impurities are the following: laboratory air, laboratory vessels, water, and reagents. These questions have widely been discussed by Thiers [18].

### 1. Hermetization of Operations

The air of any analytical laboratory and the analyst himself (e.g. creams and other cosmetics contain the mineral components Al, Zn, B, and Si) can be a serious source of secondary contamination of the analyzed sample. The air is contaminated by ordinary dust and in addition by metallic parts of laboratory devices (burners, cocks, etc.) which undergo corrosion when in contact with the vapors of volatile acids. Lead in the atmosphere of towns originates from the combustion of lead tetraethyl [19].

Table 3 presents data on the determination of various impurities in silicon and nitric acid, the data being indicative of the important positive influence of the hermetization of analytical operations. Figure 4 shows the dispersion of results obtained in the spectrochemical determination of impurities in high purity aluminum. The circles denote the results obtained without hermetization; the crosses denote the results when all analytical operations were done in hermetic boxes [20].

TABLE 3. The influence of laboratory atmosphere on the results of trace determinations. All results in  $10^{-7}\%$  [17].

Sample	Conditions	Contaminations determined						
		Al	Fe	Ca	Cu	Mg	Mn	Ni
Silicon <sup>a</sup>	A	10	10	10	0.4	10	< 0.2	< 0.5
	B	50	300	50	2	50	2	2
Nitric acid	All operations hermetized	1	8	3	< 0.1	5	0.1	< 0.1
	All operations in laboratory atmosphere	50	30	50	5	30	0.6	0.7

<sup>a</sup> The traces were enriched on graphite powder and the first part (A) was excited immediately after enrichment, the second (B) after 1 week storage in normal laboratory atmosphere.

Chow and McKinney [21] have determined lead from the air introduced into a 500 ml hydrochloric acid sample and evaporated during a long time under varying conditions. From the data in Table 4 it is seen that hermetization in a purified air stream diminishes the lead contamination of the sample by a factor ranging from 10 to 40.

Hermetization of analytical operations can be readily accomplished in glove-boxes made from plexiglass and adapted individually for the operations intended. This enables separation of the particular actions connected with studies of various materials. For example, there may be separate boxes for the processing of boron samples, separate ones for silicon, aluminum, etc., thus permitting the adaptation of the sizes and shapes of boxes to a given analytical operation. It is also possible with such boxes to change quickly the range of work in the same laboratory area.

## 2. Laboratory Vessels and Containers

The main materials used for laboratory vessels and containers include glass, quartz, platinum, and organic plastics such as polyethylene,

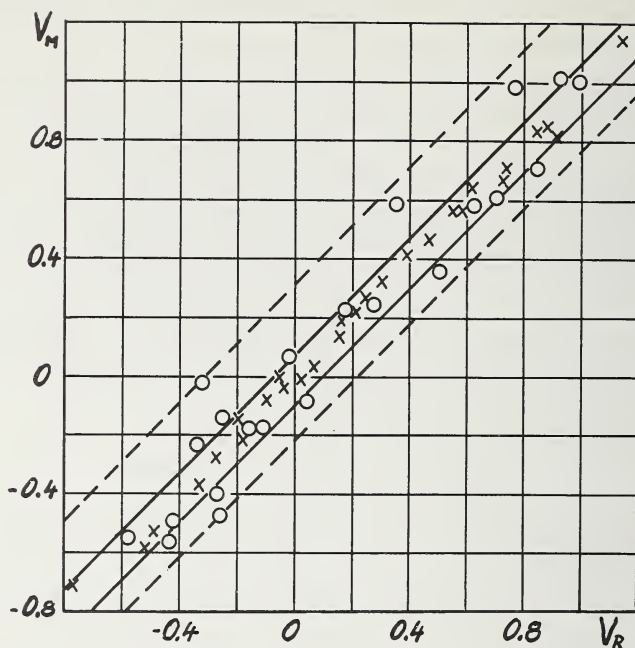


Figure 4. The dispersion of results of the spectrochemical determination of trace impurities in 5N aluminum. Blackening value measured ( $V_M$ ) versus value taken from the regression line ( $V_R$ ). Circles—without hermetization; crosses—in hermetic boxes.

TABLE 4. Lead contamination from air [21].

Beaker	Condition	Laboratory	Time	Amount of lead
Teflon	Open	ordinary	8	4.07
				2.32
	Nitrogen flushed container	ordinary	8	1.13
				0.44
	Open	pure air	8	0.18
0.13				
Nitrogen flushed container	pure air	1	0.02	
			0.03	
Borosilicate glass	Nitrogen flushed container	pure air	1	

polypropylene, and fluorine derivatives. These materials, when in contact with a sample can influence the concentration of trace components in solution by the following three ways: (1) by the sorption of trace components they can diminish the concentration of the traces in the solution examined, (2) by leaching, the solution can be enriched in mineral components, thereby increasing the concentration of traces, (3) the components previously adsorbed by the walls of the vessel can pass into the sample solution.

Studies carried out on these effects permit the establishment of a series of the applicability of the use of the above mentioned materials in trace analysis: Teflon and other fluorine plastics > polyethylene > quartz > platinum > glass. Obviously this is an average series of the applicability of the materials. In individual cases appreciable deviations may occur. These effects are such that on the average the composition of solutions may be assumed to be unchanged within a limiting concentration of up to  $10^{-4}\%$ . However, changes in concentration are very likely to occur in solutions of lower concentrations such as of the order of  $10^{-7}\%$ .

The equilibria of sorption, dissolution, and desorption at the above concentrations usually establish very slowly. Therefore these effects are of considerably greater importance in considering the preservation of standard solutions and reagents than in the course of ordinary short-time analytical operations. In the latter case prolonged dissolution and evaporation at elevated temperatures are particularly undesirable.

Studies of sorption and desorption equilibria on surfaces of various materials have been developed appreciably during the last years. In the field of application of radioisotopes this is connected with an acute problem of contamination and decontamination of materials in radiochemical laboratories. Although it is necessary to consider that radioisotopes, differing energetically from stable isotopes, can behave differently in these processes than the ordinary isotopes, nevertheless use can be made of these studies in trace analysis.

Attempts have been made to formulate simple mathematical relations [22] to express the concentration of the isotope adsorbed on the surface of a vessel and in the solution as a function of the partition coefficient, volume of the solution, and the contacting surface of the vessel with the solution. It is worthy of notice that the latter parameters, and in particular the ratio of volume of the solution to surface area of the vessel, change by a factor of two when going from a beaker of 50 ml capacity to a beaker (bottle) of 1000 ml capacity, in favor of the latter.

It should be emphasized that glass is entirely unsuitable for work with traces. The components of glass readily pass into any solution, the concentration of the passed components easily reaching  $10^{-4}\%$ . A watch glass used to cover a dish in which water was boiling gave up to

1 mg of SiO<sub>2</sub> during one hour, and 1.4 mg of SiO<sub>2</sub> in 30 min when an ammonia solution was boiled [23]. Even such trace components of glass as lead are in quantities high enough to pass into the solution analyzed. Chow and McKinney [21] have found that the latter impurity may increase up to 0.1 μg during the normal course of analysis.

So called heavy metals easily undergo adsorption on glass the surface of which, particularly after prolonged contact with aqueous solutions, becomes soft and then behave similarly to an ion exchanger.

Quartz possesses much better properties and is more chemically resistant than glass. In connection with the production of semiconductor materials, quartz of high purity now is widely available for analytical work.

Platinum vessels also seem not to be quite safe for work with traces because they can cause considerable contamination of the solutions examined. Vasilevskaya [17] has reported results of analyses of hydrofluoric, hydrochloric, and nitric acids after evaporation in dishes made from Teflon, platinum, and from the ordinary quartz. It is seen from Table 5 that after evaporation in a platinum dish the content of some impurities increased by 0.5–1.0 order of magnitude. The acids evaporated from the ordinary quartz exhibited a still higher degree of contamination.

TABLE 5. Results of spectrochemical analysis of HF, HCl, and HNO<sub>3</sub> after evaporation in Teflon, platinum, and quartz dishes. All results in 10<sup>-7</sup>% [17].

Acid	Material	Elements determined										
		Al	Fe	Ca	Cu	Mg	Mn	Ni	Pb	Ti	Cr	Sn
HF	Teflon platinum	3	3	1	< 0.04	< 3	0.1	< 0.4	< 0.1	0.1	< 0.4	N.D. <sup>a</sup>
		10	10	10	0.4	10	0.2	0.3	0.5	1	0.5	N.D. <sup>a</sup>
HCl	Teflon	< 4	3	5	0.2	3	0.1	N.D. <sup>a</sup>	< 0.4	N.D. <sup>a</sup>	N.D. <sup>a</sup>	N.D. <sup>a</sup>
	platinum	2	2	10	1	6	0.2	0.6	< 0.4	0.4	Tr. <sup>b</sup>	< 0.4
	quartz	10	10	60	1	10	0.4	2	0.5	2	0.6	0.4
HNO <sub>3</sub>	Teflon	2	8	4	< 0.01	7	0.1	N.D. <sup>a</sup>	N.D. <sup>a</sup>	Tr. <sup>b</sup>	N.D. <sup>a</sup>	N.D. <sup>a</sup>
	platinum	20	20	30	0.4	20	0.6	Tr. <sup>b</sup>	1	0.8	N.D. <sup>a</sup>	N.D. <sup>a</sup>
	quartz	20	20	60	0.1	20	0.6	N.D. <sup>a</sup>	1	0.3	N.D. <sup>a</sup>	N.D. <sup>a</sup>

<sup>a</sup> N.D. = not detected.

<sup>b</sup> Tr. = traces, not evaluated quantitatively.

Plastics, in particular polyethylene which has widely been introduced as a package for reagents, and Teflon with other fluorine plastics, surely are the most suitable materials for trace analysis. Here also, however, solutions may be contaminated with metal traces.

In the case of fluorine materials the eventual adsorption of traces should be taken into account; this may be brought about by the complexing ability of fluorine with respect to some metals. This however seems to play no major role in practice.

Of particular concern, when working with traces, is the washing of laboratory vessels. The traditional chromium mixture should not be used since, for example, as Butler and Johnston [24] have found, the adsorption of chromium on Pyrex glass amounted to 10 ng per cm<sup>2</sup>. It has long been shown by Lang [25] that the washing away of chromium traces with water is very difficult. Thiers [18] recommended for this purpose a mixture of concentrated sulphuric and nitric acids and Häberli [26] a hot ammoniacal solution of EDTA, advising, however, even after this operation that the purity be checked by means of a dilute dithizone solution (in case the heavy metals are to be determined).

### 3. Reagents

The reagents used in the course of trace analysis are the most important source of contamination and their preparation in a state of suitable purity frequently is a chemically more difficult problem and more laborious than the trace determination itself. Although reagents of special purity are at present produced, for example, the so called "transistor grade" (B.D.H.), "Suprapur" (Merck), etc., their selection is rather poor and their purity (usually the content of the particular impurity is not better than 10<sup>-6</sup>-10<sup>-7</sup>%) sometimes is unsatisfactory.

The required purity of the reagent used in the course of trace analysis depends, of course, on the content of the impurity to be determined and on the mutual weight ratio of the sample to the reagent. The content of impurities in a reagent should, however, be lower by one order of magnitude than that to be determined in the sample.

In the course of analysis the most important reagents are: water of high purity, acids (HCl, HF, HBr, H<sub>2</sub>SO<sub>4</sub>, HNO<sub>3</sub>, CH<sub>3</sub>COOH) bases (NaOH, NH<sub>3</sub> aq), buffer solutions, and solvents, the latter being used in large quantities.

The purification of water by means of ion exchangers (mixed bed columns) and by double distillation from quartz or platinum vessels now does not afford any difficulty.

For the removal of SiO<sub>2</sub> traces, Wickbold [27] proposes the use of strongly basic anion exchangers (Permutite ES). The content of SiO<sub>2</sub>, after the water sample was passed through the above exchanger, did not exceed 1.5 μg/l.

Irving and Cox [28] have widely discussed the preparation of HCl and  $\text{NH}_3$  solutions of highest purity by isopiestic distillation. They obtained  $\sim 10 N$   $\text{NH}_3$  and  $\sim 5 N$  HCl solutions the purity of which was equal to that of water applied for the absorption. Similar results can be obtained in the case of ammonia solutions by saturating the water with gaseous  $\text{NH}_3$  from a bottle, the gas being passed, as suggested by Häberli [26], through three washing bottles with an ammoniacal solution of EDTA.

Greater difficulties are encountered with the purification of hydrogen fluoride. The slow distillation method has been applied for that purpose in silver and palladium vessels, collecting the middle fraction (50%) which demonstrated the highest degree of purity. In order to obtain hydrogen fluoride without silicon, Stegeman [29] suggested the passage of gaseous hydrogen fluoride from a bottle in a nitrogen stream through a polyethylene assembly consisting of five bottles connected in a series. The first bottle contained an aqueous layer with polyethylene pellets, the second and the third contained polyethylene pellets and an aqueous suspension of sodium fluoride (to combine fluorosilicic acid) the fourth contained an air buffer, and the fifth contained pure water in which absorption proceeded.

Solutions of many reagents can be freed from the heavy metals by means of dithizone. This method is unsuitable for the purification of sodium hydroxide solutions. Such solutions, as proposed by Nazarenko and Fliantikova [30] can be prepared, using sodium of special purity (distilled), dissolved in high purity water.

### III. Concentration and Separation of Traces

To isolate, concentrate, and separate trace impurities all the known methods of partition are applied [31]. The methods are based on precipitation, coprecipitation, and solvent extraction. They also include chromatographic methods, electrolytic methods, based on the difference in volatility of substances, and other more specific methods which are applied occasionally.

Two principally different procedures consist either in separating the main component (the matrix) of the sample, the trace component remaining in the mother solution (macro-micro separation), or in separating trace components, the matrix remaining in the solution (micro-macro separation). In addition, some methods require the trace components to be separated from each other (micro-micro separation).

When discussing particular groups of methods, the role of two fields of chemistry in their development must be emphasized. These are: complexing compounds and organic reagents applied in inorganic analysis. In the last twenty years the development of both these very closely related fields has introduced to analytical chemistry in general, and to

the separation methods in particular, a very great number of new organic complexing reagents and a good deal of information on the mechanism and kinetics of complexing reactions. A thorough knowledge of these two fields makes possible the solution of very difficult separation problems of any mixture of ions in a wide range of concentration.

The basic data on the theory of complexing reactions with the purpose of determining stability constants and of using complexing agents in analytical chemistry can be found in papers of Bjerrum, Schwarzenbach and Sillen [32], Jacimirski and Vasil'ev [33], and Ringbom [34]. Schwarzenbach [35] in his studies gave an excellent generalization of the relationship between the location of an element in the Periodic Table, i.e. between its electronic configuration, and the ability of the element to form complexes with different ligands. This is of particular importance when looking for suitable complexing agents for complicated separation processes.

In the course of concentration and separation of traces, particularly with chemical methods, an important role is played by masking reactions. For this reason these reactions will be discussed first.

#### A. MASKING

An appropriate choice of a masking agent in micro-macro separations makes isolation of trace components possible while the main component remains in the solution. The choice permits the attainment of a better selectivity or even specificity of the reaction in micro-micro separations. A better understanding of the theory of complexing renders it possible to derive theoretical principles of masking. Studies of Cheng [36] and Hulanicki [37] gave the theoretical basis of application of masking agents in analytical problems.

In Table 6 the possibilities of the application of twelve most important masking agents are presented. Taking into account the great similarity, some complexing agents are considered jointly, e.g. oxygen complexes (e.g.  $\text{MnO}_4^-$ ,  $\text{WO}_4^{2-}$ ) and hydroxylic complexes  $\text{Al}(\text{OH})_4^-$ ,  $\text{Zn}(\text{OH})_4^{2-}$ , cyanide and ammonia complexes, citrate and tartrate complexes (citrate complexes are, in general, more stable in acid solutions, tartrate complexes in alkaline solutions).

The following are interesting examples of masking. Large quantities of zinc, nickel, manganese, copper, silver, and other elements are held in solution after being transformed into the complexes during the precipitating separation of traces of Ca and Mg (with carriers) as the phosphates [38].

For the analysis of trace admixtures in uranium, sodium carbonate can be used as the masking agent. The latter isolates a majority of the traces involved in the form of hydroxides or carbonates, while transforming the uranium into a soluble carbonate complex.



of bismuth iodide [42] or as the basic nitrate, mercury after being reduced in a nitric acid solution by means of formic acid [44], molybdenum as the benzoinoximate [45], and zirconium as a salt of amygdalic acid [46].

Listed in Table 7 are the most important methods of removing the main component in the form of difficultly soluble precipitates. The largest group contains the elements which can be isolated from solutions in the elemental form by means of reduction, the most frequently applied being electrochemical reduction. Electrolytical isolation of a metal from an acid solution at a stable cathode is limited to the noble metals and the half-noble metals of lower, under given conditions, decomposition potential than hydrogen. The application of a mercury electrode that possesses a high overvoltage potential for hydrogen allows one to isolate from solution the less noble metals: iron, nickel, copper, zinc, and lead. The noble metals and some other elements, for example, selenium and tellurium, can be precipitated from solution in the elemental form during the reduction by chemical means.

Coprecipitation of traces with macroquantities of a precipitate, the phenomenon that is so unfavorable during the removal of microcomponents, is widely used to isolate microcomponents by their precipitation on carriers.

Although the action mechanism of carriers, and the coprecipitation process in general, have been the subjects of numerous papers, many papers possess only an empirical character.

TABLE 7. Separation of matrix using precipitation [31].

Li b																		
Na b												Si d						
K b	Ca c				Cr a	Mn a	Fe a	Co a	Ni a	Cu ab	Zn a	Ga a	Ge a		Se a			
Rb b	Sr c		Zr d	Nb d	Mo a		Ru a	Rh a	Pd a	Ag ab	Cd a	In a	Sn a	Sb a	Te a			
Cs b	Ba c			Ta d	W d		Os a	Ir a	Pt a	Au a	Hg ab	Tl ab	Pb cb	Bi ab				

The elements are separated:

- a—in elemental form
- b—as halogenides
- c—as sulphates
- d—as oxygen compounds



and tungsten using the benzoinoxime. The traces of sulphur mentioned in Table 8 can be isolated in the form of sulphates together with dichromate ions precipitated jointly by barium.

It follows from Table 8 that for the majority of elements convenient and simple forms can be found for the isolation of their microquantities from solutions on suitable carriers.

Elements with properties similar to the trace elements but not interfering in the course of further analysis are most frequently chosen as suitable carriers. For elements precipitated as hydroxides the following elements can be used: iron (III), aluminum, and titanium. The carrier properties of lanthanum are noteworthy [50]. Lanthanum is a relatively rare element, exhibits no chromophoric properties and, as a rule, is not being determined in high purity materials.

When looking for an appropriate carrier for the coprecipitation of silicon, Marczenko and Kasiura [51] have used niobium, taking into account the close chemical and physical properties of niobic and silicic acids. To the sample solution containing traces of silicon, niobium was introduced as a solution of its oxalate complex. During evaporation with perchloric acid the niobium complex is decomposed, the silicon is dehydrogenated and the niobic acid with traces of silica gel simultaneously precipitated.

The carrier need not always be similar to the trace substance to achieve quantitative isolation of the trace from solution. The direct turbidimetric determination of chloride traces in samples dissolved in water frequently is impossible because of too low concentration of the chlorides or because of the negative influence exerted by the main component of the sample on the chloride traces. It was found that for chloride ions good results could be obtained with barium sulphate as the carrier [52]. To the sample dissolved in dilute nitric acid, sulphate ions were added followed by a solution of barium and silver nitrates. From the combined precipitate of barium sulphate and the traces of silver chloride the latter undergoes complete leaching by ammonia due to the formation of a soluble ammonia-silver complex.

The quantity of the carrier element introduced to the solution before precipitation must be large enough that the carrier element is precipitated quickly in a visible quantity convenient for separation (by filtration or centrifugation) and washing. On the other hand the quantity of the carrier should be small enough as to neglect the adsorption by the precipitate of these ions which should remain in the solution tested. The carrier quantity should be chosen with respect to the volume of the precipitate formed. This quantity may be lower in the case of precipitating an element in the form of 8-hydroxyquinolate than during precipitation of the element as the hydroxide. It has been found experimentally that 1-3 mg of a carrier element is a suitable quantity for a solution of 50-250 ml.

Kusnietsov [53] and his coworkers for over ten years have been using organic compounds to isolate trace quantities of inorganic ions. Their methods can be used to enrich traces both in a group way and specifically. The organic compounds applied, of basic and acid character, are chosen appropriately to the chemical character of the traces to be determined with which they form compounds of the salt or ion-pair type, e.g.  $\text{Me}^+\text{R}^-$ ,  $\text{R}^+\text{MeO}_n^-$ , or  $\text{R}^+\text{MeCl}_n^-$ . The organic substance is introduced as an aqueous solution of a suitable  $p\text{H}$  value or in an organic solvent, e.g. in ethanol. Under the precipitation conditions the solubility of the organic substance is decreased causing the onset of its precipitation together with the traces of interest. One of the advantages that is demonstrated by organic carriers is the fact that the carrier can easily be separated from inorganic traces by simple ignition. The latter may, however, be accompanied by losses of nonvolatile trace elements due to the formation of light aerosols which can be lost from the ignition vessel by a weak thermal movement of the air.

A systematic discussion of various kinds of organic carriers and ways of their application can be found in a recently published paper by Miasoyedova [54].

### C. EXTRACTION

The extraction process, applied very frequently to the isolation of both the main and trace components from a solution of the sample examined, is based on the difference in the solubility of the substance extracted in the organic and aqueous phases. If the partition coefficient is high enough to afford a high percentage extraction then the process is useful for analytical purposes and enables one to extract quantitatively the required components from aqueous solutions into organic solvents or to reextract them from the organic phase into the aqueous one [55-61].

More information about complexing reactions has appreciably broadened on one hand the possibility of applying the extraction process for isolating and concentrating traces and on the other hand it revealed that the extraction mechanism is very complex. This is taking place particularly in analytical applications where almost always complicated solutions of mixtures are encountered.

The inorganic ions to be extracted should be transformed into a form that is soluble in the organic phase. Attention must be paid to the reactions and interactions which occur between the ion extracted and the complexing agent, solvent (diluent), and foreign species present in the solution. The eventual dissociation and association should also be taken into account. The effective rate of the extraction process is limited by the kinetics of the processes mentioned and by the rate of passing the extracting species into the organic phase. Thus only a full knowledge of all the partial processes occurring in both the phases makes possible a forecast of the overall extraction process that is essential from the analytical point of view.

Theoretical studies of the extraction process, and particularly those of the theory of electrolyte and nonelectrolyte solutions, have explained a number of extraction principles. As a result both the synergistic and antagonistic effects discovered are being applied in analytical chemistry [62-64]. Extraction studies have shown that the extraction process may be accompanied by coextraction [65]. The facts hitherto found on coextraction do not yet give us a theoretical explanation of the phenomenon. The small number of papers on coextraction seem to indicate that the phenomenon has no wider meaning.

The monograph by Morrison and Freiser [66] on the theoretical basis of extraction and on various aspects of its application in analytical chemistry excellently classifies the trends and possibilities of application of the process including the separation and concentration of traces.

An element in an aqueous solution can be extracted into an organic phase in the elemental form, in the form of a simple covalent compound, as an inner chelate, or as an association complex with the element of interest in its cation or anion forms. The extraction of elements in the elemental form is characteristic for some elements (see Table 9) and cannot be influenced by us. On the other hand owing to the great number of known organic complexing agents, extraction of other chemical forms of elements can be accomplished and is widely applied.

The application of extraction to the separation of the main component or to the isolation of trace components, differs basically in the requirements with respect to the solubility of the extracting species in the organic phase. In the case of separation of a macrocomponent the solubility must be high, in the second case, low solubilities suffice.

Considering the above, the extraction process can be divided into two classes. The high solubility in the organic phase is a characteristic feature of some elements, covalent compounds with simple inorganic ligands, and of ion-association systems. On the other hand, the solubility of inner chelates in organic solvents is low and these systems are mainly used for the extraction of traces.

In Table 9 are listed elements which can be extracted as the main component. Bromine, iodine, and sulphur can be extracted and separated in the elemental form. The following elements can be extracted as simple covalent halogen-compounds: germanium [67], arsenic (III) as chlorides into carbon tetrachloride or benzene, mercury (II) as iodide into cyclohexanone [68], ruthenium and osmium as tetraoxides into carbon tetrachloride.

The extraction based on the oxonium mechanism is the most widely applied for the separation of a considerable number of metals in the form of anion halogen-complexes, nitrates, and others into oxygen containing solvents. As a classic example the extraction of uranyl nitrate into diethyl ether or tri-*n*-butyl phosphate can be mentioned, the extraction being conducted in order to determine traces in the residue [69].

TABLE 9. Separation of matrix using extraction [31].

	Be																		
																	Sc		
					Cr d		Fe a	Co a	Ni a	Cu a	Zn a	Ga a	Ge a	As a	Se ca	Br c			
				Nb a	Mo a		Ru ad	Rh a	Pd a	Ag a	Cd a	In a	Sn a	Sb a	Te a	I c			
				Ta a	W a	Re d	Os ad		Pt a	Au ab	Hg a	Tl a	Pb a	Bi a					
				Ce b	Th b	U b													

The elements are extracted as:

a—halogen-compounds

b—nitrates

c—elements

d—oxygen-compounds

In the ion-association systems attention should be paid to the extraction by aliphatic amines which are relatively poorly applied in analytical separations [70].

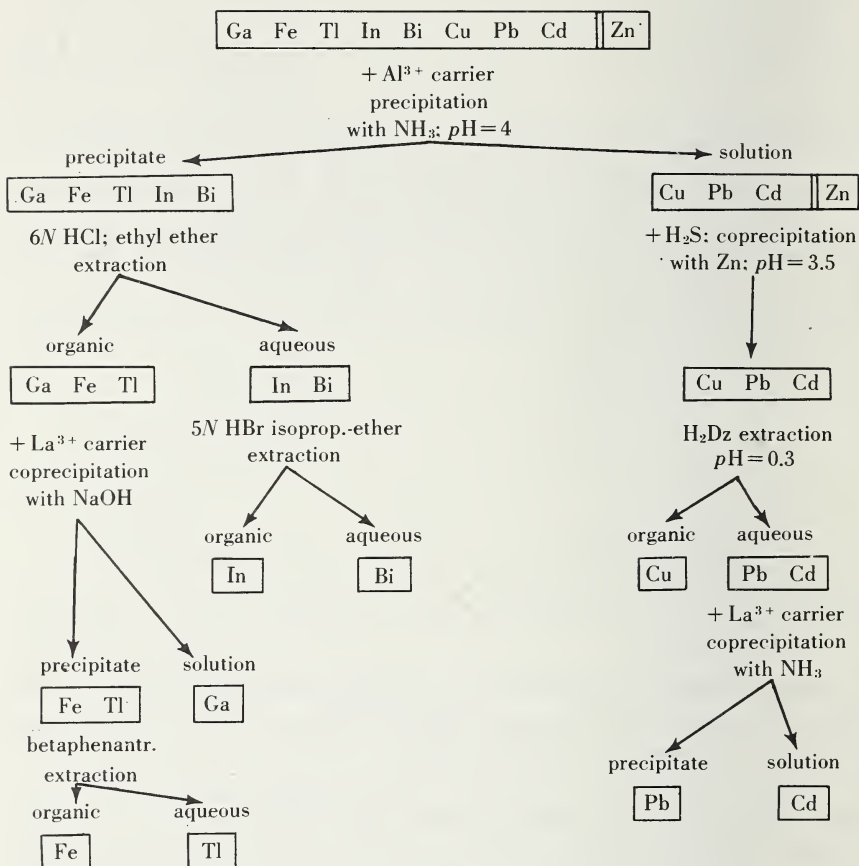
As examples of specific extractive separations, the isolation of macro-quantities of beryllium in the form of a hydroxo-acetic complex into chloroform [71] or a separation of chromium as a peroxide compound into diethyl ether should be mentioned.

In Table 10 are listed more important extractive methods for the isolation of trace elements. Beside the methods that have already been mentioned and which are being applied also to the extraction of trace impurities, the main role is played by the extraction of inner chelates. The most important are here organic reagents that form inner chelates with metal ions, the chelates being soluble in chloroform, carbon tetrachloride, and other organic solvents. Table 10 presents some examples of chelating agents. Dithizone and DDTC are given as representatives of reagents in which the sulphur atom is the main ligand atom. These reagents are used for the extraction of metals forming difficultly soluble sulphides. Cupferron and oxine containing oxygen as the main ligand atom are suitable for the extraction of metals which are apt to react with hydroxylic groups.

These reagents and their mixtures have been used for group separations of metals, e.g. dithizone has been used for the determination of traces in antimony of high purity [72], and dithizone, oxine, and diethyldithiocarbamic acid for the separation of twenty-six trace elements in aluminum, titanium, zirconium, and selenium of high purity [73].



TABLE 11. Separation and concentration of trace contaminants in zinc sulphide [81].



1 g of a high purity substance, a complete isolation and separation of a dozen or so impurities can be achieved, the determination being done colorimetrically on an average level of  $10^{-6}\%$ .

#### D. CHROMATOGRAPHY

Chromatographic processes, consisting in the application of the different behavior of the component to be determined in the system: stationary phase—mobile phase, frequently are used in the course of isolating and concentrating traces.

For macro-micro and micro-macro separations, ion-exchange chromatography (the stationary phase is an ion-exchanger, the mobile liquid phase are aqueous and nonaqueous solutions) and reversed-phase partition chromatography (the stationary phase is a liquid complexing agent adsorbed on a solid supporting material, the mobile phase is an

aqueous solution of suitable composition) are mainly used. The most suitable are such systems in which a column operates as a sieve, the trace components being held, and the main component being passed through.

In addition to both the separation methods mentioned above, other chromatographic techniques are being used but they are of much less importance.

The characteristic feature of chromatographic methods, treated as a whole, is their universality. If gas chromatography is included, the methods cover almost all the elements of the Periodic Table.

The most commonly used is ion-exchange chromatography. The recently published monograph of Tremillon [82] widely discusses separation methods based on ion-exchangers taking into account also the problem of traces. In connection with the latter the most frequently used are anion-exchangers and cation-exchangers. Chelating ion-exchangers have also been investigated, as can be found in exhaustive reviews of Bayer [83] and Schmuckler [84]. The same applies to inorganic exchangers which have been discussed by Rein [85].

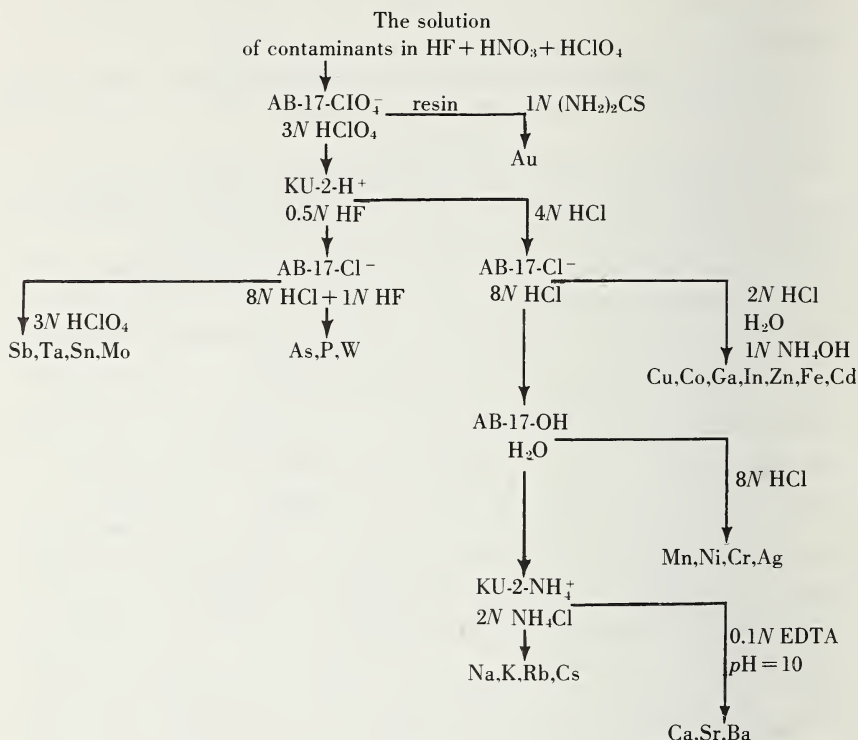
To give an example one can mention the isolation of the main components in gallium arsenide [86] for the successive determination of impurities, and an interesting application of a special technique called "precipitation ion-exchange" [87], which allows for an easy isolation of the sum of trace impurities from chloride solutions, e.g. of the alkali metals. By means of ion-exchangers a fairly specific isolation of particular trace components can be achieved, e.g. the isolation of cesium traces from potassium and sodium salts [88], and the isolation of nickel and copper traces from cadmium, zinc, and iron (III) [89].

A classic example of the application of ion-exchangers for group separation is reported by Kalinin et al., [90] who separated 25 trace elements in a sample of semiconductor silicon in the course of determining them by neutron activation. After the silicon had been distilled off as  $\text{SiF}_4$ , the solution was separated entirely by means of cation and anion exchangers, according to the scheme given in Table 12. The elements in the groups obtained were determined by gamma-spectrometric measurements and needed no further separation.

Ion-exchange has also been applied in studies of the purity of rare earth concentrates [91].

The possibilities of ion-exchange for the enrichment of traces are best illustrated by Brooks [92], who, using a small anion exchanger column, has isolated and determined 1.5  $\mu\text{g}$  of gold in a 250-l portion of sea water. The determinability was  $10^{-10}\%$  in this case.

Reversed-phase partition chromatography is, in principle, an extraction process performed in a continuous and multistage way on a column. The method can also be interpreted as chromatography on liquid anion-exchangers. The main trends of application developed by Siekierski

TABLE 12. Scheme of separation of semiconductor-silicon contaminants [90].<sup>a, b</sup>

<sup>a</sup> AB-17—anion exchange resin

<sup>b</sup> KU-2—cation exchange resin

and his coworkers include systems in which the organic stationary phases were mainly acidic and neutral esters of phosphoric acids, and amines. They have shown the usefulness of this process to numerous radiochemical separations which often can directly be employed for the isolation and separation of traces. For instance, columns with TBP absorbed on siliconated kieselguhr were used to separate traces of arsenic from germanium [93], and traces of scandium from calcium [94]. This same system has been used for analytical separation of traces of niobium from molybdenum [95]. Good results were obtained by Siekierski and Fidelis [96, 97] in micro-micro separations, e.g. with mixtures of rare earth elements. Smulek et al., using columns with tri-*n*-octylamine separated traces of cobalt from nickel [98], and traces of iron (III) from manganese [99].

It seems that application of this method can be considerably widened, especially with the use of relatively highly dissociated agents, such as those mentioned above, as the organic phase.

## E. VOLATILITY

Separation and isolation methods based on distillation make use of the difference in the volatility of elements or their corresponding compounds. These methods can be applied in three variants. The fractional distillation is applied from a solution of a proper composition, or a solid sample is distilled making use of the difference in the volatility of the sample components, or, finally, a solid sample is attacked with reagents in the gaseous phase at suitably selected temperatures. The latter procedure, consisting of the attack of the sample with such agents as fluorine, chlorine, bromine, hydrogen fluoride, hydrogen chloride, vapours of nitric acid, etc., although usually technically complicated has the advantage that the reagents in gaseous phase carry with them the smallest quantity of impurities; they give the smallest blank.

Direct distillation of the components of the tested sample, as a method for the isolation of traces, has found its classical application in the method of Scribner and Mullin [100], the so-called "carrier distillation" in spectrography, in which traces are distilled off from a difficultly volatile matrix directly to the excitation zone, and in the method of Mandelshtam et al. [101] and Zaidel et al. [102] who distilled traces from a difficultly volatile matrix and condensed them at an auxiliary electrode from which the traces were excited.

Direct distillation of a more volatile metal (the main component) from a sample in a special (usually vacuum) apparatus has been performed. The less volatile components remained in the residue, affording an appreciable degree of concentration (usually  $\sim 100$  times). This procedure has been applied for the concentration of impurities in zinc [103] and cadmium [104]. The reversed operation—distillation of traces—has been used by Neeb for the separation of zinc traces in aluminum of high purity [105], and by Joungdahl and Deboer for the isolation of manganese from aluminum [106].

Volatilization either of the main component of a sample, or of trace impurities from a matrix, under the influence of gaseous reagent, may involve, in principle, all the elements listed in Tables 13 and 14. These methods are technically complicated because they require manipulation with gaseous substances which are strongly toxic and corrosive, especially at elevated temperatures. Therefore suitable construction materials, that do not cause secondary contamination, and hermetization of the process are needed. Despite these difficulties a number of such methods are described in the literature. Fratkin and Shebunin [107] used gaseous hydrogen fluoride at  $350^\circ\text{C}$  to distill the main component of the tested sample as the fluoride or oxyfluoride. They examined, under these conditions, the distillation of boron, vanadium, tungsten, germanium, silicon, molybdenum, selenium, antimony, tantalum, and titanium. With respect to titanium Fratkin [108], using initially a 1 g



sample determined spectrographically the following elements: Mn, Mg, Cu, Cr, Al, Fe, Pb, Ca, Ni, and Sn in the range from  $1 \times 10^{-5}$  –  $1 \times 10^{-6}$  %.

Karabash et al. [109] have applied chlorination for the removal of titanium as the main component, the fourteen elements in the residue being determined spectrally.

Geilmann and Neeb [110] have proposed and proved the isolation of ten elements from mineral samples by means of roasting in a hydrogen atmosphere at 1000 °C. It may be assumed that this method could be applied to some materials of high purity, e.g.  $\text{SiO}_2$  and  $\text{Al}_2\text{O}_3$ .

In order to remove nickel, as the main component, Shvarts [111] has even applied the action of carbon monoxide on a powdered sample in an autoclave (150 atm) at an elevated temperature, transforming the nickel into a volatile nickel carbonyl.

Distillation of inner chelate compounds, many of which are fairly volatile, has as yet been rarely applied. Nazarenko et al. [30] have used gallium oxinate for the removal of gallium as the main component. Baudin, Lorrain, and Platzer [112] have distilled beryllium as the acetylacetonate.

Distillation from solutions mainly involves easily volatile elements and those in which covalent bonds prevail (an analogy to extraction by nonpolar solvents). The compounds involved include those of hydrogen, oxygen, halides, and inner chelates, e.g. ( $\text{AsH}_3$ ,  $\text{GeCl}_4$ ,  $\text{OsO}_4$ , gallium oxinate). These compounds may have sufficiently low boiling temperature so that their distillation from solutions is feasible. A classic example of isolating the main component by distillation from solution is the distillation of germanium tetrachloride [113], or arsenic trichloride, in the course of preparation of semiconductor germanium and gallium arsenide for spectrochemical analysis. Also the analysis of boron of high purity requires a previous isolation of the main component which is achieved by distilling boron as methyl borate [114].

This way is suitable for the removal of chromium as chromyl chloride [115, 116] in the case where spectrographic or colorimetric determination of traces is to follow. The same applies to selenium removed as  $\text{SeBr}_4$  and  $\text{SeO}_2$ .

Finally, the ignition or wet oxidation of organic compounds should be considered as the removal of the main component by volatilization. During investigations of high purity materials this operation is frequently involved when examining the purity of organic reagents or graphite. The course of ignition, when determination of traces is to be followed, also requires some precautions. For instance, carriers sometimes must be used to prevent the losses of material due to convection [117–119].

A classic example of isolating traces in the form of volatile compounds is the isolation of traces of arsenic as  $\text{AsH}_3$ , according to the method of

Gutzeit. This method, when combined with neutron activation, allows fully specific determination up to  $10^{-9}\%$  of arsenic in semiconductor materials [120]. The isolation of sulphur as  $H_2S$  for its successive colorimetric determination by the methylene blue method can also be quoted as another example [121].

Classical methods for the determination of trace contents of gases in metals are also based on volatility. After being removed by the melting method in vacuum the gasses are then determined by different methods.

If the main component of a sample can be removed due to its volatilization (distillation, sublimation), particularly with no additional reagents added, or if it can be attacked by gaseous reagents, then an exceptionally favorable concentration coefficient can be obtained, which may reach even a value of 1000 (i.e. from a 10 g sample a 10 mg portion of the concentrate is obtained).

During the course of evaporation it should be remembered that microgram quantities of some components may undergo partial distillation in spite of their low volatility. For instance, an aqueous solution of microquantities of boric acid can be concentrated by evaporation without appreciable losses of boron. However, a solution of traces of the acid can be evaporated without losses only after the solution has been made alkaline. During the determination of traces of boron in silicon, the latter is removed as  $SiF_4$ . To avoid the losses of  $BF_3$  by distillation, the boron must be combined with mannite to form a nonvolatile compound.

#### F. ZONE MELTING

Among the methods which do not belong to any of the above mentioned, zone melting should be mentioned [122]. During this process some impurities are concentrated at the end of a block of the tested substance. These impurities can then be directly determined. The method is, no doubt, of real value because no reagents are added to contaminate the sample. Automation of the apparatus used permits the concentration of traces automatically. The disadvantage of the method is a different partition coefficient between the crystalline and liquid phases of various elements, followed by difficulties in obtaining a high and full concentration (e.g. by a factor of 100) for a large number of impurities. Also some secondary processes, as volatility or oxidation of the particular impurities may influence the course of the concentration process. Nevertheless the method has been applied successfully for concentration purposes in the analysis of high purity materials [123-125] and wider and wider application and new approaches seem to indicate that the method is not as yet fully exploited. Recently Konovalov and Peyzulayev [126] have used the method for the determination of silver, thallium, and copper traces in bismuth and lead of high purity. These authors in their extensive paper discuss all the factors influencing the

course of the concentration process, taking the analysis of bismuth as an example.

#### IV. Final Remarks

The methods discussed above for isolation, concentration, and separation of trace admixtures in high purity materials indicate that the problem has to a significant degree been overcome. Thus, chemical laboratories can, in principle, separate trace impurities of any required sample enabling quantitative determination of the traces by one of the known methods. Further development of these methods, however, is required for further progress and must include a better understanding of the chemical reactions on which the methods depend, coupled with the introduction of new specific complexing agents, the development of techniques for obtaining substances of high purity (reagents), and the introduction of new materials into chemical laboratories.

One problem that is important in the analytical chemistry of traces still needs some comment. This is the problem of accuracy and precision of the discussed processes, the lower limit of traces that it is possible to isolate, and a general evaluation of the pre-concentration methods.

By applying the method of radioactive tracers it is possible to verify accurately whether the separation and concentration takes place quantitatively with a yield sufficiently close to 100%.

The limiting factor of application of the methods described above is, in general, the so called blank test, i.e. the amount of the component to be determined that is introduced with the reagents, from the air from the materials of containers, etc. to the sample during its processing. The blank test determines the lower limit of concentrating the components to be isolated. The variation of the blank test limits the precision of the obtained results after pre-concentration.

The final precision of the results is affected by the dominating effects of enrichment and separation of traces, taking into account an average performance of analysis.

For this reason these methods need constant control which can relatively easily be ensured by a parallel analysis and identical treatment of the sample and a blank to which known and comparable quantities of the components to be determined are added.

Certain disadvantages of preconcentration and separation processes are that they are time-consuming, and require that processes be performed by significantly better educated personnel to be sure that the particular operations are correctly performed. The personnel should be able to modify the way of treatment, if the normal course of analysis would be disturbed by an unexpected change, for example, in composition of the traces to be determined.

Despite these disadvantages, the pre-concentration methods, combined with appropriate instrumental determination methods, are of real

value in industrial laboratories, and may be particularly useful in research laboratories which must analyze samples of different and variable composition.

### V. Acknowledgements

The author wishes to thank both the staff of the Department of Analytical Chemistry of Technical University of Warsaw and the staff of the Analytical Department of the Institute of Nuclear Research for their help in preparing this paper. The author in particular is deeply indebted to Dr. Z. Marczenko, assistant professor of the Technical University of Warsaw, for valuable discussions and remarks.

### VI. References

- [1] Yoe, J. H., Koch, H. J., Trace Analysis, J. Wiley & Sons Inc., New York, 1957.
- [2] Burriel-Marti, F., *Experientia Suppl.* **5**, 71 (1956).
- [3] Alimarin, I. P., *Pure Appl. Chem.* **7**, 455 (1963).
- [4] Minczewski, J., *ibid.* **10**, 567 (1965).
- [5] Specker, H., Harthamp, H., *Angew. Chem.* **67**, 173 (1955).
- [6] Claassen, A., *Chem. Weekbl.* **53**, 33 (1962).
- [7] Specker, H., *Z. Erzbergbau Metallhüttenwesen* **17**, 132 (1964).
- [8] Ehrlich, G., Rexer, E., *Wiss. Z., Techn. Hochsch. Chem. Leuna-Merseburg* **6**, 207 (1964).
- [9] Minczewski, J., *Chim. Anal. (France)* **47**, 401 (1965).
- [10] Lipis, L. V., *Usp. Fiz. Nauk.* **68**, 71 (1959).
- [11] Nedler, V. V., Arakelian, N. A., *Zavod. Lab.* **23**, 672 (1962).
- [12] Konovalov, E. E., Peyzulayev, Sh. I., *Trudy Komm. Anal. Khim.* **15**, 375 (1965).
- [13] Radwan, M., *Freiberger Forschungshefte, Heft B 111*, December 1965, p. 167.
- [14] Strzyżewska B., *Chem. Anal. (Warsaw)* **11** (1966) in press.
- [15] Kane, P. F., *Anal. Chem.* **38**, No. 3, 29a (1966).
- [16] Ducret, L., *Anal. Chim. Acta* **17**, 213 (1957).
- [17] Vasilevskaya, L. S., *Metody Analiza Veshchestv Vysokoi Chistoty*, Nauka, Moskva 1965, p. 16.
- [18] Thiers, R. E., item 1., p. 637.
- [19] D'Ambrosio, A., *Mikrochim. Acta* **1961**, 927.
- [20] Strzyżewska, B., Radwan, Z., *Chem. Anal. (Warsaw)* **11** (1966) in press.
- [21] Chow, T. J., McKinney, C. R., *Anal. Chem.* **30**, 1499 (1958).
- [22] Kokotov, Yu. A., *Radiokhimicheskiye Metody Opredeleniya Mikroelementov*, Nauka, Moskva 1965, p. 54.
- [23] Knižek, M., Provaznik, J., *Chem. Listy* **55**, 389 (1961).
- [24] Butler, E. B., Johnson, W. H., *Science* **120**, 543 (1954).
- [25] Lang, E. P., *Ind. Eng. Chem., Anal. Ed.* **6**, 111 (1934).
- [26] Häberli, E., *Z. Anal. Chem.* **160**, 15 (1958).
- [27] Wickbold, R., *ibid.* **171**, 81 (1959).
- [28] Irving, H., Cox, J. J., *Analyst* **83**, 526 (1958).
- [29] Stegeman, H. Z. *Anal. Chem.* **157**, 267 (1957).
- [30] Nazarenko, V. A., Fliantikova, G. V., *Zavod. Lab.*, **24**, 663 (1958).
- [31] Marczenko, Z., *Zeszyty Naukowe Politechniki Warszawskiej (Warsaw)* **115**, *Chemia*, No. 3, 1965.
- [32] Bjerrum, J., Schwarzenbach, G., Sillen, L. G., *Stability Constants of Metal Complexes with Solubility Products of Inorganic Substances. I. Organic Ligands, II. Inorganic Ligands*, The Chemical Society, London 1957-58.
- [33] Jacimirski, K. W., Vasil'ev, W. P., *Instability Constants of Complex Compounds*, Pergamon Press, Oxford 1960, transl. from Russian.

- [34] Ringbom, A., *Complexation in Analytical Chemistry*, J. Wiley & Sons, New York, 1963.
- [35] Schwarzenbach, G., *Experientia Suppl.* **5**, 162 (1956); *Angew. Chem.* **70**, 451 (1958).
- [36] Cheng, K. L., *Anal. Chem.* **33**, 783 (1961).
- [37] Hulanicki, A., *Talanta* **9**, 549 (1962).
- [38] Gorbach, G., Pohl, F., *Mikrochemie* **3637**, 486 (1951).
- [39] Marczenko, Z., Kasiura, K., *Chem. Anal. (Warsaw)* **9**, 87 (1964).
- [40] Karabash, A. G., Bondarenko, L. S., Mozozova, G. G., Peyzulayev, Sh. I., *Zh. Anal. Khim.* **15**, 623 (1960).
- [41] Degtiareva, D. F., Ostrovskaya, M. F., *ibid.* **20**, 814 (1965).
- [42] Baronova, L. L., Solodovnik, S. M., *ibid.* **19**, 588 (1964).
- [43] Krauz, L. S., Karabash, A. G., Peyzulayev, Sh. I., Lipatova, V. M., Moleva, V. S., *Trudy Komm. Anal. Khim.* **12**, 175 (1960).
- [44] Mayer, J., *Z. Anal. Chem.* **219**, 147 (1966).
- [45] Karabash, A. G., Samsonova, Z. N., Smirnova-Averina, N. I., Peyzulayev, Sh. I., *Trudy Komm. Anal. Khim.* **12**, 255 (1960).
- [46] Sotnikova, N. P., Romanovich, L. S., Peyzulayev, Sh. I., Karabash A. G., *ibid.* **12**, 151 (1960).
- [47] Silvey, W. D., Brennan, R., *Anal. Chem.* **34**, 784 (1962).
- [48] Pickett, E. E., Hankins, B. E., *ibid.* **30**, 47 (1958).
- [49] Marczenko, Z., Krasiejko, M., *Chem. Anal. (Warsaw)* **9**, 291 (1964).
- [50] Marczenko, Z., Kasiura K., *ibid.* **10**, 449 (1965).
- [51] Marczenko, Z., Kasiura, K., *ibid.* **9**, 321 (1964).
- [52] Chwastowska, J., Marczenko, Z., Stolarczyk, U., *ibid.* **8**, 517 (1963).
- [53] Kusnietsov, V. I., *Zh. Anal. Khim.* **9**, 199 (1954).
- [54] Miasoyedova, G. V., *ibid.* **21**, 598 (1966).
- [55] Green, H., *Metallurgia* **70**, 143, 201, 254, 299 (1964).
- [56] Stary, J., *Anal. Chim. Acta* **28**, 132 (1963).
- [57] Stary, J., Hladky, E., *ibid.* **28**, 227 (1963).
- [58] Stary, J., Smizanska, J., *ibid.* **28**, 545 (1963).
- [59] Zolotov, Yu. A., *Trudy Komm. Anal. Khim.* **15**, 3 (1965).
- [60] West, T. S., *Anal. Chim. Acta* **25**, 405 (1961).
- [61] Babko, A. K., Zharovskii, F. G., *Zavod. Lab.* **28**, 1287 (1962).
- [62] Specker, H., Cremer, M., Jackwerth, E., *Angew. Chem.* **71**, 492 (1959)
- [63] Siekierski, S., Taube, M., *Nukleonika (Warsaw)* **6**, 489 (1961).
- [64] Walker, W. R., Li N. C., *J. Inorg. Nucl. Chem.* **27**, 411 (1965).
- [65] Alimarin, I. R., Zolotov, Ju. A., Shakhova, N. V., *Trudy Komm. Anal. Khim.* **14**, 24 (1963).
- [66] Morrison, G. H., Freiser, H., *Solvent Extraction in Analytical Chemistry*, J. Wiley & Sons Inc., New York, 1957.
- [67] Green, D. E., Haslop, J. A. B., Whittey, J. E., *Analyst* **88**, 522 (1963).
- [68] Jackwerth, E., *Z. Anal. Chem.* **202**, 81 (1964).
- [69] Czakow, J., Kucharzewski, B., *Chem. Anal. (Warsaw)* **12** (1967), in press.
- [70] Green, H., *Talanta* **11**, 1561 (1964).
- [71] Karabash, A. G., Peyzulayev, Sh. I., Slusarieva, P. L., Lipatova, V. M., *Trudy Komm. Anal. Khim.* **12**, 331 (1960).
- [72] Häberli, E., *Z. Anal. Chem.* **160**, 15 (1958).
- [73] Koch, O. G., *Mikrochim. Acta* **1958**, 92, 347.
- [74] Chwastowska, J., Minczewski, J., *Chem. Anal. (Warsaw)*, **8**, 157 (1963), **9**, 791 (1964).
- [75] Shigematsu, T., Tabushi, M., *Bull. Inst. Chem. Res. Kyoto Univ.* **39**, 35 (1961).
- [76] Moore, F. L., *A.S.T.M. Spec. Tech. Publ. No. 238*, 13 (1959).
- [77] Karczewska, B., Minczewski, J., Marczenko, Z., *Chem. Anal. (Warsaw)* **6**, 501 (1961).
- [78] Minczewski, J., Chwastowska, J., Marczenko, Z., *ibid.* **6**, 509 (1961).
- [79] Haas, C. S., Pellin, R. A., Everingham, M. R., *Anal. Chem.* **36**, 245 (1964).

- [80] Lancaster, W. A., Everingham, M. R., *ibid.* **36**, 246 (1964).
- [81] Marczenko, Z., Kasiura, K., private communication.
- [82] Tremillon, B., *Les Separations par les Resines Exchangeuse d'Ions*, Masson et Cie., Paris 1965.
- [83] Bayer, E., *Angew. Chem.* **76**, 76 (1964).
- [84] Schumuckler, G., *Talanta* **12**, 281 (1965).
- [85] Rein, J. E., paper presented at 150th Meeting ACS., Atlantic City, N.J., 1965.
- [86] Kataev, G. A., Otmakhova, Z. I., *Zh. Anal. Khim.* **18**, 339 (1963).
- [87] Tera, F., Ruch, R. R., Morrison, G. H., *Anal. Chem.* **37**, 358 (1965).
- [88] Dybczyński, R., Sterliński, S., *Proc. Anal. Chem. Conference, Budapest 1966*, p. 398.
- [89] Fritz, J. S., Abbink, J. E., *Anal. Chem.* **37**, 1274 (1965).
- [90] Kalinin, A. I., Kusnetsov, R. A., Moyssev, V. V., *Radiokhimiya* **4**, 575 (1962).
- [91] Dybczyński, R., Minczewski, J., *Chem. Anal. (Warsaw)* **11** (1966), in press.
- [92] Brooks, R. P., *Analyst* **85**, 745 (1960).
- [93] Fidelis, I., Gwóźdź, R., Siekiński, S., *Nukleonika (Warsaw)* **8**, 320 (1963).
- [94] Siekiński, S., Sochacka, R. J., Institute for Nuclear Research, Warsaw, Report No. 262/V (1964).
- [95] Minczewski, J., Różycki, C., *Chem. Anal. (Warsaw)* **10**, 965 (1965).
- [96] Siekiński, S., Fidelis, I., *J. Chromatog.* **4**, 60 (1960).
- [97] Fidelis, I., Siekiński, S., *ibid.* **5**, 161 (1961).
- [98] Smulek, W., Zelenay, K., Institute for Nuclear Research, Warsaw, Report No. 677/V/XIII/, (1965).
- [99] Smulek, W., *Nukleonika (Warsaw)* **11** (1966), in press.
- [100] Scribner, B. F., Mullin, H. R., *J. Research NBS* **37**, 378 (1946).
- [101] Mandelsham, S. L., Semenov, N. N., Turvotseva, Z. M., *Zh. Anal. Khim.* **11**, 9 (1956).
- [102] Zaidel, A. V., Kaliteevski, N. S., Lipis, L. V., Chayka, M. B., Beliaso, Yu., *ibid.* **11**, 21 (1956).
- [103] Shvarts, D. M., Kaporskii, L. N., *Zavod. Lab* **23**, 11 (1957).
- [104] Gerken, E. B., *Sbornik Trudov Gintsvetmeta* **19**, 800 (1962).
- [105] Neeb, K. H., *Z. Anal. Chem.* **194**, 255 (1963).
- [106] Joungdahl, C. A., Deboer, F. E., *Nature* **184**, 54 (1959).
- [107] Fratkin, E. G., Shebunin, V. S., *Trudy Komm. Anal. Khim.* **15**, 127 (1965).
- [108] Fratkin, E. G., *Zavod. Lab.* **30**, 170 (1964).
- [109] Karabash, A. G., Peyzulayev, Sh. I., Sotnikova, N. P., Sazanova, S. K., *Trudy Komm. Anal. Khim.*, **12**, 108 (1960).
- [110] Geilmann, W., Neeb, K. H., *Z. Anal. Chem.* **160**, 410 (1958); **165**, 251 (1959).
- [111] Shvarts, D. M., *Zavod. Lab.* **26**, 966 (1960).
- [112] Baudin, G., Lorrain, S., Platzer, R., *Travaux XXXV Congrès Intern. Chimie. Ind., Varsovie 1965*.
- [113] Rutkowski, W., Wasowicz S., *Chem. Anal. (Warsaw)* **11** (1966), in press.
- [114] Marczenko, Z., *ibid.* **9**, 1093 (1964).
- [115] Minczewski, J., Chwastowska, J., *ibid.* **6**, 715 (1961).
- [116] Chwastowska, J., *ibid.* **7**, 731 (1962).
- [117] Pijck, J., Hoste, J., Gillis, J., *Proc. Intern. Symp. Microchem., Birmingham, 1958*, p. 48.
- [118] Schulek, E., Laszlovsky, J., *Microchim. Acta* **1960**, 485.
- [119] Gorsuch, T. T., *Analyst* **87**, 112 (1962).
- [120] Földzińska, A., Malinowski, J., *Nukleonika (Warsaw)* **7**, 153 (1962); **8**, 233 (1963).
- [121] Marczenko, Z., Choluj-Lenarczyk, L., *Chem. Anal. (Warsaw)* **10**, 729 (1965).
- [122] Pfann, W. G., *Zone Melting*, J. Wiley & Sons, New York, (1959).
- [123] Downarowicz, J., *Chem. Anal. (Warsaw)* **4**, 643 (1959).
- [124] Pfann, W. G., Theuerer, H. C., *Anal. Chem.* **32**, 1574 (1960).
- [125] Konovalov, E. E., Peyzulayev, Sh. I., Emelyanov, V. P., *Zh. Anal. Khim.* **18**, 1500 (1963).
- [126] Konovalov, E. E., Peyzulayev, Sh. I., *Trudy Komm. Anal. Khim.* **15**, 375 (1965).

# PRECONCENTRATION, SAMPLING, AND REAGENTS

## Contributed Papers and Discussion

GEORGE H. MORRISON

*Cornell University, Ithaca, New York 14850*

### I. Introduction

Any symposium concerned with the techniques for trace characterization would be incomplete without a session on the chemical and/or physical methods of pretreatment of samples. Although we have heard much of the capabilities of the various instrumental techniques for trace analysis, the full realization of their potentialities for the compositional characterization of complex materials can, in many cases, be accomplished only by coupling the techniques with preconcentrations and separations to remove or minimize the ever-present possibility of interferences or to provide adequate microconstituent for the measurement to be employed.

The lecture by Professor Minczewski presented earlier has reviewed the various methods of concentration and separation of traces and the problems of contamination associated with these methods. The contributed papers in this session describe some new developments in the field, as well as provide reviews of specific methods. Before discussing this material, however, a few additional comments on the general subject may provide a better perspective for their role in trace analysis.

All analytical methods can be divided into three component steps: sampling, chemical and/or physical pretreatment, and instrumental measurement. These steps are interrelated and require different degrees of emphasis depending upon the individual analytical situation. But, in all cases, one is interested in finally measuring a signal which can be related to the concentration of a particular species in the original sample. Therefore, in order to properly evaluate the requirements of preconcentration, separation, and sampling, it would be most meaningful to start with an examination of the last component step of analysis, i.e., instrumental measurement.

The usefulness of the various measurement techniques to trace characterization is governed to a considerable extent by the detection limits that can be achieved for the elements of interest in a given system, i.e.,

the smallest quantity or concentration that can be detected with a certain stated confidence. Figure 1 [1]<sup>1</sup> graphically summarizes the detection limits that can be experimentally achieved with a number of trace techniques under conditions of little or no interference by the matrix or by other elements. The original reference should be consulted for details for specific elements and experimental conditions. It can be seen that in the absence of interferences all of the techniques included are generally applicable to the determination of most elements down to 100 ng. Although many of the techniques are applicable to a more limited number of elements in the range of 0.01–100 ng, only spark-source mass spectrometry and activation analysis are generally applicable below this. These limits, therefore, represent the capabilities of the measurement steps for the various techniques. Failure to achieve them in the analysis of actual samples arises because of interferences by the matrix or other trace elements or because of the diluting effect of the matrix.

The specific requirements for preconcentration and separation are intimately related to the sample under consideration and the technique of measurement employed. There are two important terms in separations in trace analysis that should be defined at this point [2].

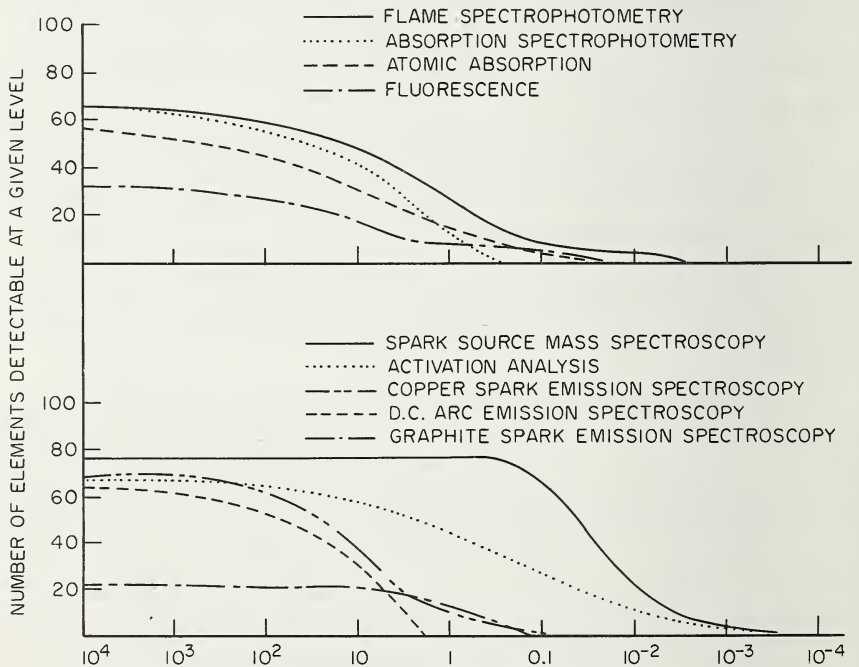


Figure 1. Summary of detection limits in nanograms, for a number of trace techniques under conditions of little or no interference by matrix or other elements.

<sup>1</sup> Figures in brackets indicate the literature references at the end of this paper.

One is the recovery or yield ( $R_A$ ) of a desired trace element A, and the other is the separation factor ( $S_{B/A}$ ) for an undesired constituent B with respect to a desired trace element A. The definitions are as follows:

$$R_A = Q_A/Q_A^\circ \times 100 (\%) \quad (1)$$

$$S_{B/A} = (Q_B/Q_A)/(Q_B^\circ/Q_A^\circ) \quad (2)$$

where  $Q_A^\circ$  the quantity of A in the sample;  $Q_B^\circ$  = the quantity of B in the sample;  $Q_A$  = the quantity of A after the separation;  $Q_B$  = the quantity of B after the separation.

The reciprocal of  $S_{B/A}$  is called the concentration factor or the enrichment factor of A when B is the matrix. The ideal separation has a recovery of 100% and separation factors of zero. Actually, these two factors depend on the nature of the sample as well as on the method of separation. Knowing the limits of detection of the various methods of measurement, one can then select an adequate sized sample and a method of appropriate separation and recovery factors to achieve adequate sensitivity and precision in the trace analysis. Time and effort can usually be conserved by selecting methods which do not require complete separation.

## II. Preconcentration and Separation Methods

Professor Minczewski has surveyed the various methods of separation. Because of the broad scope of the subject, only an abbreviated treatment was possible in the time allotted for presentation. Of particular value, however, is the citing of numerous applications of the various methods, principally from papers not readily accessible to the Western world. The separation methods included in the treatment are precipitation and coprecipitation, extraction, chromatography, volatilization, and zone melting.

A number of the contributed papers in this session further illustrate the effectiveness of a few of these methods of preconcentration and separation to the determination of trace elements. With regard to precipitation methods, the paper by Alvarez illustrates the value of electrolytic methods of preconcentration. In this study submicrogram amounts of silver have been isolated from macro amounts of zinc matrix by electrodeposition on high purity graphite or pyrolytic graphite cathodes followed by washing for eventual determination by graphite-spark emission spectroscopy. Many preconcentration procedures produce extremely dilute solutions of the trace elements, resulting in sorption losses; however, trace elements having suitable electrodeposition potentials can be deposited directly on the cathode from a concentrated solution of the matrix, thus virtually eliminating errors of this type.

Ion exchange methods hold considerable promise for preconcentration of trace elements and Professor Minczewski has discussed a number of applications. Most applications in the past, however, use ion exchange in a more or less conventional fashion taking advantage of the different distribution coefficients of the species to be separated in a given system. I would like to take this opportunity to refer to a novel approach to preconcentration of multielement traces by ion exchange which was developed in our laboratory and which we refer to as "precipitation ion exchange" [3, 4]. By combining precipitation and ion exchange simultaneously on the resin column useful separations are made possible. In this approach the matrix and trace elements are first sorbed on a cation exchange column, the matrix is then precipitated by an organic-hydrochloric acid eluent, followed by nonselective elution of the traces. The separation is based on the insolubility of the matrix and low selectivity of the traces in 70% p-dioxane-30% concentrated hydrochloric acid (v/v). As many as 40 trace elements may be preconcentrated in greater than 90% yields, matrix-free or with only small amounts of matrix from the following matrices: lithium, sodium, potassium, rubidium, magnesium, calcium, strontium, barium, scandium, yttrium, and lanthanum. Using 81% dioxane-10% ethanol-9% concentrated hydrochloric acid as eluent, matrices such as nickel, chromium, manganese, lead, and aluminum demonstrate sufficient insolubility and delayed column breakthrough, as well as favorable trace recovery, to be of value in preconcentration.

The paper by Burnett et al., describes a novel paper disk anion exchange column that shows promise for the rapid separation of radio-nuclides in neutron activation analysis. Their study has been directed towards the decontamination of complexes of radioactive traces from sodium-24, based on the sorption on the paper disks of anion complexes of these metals formed in hydrochloric acid media.

Again I would like to cite a recent study in our laboratory concerned with a general approach for the rapid separation of radioactive species, which has particular application to matrix removal in activation analysis [5]. The method, which is called "isotopic ion exchange", can effect rapid multi-element trace separations from large amounts of a radioactive matrix element, thereby permitting gamma spectrometric measurement of the traces. The approach is applicable to a variety of matrices, and separations can be achieved in a matter of minutes.

A novel volatilization method of preconcentration that may have considerable impact on the determination of trace elements in organic and biological materials is presented in the paper by Bersin, Hollahan, and Holland. Excited atomic and molecular oxygen produced in a radio frequency discharge permit the low temperature ashing of the organic matrix. The net effect is to provide a low temperature environment for removing oxidizable material from the sample without introducing con-

taminants. Thereby, one avoids sintering, melting, volatilization and other consequences of high temperature which can destroy crystallinity or other structural characteristics of the developed ash, or create loss of volatile elements. This low temperature ashing is accomplished at a rate practical for analytical requirements. The coupling of this approach with a variety of measurement techniques is possible, permitting both compositional and structural characterization.

Other separation methods described in papers for this session include a review of the ring-oven technique by Mukherji, and the application of the zone-melting process to metal chelate systems by Kaneko, Kobayashi, and Ueno.

The application of a variety of conventional separation and preconcentration methods to the trace analysis of several important materials is also presented in papers for this session. Thus, the determination of parts per million and parts per billion amounts of a number of impurities in very pure rare earth oxides and metals is described in the paper by Banks et al., in which extraction chromatography and solvent extraction, among other methods, are coupled with atomic absorption and spectrophotometric methods of determination. These determinations permit the evaluation of more direct methods of trace analysis such as emission spectroscopy and spark source mass spectrometry.

An excellent review of preconcentration methods for the determination of trace elements in sea water is provided in the paper by Joyner et al., involving cocrystallization, coprecipitation, solvent extraction, and chromatography.

Much emphasis in this session has been placed on separations for the trace analysis of solid and liquid samples. Of particular importance in materials research is the use of ultrapure gases, and Roboz describes several preconcentration methods for trace elements in gas matrices used in conjunction with mass spectrometric determinations. Included is the removal of matrix hydrogen by diffusion through a palladium membrane, removal of matrix carbon dioxide by freeze-out, and removal of oxygen matrix using sodium-potassium alloy.

### III. Reagents

Any discussion of the chemical preconcentration and separation of trace elements at the nanogram level in aqueous systems would be meaningless unless the problem of contamination by reagents and/or container material is objectively evaluated. In their paper Freeman and Kuehner discuss the mechanisms of contamination, the principles of contaminant separation, and specific studies of reagent purification. Attention has been given to the purification of water which is broadly needed for reagent preparation, to hydrochloric acid which is one of the common acid reagents, and to the comparative decontamination of silica gel.

#### IV. Sampling and Sample Preparation

Finally I would like to discuss the first and perhaps most critical step in an analytical method, namely sampling and sample preparation. One of the most serious sources of error in analysis is that introduced by improper sampling. The situation is particularly acute in the case of trace characterization in materials research where the trace elements at the parts per million and parts per billion levels are almost invariably distributed in the solid state material in a heterogeneous fashion as has been shown by Professor Minczewski.

The paper by Skogerboe and Morrison examines a number of the problems in terms of sampling theory and shows their effect on various trace analytical techniques. In view of the many factors influencing sampling errors, it is understandable why analysts encounter difficulties when they try to compare the analytical results obtained by different trace techniques. Table I presents generalized data to illustrate the sampling capabilities of some of these techniques. The data may be regarded as typical since they represent the most common practice, usage, and results, as determined from the general literature. It can be seen that the combined pretreatment and measurement errors for all methods listed are in the same range of 1-5% depending upon the care taken in the analysis. All of these techniques involve either electronic or photographic detection in the measurement step and relative standard deviations of 1-5% are reasonable.

With regard to the total error involved in the various methods, it is readily apparent that techniques utilizing solutions consistently result in a reported overall error which is better than that observed for direct techniques. It should be noted that solution techniques normally utilize a relatively large sample with a resultant reduction in the sampling error observed. Also, it is a common practice to make several measurements on the same homogenized solution and use these data to obtain a precision estimate. In reality this estimates the measurement precision only and tends to place the technique in a more favorable, but false, position when compared with other techniques.

A similarly misleading practice is encountered in publications involving the nondestructive techniques such as neutron activation and x-ray fluorescence. Either the square root of the observed count or the reproducibility of subsequent measurements on the same sample are frequently taken as representative of the total error. The first approach estimates only the measurement precision, while the latter partially estimates the combined pretreatment-measurement errors if neutron or x-ray bombardment is considered as a part of the pretreatment stage. Explicitly, these usages tend to delete sampling error by ignoring it or to reduce it by using a large sample together with homogenization.

The overall reproducibilities of direct methods of analysis are frequently less favorable because the techniques use smaller samples

TABLE 1. Distribution of errors of trace methods.

Technique	Typical Sample Size, Mg	Most Common Mode of Sample Pretreatment	Typical Relative Standard Deviation, %	
			Pretreatment and Measurement	Total
Spectrophotometry				
Absorption	100-1000	homogenization by dissolution	1-5	1-5
Fluorescence	100-1000	homogenization by dissolution	1-5	1-5
Flame	100-1000	homogenization by dissolution	1-5	1-5
Atomic absorption	100-1000	homogenization by dissolution	1-5	1-5
Neutron activation	10-1000	direct or homogenization by dissolution	1-5	1-15
Emission spectrography	1-50	direct or homogenization by dissolution	1-5	5-30
Spark source mass spec	0.1-10	direct	1-5	5-30
Microprobe	0.01-1	direct	1-5	5-30
X-Ray fluorescence	10-1000	direct or homogenization by dissolution or fusion	1-5	5-30

subject to greater sampling error. Also, these techniques are often not amenable to prehomogenization practices. While it is true that the lack of control of dc arc or the spark in emission or mass spectrography contributes to the total error, these same "uncontrolled" sources are often used on samples known to be homogeneous to obtain a total error equivalent to the combined pretreatment measurement errors. Such results are numerous in emission and mass spectrometry, and indicate that although these techniques do not provide the best estimate of the bulk

concentration of heterogeneous samples, they should be very useful in giving a good estimate of the localized concentrations in the fashion of a probe. It should be apparent from this discussion that comparison of the indicated reliabilities of analytical results obtained by independent methods may be invalidated by the difference in the capabilities of the methods with regard to the inference of heterogeneity and/or misrepresentation of the total error reported.

In connection with sampling, the preparation of solids for further study and characterization is a very important step, and the paper by Hill, Morris, and Frazer describes a cathodic etching method that has been developed to clean the surfaces of metal samples prior to oxygen determination by vacuum fusion. The sample is made the cathode in a low pressure argon-ion discharge. The argon ions bombard the surface of the sample and remove the oxide film by an etching process. The oxygen content of metal samples such as high purity uranium and iron cleaned by cathodic etching is consistently lower than that achieved using acid etching or filing.

A somewhat related study by Yates and Madey describes the preparation of atomically clean surfaces. Details are presented on the production and measurement of ultrahigh vacuums, the purification and handling of gases for adsorption studies under these conditions, as well as the production and characterization of clean surfaces.

Finally, an example of the problem of losses of trace elements in solution samples by adsorption is treated in the paper by F. K. West and P. W. West. A study is described to evaluate the adsorption of silver in potable water samples on various storage container materials and the use of ligands to complex the traces of silver to prevent losses.

## V. Discussion

Margoshes (NBS) agreed with the general feeling that separations and preconcentrations at the nanogram level are to be avoided in general analysis because of the dangers of contamination. There are, however, situations where they are essential and he cited the situation discussed in the paper by Alvarez where it was necessary to remove the matrix in order to accurately determine traces of elements in certified standard samples of zinc. Here every effort must be made to provide very dependable certification.

Grant of the University of New Hampshire commented on the problem of sampling errors and cited the example of the original sampling of biological systems where errors of  $\pm 25\%$  are not uncommon before the analyst receives the laboratory sample.

Morrison raised the question of the validity of the designation of commercially available high-purity materials as 5-9's or 6-9's purity. In many cases emission spectroscopy is used to characterize these materials and the presence of many impurities is missed because of the ineffec-

tiveness of the method. Comments from the audience indicated that most analysts recognized these designations as being meaningless and understood the necessity of analyzing these materials for the specific application at hand.

Honig of RCA raised the question of reporting analytical results in units of parts per million on a weight basis versus an atomic basis. It was concluded that the preferred units depended upon the particular application involved. In any case, it is a simple matter to convert from one form to the other.

Considerable interest was expressed in a novel approach to reagent purification described by Freeman of the NBS. The method includes the storage of high purity reagents in their frozen state. Water, sulfuric acid and sodium hydroxide are maintained at  $-25^{\circ}\text{C}$  and facilities are being constructed for the frozen storage of aqueous mineral acid solutions.

## VI. References

- [1] Morrison, G. H. and Skogerboe, R. K., "General Aspects of Trace Analysis", in Trace Analysis: Physical Methods, G. H. Morrison, editor, Interscience Publishers, N.Y., 1965, p. 16.
- [2] Mizuike, A., "Separations and Preconcentrations", in Trace Analysis: Physical Methods, G. H. Morrison, editor, Interscience Publishers, N.Y., 1965, p. 104.
- [3] Tera, F., Ruch, R. R., and Morrison, G. H., *Anal. Chem.* **37**, 358 (1965).
- [4] Ruch, R. R., Tera, F., and Morrison, G. H., *Anal. Chem.* **37**, 1565 (1965).
- [5] Tera, F., and Morrison, G. H., *Anal. Chem.* **38**, 959 (1966).



# THE STUDY OF CRYSTAL IMPERFECTIONS BY MEANS OF OPTICAL METHODS AND BY MEANS OF ELECTRON MICROSCOPY AND ELECTRON DIFFRACTION

S. AMELINCKX<sup>1</sup>

*Centre d'Etude Nucléaire, Mol, Donk, Belgium*

## I. Introduction

In this paper a survey will be given of optical and electron optical methods for revealing dislocations and other crystal defects. In a first part we shall sketch the historical development of the so-called methods for "direct observation" of crystal defects. By a "direct" method is meant a method which allows to localize the defect and to determine at least some of its geometrical characteristics. This is in contrast with indirect methods for the study of dislocations such as X-ray line broadening, internal friction, etc. From what follows it will become clear that the term "direct" is somewhat relative because for most of the methods which are termed direct one does in fact not see the dislocation or defect itself, but some more or less adequate image which may be a row of particles in the case of the decoration method or a fringe pattern in the case of electron microscopy.

The second part is devoted to a brief discussion of some of the properties of dislocations, stacking faults and other lattice defects. Only these properties will be mentioned which are relevant for our purpose, for instance because one of the methods of studying dislocations is based on it. A brief description will be given also of some of the geometrical features which lend themselves easily to a study of direct methods.

In a third part a systematic discussion is presented of the different optical and electron optical methods for the study of lattice imperfections. In particular we shall emphasize the techniques, rather than the results obtained by them. Consequently neither is an attempt made to give a complete survey of all results, nor is it possible to include all references to such work. Special attention will be paid to the limitations of each of the methods and specific fields of application shall be indicated.

---

<sup>1</sup> Also at: Laboratorium Fysika Vaste Stof, Rijksuniversitair Centrum, Middelheimlaan 1 Antwerpen.

## II. Historical Survey

The discovery of X-ray diffraction and of methods for structure determination has laid the emphasis on the perfect three dimensional periodicity of crystals. However it was soon found that real crystals show deviations from strict three dimensional periodicity. This follows already from a comparison of the observed intensity of the X-rays diffracted by a crystal with that calculated for a perfect crystal. It is only very recently that crystals have been found which behave as perfect crystals should according to the dynamical theory of X-ray diffraction.

The properties which are most sensitive to the presence of geometrical imperfections are however the mechanical properties such as yield stress. It was in fact in an attempt to explain the slip process in crystals that dislocations were first introduced by Taylor [1]<sup>2</sup> and Burgers [2]. The basic idea was a very simple one. The reason why the calculations based on the perfect crystal assumption failed in predicting the strength of crystals was that in a perfect crystal one had to accept that a *whole* crystal plane of atoms slipped *at once* over a similar plane. This process obviously requires a large force since all atoms have to go simultaneously over the potential hills constituted by the other layer of atoms. This "one shot" process can be replaced by a progressive motion of a small number of atoms at any time if one assumes the presence of a dislocation. It was this idea which lead the theoreticians to postulate possible models for linear defects so called *dislocations*, which would be capable of performing the required atom movement on propagating between two crystal planes.

For a long time the study of dislocations remained the privilege of theoreticians and large chapters of dislocation theory were written without even a single observation proving that dislocations really exist in crystals. This situation persisted until 1950, when, again on theoretical grounds, it was predicted that dislocations should play an important role in the growth of crystals [3]. The importance of the dislocation theory of crystal growth lies in the fact that it predicted an unambiguously defined and in principle easily observable surface feature: the *growth spiral*. The observation of growth spirals provided a simple means for localizing the emergence points of dislocations in the surface of crystals. The scale of these surface features was such that the optical microscope was quite adequate, especially if phase contrast is used, to improve the visibility of surface steps. For this reason optical methods have played an important role in the direct observation of dislocations at least in the initial stage.

The study of growth features requires for obvious reasons growth faces. Furthermore the growth steps to be revealed are of the scale of the unit cell, which means that almost atomically flat growth faces are

---

<sup>2</sup> Figures in brackets indicate the literature references at the end of this paper.

required for the study of the growth spirals. For this reason it is clear that the use of growth spirals as "indicators" for the emergence points of dislocations can only be of limited application.

The logical step forward was obviously to try whether the reverse phenomena of growth, i.e., dissolution, etching or evaporation would also be sensitive to the presence of dislocations. On etching crystals exhibiting growth spirals or growth hills it was found that pits were produced at the centers of growth spirals or at the tops of growth hills proving clearly that etchpits are formed preferentially at the emergence points of the same dislocations that gave rise to growth spirals [4]. Moreover it was discovered that pits were produced also at sites other than those marked by the emergence points of screw dislocations. This observation was in agreement with the fact that according to the dislocation theory of crystal growth not all dislocations give rise to spirals, but only those for which  $\mathbf{b} \cdot \mathbf{n} \neq 0$  ( $\mathbf{n}$  = unit normal on crystal face under observation,  $\mathbf{b}$  = Burgers vector of the dislocation). The etch pitting technique for revealing the emergence points of dislocations has now been developed to the stage where it has become a standard method for the quasi-non-destructive determination of crystal perfection, mainly in the semi-conductor field.

Also evaporation has found application as a means of studying the dislocation geometry. Since the scale of the phenomena is however at the limit of resolution of the optical microscope, it is more successfully used in conjunction with electron microscopy [5] although the first observations were made with optical microscopy [6].

All the methods mentioned so far are surface methods and therefore only reveal the emergence points. As a result only a limited amount of information can be obtained from them. The first method capable of revealing dislocations along their length in the interior of transparent crystals was the so called "decoration" method. It reveals the dislocations by causing particles of a second phase or of the stoichiometric excess of one of the constituents to separate out along them. The method was discovered as a by-product of a study of the photographic process by Hedges and Mitchell [7]. When subjecting crystals of silver bromide to the print out process they discovered that specks of photolytic silver were formed preferentially along dislocations. The method was afterwards adapted and used intentionally for the study of dislocations in alkali halides [8], in silicon [9] and other crystals [10].

Comparing etchpits with internal decoration patterns it was found as well for alkali halides as for silver bromide and for silicon, that the etchpits do form at the emergence points of dislocations in the surface, proving the relation between the two methods [11].

Also the decoration technique has limitations. The most obvious one is that since optical microscopy is used for the observation, one is limited by the resolution of the optical microscope. However as we

shall see below other factors limit the use of the method. The crystals should furthermore be transparent either to visible light or to some other easily detectable radiation (e.g., infra red) which limits practically the application to non-metals. However it has been shown recently that use can be made of the fact that certain metals are transparent in the ultra violet [12].

The decoration methods do not allow to see "bare" dislocations; the presence of dislocations can only be inferred from the presence of linear arrangements of fine precipitate particles which scatter light and which are assumed to "decorate" the dislocations.

"Bare" dislocations can nevertheless be observed optically as a result of stress birefringence [13]. Comparison between the etch pattern, the decoration pattern and the birefringence pattern for the same dislocation arrangement in silicon has shown perfect one to one correspondence giving confidence in the three methods [14].

The most versatile method for the direct study of dislocations is undoubtedly electron microscopy in transmission. After some partly successful attempts by Heidenreich [15] and Castaign [16], transmission electron microscopy was shown to be a method capable of revealing dislocations and other crystal defects by Hirsch and coworkers [17] and independently by Bollmann [18]. The contrast is *not* due to absorption, as in the case of replica, but instead it results from diffraction phenomena at the deformed region of the crystal around the dislocation.

For a correct interpretation of the image produced in the electron microscope at imperfections a fairly good knowledge of diffraction contrast theory is required. If one wishes to extract all the information which is contained in an electron micrograph a complete knowledge of the exact diffraction conditions is necessary. It is therefore useful to combine direct observation with electron diffraction and correlate the information obtained from both.

Almost simultaneously Menter [19] showed that the periodic arrangement of molecules in certain organic crystals (Pt-phthalocyanine) could be imaged directly in the electron microscope. From the local disturbance of the lattice rows one can then conclude to the presence of dislocations.

Pashley, Menter and Bassett [20] also developed methods to produce a "geometrical" magnification of crystal lattices so as to bring the detailed structure of the resulting pattern within the resolving power of the electron microscope. The method consists in superposing thin films formed by metals with slightly different lattice parameters or with a slightly different orientation. The so called "moiré pattern" gives a magnified representation of the actual crystal lattice. A dislocation in the lattice of one of the constituent crystals of the sandwich is revealed as a dislocation in the moiré pattern.

As well the formation of "lattice fringes" as the formation of "moiré fringes" is the result of a diffraction phenomena. Considerable care is therefore needed in interpreting discontinuities and disturbances of fringes in terms of lattice defects. Some of the difficulties are discussed below.

Perhaps the ultimate technique for the study of dislocations and even individual point defects is the field ion microscope developed by Müller [21]. It allows to reveal patterns of individual atoms in the surface of fine tips of refractory metals. The application of high electrostatic fields allows to "peel off" monolayers of atoms and as a result it becomes possible to explore the crystal in depth.

Parallel with the electron optical methods a number of X-ray methods for mapping dislocations have been developed. A review of these is the subject of another paper and we shall therefore not discuss them.

### III. Structural Defects

In this chapter we shall only give a very elementary survey of some notions of dislocation theory which are required for an understanding of the remaining part of the paper. For a more complete treatment of the theory we refer to the well known textbooks [21b].

#### A. DISLOCATIONS

##### 1. *Definition, Displacement Vector*

First an intuitive definition of the concept of a dislocation will be given. The definition merely states how a dislocation can be introduced into a perfect crystal. Consider the ideal crystal with a primitive lattice of Figure 1a. Imagine a cut along one of the cube planes. Displace now the two parts I and II, underneath and above the cut, one with respect to the other, over a vector  $\mathbf{b}$ . This can be done in three different ways without destroying the homogeneity of the crystal: (1) by shearing in the  $x$ -direction (Figure 1b); (2) by shearing in the  $y$ -direction (Fig. 1d); (3) by pulling the two parts apart in the  $z$ -direction and inserting a supplementary half plane (Fig. 1c). It is evident from Figure 1 that the operations (1) and (3) lead to the same configuration, which is termed an *edge dislocation*; operation (2) gives a different configuration called a *screw dislocation*. In all cases a line discontinuity  $XY$  is created, which is in cases (1) and (3) the edge of a supplementary half plane, and in case (2), the axis of the helicoidal surface formed by the  $(xz)$  "planes". In cases (1) and (3) this line, called the *dislocation line*, is the limit between the part of the crystal plane,  $(xy)$  in this case, where glide has occurred, and the part that remained unaltered. This plane is the *glide plane* and for the edge dislocation this is unambiguously determined, since it passes through the line and is perpendicular

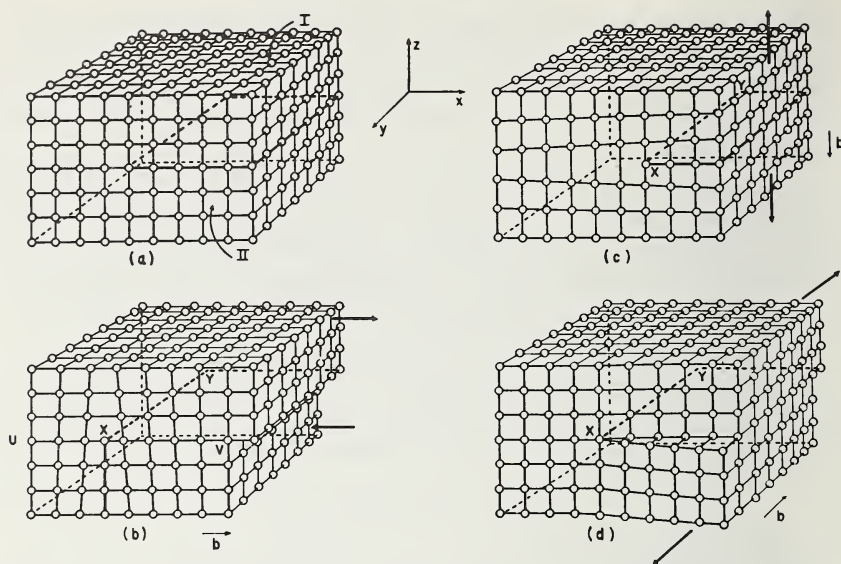


Figure 1. (a) Perfect crystal. (b) Crystal containing an edge dislocation  $XY$  introduced by shearing in the  $x$ -direction along the plane  $XYV$ . (c) Crystal containing an edge dislocation  $XY$  introduced by inserting a supplementary half plane ( $yz$ ). (d) Crystal containing a screw dislocation  $XY$  introduced by shearing in the  $y$ -direction.

to the supplementary half plane. The configuration (3) could also result from glide on a plane ( $zy$ ) perpendicular to the inserted half plane. For the screw dislocation, every plane passing through the line could function as a glide plane (the configuration has axial symmetry in an isotropic medium).

For an edge dislocation  $\mathbf{b}$  is perpendicular to the line, whereas in the case of a screw dislocation,  $\mathbf{b}$  is parallel to the line. In both cases the glide plane contains the line and  $\mathbf{b}$ .

The definitions introduced here are not very rigorous. The main purpose is to demonstrate that one can distinguish only two different types of pure dislocations, differing only in the relative orientation of the displacement vector  $\mathbf{b}$  and the line. It is possible to consider all intermediate orientations; this leads to dislocations of mixed character.

## 2. Burgers Circuit—Burgers Vector

More rigorous definitions can be formulated in a geometrical way, without thinking of a deformation, by comparing the real crystal with an ideal crystal, and introducing the concept of *corresponding paths*. Consider first an edge dislocation, which can be represented in two dimensions. Let Figure 2a represent the crystal containing an edge dislocation (perpendicular to the plane of the figure at  $D$ ) and Figure 2b an ideal crystal. One can now consider a path in the ideal crystal de-

fined by a prescription of the following kind:  $x$  unit distances to the left,  $y$  downward,  $z$  to the right, etc. As long as one stays in "good" parts, there is no difficulty in finding a path given by the same prescriptions in the real crystal. These are corresponding paths.

Consider now a *closed* path in a *real* crystal, going all the way through the good crystal but possibly surrounding dislocations, such a path is called a *Burgers circuit*. The corresponding path may either be closed also (e.g. path 1) or it may fail to close (e.g. path 2); this depends upon whether the Burgers circuit surrounds a dislocation or not. The closure failure i.e., the vector  $\mathbf{A'B'} = \mathbf{b}$  is the Burgers vector of the dislocation surrounded by the Burgers circuit,  $\mathbf{b}$  is perpendicular to the dislocation line. It is further evident that  $\mathbf{b}$  is identical with the displacement vector introduced in section III.A.1. For a pure screw dislocation the Burgers vector is parallel to the dislocation line. When a Burgers circuit surrounds more than one dislocation, the closure failure is the sum of the Burgers vectors of all the individual dislocations surrounded by the circuit.

It is clear that the definition of the Burgers vector as given here still depends on a number of arbitrary conventions. The set of conventions which is usually adopted is the so called FS/RH rule. It consists in applying the following prescriptions:

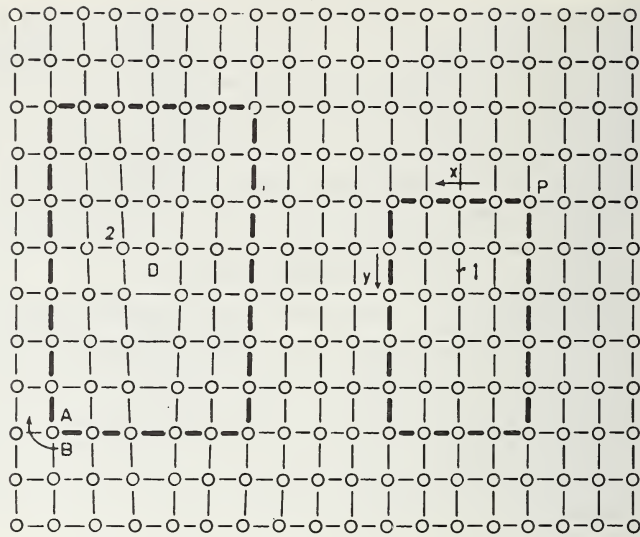
- (i) Choose an *arbitrary positive sense* along the dislocation.
- (ii) Make a *closed Burgers circuit* in the deformed crystal.
- (iii) The circuit should be *right handed* (RH) when viewed along the *positive sense* of the dislocation.
- (iv) The corresponding circuit is constructed in the perfect crystal.
- (v) The closing vector, which is the Burgers vector of the dislocation, connects the final point (F) with the starting point (S) of the circuit.

Once a positive sense is chosen along the dislocation the Burgers vector is unambiguously defined.

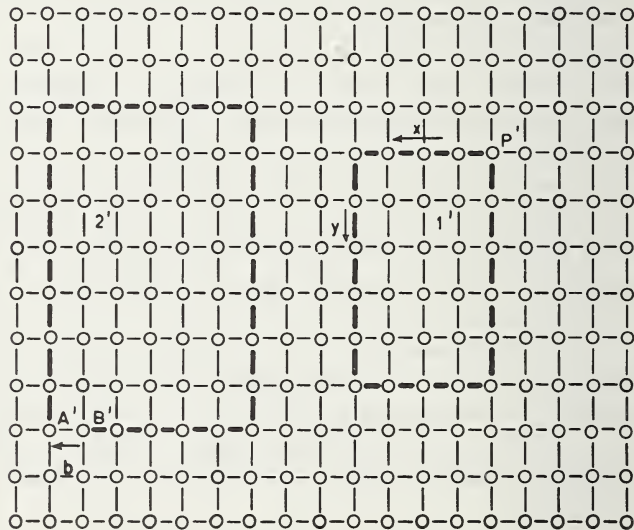
Both kinds of dislocations can be positive or negative. When the edge dislocation of Figure 1b with supplementary half plane above the plane  $UV$ , is called positive, an edge dislocation with the supplementary half plane under  $UV$  would be called negative. Positive and negative screw dislocations can be defined as the axis of right- and left-handed helicoidal surfaces.

### 3. Dislocation Loops

For topological reasons a dislocation line either emerges with both ends at the surface or it forms a closed loop. When the dislocation line branches, the sum of the Burgers vectors of the three (or more) components is zero:  $\mathbf{b}_1 + \mathbf{b}_2 + \mathbf{b}_3 = 0$ . This last relation implies that the positive sense of the dislocations is chosen away from the branching point.



(a)



(b)

Figure 2. Burgers circuit for an edge dislocation  $D$ ;  $1$  is a circuit not surrounding the dislocation, the corresponding circuit  $1'$  is closed; circuit  $2$  surrounds the edge dislocation,  $2'$  is not closed, the closure failure is vector  $A'B'$ .

A dislocation loop has the same Burgers vector along its whole length. As a consequence the line changes its character (edge or screw) along different parts of the loop.

Consider *e.g.*, the cut ABCD (Fig. 3) along a glide plane in a primitive lattice and displace the material contained in the parallelepiped ABCDA'B'C'D' with respect to the surrounding material over a vector  $\mathbf{b}$  parallel to DC. The resulting situation is shown in Figure 4b. Figure 4a is a cut along XY. It is evident that the square dislocation loop so obtained consists of two edge parts BC and AD and two screw parts AB and DC, both being of opposite sign. Such a loop is "glissile."

One could also compress the parallelepiped into the crystal over a vector  $\mathbf{b}$  parallel to AA', creating a square step on the upper surface and a square dislocation loop ABCD in the interior of the crystal. The loop now has edge character along its whole length; this is shown in Figure 5 which represents an arbitrary cut. It is termed a *prismatic dislocation*.

#### 4. Displacement Fields

It is clear that in the vicinity of a dislocation the atoms are not at the sites which they would occupy in a perfect crystal. One can describe the displacements of the atoms around a dislocation by means of a vector field represented by a *displacement function*  $R(r)$ . For a screw dislocation in an infinite medium all displacements are parallel to the line. If the screw dislocation is along the  $z$ -axis the components of  $R$  are

$$R_x = R_y = 0 \quad R_z = (b/2\pi) \arctg(y/z)$$

For an edge dislocation along the  $z$ -axis and with a Burgers vector along the  $x$ -axis, the supplementary half plane being along the positive part of the  $y$ -axis, one finds for the displacement field

$$R_x = (b/2\pi) [\arctg(y/x) + xy/2(1-\nu)(x^2 + y^2)]$$

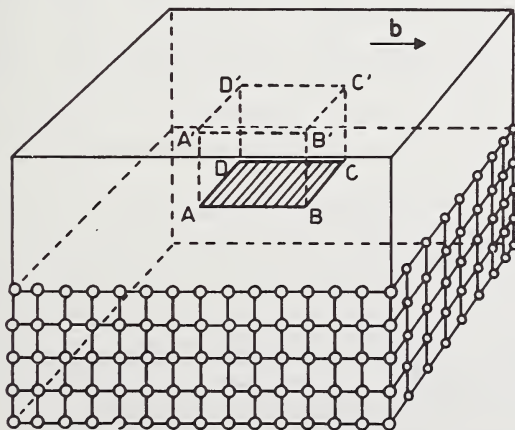


Figure 3. Cut in a perfect crystal leading to the formation of a dislocation loop.

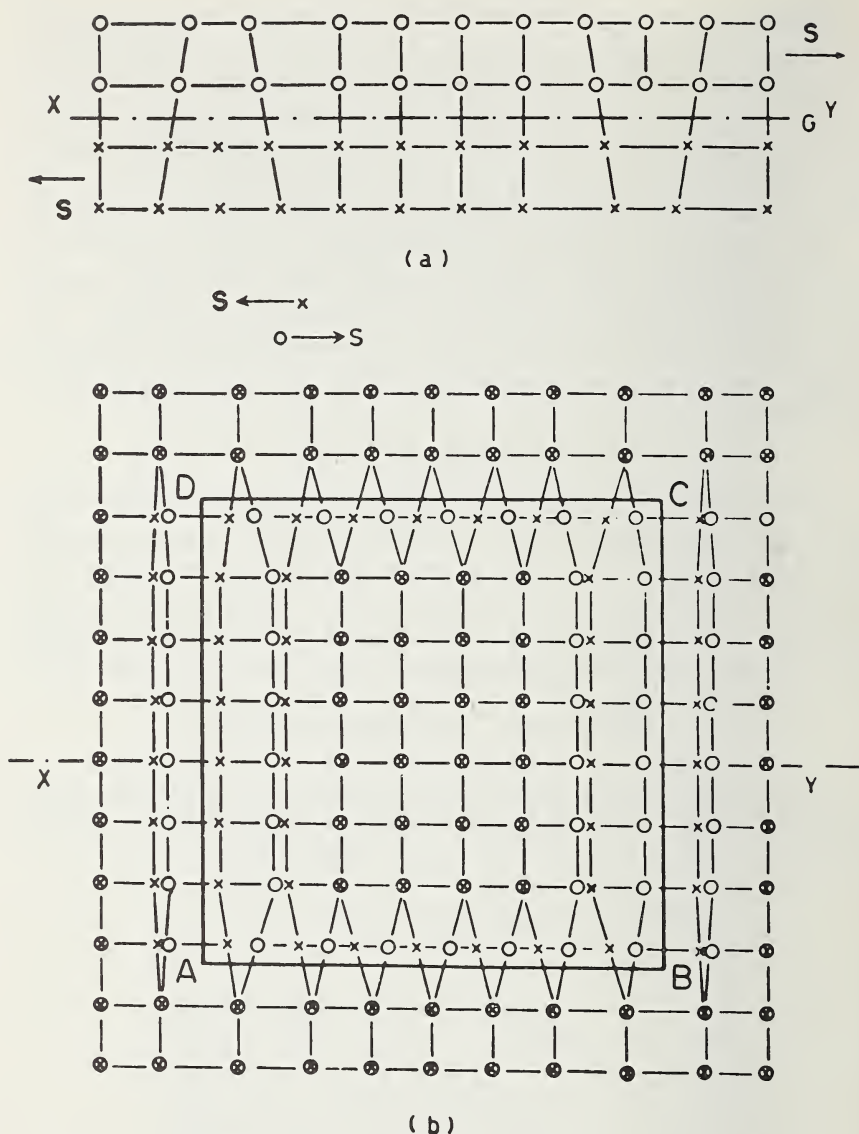


Figure 4. Glissile square dislocation loop; (b) in projection, (a) cut along XY.

$$R_y = [-b/8\pi(1-\nu)] [(1-2\nu) \ln(x^2 + y^2) + (x^2 - y^2)/(x^2 + y^2)]$$

$$R_z = 0.$$

Note that in the vicinity of the dislocation there is a displacement in a direction perpendicular to the glide plane, this causes the glide plane to present a bump at the position of the dislocation.

The displacement fields of screws and edges are found to be "orthogonal"; as a result the displacement field of a mixed dislocation is just

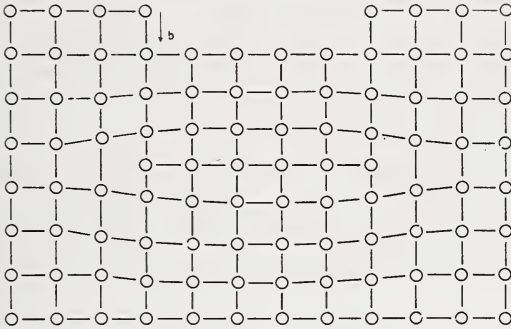


Figure 5. Cross section of prismatic dislocation made by "punching".

the superposition of the displacement fields of the edge and screw components.

Dislocations are seen in the electron microscope because of their displacement fields. Pictorial views of the lattice deformations around dislocations are given below (Figs. 32, 33).

### 5. Stress Fields—Cottrell Interaction

With the displacement field a stress field is associated. The stress field around a screw dislocation in an infinite isotropic medium only contains shear stresses on planes which are not perpendicular to the dislocation line. The stress field has axial symmetry.

On the other hand the stress field due to an edge dislocation is more complicated. It has dilatational and shear components. The dilatational stress is compressive on that side of the glide plane where the supplementary half plane is situated; it has tensile character on the other side of the glide plane. As a result of this oversized and undersized impurity atoms are attracted respectively to the regions of tensile and compressive stress. This effect is called "Cottrell interaction" and it plays an important role in decoration and etching.

The stress fields of all dislocations decrease as  $1/r$ ; where  $r$  is the distance from the dislocation core.

### 6. Energy of a Dislocation

A certain amount of energy per unit length is associated with a dislocation. This energy has its origin partly in the distorted core, but for the largest part in the elastic strain field in the region around the dislocation. It can be shown that the energy per unit length is proportional to the square of the Burgers vector. This is reasonable since it cannot depend on the sign of  $\mathbf{b}$ . It depends on the character of the dislocation, being smallest for screw dislocations and largest for edge dislocations, at least in an isotropic medium.

Two meeting dislocations may form a single dislocation if this process is accompanied by a decrease in energy. In such a reaction the Burgers vector  $\mathbf{b}_3$  of the newly formed dislocation is equally the sum of the Burgers vector of the reacting dislocations  $\mathbf{b}_1$  and  $\mathbf{b}_2$ :  $\mathbf{b}_3 = \mathbf{b}_1 + \mathbf{b}_2$ . One can say as a rough approximation that the reaction will give rise to energy gain provided  $b_3^2 < b_1^2 + b_2^2$ .

Reactions of this kind are responsible for the formation of three-fold nodes at the intersection points of two dislocations.

Since the total energy associated with a dislocation is proportional to its length it will tend to shorten giving rise to a certain "line tension."

### 7. Force on a Dislocation; Motion of Dislocations

A dislocation being only a configuration of atoms the concept of "force on a dislocation" is of course quite different from the Newtonian notion of force on a mass. In fact forces act on *atoms* and *not* on the dislocation.

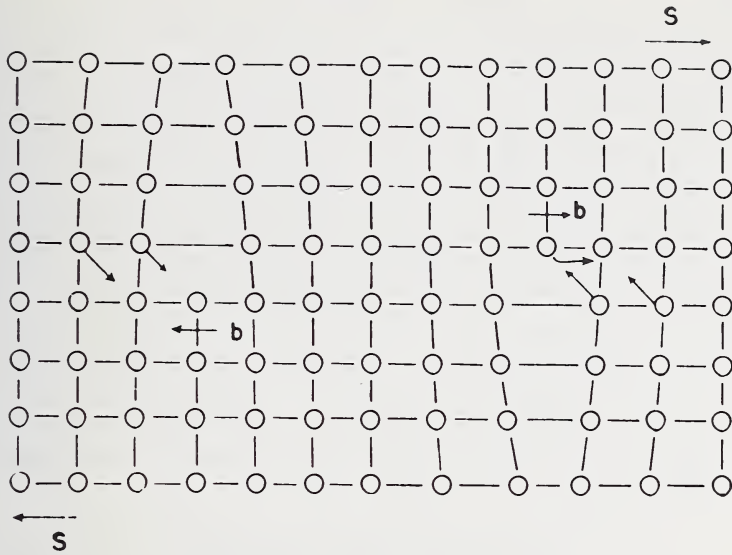
Figure 6a represents a crystal containing two edge dislocations of opposite sign. Under the influence of the shear stresses  $S$  the forces on the atoms will cause the rearrangements as indicated by the arrows and as a result the dislocations move. It is clear that dislocations of opposite sign move in the opposite sense. Where they reach the surface, they are eliminated and steps result (Fig. 6b). Inversion of the stresses inverts the sense of the movement of the two dislocations. When the two supplementary half planes come one above the other, the two dislocations *annihilate mutually* if they are in the same glide plane. A pure edge dislocation moves in the direction of its Burgers vector (i.e., perpendicular to its line).

When a shear stress  $S$  is applied to a screw dislocation, it moves in a direction normal to its Burgers vector. Here again an inversion of the sense of the shear stresses changes the sense of the movement. When the two dislocations are in the same glide plane, they will also annihilate mutually on meeting.

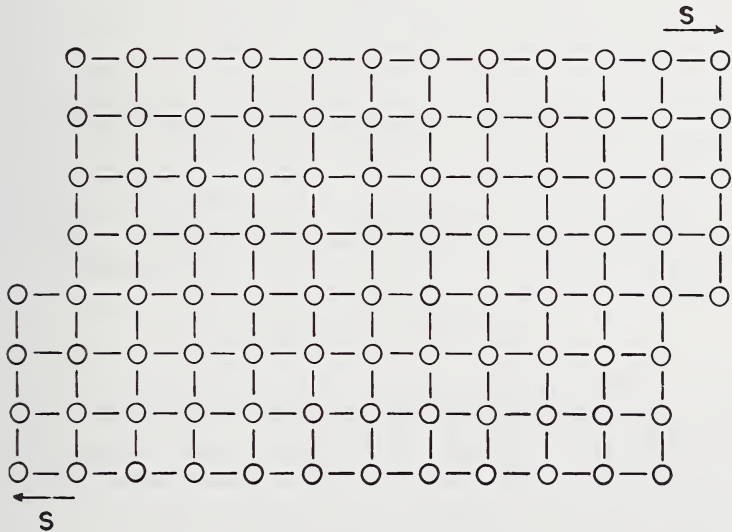
As a result of the movement of a dislocation under the influence of the applied shear stresses the crystal yields i.e., one part of the crystal is displaced with respect to the other over the Burgers vector and therefore work is done by the applied forces. Also the "force" acting on the dislocation has performed work since the dislocation has been displaced over the slip plane. Equating these two amounts of work yields an expression for the force  $F$  on a dislocation. In the simplest case  $F = b\sigma$  where  $\sigma$  is the shear stress on the glide plane.

The force always acts in a direction perpendicular to the dislocation line.

Consider now the square loop of Figure 4b. Under the applied shear stress  $S$  the two edges move outwards, as well as the two screws, and as a consequence the loop expands. Inversion of the stresses inverts



( a )



( b )

Figure 6. Movement of two edge dislocations of opposite sign. When the dislocations leave the crystal surface steps result.

the movement of every component of the loop, which will thus contract and might finally disappear.

The case of the prismatic dislocation of Figure 5 is different as every section is edge. Each dislocation now has a different glide plane, defined by the line itself and its Burgers vector. The loop is thus

mobile only on the cylindrical surface defined by the square loop and with generators parallel to  $\mathbf{b}$ . By generalizing the previous considerations, one formulates the general rule: a dislocation is mobile on the cylindrical surface that contains the line and its Burgers vector.

Up till now only conservative motion, i.e., motion involving only glide, has been considered. Edges are, however, capable of a diffusive type of motion. The arrival or the departure of vacancies at or from the dislocation will shorten or lengthen the supplementary half plane, and this changes the glide plane of the dislocation. This phenomenon is called climb. Edge dislocations can thus act as sources or sinks for vacancies. The removal or the absorption of vacancies takes place at *jogs*, which as a consequence move sideways along the line. A jog in an edge is a site at which the supplementary half plane becomes one unit longer or shorter, i.e., where the line changes its glide plane. Jogs in screw dislocations can move in a conservative way along the line.

### 8. Forces Between Dislocations

The stress field due to one dislocation causes a force on other dislocations in its vicinity: they interact one with the other. The force laws for dislocations show a large analogy with those between electrically charged lines. For parallel dislocations with the same character the force may be either repulsive or attractive depending on whether the Burgers vectors have the same or opposite sign. The forces between parallel dislocations in the same glide plane vary as  $1/r$ , the proportionality coefficient being a function of the magnitude of the Burgers vector and of the elastic constants. If the Burgers vectors enclose an acute angle there is repulsion; otherwise there is attraction.

### 9. Multiplication of Dislocations

One can now describe a mechanism for the multiplication of dislocations, which is of fundamental importance. In practice, dislocations will be curved and may not even be plane. As a consequence it is to be expected that some parts of a dislocation will satisfy the mobility condition, others not. Consider the situation where only a part AB of a dislocation line is mobile in the plane of the drawing, i.e., the glide plane; suppose it is of the edge type (Fig. 7a). Under the influence of the applied stress the dislocation line will successively adopt the shapes 1, 2, 3, . . . and finally (situation 4), two screws of opposite sign will annihilate, and an expanding loop of the kind discussed in section III.A.3 will be formed. At the same time the original line AB will be reformed, so that the process can start over again. The area within the loop is hereby displaced in the direction and the sense indicated by  $\mathbf{b}$ , with respect to the outside. If at a point  $n$  loops have passed, the

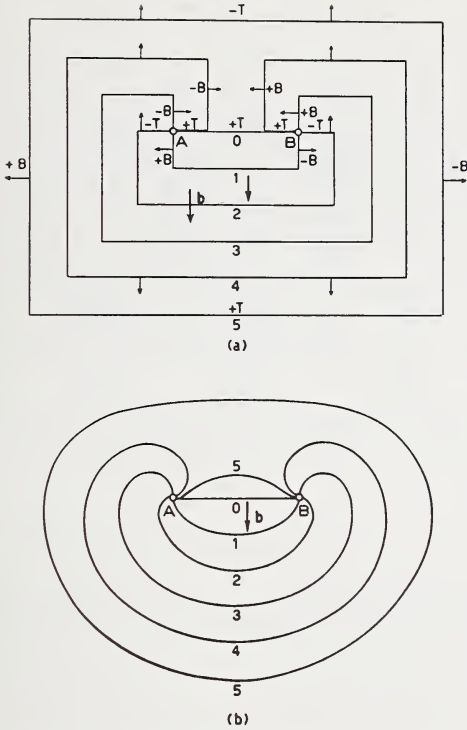


Figure 7. Frank-Read source of dislocations. Edge components are marked  $T$ , screw components  $B$ . (a) Schematic, (b) more realistic.

displacement is  $nb$ . It is theoretically possible to obtain an unlimited amount of slip from a single "source" AB. In reality the dislocation loops will not be square, but curved (Fig. 7b). They may adopt complicated shapes as a consequence of their interaction with other dislocations.

### B. STACKING FAULTS. PARTIAL DISLOCATIONS

If the displacement vector or Burgers vector of the dislocation is *not* a lattice vector the dislocation is called *partial*. The plane  $YXV$  of Figure 1, over which slip has occurred would then be a plane of misfit or a *fault plane* and the partial dislocation forms the edge of the faulted region. Such a situation often occurs because slip usually takes place between close packed planes. A simple experiment with layers of hard spheres will show us how such slip motion can occur. Such a layer of spheres is represented in Figure 8. It presents two kinds of hollows:  $\triangle$  hollows and  $\nabla$  hollows. A second layer of the same kind would fill completely one family of hollows only. In the f.c.c. structure all successive layers fill hollows of the same kind in the underlying layer. The perfect dislocation which would perform

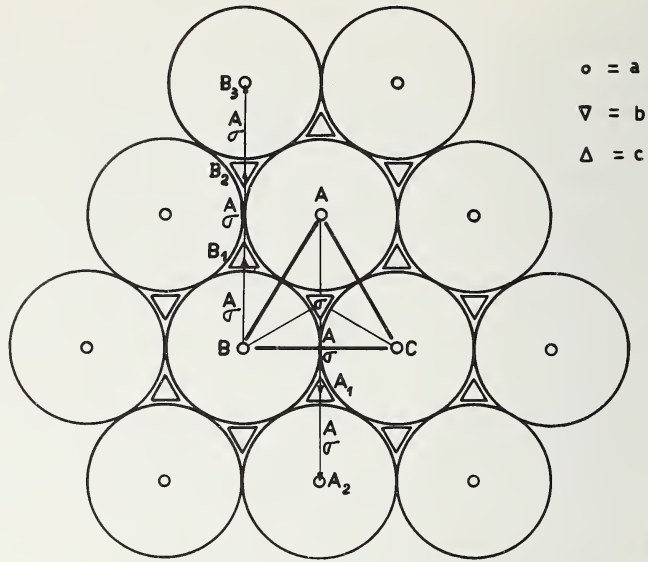


Figure 8. Close packed planes of balls illustrating the concept of Shockley partials. Glide from A to B proceeds in two steps:  $A\sigma$  and  $\sigma B$ .

slip between two such layers would have a Burgers vector of the type  $AB$ . However it is clear that the slip process will become easier if it is performed in two steps. The first step brings the layer from the  $\Delta$  hollow into the  $\nabla$  hollow, i.e., in a faulted position. The second step completes the slip motion and brings the layer from the  $\nabla$  hollow again into the  $\Delta$  hollow. In dislocation language one describes this two step process by saying that slip is performed by the passage of an *extended dislocation* or *dislocation ribbon*. The ribbon consists of two partial dislocations (so called Shockley partials) separated by a stacking fault. The first partial with  $\mathbf{b} = A\sigma$  causes on passing the first slip motion creating a stacking fault. The second partial with  $\mathbf{b} = \sigma B$  removes the stacking fault and completes the slip process. The perfect dislocation with  $\mathbf{b} = AB$  is said to have dissociated according to the dislocation reaction  $AB = A\sigma + \sigma B$ . The two vectors  $A\sigma$  and  $\sigma B$  enclose an acute angle ( $60^\circ$ ) as a result the two partials repel. They are kept together by the stacking fault between them. In more complicated structures the slip process may break up in more than two steps giving rise to multiribbons. Examples of this are shown below.

Stacking faults may also result during growth or as a result of the formation of point defect loops. This is discussed below.

A certain amount of energy is associated with a stacking fault. The energy per unit area of fault is called the stacking fault energy.

## C. ARRAYS OF DISLOCATIONS

The contact zone between two differently oriented crystallites is called a *grain boundary*. There is now convincing evidence that they can be described as arrays of dislocation lines, at least when the orientation difference is small. A general grain boundary is defined by means of five parameters:  $\mathbf{n}$  the unit vector normal on the contact plane,  $\mathbf{u}$  the unit vector along the rotation axis, and  $\theta$  the rotation angle. Two ideal cases are

- (i) the pure tilt boundary:  $\mathbf{n} \cdot \mathbf{u} = 0$
- (ii) the pure twist boundary:  $\mathbf{n} \times \mathbf{u} = 0$ .

Two examples of the first kind are shown in Figure 9 in the case of a primitive lattice. Figure 9a represents the symmetrical pure tilt

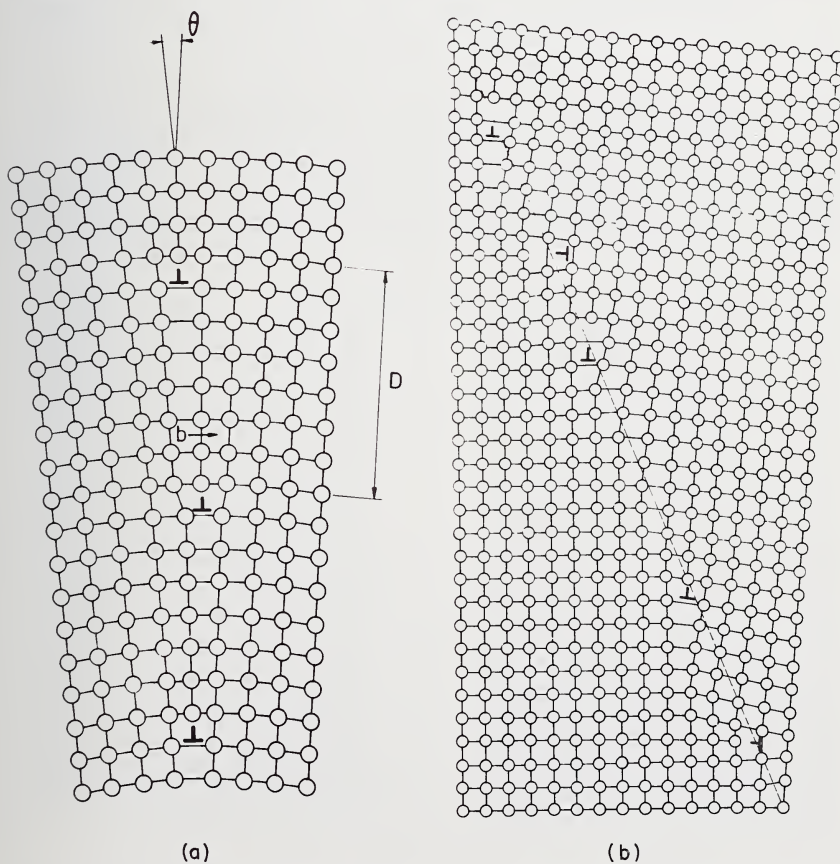


Figure 9. (a) Symmetrical type tilt boundary in primitive lattice. (b) Asymmetrical pure tilt boundary.

boundary. The contact plane is a symmetry plane for the bicrystal. The model consists of a set of equidistant (separation  $D$ ) parallel and straight edge dislocations all having the same Burgers vector  $\mathbf{b}$ , where

$$D = b/\theta.$$

When the contact plane forms an angle  $\phi$  with the symmetry plane, the boundary still consists of parallel edges but they have mutually perpendicular Burgers vectors (Fig. 9b). The two kinds of dislocations are both at characteristic distances given by

$$D_1 = b/\theta \sin \phi \quad D_2 = b/\theta \cos \phi.$$

Figure 10 represents a pure twist boundary in a primitive lattice. Vectors  $\mathbf{u}$  and  $\mathbf{n}$  are both normal to the simple lattice plane, which is in the plane of the drawing. The scheme in (a) represents two undistorted lattice planes on both sides of the contact plane; (b) shows the configuration after a small relaxation of the atoms towards equilibrium. There is now a crossed grid of screws, the mesh size being  $D = b/\theta$ .

For more general grain boundaries the models become increasingly more complicated and they can no longer be derived on a purely geometrical basis. For actual crystal lattices the described models become slightly more complicated. The pure twist boundary in a (111) plane of a face centered cubic lattice will be a hexagonal net (Fig. 11); a

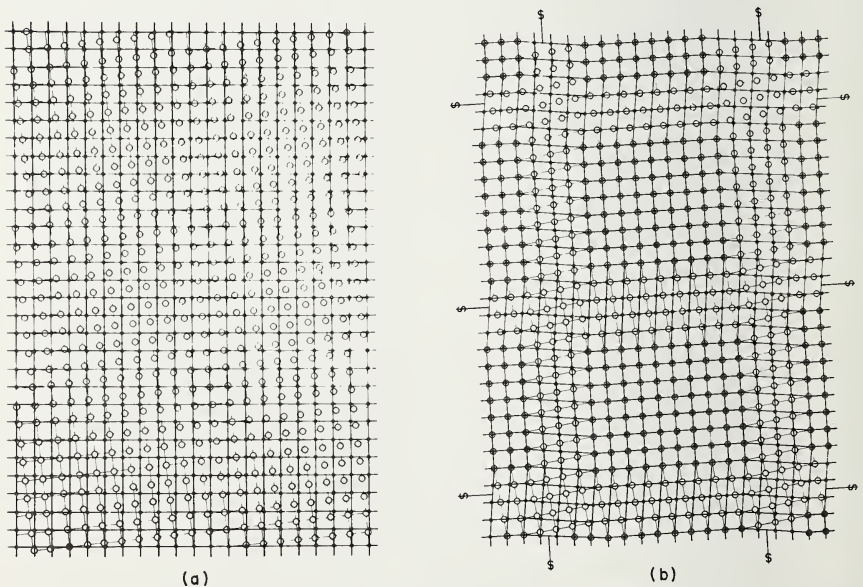


Figure 10. Pure twist boundary on cube plane in primitive lattice. (a) after twisting (b) the atoms have relaxed.

pure twist boundary in a (100) plane will be the simple square grid of Figure 10.

If the dislocations can dissociate twist boundaries situated in close packed planes acquire a somewhat more complicated geometry. We shall only consider face centered cubic crystals. If the stacking fault energy is small, half or all of the nodes of hexagonal networks become extended (Fig. 12): small triangular regions of stacking fault are formed. The degree of extension is determined by the balance between the increase in energy that accompanies the creation of the stacking fault region, and the decrease in energy resulting from the shortening of the dislocations. The extended nodes contain alternatively *intrinsic* and *extrinsic* faults (see paragraph V. C.1). If both have small energy all nodes will dissociate; if only one type of fault has low energy only one family of nodes dissociates. In silicon the first situation prevails; in face centered cubic alloys usually one family of nodes only is dissociated. However recently it has been found that also in f.c.c. metal alloys both types of nodes may be visibly dissociated.

#### D. POLYGONIZATION

Pure tilt boundaries can be introduced by bending a crystal about an axis lying in a glide plane, normal to the Burgers vector, followed by annealing. The formation of these boundaries is known as polygonization because curved lattice planes become polygonal during this process (Fig. 13). The phenomenon consists in a rearrangement of dislocations in their glide plane, as well as normal to it; this implies the occurrence of "climb". The final stable configuration is one in which

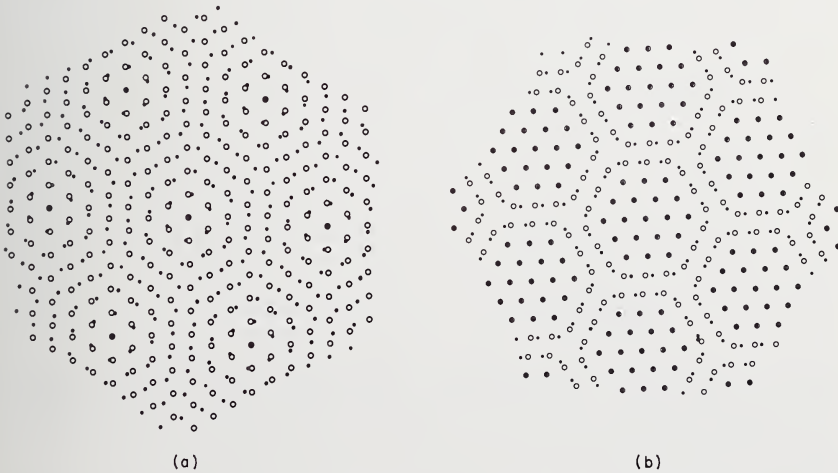


Figure 11. Model for a hexagonal grid of screw dislocations in the (111) plane of a f.c.c. crystal. (a) after twisting about the [111] axis (b) after the atoms have relaxed.

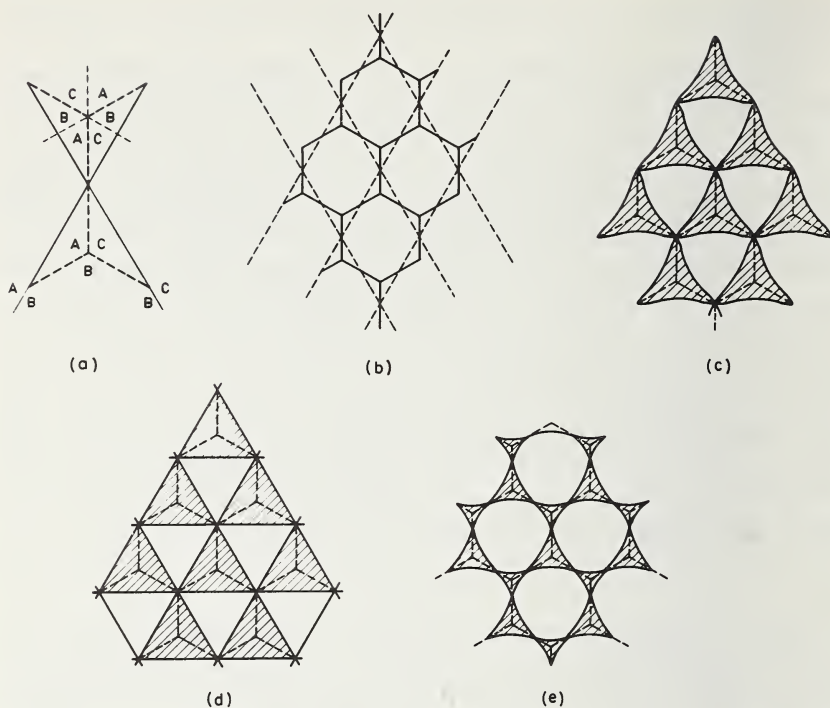


Figure 12. Generation of networks. (a) Interaction of two dislocation segments with vector  $AB$  and  $BC$ , with formation of new segments, with vector  $AC$ . (b) Formation of hexagonal meshes from the intersection of 2 families of dislocations. (c) Net after one family of nodes has become extended (d) If the stacking fault energy is very small the network consists of an alternation of faulted and unfaulted triangular regions. (e) If both the intrinsic and extrinsic faults have small energy doubly dissociated nets result.

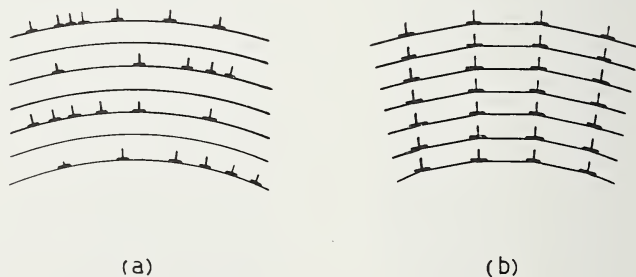


Figure 13. Polygonization. (a) Distribution of dislocations immediately after bending. (b) Stable configuration of dislocations resulting from a rearrangement in the glide plane as well as from climbing.

the dislocation walls (pure tilt boundaries) are normal to the active glide planes.

## IV. Observation Methods

## A. SURFACE METHODS

## 1. Growth Spirals [21, b]

As we have mentioned above the first phenomenon which was shown to be directly related to the presence of dislocations was the occurrence of growth spirals centered on the emergence points of dislocations of which the Burgers vector has a component normal to the crystal face under consideration. We now summarize briefly the underlying theory [3]. It is obvious that a perfect crystal could only grow by the addition of complete layers of growth units. In order to start a new layer on a close packed plane a two dimensional nucleus has to be formed. However the probability for the formation of a two dimensional nucleus of the critical size or larger is negligibly small at the low supersaturations where crystals are found to grow at observable rates. This difficulty can be removed by taking into account that crystals contain dislocations emerging in the surface. For geometrical reasons a surface step of height  $h = \mathbf{b} \cdot \mathbf{n}$  is attached to each dislocation with Burgers vector  $\mathbf{b}$  emerging in a crystal face with unit normal  $\mathbf{n}$ . Under conditions where growth occurs this step will tend to acquire growth units and thereby it tends to move parallel to itself. However since the step is anchored in  $P$  (Fig. 14), it can only adopt the shapes shown in Figure 14. On further growth each part of the curved step is displaced further outwards. As a result the step winds up into spiral shape, but it never grows away as an ordinary surface step, not attached to a dislocation,

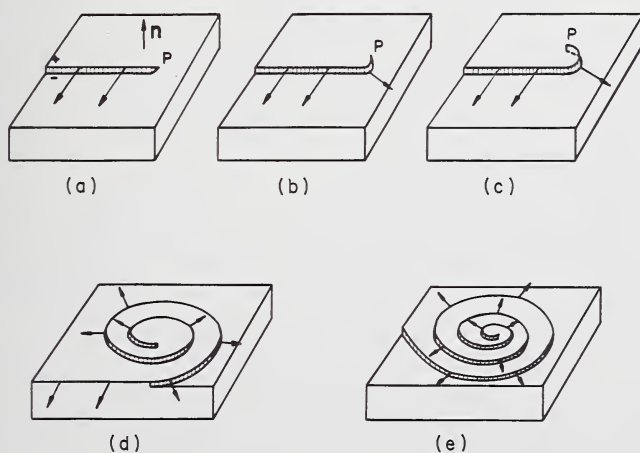


Figure 14. (a) Step attached to the emergence point  $P$  of a dislocation with a Burgers vector which is not parallel to the surface. The step height  $h = \mathbf{b} \cdot \mathbf{n}$  where  $\mathbf{n}$  is the unit normal on the surface. (b) Under the influence of a supersaturation the step in (a) winds up into a spiral centered on  $P$ . (d and e).

would do. On continued growth each part of the spiral is displaced outwards and the spiral apparently rotates around its center maintaining a stationary shape. After the cessation of growth one thus expects to find crystal faces exhibiting spirally shaped growth hills the centers of which are the emergence point of a dislocation.

It is clear that one can exploit this phenomenon and use the growth spirals as "indicators" for the emergence points of dislocations. Furthermore, the step height, which can be measured by multiple beam interferometry, gives the component of  $\mathbf{b}$  perpendicular to the crystal face. Steps as small as  $7.5 \text{ \AA}$  can be observed by reflection phase contrast microscopy and using sufficiently well developed spirals, step heights of the same magnitude can be measured by means of multiple beam interferometry (Fig. 15).

On moving, a dislocation creates in its wake a surface step (a so called slip step) of which the step height is again  $h = \mathbf{b} \cdot \mathbf{n}$ . Such unit slip steps can be observed in the same way as the spiral steps; they sometimes start at the centre of the growth spirals giving rise to characteristic step configurations from which the path of the moving dislocation can be inferred [22].

It is clear that only a limited amount of information can be obtained from the observation of growth spirals:



Figure 15. Growth promoted by a number of spirals of the same sense originating in a group of dislocations with components perpendicular to the  $c$ -face of the same sign. The step heights are  $13 \text{ \AA}$ .

(i) One can estimate the density of dislocations having a component perpendicular to the crystal face under examination and one can measure this component.

(ii) The sense of winding of the spirals depends on the sign of  $\mathbf{b} \cdot \mathbf{n}$ , i.e., on the sign of the dislocation. One can as a result determine the relative densities of dislocations for which the normal component of  $\mathbf{b}$  has a given sign.

(iii) Some information on the motion of dislocations can be obtained. For instance the mutual annihilation on moving together of two dislocations of opposite sign could be deduced from growth patterns [23].

The method is obviously of very limited use because very clear and perfect growth faces are needed to make the observations possible. Furthermore not all the dislocations are revealed and only the emergence points are detectable.

## 2. Evaporation Spirals

The reverse phenomena, i.e., evaporation under conditions of low undersaturation also produces spiral steps of which the center is now the lowest point. These spirals can be used in exactly the same way as the growth spirals. However it is difficult to create undersaturations low enough so as to produce spiral depressions with widely spaced turns which can be resolved in the optical microscope. The method is therefore used with greater success, in conjunction with electron microscopy [5].

The technique as applied to alkali halides, is as follows. After the alkali halide crystal has been subjected to evaporation a very thin layer of gold is evaporated onto the surface, which is kept at a temperature of about 150–200 °C (for NaCl). Under these circumstances the gold does not form a continuous layer but instead small gold particles nucleate epitaxially in a highly preferential way along surface steps. A layer of carbon is then deposited on top of the gold layer. On dissolving the alkali halide crystal the gold particles remain imbedded in the carbon replica, which is then examined in the electron microscope. In this way monoionic steps can be revealed with very high contrast (Fig. 16). This technique has been developed to a high degree of perfection by Betghe and coworkers [5]. Recently they succeeded in obtaining decoration whilst deforming the crystal. In order to introduce the parameter 'time' into their experiments, they used the double decoration technique, which consists in evaporating two different metals at different times during the deformation process.

The main limitation of the technique is obviously that again only emergence points are observed. However it turns out that possibly also dislocations which have a Burgers vector parallel to the crystal face can be revealed; their presence can be inferred from the presence of sequences of closed contours of monosteps nucleated apparently at their emergence points.

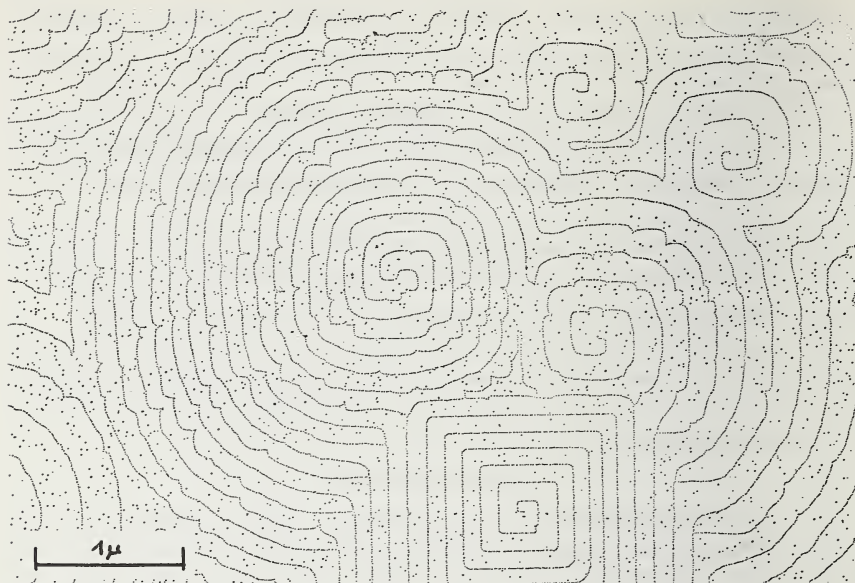


Figure 16. Evaporation spirals observed on the cube plane of sodium chloride. The steps are decorated by means of small gold particles. Note that the step height of the square spiral is twice that of the rounded double spiral. This is concluded from the way the steps fuse. Courtesy Betghe and coworkers.

The resolution of the method is determined not only by the resolution of the electron microscope but mainly by the quality of the decoration, i.e., by the size of the decorating particles and the degree of preferential nucleation of these along steps. The main parameters which determine the quality of the decoration are: the nature of the metal used and the temperature of the crystal face during deposition of the metal.

It is to be expected that this method can be adapted to other crystals. The type of information that can be obtained by the use of this method is of course similar to that obtainable from growth spirals. A big advantage however is that no growth faces are required and that the high resolution of the electron microscope can be used.

### 3. Etching

Etching as well as evaporation is essentially the reverse of growth. It consists simply in dipping the crystal in a suitable medium mostly a liquid but possibly also a gas or another solid. It is then found that small pits develop at the emergence points of the dislocations; the pits can be observed by means of reflection optical microscopy. Under conditions of high undersaturation such as those prevailing during etching, no resolvable dissolution or evaporation spirals develop since the distance between successive turns would be too small. Instead a pit

results which is easily observable only if the slope of its side faces is sufficiently large. This slope is determined by the ratio  $v_1/v_n$ , where  $v_1$  is the lateral growth rate of the pit, whereas  $v_n$  is the depth growth rate. For good etch pits  $v_1/v_n$  should be smaller than about 10. The ratio  $v_1/v_n$  can be influenced by adding small amounts of impurities to the etchant.

The formation of etch pits at dislocations with a Burgers vector which has a component normal to the etched crystal face can be considered as resulting from the same process that generates growth spirals except that the dissolution fronts move and are curved in the opposite sense of the growth fronts [24]. As a result the center of the dissolution spiral is lower than the original crystal face. On the basis of this view one expects etch pits at the centers of the growth spirals. This is indeed the case as e.g., in Figure 17. However one also finds pits at other sites; these are associated with the emergence points of dislocations for which  $\mathbf{b} \cdot \mathbf{n} = 0$ . This assumption is e.g., born out by observations on deformed alkali halide crystals where one can develop in a controlled way slip bands in which dislocations emerge for which  $\mathbf{b} \cdot \mathbf{n} = 0$  [25, 26]. With the emergence points of such dislocations no surface steps are associated. The previous considerations are therefore not of application. It is now assumed that the gain in strain energy



Figure 17. Etch pattern on the *c*-face of silicon carbide. Pits located at the centers of growth spirals, as well as pits located elsewhere can be seen. The growth spirals have become visible as a consequence of preferential attack along the growth steps. Single steps are only 7 Å high.

resulting from the dissolution of the disturbed region around the dislocation core is sufficient to cause preferential dissolution at the emergence point of the dislocation [24]. The same argument is of course valid for dislocations for which  $\mathbf{b} \cdot \mathbf{n} = 0$ . The formation of etchpits is therefore a somewhat more complex phenomenon than the formation of growth or evaporation spirals.

It is found that dislocations freshly introduced by deformation etch usually differently from grown-in dislocations [25, 26]. This seems to suggest that the segregation of impurities at dislocations plays a role, although not a vital one. This fact can be exploited to distinguish fresh and old dislocations, which may be a desirable feature of the technique, e.g., when studying dislocation motion.

The effect of impurities in the etching solution seems to be more pronounced. The addition of suitable impurities slows down the lateral displacement rate of steps and as a result it increases the slope of the sides of the pits and therefore increases their visibility. In the extreme case etch tunnels can be formed all along the dislocations [27].

Etching seems to work best on close packed and low index crystal faces, e.g., {100} for alkali halides; {111} for calcium fluoride etc. This is not well understood at present.

An important question which naturally arises is whether or not all dislocations are revealed by etch pits. This question can be answered for a particular crystal-etchant pair by performing a few simple tests. One can introduce known densities and configurations of dislocations e.g., by bending a crystal to a given radius of curvature, and afterwards one can compare the obtained density and configuration of etchpits with the theoretical configuration. An even simpler test is possible for crystals which cleave such as the alkali halides. It is now possible to compare the etch patterns on the matching faces of a cleaved crystal; they should very approximately be mirror images [28] (Fig. 18). For metal specimens successive attacks alternated with electropolishing should consistently reveal almost the same pattern of pits.

Alkali halides are also particularly suitable for comparing pits due to edge dislocations with those due to screw dislocations. As a result of the particular glide geometry (slip vector  $\mathbf{a}$  [100], slip plane (110)) the slip traces which are at an angle of  $45^\circ$  to the cube edge are generated predominantly by edge dislocations, whereas the dislocations that emerge along slip lines parallel to the cube edge have predominantly screw character [29].

The conclusion from such experiments is that there is evidence that some pits are *not* due to dislocations; precipitates may for instance cause etching, also fission tracks in ionic crystals can be etched. Some caution is therefore needed in interpreting etch patterns in terms of dislocations.

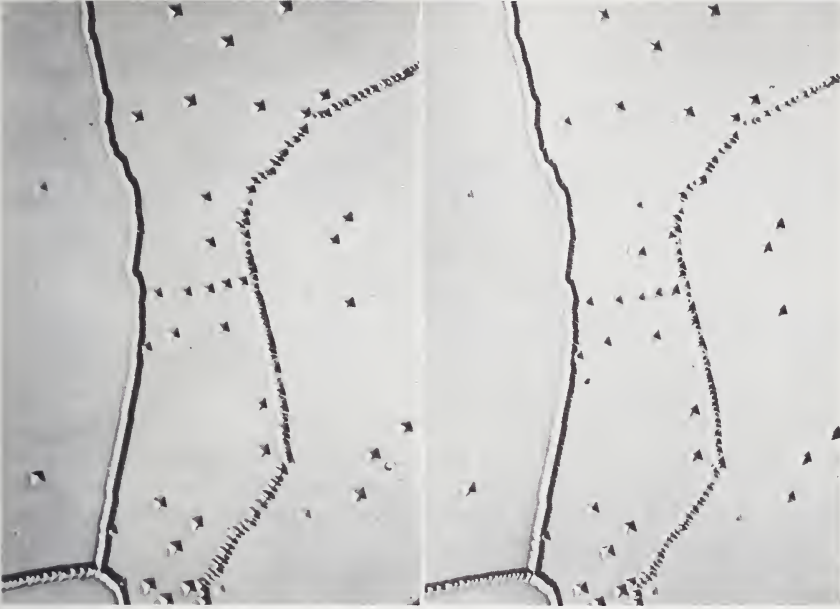


Figure 18. The etch pattern on two matching halves of a cleaved lithium fluoride crystal. The patterns are mirror images, but on printing one image has been reversed so that they become identical. Courtesy of Gilman and Johnston.

We shall now discuss what type of information can be obtained from etch patterns. Although etching is essentially a surface method we can obtain somewhat more than just the emergence points of dislocations. When making the reasonable assumption that the pit is always centered on the instantaneous position of the dislocation, the detailed shape of the etch pit can inform us on the general direction of the dislocation line, as represented in Figure 19. When using alternatively polishing and etching we can explore the pattern of dislocations in depth. It is also possible to etch the crystal several times without polishing and reveal for instance the positions of dislocations before and after application of stress or before and after heat treatment. Etch pits left behind by the dislocations that gave rise to them and which subsequently moved away, will on further etching, develop a flat bottom since the pits only extend laterally, but not in depth. In such a way the successive positions of a dislocation which moved during etching can be revealed, as shown schematically in Figure 20. Using this technique the glide motion of dislocations can be studied. Gilman and Johnston [30] used this technique to establish the stress-velocity relationship for edge and screw dislocations.

In some exceptional cases it is found that dislocations which are parallel to the surface over some distance are revealed as etch grooves [31]. Apparently the strain is sufficient to cause etching along that part of the dislocation where it is close to the surface.

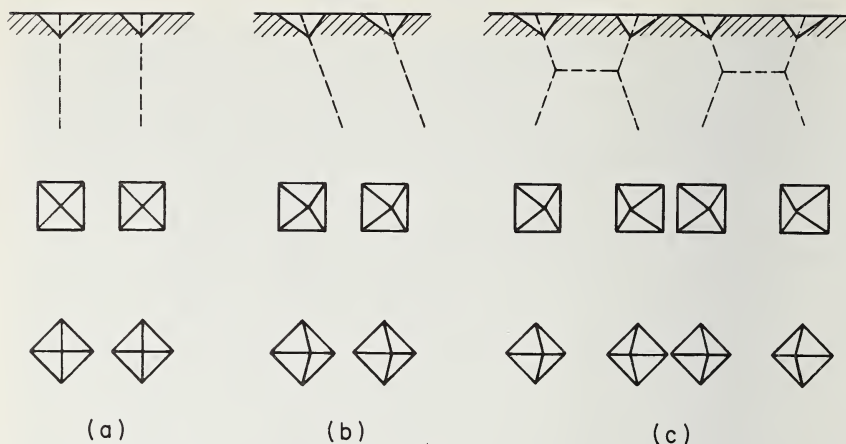


Figure 19. Asymmetry of etch pits due to the inclination with respect to the surface of the dislocation lines giving rise to them. (a) Parallel lines perpendicular to the surface produce symmetrical pits. (b) Parallel lines inclined with respect to the surface, as in a tilt boundary, produce asymmetrical pits all oriented in the same way. (c) Pits formed at the emergence points of a hexagonal grid of dislocation; the pits are asymmetrical and successive pits are oriented differently.

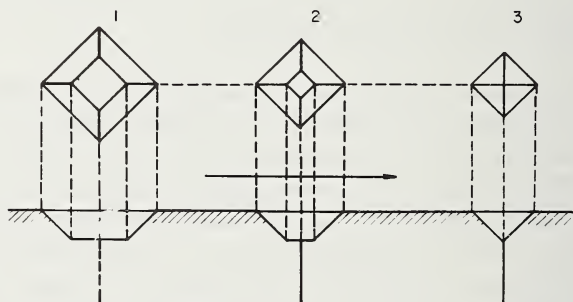


Figure 20. Etch pits due to moving dislocations. The flat bottomed pits (1) and (2) correspond to intermediate positions of the dislocations. The final position of the dislocation is marked by the centered pit (3).

We shall now enumerate some typical problems which can successfully be studied by means of etch pits. It is clear that all problems which involve the study of static configurations of dislocations can in principle be solved. Also problems where the successive positions of the same dislocations are required can be tackled.

(i) Deformation problems: the distribution of dislocations in slip planes (pile-ups); multiplication of dislocations in glide bands [32] [33]; the movement of single dislocations with the possibility of determining the stress velocity relation for single edge and screw dislocations [30].

(ii) Equilibrium configurations of dislocations: the geometry of dislocations in subboundaries [25], the arrangement and the evolution

of the configuration of dislocations on polygonization after bending and heat treatment.

(iii) Fracture problems. The relationship between the nucleation and propagation of cracks and the pile up in glide bands [34].

(iv) Fission tracks [35]. The possibility to etch fission tracks as well as tracks caused by high energy heavy ions in materials such as mica, has led to applications in the field of particle detection and of trace analysis of fissionable nuclei. The method allows for instance to detect energetic heavy particles in the presence of a background of light particles; only the former leave etchable tracks in mica. For the trace analysis of uranium or other fissionable nuclei it is sufficient to irradiate the specimen in contact with mica by means of thermal neutrons, and then count the number of fission tracks [36]. From a knowledge of the cross sections one can then calculate the concentration of fissionable nuclei.

For a more complete summary of results obtained with the etch pitting technique we refer to [37] and [38]. We reproduce here a table of etchants (table I) which have been used in revealing dislocations. A more extensive list can be found in ref. [38].

The great simplicity of the etching method, especially for determining dislocation densities and dislocation distributions makes it an attractive method for routine checks. As such, and also as a research tool, it will undoubtedly be used further in the future. Whereas electron microscopy (see below) can yield much more detailed information on individual defects, it is clear that the overall picture may be lost. Etch pitting is then an excellent complementary technique for providing this overall picture.

## B. BULK METHODS

### 1. *Decoration*

The technique consists in treating a crystal in such a way as to cause the formation of small, but visible particles, along the dislocation lines. The particles should be small enough so as to draw with sufficient resolution the pattern of dislocations. However they should be large enough to scatter enough light so as to become visible in dark field optical microscopy or even in transmission microscopy.

The possibility to produce decoration is connected with the following properties of dislocations. Cottrell interaction causes an elastic attraction between the impurities and dislocations. Along dislocation lines diffusion is enhanced, which favours the preferential nucleation of particles there. Also the dislocations can act as sources of vacancies and hence enable the precipitate to grow. Since the migration of atoms over several atomic distances is involved, heat treatment is usually required to cause decoration. Impurities which diffuse along interstitial sites usually migrate rapidly already at relatively low tempera-

TABLE I. Etchants<sup>a</sup>

Crystals	Etchant	Remarks	References
Aluminum	47% HNO <sub>3</sub> , 50% HCl, 3% HF, temp: room.	With Fe impurity	S. Amelinckx, <i>Phil. Mag.</i> <b>44</b> , 1048 (1955).
Antimony	(1) CP 4—temp: room, time: 2–3 sec, plane (111). (2) 1 pt HF, 1 pt Superoxall, 4 pt H <sub>2</sub> O, temp: room, time: 1 sec, plane (111)	Cleaved surface	J. H. Wernick, et al., <i>J. Appl. Phys.</i> , <b>29</b> , 1013 (1958). Idem
Bismuth	1% I <sub>2</sub> in methanol, temp: room; time: 15 sec, plane: (11).	After prepolishing	I. C. Lovell and J. H. Wernick, <i>J. Appl. Phys.</i> <b>30</b> , 234 (1959).
Brass	0.2% Na <sub>2</sub> S <sub>2</sub> O <sub>4</sub> ; temp: room; time: 60 sec, plane: (111).	Electrolytic: 0.1 A cm <sup>-2</sup>	P. A. Jacquet, <i>Compt. Rend.</i> <b>237</b> , 1248 (1953).
Cadmium	(1) 2 pt orthophosphoric acid, 2 pt glycerine, 1 pt. water, time: 20–40 sec (2) Sat. sol. of picric acid in acetone; time: 2 min.	Electrolytic: 0.9–10 v after polishing in same bath at 2.1–2.2 v for 9–12 min.	A. A. Predvohitiv and N. A. Tiapunia, <i>Phys. Metals Metallog. (USSR)</i> (Engl. trans <b>7</b> , n° 6, 55 (1959)). J. George, <i>Nature</i> <b>189</b> , 743 (1961).
Copper	(1) Impure: 60% H <sub>3</sub> PO <sub>4</sub> in H <sub>2</sub> O, temp: room, time: 10 sec. (2) Pure: 4 pt aqueous FeCl <sub>3</sub> , 4 pt HCl, 1 pt acetic acid plus few drops bromine; temp: room; time: 15–30 sec.	Electrolytic Rinse in NH <sub>4</sub> OH, prepolishing necessary.	F. W. Young and N. Cabrera, <i>J. Appl. Phys.</i> <b>28</b> , 339 (1957). L. C. Lovell and J. H. Wernick, <i>J. Appl. Phys.</i> <b>30</b> , 590 (1959).

Germanium	(3) Several etchants planes: (111) (110) (100). (1) CP 4; time: 1 min; planes: (111) (100). (2) 40 ml HF, 20 ml HNO <sub>3</sub> , 40 ml H <sub>2</sub> O 2 gm Ag <sub>2</sub> O <sub>3</sub> ; time: 1 min, planes (111) (110).	Distinguish fresh dislocations and dislocations with Cottrell atmosphere.	F. W. Young, J. Appl. Phys. <b>32</b> , 192 (1961).
Iron	(1) 2% Nital containing 2% saturated picral; time: 15 min. (2) Saturated picral—time: 4 min.	Anneal at 1750 °C to decorate dislocations.	W. C. Johnston, G. E. Report 61-RL-2649M (1961); Progr. Ceramic Sci. <b>2</b> , 1 (1962).
Silicon-iron	(1) 133 ml acetic acid 25 mg CrO <sub>3</sub> , 7 ml H <sub>2</sub> O; temp: room; time: 5-20 min. (2) Dilute phosphoric acid (200 gm/lit H <sub>3</sub> PO <sub>4</sub> ) temp: 20-25 °C; time: 4-12 min.	Electrolytic: 30 mA/cm <sup>2</sup> after predecoration. Electrolytic: 0.15 A/cm <sup>2</sup>	R. D. Heidenreich, U.S. Patent, 2, 619, 414 (1952); F. L. Vogel et al, Phys. Rev. <b>90</b> , 489 (1953).
Nickel-Manganese	100 cc H <sub>3</sub> PO <sub>4</sub> , 100 cc ethanol; temp: 40 °C; time: 2 min.	Electrolytic: 2 A/cm <sup>2</sup> Cu-cathode	L. C. Lovell, F. L. Vogel and J. H. Wernick, Metall. Progr. <b>75</b> , N° 5, 96 (1959). Idem.
Niobium	(1) 10 cc H <sub>2</sub> O, 10 cc H <sub>2</sub> SO <sub>4</sub> , 10 cc HF, few drops superoxil; temp: room. (2) H <sub>2</sub> SO <sub>4</sub> (95%), HNO <sub>3</sub> (70%), HF (48%) in ratio 5 : 2 : 2	Agitate specimen in solution Strongly orientation dependent	W. R. Hibbard and C. G. Dunn, Acta Met. <b>4</b> , 306 (1956). S. Felin and G. Castro, Acta Met., <b>10</b> , 543 (1962).
			T. Taoka and S. Aoyagi, J. Phys. Soc. Japan, <b>11</b> , 522 (1956).
			A. B. Michael and F. J. Huegel, Acta Met. <b>5</b> , 339, (1957).
			R. Bakish, Trans. Aime <b>212</b> , 818 (1958).

TABLE I. Etchants <sup>a</sup>—Continued

Crystals	Etchant	Remarks	References
Silicon	(1) 1 HF, 3 HNO <sub>3</sub> , 10 CH <sub>3</sub> COOH time: 10 min to "overnight" (2) 10 cc Hydrofluoric acid (37–38%) 10 cc HNO <sub>3</sub> , 10 cc glacial acetic acid; temp: 30–35 °C, time: 2–3 min.	Adding 15 cc double distilled water reduces time to 1.5–2 min.	W. C. Dash, J. Appl. Phys. <b>27</b> , 1193 (1956). N. N. Sirota and A. A. Tonoyan, Proc. Acad. Sci. USSR, Phys. Chem. Sect. (Engl. transl.) <b>134</b> , 987 (1960).
Tantalum	5 pt H <sub>2</sub> SO <sub>4</sub> , 2 pt HNO <sub>3</sub> , 2 pt HF, temp: room; plane: (112).	After predecoration	R. Backish, Acta Met. <b>6</b> , 120 (1958).
Tellurium	(1) 3 pt HF, 5 pt HNO <sub>3</sub> , 6 pt acetic acid, time: 1 min, temp: room; plane: (1010). (2) Conc. HNO <sub>3</sub> (3) 43 gm H <sub>3</sub> PO <sub>4</sub> ( <i>d</i> = 1.55) 1 cc conc. H <sub>2</sub> SO <sub>4</sub> , 5 mg CrO <sub>3</sub> ; time: 1–3 min; temp: 90–100 °C.	Cleaved surface  Another etchant with nearly the same composition (84.4 gm H <sub>3</sub> PO <sub>4</sub> , 2 cc H <sub>2</sub> SO <sub>4</sub> , 4.4 gm CrO <sub>3</sub> ) works at 150–160 °C.	L. C. Lovell, J. H. Wernick and K. E. Benson, Acta Met. <b>6</b> , 716 (1958).  A. I. Blum, Sov. Phys-Solid State <b>2</b> , 1509 (1961).
Tungsten	(1) 2 pt CuSO <sub>4</sub> (25%), 1 pt conc. NH <sub>4</sub> OH. (2) 32.7 gm K <sub>3</sub> Fe(CN) <sub>6</sub> , 4.78 gm NaOH 107 ml H <sub>2</sub> O; plane: (110).	No guarantee that all pits cor- respond to dislocations.	U. E. Wolff, Acta Met <b>6</b> , 559 (1958).  I. Berlec, J. Appl. Phys. <b>33</b> , 197 (1962).

Uranium	170 cc H <sub>2</sub> SO <sub>4</sub> (98%), 100 cc H <sub>2</sub> O (dist) 5 gm CrO <sub>3</sub> , 25 cc dehydrated glycerol; time: 60 sec.	Electrolytic 2 A/cm <sup>2</sup> similar etchants are given in ref.	A. Bassi, S. Granata and H. Imarisio, <i>Energie Nucl.</i> <b>8</b> , 744 (1961).
Zinc	(1) 160 gm chromic acid, 5P gm hydrated sodium sulfate, 500 ml H <sub>2</sub> O. (2) 2 gm NH <sub>4</sub> (NO <sub>3</sub> ) <sub>2</sub> , 10 cc NH <sub>4</sub> OH, 50 cc deionized water; time: 10 sec; temp: room.	Rinsed in water and methyl alcohol and dried in stream of air.	J. J. Gilman, C. E. Report, 56-RI-1575 (1956); <i>J. Metals</i> <b>8</b> , 998 (1958). P. P. Sinha and P. A. Beck, <i>J. Appl. Phys.</i> <b>33</b> , 625 (1962).
Nonmetals: CaCO <sub>3</sub>	HCl (10%); time: 10-60 sec; plane: (010) cleavage.		R. D. Stanley, <i>Nature</i> <b>183</b> , 1548 (1959).
CaF <sub>2</sub>	Conc. H <sub>2</sub> SO <sub>4</sub> ; time: 10-30 min plane: (111).		W. Bontinek, <i>Phil. Mag.</i> <b>2</b> , 561 (1957).
CdS	Vapor of conc. HCl; time: 5-10 sec; plane: (0001). Other etchants: see ref.		D. C. Reynolds and L. C. Greene, <i>J. Appl. Phys.</i> <b>29</b> , 559 (1958). J. C. Nishimura, <i>J. Phys. Soc. Japan</i> , <b>15</b> , 232 (1960). J. Woods, <i>Brit. J. Appl. Phys.</i> <b>11</b> , 296 (1960).
GaAs	2 HCl, 1 HNO <sub>3</sub> , 2H <sub>2</sub> O; time: 10 min; plane: (111). Other etchants: see references		A. Eland, <i>Philips. Techn. Rev.</i> <b>22</b> , 228 (1961). Z. G. Pizarenko and M. K. Sreinkam, <i>Sov. Phys. Solid State</i> <b>3</b> , 838 (1961). J. G. White and W. C. Roth, <i>J. Appl. Phys.</i> <b>30</b> , 946 (1959). H. A. Shell, <i>Z. Metallk.</i> <b>48</b> , 158 (1957). J. L. Richards, <i>J. Appl. Phys.</i> <b>31</b> , 600 (1960).

TABLE I. Etchants<sup>a</sup>—Continued

Crystals	Etchant	Remarks	References
InAs	0.4 N Fe <sup>++</sup> in conc. HCl; time: 3 min; temp. 25 °C; plane: (111). Other etchants: see references		J. L. Richards and A. J. Crocker, J. Appl. Phys. <b>31</b> , 611 (1960). H. C. Gatos and M. C. Lavine, J. Electrochem. Soc. <b>107</b> , 427 (1960). J. W. Faust and A. Sagar, J. Appl. Phys. <b>31</b> , 331 (1960). E. P. Warekois and P. H. Metzger, J. Appl. Phys. <b>30</b> , 960 (1959).
InSb	25 HNO <sub>3</sub> , 20 CH <sub>3</sub> COOH, 10 HF, 1 BR <sub>2</sub> ; time: 5 sec; plane: (111). Other etchants: see references	Stop etching by adding H <sub>2</sub> O	W. Bardsley and R. L. Bell, J. Electrochem. Control <b>3</b> , 103 (1957). J. W. Allen, Phil. Mag. <b>2</b> , 1475 (1957). R. E. Maringer, J. Appl. Phys. <b>29</b> , 1261 (1958). J. D. Venables and R. M. Broudy, J. Appl. Phys. <b>29</b> , 1025 (1958). H. C. Gatos and M. Lavine, J. Appl. Phys. <b>31</b> , 743 (1960); J. Electrochem. Soc. <b>107</b> , 433 (1960).
KBr	Glacial acetic acid; time: 3 sec; plane: (100). Other etchants: see references	Rinse in CCl <sub>4</sub>	P. R. Moran, J. Appl. Phys. <b>29</b> , 1768 (1958). J. S. Cooks, J. Appl. Phys. <b>32</b> , 2492 (1961).

KCl

Conc. sol. polyvinyl butyrol in butyl or ethyl; time: 5-7 sec; plane: (100).  
Other references: see KBr and

KI

Isopropyl alcohol; time: 25 sec; plane: (100).

LiF

$H_2O + FeF_3$  ( $2 \times 10^{-6}$  molar); time: 1 min, plane (100).  
Other etchants: see references

M. P. Shaskolskaya, W. Yang-Wen and K. Shu-Chao, *Sov. Phys-Cryst* (English transl.) **6**, 220 (1961).  
S. A. Slack, *Phys. Rev.* **105**, 832 (1957). M. Sakamoto and S. Kobayashi, *J. Phys. Soc. Japan* **13**, 800 (1958). L. W. Barr et al., *Trans. Faraday Soc.* **56**, 697 (1960).  
J. J. Gilman et al, *J. Appl. Phys.* **29**, 747 (1958).  
P. R. Moran, *J. Appl. Phys.* **29**, 1768 (1958).

J. J. Gilman and W. G. Johnston, *Dislocations and Mechanical Properties of Crystals*, p. 116 (Wiley, New York, 1957).

J. J. Gilman and W. G. Johnston, *J. Appl. Phys.* **27**, 1018 (1956). L. S. Birks and R. T. Seal, *J. Appl. Phys.* **28**, 541 (1957). A. A. Urusovshata, *Sov. Phys-Cryst* (English Transl.) **3**, 731 (1958). A. P. Kapustin, *Sov. Phys-Cryst* (English Transl.) **4**, 247 (1959). M. P. Ives and J. P. Hirth, *J. Chem. Phys.* **33**, 517 (1960). A. R. C. Westwood, H. Opperhauser and D. L. Goldheim, *Phil. Mag.* **6**, 1475 (1961).

Distinguishable between aged and fresh dislocations.

Same as one mentioned for KCl.

NaF

TABLE I. Etchants<sup>a</sup>—Continued

Crystals	Etchant	Remarks	References
MgO	1 H <sub>2</sub> SO <sub>4</sub> , 1 H <sub>2</sub> O, 5 NH <sub>4</sub> Cl sat. sol.; time: 15 min; plane: (100). Other etchants: see references	Distinguished between fresh and aged dislocations.	R. J. Stokes, T. L. Johnston and C. H. Li, <i>Phil. Mag.</i> <b>3</b> , 718 (1958). R. J. Stokes, T. L. Johnston and C. H. Li, <i>Phil. Mag.</i> <b>4</b> , 137 (1959). J. Washburn, A. E. Gorum and E. R. Parker, <i>Trans. AIME</i> <b>215</b> , 718 (1958). T. K. Ghash and F. Clark, <i>Brit. J. Appl. Phys.</i> <b>12</b> , <b>44</b> , (1961). A. S. Keh, <i>J. Appl. Phys.</i> <b>31</b> , 1538 (1960).
NaCl	Glacial acetic acid; time: 0.1 sec; plane: (100). Other etchants see references		B. Jessensky, <i>Nature</i> <b>181</b> , 559 (1958). S. Amelinckx, <i>Acta Met.</i> <b>2</b> , 848 (1954); S. Mendelson, <i>J. Appl. Phys.</i> <b>32</b> , 1579 (1961); M. P. Shas- kolskaya and S. Jui-Fang, <i>Sov. Phys- Cryst. (English Transl.)</i> <b>4</b> , 74 (1960).
NiO	Hot nitric acid Other etchants: see references		T. Takeda and H. Kondoh, <i>J. Phys. Soc. Japan</i> <b>17</b> , 1315 (1962); <i>J. Phys. Soc. Japan</i> <b>17</b> , 1317 (1962).
PbTe	10 ml H <sub>2</sub> O + 5 gm NaOH + 0.2 gm I <sub>2</sub> ; time: 5 min; temp: 94–98 °C; plane: (100) cleavage. Other etchants: see references	Rinse in water	B. B. Houston and M. K. Norr, <i>J. Appl. Phys.</i> <b>31</b> , 615 (1960). G. P. Tilly, <i>Brit. J. Appl. Phys.</i> <b>12</b> , 524 (1961).

SiC	Fused borax: temp: 800–1000 °C; plane: (0001). Other etchants see reference	R. Gevers, S. Amelinekx and W. Dekeyser, <i>Naturwiss</i> <b>39</b> , 448 (1952). F. H. Horn, <i>Phil. Mag.</i> <b>43</b> , 1210 (1952).
UO <sub>2</sub>	H <sub>2</sub> O <sub>2</sub> , H <sub>2</sub> O, and conc. H <sub>2</sub> SO <sub>4</sub> in proportion 6 : 3 : 1 by volume; time: 3 min; temp: 20 °C; plane: (111) (100).	A. Briggs, Harwell Report AERE-M 859 (1961).
ZnS	Aqueous H <sub>2</sub> O <sub>2</sub> solutions of 7.5% to 30%; time: 10 min–1 hr; temp: 60–80 °C.	P. Goldberg, <i>J. Appl. Phys.</i> <b>32</b> , 1520 (1961).

Wash with KCN solution, water, acetic acid, water, dry at 100 °C.

<sup>a</sup> After: S. Amelinekx, *The Direct Observation of Dislocations*, Suppl. 6—Solid State Physics, F. Seitz and D. Turnbull, eds. (Academic Press, New York, 1964).

tures where self-diffusion is still insignificant, they are therefore good decorating agents. Also the solubility of the impurity should decrease with decreasing temperature. The stoichiometric excess of one of the constituents of the crystal may also function as a decorating agent, this is e.g. the case in silver bromide where on illumination silver specks form along the dislocations [40]. It is also possible to cause a chemical reaction inside the crystal, the reaction product being insoluble and hence precipitating; this is e.g., the case in  $\text{CaF}_2$  heat treated in moist air [41].

The inherent limitations of the method are obviously that the heat treatment presumably modifies the dislocation configurations and further that the dislocations are pinned by the impurities and therefore become immobile. The method is clearly well suited for the study of annealing structures. Nevertheless, if using rapidly diffusing impurities in well chosen crystals it is possible to reveal deformation structures as well. The best examples of Frank-Read sources were in fact found by using copper decoration in deformed silicon single crystals [39] (Fig. 21).

The method allows with very simple means (i.e., optical microscopy) to study the spatial arrangements of dislocations. The resolution limiting factor is the particle size of the decorating agent rather than the resolution of the microscope. For many purposes the resolution which can be achieved is sufficient to study crystals with moderately high dislocation densities ( $10^5/\text{cm}^2$ ). In some cases "double" decora-

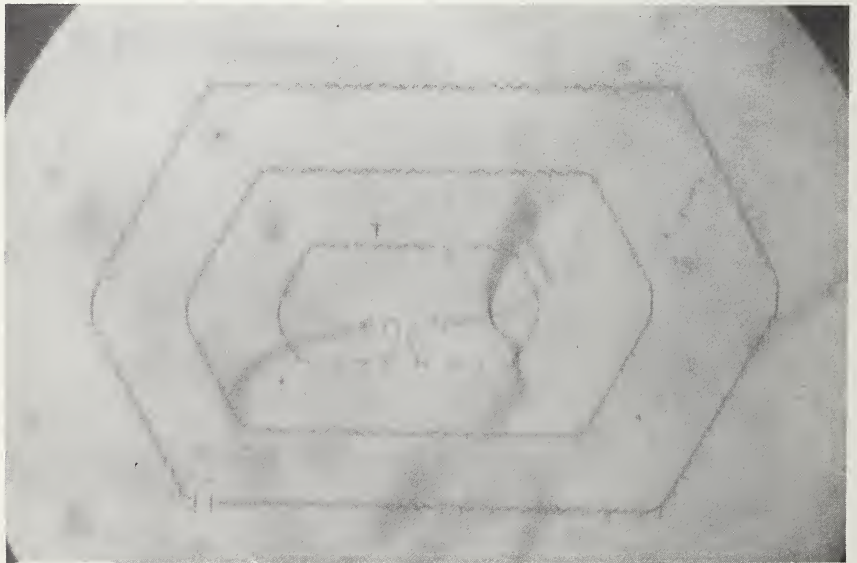


Figure 21. Double ended Frank-Read source in silicon made visible by copper decoration. Courtesy of W. Dash.

tion can be achieved which means that successive positions of the same dislocation can be imaged. In table II a number of decoration methods for specific crystals has been summarized.

A short summary will finally be given of some typical applications of decoration methods.

(i) *The geometry of subboundaries.* This is perhaps the most ideally suited problem to be studied by means of decoration techniques because we are now interested in equilibrium configurations resulting from heat treatments such as those used for the decoration process. Detailed studies have been made of networks of dislocations in the alkali halides [45]. Figure 22 shows an example of these.

(ii) *Dislocation climb.* The use of decoration techniques lead to the discovery that screw dislocations, adopt helical shape when subject to climb, i.e., to a supersaturation or an undersaturation of point defects. The phenomenon was first discovered in calcium fluoride, in

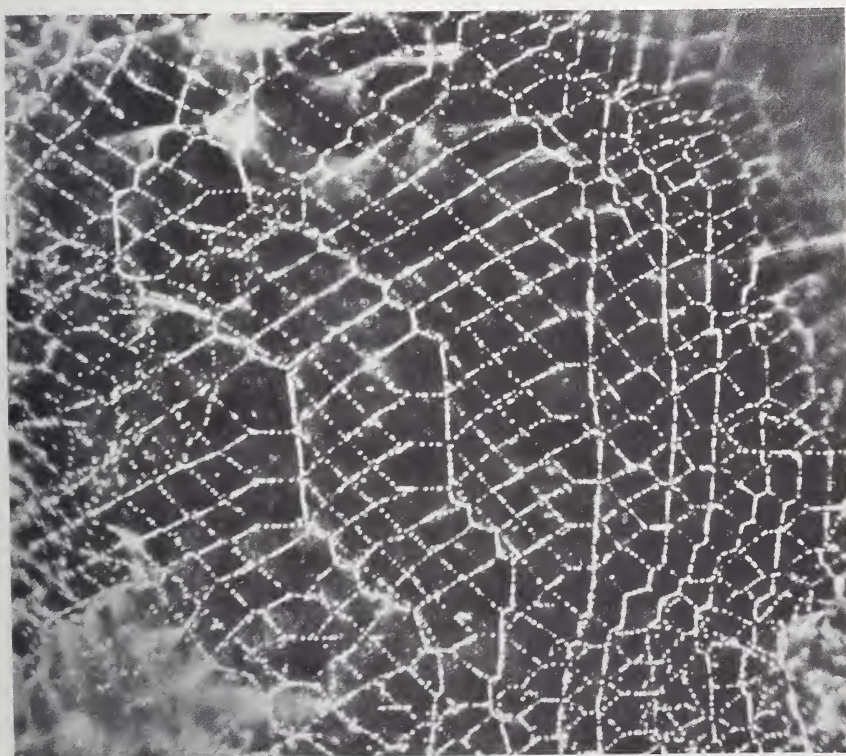


Figure 22. Dislocation network of a mixed type in potassium chloride (dark field image). The decorating particles are silver. They result from an anneal in hydrogen of a silver doped crystal. Note the zig-zag shaped dislocation lines.

TABLE II. Decoration methods for specific crystals

Crystal	Decorating agent	Decoration treatment
Silver halides: Silver bromide Silver chloride	Silver Silver	Exposure to absorbed light [40] Sweeping photo-electrons into the crystal with an electric field [40b, 42]
Alkali halides: Sodium chloride	Colloidal sodium	Heavy additive colloration [43]. Heavy colloration by electron irradiation [44]. Annealing in hydrogen or in sodium vapour of crystals doped with the corresponding silver halide [45].
Sodium chloride Potassium chloride Potassium bromide Potassium chloride Potassium bromide Sodium chloride Lithium fluoride Potassium bromide Sodium chloride Calcium fluoride	Silver particles  Cavities Barium or calcium chloride Calcium fluoride Gold Calcium oxide	Crystal doped with $\text{AgNO}_3$ is X-irradiated and subsequently heat treated [46]. Addition of divalent impurity to the melt followed by suitable heat treatment [47, 48]. Diffusing in of $\text{H AuCl}_4$ or $\text{H AuBr}_4$ in an evacuated quartz tube [49]. Heating in moist air; 30 min at 800 °C [41, 50].
Silicon	Copper	Diffusing in copper at 900 °C (copper nitrate is put on the surface and the crystal is annealed in hydrogen; observation in infra-red.) [39, 53]. (Far infra-red image converter is required for observations). [51].
Germanium	Lithium	
Aluminium oxide	Thorium oxide	Crystal is doped with 1% $\text{ThO}_2$ on growth by the Verneuil method [52].

which the dislocations were decorated using the procedure summarized in table II [41]. Also in silicon the phenomenon could be demonstrated and from the sense of winding of the helical dislocations it could be concluded that interstitials were responsible for the climb process [53]. Harvey observed large prismatic loops due to climb in sodium chloride doped with barium chloride and quenched from a high temperature [53, b].

(iii) *Deformation patterns.* The most spectacular images of Frank-Read sources were observed by Dash [39] in silicon crystals in which the dislocations were made visible by copper decoration (Fig. 21). Deformation by prismatic punching was studied by Jones and Mitchell [54] in silver chloride in which the dislocations were revealed by printing out.

(iv) *Dislocations in whiskers.* The gold decoration technique referred to in table II has been applied successfully to sodium chloride whiskers [55]. It was found that some of the whiskers did contain the theoretically predicted axial dislocation, but others contained many parallel dislocations.

(v) *Prismatic loops.* Prismatic loops, presumably due to the precipitation of vacancies were revealed by silver decoration in potassium chloride [38]. Similar loops, but presumably due to interstitials, were made visible by decoration in silicon. [56].

## 2. Birefringence

It is well known that isotropic crystals become birefringent when stressed. This can e.g., be observed in deformed sodium chloride. Since dislocations have a stress field around them one might expect to be able to reveal the birefringence due to single dislocations. Birefringence can easily be observed with polarizing microscopes, supplemented with an additional sensitive tint plate. Unfortunately it turns out that the resolution of the method is poor. As a result it can only be applied successfully to almost perfect crystals which moreover have large strain-optic coefficients. Silicon turns out to satisfy both criteria and the first observations in this field were made by Bond and Andrus in this crystal [13]. Similar observations were made on rochelle salt [57]. Birefringence associated with groups of dislocations in deformation bands was studied in LiF by Kear and Pratt [58], who also correlated the birefringence bands with etch patterns.

Perhaps the most convincing observations were made on silicon by Indenbohm and coworkers [59]. Some of their pictures are reproduced in Figure 23; this figure provides at the same time a good comparison of three different techniques applied to the same specimen: etching, decoration and birefringence.

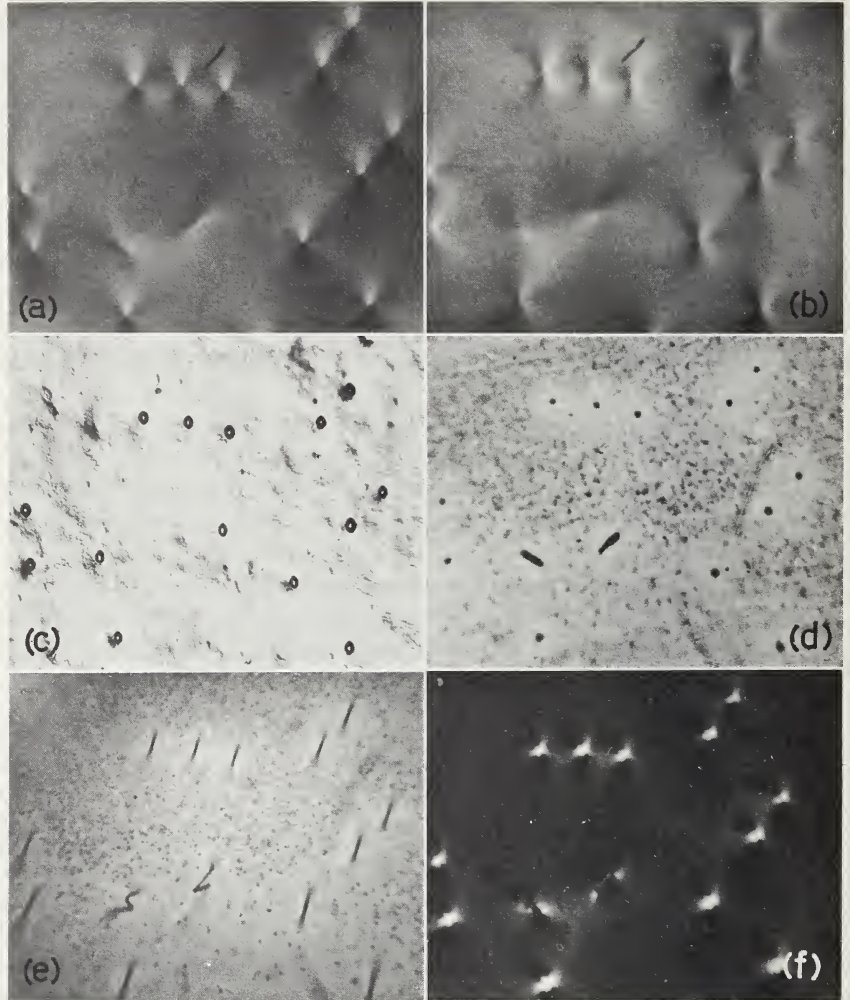


Figure 23. Dislocations in silicon seen by stress birefringence and other methods. All pictures refer to the same area (a) Stress pattern around dislocation ( $\alpha = 0^\circ$ ). (b) Stress pattern around dislocation ( $\alpha = 45^\circ$ ) (c) Etch pits (d) Decorated dislocations seen end on (e) Decorated dislocations seen at small inclinations (f) Stress pattern around decorated dislocations. Courtesy of Indenbohm.

## V. Electron Microscopy and Electron Diffraction

### A. TRANSMISSION ELECTRON MICROSCOPY

#### 1. Introduction

In recent years electron microscopy has become an extremely useful tool for the detailed study of individual crystal imperfections. Considerable progress has been made in the theory of contrast at defects [60]. The results of these theories are of great importance if one wishes

to extract all the information contained in an electron micrograph. It will be briefly shown what information can be obtained and how this can be applied to the study of defects. We shall only make use of intuitive pictures; for a more rigorous theoretical foundation we shall refer to the original papers.

We shall first discuss briefly the various experimental techniques used for the observation and the preparation of specimens and we shall illustrate the interpretation of micrographs by specific examples. It is not intended to give an exhaustive review of the literature; for a more complete review on the observation of lattice defects by means of transmission electron microscopy we refer to [38].

## 2. Principle of the Method

The technique is in fact extremely simple. The specimen is a thin foil ( $\leq 5000 \text{ \AA}$ ) transparent to electrons. Usually an acceleration voltage of 100 kV is used to have high penetrating power. Recently microscopes working under much higher voltages, e.g., 1 MeV, have been built [61]. The specimen is mounted on a grid like a conventional replica. A diffraction pattern is obtained from a transparent region and the aperture is put around the selected beam, usually the direct beam. The image is then magnified to the desired level; it is in fact a representation of the intensity distribution in the selected beam.

If the direct beam is selected, the image is called a "bright field" image; if a diffracted beam is used, the image is called a "dark field" image (Fig. 24). Since dark field images are formed from nonaxial beams they are usually slightly deformed and diffuse. This can be overcome by tilting the electron gun or by using a bias on deflector plates.

Optimum contrast is achieved by choosing the correct tilting angle. The simplest type of contrast is obtained if there is only one strongly diffracted beam; the most intense spot is then responsible for the contrast; such a situation is called a two beam case and most of the theory is made on this assumption. The diffraction vector  $\mathbf{g}$  which is perpendicular to the diffracting planes, and which has a length inversely proportional to the interplanar distance, connects the center of the diffraction pattern with the diffraction spot. The knowledge of the diffraction vector of the contrast producing reflection is of great importance for the interpretation of the images. Dark field images are of special interest since their use allows to be sure which beam is producing the contrast. Whereas the contrast in the direct beam is "subtractive" it is "additive" in the dark field image. In very thin samples the dark field image has usually better contrast.

Specimen heating by the electron beam, especially in insulating crystals, is often a problem. For metal specimens the temperature rise is small (10–20 °C).

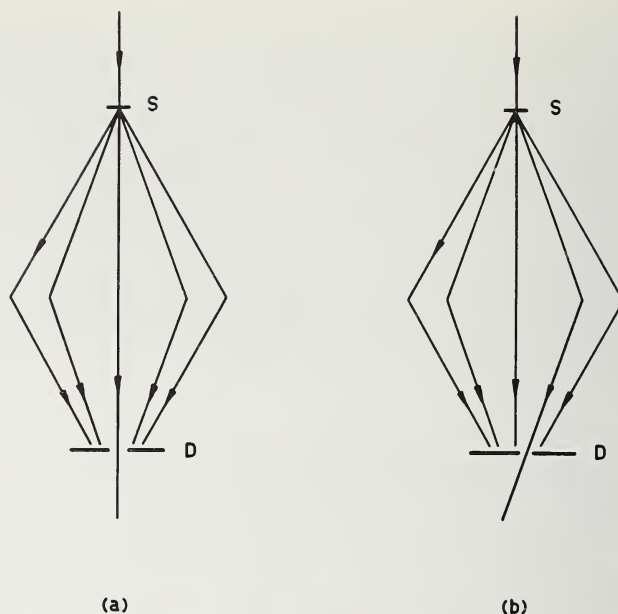


Figure 24. The image formation in the electron microscope. (a) Bright field image (b) dark field image.

Attachments for special purposes are available for most microscopes, e.g., cooling and heating stages, straining devices, double tilting specimen holders, etc.

### 3. Specimen Preparation

The thinning of specimens to a suitable thickness (500–5000 Å) depending on the nature of the material, is an important and sometimes difficult problem that arises in the application of this technique. Metals are usually thinned in successive stages by rolling alternated with annealing treatments and finally electro-polishing. Bulk specimens can first be reduced to thin plates by acid sawing or by spark cutting. We refer to Kelly and Nutting for an excellent review of these techniques [62].

Some layered crystals, e.g., graphite can be cleaved to thin foils [63]. Other crystals develop as sufficiently thin plates when grown by sublimation, e.g., zinc, cadmium, tin disulfide, chromium chloride, etc. Chemical thinning can be applied to uranium dioxide [64], magnesium oxide [65], silicon, germanium [66], etc. Annealed beaten foils of gold [67] and platinum [68] have been used in radiation damage studies. Extensive use has also been made of very thin evaporated metal films [69]. Thin layers of fine grained oxides (such as  $\text{TiO}_2$  and  $\text{Ta}_2\text{O}_5$ ) can often be recrystallized in the microscope by electron beam heating [70, 71] which produces large foils of uniform thickness.

4. *Electron Diffraction in Perfect Crystals*

We shall not develop the theory of electron diffraction. We only summarize the fundamentals required for an understanding of the technique. The condition for diffraction is usually expressed by Bragg's "reflection" law

$$2d_{hkl} \sin \theta = k\lambda \quad (1)$$

where  $d_{hkl}$  ( $=1/g$ ) (2) is the interplanar distance of the lattice planes which "reflect,"  $\theta$  is the Bragg angle,  $k$  is an integer and  $\lambda$  is the wave length of the radiation used. In the case of electrons  $\lambda = 0.04 \text{ \AA}$  for 100 kV electrons, and the Bragg angles are very small (a few degrees), so that  $\sin \theta \approx \theta$ .

Using the reciprocal lattice concept the diffraction condition can be formulated as follows. Let 0 be the origin of the reciprocal lattice (Fig. 25a). From 0 we draw a vector  $-\mathbf{k}_0$  where  $\mathbf{k}_0$  is the wave vector of the incident beam. This gives the point C. With C as a centre, we construct a sphere with radius  $1/\lambda = |k_0|$ . If this sphere, called Ewald's sphere, passes through the node point N of the reciprocal lattice, the diffracted beam will have the direction CN; its diffraction vector is  $\mathbf{g} = \overline{0N}$ . In electron diffraction the radius of the reflecting sphere is large compared to the mesh size of the reciprocal lattice, which is of the order of one reciprocal Ångström. For many practical purposes the reflecting sphere can therefore be considered as planar.

In a thin foil Bragg's condition is considerably relaxed, i.e., the angle over which reflection takes place is relatively large. This is described in terms of the reciprocal lattice, by saying that the reciprocal lattice nodes are not points, but "regions" in reciprocal space corresponding to large diffracted intensities. For a thin foil these regions are rods perpendicular to the foil surface. The rods intersect Ewald's sphere over a certain angular range. The intensity of the diffracted wave depends on the exact point where the rod is intersected by Ewald's sphere. The deviation from the exact Bragg position is described by the vector  $\mathbf{s}$  (Fig. 25b) called excitation error. The vector  $\mathbf{s}$  goes from the considered reciprocal lattice point to Ewald's sphere. It is counted positive in the sense of the incident beam, i.e.,  $s > 0$  when the reciprocal lattice point is inside Ewald's sphere.

For a perfect crystal the amplitude of the transmitted beam is given, according to the two-beam dynamical theory, neglecting anomalous absorption by

$$A_T = (\cos \pi\sigma z_0 - i \frac{s}{\sigma} \sin \pi\sigma z_0) e^{\pi i s z_0} \quad (3)$$

where  $z_0$  is the thickness of the crystal. The quantity  $\sigma$  is defined by

$$\sigma t_g = \sqrt{1 + (st_g)^2}, \quad (4)$$

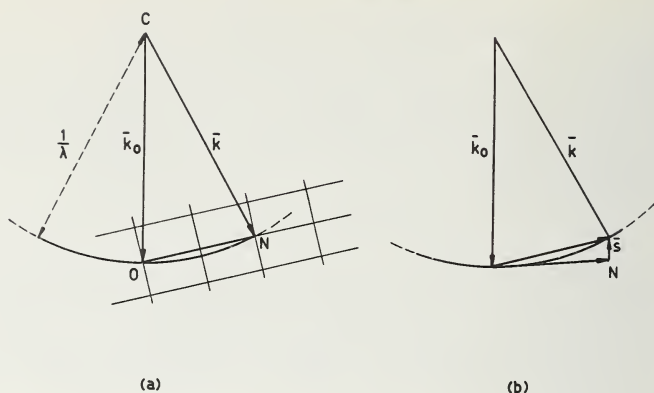


Figure 25. Reciprocal lattice construction of the diffracted beam. O is the origin of the reciprocal lattice. C is the center of Ewald's sphere. CN is the direction of the diffracted beam for a reflection with diffraction vector ON.

where  $t_g$  is the extinction distance,  $t_g$  has the dimensions of a length, it is related directly to the Fourier coefficient of the lattice potential which corresponds to the operating reflection. Anomalous absorption is taken into account phenomenologically by making  $t_g$  complex, i.e., by making the substitution  $\frac{1}{t_g} \rightarrow \frac{1}{t_g} + \frac{i}{\tau_g}$  [72], where  $\tau_g$  is the absorption length. Usually  $\tau_g$  is 10–15 times the extinction distance  $t_g$ .

The amplitude of the scattered beam is similarly given by:

$$A_S = \frac{i}{\sigma t_g} \sin \pi \sigma z_0 e^{\pi i s z_0} \quad (5)$$

and the intensity of the scattered beam is

$$I_S = [1/(\sigma t_g)^2] \sin^2 \pi \sigma z_0 \quad (6)$$

without absorption

$$I_T = 1 - I_S. \quad (7)$$

This expression is represented in Figure 26(1) as a function of  $s$ . If anomalous absorption is taken into account the curve (rocking curve) for the intensity of the transmitted beam  $I_T$  becomes as shown in Figure 26(2). The curve is now asymmetrical; for  $s > 0$  the intensity is much larger than for  $s < 0$  (this is the Borrmann effect).

##### 5. Kikuchi Lines—Determination of $s$

For several problems it is of interest to know at least the sign of  $s$ ; the magnitude is usually not required. This information can easily

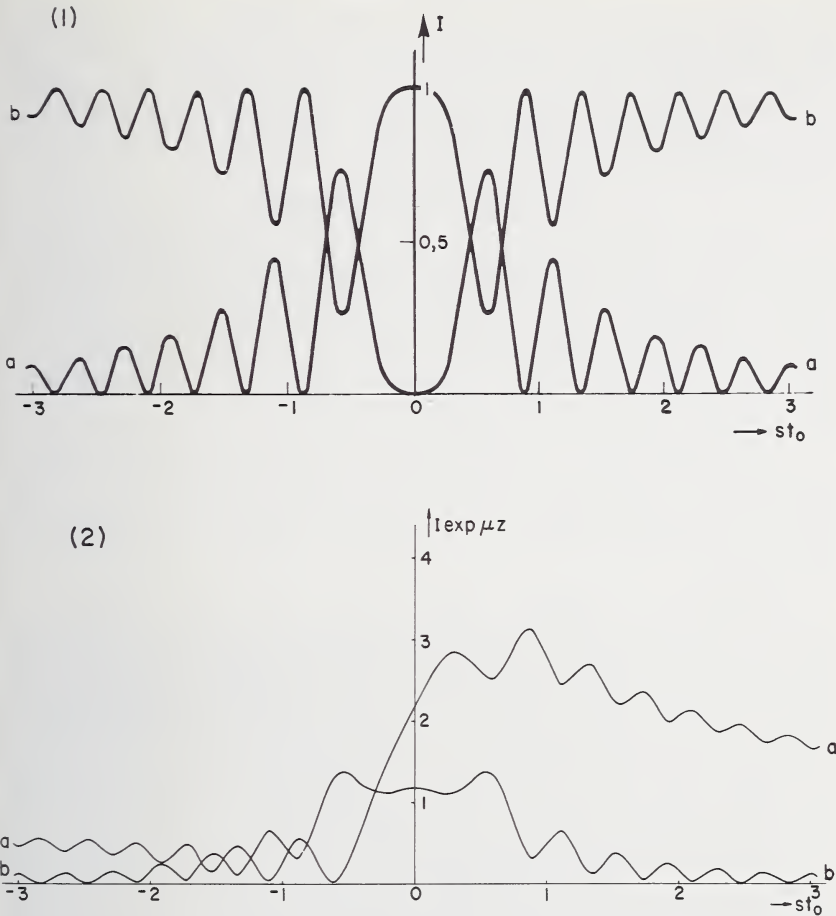


Figure 26. Intensity of the transmitted and scattered beam for a perfect crystal, as a function of the excitation errors. (1) without anomalous absorption (a) transmitted, (b) scattered. (2) with anomalous absorption (a) transmitted (b) scattered.

be deduced from the pattern of Kikuchi lines which is usually observed in relatively thick crystals. Kikuchi lines are due to Bragg reflection of inelastically scattered electrons, which are incident under all possible angles. The geometrical locus of the Bragg reflected beams is a very wide cone with an opening angle of  $90^\circ - \theta$ . This cone intersects the photographic plate along part of a hyperbola, which becomes in fact very nearly a straight line. If the crystal is in the exact reflecting position, the Kikuchi line corresponding to a given set of lattice planes passes through the diffraction spot corresponding to the same set of planes. If the foil is now rotated over a small angle  $\Delta\theta$  the position of the spot does not change appreciably, but the beam producing the Kikuchi line rotates over the same angle  $\Delta\theta$ . The Kikuchi line is thus

displaced with respect to the spot over some distance. This displacement is outwards if the reciprocal lattice point is rotated towards the interior of Ewald's sphere, it is inwards for a rotation in the opposite sense. When the sign convention adopted in section V.A.4 is used the situation can be summarized by Figure 27.

### 6. Extinction Contours [73]

According to the two-beam dynamical theory, neglecting anomalous absorption, the intensity of the transmitted beam is given by eqs (6) and (7). The magnitude of  $t_g$  depends on the operating reflection. In metals it is usually of the order of 2–400 Å. From this formula it is clear that  $I_T$  depends on the specimen thickness  $z_0$  in a periodic way. It also depends in an oscillating way on  $s$  (Fig. 26).

Most specimens used in transmission work are very thin and therefore deformed; moreover they have a non-uniform thickness. As a result of this, dark bands become visible. They are the geometrical loci for  $z_0 = \text{constant}$  (thickness contours) or for  $s = \text{constant}$  (inclination contours).

**a. Thickness Contours.** Along the lines where the crystal has a thickness given by  $(r + \frac{1}{2}) t'_g$  with  $t'_g = 1/\sigma$  the intensity of the transmit-

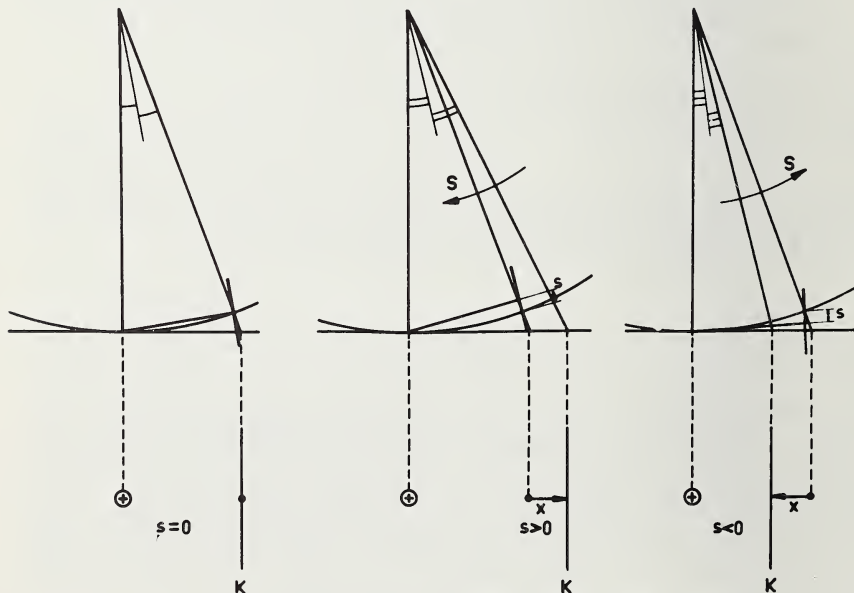


Figure 27. The relation between the position of a diffraction spot and that of the corresponding Kikuchi line (K).  $S$  indicates the sense into which the lattice has to rotate in order to approach the exact Bragg position.

ted beam is minimum and a black contour is observed in the bright field image. The positions of the contours of this type are not sensitive to the tilt of the specimen; their intensity of course is. Since  $t_g$  changes with the operating reflection the depth distance between contours changes with the diffraction vector. Knowing the extinction distance the number of fringes gives an easy measure of the thickness. Figure 28 shows typical thickness contours in a wedge shaped crystal.

**b. Inclination or Bend Contours.** The points for which the Bragg condition is satisfied, i.e., for which  $s \approx 0$  form continuous curves, which are called bend contours. Along these lines the intensity of the transmitted beam is minimum and a black line is observed in the bright field image. These contours are very sensitive to changes in orientation of the specimen; they are observed to migrate on tilting. In nearly perfect foils the bent contours are very broad and hardly visible; in metal specimens they are usually much sharper. In thick foils the contours become very broad as a result of anomalous absorption. Along the main contours one has  $s \approx 0$ ; on passing the contours,  $s$  changes sign.



Figure 28. Thickness contours in a wedge shaped silicon foil.

The fine structure described by eq (6) can sometimes be revealed as secondary contours along which  $s = \text{constant}$ . From the fringe spacing in this fine structure the foil thickness can be deduced.

Figure 29 is a dark field image of inclination contours.

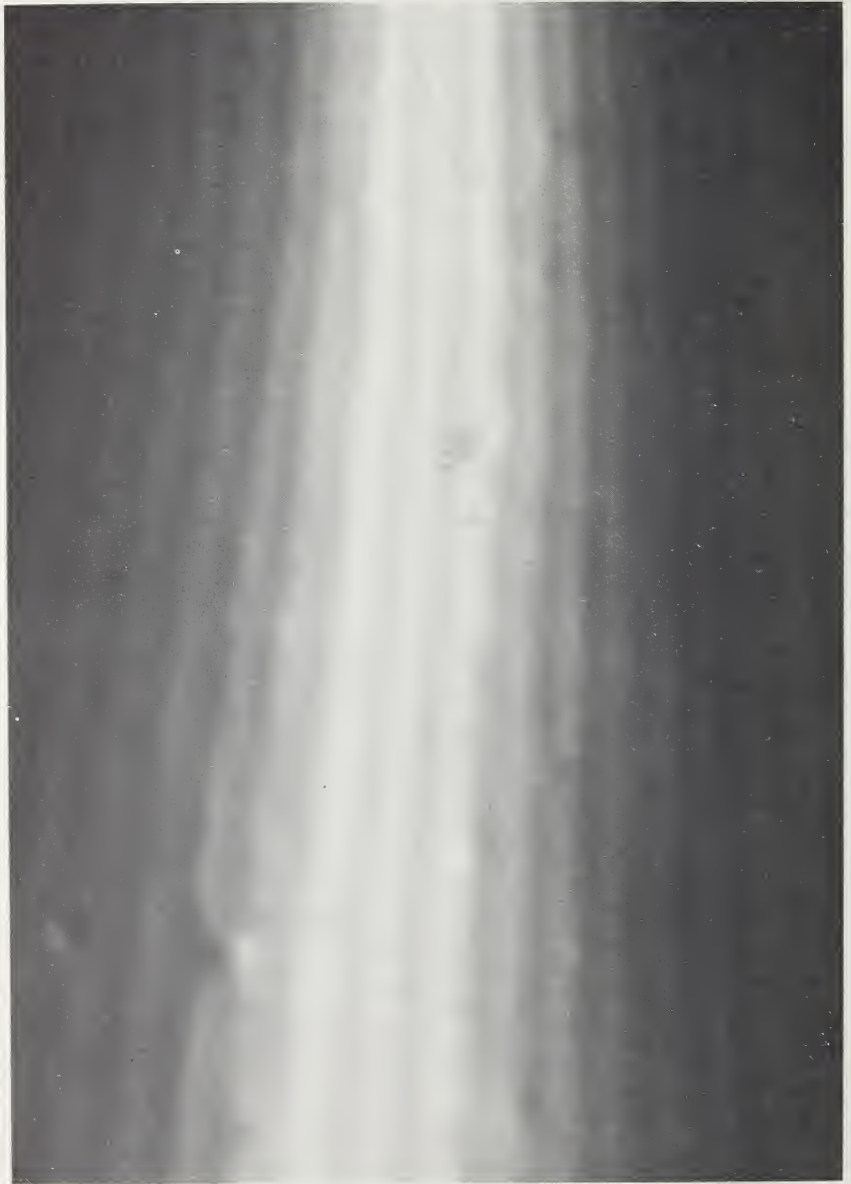


Figure 29. Dark field image of inclination contours in a bent graphite foil.

## B. CONTRAST AT DISLOCATIONS [74, 75, 76]

1. *Origin of the Contrast*

We shall only use the intuitive approach, which is sufficient for most purposes. Let us assume that the thin foil  $F$  contains an edge dislocation parallel to the foil plane in  $E$  (Fig. 30). We further suppose that the set of lattice planes represented in Figure 30 is near the reflecting position. For a thin foil Bragg reflection takes place over an appreciable angular range. This is pictured in reciprocal space by saying that points have become rods perpendicular to the foil plane. Let us assume that the center of gravity of the reciprocal lattice rod is outside the Ewald sphere. A rotation in the sense  $S$  indicated in Figure 27 is then required to bring the crystal into the Bragg position. In the perfect region of the foil, part of the intensity is transmitted and another part is diffracted: this is indicated by the relative thickness of the lines in Figure 30. The bright field image is now formed by observing the intensity distribution in the direct beam; the scattered beams being intercepted by an aperture like in Figure 24.

To the left of  $E$  the deformation of the lattice planes due to the presence of the dislocation is such that Bragg's condition is better satisfied and hence the intensity of the scattered beam is locally larger. At the other side of the dislocation the deformation is in the opposite sense and the intensity of the scattered beam is consequently less. As a result a lack of intensity will be noted in the bright field image, on one side of the dislocation, and a black line will be observed. The same

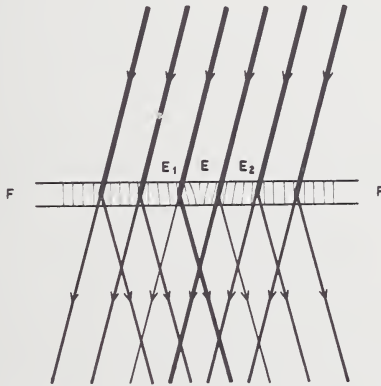


Figure 30. Illustrating the image formation at an edge dislocation. The thickness of the lines is a measure for the intensity.

type of reasoning is valid for a screw dislocation. Summarizing we can say that for  $s \neq 0$  and relatively large, the image side for a dislocation is that side for which the lattice rotation is such as to bring the lattice planes into the Bragg position.

From this picture which is essentially a kinematical approach, it is clear that changing the sign of the edge dislocation changes the image side for a given sign of  $s$ . This is visualized in Figure 31. Changing the sign of  $s$  or changing the sign of the diffraction vector changes the image side. The same reasoning can be made for a screw dislocation; the result is also shown in Figure 31. It is clear that the results of this paragraph can be used to determine the sign of a dislocation. We shall describe the procedure further below. Although the picture given here is certainly not correct quantitatively, it gives the right qualitative answer, which is sufficient for most purposes.

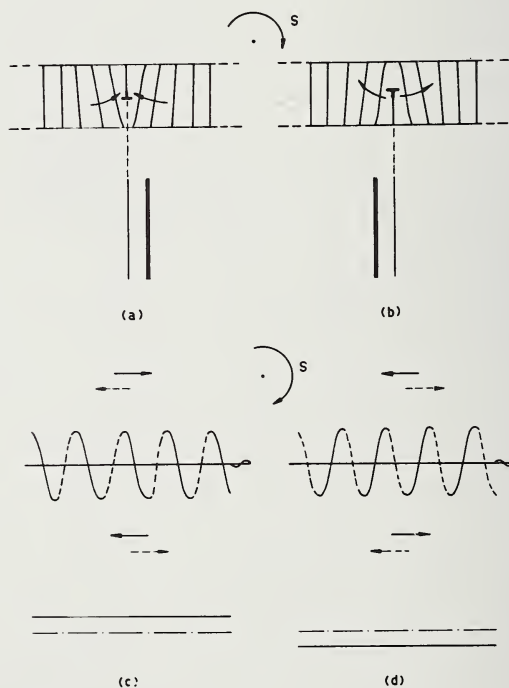


Figure 31. Image formation at edge and screw dislocations of both signs. The images (heavy lines) are on opposite sides of the true positions of the dislocations for dislocations of opposite sign. (a) and (b) edge dislocations (c) and (d) screw dislocations.

## 2. Determination of the Direction of the Burgers Vector. Extinction Conditions

Intuitively one can see that if the contrast-producing reflection corresponds to a set of lattice planes which is not deformed by the presence of the dislocation, the latter will remain invisible. This is shown specifically for an edge dislocation in Figure 32. The planes with diffraction vector  $\mathbf{g}_1$  are deformed by the presence of the dislocation and reflection by these planes does reveal the dislocation. On the other hand the dislocation can be considered as resulting from the superposition of planar arrangements perpendicular to the vector  $\mathbf{g}_3$ . This evidently shows that on reflection with a diffraction vector  $\mathbf{g}_3$  no contrast will be seen. The planes perpendicular to  $\mathbf{g}_2$  (i.e., the planes parallel to the glide plane), are slightly deformed, the glide plane having a little bump at the position of the dislocation, and hence only very weak contrast will be produced by reflection with a diffraction vector  $\mathbf{g}_2$ .

The same reasoning is shown for a screw in Figure 33. Planes intersecting the axis of the screw are deformed, whilst planes passing through the screw axis remain flat to a first approximation. If the end effects are taken into account for a screw intersecting the surface, these planes are in fact transformed into helicoidal surfaces.

One can summarize these considerations by the following rule: if  $n \equiv \mathbf{g} \cdot \mathbf{b} = 0$  the dislocation shows no contrast. The quantity  $n$  is an integer in the case of a perfect dislocation, since  $\mathbf{g}$  is a reciprocal lattice vector and  $\mathbf{b}$  a lattice vector. For a partial dislocation  $\mathbf{b}$  is no

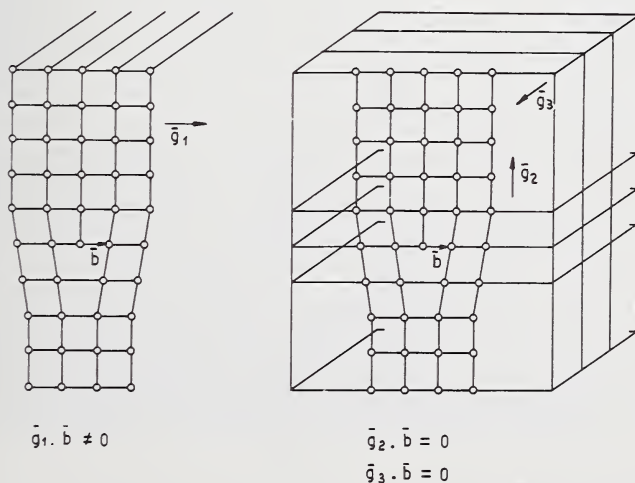


Figure 32. Deformation of different families of lattice planes by the presence of an edge dislocation. Only families of lattice planes which are deformed by the presence of the dislocations give rise to contrast.

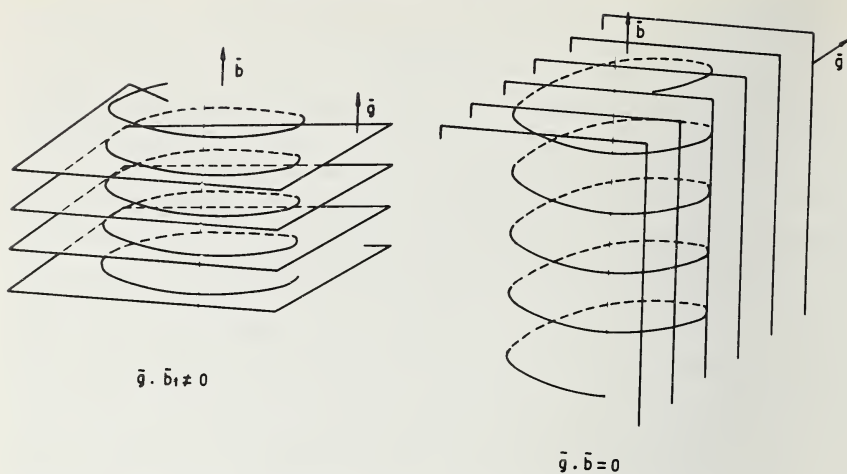


Figure 33. Deformation of different families of lattice planes by the presence of a screw dislocation.

longer a lattice vector and  $n$  may become fractional. For  $n \leq 1/3$  the dislocation is invisible [75, 76]. Some care is therefore required when using the absence of contrast as a criterion to decide that  $n=0$ .

There is another case where special care is needed (Fig. 34a). If the dislocation has a Burgers vector perpendicular to the foil plane, and if the foil plane is perpendicular to the incident beam, the only operating reflections have diffraction vectors that satisfy the criterion  $\mathbf{g} \cdot \mathbf{b} = 0$ . No contrast would therefore be expected. However, as pointed out

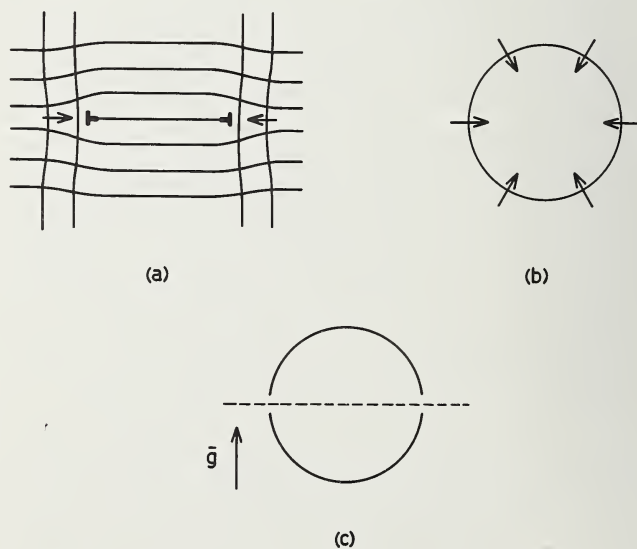


Figure 34. Image formation at a prismatic loop. The displacements are radial. The diffracting planes are parallel to the line joining the segments of no contrast.

already above, the planes parallel to the glide plane, are, for an edge dislocation, slightly deformed. For a prismatic loop, parallel to the foil plane a radial displacement is produced as a result of this (Fig. 34b). This radial displacement is either inwards or outwards depending on the sign of the Burgers vector. This deformation is sufficient to produce contrast for small  $s$ -values [77]. Contrast is however completely absent for these segments of the dislocation loop where the displacement is perpendicular to the operating diffraction vector. As a result a prismatic loop with Burgers vector perpendicular to the loop plane will show contrast except for two segments. The diffracting lattice planes are parallel to the line connecting these two segments (Fig. 34c).

If the Burgers vector is inclined with respect to the loop plane, whilst the loop is in the foil plane, contrast will only be "residual" for the set of lattice planes parallel to this inclined vector. For other reflections the whole loop exhibits contrast. An example of this is represented in Figure 35, which shows loops in the basal plane of coldworked zinc. Some show residual contrast; others are in full contrast.

It is now evident how the extinction conditions can be used to determine the direction of the Burgers vector. If a perfect dislocation is



Figure 35. Loops in the basal plane of zinc. Two types of images are visible. The Burgers vector of the loops is inclined with respect to the basal plane. The inset shows stacking fault fringes for loops which are inclined with respect to the foil plane. Courtesy Stals.

out of contrast for two diffraction vectors,  $\mathbf{g}_1$  and  $\mathbf{g}_2$ , the Burgers vector is parallel to  $\mathbf{g}_1 \times \mathbf{g}_2$ . An example of a complete Burgers vector determination for a dislocation network in graphite is shown in Figure 36, where use is made of the bright field image. The foil has been inclined at different small angles with respect to the electron beam so as to bring the three families of partial dislocations successively out of contrast.

The bright field method is difficult to apply in thin crystals because one cannot easily obtain the two beam situations required for extinction. It is then advisable to use the dark field method which consists in making dark field images using the different low order diffraction vectors. This method has successfully been applied to the study of dislocation

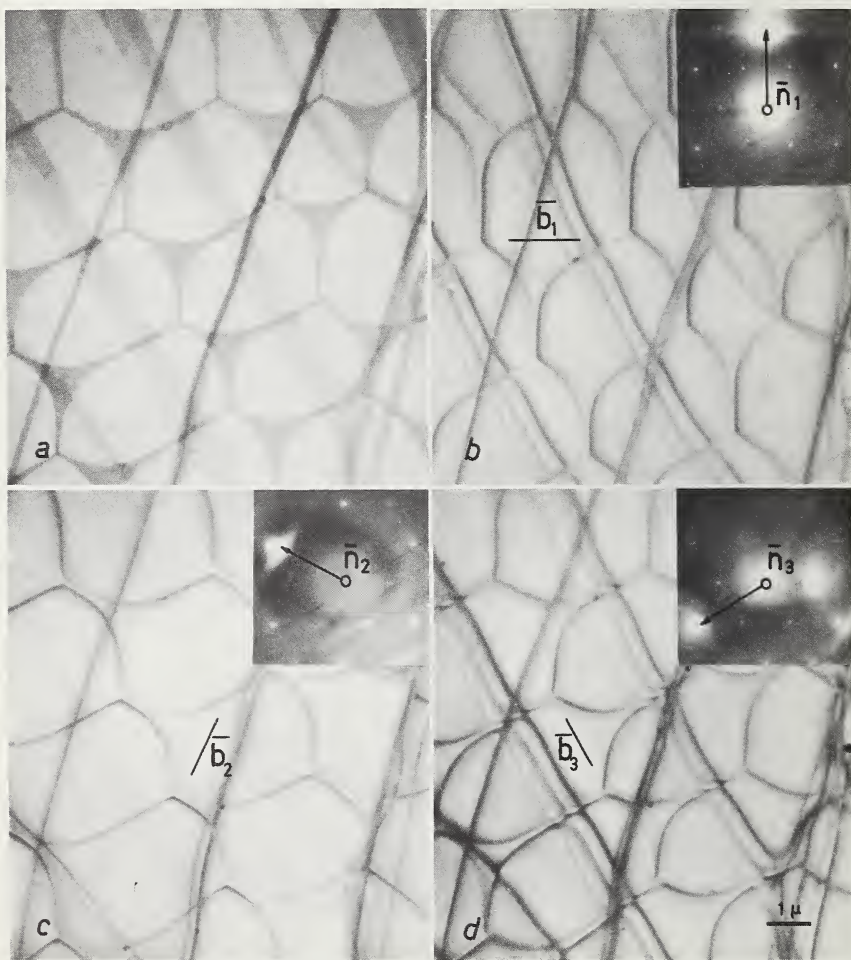


Figure 36. Determination of the direction of the Burgers vectors for a network in graphite. The different families of dislocations go successively out of contrast.

networks in extremely thin polyethylene single crystals [78]. Figure 37 reproduces one of the sequences of photographs obtained in this study, whilst Figure 38 shows the resulting Burgers vector analysis of the network which turns out to contain partial dislocations.

For the loops in zinc, shown in Figure 35, it is possible to conclude that the vector is inclined with respect to the basal plane because otherwise the loops would always exhibit residual contrast, which is obviously not the case. In this case there is additional evidence that the Burgers vector is inclined: the loops also contain a stacking fault.

### 3. *Determination of the Sign of the Dislocations (i.e., the Sense of the Burgers Vector) [79, 80]*

We describe the procedure for the simple case where the dislocation is in the foil plane. The following information is required:

- (i) the image side,
- (ii) the sign of  $s$ ,
- (iii) the direction of the Burgers vector.

The image side is determined by comparing photographs taken with two different signs of  $s$  and the same  $\mathbf{g}$ -vector or with two different signs of the  $\mathbf{g}$ -vector for  $s$ -values of the same sign. The image side changes in both cases, the true position of the dislocation is between the two images. Since the best bright field images are obtained for positive  $s$ -values, it is often easiest to produce images for  $+g$  and  $-g$ .

The sign of  $s$  is determined in the manner described in subsection V.A.5. As already mentioned it is usually positive for good contrast.

The direction of the Burgers vector is found by means of the procedure outlined in subsection V.B.2.

In the light of these three pieces of information, Figure 31 tells us immediately the sign of the dislocation i.e., the sense of the Burgers vector. The application of this procedure to small loops is discussed below.

According to the dynamical theory and adopting the FS/RH convention, the image side in the bright field image is left if  $(\mathbf{g} \cdot \mathbf{b})s > 0$ . This relation can obviously also be used to determine the sign of  $\mathbf{b}$  if  $\mathbf{g}$  and  $s$  are known and if the direction of  $\mathbf{b}$  is known [81].

### 4. *Determination of the Length of the Burgers Vector*

The image profile of a dislocation depends on the value of  $n$  [74, 75, 76]. In particular the change in aspect of the profile on crossing extinction contours where the sign of  $s$  changes, is different for  $n=1$  and  $n=2$  [76]. The behaviour is shown schematically in Figure 39. This behaviour follows from the fact for  $n=1$  the image is a symmetrical peak at the position of the dislocation for  $s=0$  (i.e., in the contour). For  $n=2$  the image is double peaked for  $s=0$ : the center of the image has the same

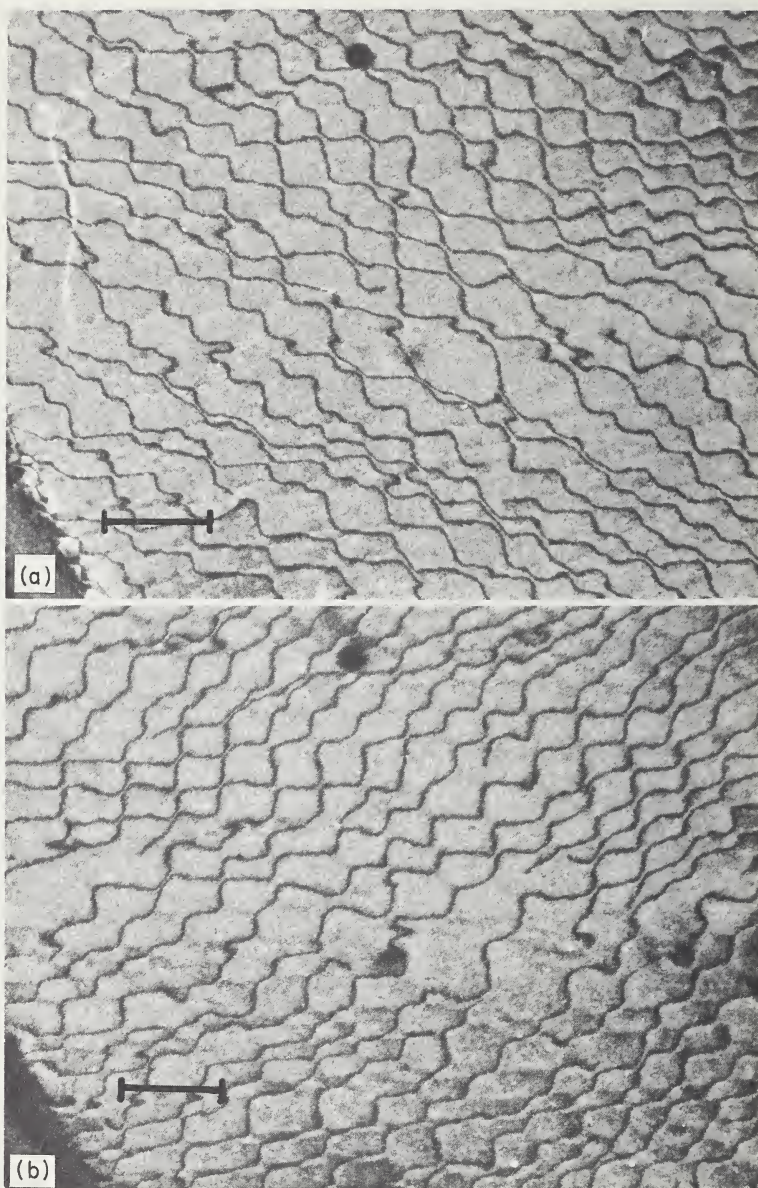
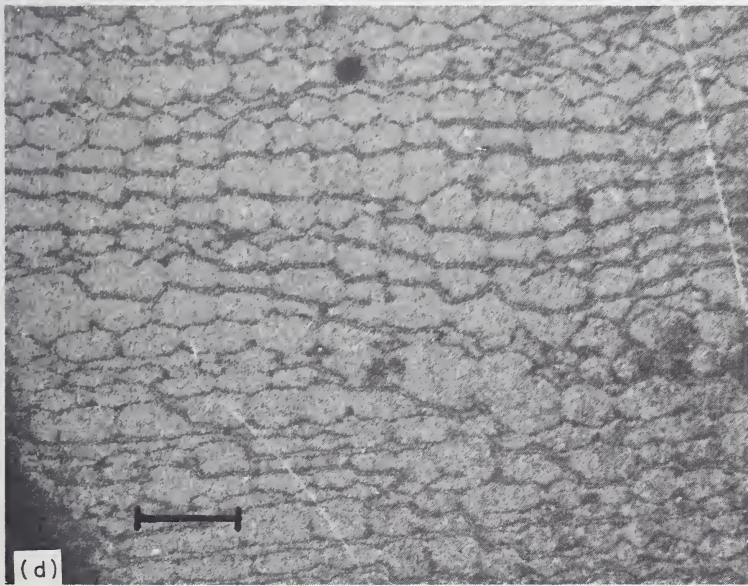
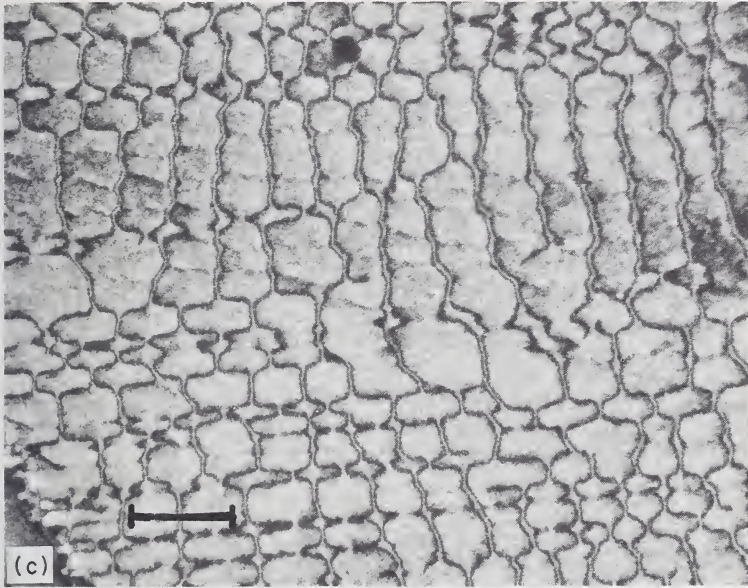


Figure 37. The same area of a network in a polyethylene single crystal imaged by different diffraction vectors (dark field images) (a)  $[110]$  (b)  $[1\bar{1}0]$  (c)  $[200]$  (d)  $[020]$ . Courtesy of Holland and Lindemeyer.



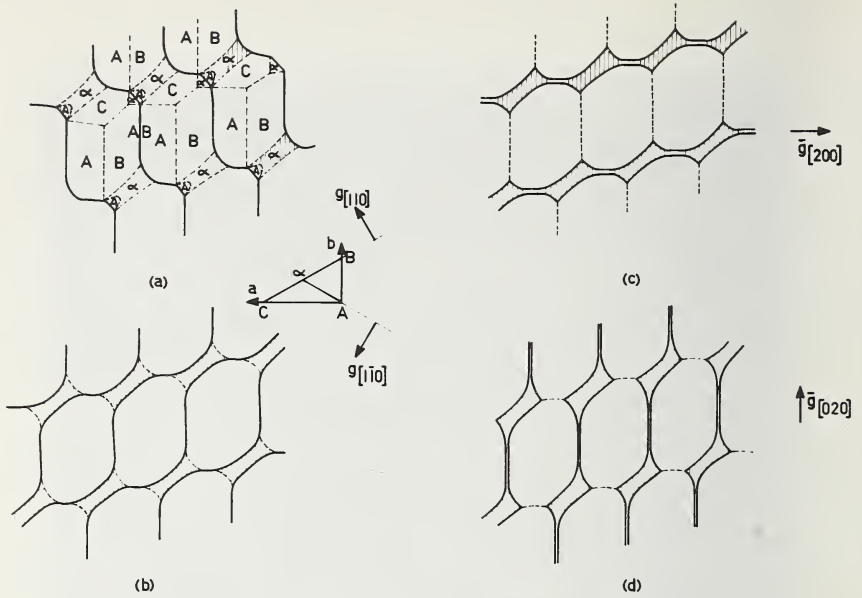


Figure 38. Lettering pattern of a network of dislocations such as in Fig. 37 with all segments represented. The different diagrams represent the dark field patterns as imaged by the different reflections. Dotted lines represent dislocations which are out of contrast; double lines represent double images. These diagrams are to be compared with the DF image of Fig. 37.

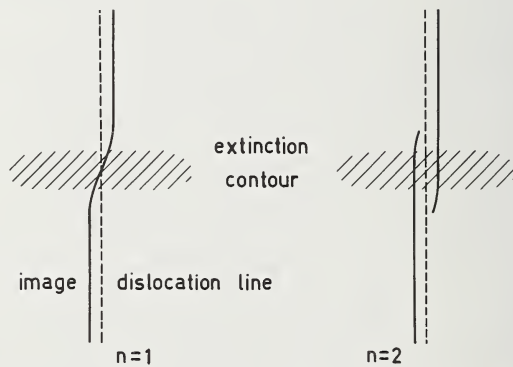


Figure 39. Difference in behaviour on crossing an extinction contour for dislocation images with  $n = 1$  and  $n = 2$ .

intensity as the background. By observing the change in profile for a given dislocation image it is therefore possible to determine whether  $n$  is equal to 1 or to 2. If we know already the direction of  $b$  for this particular dislocation and knowing  $g$  it is possible to determine the length of  $b$ :  $b = n/g \cdot e_b$ , where  $e_b$  is the unit vector along  $b$ . In fact the knowledge of  $n$  is equivalent to knowing the length of the projection of  $b$  onto  $g$ .

5. *Dislocations Inclined With Respect to the Foil; Oscillating Contrast* [76, 77]

The image profile of a dislocation parallel to the foil plane depends, especially for small  $s$ -values, on its distance from the surfaces. The profile varies in a periodic way with the distance, the period being  $t'_g$ . Figure 40 shows the variation of the image profile as a function of depth, for a screw dislocation parallel to the foil plane [76]. Bright and dark sides are seen to alternate periodically with depth. If the dislocation is now inclined with respect to the surface, the image profile changes periodically with depth. An example of such oscillating images is visible in Figure 41.

The phenomenon is of importance because it provides a depth scale which is otherwise completely lacking in the electron microscope, as a result of the large depth of focus. It can for instance be used to estimate the distance from the surface of a segment of a dislocation line which intersects the surface [79]. It is sufficient to count the number of periods between the emergence point in the surface and the segment of interest. The phenomenon can also be used to determine the foil thickness.

As a result of anomalous absorption, oscillating dislocation images are similar at the top end of the foil, but pseudo-complementary at the bottom end (cfr. stacking fault fringes section V.C.3). This remark allows to distinguish both ends of the dislocation line. The oscillations disappear for sufficiently large values of  $s$ . It is clear that only for such values of the  $s$  the image side has a meaning and can be used to determine the sign of  $\mathbf{b}$ .

6. *Dislocations Seen End on* [38, 82, 83, 84]

The contrast due to the dislocations seen end on cannot be interpreted by means of the simple image of section V.B.1. It is therefore considered separately here.

For an edge dislocation seen end on the contrast may be considered to arise from the difference in lattice parameter in the compressed and expanded regions of the dislocation. If the Bragg condition is better satisfied than in the perfect part provided the lattice parameter were smaller the compressed region will show up black in the bright field image, whilst the expanded region will show up bright. The reverse will be true after a change of the sign of  $s$ . The image therefore consists of a black-white dot. It is clear that these considerations allow a determination of the sign of the dislocation. The effects mentioned are small and it is not sure whether edge dislocations of this type can be observed.

For a screw dislocation in an infinite medium, all displacements are parallel to the axis of the screw. No contrast is therefore to be expected for a screw dislocation perpendicular to the foil plane, i.e.,

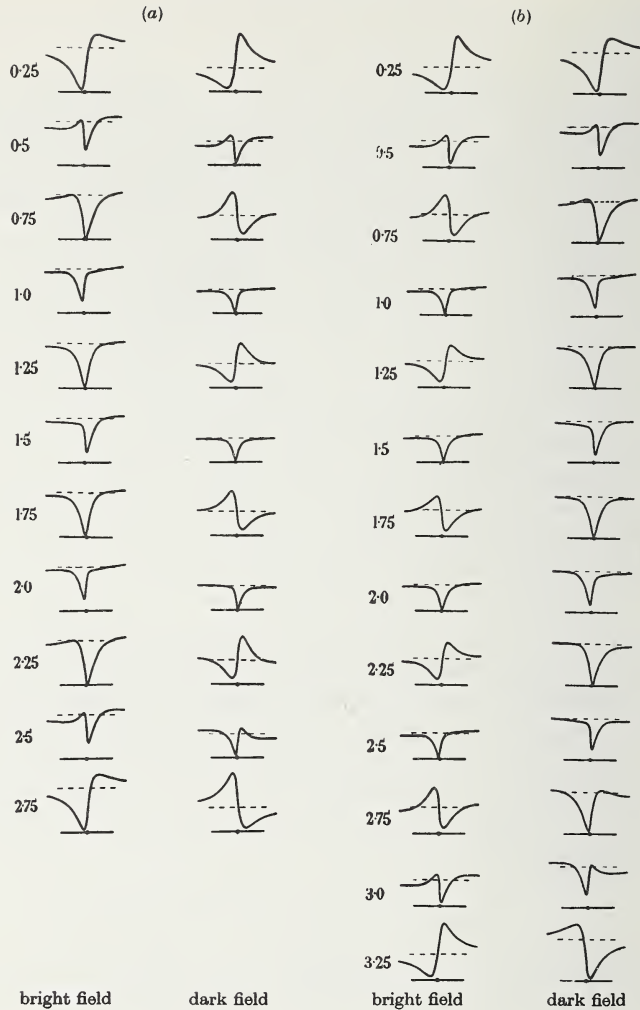


Figure 40. The image profile for a screw dislocation as a function of its distance from the surface. Courtesy Howie and Whelan. The sequence (a) refers to a foil of thickness  $3 t_g$  and the sequence (b) to the foil of thickness  $3.5 t_g$ .

parallel to the electron beam. However, as a result of surface relaxation the planes parallel to the screw axis are transformed into helicoidal surfaces and contrast arises (Fig. 42). Let us consider as in Figure 42 diffracting planes perpendicular to  $g$ . Behind the screw of Figure 42 (in C) the lattice planes are then rotated towards  $s > 0$  whereas in front of it (in D) they are rotated towards  $s < 0$ . If in the perfect crystal part  $s < 0$  it follows that behind the screw (in C) the crystal locally approaches the Bragg position, whereas in front of the screw (in D) the crystal is locally turned away from the Bragg position. It then follows that in the bright field image a dark dot will be seen behind the dislocation and a

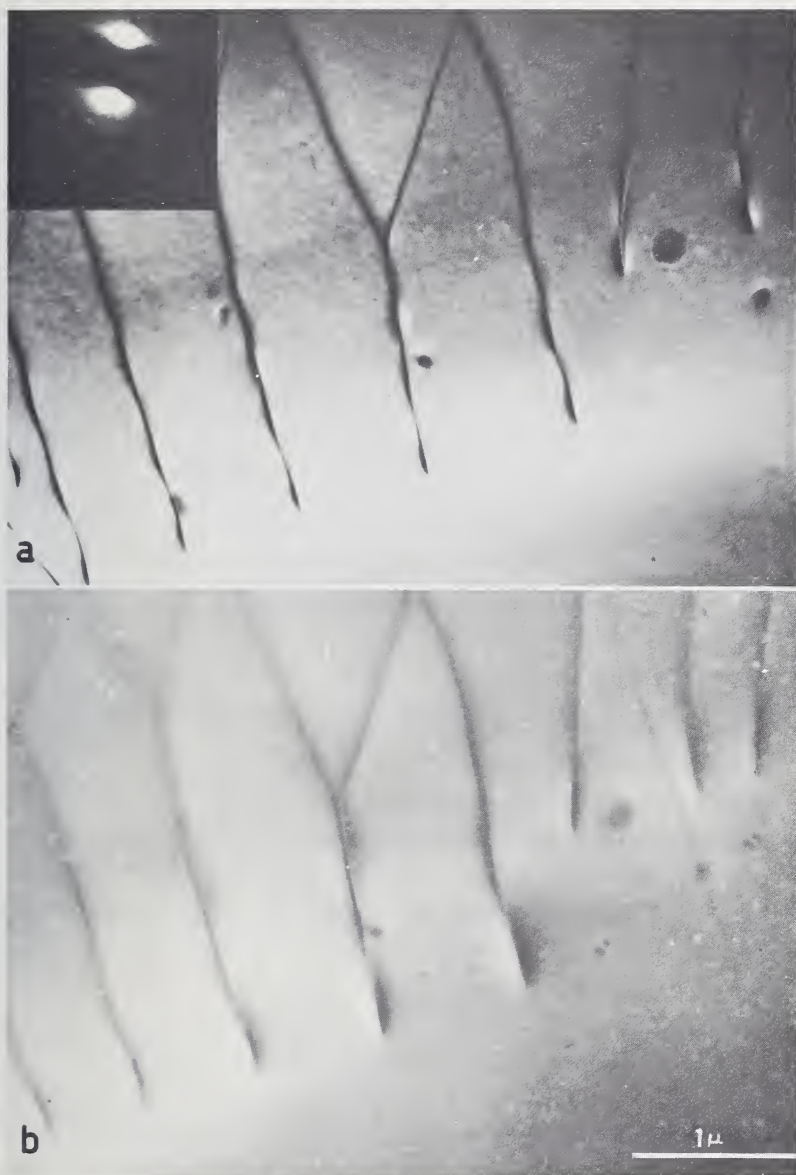


Figure 41. Oscillating contrast at dislocations approaching the surface in a tin disulfide single crystal. (a) Bright field image. (b) Dark field image.

bright one in front of the dislocation. This is reversed for a screw dislocation of the opposite sign (Fig. 42e). The line of no contrast is parallel to the diffraction vector. It is again clear how the sign of the dislocation can be determined. The same rule can still be applied to dislocations which are not quite perpendicular.

Images of this type are visible in Figure 43.

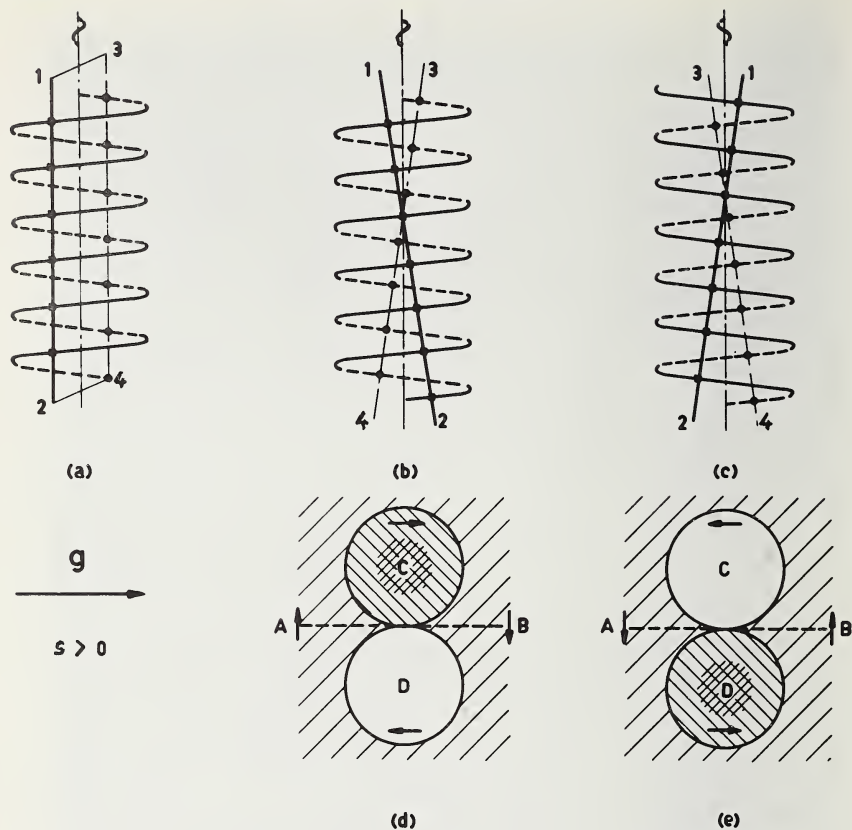


Figure 42. Image formation at a screw dislocation seen end on.

In Figure 43c the dislocations are out of contrast in the central part of the foil, but the ends are visible as a result of surface relaxation alone.

### C. STACKING FAULTS

#### 1. Types of Stacking Faults

**a. In f.c.c. Crystals.** In face centered cubic crystals stacking faults can be generated in at least two ways:

(i) by the passage of a partial dislocation, e.g., resulting from the splitting of a perfect dislocation into Shockley partials on the (111) glide planes.

(ii) by removing or inserting part of a (111) lattice plane.

The mechanism (ii) suggests that two different types of stacking faults can be considered. The fault resulting from the removal of a single (111) layer can be described by the stacking symbol

$$a b c a b \underbrace{c a c}_{\text{fault}} a b c \dots \quad (8)$$

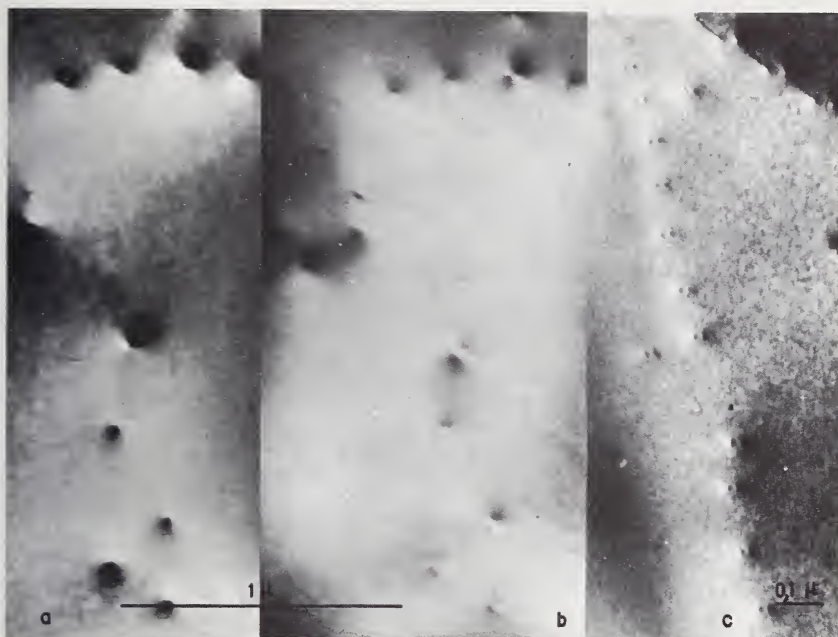


Figure 43. (a) and (b): Dislocations seen end on in uranium dioxide. The images consist of black-white dot pairs. The line of no contrast is parallel to the diffraction vector. (a) Bright field image (b) Dark field image (c) Dislocations in platinum. The dislocations are out of contrast in the central part of the foil; the ends are visible as a result of surface relaxation. Courtesy Ruedl.

It contains one lamella which is hexagonally close-packed and is called *intrinsic*. Another fault can be generated by inserting a single (111) layer; such a fault is characterized by the layer sequence

$$a \ b \ c \ a \ \underline{b \ c} \ \underline{b \ a} \ b \ c \ . \ . \ . \quad (9)$$

It contains again two triplets, in the hexagonal arrangement, but they are one layer further apart than for the intrinsic fault. Such a fault is called *extrinsic*.

The intrinsic fault can be generated by the passage of a single partial of the Shockley type, i.e., with Burgers vector of the type  $\frac{1}{6}a$  [112]. After glide between the indicated layers in the sequence

$$a \ b \ c \ a \ b \ c \ a \ b \ c \ a \ b \ c \ . \ . \ . \quad (10)$$

↑

the layer sequence becomes

$$a \ b \ c \ a \ b \ c \ a \ c \ a \ b \ c \ a \ b \ c \ . \ . \ . \quad (11)$$

↑

which is obviously equivalent to (8). This is not possible for the extrinsic fault, which may have lower energy however.

The edge of a faulted region is a partial dislocation which in the case of a prismatic loop has a vector  $\frac{1}{3}\mathbf{a}$  [111] or its negative. Such a dislocation is called a Frank sessile. For a stacking fault generated by glide the boundary partial has a vector of the type  $\frac{1}{6}\mathbf{a}$  [112]. The shear vector of the stacking fault, characterizing the displacement that brings the perfect crystal into the faulted position is alternatively  $\frac{1}{3}\mathbf{a}$  [111] or  $\frac{1}{6}\mathbf{a}$  [112]. Both formulations are equivalent since e.g.,

$$\frac{1}{3}\mathbf{a} [111] + \frac{1}{6}\mathbf{a} [11\bar{2}] \rightarrow \frac{1}{2}\mathbf{a} [110] \quad (12)$$

which is a lattice vector.

**b. In h.c.p. Crystals.** Also in hexagonal close packed crystals one can distinguish different types of stacking faults. The normal stacking can be represented by the symbol sequence: a b a b a b . . . . The *single* fault is then described by a sequence which contains only one infraction against the stacking rule, e.g.

$$\dots a b a b \underbrace{a b c} b c b c \dots$$

Such a fault can for instance be generated during growth. The displacement vector is the sum of a vector associated with a Shockley partial ( $\mathbf{p}$ ) and the vector  $\mathbf{c}/2$  in the direction of the  $c$  axis, i.e.,  $\mathbf{R} = \mathbf{p} + \frac{\mathbf{c}}{2}$ .

The double fault is described by a sequence containing two violations of the normal stacking, i.e.,

$$\dots a b a b \underbrace{a b c} \underbrace{a c a c} a \dots$$

Such a fault results on deformation by the passage of a Shockley partial, its displacement vector is  $\mathbf{p}$ .

Finally one can imagine *triple faults* such as

$$a b a b \underbrace{a b c a} \underbrace{b a b a} \dots$$

The displacement vector is now  $\frac{1}{2}\mathbf{c}$ .

**c. Antiphase Boundaries; Periodic Antiphase Boundaries and Stacking Faults.** A particular type of stacking fault occurs in ordered alloys. When ordering starts simultaneously in different parts of a disordered alloy it is to be expected that on meeting different ordered domains may be "out of step." If this is the case the contact plane is called an "antiphase boundary." It is shown schematically in Figure 44(1) for the CuAu alloy. Antiphase boundaries are generated also when dislocations, which are perfect with respect to the disordered structure, but partial with respect to the ordered structure, move through the crystal (Fig. 44(2)). A strip of antiphase boundary then connects two dislocations, very much like a strip of stacking fault connects two partial dislocations.

In a number of alloys periodic arrangements of antiphase boundaries occur; they can be revealed directly in the image as a periodic line structure [85] (Fig. 45a).

The nonperiodic antiphase boundaries exhibit fringe contrast similar to stacking faults (Fig. 45b). However in ordered alloys the contrast is due to a superlattice reflection. Since these reflections have usually long extinction distances only a small number of fringes is visible [86].

It has been found recently that certain ordered alloys contain periodically arranged stacking faults giving rise to complicated regular stacking sequences, with long periods. These long periods can be resolved directly in the electron microscope [87].

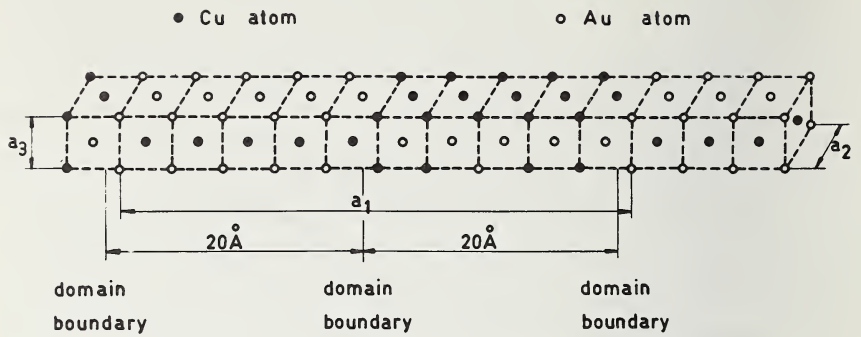
## 2. Origin of the Contrast

With respect to diffraction a stacking fault is characterized by its displacement vector  $\mathbf{R}$  describing the displacement of the exit part of the foil, with respect to the entrance part. With  $\mathbf{R}$  corresponds the phase angle  $\alpha = 2\pi \mathbf{g} \cdot \mathbf{R}$ . For a face centered cubic crystal only reflections  $hkl$  for which the indices are either all even or all odd have a non-zero intensity. Taking the shear vector as  $\frac{1}{6} \mathbf{a} [112]$  one finds

$$\alpha = 2\pi \frac{1}{a} [hkl] \cdot \frac{1}{6} \mathbf{a} [112] = \frac{2}{6} \pi(h+k+2l) = \pm \frac{2}{3} \pi(\text{mod } 2\pi). \quad (13)$$

The result of the presence of a stacking fault is to cause a phase shift of the amount  $\alpha$  between waves diffracted by the part of the crystal above the fault plane with respect to the waves diffracted by the part below the fault plane. The resulting intensity at the back surface of the foil depends in a periodic way on the fault position. If the fault is parallel to the foil plane, a different intensity will in general be found within the faulted area as compared to that in the perfect part. For an inclined fault plane this results in the formation of a fringe pattern. The detailed intensity distribution in this fringe pattern is studied in ref. 87b. An example of stacking fault fringes in a copper gallium

(1)



(2)

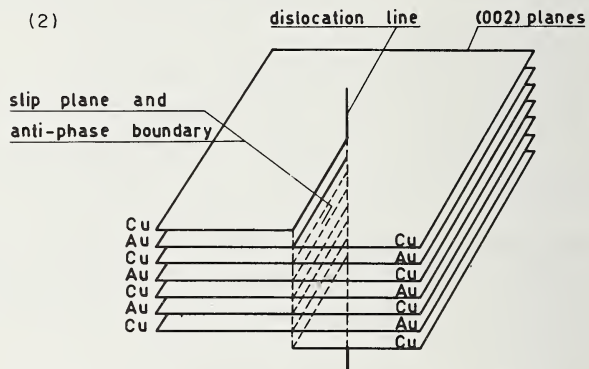


Figure 44. (1) One unit cell of the ordered alloy CuAu II. Courtesy Johansson and Line.  
(2) Illustrating the relation between dislocations and antiphase domain boundaries in the alloy CuAu I.

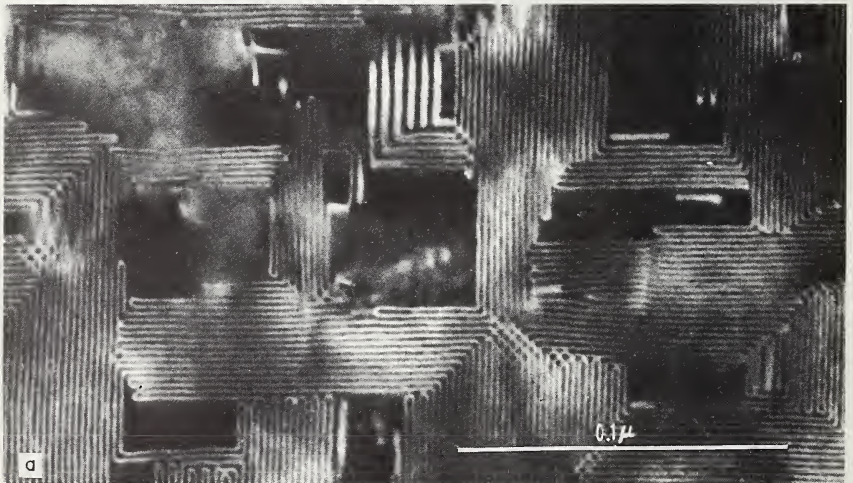


Figure 45(a). Periodic antiphase boundaries in CuAu II. Courtesy Pashley.



Figure 45(b). Antiphase boundaries in Tealite ( $\text{SnPbS}_2$ ). Courtesy Marinkovic.

alloy of low stacking fault energy is reproduced in Figure 46. The depth distance between successive fringes close to the surface is

$$t'_g = t_g / \sqrt{1 + (st_g)^2}. \quad (14)$$

If  $t_g$  and  $s$  are known, the foil thickness can be deduced from the number of fringes. Inversely if the foil thickness is known  $t'_g$  can be measured.

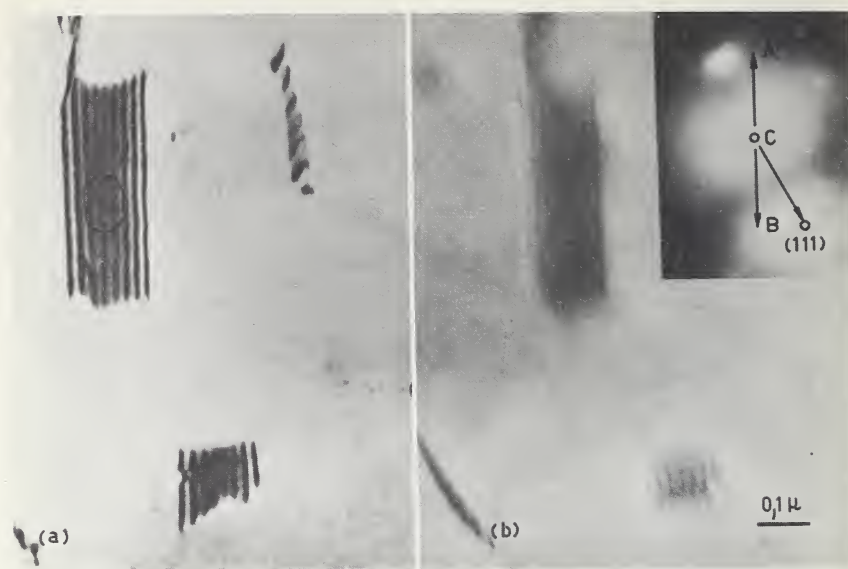


Figure 46. Fringe patterns due to stacking faults in a copper gallium alloy of low stacking fault energy. The fault is intrinsic. Courtesy Art.

### 3. Some Properties of Stacking Fault Fringes [88, 89, 90, 91]

Some important conclusions of the dynamical two beam theory of stacking fault fringes, taking into account anomalous absorption, are now mentioned (first for fringes with  $\alpha = \pm \frac{2\pi}{3}$ ).

(i) The fringe pattern is symmetrical with respect to the foil centre in the bright field image, but asymmetrical in the dark field image.

(ii) The front part of the pattern is similar in the bright field and the dark field image, whereas the back part is pseudo-complementary.

(iii) The nature of the outer fringes only depends on the sign of  $\alpha$  and not on the foil thickness  $z_0$ , provided the foil is sufficiently thick (i.e.,  $z_0 \geq 4t_g$ ). If  $\alpha = \pm \frac{2}{3}\pi$  the extreme fringes in the bright field image

are bright, whereas they are dark if  $\alpha = -\frac{2}{3}\pi$ .

(iv) The fringes are parallel to the nearest surface: new fringes are generated in the centre of the pattern.

These properties are illustrated by Figure 46. They result essentially from the effect of the anomalous absorption. We shall show below how they can be used to determine the type of stacking fault in f.c.c. metals.

Fringes for which the phase angle  $\alpha = \pi$  have very characteristic properties which allow to recognize them almost immediately [92]. Some of their specific properties are:

(i) For  $s=0$  the fringes are parallel to the central line of the foil, rather than to the surface like for  $\alpha = \pm \frac{2\pi}{3}$ . As a result new fringes are born at the surface rather than in the centre of the foil like for  $\pm \frac{2\pi}{3}$ . However for large values of  $s$  the fringes become again parallel to the surfaces.

(ii) For  $s=0$  the depth spacing of the fringes is  $\frac{1}{2}t_g$  and not  $t_g$  as for  $\pm \frac{2\pi}{3}$  fringes.

(iii) For  $s=0$  the bright and dark field images are complementary on both ends of the pattern, even with anomalous absorption present.

(iv) In bent foils the fringes are always continuous, i.e., a bright fringe in one part of the fault, continues as a bright fringe in the other part of the bend.

These properties are illustrated in the set of Figures 47, 48. They can be used to decide that for a given diffraction vector the phase angle  $\alpha = \pi \pm 2k\pi$  ( $k$ :integer). This information is helpful in determining the displacement vector (see next paragraph).

#### 4. Displacement Vector Determination

The determination of the displacement vector  $\mathbf{R} = [u, v, w]$  of a stacking fault or antiphase boundary is similar to the Burgers vector determination of a dislocation. There is an important difference however. Whereas a dislocation goes out of contrast (to a first approximation) if  $\mathbf{g} \cdot \mathbf{b} = 0$  the extinction criterion for a stacking fault is  $\mathbf{g} \cdot \mathbf{R} = 0$  or an integer. In practice one looks for a number of diffraction vectors  $\mathbf{g}_i (h_i k_i l_i)$  for which the fringes disappear. This leads to a set of equations  $h_i u + k_i v + l_i w = n$  where  $n$  is zero or an integer. It is further possible that one may be able to identify a number of reflections for which  $\alpha = \pi$  (using the criteria given in the previous paragraph). Such observations lead to additional equations of the type

$$h_j u + k_j v + l_j w = 1/2 \pm n. \quad (15)$$

One then tries to satisfy all these equations with the smallest possible values of  $n$ ,  $v$ , and  $w$ . This determines usually the displacement vector to within a lattice vector of course. Examples of displacement vectors determination can be found in ref. [93] and [94].

#### 5. Determination of the Type of Stacking Fault

**a. In f.c.c. Crystals.** The displacement vector of a stacking fault can also be taken as  $\frac{1}{3} \mathbf{a}$  [111]. In view of the relation (12) this does not change the value of  $\alpha$  since the vector  $\frac{1}{2} \mathbf{a}$  [110] only contributes an integer

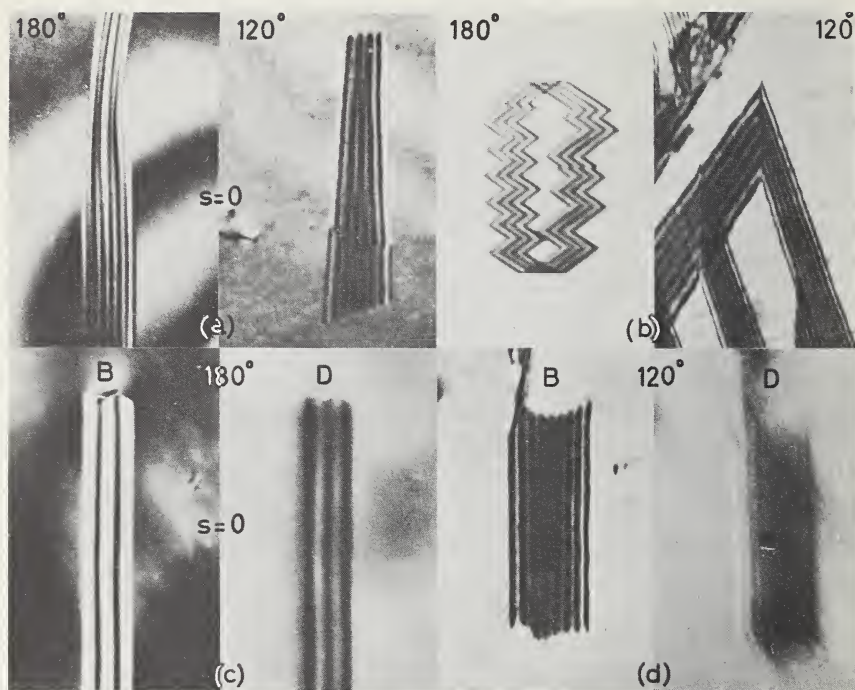


Figure 47. Comparison of fringe characteristics for  $180^\circ$  and  $120^\circ$  faults. Examples are taken from APB in rutile ( $180^\circ$ ) and stacking faults in Cu-Ga alloy. (a) Behaviour for varying foil thickness. Note that for  $\alpha = 180^\circ$  and  $s = 0$  the fringes are added at the outside of the pattern whilst in the case  $\alpha = 120^\circ$  forking of the inner fringes is observed. (b) Contrast at bends. Note that for  $180^\circ$  the fringes continue at the bend whereas for  $120^\circ$  a shift between the two fringe systems is present. (c) and (d) Characteristics of bright (BF) and dark (DF) field images (c)  $\alpha = 180^\circ$  and  $s = 0$ , the dark field image is complementary to the bright field image and thus also symmetrical. (d) for single faults with  $\alpha = 120^\circ$  the dark field image is always similar to the BF at the front surface whereas it is complementary at the bottom; this result is an asymmetrical DF image.

$x 2\pi$ . It is now easy to see that intrinsic and extrinsic faults correspond to displacement vectors of the type  $\frac{1}{3} \mathbf{a} [111]$  which are opposite in sign and hence give an opposite sign to  $\alpha$  for the same  $\mathbf{g}$ . It is therefore possible in principle to distinguish between intrinsic and extrinsic faults on the basis of the nature of the extreme fringes since from this the sign of  $\alpha$  can be deduced. A practical method for doing this has been worked out [90, 91]. The resulting rule is as follows.

Orient the image in such a way that the operating diffraction vector points to the right of the intersection line of the fault plane and the foil plane. This is always possible. One should make sure that the image and the diffraction pattern have the correct relative orientation. If the reflection belongs to class A, and if the diffraction vector points towards the bright fringe in the dark field image the fault is intrinsic. The

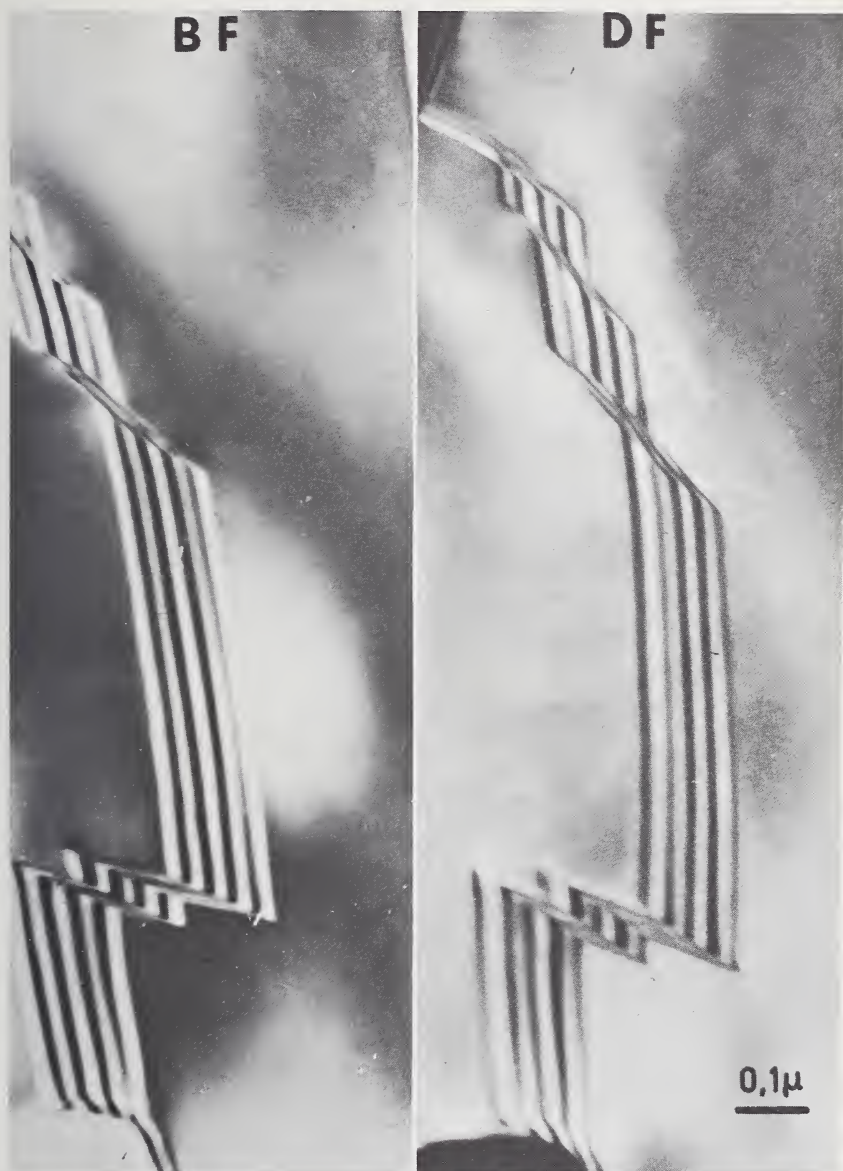


Figure 48. Bright and dark field images are complementary for  $\alpha = \pi$  and  $s = 0$ .

reverse is true for reflections belonging to class B. Reflections of class A are 200 and 222, those of class B are 400, 220, and 111. Application of this rule to Figure 46 leads to the conclusion that the fault is intrinsic. From this rule it is evident that the dark field image alone is sufficient to make the determination. If both bright and dark field images are available, one can determine top and bottom end of the foil as well. At the

top part the fringe patterns are similar, while they are pseudo-complementary at the exit face.

The rule can be deduced from Figure 49 which shows all the logically possible configurations and the corresponding bright and dark field images for class A and class B reflections. The displacement vector is

taken as  $D = \pm \frac{1}{3} \mathbf{a}$  [111] since, apart from its sign, this vector is unambiguously defined in contrast to the shear vector  $\frac{1}{6} \mathbf{a}$  [112]. This vector

describes the displacement of the cross hatched back part with respect to the front part; it is perpendicular to the fault plane. For a derivation of the rule we refer to [90].

**b. Hexagonal Close Packed Crystals.** The triple fault can easily be distinguished from single and double faults because different extinction criteria apply to it. However, single and double faults obey the same extinction criteria and they can therefore not be distinguished on such a basis. A method has been worked out based on the nature of the outer fringes. For the derivation of the method we refer to the original paper [95]; but we shall give the practical rule. If the nature of the

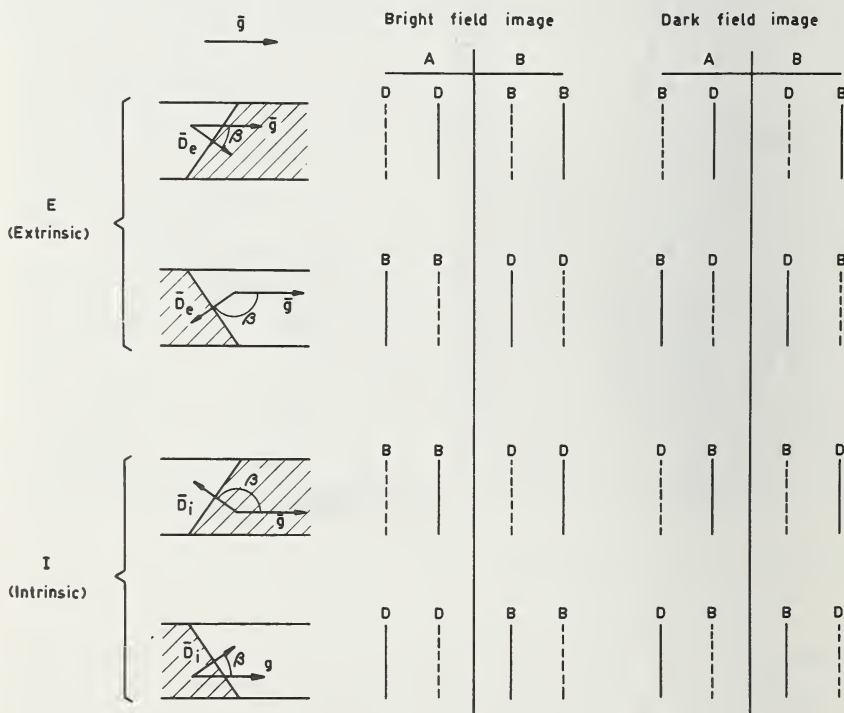


Figure 49. Schematic representation of the fringe pattern for intrinsic and extrinsic stacking faults in f.c.c. metals. A full line represents the first fringe (at the top) and a dotted line the last fringe. The nature of these fringes is indicated by B (bright) and D (dark).

outer fringes is different for dark field images with  $l$  even and with  $l$  odd but for the same  $h - k$  value, the fault is single. If the nature of the outer fringes does not depend on whether  $l$  is odd or even, the fault is double. An example of application to faults in wurtzite is shown in Figure 50. The nature of the outer fringes is different, for the dark field images taken with  $l=1$  and  $l=2$  and therefore one concludes that the faults are single.

### 6. The Measurement of Stacking Fault Energies [96, 38]

One of the typical applications where transmission electron microscopy has been particularly successful is the measurement of stacking fault energies,  $\gamma$ , i.e., the excess energy per unit area associated with a stacking fault. Electron microscopy provided in fact the first direct methods for such measurements. In principle one can make use of any equilibrium configuration of partial dislocations which is observable in the microscope and which lends itself to theoretical treatment. We shall discuss some of these configurations.

**a. Ribbons.** By far the simplest one is the dislocation ribbon or extended dislocation. According to isotropic elasticity theory in an infinite solid the two partials in the ribbon repel each other following an inverse distance law

$$F_r = \frac{\mu b}{2\pi d} \left( b_{1s}b_{2s} + \frac{b_{1e}b_{2e}}{1-\nu} \right) \quad (16)$$

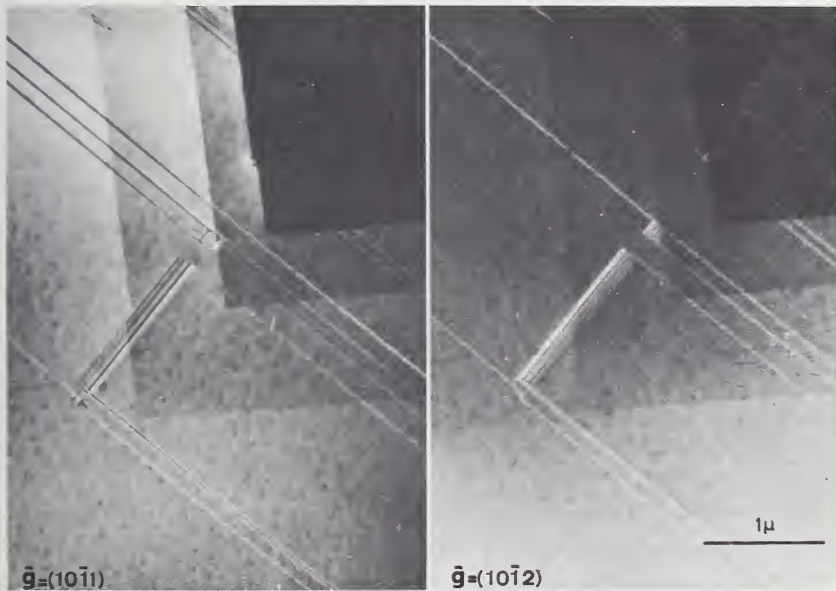


Figure 50. Dark field images of stacking faults in wurtzite (ZnS). The nature of the outer fringes is different for  $\mathbf{g}=(10\bar{1}1)$  and for  $\mathbf{g}=(10\bar{1}2)$ .

where  $d$  : distance between partials

$\mu$  : shear modulus

$\nu$  : Poisson's ratio

$b_{1s}$  and  $b_{2s}$  : the screw components of the Burgers vectors of the two partials

$b_{1e}$  and  $b_{2e}$  : are similarly the edge components.

On the other hand the two partials are kept together by the stacking fault between them, which exerts a constant attractive force equal numerically to  $\gamma$ , the stacking fault energy. An equilibrium separation therefore necessarily results (Fig. 51). The equilibrium distance, in the case of Shockley partials, is given by

$$d = d_0 \left( 1 - \frac{2\nu}{1-\nu} \cos 2\phi \right) \quad (17)$$

$$d_0 = \frac{\mu b^2}{8\pi\gamma} \frac{2-\nu}{1-\nu} \quad (18)$$

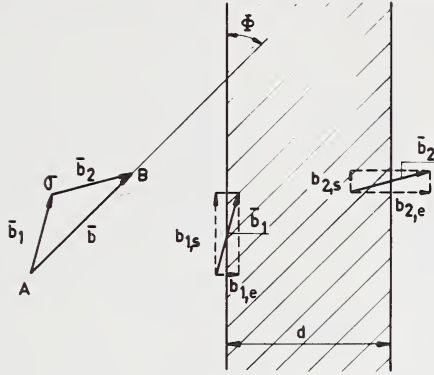
where  $\gamma$  is the angle between the total Burgers vector  $\mathbf{b} = \mathbf{b}_1 + \mathbf{b}_2$  and the direction of the ribbon. For a general ribbon this relation becomes somewhat more complicated; it is given in ref. [78].

If the ratio  $\gamma/\mu b$  becomes too large the spacing between partials becomes too small to be measured with any accuracy. The extended node discussed below should then be used.

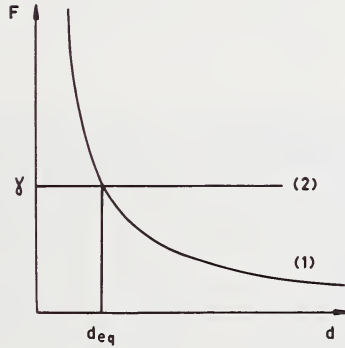
The ribbon formula can easily be extended to the case of multiple ribbons. The triple ribbon resulting from the interaction of two single ribbons is a particularly interesting configuration. It consists of three dislocations with the same Burgers vector. A model for such ribbons in hexagonal crystals is shown in Figure 52. The two halves of the symmetrical ribbon contain stacking faults with the same energy, since they are crystallographically equivalent. Because of their large width triple ribbons are more sensitive probes than single ribbons and therefore they allow more accurate measurements [38, 97]. However one has to be aware of possible surface effects which may lead to too high values for  $\gamma$  [98]. An example of a triple ribbon is shown in Figure 53.

Such triple ribbons have now also been observed in face centered cubic Ag-In alloys with low stacking fault energy. One half contains an intrinsic fault and the other half an extrinsic fault. The ratio of the width of the two halves allows to determine the ratio of the two stacking fault energies [97, 99].

In complex crystals such as talc [100] and the chromium halides [101] ribbons consisting of four and six partials occur (Fig. 54). From the spacings of the partials one can deduce the values of all different stacking faults provided the elastic constants are known.

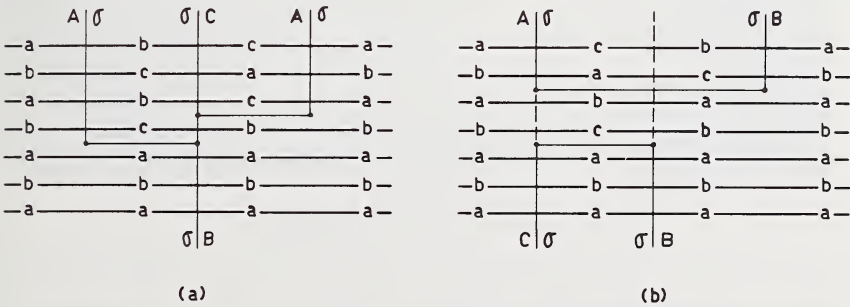


(a)



(b)

Figure 51. (a) Model for ribbons of partial dislocations of the Shockley type. The angle between the direction of the ribbon and the Burgers vector is called  $\phi$ . (b) The repulsive force between partials (curve 1) goes as  $1/d$  whereas the force due to the stacking fault is constant (curve 2). The intersection point gives the equilibrium separation  $d_{eq}$ .



(a)

(b)

Figure 52. Arrangement of layers in threefold ribbons in the hexagonal structure, in particular in graphite; the 3 partials have parallel Burgers vectors (a) symmetrical (b) asymmetrical.

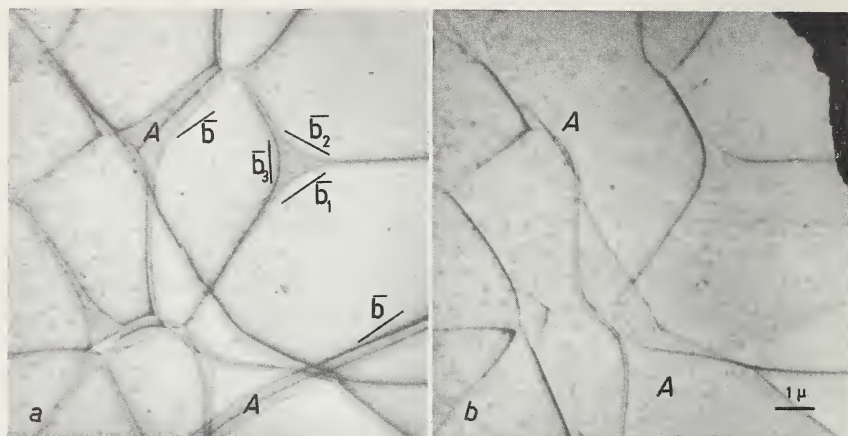


Figure 53. Dislocation pattern in graphite. (a) isolated extended node and threefold ribbon. All partials are in contrast. (b) the same region as (a) but with some of the lines out of contrast; particularly the threefold ribbon is out of contrast. The direction of the Burgers vector is indicated.

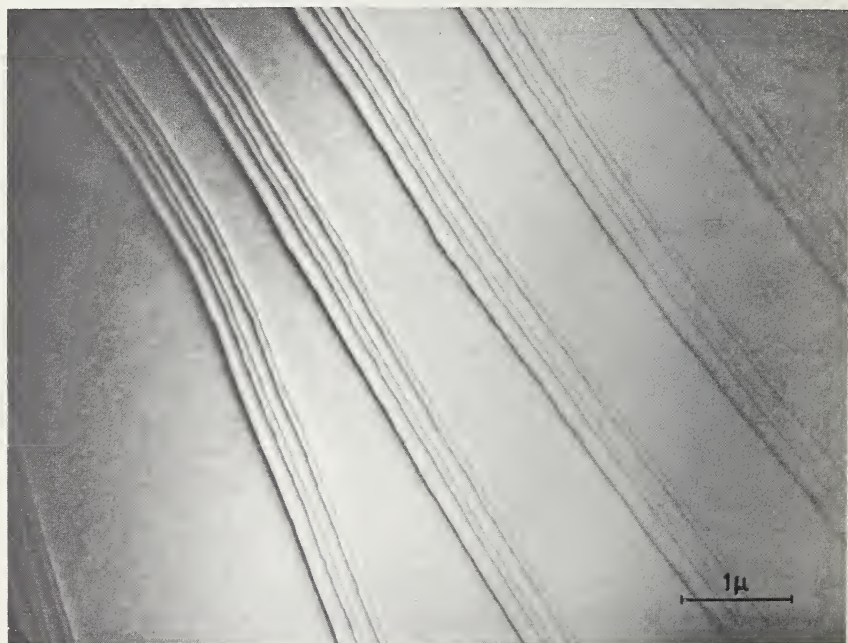


Figure 54. Sixfold ribbons in chromium chloride.

**b. Extended Nodes.** Isolated extended nodes are generated by the reaction between two ribbons which have a common partial. This dislocation reaction is shown in Figure 55. One can now measure either

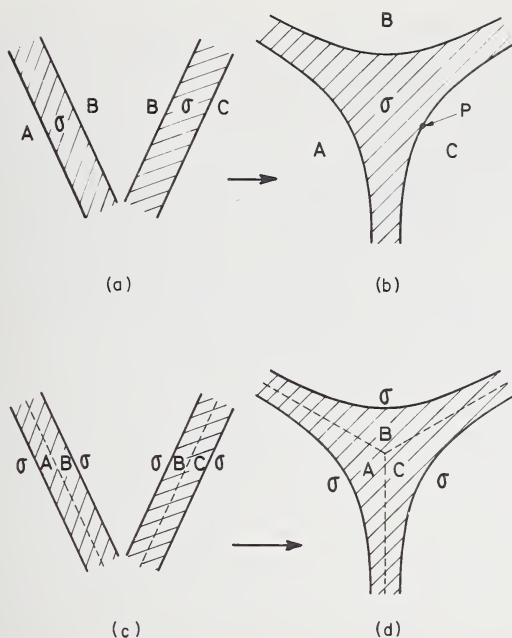


Figure 55. Fusion of two ribbons giving rise to an isolated extended node.

the radius of curvature ( $R$ ) or the radius of the enscribed circle ( $y_0$ ), the latter measurement is in practice the more accurate one.

The stacking fault energy is related to the radius of curvature of the partials by the relation

$$\gamma = \frac{\mu b^2}{2R}. \quad (19)$$

This relation expresses the equilibrium curvature of an isolated partial, under the influence on the one hand of the effective shear stress  $\gamma/b$  exerted by the stacking fault inside the node, and on the other hand of the "line tension" of the partial [102].

A more accurate solution of the node problem requires taking into account the interaction between the different partials in the node. An analytical solution to this problem was given by Siems et al. [103], and the result is summarized here.

The stacking fault energy is now given by

$$\gamma = K\psi_0/y_0 \sqrt{3} \quad (20)$$

where  $K = \frac{\mu b^2}{8\pi} \frac{2+\nu}{1-\nu}$  (21) for edge ribbons and  $K = \frac{\mu b^2}{8\pi} \frac{2-3\nu}{1-\nu}$  (22) for screw ribbons. The dimensionless quantity  $\psi_0$  is the solution of the following equation

$$\ln \psi_0 = \psi_0 - 1 - 0.267(\epsilon/K) \quad (23)$$

$\epsilon$  is the line energy; one has  $\epsilon/K = 8.95 \frac{2}{2+\nu}$  for edge ribbons and  $\epsilon/K = 8.95 \frac{2}{2-3\nu}$  for screw ribbons.

For dislocations in the basal plane of hexagonal crystals the anisotropy can easily be taken into account as well as in formula (17) as in formula (20) by using the appropriate expressions for  $\mu$  and  $\nu$  (see ref. [38, 103]). Also for dislocations in the (111) plane of cubic crystals it is possible to give approximate expressions for the effective values of  $\mu$  and  $\nu$  [104].

More recently Siems [105] has improved this analytical treatment by taking into account the orientation dependence of the line energy.

Numerical solutions of the node problem have been given independently by Brown and Thölen [106] and by Jøssang, Stowell, Hirth and Lothe [107]. The results of Brown and Thölen can be summarized in "empirical" formulae which are accurate to about 10%:

$$\frac{\gamma R}{\mu b^2} = 0.27 - 0.08 \left( \frac{\nu}{1-\nu} \right) \cos 2\alpha + \left\{ 0.104 \left( \frac{2-\nu}{1-\nu} \right) + 0.24 \frac{\nu}{1-\nu} \cos 2\alpha \right\} \log_{10} \frac{R}{\epsilon} \quad (24)$$

$$\frac{\gamma \gamma_0}{\mu b^2} = 0.055 \left( \frac{2-\nu}{1-\nu} \right) - 0.06 \left( \frac{\nu}{(1-\nu)^2} \right) \cos 2\alpha + \left\{ 0.018 \left( \frac{2-\nu}{1-\nu} \right) + 0.036 \frac{\nu}{1-\nu} \cos 2\alpha \right\} \log_{10} \frac{R}{\epsilon} \quad (25)$$

where the meaning of the symbols is as follows:

**b**: Burgers vector of the partial dislocation,

$\alpha$ : describes the character of the partial at the point of closest approach to the node center ( $\alpha = \frac{\pi}{2}$  for edge nodes,  $\alpha = 0$  for screw nodes),

$\epsilon$ : arbitrary parameter related to the core radius.

With these formulae the stacking fault energies can be derived either from the radius of curvature ( $R$ ) or from the radius of the escribed circle ( $\gamma_0$ ) provided the Burgers vector of the partials has been determined so that  $\alpha$  is known.

Extended nodes usually occur in networks of the type shown in Figure 56 and which are in fact twist boundaries. Such a network usually contains extended and contracted nodes. However in silicon [104] and in certain f.c.c. metal alloys [97, 99] it is found that all nodes are dissociated. Only one family of nodes say the  $\Delta$  nodes then contains an intrinsic fault, the other family say the  $\nabla$  nodes, containing an extrinsic



Figure 56. Network of extended and contracted nodes in a copper-gallium alloy.  
Courtesy Art.

fault. From the geometry of both types of nodes one can deduce the  $\gamma$ -values for the two types of faults.

The same methods can of course be used to measure antiphase boundary energies.

The methods described here allow to study problems such as the variation with composition of the stacking fault energy in binary alloys.

Also the variation with temperature can conveniently be studied [108]. Continued interest in the method is to be expected in the future.

**c. Other Methods Based on Electron Microscopy.** Theory shows that the maximum size of a stacking fault tetrahedron (see paragraph V.E.2b) is a function of the stacking fault energy. Measuring this maximum size thus allows to determine the stacking fault energy. Unfortunately it is difficult in practice to decide whether the tetrahedra in a quenched foil have reached their maximum size or not. The method was applied to gold and to cobalt-nickel alloys [108a], and acceptable values were obtained.

Another interesting method which is particularly suited for measuring high stacking fault energies, has recently been proposed. It is based on a measurement of the climb rate of faulted loops. The stress exerted by the stacking fault in the interior of the Frank sessile loops, constitutes the main driving force inducing the loop to shrink by climb at temperatures where self diffusion becomes appreciable. The climb rate is thus a function of  $\gamma$  [108b]. If one measures the climb rate of faulted and unfaulted loops under the same circumstances; knowledge of the activation energy for self diffusion is not required [108c]. The method has been applied to aluminum [108b] aluminum alloy [108c] and to magnesium and zinc [108d], [108c].

#### D. CONTRAST AT SLIP TRACES [76]

Dislocations moving in a thin foil, which is being examined in the microscope, leave traces at the upper and lower surfaces of the foil. This phenomenon is seen in most metals, although the stability of the contrast is larger in one metal than in the other. In aluminium the contrast disappears after a few minutes, in other metals it may be almost permanent. This contrast effect has been attributed to dislocations left behind at the interface between an oxide layer and the metal itself. In some cases this dislocation can actually be observed. In others this is not so. The image profile calculated for a dislocation dipole having the surface as a symmetry plane leads to results in agreement with experiment [76].

From a comparison of bright and dark field images top and bottom of the foil can be determined. The images are again similar at the top and complementary at the bottom end of the foil.

The effect can be used to study the geometry of slip. Cross slip is revealed in a very striking way, as illustrated in Figure 57 which refers to aluminium. If the slip planes in a given metal are known, e.g., (111) planes in f.c.c. metals, the effect can be used to determine the foil thickness. This is an important parameter if one wishes to estimate defect densities for instance.



Figure 57. Cross slip pattern observed in quenched aluminum foil. From the slip traces the foil thickness can be computed. Anomalously wide images due to loops close to the surface can be observed also. Courtesy of R. Cotterill.

### E. POINT DEFECTS AND DISLOCATIONS

In recent years the electron microscope has greatly contributed to our understanding of the formation of point defect clusters and their relation

to dislocations. Dislocation loops or other point defect clusters can be introduced by the following processes:

- (i) quenching,
- (ii) irradiation with energetic particles or with ionizing radiation,
- (iii) deviations from stoichiometry,
- (iv) cold work,
- (v) prismatic punching.

We shall only discuss briefly some of these processes.

### 1. *Processes Giving Rise to Point Defect Clusters*

We first discuss some of the processes that lead to the formation of point defect clusters. Afterwards we describe the nature of the resulting clusters and dislocation configurations.

**a. Quenching.** At each temperature a certain concentration of point defects is in thermal equilibrium. The concentration of vacancies in a metal is for instance given by an expression of the form

$$C_v = e^{\Delta S/k} e^{-U_F/kT} \quad (26)$$

where  $\Delta S$  is the entropy of formation and  $U_F$  is the energy of formation of a vacancy;  $\Delta S$  is usually a few times  $k$ , whilst  $U_F$  is of the order of 1 eV. As a consequence, at temperatures close to the melting point,  $C_v$  may become of the order of  $10^{-3}$ . If the solid is cooled rapidly enough this concentration of vacancies may be frozen in, at least partly. Vacancies may disappear at sinks such as grain boundaries and dislocations, the rest may be trapped as isolated vacancies, or associated with impurity atoms. A certain fraction form agglomerates of different size and shape, depending mainly on the stacking fault energy of the metal considered [109]. It is easy to see from simple arguments that from a certain size on it becomes energetically more favourable to form a dislocation loop rather than a disc shaped cavity. The energy of a cavity with diameter  $d$  is given by

$$E_c = \frac{1}{2} \pi d^2 \sigma \quad (27)$$

where  $\sigma$  is the surface energy. The energy of the loop is, on the other hand, given approximately by

$$E_1 = \mu b^2 d + \frac{1}{4} \pi d^2 \gamma \quad (28)$$

where  $\sigma$  is the shear modulus and  $\gamma$  the stacking fault energy. This last term disappears if the loop does not contain a stacking fault. One notices that  $E_c > E_1$  provided

$$d > 4\mu b^2/[\pi(2\sigma - \gamma)]. \quad (29)$$

The agglomerate is presumably more or less spherical in the initial stage. On transforming into a dislocation loop it has to pass through the disc-shaped configuration, which has a higher energy, due to the increased surface area. Some activation energy is required for this process. In substances with a large surface energy it is possible that small cavities remain. This is presumably the case in platinum [83] where small cavities are found after quenching. The geometry of the loops depends on the structure and on the stacking fault energy. We shall consider different structures below.

**b. Irradiation.** The irradiation of crystalline solids with energetic particles such as neutrons,  $\alpha$ -particles, fission fragments, etc. produces knocked on atoms, which give rise to displacement cascades with the simultaneous creation of vacancies and interstitials. At temperatures where these defects become mobile they may disappear by mutual annihilation, or by migrating to sinks or finally they may agglomerate and form clusters such as those found on quenching. However, where as on quenching the defects are presumably always derived from vacancies (at least in metals), we now expect clusters of two types and it becomes a meaningful problem to determine the nature of the individual clusters.

**c. Plastic Deformation.** As early as 1952, Seitz [110] suggested that plastic deformation would lead to the formation of point defects as a result of the intersection of dislocations. The original idea was inspired by the experiments of Guylai and Hartly [111] on the influence of plastic deformation on the ionic conductivity of alkali halides and by some experiments by Molenaar and Aarts [112] on the increase of the residual electrical resistance of metals after plastic deformation. Evidence from direct observation methods, decoration, etching and electron microscopy, has shown that indeed some defects are left behind by moving dislocations. Depending on the process responsible for their formation, these defects should either be vacancies or interstitials or both [113]. It is therefore again of interest to determine the character of the clusters.

**d. Deviations From Stoichiometry.** In some binary systems which crystallize as layer structures it has been found that deviations from stoichiometry can be accommodated under the form of large dislocation loops, lying in the layer plane. This is e.g. the case in  $Sb_2Te_3$  containing an excess of Sb [114] and in InSe containing an excess of In [115] (Fig. 58). In both systems this excess can be accommodated either as interstitial loops of metal or as vacancy loops of nonmetal. Again a determination of the loop character is necessary to settle this question. Such a determination for the InSe system leads to the conclusion that they are vacancy loops [115].

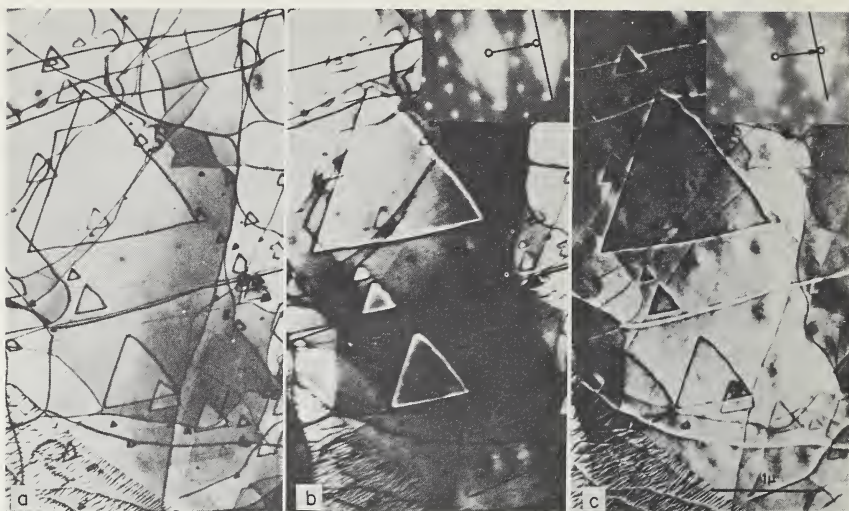


Figure 58. Loops in InSe due to non-stoichiometry. Three different contrasts allowing a determination of the loop character. Courtesy Marinkovic.

## 2. Nature of the Defect Clusters

**a. Dislocation Loops**—*i. Face Centered Cubic Metals.* Vacancies as well as interstitials can precipitate in a single sheet presumably on the (111) planes since these are the closest packed planes. If a cavity so formed collapses, a sessile dislocation loop with a Burgers vector  $\frac{1}{3}\mathbf{a}$  [111] and surrounding an intrinsic stacking fault results. It can be eliminated if the loop is swept by a partial with a Burgers vector of the type  $\frac{1}{6}\mathbf{a}$  [111]. The resulting loop is then a perfect dislocation with Burgers vector

$$\frac{1}{3}\mathbf{a} [111] + \frac{1}{6}\mathbf{a} [11\bar{2}] \rightarrow \frac{1}{2} [110] \quad (25)$$

inclined with respect to the original loop plane. Such a loop can glide on a cylinder parallel to the Burgers vector. For an interstitial loop the fault is of the extrinsic type, two partials have to sweep the loop in order to remove the stacking fault, one in a glide plane just above the loop plane the other in the (111) plane below the loop plane.

The condition for removing the stacking fault is roughly that the energy of the perfect loop should be smaller than that of the faulted one. The partial dislocation sweeping the loop has apparently to be nucleated at the edge of the loop. The shear stress available for doing this originates from the energy of the stacking fault; the equivalent shear stress is  $\gamma/b$ . With a value of  $\gamma \approx 100$  erg/cm<sup>2</sup> and  $b = 2 \times 10^{-8}$  this becomes 50 kg/mm<sup>2</sup>.

For vacancy loops in nominally pure aluminium removal of the stacking fault by the process described above seems to take place [116]. The loops do not contain a stacking fault, moreover they are found to be glissile. However, in hyperpure aluminium, most of the loops retain the stacking fault, presumably because of the difficulty of nucleation of the partial [117]. This last hypothesis is supported by the observation that some loops lose their fault whilst under observation in the microscope (Fig. 59). In some aluminium-silver alloys the stacking fault energy seems to be too small to remove the fault; in this case faulted loops remain [118].

*ii. Hexagonal Metals.* In quenched magnesium, large vacancy loops are formed in the basal plane [120]. The loops contain a stacking fault. Their Burgers vector is presumably of the type TA in the notation of Berghezan et al. [119]. The activation energy of annealing found by measuring the rate of shrinking of loops corresponds to the activation energy for self diffusion [120].

*iii. Body-Centered Metals.* Quenched in vacancy loops have been observed in molybdenum quenched from 2600 °C and annealed for 1 hour at 400 °C [120 b].

*iv. Graphite* [121, 122]. After a quench from 3000 °C followed by an aging treatment at 1300 °C loops are formed in graphite. The

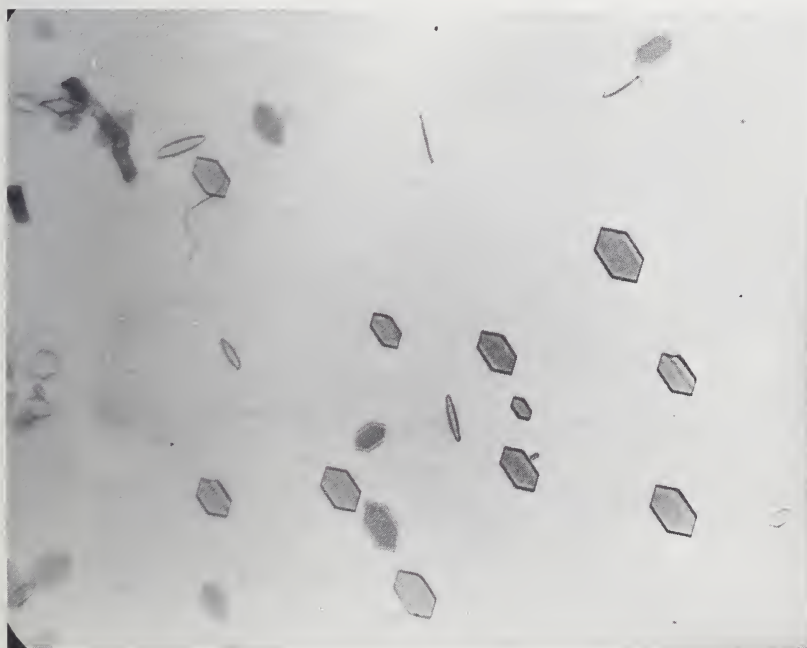


Figure 59. Faulted loops in quenched aluminum. Some have lost their fault.  
Courtesy Cotterill.

Burgers vectors of these loops appears to be inclined and the loops contain a stacking fault. Using the argument developed in subsection V.F.5 it was concluded that these loops were vacancy loops.

**b. Stacking Fault Tetrahedra.** It has been shown by Silcox and Hirsch [123] that in gold, quenched from 950 °C and aged for one hour at 100–250 °C, the vacancies cluster into spatial defects. An analysis of the contrast effects shows that the defect is a tetrahedron limited by stacking faults on (111) planes. The edges are stair rod dislocations with a Burgers vector of the type  $\frac{1}{6} \mathbf{a}$  [110]. An example is reproduced in Figure 60 whilst Figure 61 is a schematic view. Similar tetrahedra have been observed in silver [124] and in quenched nickel-cobalt alloys [125].

Silcox and Hirsch [123] have given the following mechanism by which the tetrahedra can be generated. Let us assume that originally the vacancies form a triangular sessile loop with a  $\frac{1}{3} \mathbf{a}$  [111] =  $A\alpha$  vector<sup>3</sup> and on a (111) plane. The edges of the triangle are parallel to the  $[1\bar{1}0]$ ,

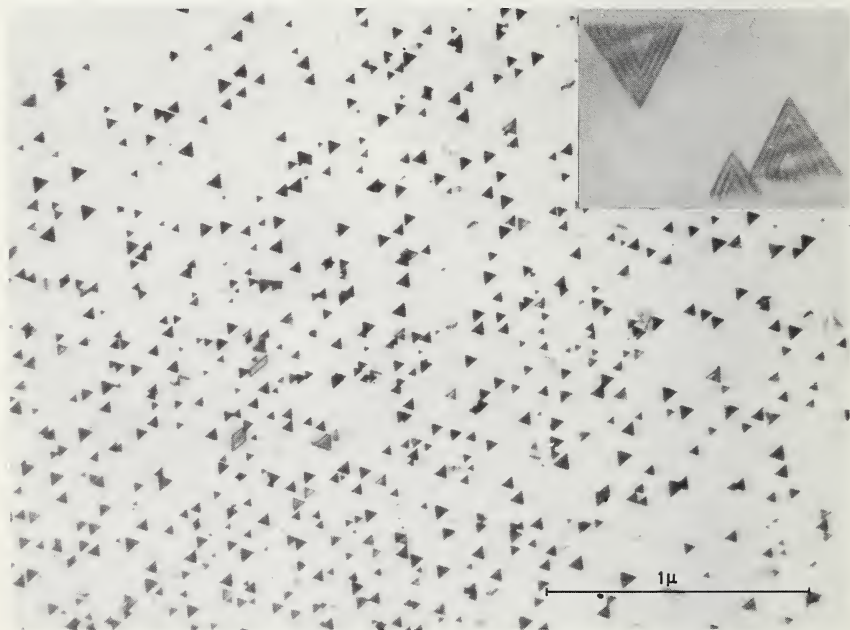


Figure 60. Quench tetrahedra in gold. The fault fringes can easily be recognized for the tetrahedron in the inset. Courtesy Cotterill.

<sup>3</sup> Use is made of Thompson's notation for Burgers vectors in the f.c.c. lattice.

$[10\bar{1}]$ , and  $[01\bar{1}]$  directions. The partials limiting the loop can now split on the different  $[111]$  planes according to the schemes:

$$\alpha A \rightarrow \alpha\beta + \beta A \text{ (in the } b\text{-plane)}$$

$$\alpha A \rightarrow \alpha\gamma + \gamma A \text{ (in the } c\text{-plane)}$$

$$\alpha A \rightarrow \alpha\delta + \delta A \text{ (in the } d\text{-plane)}. \quad (29)$$

The dissociation is accompanied by a gain in energy, according to the "Burgers vector squared" criterion. The Shockley partials with vector  $\beta A$ ,  $\gamma A$ , and  $\delta A$  bow out in their respective  $(111)$  planes being repelled by the stair rods with vectors  $\alpha\beta$ ,  $\alpha\gamma$ , and  $\alpha\delta$ . In this way they generate stacking faults on these planes. Along the intersection lines of the  $(111)$

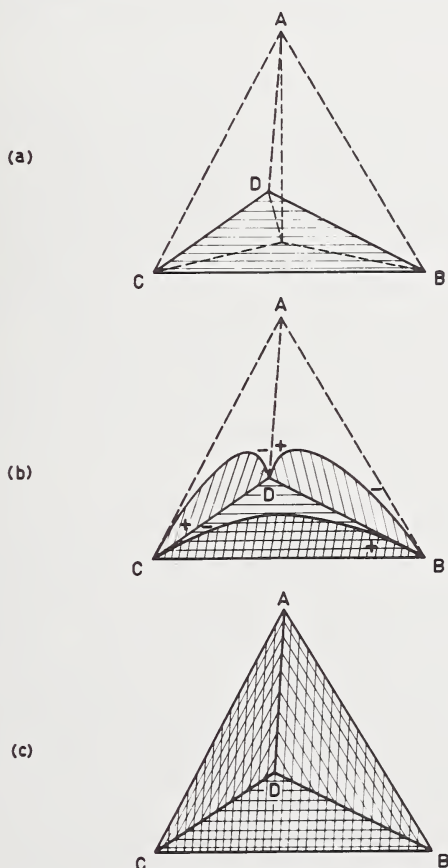


Figure 61. The formation of a tetrahedron. Courtesy Silcox and Hirsch. a) Triangular sessile loop in the  $(111)$  plane resulting from the collapse of a disc of vacancies. b) The partials bordering the loop dissociate and the Shockley partials bow out in the other  $(111)$  planes. c) Final shape of the tetrahedron. The edges are stair rod dislocations. The side faces contain stacking faults.

planes the Shockley partials meet and react to form new stair rod dislocations according to the reactions



The tetrahedron is now complete. This formation mechanism is represented in Figure 61. It can easily be shown that the total energy associated with the tetrahedron is smaller than that associated with the initial sessile loop  $E_S$  for tetrahedra which are smaller than some critical dimension. For gold the critical dimension is  $\approx 430 \text{ \AA}$ .

The mechanism discussed here demonstrates clearly the geometry of the defect, however there is no real evidence that the tetrahedra are generated in this way. It is also difficult to see how the tetrahedra grow. A possible nucleation and growth mechanism which does not imply the formation of an intermediate loop has been proposed by De Jong and Koehler [126], and modified by Kimura et al. [127].

**c. Cavities.** There is accumulating evidence that on quenching under certain conditions cavities are formed rather than dislocation loops [128, 129]. In many cases the polyhedral shape of the cavities can be recognized. It is not always clear whether these cavities are really empty or contain gas which stabilizes them. If they are empty they can be used for the study of clean surfaces, in particular ratios of the surface energies of different crystal faces can be deduced from the equilibrium shape of the cavities [130]. The contrast at cavities is discussed in ref. [131].

**d. Helices.** On quenching dislocations act as sinks creating denuded zones in their vicinity. Screw dislocations are hereby driven into helices [132, 133]. Such helices were first observed by means of decoration techniques [134], but electron microscopy has demonstrated their occurrence in many quenched alloys [135]. The reason why they are apparently more easily formed in alloys than in elemental metals, is not completely clear. However a plausible explanation is that in alloys the interaction of the vacancies with solute atoms prevents clustering and makes it more favourable for vacancies to disappear at existing dislocations.

## F. METHODS TO DETERMINE THE CHARACTER OF THE LOOPS

For many problems in relation with point defects it is of particular interest to be able to distinguish between vacancy and interstitial loops. Methods have been developed which are based on diffraction effects only; we shall summarize these.

Vacancy and interstitial loops may differ by:

- (i) the sign of their Burgers vector,
- (ii) the type of stacking fault they contain,
- (iii) the direction of their Burgers vector.

The diffraction methods make use of one of these features. The first feature is the more general one and a number of methods have been developed to determine the sense of the Burgers vector, in particular for loops. The theory of contrast formation predicts that for  $s$  different from zero the image side for a dislocation is essentially determined by the sign of the quantity  $(\mathbf{g} \cdot \mathbf{b})s$  (ref. [76]). If  $(\mathbf{g} \cdot \mathbf{b})s > 0$  the image is left. Provided the *FS/RH* convention for defining  $\mathbf{b}$  is adopted. Apparently it is therefore required to know all three quantities involved. In practice one can often avoid a Burgers vector determination in the strict sense. We now discuss these methods.

### 1. *The Geometrical Method*

Probably the simplest to expose is the procedure outlined by Groves and Kelly [136], by Siems et al. [79], and Ruedl et al. [137]. In subsection V.A.5 it was shown how the sign of  $s$  can be determined from the relative position of the diffraction spot and the corresponding bright Kikuchi line with respect to the centre of the diffraction pattern. In many cases, especially in thick foils, use is made of the phenomenon of easy transmission. In such cases loop contrast will be best for  $s$  positive. In platinum it was even found [138] that good pictures are practically only obtained for positive values of  $s$ . In order to determine the image side, it is therefore best to change the sign of  $\mathbf{g}$ . The image side can also be deduced from the asymmetry of the dislocation image; the profile is steepest at the side of the dislocation [139]. From the sign of  $s$  and from the image side one can deduce the sign of  $\mathbf{g} \cdot \mathbf{b}$ . The diffraction vector can readily be determined in two beam cases: it is sufficient to join the centre of the diffraction pattern and the only active spot. If the direction of  $\mathbf{b}$  is known its sign follows directly from the sign of the dot product. However, here arises the main difficulty associated with the method; it is often difficult to determine the direction of the Burgers vector because two extinctions are required for this. Even if the sign of  $\mathbf{b}$  is known one has still to go through a consistent system of arbitrary conventions to relate the sign of  $\mathbf{b}$  with the loop character or with the dislocation geometry. Mazey, Barnes, and Howie [140] have described completely the formalism used in this method. We refer to their work for a detailed account. Instead we will describe the more intuitive geometrical method, which makes use of the loop plane rather than of the Burgers vector and which is equivalent to the formal method. This geometrical method is an extension of the one outlined for single straight dislocations [137].

Let  $s$  be different from zero and let us assume that the sense into which the contrast producing lattice planes have to be rotated in order to approach the Bragg position is as indicated in Figure 31. Let us further assume that we have purely prismatic loops situated in inclined planes. The four possibilities are shown in Figure 62. It is now easy to deduce for each case whether the image will be inside or outside of the loop. It is found e.g., that for a vacancy loop, in a plane sloping upwards to the right and with a diffraction vector to the right, the image is outside because the lattice rotations are in the right sense (S) outside. Similar conclusions can be drawn for the other cases, the result is shown in Figure 62. It is evident how on inverting the reasoning the loop character can be deduced. The conclusion is clearly based on the assumption that the loops are purely prismatic, i.e., that the direction of the Burgers vector is known and perpendicular to the loop plane. Only in this case we can deduce the sign of  $\mathbf{b}$  once the sign of  $\mathbf{g} \cdot \mathbf{b}$  and that of  $\mathbf{g}$  is known. However, if the loop is not purely prismatic the conclusion is still valid if the angle  $\phi$  between the normal to the loop plane and the direction of  $\mathbf{b}$  is small enough so as to make sure that  $\mathbf{g} \cdot \mathbf{b}$  has the same sign as for

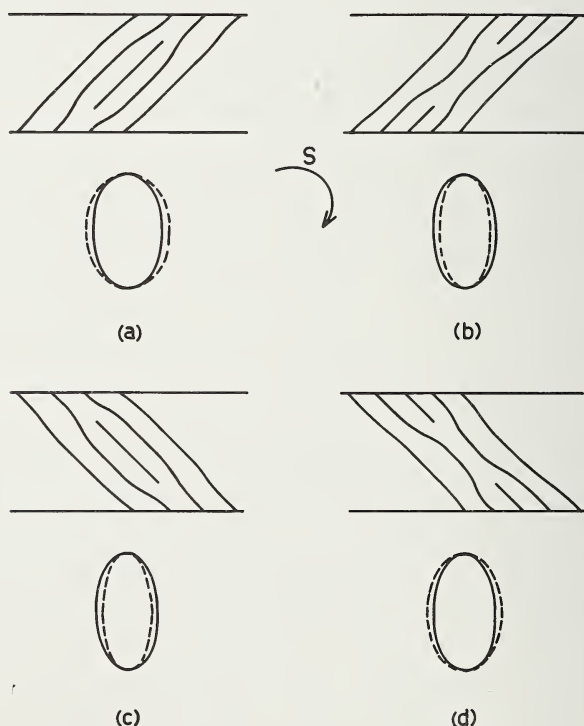


Figure 62. Determination of the loop character by the diffraction method. The four possible configurations are shown. The true position of the loop is indicated by a dotted line; the image is represented as a full line.  $S$  is the sense into which the lattice has to be rotated in order to bring it into the exact Bragg position.

a purely prismatic loop whatever the position of  $\mathbf{b}$  on the cone with angle  $\phi$  around the loop normal. For instance for  $\{012\}$  loops in f.c.c. metals  $\phi = 18^\circ$ ; for faulted loops in the basal plane of zinc  $\phi = 31^\circ$ , for loops in graphite  $\phi = 22^\circ$ . If in the case of zinc e.g., the loop plane makes an angle of  $45^\circ$  with the electron beam and if the diffraction vector forms an angle of at least  $45^\circ$  with the line of intersection of the loop plane and the plane normal to the beam, the procedure still works without ambiguity.

One question remains to be answered. How do we know in which plane the loop is lying? For loops in zinc [119] or in graphite [141] this is the basal plane, but in face centered cubic metals, as a consequence of the higher symmetry more possibilities arise. In order to discriminate between these, the foil is mounted once normal to the beam and once in an inclined position (e.g.,  $45^\circ$  to the beam). The change in shape of the loops will allow to determine the sense of sloping of the loop plane, as well as the indices of the loop plane.

In order to put the foil in an inclined position the grid is mounted between two wedge shaped rings [136]. If the loops are in the foil plane as it is the case for layer structures or for hexagonal metals it is still required to mount the foil in an inclined position in order to apply the procedure. The situation is shown in Figure 63. If mounted under  $45^\circ$  the sign of  $\mathbf{g} \cdot \mathbf{b}$  is the same for the six possible orientations of  $\mathbf{b}$ , and for a suitable  $\mathbf{g}$ -vector as pointed out above. In f.c.c. metals the assumption that the loops are purely prismatic, i.e., that  $\phi = 0$  instead of  $\phi = 18^\circ$  will lead to the correct result provided the loop plane is again sufficiently inclined.

It may be worth while to remind the reader that the reasoning presented above has to be made looking along the line of intersection of the loop plane and the plane normal to the electron beam, with the  $\mathbf{g}$  vector to the right of this line. It is of course always possible to orient the photograph this way. The intersection line which is equivalent to the rotation axis, can be deduced by measuring distances between equivalent points on pictures in the normal and in the inclined positions [137]. The

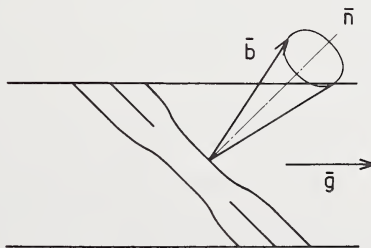


Figure 63. Loop in a foil mounted in an inclined position. The Burgers vector  $\mathbf{b}$  lies on a cone which has the loop normal as its axis. For all possible positions of  $\mathbf{b}$  on this cone the sign of  $\mathbf{g} \cdot \mathbf{b}$  is the same.

largest shortening evidently occurs in the direction perpendicular to the rotation axis.

Although the reasoning is made for loops lying in a plane parallel to the rotation axis, not too large a deviation from this does not influence the result. Loops lying approximately in the foil plane are apparently the best choice for all operations. Moreover such loops usually have their Burgers vector nearly normal to the foil, which makes it easy to determine its direction. Although this information is not absolutely required it is of great help to remove ambiguity.

## 2. *The Tilting Method* [142]

If a tilting device that allows rotation over a large angle is available, the following method can be used. Suppose that we have a prismatic loop in a plane almost parallel to the beam, the image is then very narrow. Let us further assume that the contrast producing reflection is to the right of the rotation axis and that we rotate the crystal through the Bragg position. As one turns the foil the loop becomes wider for purely geometrical reasons. As one approaches the reflecting position it is evidently positive and the image is inside for an interstitial loop and outside for a vacancy loop (Fig. 64). On passing through the reflecting position the image side changes i.e. the image becomes outside for the interstitial loop and inside for the vacancy loop. We can conclude that the image of the interstitial loop grows continuously in size as we rotate the crystal in the positive sense, whilst the image of the vacancy loop first grows and temporarily shrinks on going through the reflecting position before growing further for geometrical reasons. Before the next reflection arrives the image side changes because we start for this next reflection again with  $s > 0$ . However, in general the image of the interstitial loop will not shrink as a consequence of this because of the geometrical effect. The image of the vacancy loop in any case increases in size. The same type of reasoning can be made for a rotation in the other sense and for a reflection at the left; the conclusion is the same. Fig. 64 is made for a purely prismatic loop and for a rotation axis perpendicular to the diffraction vector and parallel to the loop plane. In practice these conditions are not so strict. However, in order to have a noticeable geometrical effect one should start with a loop in a rather steeply inclined plane.

## 3. *Loops Seen Edge On*

In this special case one can make use of a method due to Ashby and Brown [143]. These authors made calculations for the contrast effects associated with coherent precipitates that are under positive or negative hydrostatic pressure. An interstitial loop can be considered as a special case of a precipitate platelet that gives rise to outward lattice displacements whereas a vacancy loop does the reverse. From machine calcula-

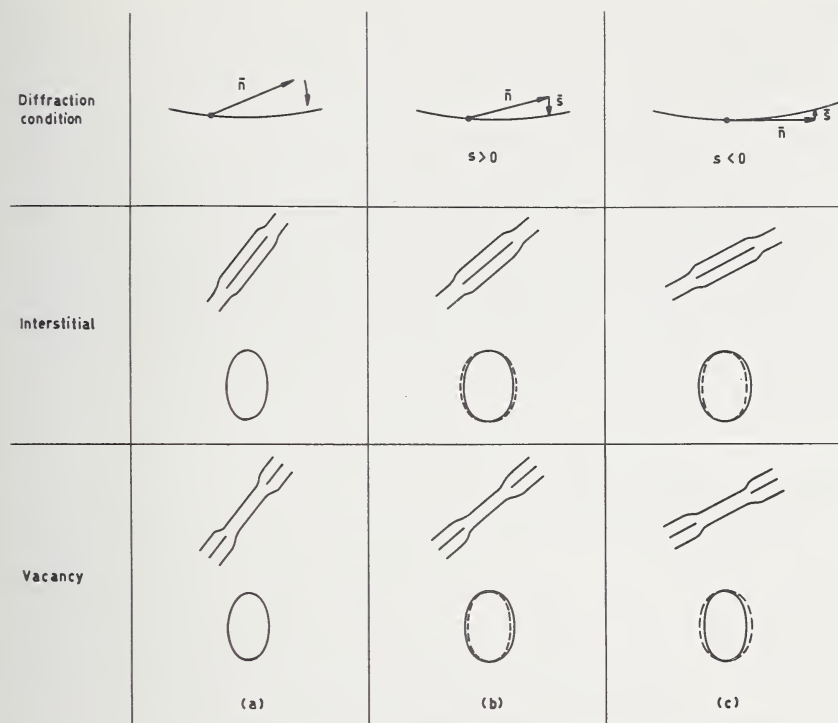


Figure 64. Determination of the loop character by the tilting method. The width of an interstitial loop is seen to increase continuously whereas the width of a vacancy loop increases first and then decreases as one passes through the reflecting position. The full line represents the image; the dotted line is the true position of the loop.

tions based on the dynamical theory the authors conclude that the images of loops seen edge on and which are close to the surface are "anomalously wide" and asymmetrical. Examples are visible in Figure 57. One side consists of a bright crescent, the other side of a dark one. The line of no contrast is perpendicular to the diffraction vector. In the bright field image this asymmetry is in the opposite sense near top and bottom surface. However, in the dark field image the asymmetry is in the same sense near top and bottom of the foil as a consequence of anomalous absorption. The asymmetry is such that in the dark field image the white crescent is in the positive sense of the diffraction vector for a vacancy loop and in the opposite sense for an interstitial loop. Recently it has been pointed out that considerable caution is required when applying this method to loops [144, 145, 146].

#### 4. Stacking Fault Method

In f.c.c. metals the interstitial loops may contain an extrinsic stacking fault provided the stacking fault energy is small enough. Under the same circumstances a vacancy loop would contain an intrinsic stacking

fault. As we have pointed out it is possible to deduce the nature of stacking faults in the face centered cubic metals from the nature of the first fringe at the surface in the dark field image. In principle it is therefore possible to distinguish loops on this basis. However, the use of the method is restricted by the fact that the loops have to be large enough to contain at least a few fringes and secondly they have to intersect the surface. Nevertheless Hirsch et al. [148], have shown in this way that proton irradiated copper contains interstitial loops.

As mentioned above it is also possible for some intermediate value of the stacking fault energy that interstitial loops contain a stacking fault, whereas it could be removed from vacancy loops. In such a material the distinction would be immediate. It was suggested that this is the case in platinum [137]. It is possible that these circumstances are also realized for copper, where fault free loops have been observed in neutron irradiated specimens [147], whereas faulted loops were found in proton-irradiated material [148].

The nature of loops in hexagonal crystals can also be determined by similar methods. In low stacking fault energy hexagonal metals or alloys vacancy loops would contain single faults whereas interstitial loops would contain triple faults. The two types of loops can be distinguished on the basis of a Burgers vector determination, or by noting that the vacancy loops show fault contrast for certain reflections belonging to the zone [0001] whereas the interstitial loops do not.

If the stacking fault energy is high both loops contain single faults because the triple fault is removed by the passage of a partial; the remaining single fault cannot be removed however [119]. The loops have then to be distinguished by determining the sign of the Burgers vector of the bordering partials.

### 5. *The Burgers Vector Method [121, 122]*

In low stacking fault energy hexagonal metals, as well as in graphite, still another method is available to distinguish vacancy and interstitial loops. The stacking in such crystals can be represented by the letter sequence

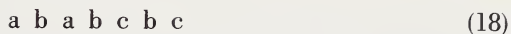
$$a \ b \ a \ b \ a \ b. \quad (16)$$

If one layer is removed like in a vacancy loop a fault

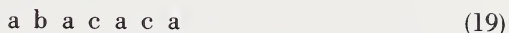
$$a \ b \ a \ a \ b \ a \ b \quad (17)$$

↑

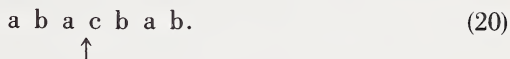
would be generated. This has a very large energy and will be removed by shear along the basal plane. The stacking sequence becomes



or



in either case a fault, with smaller energy remains. The fault cannot be removed completely by glide. The Burgers vector of the loop has now become inclined with respect to the basal plane (Fig. 65). If on the other hand a layer is inserted as for an interstitial loop this layer can go in c-position, i.e., the stacking sequence could become



If the stacking fault energy is small enough there is no shear movement and the Burgers vector of the loop remains perpendicular (Fig. 65).

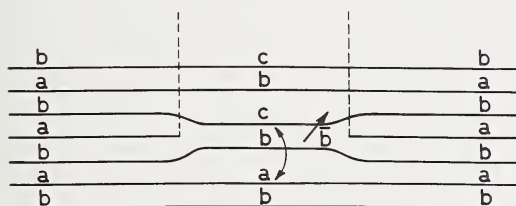


Figure 65. Prismatic loop in graphite: Vacancy loop: the Burgers vector is inclined with respect to the c-plane.

It is clear that the distinction can now be made on the basis of a determination of the direction of the Burgers vector. This method was applied to quenched graphite. The stacking fault energy in graphite is very small:  $0.7 \text{ erg/cm}^2$  [149]. Graphite was in fact the first material for which the distinction could be made [121]. The situation is especially favourable since the loops are in the foil plane. Interstitial loops would only show residual line contrast in the normal orientation of the foil, whatever the operating reflection. On the other hand vacancy loops would show stacking fault contrast for certain reflection (when the fault is at the right depth in the foil) and line contrast for other reflections. The vacancy loops would go out of contrast for reflection against a set of planes parallel to the Burgers vector. By making dark field images with these reflections [1120] it was found that certain loops only exhibited residual contrast whereas others were in full line contrast, in accord with the fact that the inclined Burgers vector can lie in three different planes of this type. From this observation and also from the fact that fault contrast is observed one can conclude that the loops are vacancy

loops as one would expect in quenched graphite. It is perhaps worth mentioning that due to the large anisotropy of graphite the residual contrast is very weak and the loop goes out of contrast completely.

## G. DOMAIN BOUNDARIES

Ferromagnetic, anti-ferromagnetic, ferroelectric and anti-ferroelectric crystals are usually broken up into domains. The interfaces between such domains shall be called "domain boundaries".

### 1. *Ferroelectric Domains*

We shall discuss as a specific example the domain structure of barium titanate. Above the ferroelectric transition temperature barium titanate is cubic and it has the perovskite structure which consists essentially in a close packed arrangement of oxygen ions, a fraction of the oxygen ions being replaced by barium ions. The titanium ions occupy the centers of the oxygen octahedra (Fig. 66-1(a)). Below the ferroelectric transition temperature (120 °C) the crystal becomes tetragonal, as a result of the fact that the titanium ions no longer occupy the centers of the oxygen octahedra. They are displaced along one of the cube directions which now becomes the  $c$  axis of the tetragonal form (Fig. 66-1(b)). This displacement also causes the ferroelectric polarization. Since there are three equivalent cube directions, and since furthermore the  $c$  axis becomes a polar axis there are three possible orientations, each having two senses for the  $c$  axis as referred to the cubic structure. On cooling through the transition temperature polarization starts simultaneously in different parts of the crystal. In each part the  $c$  axis adopts hereby one out of the six possibilities, thereby creating a domain structure. Also it can be shown that it is energetically more favourable for the crystal to break up into domains rather than to form a single domain.

As a consequence one can consider two kinds of domain boundaries:

- (i) 90° boundaries: the  $c$  axis of the domains on both sides of the boundary are mutually perpendicular.
- (ii) 180° boundary: the  $c$  axis of the domains on both sides of the boundary are anti-parallel.

For the first kind of interface, the 90° boundary, the lattice is twinned, the twinning vector being very small. Figure 66-2(b) shows in a highly exaggerated way the lattices on both sides of the boundary.

We shall now discuss how fringe contrast arises at such boundaries and what information can be obtained from the fringe patterns. From Figure 66-2 it is clear that since the lattices are slightly different on both sides of the boundary, also the simultaneously operating diffraction vectors  $\mathbf{g}_1$  and  $\mathbf{g}_2$  are slightly different. It can be shown that for a coherent twin boundary the vector  $\Delta\mathbf{g} = \mathbf{g}_2 - \mathbf{g}_1$ , is perpendicular to the boundary plane [150]. The main consequence of this is a difference in excitation error  $\Delta s = s_1 - s_2$  for the crystal parts on both sides of the

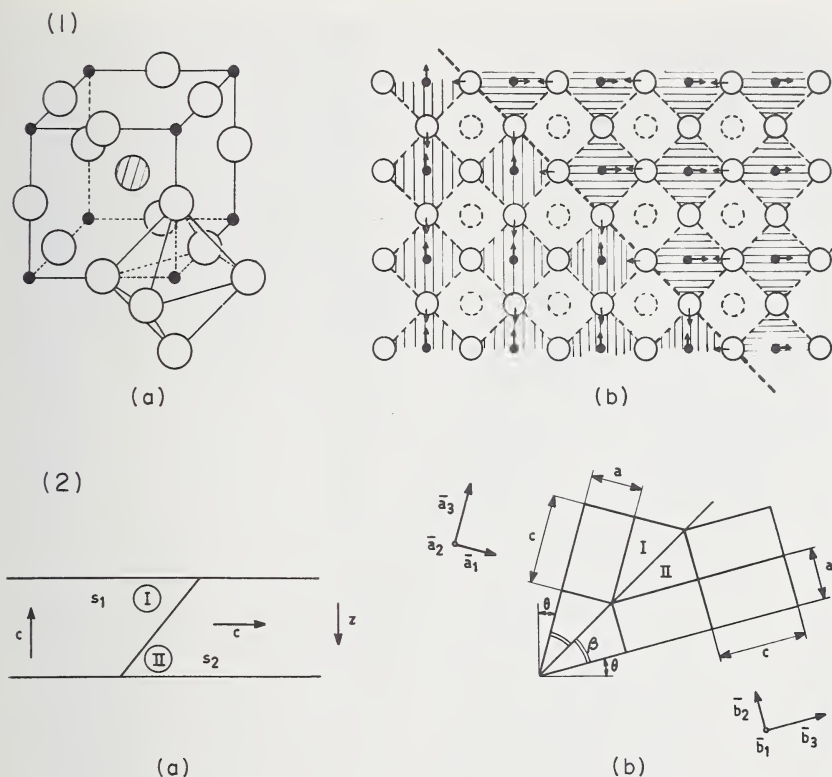


Figure 66. (1) a) structure of barium titanate, b) Displacements of the titanium ions giving rise to domain formation. (2) a) Schematic cross section of a foil containing a domain wall in barium titanate. In part I the diffraction conditions are determined by  $s_1$ , part II by  $s_2$ . In part I the  $c$ -axis is perpendicular to the foil, whereas it is parallel to the foil in part II; b) Cross section of the lattice of barium titanate perpendicular to the twin plane and containing the tetragonal axis. The tetragonal deformation is highly exaggerated.

domain boundary,  $\Delta s$  being in length equal to the component of  $\Delta \mathbf{g}$ , perpendicular to the foil plane ( $s_1$  and  $s_2$  are the excitation errors in part I and II of the crystal; part I is first met by the electrons). It can be shown that a fringe pattern results if the boundary plane is inclined with respect to the foil plane. These fringe patterns have been called  $\delta$ -fringes [151], they have properties which are quite different from those due to stacking faults and it is therefore easy to distinguish between stacking faults and domain boundaries. The main properties of  $\delta$ -fringes are summarized here (Fig. 67):

(i) In the bright field image the outer fringes have opposite nature; in the dark field image they have the same nature.

(ii) The fringe spacing may be slightly different at the top and bottom end of the fringe pattern, it is only equal in the "symmetrical" case, i.e., if  $|s_1| = |s_2|$ .

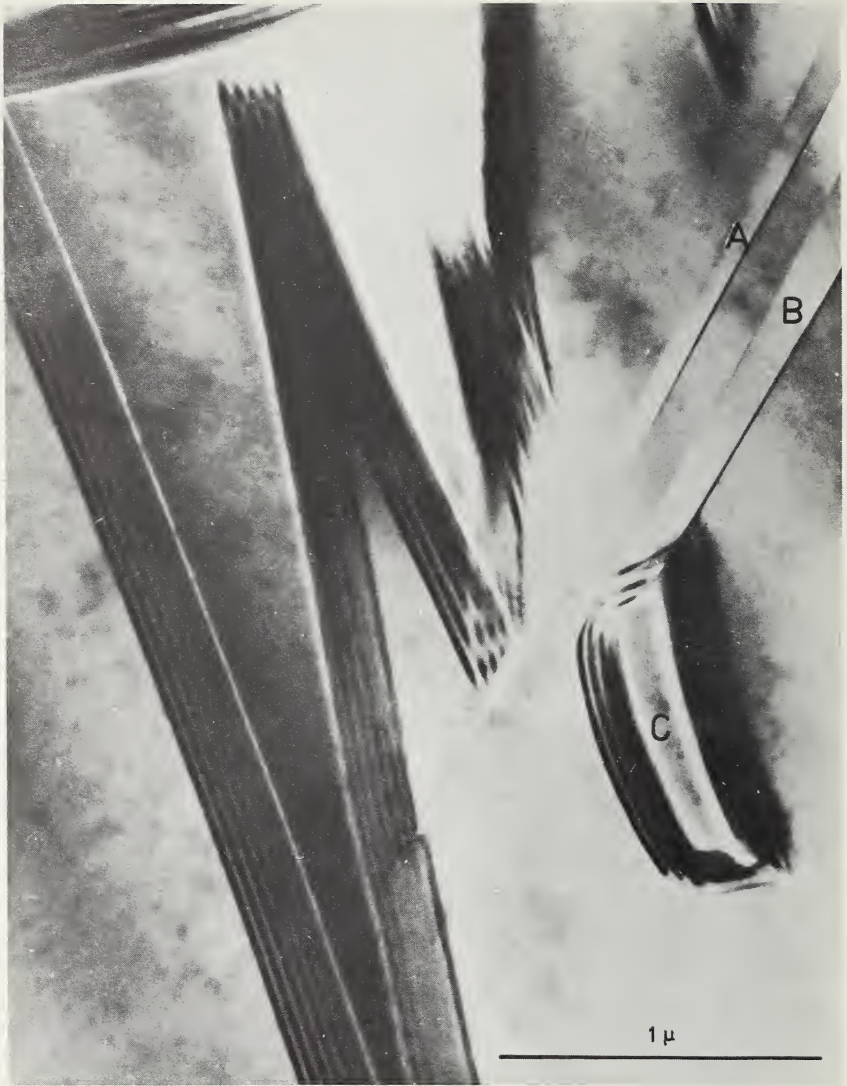


Figure 67. Ferroelectric domain boundaries in barium titanate. The fringe patterns are due to boundaries inclined with respect to the foil plane. The first and last fringes are opposite in nature. In A and B domain walls are perpendicular to the foil plane. Notice the closed loop of boundary in C.

(iii) The fringe system is similar in the bright and in the dark field image at the top end, but pseudo-complementary at the bottom end of the pattern. This property is common to all contrast effects in "thick foils"; it results from anomalous absorption.

(iv) The first fringe in the bright field image is bright if  $\Delta s > 0$ ; it is dark if  $\Delta s < 0$ .

## 2. *Anti-Ferromagnetic Domain Boundaries*

Similar domain boundaries occur in anti-ferromagnetic crystals such as nickel oxide and cobaltous oxide. Nickel oxide is cubic above the Néel point (550 °C) and it has then the sodium chloride structure. Below this temperature the magnetic moments of the nickel ions order into ferromagnetic sheets parallel to the (111) plane. The coupling between successive ferromagnetic sheets is antiferromagnetic. As a result of the spin ordering a contraction takes place along a [111] direction of the cubic structure, causing in this way a rhombohedral deformation. Since there are four possible [111] directions in the cubic structure, the contraction can take place along different directions in different parts of the crystal and a domain structure results. Again the lattices on both sides of the domain boundaries are in a twin relationship and  $\delta$ -fringes result [152].

In cobaltous oxide the lattice deformation as a result of spin ordering is similar to that in barium titanate; the crystal becomes tetragonal the  $c$  axis coinciding with one of the cube axes of the NaCl structure. Also the anti-ferromagnetic domain structure is therefore analogous to the ferro-electric domain structure in barium titanate [153].

Bright and dark field images due to domain boundaries in nickel oxide are shown in Figure 68. It is easy to verify the properties of the  $\delta$ -fringes mentioned above.

## 3. *Domains Due to Interstitial Ordering*

The ordering of interstitial atoms or ions in body centered metals leads to a domain structure as well [154]. The interstitials when occupying for instance one family of octahedral interstices cause a tetragonal deformation of the lattice, the  $c$  axis being along one of the cube directions. Since there are three different families of octahedral interstices a tetragonal deformation can be caused along the three different cube directions and therefore the formation of domains is again to be expected. Domains have actually been observed in oxygen containing niobium [154], in hydrogen loaded titanium [155] and in carbon containing tantalum [156].

A detailed study of the fringe patterns, making use of the properties mentioned above, allows to determine the complete geometrical characteristics of domain boundaries. Figure 69 summarizes for instance the results of such a study for barium titanate [150]. Comparing the observed fringe patterns with this figure one can immediately determine the orientation of the  $c$  axis in the two crystal parts, as well as the sense of sloping of the boundary plane. A similar analysis has been made for the anti-ferromagnetic domain walls in nickel oxide [150].

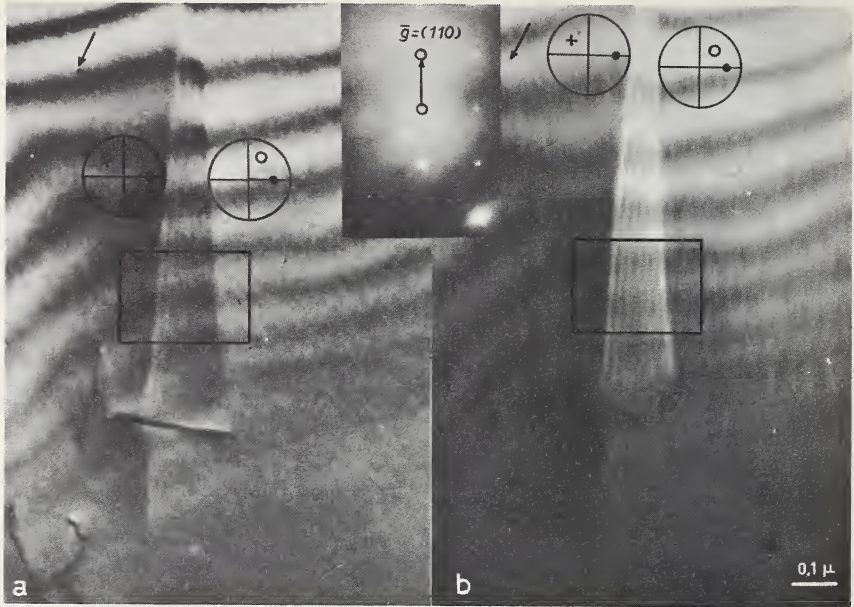


Figure 68. Bright (a) and dark field (b) image of the same boundary in nickel oxide. Notice that in the dark field image the outer fringes have both the same nature. The contraction direction and the contact plane of the boundary have been determined, the result is shown by means of a stereographic projection. The black full dot represents the contact plane and the open dot and cross the contraction direction [150, 151].

#### 4. Ferromagnetic Domain Walls

Ferromagnetic domain walls can be revealed in the electron microscope as a result of "Lorentz contrast" [157]. The image consists of either a bright or a dark line at the position of the wall (Fig. 70). It results from the "Lorentz force" exerted on the electrons by the magnetic field within the domains. Since the magnetic field changes sign at the domain walls the sense of the deflection also changes and locally either convergence or divergence of the electron beam will result. If for a wall causing convergence the focal plane of the microscope is located behind the specimen an excess of electrons will be noted, i.e., one will observe a bright line. If on the contrary the focal plane is located in front of the specimen an absence of electrons, i.e., a black line will be noted. The reverse will be true for a wall causing divergence. This mechanism of contrast formation is shown schematically in Figure 71.

Ferromagnetic domains can also be imaged by diffraction contrast. Due to the presence of the magnetic field within the domains the electrons are deflected and describe curved paths. The effect of this on the intensities of the scattered and the transmitted beam is the same as if the crystal were deformed, the displacement being proportional to the square of the distance from the entrance face [158]. This equivalent



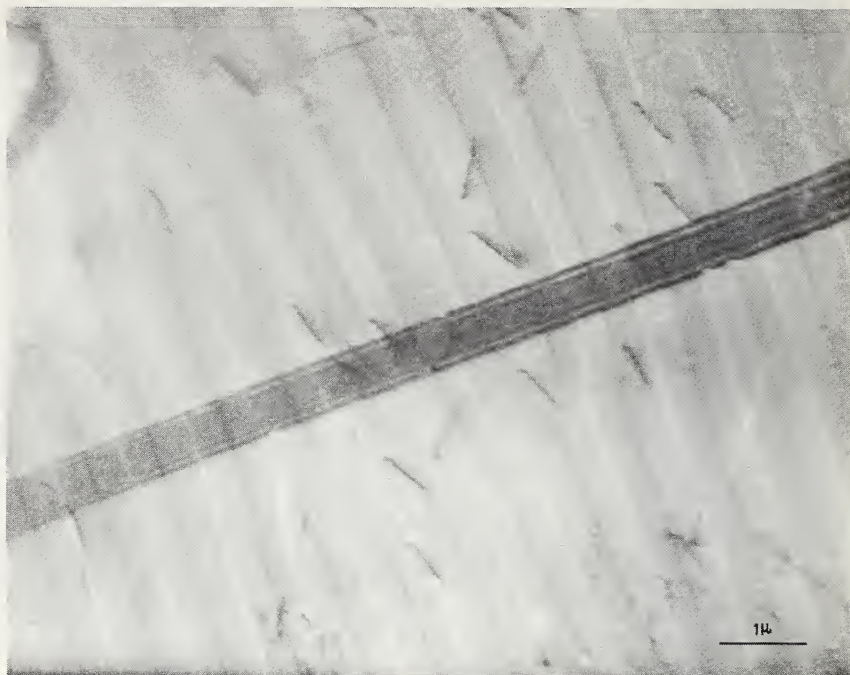


Figure 70. Sequence of ferromagnetic walls in cobalt. Stacking faults and dislocations are visible simultaneously. The domain walls are lying along the "easy" axis [0001]. Courtesy of Silcox.

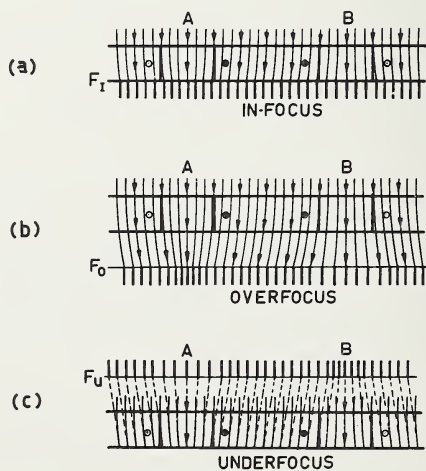


Figure 71. Origin of black and white lines at magnetic domain walls. (a) In focus: no contrast (b) Over focus: A is marked by a black line, B by a white line (c) Under focus: A is marked by a white line, B by a black line.

As a result one finds that different domains show up with a different intensity in the dark field image, but not in the bright field image [158].

#### H. OTHER PLANAR DEFECTS

The contrast effects due to more complicated planar defects have been studied as well. [159, 160, 161].

In crystals which exhibit polytypism the contact between two different polytypes usually takes place along a planar interface parallel to close packed planes. In zinc sulfide for instance the interfaces between cubic (sphalerite) and hexagonal (wurtzite) parts and between wurtzite and 4H regions have been studied [162]. Such interfaces are again revealed as fringe patterns with characteristic properties which are different from those of stacking faults and of domain boundaries.

Very often planar interfaces overlap which gives rise to more complicated fringe patterns. This is for instance the case for thin twin lamella. Methods have been worked out to distinguish thin twin lamella from overlapping stacking faults [160]. The contrast effects associated with overlapping domain walls have been studied as well, both from the theoretical and from the experimental point of view [161].

Such studies are necessary for a complete understanding of the sometimes very complicated contrast effects observed in the electron microscope.

#### I. DIRECT LATTICE RESOLUTION

In a number of crystals the distances between planes of molecules or atoms are large enough to be resolved in the electron microscope. Menter [163] was the first to demonstrate this possibility with platinum phthalocyanine crystals. In order to obtain an image of a periodic structure it is necessary, by analogy to the Abbe theory of optical image formation, that apart from the directly transmitted beam at least the first order diffracted beam is allowed to pass through the selector aperture. It is the interference between these two beams which produces the fringe pattern. The fringes are perpendicular to the diffraction vector of the diffracted beam used for imaging the lattice rows; they have the same spacing as the corresponding lattice planes. It is easy to demonstrate this experimentally by selecting only one beam; in this case the line pattern disappears. By admitting more high order diffracted beams a better resolution of the crystal lattice can theoretically be achieved; usually however the contrast decreases.

The line pattern cannot be considered as just the projection of the lattice rows. According to the dynamical two beam theory the interference between the direct beam and the scattered beam produces fringes which have the same spacing as the corresponding lattice planes, however their position in space depends on the diffraction conditions, and on the crystal thickness. The dark fringes therefore do not mark

lines of maximum mass-thickness; there is a phase shift with respect to such lines. This phase shift varies with  $s$  and with the crystal thickness. For a wedge shaped crystal with the fringes perpendicular to the edge of the wedge, one finds that black fringes change over into white fringes for a thickness change of  $1/2 t_g$ . In bent crystals where the fringes are parallel to the axis of bending spacing anomalies occur. Also the fringe spacing is then different from the lattice spacing [164, 38, 165].

The resolution conditions for periodic structures seem to be less stringent than those for point to point resolution; it is therefore not completely fair to use lattice resolution as a test. With present day microscopes even the (111) (2.35 Å) and (200) (2.04 Å) spacings of gold can be resolved as shown by Komoda [166].

It is clear that this technique opens the possibility for the direct observation of the geometry of lattice planes around dislocations, in particular it becomes possible to reveal the presence of supplementary half planes associated with dislocations. Figure 72 shows examples of such dislocations in tantalum pentoxide, where the fringes reveal the superlattice spacing of about 35 Å.

The Burgers vector can in principle be determined directly as well in direction as in magnitude by imaging the dislocation using three different families of lattice planes not belonging to the same zone. The determination is based on the fact that the number of supplementary half fringes associated with the dislocation is  $n = \mathbf{g} \cdot \mathbf{b}$ . For a perfect dislocation  $n$  is an integer; this is not the case for a partial dislocation. With three different non coplanar  $\mathbf{g}_j$  vectors one can determine the three components  $n_j = \mathbf{g}_j \cdot \mathbf{b}$  of the vector  $\mathbf{b}$ .

The sign of the dislocation is of course immediately evident. Stacking faults in planes intersecting the foil surface, as well as the fringe system, are revealed by discontinuities in the fringes along a line segment, the endpoints of which are the emergence points of the partial dislocations. However considerable care should be taken not to interpret fringe anomalies resulting from buckling or from thickness changes as being due to dislocations or stacking faults.

With the constantly improving resolution of the electron microscopes it is to be expected that this method will be extended to crystals with smaller lattice spacing; the method will therefore presumably grow in importance.

#### J. MOIRÉ PATTERNS [167, 168]

In cases where the lattice resolution becomes difficult to achieve, because of the small interplanar distance involved, like in pure metals, one can in a sense artificially increase the spacing to be resolved by making use of the "moiré fringes" formed by two overlapping crystal films.



Figure 72. Lattice fringes in tantalum pentoxide. Note the presence of dislocations and sub-grain boundaries. Courtesy Spyridelis.

The formation mechanism of moiré fringes can be demonstrated by means of an optical analogue consisting of two superposed line gratings, which differ either in spacing or in orientation [167]. Also both spacing and orientation may be different. The moiré pattern is in fact just the

“coincidence” pattern of the two gratings. At regular intervals the lines in the two gratings are in coincidence. The coincidence points form again a line grating which has a larger spacing however and which can therefore be resolved in the electron microscope (Fig. 73).

For a moiré pattern resulting from the superposition of two parallel gratings (a so-called parallel “moiré pattern”) the fringe spacing  $D_p$  is given by

$$D_p = \frac{d_1 d_2}{d_1 - d_2}$$

where  $d_1$  and  $d_2$  are the line spacings of the superposed gratings.

For a moiré pattern resulting from the superposition of two identical gratings (i.e.,  $d_1 = d_2 = d$ ) differing only in orientation by an angle  $\vartheta$ , (a so-called “rotation moiré” pattern) the fringe spacing becomes

$$D_r = d/\vartheta$$

For a general moiré pattern where there is as well an orientation difference as a spacing difference one finds for the moiré spacing

$$D = d_1[(d_1 - d_2)^2/d_2^2 + \vartheta^2]^{-1/2}.$$

Also the orientation of the fringes is different in both cases. For a parallel moiré pattern the moiré fringes are parallel to the lines of both gratings; for a rotation moiré pattern the moiré fringes are perpendicular to the average orientation of the lines in the two gratings.

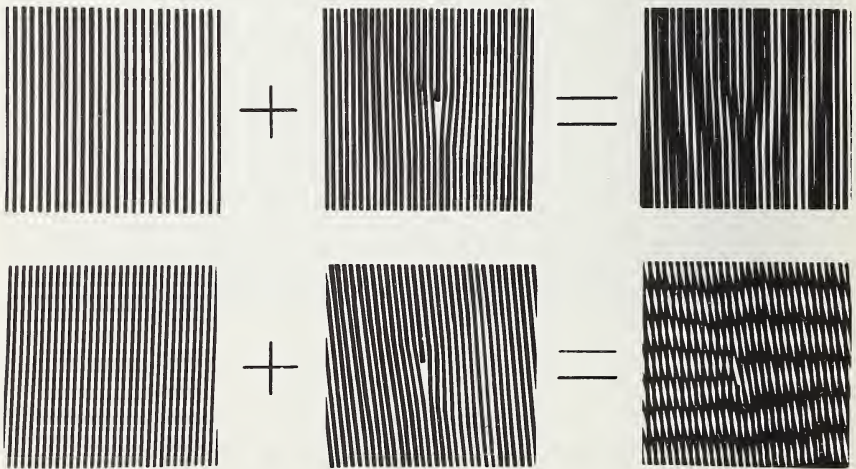


Figure 73. Optical analog illustrating the formation of Moiré fringes by superposition of two lattices. First row: parallel Moiré pattern, Second row: rotation Moiré pattern. Courtesy J. Menter.

The moiré fringes due to superposed crystals result from double diffraction. The bright field image is formed by the interference between the beam transmitted through both crystals and the beam scattered by both crystals. Let  $\Delta\mathbf{g} = \mathbf{g}_1 - \mathbf{g}_2$  be the difference between the operating diffraction vector in both crystal parts. In general  $\Delta\mathbf{g}$  will be parallel to the foil plane. For double diffraction to occur  $\Delta\mathbf{g}$  must be small. One can then show that there is a phase difference  $2\pi\Delta\mathbf{g} \cdot \mathbf{r}$  between the doubly transmitted and the doubly diffracted beam ( $\mathbf{r}$  is a position vector in the foil plane) [162].

It is obvious that this phase difference is position dependent. The phase difference and hence the total transmitted intensity will be the same along lines for which  $\Delta\mathbf{g} \cdot \mathbf{r}$  is constant. This equation represents the fringes, which are straight lines perpendicular to  $\Delta\mathbf{g}$ .

The spacing is further given by  $D = 1/|\Delta\mathbf{g}|$ . It is easy to verify that this formula leads as well for the parallel moiré as for the rotation moiré to the same expressions for the spacing as those given above and which were based on the optical analogue. From these formula we can conclude that for a small difference in lattice parameter or for a small rotation angle  $\vartheta$  (in general for small  $\Delta\mathbf{g}$ ), the moiré spacing may become fairly large and easily resolvable in the electron microscope.

The first moiré patterns were observed on sandwiches which were generated by chance during the preparation of specimens of layer crystals. Bassett et al. [168], worked out a technique which allows to make specimens in a reproducible way. The technique is based on the epitaxial growth of metal films. A first metal film is epitaxially grown, e.g., on sodium chloride or on mica, a film of a second metal with a slightly different lattice parameter is grown epitaxially on the first metal film. The sandwich of metal films is then removed from the substrate and used as a specimen. Such specimens produce parallel moiré patterns. Careful superposition of two films of the same metal leads to rotation moiré specimens. An example of such a moiré pattern is shown in Figure 74; the sandwich consists of superposed layers of gold and palladium.

A more recent approach consists in using a single crystal foil of a layer crystal (e.g., molybdenite or mica) prepared by cleavage, as a substrate for the epitaxial growth of metal films. Good systems are molybdenite with gold or silver. Usually the evaporation of the metal is performed in the microscope itself whilst the substrate is being observed [170].

Using the optical analogue one can readily show that an edge dislocation in one of the components of the sandwich will be imaged as an edge dislocation in the moiré pattern. In the case of a parallel moiré the supplementary halfplane in the moiré pattern will be parallel to the supplementary halfplane in the crystal as seen by the same diffraction vector. The reverse is not true however.

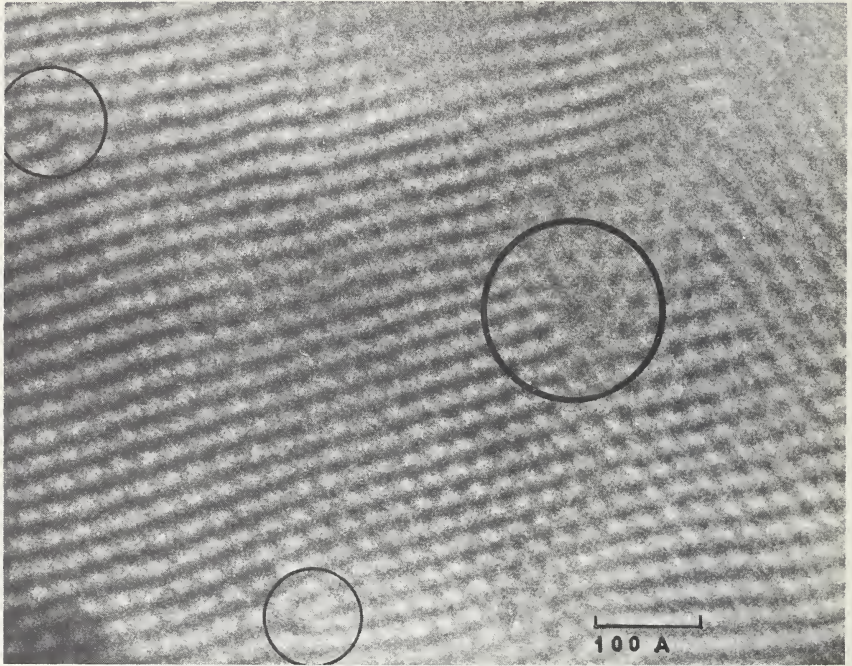


Figure 74. Moiré pattern from a sandwich of palladium-gold. The encircled areas contain dislocations. In this case two different operating reflections produce a two-dimensional dot pattern. Courtesy of Bassett, Menter and Pashley.

Ending moiré fringes do not necessarily correspond to ending half-planes. Also screw dislocations will be imaged as terminating fringes. The number of terminating fringes is, like in the case of lattice resolution, given by  $n = \mathbf{g} \cdot \mathbf{b}$ . For a partial dislocation the fringes undergo a phase shift at the intersection line of the associated fault plane and the foil plane. The phase shift expressed as a fraction of the inter fringe spacing is again given by  $\mathbf{g} \cdot \mathbf{b}$ , where  $\mathbf{g} \cdot \mathbf{b}$  is now fractional since  $\mathbf{b}$  is not a lattice vector. It is clear that application of this remark allows to determine the Burgers vector of dislocations in magnitude and in direction [168]. The determination becomes especially simple if one uses multiple beam moiré patterns imaging these different families of lattice planes simultaneously.

Although very elegant and attractive, the technique is not generally applicable because of the difficulty in specimen preparation. Also the interpretation of moiré patterns in terms of defects is not always obvious. More theoretical work is needed before the same level of interpretation, which is now possible in transmission electron microscopy, will be reached.

## K. THE EFFECT OF THE PRESENCE OF DEFECTS ON THE DIFFRACTION PATTERN

We shall only consider the effect of geometrical effects such as dislocations, stacking faults and domain boundaries on the fine structure of diffraction spots.

It was already realized by Hirsch and Whelan [171] that the presence of even a single stacking fault causes beam splitting. More recently the effect of single stacking faults, domain boundaries and dislocations on the fine structure of diffraction spots has been studied in detail both from the experimental and from the theoretical point of view [172, 173]. For the planar defects the intensities and the geometry of the different satellites were calculated for the two beam case taking into account anomalous absorption [172]. For stacking faults it was found that for small  $s$ -values as well the transmitted as the scattered beam is split into three components, the main beam which remains at the same position as in the perfect crystal, and a satellite beam on each side of it. For large  $s$ -values one of the two satellites becomes much weaker than the other so that effectively one satellite only will be observed. The  $s$ -dependence of the intensities and positions of the satellites are conveniently represented in reciprocal space by means of the curves of Figure 75a and 75b. One of the asymptotes of these curves is perpendicular to the fault plane, the other one is asymmetrical with respect to the normal on the foil plane. The positions of the satellite spots around the scattered beam are found by intersecting the curve of Figure 75a, which has to be imagined centered on the reciprocal lattice node point, by means of Ewald's sphere. The directions of the scattered beams are then found by connecting the centre of Ewald's sphere with the intersection points. The width of the shaded region around the curve is a measure for relative intensity of the three beams. From this curve we deduce that for large  $s$ -values apparently a rod of intensity perpendicular to the fault plane is created.

One can use this remark to determine the sense of sloping of the fault plane from the relative position of the main spot and the satellite with respect to the center of the diffraction pattern. Once the sense of sloping is known one can determine the nature of stacking faults in face centered cubic metals from the bright field image along [174].

For the transmitted beam one can similarly describe the beam splitting by means of the curve of Figure 75b which has to be thought around the origin of reciprocal space. It is to be noted that both satellites have now the same intensity independent of the value of  $s$ .

It is clear that a close relationship exists between the fringe pattern observed in the image and the fine structure of the diffraction spot. The fringe pattern in the dark field image results in fact from the interference between the different components of the scattered beam. Similarly

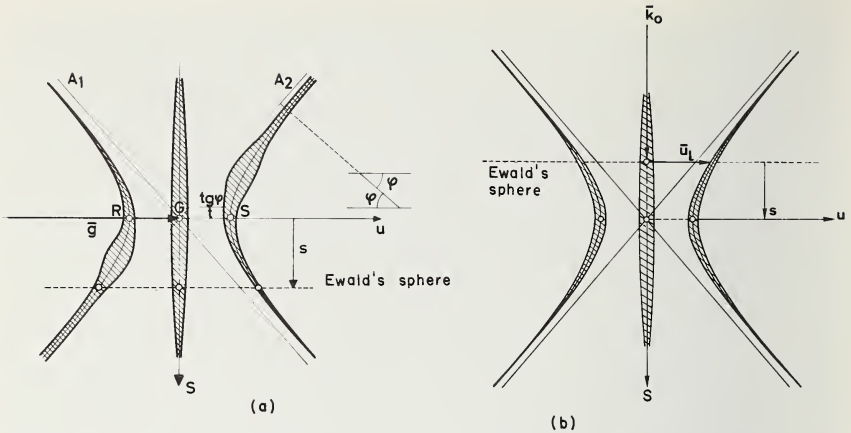


Figure 75. (a) Geometry and intensity of the satellites in the case of stacking faults. From this drawing the position and intensity of the satellites can be deduced as a function of  $s$ . The width of the cross hatched part along the hyperbola is a measure of the intensity variation as a function of  $s$ , (b) Graphical representation for the positions of the satellites around the transmitted beam. The widths of the cross hatched strip is a measure for the intensity variation.

the bright field image results from the interference between the different components of the transmitted beams.

The effect of the presence of a domain boundary is to cause splitting of the scattered and the transmitted beams into four components. For a discussion we refer to the original paper [172].

Finally the effect of dislocations is to cause fine streaking of the diffraction spots in a direction perpendicular to the direction of the dislocations [175].

Figure 76 illustrates some of the effects discussed here with observations made on single stacking faults. If many stacking faults are present in parallel planes their effect is to cause streaking along certain reciprocal lattice rows perpendicular to the interfaces. Kinematical theories have been developed for the X-ray case, assuming different types of faults to be present. However these theories are inadequate for the electron case because of dynamical effects.

Much work remains to be done in this field before the streaking in electron diffraction patterns from faulted crystals can be interpreted in detail. Combining the information derived from the different diffraction patterns, with the results obtained from the image should be a fruitful approach capable of yielding a detailed description of the fault structure of crystals.

## L. DISCUSSION

Transmission electron microscopy has already acquired the status of a routine technique in materials science in general and in physical

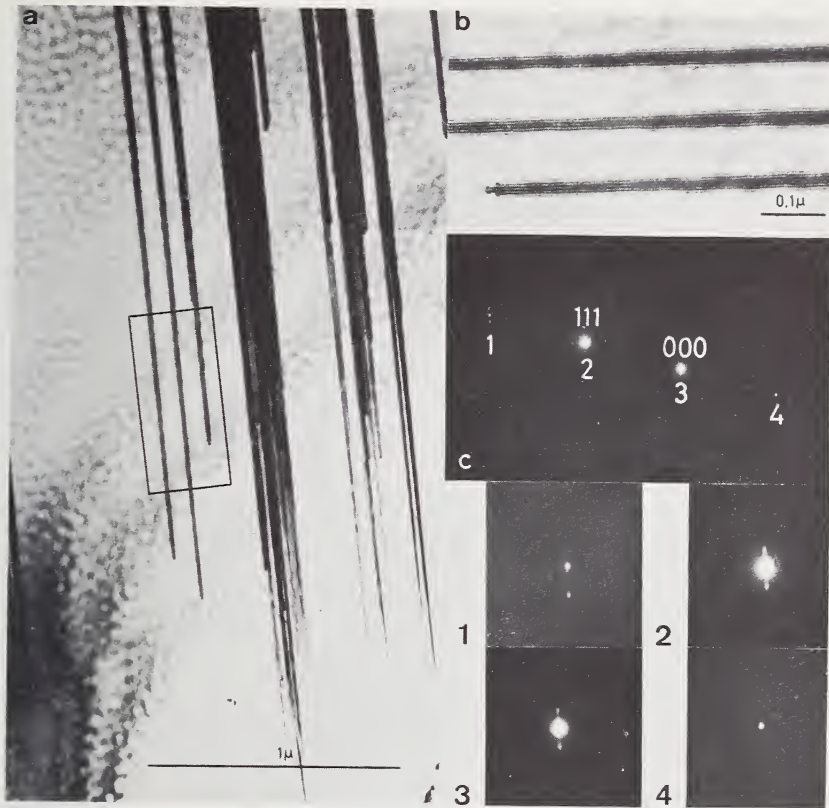


Figure 76. Bright field image of stacking faults in steel (a) and the associated diffraction pattern (c). An enlargement of the selected area is given in (b). The diffraction pattern (c) is in correct orientation with respect to (b). Insets 1, 2, 3 and 4 show enlargements of the four spots. The two satellites at the transmitted and 'dynamical' spots are clearly seen in insets 2 and 3. In spot 1 and 4 only one satellite is visible.

metallurgy research in particular. As further progress is made in the interpretation of the contrast effects more and also more detailed information can be gained. Like any other method it has obviously some limitations.

In the first place we have to be aware of the fact that we are working with a thin foil and that as a consequence of this the results may not always be representative for bulk material. A striking example of this is the difference in the habit of precipitates depending on whether the precipitation takes place in the bulk or in a thin foil. Also the width of dislocation ribbons depends on the foil thickness and when measuring stacking fault energies this can introduce serious errors. With the use of high voltage microscopes thicker specimens will be used and this drawback can be minimized. However the use of high voltage microscopes makes the application of two-beam dynamical theory more ques-

tionable. The need for multiple beam calculations for a detailed interpretation of the contrast becomes then more urgent.

Some materials are not stable under electron irradiation; such materials are obviously difficult to study by this technique. Here again the situation may improve with the use of high voltage microscopes.

New developments, extending greatly the range of possible applications are being made at present: small angle electron scattering and energy loss spectroscopy are two of them. This last technique may become very useful for identification purposes. For the same purpose X-ray fluorescence analysis can now be combined with transmission electron microscopy to yield information of a chemical nature.

One of the main advantages of the technique, its great resolution, turns out to be sometimes a drawback. One observes only small areas of the specimen at a time, which may lead to "selected area interpretation". For this reason transmission electron microscopy is *not* a good technique to judge the quality of relatively perfect crystals. Here some of the X-ray mapping techniques, or even etching, is superior.

With improving resolution, methods based on direct imaging of the lattice will presumably gain importance, also for the study of perfect crystals.

## VI. Acknowledgments

I would like to express my gratitude to those authors who supplied me with photographs for use as illustrations in this article. In this connection special thanks are due to Dr. P. Delavignette who supplied me with a large number of photographs.

I also wish to thank the Academic Press and North Holland Publishing Company for their kind permission to reproduce illustrations.

## VII. References

- [1] Taylor, G. I., Proc. Roy. Soc. **A145**, 362 (1934).
- [2] Burgers, J. M., Proc. Acad. Sci. Amsterdam **42**, 293 (1939).
- [3] Burton, W. K., Cabrera, N., and Frank, F. C., Phil. Trans. Roy Soc. **A243**, 299 (1951).
- [4] Gevers, R., Amelinckx, S., and Dekeyser, W., Naturwiss. **39**, 448 (1952); Gevers, R., J. Chim. Phys. **50**, 321 (1953); Gevers, R., Nature **171**, 171 (1953); Horn, F. H., Phil. Mag. **43**, 1210 (1952).
- [5] Sella, C., Conjeaud, P., Trillat, J. J., Compt. Rend. **249**, 1978 (1959); Bassett, G. A., Phil. Mag. **3**, 1042 (1958); Betghe, H., and Keller, W., Z. Naturforsch. **15a**, 271 (1960); Betghe, H., and Keller, W., Proc. European Reg. Conf. on Electron Microscopy, Delft 1960, Vol. **1**, p. 266 (1961); Betghe, H., Proc. 4th Intern. Conf. on Electron Microscopy, Berlin 1958 Vol. **1**, p. 409 (1960).
- [6] Amelinckx, S., and Votava, E., Nature **172**, 538 (1953).
- [7] Hedges, J. M., and Mitchell, J. W., Phil. Mag. **4**, 223, 357 (1953).

- [8] Amelinckx, S., Meanhout-Van der Vorst, W., Gevers, R., and Dekeyser, W. *Phil. Mag.* **46**, 450 (1955); Amelinckx, S., *Phil. Mag.* **1**, 269 (1956).
- [9] Dash, W. C., *J. Appl. Phys.* **27**, 1193 (1956).
- [10] Bontinck, W., and Amelinckx, S., *Phil. Mag.* **2**, 1 (1957).
- [11] Jones, D. A., and Mitchell, J. W., *Phil. Mag.* **2**, 1047 (1957); Amelinckx, S., *Phil. Mag.* **1**, 269 (1956).
- [12] Forth, A. J., *Phil. Mag.* **8**, 663 (1963).
- [13] Bond, W. L., and Andrus, J., *Phys. Rev.* **101**, 1211 (1956).
- [14] Indenbohm, V. L., *Fis. Tverd. Tela* **4**, 231 (1962); Indenbohm, V. L., *Dokl. Akad. Nauk SSSR* **141**, 1360 (1961).
- [15] Heidenreich, R. D., *J. Appl. Phys.* **20**, 993 (1949).
- [16] Castaigne, R., *Proc. 3rd Intern. Conf. on Electron Microscopy*, 1954 London, p. 379 (1956).
- [17] Hirsch, P. B., Horne, R. W., and Whelan, M. J., *Phil. Mag.* **1**, 677 (1956); Hirsch, P. B., Howie, A., and Whelan, M. J., *Phil. Trans. Roy. Soc.*, **A252**, 499 (1960); Hirsch, P. B., Howie, A., and Whelan, M. J., *Proc. 4th Intern. Conf. on Electron Microscopy*, Berlin 1958, Vol. **1**, 527 (1960).
- [18] Bollmann, W., *Phys. Rev.* **103**, 1588 (1956).
- [19] Menter, J., *Proc. Roy. Soc.* **A236**, 119 (1956).
- [20] Pashley, D. W., Menter, J. W., and Bassett, G. A., *Nature* **179**, 752 (1957); Bassett, G. A., Menter, J. W., and Pashley, D. W., *Proc. Roy. Soc.* **A246**, 345 (1958).
- [21] Müller, E. W., *Z. Physik* **131**, 136 (1951).
- [21b] Read, W. T., *Dislocations in Crystals* (McGraw-Hill, New York, 1955); Cottrell, A. H., *Dislocations and plastic flow in crystals*, Oxford University Press., 1953; Friedel, J., *Dislocations*, Addison-Wesley, 1964; Weertman, J., and Weertman, J. R., *Elementary Dislocation theory*, Macmillan Series in Materials Science, 1964; Hull, D., *Introduction to Dislocations* (Pergamon Press, 1965).
- [22] Griffin, L. J., *Phil. Mag.* **41**, 196 (1950); Griffin, L. J., *Phil. Mag.* **42**, 775 (1951); Griffin, L. J., *Phil. Mag.* **43**, 651 (1952).
- [23] Dawson, I. M., and Vand. V., *Proc. Roy. Soc.* **A206**, 555 (1951); Anderson, N. G., and Dawson, I. M., *Proc. Roy. Soc.* **A218**, 255 (1953); Dawson, I. M., *Proc. Roy. Soc.* **A214**, 72 (1952).
- [24] Cabrera, N., and Levine, M. M., *Phil. Mag.* **1**, 450 (1956); Cabrera, N., Levine, M. M., and Plaskett, J., *Phys. Rev.* **96**, 1153 (1954).
- [25] Amelinckx, S., *Acta Met.* **2**, 848 (1954).
- [26] Gilman, J., and Johnston, W. G., in *Dislocations and Mechanical Properties of Crystals* (Fisher, J. C. et al., eds) p. 116 (Wiley, New York, 1957).
- [27] Sears, G. W., *J. Chem. Phys.* **32**, 1317 (1960).
- [28] Gilman, J. J., and Johnston, W. G., in *Dislocations and Mechanical Properties of Crystals*, p. 116 (J. Wiley, New York, 1957).
- [29] Gilman, J. J., and Johnston, W. G., *J. Appl. Phys.* **27**, 1018 (1956).
- [30] Johnston, W. G., and Gilman, J. J., *J. Appl. Phys.* **30**, 129 (1959); Gilman, J. J., and Johnston, W. G., *J. Appl. Phys.* **29**, 877 (1958).
- [31] Dash, W. C., *J. Appl. Phys.* **29**, 705 (1958).
- [32] Amelinckx, S., and Strumane, G., *Silicon Carbide* (J. R. O'Connor and Smiltens, J., eds) p. 162 (Pergamon Press, New York, 1960).
- [33] Jacquet, P. A., *Acta Met.* **2**, 725, 770 (1954).
- [34] Stokes, R. J., Johnston, T. L., and Li, C. H., *Phil. Mag.* **3**, 31 (1958); Stokes, R. J., Johnston, T. L., and Li, C. H., *Phil. Mag.* **4**, 137 (1959).
- [35] Silk, E. C. H., and Barnes, R. S., *Phil. Mag.* **4**, 970 (1959).
- [36] Price, P. B. and Walker, R. M., *Appl. Phys. Letters* **2**, 23 (1963); *J. Appl. Phys.* **33**, 3407 (1962); *ibid.* **33**, 3400 (1962); *Phys. Letters* **3**, 113 (1962).
- [37] Johnston, W. G., *Dislocation etch pits in nonmetallic crystals*, *Progress in Ceramic Science* (Burke, J. E., ed) Vol. **2**, Pergamon Press, New York, 1962.

- [38] Amelinckx, S., The Direct Observation of Dislocations. Solid State Physics, Suppl. 6 (Seitz, F. and Turnbull, D., eds) Academic Press, New York, 1964.
- [39] Dash, W. C., J. Appl. Phys. **27**, 1193 (1956).
- [40] Hedges, J. M., and Mitchell, J. W., Phil. Mag. **44**, 223, 357 (1953).
- [40b] Childs, C., Thesis University of North Carolina 1959; Childs, C., and Slifkin, L., Phys. Chem. Solids **12**, 119 (1959); Childs, C., and Slifkin, L., Phys. Rev. Letters **5**, 502 (1960).
- [41] Bontinck, W., and Amelinckx, S., Phil. Mag. **2**, 1 (1957); Bontinck, W., Phil. Mag. **2**, 561 (1957).
- [42] Miller, M. G., Thesis University of North Carolina, 1961.
- [43] Amelinckx, S., Phil. Mag. **1**, 269 (1956).
- [44] Kubo, K., and Katano, Y., J. Phys. Soc. Japan **16**, 347 (1961).
- [45] Amelinckx, S., Acta Met. **6**, 34 (1958).
- [46] Amelinckx, S., Maenhout-Van der Vorst, W., and Dekeyser, W., Acta Met. **7**, 8 (1959).
- [47] Amelinckx, S., Maenhout-Van der Vorst, W., and Dekeyser, W., Phil. Mag. **46**, 450 (1955).
- [48] Washburn, J., and Nadeau, J., Acta Met. **6**, 665 (1958); Washburn, J., in "Growth and Perfection of Crystals" (Doremus, R. H., et al.), p. 342 Wiley and Sons, New York, 1958.
- [49] Barber, D. J., Harvey, K. B., and Mitchell, J. W., Phil. Mag. **2**, 704 (1957); Amelinckx, S., in "Growth and Perfection of Crystals" (Doremus, R. H., et al.), p. 139 Wiley, New York, 1958.
- [50] Bontinck, W., Physica **24**, 650 (1958).
- [51] Tyler, W. W., and Dash, W. C., J. Appl. Phys. **28**, 1221 (1957).
- [52] Bond, H. E., and Harvey, K. B., J. Appl. Phys. **34**, 440 (1963).
- [53] Dash, W. C., J. Appl. Phys. **31**, 2275 (1960).
- [53b] Harvey, K. B., Phil. Mag. **8**, 435 (1963).
- [54] Jones, D. A., and Mitchell, J. W., Phil. Mag. **3**, 1 (1958).
- [55] Amelinckx, S., "Growth and Perfection of Crystals" (Doremus, R. H., et al.), p. 139 Wiley and Son, New York, 1958.
- [56] Dash, W. C., Phys. Rev. Letters **1**, 400 (1958).
- [57] Indenbohm, V. L., and Chernycheva, M. A., Dokl. Akad. Nauk. SSSR **111**, 596 (1956); Indenbohm, V. L., and Tomilovskii, G. E., Kristallografiya **2**, 190 (1957).
- [58] Kear, B. H., Taylor, A., and Pratt, P. L., Phil. Mag. **4**, 665 (1959).
- [59] Indenbohm, V. L., Fis. Tverd. Tela **4**, 231 (1962); Indenbohm, V. L., Dokl. Adam. Nauk. SSSR **141**, 1360 (1961).
- [60] Hirsch, P. B., Howie, A., and Whelan, M. J., Phil. Trans. Roy. Soc. **252**, 499 (1960); Hirsch, P. B., Howie, A., and Whelan, M. J., Proc. 4th Int. Conf. Electron Microscopy, 1958, Vol. 1 (Springer Verlag, Berlin, 1960) p. 527; Howie, A., and Whelan, M. J., Proc. Roy. Soc. **263**, 217 (1961); Whelan, M. J., and Hirsch, P. B., Phil. Mag. **2**, 1121, 1303 (1957); Hashimoto, H., Howie, A., and Whelan, M. J., Proc. Eur. Reg. Conf. Electron Microscopy, Delft 1960, p. 207; Hashimoto, H., Howie, A., and Whelan, M. J., Phil. Mag. **5**, 967 (1960); Howie, A., and Whelan, M. J., Proc. Roy. Soc. **A263**, 217 (1961); Howie, A., and Whelan, M. J., Proc. Roy. Soc. **A267**, 206 (1962).
- [61] Dupouy, G., Perrier, F., Compt. Rend. **253**, 2435 (1961); Dupouy, G., Perrier, F., and Fabre, R., Compt. Rend. **252**, 627 (1961); Dupouy, G., Perrier, F., and Durrieur, C., Compt. Rend. **251**, 2836 (1960).
- [62] Kelly, P. M., and Nutting, J., J. Inst. Metals **87**, 385 (1958-59).
- [63] Amelinckx, S., and Delavignette, P., Proc. Am. Inst. Mining Engrs.—St. Louis 1961 (Interscience Publishers, New York, 1962) p. 295.
- [64] Blank, H., and Amelinckx, S., J. Appl. Phys. **34**, 2200 (1963).
- [65] Washburn, J., Groves, G. W., Kelly, A., and Williamson, G. K., Phil. Mag. **5**, 991 (1960).

- [66] Aerts, E., Delavignette, P., Siems, R., and Amelinckx, S., *J. Appl. Phys.* **33**, 3078 (1962).
- [67] Hirsch, P. B., Kelly, A., and Menter, J. W., *Proc. 3rd Int. Conf. Electron Microscopy, London 1954*, p. 231.
- [68] Ruedl, E., Delavignette, P., and Amelinckx, S., *J. Nucl. Mat.* **6**, 46 (1962).
- [69] Kelsch, J. J., Kammerer, O. F., and Buhl, P. A., *J. Appl. Phys.* **11**, 555 (1960); Kelsch, J. J., Kammerer, O. F., Goland, A. N., and Buhl, P. A., *J. Appl. Phys.* **33**, 1475 (1962).
- [70] Van Landuyt, J., Gevers, R., and Amelinckx, S., *Phys. Stat. Sol.* **7**, 307 (1964).
- [71] Spyridelis, J. (private communication).
- [72] Hashimoto, H., Howie, A., and Whelan, M. J., *Proc. Eur. Reg. Conf. on Electron Microscopy, Delft 1960*, p. 207; Hashimoto, H., Howie, A., and Whelan, M. J., *Phil. Mag.* **5**, 967 (1960).
- [73] Heidenreich, R. D., *J. Appl. Phys.* **20**, 993 (1949).
- [74] Hirsch, P. B., Howie, A., and Whelan, M. J., *Phil. Trans. Roy. Soc.* **252**, 499 (1960).
- [75] Gevers, R., *Phil. Mag.* **8**, 769 (1963).
- [76] Howie, A., and Whelan, M. J., *Proc. Roy. Soc.* **A267**, 206 (1962).
- [77] Howie, A., and Whelan, M. J., *Proc. Eur. Reg. Conf. Electron Microscopy, Delft 1960*, p. 194.
- [78] Holland, V. F., Lindenmeyer, P. H., Trivedi, R., and Amelinckx, S., *Phys. Stat. Sol.* **10**, 543 (1965).
- [79] Siems, R., Delavignette, P., and Amelinckx, S., *Phys. Stat. Sol.* **2**, 421 (1962).
- [80] Groves, G. W., and Whelan, M. J., *Phil. Mag.* **7**, 1603 (1962).
- [81] Groves, G. W., and Kelly, A., *Phil. Mag.* **6**, 1527 (1961).
- [82] Hashimoto, H., and Mannami, M., *Acta Cryst.* **13**, 363 (1960).
- [83] Ruedl, E., Delavignette, P., and Amelinckx, S., *J. Nucl. Mat.* **6**, 46 (1962).
- [84] Hunstall, W. J., Hirsch, P. B., and Steeds, J., *Phil. Mag.* **9**, 99 (1964).
- [85] Glossop, A., and Pashley, D., *Proc. Roy. Soc.* **A250**, 132 (1959); Ogawa, S., Watanabe, D., Watanabe, H., and Komoda, T., *Acta Cryst.* **11**, 872 (1958); Pashley, D., and Presland, P., *J. Inst. Metals* **87**, 419 (1958-1959).
- [86] Fisher, R. M., and Marcinkowski, M. J., *Phil. Mag.* **6**, 1385 (1961).
- [87] Sato, H., and Toth, R. S., in *Alloying behaviour and Effects in concentrated Solid Solution* ed. T. B. Massalski (Gordon and Breach, 1965) p. 295.
- [88] Howie, A., *Met. Rev.* **6**, 467 (1961).
- [89] Hashimoto, H., Howie, A., and Whelan, M. J., *Proc. Roy. Soc.* **A269**, 80 (1962).
- [90] Gevers, R., Art, A., and Amelinckx, S., *Phys. Stat. Sol.* **3**, 1563 (1963).
- [91] Art, A., Gevers, R., and Amelinckx, S., *Phys. Stat. Sol.* **3**, 697 (1963).
- [92] Van Landuyt, J., Gevers, R., and Amelinckx, S., *Phys. Stat. Sol.* **7**, 519 (1964).
- [93] Drum, C. M., *Phil. Mag.* **11**, 313 (1965).
- [94] Van Landuyt, J., *Phys. Stat. Sol.* **16**, 585 (1966).
- [95] Blank, H., Delavignette, P., Gevers, R., and Amelinckx, S., *Phys. Stat. Sol.* **7**, 747 (1964).
- [96] An excellent survey of different methods for measuring stacking fault energies is given in the paper by Christian, J. W., and Swann, P. R.: *Stacking faults in Metals and Alloys, in Alloying behaviour and effects of concentrated solid solutions* (Gordon and Breach) ed. T. B. Massalski (1963).
- [97] Gallagher, P. C. J., *Phys. Stat. Sol.* **16**, 95 (1966).
- [98] Siems, R., Delavignette, P., and Amelinckx, S., *Phys. Stat. Sol.* **2**, 636 (1962).
- [99] Ives, L. K., and Ruff, A. W., *J. Appl. Phys.* **37**, 1831 (1966).
- [100] Amelinckx, S., and Delavignette, P., *J. Appl. Phys.* **32**, 341 (1961).
- [101] Delavignette, P., and Amelinckx, S., *Trans. Brit. Ceram. Soc.* **62**, 687 (1963).
- [102] Whelan, M. J., *Proc. Roy. Soc.* **A249**, 114 (1958).
- [103] Siems, R., Delavignette, P., and Amelinckx, S., *Z. Physik* **165**, 502 (1961).
- [104] Aerts, E., Delavignette, P., Siems, R., and Amelinckx, S., *J. Appl. Phys.* **33**, 3078 (1962).

- [105] Siems, R., in *Dislocations in Solids*, The Faraday Society, 1964, p. 42.
- [106] Brown, L. M., and Thölen, A. R., in *Dislocations in Solids*, The Faraday Society, 1964, p. 35.
- [107] Jøssang, T., Howell, M. J., Hirth, J. P., and Lothe J., *Acta Met.* **13**, 279 (1965).
- [108a] Czjzek, G., Seeger, A., and Mader, S., *Phys. Stat. Sol.* **2**, 558 (1962).
- [108b] Edington, J. W., and Smallmann, R. E., *Phil. Mag.* **11**, 1109 (1965).
- [108c] Kannan, V. C., and Thomas, G., *J. Appl. Phys.* **37**, 2363 (1966).
- [108d] Harris, J. E., and Masters, B. C., *Proc. Roy. Soc.* **A292** 240 (1966).
- [108e] Dobson, P. S., and Smallmann, R. E., *Proc. Roy. Soc.* **A293**, 423 (1966).
- [109] Kuhlmann-Wilsdorf, D., *Phil. Mag.* **3**, 125 (1958).
- [110] Seitz, F., *Advances in Phys.* (Phil. Mag. Suppl.) **1**, 43 (1953).
- [111] Gyulai, Z., and Hartly, D., *Z. Physik* **51**, 378 (1928).
- [112] Molenaar, J., and Aarts, W. H., *Nature* **166**, 690 (1950); Druyvestein, M. J., and Manintveld, J. A., *ibid.* **168**, 868 (1951).
- [113] Cottrell, A. H., in *Dislocations and Mechanical Properties of Crystals* (Fisher, J. C., et al., eds.), p. 509. Wiley, New York, 1957.
- [114] Delavignette, P., and Amelinckx, S., *Phil. Mag.* **6**, 601 (1961); Bierly, J. N., *Proc. 5th Intern. Conf. on Electron Microscopy*, Philadelphia, 1962, **1**, J-14 (1962).
- [115] Marinkovic, V., Thesis, Ljubljana (1965).
- [116] Hirsch, P. B., Silcox, J., Smallmann, R., and Westmacott, K., *Phil. Mag.* **3**, 897 (1958); Silcox, J., *Proc. 4th Intern. Conf. Electron Microscopy*, Vol. **1**, p. 548 (1958).
- [117] Cotterill, R. M. J., *Phil. Mag.* **6**, 1351 (1961); Yoshida, S., Kino, T., Kiritani, M., Kabemoto, S., Maeta, H., and Shimomura, Y., *Proc. Intern. Conf. Crystal Lattice Defects*, *J. Phys. Soc. Japan* **18**, suppl. 3, 98 (1963).
- [118] Nicholson, R. B., and Nutting, J., *Acta Met.* **9**, 332 (1961).
- [119] Berghezan, A., Fourdeux, A., and Amelinckx, S., *Acta Met.* **9**, 464 (1960).
- [120] Price, P. B., *Electron microscopy and strength of crystals* (Interscience Publishers, New York, 1963) p. 41.
- [120b] Meakin, J. D., Lawley, A., and Koo, R. C., *Appl. Phys. Letters* **5**, 133 (1964).
- [121] Amelinckx, S., and Delavignette, P., *Phys. Rev. Letters* **5**, 50 (1960).
- [122] Williamson, G., and Baker, C., *Phil. Mag.* **6**, 313 (1961).
- [123] Silcox, J., and Hirsch, P. B., *Phil. Mag.* **4**, 72 (1959).
- [124] Smallmann, R. E., Westmacott, K. H., and Cooley, J. A., *J. Inst. Metals* **88**, 127 (1959); Smallmann, R. E., and Westmacott, K. H., *J. Appl. Phys.* **30**, 603 (1959).
- [125] Mader, S., and Sims, E., *Proc. Eur. Rég. Conf. Electron Microscopy*, Delft, 1960, Vol. **1**, p. 379.
- [126] De Jong, M., and Koehler, J. S., *Phys. Rev.* **129**, 49 (1963).
- [127] Kimura, H., Kuhlmann-Wilsdorf, D., and Maddin, R., *Appl. Phys. Letters* **3**, 4 (1963).
- [128] Yoshida, S., Kiritani, M., and Shimomura, Y., *Intern. Conf. on Electron diffraction and Crystal defects*, Melbourne 1965, II, G-4.
- [129] Ruedl, E., and Amelinckx, S., *J. Nucl. Mat.* **9**, 116 (1963).
- [130] Nelson, R. S., Mazey, D. J., and Barnes, R. S., *AERE-R4564* (1964).
- [131] Van Landuyt, J., Gevers, R., and Amelinckx, S., *Phys. Stat. Sol.* **10**, 319 (1965).
- [132] Amelinckx, S., Bontinck, W., Dekeyser, W., and Seitz, F., *Phil. Mag.* **2**, 1 (1957).
- [133] Weertman, J., *Phys. Rev.* **107**, 1259 (1957).
- [134] Bontinck, W., and Amelinckx, S., *Phil. Mag.* **2**, 1 (1957).
- [135] Thomas, G., and Whelan, M. G., *Phil. Mag.* **6**, 1103 (1961).
- [136] Groves, G., and Kelly, A., *Phil. Mag.* **6**, 1527 (1961).
- [137] Ruedl, E., Delavignette, P., and Amelinckx, S., *Proc. IAEA Symp. on Effects of Radiation Damage in Solids and Reactor Materials*, Venice 1962 (Intern. Atomic Energy Agency, Vienna, 1962) p. 363.
- [138] Ruedl, E., and Amelinckx, S., *Proc. Intern. Conf. Crystal Lattice Defects 1962*, *J. Phys. Soc. Japan* **18**, suppl. 3, 195 (1963).
- [139] Makin, M. J., and Hudson, B., *Phil. Mag.* **6**, 447 (1963).

- [140] Mazey, D. J., Barnes, R. S., and Howie, A., *Phil. Mag.* **7**, 1861 (1962).
- [141] Amelinckx, S., and Delavignette, P., *Phys. Rev. Letters* **5**, 50 (1960).
- [142] Edmundson, B., and Williamson, G. K., *Phil. Mag.* **9**, 277 (1964).
- [143] Ashby, M. E., and Brown, L. M., *Proc. Intern. Conf. Electron Microscopy, Philadelphia 1962* (Academic Press, New York, 1962) p. K-5.
- [144] Rühle, M., and Wilkens, M., *Phys. Stat. Sol.* **16**, K 105 (1966).
- [145] Essmann, U., and Wilkens, M., *Phys. Stat. Sol.* **4**, K53 (1964).
- [146] Rühle, M., Wilkens, M., and Essmann, U., *Phys. Stat. Sol.* **11**, 819 (1965).
- [147] Silcox, J., and Hirsch, P. B., *Phil. Mag.* **4**, 1356 (1959).
- [148] Hirsch, P. B., Cotterill, R. M. J., and Jones, M. W., *Proc. 5th Intern. Congr. Electron Microscopy, Philadelphia 1962* (Academic Press, New York, 1962) p. F-3.
- [149] Siems, R., Delavignette, P., and Amelinckx, S., *Z. Physik* **165**, 502 (1962).
- [150] Gevers, R., Delavignette, P., Blank, H., and Amelinckx, S., *Phys. Stat. Sol.* **4**, 383 (1964).
- [151] Gevers, R., Van Landuyt, J., and Amelinckx, S., *Phys. Stat. Sol.* **11**, 689 (1965).
- [152] Delavignette, P., and Amelinckx, S., *Appl. Phys. Letters* **2**, 236 (1963).
- [153] Remaut, G., Lagasse, A., and Amelinckx, S., *Phys. Stat. Sol.* **7**, 497 (1964).
- [154] Van Landuyt, J., Gevers, R., and Amelinckx, S., *Phys. Stat. Sol.* **13**, 467 (1966).
- [155] Fisher, R. M., and Swann, P. R., *Annual EMSA Meeting Denver* (1963).
- [156] Villagrana, R., and Thomas, G., *Appl. Phys. Letters* **6**, 61 (1965).
- [157] Fuller, H. W., and Hale, M. E., *J. Appl. Phys.* **31**, 238 (1960).
- [158] Jakubovics, J. P., *Phil. Mag.* **10**, 277 (1964); Wilkens, M., *Phys. Stat. Sol.* **9**, 255 (1965); Hirsch, P. B., Howie, A., and Jakubovics, J. P., *Int. Conf. on Electron diffraction and crystal defects. Melbourne, 1965 B-5*.
- [159] Van Landuyt, J., Gevers, R., and Amelinckx, S., *Phys. Stat. Sol.* **9**, 135 (1965).
- [160] Remaut, G., Gevers, R., Lagasse, A., and Amelinckx, S., *Phys. Stat. Sol.* **10**, 121 (1965).
- [161] Remaut, G., Gevers, R., Lagasse, A., and Amelinckx, S., *Phys. Stat. Sol.* **13**, 125 (1966).
- [162] Secco d'Aragona, F., Delavignette, P., and Amelinckx, S., *Phys. Stat. Sol.* **14**, K115 (1966).
- [163] Menter, J., *Proc. Roy. Soc.* **A236**, 119 (1956).
- [164] Hashimoto, H., Mannami, M., and Naiki, T., *Phil. Trans. Roy. Soc.* **A253**, 459 (1961).
- [165] Cowley, J. M., and Moodie, A. F., *Acta Cryst.* **10**, nr. 10, 609 (1957).
- [166] Komoda, T., *Optik* **21**, 93 (1964).
- [167] Pashley, D. W., Menter, J. W., and Bassett, G. A., *Nature* **179**, 752 (1957).
- [168] Bassett, G. A., Menter, J. W., and Pashley, D. W., *Proc. Roy. Soc.* **A246**, 345 (1958).
- [169] Gevers, R., *Phil. Mag.* **7**, 1681 (1962).
- [170] Pashley, D. W., Howell, M. J., Jacobs, M. H., and Law, T. J., *Phil. Mag.* **10**, 127 (1964).
- [171] Whelan, M. J., and Hirsch, P. B., *Phil. Mag.* **2**, 1121, 1303 (1957).
- [172] Gevers, R., Van Landuyt, J., and Amelinckx, S., *Phys. Stat. Sol.* (to be published).
- [173] Fitzgerald, A. G., and Mannami, M., *Proc. Roy. Soc.* **A293**, 169 (1966).
- [174] Van Landuyt, J., Gevers, R., and Amelinckx, S., *Phys. Stat. Sol.* **18**, 167 (1966).
- [175] Willaime, C., Delavignette, P., Gevers, R., and Amelinckx, S., *Phys. Stat. Sol.* **17**, K173 (1966).



# ELECTRON AND OPTICAL MICROSCOPY

## Contributed Papers and Discussion

HEINZ G. F. WILSDORF

*Department of Materials Science  
University of Virginia, Charlottesville, Virginia*

### I. Introduction

My task, namely to discuss the contributed papers of this session, has been made easy in that the contributions are very interesting and of excellent quality. But before embarking on these discussions I would like to provide some focus on a few details related to the techniques involved.

Three methods of analysis have been employed which singly or in combination have proven to give valuable results when applied to the analysis of trace elements. They are : (i) microscopy, both light optical and electron optical, (ii) x-ray and electron diffraction, and (iii) electron probe analysis.

The usefulness of the light microscope is unchallenged and I rather would like to dwell upon some features of the electron microscope. Due to the properties of fast electrons this instrument has an inherent theoretical resolving power of about 1 atomic distance as well as the capability to enlarge an image to a size so that all the details can be easily seen with the naked eye. R. D. Heidenreich reported recently [1] a resolution of two angstroms and his micrographs show indications of the atomic arrangements of carbon in the basal plane of graphite.

This result has been obtained by viewing the specimens in transmission. It should be remembered, however, that the observation of surfaces by replica techniques will yield only a resolution of about 25 Å. Obviously, then, preparation techniques for electron microscopy must receive a great deal of attention in connection with our aim.

A case in point is the detection of small particles of a second phase in a matrix. The image contrast in such a specimen can be caused by the following effects: (1) mass-thickness effects, (2) diffraction contrast due to different reflections in matrix and particle, (3) phase changes at the interface, (4) structure factor contrast, that is: different extinction distances for the two substances, (5) production of Moiré patterns due

---

<sup>1</sup> Figures in brackets indicate the literature references at the end of this paper.

to geometrical effects at the interface, (6) strain contrast. Extensive investigations have been carried out to determine the smallest particle size visible, and the result indicates that the limit is about 40 Å [2].

Now, I have to mention some features in electron microscopy which have to be carefully taken into account when considering this method for trace analysis. Firstly, I have to point out the interaction of beam electrons with the substance to be analyzed. It is known that high speed electrons lose about 10 eV when passing through matter due to electron excitation and ionization. Although the energy provided by the electrons is too low for the displacement of atoms, it has been observed that point defects in the specimen can be expected to move through the lattice under the influence of the imaging beam. For our consideration this could mean a redistribution of point defects but no change in the overall impurity content.

The above mentioned phenomenon will lead to two additional effects namely the heating of the specimen and the contamination of the specimen. Due to the irradiation by electrons and the subsequent heating effects, the decomposition of unstable solids can occur. The contamination of the specimen will occur because of the decomposition of hydrocarbons, which are available in the vacuum, so that the remaining carbon will be deposited as a layer on the specimen.

I am proceeding now to the electron diffraction method and I will discuss a rather special case. The electron microscope also offers the opportunity to do electron diffraction after viewing the specimen simply by changing the optical path of the electron beam in the instrument. This type of electron diffraction is referred to as "selected area diffraction." It is very helpful to utilize this technique for the identification of the structure of the specimen which can be observed at high magnifications in the instrument. However, due to the spherical aberration of the lens system involved, slight changes of the area seen in the microscope can occur for the electron diffraction study. Also the distortion of the diffraction pattern is easily possible and while the accuracy is suffering from one two-hundreds of a percent for small orders of reflections, for high orders this error may amount to about 1%. It is clear that this technique has to be employed with great care for precision measurements, and the standardization of the instrument is mandatory.

Finally, I come to the electron microprobe. The actual instrument will receive our attention in some of the contributed papers so that I would like to mention at this time only an attachment which can be found already on one make of electron microscope. This microanalyzer is based on the same scientific principle as the microprobe instrument and allows the subsequent observation and analysis of the specimen in the electron microscope. The range of analysis covers elements with atomic numbers from 10-40 with the resolution of about two at

an exposure time between 30–90 sec. The smallest area which can be analyzed has approximately a diameter of 2 microns and the amount of material to be detected is on the order of  $10^{-13}$  g. Of course, the inherent resolution of the electron microscope is somewhat affected and amounts to about 100 Å.

## II. Contributed Papers

The first contributed paper to be discussed is concerned with the identification of defects in aluminum oxide which have been produced by the bombardment of neutrons. The paper is offered by D. J. Barber and N. J. Tighe of the National Bureau of Standards in Washington, D.C. The analytical tool in this investigation was the electron microscope using the transmission technique. The specimens, synthetic sapphire, were irradiated in the Oak Ridge Research reactor with a neutron dose of  $1.8 \times 10^{20}$  n.v.t. After cutting the specimens parallel to the basal plane and chemical thinning, the discs were annealed in air for 6 hours at temperatures ranging from 280 °C. to 1500 °C. Before turning to the discussion of the atomic defects, it is of interest to note the changes of a bulk property with annealing time. The dependence of hardness with annealing temperature for the neutron irradiated  $\text{Al}_2\text{O}_3$  was determined. It was shown that with increasing temperature the hardness decreases until a temperature of 1350° has been reached and then the hardness increases with further increase in temperature.

The as-irradiated specimens showed point defect clusters which with increasing annealing temperatures condensed into voids and platelike precipitates. Samples annealed at temperatures below 1200°C. showed vacancy and interstitial loops.

The strain caused by the point defect clusters and voids makes it possible for them to be seen by diffraction contrast in the electron microscope. After annealing the samples at temperatures of about 1300 °C, dislocations started to climb but impurity pinning was also in evidence. An interesting feature of the investigation was the observation of dislocation behavior when annealing specimens in the electron microscope. The authors point out, however, that the behavior of specimens in the hot stage is complicated by the fact that point defects can be created in the electron microscope through the electron beam at temperatures of about 1500 °C.

In summary one can state that the transmission technique of the electron microscope is a powerful tool for observing minute defects caused by neutron irradiation and that vacancy and interstitial clusters can be distinguished from voids and precipitates. This information, of course, is of importance when trying to interpret bulk properties as, for example, the change of hardness with annealing temperature.

The next paper is an electron microprobe and electron diffraction analysis of surface replica extractions by W. B. Estill, M. M. Robertson,

and G. H. Conrad of the Sandia Laboratory, Albuquerque, New Mexico. Three techniques, the electron microprobe, electron diffraction and electron microscopy are employed for the analysis of micro-contamination on surfaces and for sampling precipitates or particles in the matrix.

First we will discuss the sampling of micro-contamination on surfaces. After selecting a suitable surface area using optical microscopy, a thin plastic layer is cast onto this area and later on is stripped. The side of the film which shows the extracted particles is then coated with carbon by evaporation and subsequently, the plastic film is dissolved. After suitable mounting the specimen is ready for analysis with the electron microprobe. After the spectrum has been recorded with this instrument, the identical area is viewed in the electron microscope and, following this particular analysis, the electron diffraction analysis is made by the selected area diffraction technique.

For sampling precipitates or particles which are contained in a matrix, the usual extraction replica is taken and then scanned in the electron microprobe. It is worthwhile to remember that during the scanning of the electron beam a thin film of carbon is laid down on the specimen surface. This film, of course, can be used as supporting film for the electron microscope and electron diffraction study after the plastic film has been dissolved. In this way the contamination by the electron beam during electron microprobe scanning can be converted into a beneficial factor.

The introduction of the electron microprobe study preceding an electron microscope and electron diffraction investigation is of importance since it provides information on the composition of the particles. The combination of the chemical analysis as obtained by the electron microprobe plus the structure determination by electron diffraction and the determination of the shape of the particles thus can yield a complete analysis of the particles involved. This conclusion has been demonstrated in the paper by a number of typical examples, as for instance the contamination of a surface by  $K_2Cr_2O_7$ .

The paper by Charles Hays of the Franklin Institute Research Laboratories in Philadelphia, Pennsylvania and by Robert J. Gray of the Oak Ridge National Laboratory, Oak Ridge, Tennessee, reports on some methods for identification of microconstituents in metals and alloys and the application of quantitative metallography. These methods are of importance for determining the composition of phases in binary alloys. Normally, the metallurgist uses a metallographic sample which has been prepared by cutting, polishing, and etching. However, the etching technique may introduce artifacts or change the individual components of the alloy to some extent. Therefore, the authors proposed the following procedure.

Provided the secondary phase in the alloy can be attacked by chemical means, the analysis is aided by concentrating this phase through

electrolytic extraction or chemical extraction or by mechanical extraction. Depending on the size of these microconstituents, different methods of direct analysis can be utilized. If the size of the particles is less than  $3 \mu$ , electron microprobe instruments or electron microscopy must be employed. For particle sizes between 4 and  $25 \mu$  light microscopy is useful and for particle sizes larger than  $25 \mu$  light microscopic inspection and x-ray diffraction will be adequate. Table 1 lists a number of additional characterization methods for this second phase.

TABLE 1. Methods of additional analysis for quantitative metallography.

1. Electron microprobe analysis
2. X-ray microscopy
3. X-ray fluorescence
4. Electrodeposition
5. Micro-radiography
6. Auto-radiography
7. Electron or x-ray diffraction
8. Spectroscopy.

Consequently, it is proposed that extraction techniques should be utilized for concentrating a microscopic constituent following a suitable selection of the analytical techniques. The authors have worked out equations which involve the observed area, the volume, and the density of the microconstituents so that the weight percentage of one of the components in the alloy mixture can be easily calculated.

As a special application they describe the characterization of carbide inclusions in the nickel-molybdenum system. As their micrograph illustrates, spheroidal inclusions are very frequent in this alloy and the question was to determine whether these inclusions were  $M_6C$ ,  $M_{23}C_6$ , or some other complex. Using an extraction cell the carbide inclusions were concentrated and subjected to an x-ray diffraction analysis. The results showed that the particles were carbides belonging to the structural type  $M_6C$ . Following this, a spectrographic study was made which revealed the presence of molybdenum, iron, chromium and vanadium. This suggested that molybdenum and iron were the prime metallic components of these  $M_6C$  carbides.

K. F. J. Heinrich of the National Bureau of Standards, Washington, D.C. gives a critical assessment of the determination of trace elements by electron probe microanalysis. The author points out that the electron microprobe is not a typical trace analysis technique but that it is a very powerful microanalytical technique. The use of the instrument for trace analysis will be successful if trace elements can be preconcentrated and a number of possibilities are listed.

The questions which one would like to ask when thinking of the electron microprobe for the determination of trace elements are, for instance,

which are the elements that can be detected, how large is the excited specimen volume and what are the limits of detectability. The answers provided are as follows: The elements that can be detected range from boron to the transuranic elements. The excited specimen can have a volume from about one to ten cubic microns which means that the mass of specimen analyzed is between  $10^{-10}$  to  $10^{-11}$  g. The limits of detectability are given as 0.01–0.2%. This leads to the conclusion that for a limit of detection of 0.01% an absolute amount of  $10^{-14}$  to  $10^{-15}$  g can be found. Finally it should be mentioned that the accuracy of the method is from 2–10% of the amount present for major constituents.

It must be clear that in order to obtain results of such sensitivity, a considerable amount of work is needed for the preparation of samples. The author observes that systematic investigations have not been undertaken as yet to optimize the experimental conditions for this type of analysis.

The paper by W. C. McCrone, of McCrone Associates Inc., Chicago, Illinois, also concentrates on one particular technique. The paper is entitled "Trace Analysis by Microscopy." In order to prevent confusion between the terms microanalysis and trace analysis the author gives the definition of these two terms at the beginning of his paper. Microanalysis involves the determination of the major component in a very small sample, while trace analysis usually refers to the identification or determination of very small percentages of elements or compounds in a relatively large sample. When using microscopy, it is important to realize that the trace elements or trace constituents can exist in two states of aggregation or, say, dispersion. Firstly, they can be uniformly dispersed as a solid solution in a matrix or in a liquid, and secondly, they can be dispersed as small discrete particles in a very large matrix. If the trace elements are dispersed in a solid solution they ought to be identified by detecting and measuring some chemical or physical properties of the molecules or ions. In general, a concentration procedure has to be employed. For a dispersion of small discrete particles or precipitates, of course, the actual characteristics of that phase can be used for identification.

When performing a trace analysis it is mostly required to determine the percentage of the known trace constituent while the use of the microscope often enables also the identification of the minute sample. Hereby the microscope may be used only as the initial instrument and additional techniques will have to be brought into play. The article deals first with the characterization and identification of subnanogram samples. If one uses light microscopical methods subnanogram samples of ten microns down to two microns can be utilized. The weight of these specimens is on the order of  $10^{-12}$  g. The electron microscope can make visible samples down to about 100 Å and the samples then have a weight of  $10^{-18}$  g.

The advantage of using the light microscope is that a complete morphological analysis can be made and Table 2 lists the major features

TABLE 2. Observations by microscopy.

1. Shape
2. Surface Characteristics
3. Homogeneity
4. Transparency
5. Color
6. Birefringence
7. Refractive Index

that can be observed. Furthermore, the basic observations can be complimented by the measurement of physical properties, such as the measurement of density or melting point; other techniques for the study of physical properties are x-ray diffraction, ultra-microspectrometry, x-ray fluorescence and microchemical tests; also microprobe analysis and dispersion staining should be mentioned. Explanations of all of these measurements are given in the paper and I will refrain from giving a detailed account with one exception, namely, the dispersion staining technique. This technique is suitable for small particles of any transparent substance. The method is based on the appearance of very specific colors when the particles are dispersed in a particular liquid of a certain refractive index. For this investigation the microscope is used in dark-field.

The characterization and identification of dispersed trace constituents involves first the concentration of a small sample of nearly pure material. A great number of these techniques have been mentioned prior to this session and I will only refer to the author's account of some unusual techniques such as ion exchange beads, electrophoresis on a single fiber, or concentrations through biological procedures. For example, the measurement of the growth rate of microorganisms as a function of the amount of a required chemical substance in the diet can be used for such a procedure.

Not always will it be necessary nor will it be possible to provide a concentration of the trace elements. In these cases, fluorescence and radiography are two successful techniques which have been applied in the past. For radiography one distinguishes between auto- and induced radiography. Employing fluorescence techniques it is possible to detect concentrations of 1 ppm. Using radiography, particles of nuclear debris one or two microns in diameter can be detected by an exposure on x-ray film.

The paper shows convincingly that microscopy is indeed a very powerful technique for trace analysis, in particular, using the instruments in conjunction with other means of investigation.

A paper entitled "Stacking Fault Studies in Silver Alloys" by A. W. Ruff, Jr., of the National Bureau of Standards in Washington, D.C., discussed measurements of the amount and energy of stacking faults in a face-centered-cubic material. The geometrical properties of stacking faults were first reviewed. The importance of stacking faults rests primarily on the properties of (111) glide dislocations which extend to form two partial dislocations and a stacking fault ribbon. The motion and interaction of dislocations may be greatly modified by this extended configuration. It is, therefore, of fundamental importance in studying the properties of dislocated materials to know accurately the stacking fault energy  $\gamma$ . For alloy materials it is established that  $\gamma$  depends in general on solute concentration. Measurements of this variation in silver-tin solid solution alloys are reported in this paper.

Two different methods of measurement were employed. The most direct method involved the technique of transmission electron microscopy where threefold extended dislocation nodes were directly observed and measured. The second technique utilized the effect of stacking faults on the x-ray diffraction pattern from the alloy materials. Using both techniques, the absolute values of  $\gamma$  and their dependence on solute concentration were determined and compared.

Figure 1 shows examples of dislocation nodes from four alloys as observed in the electron microscope. These samples were plastically deformed a few percent before examination at 100 kV. The details of

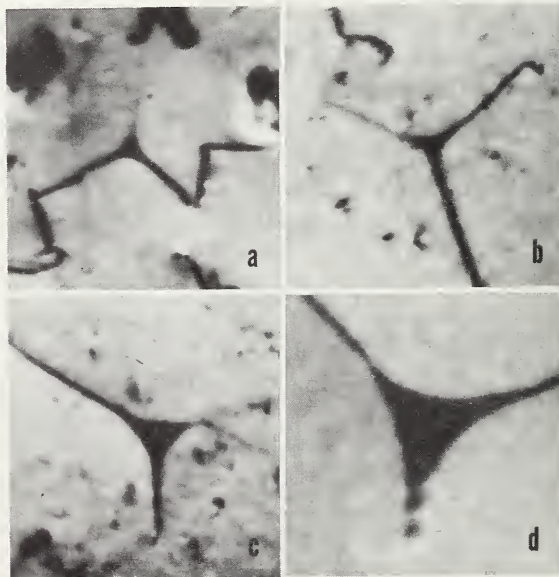


Figure 1. Faulted dislocation nodes observed by transmission electron microscopy in alloys containing (a) 0, (b) 2, (c) 4, and (d) 6 at. % tin in silver.  $M = 130,000$ .

the observation and correction procedures have been given elsewhere [3]. It is seen that the amount of node extension (i.e., the size of the central faulted region) increases with increasing solute concentration. According to theory [4], the radius  $\gamma$  of a circle inscribed within the faulted region and the stacking fault energy  $\gamma$  are related as

$$\gamma\gamma = Gb_p^2\varphi(\nu, \alpha, \epsilon).$$

Here  $G$  is the shear modulus,  $b_p$  the partial dislocation Burgers vector, and  $\varphi$  is a function of variables of the dislocation problem. The stacking fault energy  $\gamma$  was found to decrease as the amount of tin increases in the alloys. The quantitative results are shown in Figure 2 by the curve marked Nodes, determined for six different alloy compositions. These results were compared with those from other silver alloys and good agreement was found. It was pointed out that each electron micrograph examines only about  $10^{-13}$  cm<sup>3</sup> of material and the techniques of sampling are crucial if large systematic errors are to be avoided.

The x-ray diffraction measurements were performed on the same alloys but in different form. Two types of samples were studied: powders obtained from filings produced at room temperature, and bulk bar specimens that were plastically deformed in compression. The change in the Bragg diffraction angle ( $\Delta 2\theta$ ) that occurs after plastic deformation can be related to the stacking fault probability  $\alpha$  according to theory [5] as follows,

$$\alpha = f(\theta_{hkl})\Delta 2\theta.$$

Here the function  $f(\theta)$  contains variables of the diffraction problem. The fault probability  $\alpha$  can be interpreted physically as the reciprocal of the interplanar spacing between completely faulted layers. Measurements on the silver-tin alloys [6] revealed that  $\alpha$  increased smoothly with solute concentration in both types of samples. It was also possible to determine the dislocation density in the samples by further x-ray analysis or by direct electron microscope observation. An example of the observed microstructure is shown in Figure 3 for the 6 at.% alloy. Then using a particular model of the diffracting defect, the stacking fault energy  $\gamma$  can be calculated as

$$\gamma = K\rho/\alpha.$$

Here  $\alpha$  is the fault probability,  $\rho$  the dislocation density, and  $K$  includes various constants of the problem. Figure 2 shows the results obtained in this way for the two types of x-ray samples. It was emphasized that all three curves shown were determined independently in absolute value. The x-ray results for the filed samples agree fairly well with the dislo-

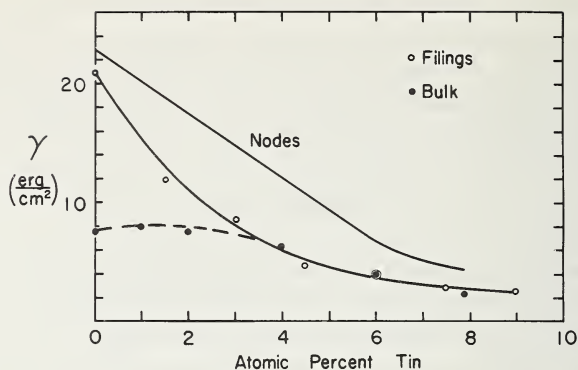


Figure 2. The stacking fault energy determined for silver-tin alloys.

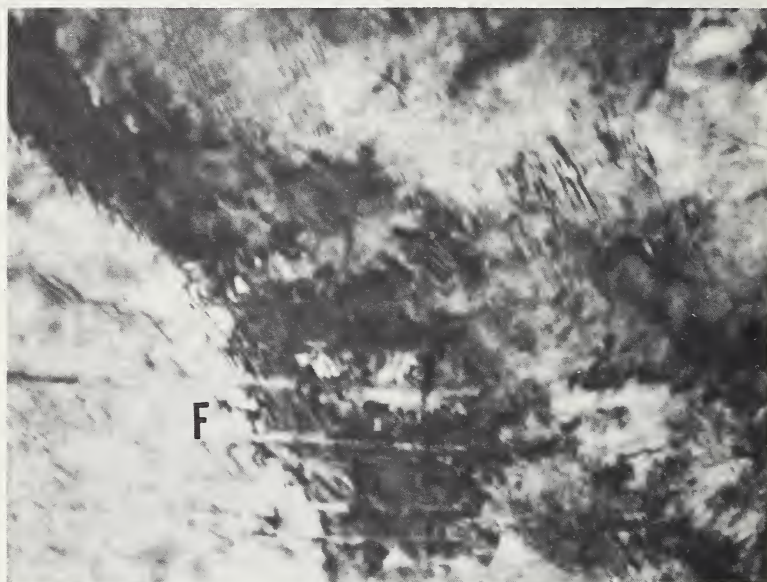


Figure 3. Transmission electron micrograph of dislocation structure in compressed x-ray specimen of 6 at. % tin.  $M=200,000$ .

cation node results for low and high tin concentrations. The agreement for intermediate values of solute concentration is not as good. The results for the bulk compressed samples diverge considerably at low tin concentrations; the reason for this difference is not yet clear. Further study using these and other measurement methods should improve the knowledge of the stacking fault energy in these materials.

The last paper is concerned with the identification of defects in oxides using transmission electron microscopy. The paper is by N. J. Tighe and A. Hyman of the National Bureau of Standards, Washington, D.C.

The substance investigated here is aluminum oxide, using two different types of this material, the analysis of which is given in Table 3. The specimens were cut up into discs 50–70  $\mu$  in thickness, and finally thinned by ionic bombardment.

TABLE 3. Analysis of two alumina samples.

$\text{Al}_2\text{O}_3$

*Sample A:* Purity 99.8%

Impurities: Mg 0.15%;

Si 0.03%; Ca 0.004%; Fe 0.002%

*Sample B:* Purity 99.7%

Impurities:  $\text{Na}_2\text{O}$  0.10%;

$\text{Fe}_2\text{O}_3$  0.10%;  $\text{SiO}_2$  0.05%;

$\text{K}_2\text{O}$  0.05%

Transmission electron microscopy yielded significant differences between the alumina designated A and B. While for alumina A the usual grain boundaries were observed and little or no evidence of impurity precipitation could be found, the grain boundaries in alumina B were irregular, and impurity precipitates and voids within the grains were clearly visible. This investigation provides further evidence that transmission electron microscopy of alumina can easily reveal important differences due to impurities between specimens.

### III. Discussion

In opening the general discussion, Dr. Newkirk remarked that there were several contributed papers in which the term x-ray microscopy was used. This may introduce a little confusion unless x-ray topography is mentioned at the same time and the two terms are clearly distinguished. To one school x-ray microscopy means projection x-ray microradiography. That is not a diffraction method at all. And to another school x-ray microscopy means diffraction topography in which the original image is not really magnified at all so that it is not really microscopy, yet the term has come to mean that occasionally. We should distinguish between x-ray topography and x-ray microradiography or x-ray microscopy.

J. B. Wachtman (NBS) asked Dr. Estill whether the technique that he described appears to be one capable of handling nanogram samples. A speaker earlier in the conference had pointed out the great difficulty in handling very small samples as opposed to the difficulty of analyzing them. The technique which Dr. Estill described in the context of a particular application to surface contamination might, however, be a way of handling very small specimens in general. Dr. Estill indicated

that he had not made any calculations on the sensitivity of the method but that this method presumably would fall in the category of trace analysis.

When asked to comment on the microprobe, Dr. Heinrich stated that it has to be realized that electron microprobe analysis is not a single method. So the limits, depending on the particular technique, are very wide. However, the instrument can analyze in many instances a single layer of atoms and, considering the amount of material that is contained in one square micron of the single layer of atoms, this is indeed an extreme micro-method. Concerning the manipulation of instruments, one of the advantages of the method is that the sample can be analyzed in situ.

The rapporteur called upon W. C. McCrone to add any comments on microscopy. Dr. McCrone emphasized the importance of the electron microprobe and pointed out that it combines both trace analysis and microanalysis. Actually a trace analysis can be made on an ultra-micro sample. In favorable circumstances when everything is lined up beautifully, analyses can be made of single particles less than  $1 \mu$  in diameter for trace elements.

J. B. Wachtman noted that specimens have to be exceedingly thin to be used for transmission electron microscopy. He asked Dr. Amelinckx to comment on this, and also on the question of what opportunity the new high voltage microscopes offer in the use of thicker specimens, and whether this higher voltage carries with it the danger of damage to the specimen.

Dr. Amelinckx commented as follows: First of all, as to the thickness of the specimens, this depends solely on the type of specimen, specifically on the Z value of the element involved. With aluminum, specimens of  $1 \mu$  thickness can be used with a 100 kV electron microscope. However, with uranium you are restricted to 400 to 500 Å.

Of course, the specimen thickness is important in that the technique in certain cases has severe limitations. You have to be aware of the fact that you are working with a thin specimen and sometimes the behavior of these specimens is not the same as that of the bulk specimens. As a concrete example, precipitation phenomena appear to be different in thin foils in comparison to bulk specimens. Also, surface effects become important. For instance, to measure stacking fault energy as shown by Dr. Ruff, you use dislocation ribbons. Then you have to be aware of the fact that, on account of the thin specimen, the repulsion forces between these dislocations are not the same as they would be in the bulk material. Consequently, if one does not correct for the presence of the surface, an error will be made.

Dr. Amelinckx referred to the second question on how can the situation be improved. One way of doing it is, of course, to use high voltage microscopy, say at 1 MeV instead of 100 kV. There is a practical limit

in the sense that whereas you still gain in resolution by going to 1 MeV, this rapidly levels off and there is not much point in going beyond 1.5 MeV. Although one still gains in penetrating power there is again a leveling off and a compromise will have to be made somewhere between 500 kV and 1 MeV. Another consequence of high voltages, of course, is the fact that you create radiation damage. By calculation we can easily see that for 1.1 MeV the threshold for the displacement of a metal atom by electrons is reached, assuming about 25 eV as the displacement energy. Radiation damage then limits again the high voltage that can be used.

Moreover, the interpretation of the micrographs becomes more difficult. Two beam situations are necessary if you want to analyze diffraction contrast phenomena quantitatively. As you go to higher voltages the Ewald sphere becomes flatter and flatter and it becomes increasingly more difficult to realize two beam situations. And so we are in need of multiple beam calculations and these are more difficult to perform than two beam calculations. These are a few advantages and drawbacks of using high voltage electron microscopy.

#### IV. References

- [1] Heidenreich, R. D., *The Bell System Technical Journal* XLV, 651 (1966).
- [2] Ashby, M. F., and Brown, L. M., *Phil. Mag.* **8**, 1649 (1963).
- [3] Ruff, A. W., Jr., Kves, L. K., *Acta Met.* (in press).
- [4] Brown, L. M., and Thólfén, A. R., *Discussions Faraday Society* **38**, 35 (1964).
- [5] Paterson, M. S., *J. Appl. Phys.* **23**, 805 (1952).
- [6] Newton, C. J., and Ruff, A. W., Jr., *J. Appl. Phys.* **37**, 3860 (1966).



## APPENDIX I. CONTRIBUTED PAPERS\*

### ELECTROCHEMICAL METHODS

- BIEDERMANN, George, NEWMAN, Leonard, OHTAKI, Hitoshi. Determination of Traces of Protolytic Impurities. Department of Chemistry, The Royal Institute of Technology, Stockholm, Sweden.
- GIERST, L., NICOLAS, E., VANDENBERGHEN, L., BIRKE, R. L. Characteristics and Potentialities of the Chlorite Catalytic Wave for Trace Analysis. Free University of Brussels, Brussels, Belgium.
- JOYCE, R. J., WESTCOTT, C. C. Evaluation of Mercury Film Electrodes for Trace Analysis of Reagent Grade Chemicals by Stripping Analysis. Beckman Instruments, Inc., Fullerton, California.
- MARK, Harry B., Jr. Application of the Catalytic Polarographic Behavior of Certain Metal Complex Systems to Trace Analysis. Department of Chemistry, University of Michigan, Ann Arbor, Michigan.
- MAIENTHAL, E. June, TAYLOR, John K. Application of Cathode-Ray Polarography and Anodic Stripping Voltammetry to Trace and Micro Analysis. NBS Institute for Materials Research, National Bureau of Standards, Washington, D.C.
- PARRY, E. P., OSTERYOUNG, R. A. Application of Pulse Polarography to Trace and Micro Analyses. North American Aviation Science Center, Thousand Oaks, California.
- PHILLIPS, Sidney L. Adsorption Electroanalysis. IBM Corporation, Poughkeepsie, N.Y.
- RECHNITZ, G. A. Ion-Specific Electrodes as Tools for Trace Analysis. Department of Chemistry, State University of New York, Buffalo, New York.

### ELECTRICAL MEASUREMENTS

- BULLIS, W. Murray. Use of the Hall Effect in Trace Analysis of Semiconductors. Institute for Applied Technology, National Bureau of Standards, Washington, D.C.
- MOULDER, John C., CLARK, Alan F., GNIEWEK, John J. Measurement of Effective Electronic Purity by the Eddy Current Decay Method. Institute for Materials Research, National Bureau of Standards, Boulder, Colorado.
- SMAKULA, A. Dielectric Properties and Defects in Single Crystals. Crystal Physics Laboratory, Massachusetts Institute of Technology, Cambridge, Massachusetts.
- SPARKS, L. L., POWELL, R. L. Metals Characterization by Low-Temperature Thermoelectric Methods. Institute for Materials Research, National Bureau of Standards, Boulder, Colorado.

### OPTICAL AND X-RAY SPECTROSCOPY

- ADAMS, P. B., NORTH, C. H. Definitions of Some Terms Pertinent to Trace Analysis. Corning Glass Works, Corning, N.Y., and National Lead Company, South Amboy, N.J.
- ADAMS, P. B., PASSMORE, W. O., CAMPBELL, D. E. The Determination of Trace Elements in Glasses and Refractory Materials by Flame Emission and Atomic Absorption Spectroscopy. Corning Glass Works, Corning, N.Y.

\*These papers were available for discussion at the Symposium but are not included in this summary volume. Publication rights remain with the authors who will make their own arrangements for publication in the scientific literature. (See also Preface.)

- ADLER, Seymour J. The Determination of the Rare Earths in Solid-State Laser Materials. RCA Laboratories, Princeton, N.J.
- CAMPBELL, William J., SPANO, Ernest F., GREEN, Thomas E. Micro and Trace Analysis Using Ion Exchange Resin-Loaded Papers and X-Ray Spectrography. U.S. Department of the Interior, Bureau of Mines, College Park Metallurgy Research Center, College Park, Maryland.
- CHAPLENKO, G., LANDON, D. O. Microspark Spectroscopy in Trace Analysis. Spex Industries, Inc., Metuchen, N.J.
- ELFERS, Lawrence A. Flame Photometric Determination of Stable Cesium in Environmental Media. Radiological Health Research Activities, Robert A. Taft Sanitary Engineering Center, Cincinnati, Ohio.
- FASSEL, Velmer A., GOLIGHTLY, Danold W. Detection Limits of the Elements in the Spectra of Premixed Oxy-Acetylene Flames. Institute for Atomic Research and Department of Chemistry, Iowa State University, Ames, Iowa.
- HOBBS, D. J., REES, Barbara J. Confident Trace Analysis Above and Below the "Limit of Spectrographic Detection. Johnson, Matthey & Co. Limited, Wembley, Middlesex, England.
- RIGDON, Lester P. The Determination of Impurities in Elemental Boron by X-Ray Fluorescence. Lawrence Radiation Laboratory, University of California, Livermore, California.
- CUNNINGHAM, J. L., RYAN, J. R. Trace Characterization of Refractory Materials by Laser Spectroscopy. Harbison-Walker Refractories Company, Garber Research Center, Pittsburgh, Pa.
- SVOBODA, V. High Purity Material Analysis Using Optical Fluorescence Excited by a Continuum Radiation Source. Institute for Research, Production and Utilization of Radioisotopes, Prague, Czechoslovakia.
- VUKANOVIC, Vladimir M., GEORGIJEVIC, Vida M. The Use of External Magnetic Fields in Spectroscopic Analysis of Traces in DC Arc. Institute of Physics, Belgrade, Yugoslavia.
- WALTERS, R. M., COSGROVE, J. F., BRACCO, D. J. X-Ray Excited Optical Fluorescence in the Analysis of Trace Rare Earths. General Telephone and Electronics Laboratories, Inc., Bayside, N.Y.
- WINEFORDNER, J. D. Atomic Fluorescence Flame Spectrometry. University of Florida, Gainesville, Florida.
- WINEFORDNER, J. D. Use of Signal-to-Noise Ratio Theory as a Simple Means of Optimizations of Experimental Conditions and Estimation of Limits of Detection in Flame Spectrometric Methods of Analysis. University of Florida, Gainesville, Florida.

## X-RAY DIFFRACTION

- BURLEY, Gordon. Improved X-Ray Atomic Scattering Factors: Effect on the Detection of Point Defects and Trace Quantities. Institute for Materials Research, National Bureau of Standards, Washington, D.C.
- DESLATTES, Richard D., PARETZKIN, Boris. Trace Characterization for Strain by Double Crystal Topography. Institute for Materials Research, National Bureau of Standards, Washington, D.C.
- van GOOL, W. Materials Characterization by Means of Predominant Defect Situations. Scientific Laboratory, Ford Motor Company, Dearborn, Michigan.
- INOUE, Tamon, NAGAMI, Hatsutarō. Application of Fourier Analysis to X-Ray Stress Measurement. Central Research Laboratory, Tokyo Shibaura Electric Co., Ltd., Kawasaki, Japan.
- PRICKETT, Robert L., VAHLDIEK, Fred W. A High Temperature Single Crystal X-Ray Camera. Air Force Materials Laboratory, Wright Patterson AFB, Ohio.

**OPTICAL METHODS**

- BAKER, John A. Calibration of Impurities in Silicon by Infrared Spectroscopy. Dow Corning Corporation, Hemlock, Michigan.
- CHANG, Te-Tse. Electron Spin Resonance Absorption as an Analytical Tool Exemplified by the Study of Several Ions in Rutile ( $\text{TiO}_2$ ). National Bureau of Standards, Washington, D.C.
- LORIMOR, O. G., SPITZER, W. G., WILLARDSON, R. K., ALLRED, W. P. Characterization and Concentration Determination of Impurities in Semiconductors from Infrared Local Mode Absorption. University of Southern California, Los Angeles, California and Bell and Howell Research Center, Pasadena, California.

**CHEMICAL SPECTROPHOTOMETRY**

- BURRELL, D. C. Trace Elements in Marine Waters by Atomic Absorption Spectrophotometry. Institute of Marine Science, University of Alaska, College, Alaska.
- CHENG, K. L. Spectrophotometric Determination of Microgram and Submicrogram Amounts of Silver with Thio-Michler's Ketone. Department of Chemistry, University of Missouri at Kansas City, Kansas City, Missouri.
- DODSON, E. M. Some Problems in the Assessment of Trace Impurities in Highly Refractory Electronic Materials with Particular Reference to Single Crystal Ruby and Sapphire for Maser and Laser Use. National Physical Laboratory, Teddington, England.
- LUDWICK, J. D. Dual Atmospheric Tracers Utilizing the Fluorescence of Fluorescein and Calcium Acetylsalicylate. Battelle Memorial Institute, Pacific Northwest Laboratory, Richland, Washington.
- LUKE, C. L. Spectrophotometric Determination of Vanadium in Steel. Bell Telephone Laboratories, Inc., Murray Hill, N.J.
- MENIS, Oscar, BURKE, R. W., RAINS, T. C. Evaluation of Absorptometric Methods for the Determination of Nanogram Quantities of Elements in High-Purity Materials. Institute for Materials Research, National Bureau of Standards, Washington, D.C.
- ROSS, H. H. Precision Photometric Analysis Using a  $\beta$ -Excited Isotopic Light Source. Analytical Chemistry Division, Oak Ridge National Laboratory, Oak Ridge, Tennessee.

**NUCLEAR METHODS**

- DEYRIS, M., REVEL, G., ALBERT, Ph. Le Dosage de l'Oxygène dans l'Aluminium par Radioactivation. C.N.R.S., Centre d'Etudes de Chimie Métallurgique, Vitry.
- BLOURI, J., CHAUDRON, Th., ALBERT, Ph. Le Dosage par Radioactivation Neutronique du Soufre et de Quelques Elements Minéraux dans le Carbazole Purifié par Zone Fondue. C.N.R.S. Centre d'Etudes de Chimie Métallurgique, Vitry et Centre d'Etudes et de Recherches de Chimie Organique Appliquée, Thiais, France.
- ENGELMANN, Ch. Analyses de Très Faibles Traces d'Eléments Légers dans les Matériaux de Très Haute Pureté par Activation dans les Photons  $\gamma$  et les Particules Chargés. Centre d'Etudes Nucléaires de Saclay, France.
- ERICKSON, N. E., KRISHNAN, S. S., PERKONS, A. K. Neutron Activation in Forensic Investigations. The Attorney General's Laboratory, Province of Ontario, Toronto, Canada.
- FISHER, D. E., RANCITELLI, L., LAWRENCE, J. F., CURRIE, R. L., BERKEY, E. Some Recent Work on Instrumental Activation Analysis of Meteorites. Cornell University, Ithaca, N.Y.
- HOLM, Dale M., SANDERS, Wm. Mort. Interference Reduction and Sensitivity Improvement in Activation Analysis. University of California, Los Alamos Scientific Laboratory, Los Alamos, New Mexico.

- KRAMER, Henry H., HAMPTON, W. J., MOLINSKI, Victor J., WAHL, Werner, H. Geographic Characterization of Chromium Ore Deposits by Elemental Analysis. Union Carbide Corporation, Sterling Forest Research Center, Tuxedo, New York.
- KRAMER, Raymond A. Characterization of Trace Amounts of Carbon in Aluminum. Aluminum Company of America, Alcoa Research Laboratories, New Kensington, Pennsylvania.
- KRUGERS, Jan. Thickness Measurement of Metal Coatings with Radioisotopes. Hewlett-Packard Company, Palo Alto, California.
- LANDGREBE, A. R., PELLA, P. A., MCCLENDON, L. T., DE VOE, J. R. The Application of Substoichiometric Radioisotopic Dilution Principles to Control Potential Coulometry and Solvent Extraction. Institute for Materials Research, National Bureau of Standards, Washington, D.C.
- LEDDICOTTE, George W. Ultratrace Element Research in the Life Sciences Using Activation Analysis. Research Reactor Facility, University of Missouri, Columbia, Missouri.
- NAGY, L. G., GIBER, J. Adsorption Effects in the Neutron Activation Analysis of High Purity Ge, Si and Ga for Trace Impurities. Polytechnical University Budapest, Budapest, Hungary.
- PERRY, K., AUDE, G., LAVERLOCHERE, J. Improvement of the Sensitivity in 14 MeV Neutron Activation Analysis. CEA-Département des Radioéléments, Centre d'Etudes Nucléaires, Grenoble, France.
- PIERCE, T. B. Experience with Analytical Methods Based on the Measurement of Prompt  $\gamma$ -Radiation Emitted During Charged-Particle Irradiation. Atomic Energy Research Establishment, Didcot, Berks, England.
- PILLAY, K. K. S., MILLER, W. W. Characteristic X-Rays from (n,  $\gamma$ ) Products and Their Utilization in Activation Analysis. The Pennsylvania State University, University Park, Pennsylvania.
- ROBERTSON, D. E., PERKINS, R. W. Trace Elements and  $^{137}\text{Cs}$  in Sea Water by Gamma-Ray Spectrometric Techniques. Batelle Memorial Institute, Pacific Northwest Laboratory, Richland, Washington.
- ROSENBAUM, H. S., ARMIJO, J. S. Fission Track Etching as an Analytical Metallographic Tool. General Electric Company, Vallecitos Atomic Laboratory, Pleasanton, California.
- SMITH, Gilbert W., BECKER, Donald A., LUTZ, George J., CURRIE, Lloyd A., DE VOE, James R. Determination of Trace Elements in Standard Reference Materials by Neutron Activation Analysis. Analytical Chemistry Division, National Bureau of Standards, Washington, D.C.
- STATNICK, R. M., SCHMIDT-BLEEK, F. Identification of Less Than  $10^8$  Molecules Via Radio-Gaschromatography. Department of Chemistry, Purdue University, Lafayette, Indiana.
- TOLGYESSY, J., KONECNY, J., BRAUN, T. Ion-Exchange Membranes in Radio-chelatometric Titrations of Traces of Metals. Slovak Technical University, Bratislava, Czechoslovakia and L. Eötvös University, Budapest, Hungary.
- YULE, Herbert P. Instrumental Reactor Neutron Activation Analysis Studies on 72 Elements Per Sample. Texas A & M University, College Station, Texas.

## MASS SPECTROSCOPY

- BOURGUILLOT, R., CAVARD, A., CORNU, A., STEFANI, R. Analysis of Traces in Beryllium and Uranium by Spark Source Mass Spectrometry. Commissariat à l'Énergie Atomique Centre d'Etudes Nucléaires de Grenoble, Grenoble (Isère), France.
- DESJARDINS, Michel. Trace Impurity Analysis by Spark Source Mass Spectrometry. Corning Glass Works, Corning, New York.

- DOAN, Arthur S., Jr. Existence of Metal Carbide Molecules in Vapor State. Lewis Research Center, National Aeronautics and Space Administration, Cleveland, Ohio.
- OBLAS, D. W., BRACCO, D. J., YEE, D. Y. Trace Analysis in Oxidic Matrices by Solids Mass Spectroscopy. General Telephone & Electronics Laboratories, Inc., Bayside, New York.
- PAULSEN, P. J., BRANCH, P. E. Electronic Analog Computer for Measuring Intensity Areas on Mass Spectrographic Plates. Spectrochemical Analysis Section, National Bureau of Standards, Washington, D.C.
- STROCK, Lester W., OBLAS, Dan. Spark Source Mass Spectrometer Analysis of Refractory Metals. Sylvania Lighting Center, Danvers, Massachusetts, and General Telephone and Electronics Research Laboratory, Bayside, New York.

## PRECONCENTRATION, SAMPLING, AND REAGENTS

- ALVAREZ, Robert. Electrodeposition of Trace Constituents as a Preconcentration Technique for Optical Emission Spectroscopy; Deposition of Silver from Zinc Solution. Spectrochemical Analysis Section, National Bureau of Standards, Washington, D.C.
- BERSIN, Richard L., HOLLAHAN, John R., HOLLAND, Walter D. Applications of Excited Gases to Trace Characterization. Research and Development Department, TRACERLAB/WEST, Richmond, California.
- BURNETT, William T., GOOD, Glenn, CARROLL, Nuala, COHAN, Morton D. An Evaluation of an Original, Plastic, Paper Disk Anion Column. Department of Chemistry, The Louisiana State University, Baton Rouge, Louisiana.
- FREEMAN, David H., KUEHNER, Edwin C. Preparation of Ultra-Pure Reagents. Institute for Materials Research, National Bureau of Standards, Washington, D.C.
- HILL, John H., MORRIS, C. J., FRAZER, Jack W. Cathodic Etching to Prepare Metals for Oxygen Determination. Lawrence Radiation Laboratory, University of California, Livermore, California.
- JOYNER, Timothy, HEALY, M. L., CHAKRAVARTI, D., KOYANAGI, T. Preconcentration for Trace Analysis of Sea Waters. Bureau of Commercial Fisheries, Biological Laboratory, Seattle, Washington.
- KANEKO, Hisamitsu, KOBAYASHI, Hiroshi, UENO, Keihei. Application of Zone Melting Process to the Metal Chelate Systems. Department of Organic Synthesis, Faculty of Engineering, Kyushu University, Fukuoka, Japan.
- MUKHERJI, Anil K. The Ring Oven Technique in Microanalysis. Drexel Institute of Technology, Philadelphia, Pennsylvania.
- O'LAUGHLIN, J. W., HANSEN, R. K., HOFER, R. J., BACHMAN, R. Z., BANKS, C. V. Determination of Trace Impurities in Pure Rare Earth Metals and Oxides by Spectrophotometric and Atomic Absorption Methods. Institute for Atomic Research and Department of Chemistry, Iowa State University, Ames, Iowa.
- ROBOZ, John. Preconcentration Techniques in the Mass Spectrometric Analysis of Trace Impurities in Inorganic Gases. Air Reduction Company, Inc., Central Research Laboratories, Murray Hill, New Jersey.
- SKOGERBOE, R. K., MORRISON, G. H. The Role of Sampling in Trace Analysis. Cornell University, Ithaca, New York.
- WEST, Foymae Kelso, WEST, Philip W., IDDINGS, Frank A. Adsorption Characteristics of Traces of Silver on Container Surfaces. Coates Chemical Laboratories and Nuclear Science Center, Louisiana State University, Baton Rouge, Louisiana.
- YATES, John T., Jr., MADEY, Theodore E. Chemisorption on Atomically Clean Surfaces. Institute for Basic Standards, National Bureau of Standards, Washington, D.C.

**ELECTRON AND OPTICAL MICROSCOPY**

- BARBER, D. J., TIGHE, N. J. Identification of Defects in Oxides by Transmission Electron Microscopy I. Radiation Damage in  $\text{Al}_2\text{O}_3$ . Institute for Materials Research, National Bureau of Standards, Washington, D.C.
- ESTILL, W. B., ROBERTSON, M. M., CONRAD, G. H. Electron Microprobe and Electron Diffraction Analysis of Surface Replica Extractions. Sandia Laboratory, Albuquerque, New Mexico.
- HAYS, Charles, GRAY, Robert J. Some Methods for the Identification of Microconstituents in Metals and Alloys and the Application of Quantitative Metallography. Franklin Institute Research Laboratories, Philadelphia, Pennsylvania and Oak Ridge National Laboratory, Oak Ridge, Tennessee.
- HEINRICH, Kurt F. J. Electron Probe Microanalysis and the Determination of Traces. Spectrochemical Analysis Section, National Bureau of Standards, Washington, D.C.
- MCCRONE, Walter C. Trace Analysis by Microscopy. McCrone Associates, Inc., Chicago, Illinois.
- RUFF, A. W., Jr. Stacking Fault Studies in Silver Alloys. Institute for Materials Research, National Bureau of Standards, Washington, D.C.
- TIGHE, N. J., HYMAN, A. Identification of Defects in Oxides by Transmission Electron Microscopy. II. Study of Polycrystalline  $\text{Al}_2\text{O}_3$ . Institute for Materials Research, National Bureau of Standards, Washington, D.C.

## APPENDIX II. SYMPOSIUM COMMITTEES

### TRACE CHARACTERIZATION Chemical and Physical

W. Wayne Meinke, General Chairman  
Roger G. Bates, Assistant General Chairman

#### Program Committee

Bourdon F. Scribner, Chairman  
Harry C. Allen                      Marvin Margoshes  
Richard D. Deslattes              Oscar Menis  
James R. DeVoe                      Robert L. Parker  
Hans Frederikse                      Elio Passaglia  
David H. Freeman                      John K. Taylor  
John B. Wachtman, Jr.

#### Arrangements Committee

John K. Taylor, Chairman  
William D. Dorko                      Thomas J. Murphy  
Rolf A. Paulson

#### Social Program Committee

David H. Freeman, Chairman  
Robert Schaffer                      David K. Snediker

#### Tours Committee

James R. DeVoe

#### Ladies' Hospitality Committee

Mrs. W. Wayne Meinke              Honorary Hostesses  
Mrs. Roger G. Bates  
Harriet L. Frush, Chairman  
Mrs. Joseph C. Richmond  
Mrs. James I. Shultz  
Mrs. Jon J. Spijkerman  
Mrs. Robert S. Tipson

#### Finance Committee

Roger G. Bates, Chairman  
Thomas B. Hoover                      John K. Taylor



## INDEX

### A

- Absorption, atomic (*see* Atomic absorption)
- Absorption spectrophotometry (*see* Spectrophotometry)
- Absorptivity, molar, 231
- Accelerator source, use of, 341
- Acid, purification of, 396, 421
- Acid, storage of, 425
- Activation analysis, 307
- accuracy and precision, 326
  - charged particle, 320, 344
  - computer techniques in, 345
  - detection limits, 311, 315, 318, 319, 321, 339
  - errors in, 339
  - fast neutron, 316, 340
  - high energy photon, 317, 320, 342
  - instrumentation for, 325
  - prompt radiation, 322
  - slow neutron, 310, 337
  - steps in, 309
- Activation energy, effect of impurity on, 36
- Activator, role of, 17
- Adsorption, losses by, 424
- role of surfaces in, 36
- Air, contamination from, 390
- Alizarin, complexes of, 225
- Alkali halides, color centers in, 16
- dislocation in, 429
  - etching on, 452
  - evaporation spirals on, 449
- Alkaline earths, determination of, 256
- Alloys, electrical measurements of, 74
- Aluminum, cross slip in, 508
- Aluminum grain growth, effect of impurities on, 29, 31
- Aluminum oxide, electron diffraction study of, 549
- identification of defects in, 556
- Aluminum purification, resistivity in, 44
- Aluminum silver alloys, stacking faults in, 513
- Ammonia, purification of, 396
- Analysis, criteria for methods of, 121, 144
- Anisotropic materials, dislocations in, 174
- Anomalous x-ray transmission, impurity effect on, 193
- intensity mapping, 171
- Antiferromagnetic domain boundaries, 527
- Antiphase boundaries, and stacking faults, 493
- Arc, detection limits in, 134
- evaporation in, 133
  - excitation in, 130
  - ionization in, 132
- Arsenate, determination of, 235
- Ashing, low-temperature, 420
- preconcentration by, 411
- Atomic absorption, 266
- assessment of, 280
  - atomizers for, 270
  - Beer-Lambert law in, 279
  - burners for, 275
  - compared to flame emission, 129
  - continuum sources in, 274
  - detection limits in, 164, 282
  - discharge lamps in, 274
  - flame in tube, 276
  - flames for, 268, 277
  - furnace for, 163, 267, 305
  - future of, 283
  - hollow cathode lamps for, 272, 278
  - hollow cathode sputtering in, 271
  - matrix effects in, 280
  - microwave sources for, 275
  - monitor for, 306
  - monochromators in, 273
  - vaporization for, 267, 271
  - wavelengths for, 279
- Atomic fluorescence, 284, 295
- burners for, 289
  - continuum sources for, 292
  - detection limits in, 149, 293
  - discharge lamps for, 291
  - equations for, 287
  - future of, 297
  - instruments for, 289
  - microwave sources for, 291
  - selectivity of, 292
  - sources for, 291
  - types of, 286

Atomic scattering factors, 206  
 Atomic substitution in crystal, 204  
 Atomizers, for atomic absorption, 270  
 Autoradiograms, to test homogeneity, 387

## B

Background, in emission spectrometry, 150  
   in mass spectrometry, 351, 355  
 Barium titanate, domains in, 524, 527, 529  
 Beer-Lambert Law, 231, 279  
 Bend contour, 475  
 Berg-Barrett method, in x-ray intensity mapping, 167  
 Beryllium, determination of impurities in, 377  
   ductility of, 24  
 Beryllium oxide, impurities in, 185  
 Biological materials, electrical measurements of, 74  
 Birefringence, 467  
 Boltzmann equilibrium (*see* Maxwell-Boltzmann equilibrium)  
 Boron, determination of, 345  
 Borrmann effect, 472  
   in x-ray intensity mapping, 171  
 Bragg angle transmission, 171  
 Bragg reflection law, 471  
 Bulk methods, role in dislocation observation, 455  
 Burgers circuit, 432  
 Burgers vector, 432  
   direction determination for, 479  
   length determination, 483  
   sense determination of, 433, 483  
 Burgers vector method, for loop character, 522

## C

Cadmium sulfide, helical dislocation  
   in, 178  
   Moiré patterns of, 190  
   impurity doped, 180  
   thermally stimulated current curves for, 66  
   x-ray diffraction topograph of, 180  
 Calcein blue reagent, 256  
 Calcium, determination of, 222  
 Camera, x-ray single crystal, 205  
 Capacitance measurement, double-layer, 105

Carrier distillation, 409  
 Cartesian Diver system, 208  
 Catalytic current polarography, 88, 113  
 Catalytic wave polarography, 112  
 Cavities, causes of, 516  
 Characterization, definition of, 5  
   for microconstituents, 550  
   importance of, 37  
   importance of defects in, 204  
   *in situ*, 211  
   types of, 6  
 Charged partial activation, 320  
   detection limits, 321  
 Chelate cage reagents, 222  
 Chelating agents (*see* Complexes)  
 Chemical equilibria, in flames, 124, 269  
 Chemical reactions in solids, 29  
 Chromatography (*see also* Ion-exchange) separation by, 406, 407  
 Chromium chloride, stacking faults in, 503  
 Chronoamperometry, 90  
 Chronocoulometry, 94  
 Chronopotentiometry, 90  
 Climb dislocation, 465  
 Climb rate technique, for stacking fault energy, 508  
 Co-activator, in phosphors, 18  
 Cobalt nickel alloys, stacking faults in, 508  
 Cobaltous oxide, domains in, 527  
 Color centers, in alkali halides, 16  
 Complexes, clathrate, 222  
   effect of pH on, 219  
   extraction with, 402  
   for fluorimetry, 254  
   in preconcentrations, 396  
   masking by, 397  
   mixed, 224  
   steric hindrance in, 221  
   ternary, 224  
 Computers, in activation analysis, 326, 345  
 Concentration method (*see* Separations)  
 Conductance, electrolytic, 104  
 Conductivity (*see also* Resistivity), 71  
 Conductometric titrations, high frequency, 104  
 Contamination, from air, 390  
   from electron irradiation, 548  
   from laboratory ware, 391, 394  
   in sampling, 388

- Continuum sources, in atomic absorption,  
274  
in atomic fluorescence, 292
- Contrast, at dislocations, 477  
at slip traces, 508  
at stacking faults, 493  
caused by planar defects, 531  
from ferroelectric boundaries, 524  
in x-ray diffraction topography, 171, 172,  
174
- Coordination number, of ions, 224
- Copper decoration, 178  
in silicon, 464
- Copper, determination of, 229, 304  
oxidation of, 30
- Copper gallium alloy, nodes in, 506  
stacking faults in, 493, 495, 496
- Copper gold alloy, boundaries in, 494
- Coprecipitation, reagents for, 400  
separation by, 398
- Corrosion reactions, 32, 37
- Cottrell interaction, 437, 455
- Coulometric titration, 93
- Coulometry, 92  
galvanic analysis, 95  
of surface layers, 92  
stripping analysis, 96  
thin layer, 92
- Coulostatic analysis, 95
- Crystal chemical fit, of foreign atom, 205
- Crystal defects (*see also* Point defects)  
electron microscopy of, 430, 431  
methods of observation of, 427, 469  
Moiré pattern method, 430
- Crystal distortion, by impurities, 194  
effects on x-ray images, 173
- Crystal growth, role of dislocations in, 428
- Crystal striations, by x-ray topography, 187,  
188
- Crystals, decoration methods for, 455,  
464-466  
defects in, 204, 207, 427  
diffusion in, 24, 25  
effect of dislocations in, 21  
Moiré patterns from, 535  
stacking faults in, 490, 492, 498  
x-ray diffraction study of, 165  
x-ray topographs of, 206  
yield point of, 21
- Cyclotron, in activation analysis, 321
- D**
- Decoration, of dislocations, 175, 204, 429,  
455
- Defect chemistry, 207
- Defect clusters, 512  
detected by electron diffraction, 549
- Defects, by optical phenomena, 212  
effect on diffraction pattern, 537  
importance in characterization, 204  
in crystals, 204, 207, 427  
in oxides, 556, 557  
point, 381  
types of, 6, 204, 205  
visibility of, 174
- Deformation, studied by decoration  
methods, 467  
studied by etch pits, 452
- Delta fringes, properties, of, 525
- Density, Cartesian Diver system for, 208  
reference material for, 208
- Density-sensitive defect properties, 208
- Derivative dilution technique, 331
- Desorption, in storage of solutions, 393
- Detection limits, activation analysis, 311,  
315, 317, 319, 321, 339  
atomic absorption, 164, 282  
atomic fluorescence, 149, 293  
contrasted to "sensitivity", 158  
definition of, 153, 154  
effect of parameters on, 153, 154, 159,  
160  
electrochemical, 75  
electron microprobe, 552  
electron spin resonance, 214  
emission spectroscopy, 134, 162, 163  
fluorimetry, 259  
improvement by replicate determina-  
tions, 156, 157  
infrared spectroscopy, 212, 213  
polarography, 76, 80, 88  
spark source mass spectrometry, 351  
spectrophotometry, 232  
stripping analysis, 98  
trace analysis methods, 418  
x-ray diffraction, 185, 206  
x-ray fluorescence, 143
- Detector, electrical, in mass spec-  
trometry, 383  
lithium drifted, 325  
phase sensitive, 86  
scintillation, 325

- Dielectric constant, measurement of, 71
- Diffraction characterization, of stacking faults, 493
- Diffraction pattern, effect of defects on, 537
- Diffusion, effects of dislocations in, 24-27  
x-ray camera for studies of, 205
- Discharge lamps, in atomic absorption, 274  
for atomic fluorescence, 291
- Dislocation densities, effect of, 21
- Dislocation loops, causes of, 513  
definition of, 433  
energy of, 510
- Dislocation theory, role in crystal growth, 428  
survey of, 431
- Dislocations, arrays of, 443  
climb, 465  
decorated, 175  
definition of, 431  
energy of, 437  
extended, 442  
force on, 437  
forces between, 440  
grain boundary, 443  
helix, 178  
inclined, 487  
in corrosion, 32  
internal methods for, 429  
in whiskers, 467  
movement of, 438  
multiplication of, 440  
observation of, 450, 453, 455, 477, 538  
one-dimensional, 204  
partial, 441  
point defect, 509, 510  
postulation of, 428  
ribbon, 442, 501  
screw, 479  
seen end on, 487  
stacking faults in, 554  
surface methods for, 429, 447  
tilt and twist types, 443, 444  
undercoated, 178  
x-ray condition for disappearance of, 174
- Displacement function, 435
- Displacement vector, 431  
determination of, 497
- Distillation, from solution, 411  
separation by, 409
- Domain boundaries, 524, 527, 538
- Double crystal method, in x-ray intensity mapping, 168  
lattice variations by, 187
- Ductility of metals, effect of impurities on, 24, 25
- Dust, contamination by, 390
- ## E
- Eddy-current method, for resistivity measurement, 57, 72
- Edge dislocation, 431
- Edge-on method, to determine loop character, 520
- Edge ribbon stacking fault, energy for, 505
- Electrical measurements, applications of, 42, 65, 66, 73, 74  
characteristics of, 40  
combined with other techniques, 48  
fundamentals of, 50  
role in trace characterization, 39, 42  
types of, 70
- Electrical properties, effect of impurities on, 7, 40  
effect of oxygen on, 74
- Electrochemical methods, adsorption, 113  
applicability of, 111  
comparison of, 105  
detection limits, 75  
future of, 105  
selectivity of, 119
- Electrodes, for stripping analysis, 115  
glass, 102, 103, 117  
impurities in graphite, 136  
in potentiometry, 101, 102  
membrane, 103  
specific ion, 103, 117, 119
- Electroluminescence, impurity interactions in, 18
- Electrolysis, separation by, 101, 399, 419
- Electrolytic conductance, 104
- Electron density map, 195
- Electron diffraction, 469, 471, 548  
analysis of surface contamination by, 550  
effects of defects on, 537
- Electron microprobe, 143, 551  
amount of sample for, 558  
detection limits, 552
- Electron microscope, resolving power of, 547

Electron microscope-microanalyzer, 548  
Electron microscopy, analysis of surface  
  contamination, 550  
  contrast in, 508, 547  
  crystal defect studies, 430, 468  
  direct lattice resolution by, 531  
  dislocation study by, 430  
  effect of voltage in, 539, 558, 559  
  fringe interpretation in, 532  
  identification of defects in oxides by,  
    556, 557  
  in trace analysis, 548  
  limitations of, 539  
  Moiré patterns in, 430, 532  
  radiation damage in, 559  
  specimen preparation for, 470  
  stacking faults by, 554  
  status of transmission, 538, 539, 547  
  study of crystal imperfections by,  
    468, 469  
  thickness of specimen in, 558  
Electron spin resonance, detection  
  limits, 214  
  impurity measurement by, 213  
Emission intensities (*see* Intensities)  
Emission spectroscopy, 121, 149  
  detection limits in, 134, 162, 163  
  in study of GaAs, 49  
  precision in, 145, 146  
Errors, in sampling and analysis, 422  
Etch patterns, information to be obtained from, 32, 453  
Etch pit formation, compared to growth and evaporation spirals, 452  
Etchants, for specific crystals, 455, 456  
Etching, effect of solution impurities, 452  
  role in dislocation observation, 429, 450  
Evaporation, role in dislocation geometry, 429  
Evaporation spirals, resolution of, 450  
  role in dislocation observation, 449  
Ewald's sphere, 471  
Extended nodes, 504  
Excitation error vector, 471  
Extinction contour, in transmission electron microscopy, 474  
Extraction, separation by, 402, 421  
Extraction techniques, for microconstituents, 551  
Extrinsic fault, 491

## F

Ferroelectric domains, 524  
Ferroelectric polarization, causes of, 524  
Ferroelectric transition temperature, 524  
Ferromagnetic domain walls, 528  
Ferromagnetic resonance, effect of impurities on, 19  
Field ion microscope, study of dislocation by, 431  
Film growth on solids, 30  
Fission tracks, studied by etch pits, 455  
Flames, burners for, 275, 289  
  chemical equilibria in, 122, 123, 269  
  comparison of emission and absorption spectra in, 129  
  excitation in, 122, 123  
  for atomic absorption, 268, 276, 277  
  higher temperature, 129, 130  
  in tubes, 276  
  ionization in, 122, 123  
  nitrous oxide-acetylene, 278  
  vaporization in, 268  
Fluorescence, atomic (*see* Atomic fluorescence)  
  delayed, 245  
  effect of parameters on, 243-246  
  energy transfer in, 258  
  inner-filter effect in, 246  
  lifetimes in, 239  
  mechanism of, 239, 250  
  quantum efficiency of, 243  
  quenching of, 243, 244, 245  
  x-ray excited, 150  
Fluoride, determination of, 225, 234  
Fluorimetry, assessment of, 259  
  compared to spectrophotometry, 252  
  detection limits in, 259  
  future of, 266  
  instruments for, 247  
  reagents for, 252, 253, 256  
  with atmospheric tracers, 304  
Fourier analysis, of powder diffraction line profiles, 205  
Fracture problems, studied by etch pits, 455  
Frank sessile loops, 492  
Frank-Read source, 440  
  in silicon, 464  
Fringe contrast, due to ferroelectric boundaries, 524

Fringe interpretation in electron microscopy, 532  
 Fringes, produced by stacking faults, 496  
 FS/RH rule, for Burgers vector conventions, 433

## G

Gallium arsenide, detection limits in, 213  
 determination of purity of, 48  
 mass spectrum of, 353  
 Gallium phosphide, effect of impurities in, 18  
 Gallium purification, resistivity in, 44  
 Galvanic analysis, 95  
 Gamma activation, 319, 320  
 Gamma ray spectra, resolution of, 325  
 Gases, analysis of, 421  
 Geometrical method, for loop character, 517  
 Germanium, determination of impurities in, 213  
 dislocations in, 21, 192  
 effect of impurities in, 194  
 effect of oxygen on, 74  
 Hall effect measurement of, 62  
 impurity distribution in, 45-47  
 lithium doped, 192  
 precipitation of Cu in, 30  
 x-ray diffraction pattern from, 182  
 Glass electrodes, 102  
 specific ion, 102, 103, 117  
 Glassware, cleaning of, 395  
 contamination from, 391, 393  
 Glide plane, 431  
 Glissile loop, 435  
 Gold, resistivity of, 12, 13  
 stacking faults in, 508, 514  
 Grain boundaries, types of, 443  
 Grain growth, effect of impurities on, 29  
 Grinding, of powders, 390  
 Graphite, Burgers vector determination in, 482  
 dislocation pattern, 503  
 impurities in, 136  
 loops in, 513, 519  
 stacking fault energy in, 523  
 Growth spirals, in crystals, 428  
 role in dislocation observation, 447

## H

Halides, determination of, 104

Hall effect, 73  
 apparatus for, 60  
 application of, 62  
 description of, 52  
 in semiconductors, 61  
 in study of GaAs, 48  
 voltage measurements, 60  
 Helical dislocations, causes of, 516  
 Hermetization, of laboratory operations, 390  
 Hollow cathode lamps, for atomic absorption, 272, 278  
 multi-element, 273  
 of high intensity, 279  
 sputtering in, 271  
 Homogeneity (*see also* Inhomogeneity)  
 methods for attaining, 387  
 of reference materials, 370  
 Hydrochloric acid, purification of, 396, 421  
 Hydrofluoric acid, purification of, 396

## I

Ilkovic equation, 76  
 Image contrast, in electron microscopy, 547  
 in x-ray diffraction topography, 174  
 Image formation, at prismatic loop, 481  
 Imperfections, due to trace impurities, 179  
 types of, 6, 7  
 Impurities, as a cause of bulk stress, 188, 189  
 clustering, 193  
 effect on dislocations, 175  
 effect on electron density distribution, 195  
 effect on intensity of x-ray diffraction, 191  
 effect on phase stability, 198  
 effect on properties, 18, 19, 40, 347  
 effect on solid state reaction kinetics, 199  
 effect on x-ray diffraction, 165, 156  
 effect on x-ray transmission, 193  
 lattice variations from, 186  
 role in physical effects, 211, 212  
 Impurity distribution, by resistivity, 46  
 Impurity segregation, x-ray topography of, 182  
 Inclination contour, 475  
 Indium selenide, loops in, 511

- Infrared spectroscopy, detection limits in, 212, 213  
trace analysis by, 212, 213
- Inhomogeneity (*see also* Homogeneity)  
effect on detection limit, 159  
in solids, 387
- Insulators, electrical measurements on, 51, 52, 65
- Intensities, calculation of emission line, 123  
effect of temperature on emission line, 125, 126
- Intensity mapping, in x-ray diffraction topography, 166
- Interstitial impurities, effect of, 19  
in solids, 26
- Interstitial ordering, domains due to, 527
- Intrinsic fault, 491
- Iodide, determination of, 232
- Ion exchange (*see also* Chromatography) 420  
membrane electrode, 103
- Ion fluctuations, in spark source, 367, 370
- Ionic conductivity, effect of point defects on, 14  
of KCl, 15  
role of, 14
- Ions, energy distribution in mass spectrometry, 361
- Iron, ductility of, 24
- Irradiation, as a cause of point defect clusters, 511  
production of centers by, 34
- Isotope derivative technique, 331
- Isotope dilution, applications of, 330  
in mass spectrometry, 384  
in radiochemical analysis, 328  
substoichiometric, 329
- Isotope displacement technique, 332
- Isotope measurement, in mass spectrometry, 357
- Isotopic methods, in mass spectrometry, 384  
in radiochemical analysis, 328, 420
- Isotropic materials, dislocations in, 174
- K**
- Kikuchi lines, determination of excitation error by, 473
- L**
- Laser probe, analysis with, 150
- Lattice expansion, caused by x-irradiation, 188
- Lattice variations, double crystal method for, 187  
from impurities, 186
- Lead, effect of impurities in, 23  
electrical measurements on, 73
- Lead sulfide, defects in, 9
- Ligands (*see* Complexes)
- Light elements, determination of, 318, 321, 343
- Lithium, dopant in germanium, 192
- Lithium fluoride, birefringence in, 467  
etch pattern on, 452
- Loops, determination of character of, 516, 517-519
- Lorentz force, contrast source in electron microscopy, 528
- Luminescence, effect of impurities and defects on, 17
- M**
- Magnesium, determination of, 223
- Magnetic properties, effect of impurities on, 18
- Masking in preconcentration, 397
- Mass spectrograph, double focusing, 349  
transmission stability of, 359
- Mass spectrometry (*see* Spark source mass spectrometry)
- Mass spectrum, molecular, 381  
of gallium arsenide, 353
- Materials sciences, growth of, 5
- Maxwell-Boltzmann equilibrium, in flames, 123
- Mechanical properties, effect of impurities on, 19  
effect of oxygen on, 22
- Metal ions, specific electrodes for, 103, 117
- Metallography, quantitative, 550
- Metals, effects of impurities on, 10, 23  
electrical phenomena in, 12  
point defects in, 12  
resistance ratios for, 59
- Methods of analysis, criteria for, 121, 144
- Microanalysis, defined, 551  
with electron microprobe, 143  
with laser probe, 150  
with spark, 150
- Micro-contamination, analysis of, 550

Microprobe (*see* Electron microprobe)  
 Microscopy (*see also* Electron microscopy,  
 Optical microscopy)  
   radiography and fluorescence techniques  
   for, 553  
 Microstrain measurements, 206  
 Microwave-powered lamps, 275, 291  
 Moiré patterns, in electron microscopy,  
 430, 532  
   in x-ray diffraction topography, 189, 208  
 Molybdenum, transition temperatures of,  
 14  
 Mössbauer effect, evaluation of, 320

## N

Neocuproine, as spectrophotometric reagent, 222  
 Neutron activation (*see* Activation analysis)  
 Neutron generators, 316  
 Neutron irradiation effects, 549  
 Neutrons, fast, 316, 317  
   thermal, 310  
 Nickel-molybdenum, inclusions in, 551  
 Nickel oxide, domains in, 527  
 Niobium, domains in, 527  
 Nitrogen, determination of, 345  
 Noise, causes and effects of, 154  
 Nomenclature, in trace analysis, 152  
 Non-destructive methods, 211, 318  
 Nuclear methods, other than activation,  
 327, 346  
   types of, 307  
 Nuclear reactor, in activation analysis, 310

## O

Optical methods, role in dislocation observation, 428  
 Optical microscopy, advantages of, 553  
   trace analysis by, 552  
 Optical phenomena, in trace characterization, 211  
   role of impurities in, 211  
 Optical properties, of solids, 15  
 Oscillatory contrast, in dislocation images,  
 487  
 Oxide layer, determination of, 92  
 Oxides, analysis of, 378  
   identification of defects in, 556  
 Oxygen, determination of, 322, 343, 344  
   effect on mechanical properties, 22  
   segregation in silicon, 182

## P

Palladium-gold, Moiré pattern of, 535  
 Partial dislocations, 441  
 Pendellösung method, 196, 207, 208  
 Permeability of iron, effect of nitrogen  
   on, 19, 21  
 Phase changes, effects on properties, 204  
 Phase sensitive detectors, in polarography, 86  
 Phase stability, influence of impurities  
   on, 198  
 Phenanthroline complex, 227  
 Phosphate, determination of, 233, 235  
 Phosphorescence, mechanism, of, 239  
   triplet states in, 242  
 Phosphorimetry, instruments for, 247  
 Phosphors, effects of impurities in, 17  
 Photographic emulsion, mass calibration  
   of, 360, 380  
   mass sensitivity of, 359  
   reciprocity of, 359  
 Photographic process, effect of chemical  
   impurities in, 33  
 Photography, reduction of fogging in, 355  
 Physical effects, role of impurities in, 211  
 Piezoelectric effect, 71  
 Planar defects, 531  
 Plastic deformation, point defects by, 511  
 Plastic vessels, contamination from, 393  
 Platinum vessels, contamination from, 393  
 Point defects, 509-511  
   strain produced by, 549  
   study of, 12  
   x-ray detection limit for, 206  
 Poisons, in phosphors, 18  
 Polarography, adsorption effects in, 88  
   alternating current, 85  
   catalytic current, 88, 113  
   catalytic wave, 112  
   cathode ray, 114  
   classical, 76  
   derivative, 79  
   derivative pulse, 82  
   detection limits, 76, 80, 88  
   elements determined by, 115  
   intermittant, 78  
   pulse, 80, 116  
   radiochemical, 86  
   radiofrequency, 84  
   square wave, 84  
 Tast, 78

- Polygonization, tilt boundary formation, 445
- Potentiometry, direct, 101  
  null-point, 103  
  trace acidity by, 118
- Powders, grinding of, 390
- Precipitates, size determination of, 181  
  strain cross section of, 180
- Precipitation, phenomena, 27  
  reagents for, 400, 402  
  separations by, 398
- Preconcentration (*see also* Separations)  
  methods for, 150
- Prismatic dislocation, 435
- Prismatic loops, 518  
  decoration methods, 467  
  image formation at, 481
- Prompt radiation activation analysis, 323
- Properties, effect of impurities on, 347  
  relation to composition, 7
- Pulse height analyzer, use of, 326
- Purification, of reagents, 395, 396  
  of water, 395  
  resistivity measurement in, 44
- Purity, measure by resistivity, 12
- Q**
- Quantum efficiency, of fluorescence, 243
- Quartz. color centers in, 188  
  impurities in, 188
- Quartz vessels, contamination from, 393
- Quenching, for point defect clusters, 510
- R**
- Radiation effects, in electron microscopy, 559  
  in solids, 33
- Radiochemical analysis (*see also* Activation analysis)  
  non-isotopic, 331  
  separations in, 323  
  using tracers, 327
- Radiofrequency polarography, 84
- Radioisotopes, in study of contamination, 393
- Radiometric titration, 333
- Radiopolarography, 86
- Radioreagent technique, 331
- Radiorelease technique, 332
- Rare earths, trace analysis of, 421
- Reaction kinetics, influence of impurities on, 199
- Reagents, chelate cage, 222  
  for coprecipitation, 402  
  for fluorimetry, 252  
  for precipitation, 400  
  for preconcentration, 404  
  for spectrophotometry, 219, 220  
  purification of, 395, 421  
  storage of, 425
- Reciprocal lattice, 471
- Reference materials (*see* Standard reference materials)
- Refractory metals, analysis of, 378
- Relative sensitivity coefficient, 362
- Residual resistivity, 44, 50  
  apparatus for, 57
- Resistance ratios, of metals, 12, 59
- Resistivity, effect of impurities on, 72  
  low temperature, 10, 11  
  of copper, 10, 11, 12  
  of gold, 12  
  of insulators, 51  
  of semiconductors, 50  
  of water, 43  
  temperature effect on, 71
- Resistivity measurement, 45, 47, 71  
  AC method for, 55  
  apparatus for, 53  
  application of, 43  
  by capacitive coupling, 55  
  by eddy-current, 57
- Resistivity probe, 54, 55
- Resistivity ratios, monitoring purity by, 59  
  of metals, 12
- Resistivity scan procedure, 54
- Resolution, improvement by Moiré patterns, 534  
  in electron microscopy, 531, 532  
  in mass spectrometry, 356
- Ribbon dislocation, 501
- Ruby, analysis of, 304
- S**
- Saha equilibrium, in flames, 124
- Sampling, contamination in, 388  
  errors in, 422, 424  
  of inhomogeneous solids, 387
- Sapphire, analysis of, 304
- Scanning transmission methods, in x-ray intensity mapping, 169

- Screw dislocation, 431, 479
- Screw ribbon, stacking fault energy for, 505
- Selenium, determination of, 294
- Semiconductors, characterization of, 9
- effect of impurities in, 9
  - electrical measurements on, 51
  - electrical properties of, 7
- Sensitivity, contrasted to "detection limit", 158
- Sensitivity coefficients, in mass spectrometry, 362, 379
- Separation methods, future of, 413
- Separations (*see also* Preconcentration)
- by chromatography, 406
  - by electrolysis, 101, 399, 419
  - by extraction, 402, 421
  - by ion-exchange, 420
  - by precipitation, 398
  - by volatilization, 409, 420
  - by zone melting, 412
  - concentration factor of, 419
  - masking in, 397
  - radiochemical, 323
  - recoveries in, 419
- Shockley partials, 442, 502
- Silica gel, purification of, 421
- Silicon, birefringence in, 467
- copper decoration in, 464
  - detection of oxygen in, 181
  - determination of impurities in, 212
  - dislocation-free, 193
  - dislocations in, 429
  - donors and acceptors in, 8
  - effect of oxygen on, 22
  - Hall effect, measurements of, 62
  - oxygen banding in, 182
  - precipitation of Li in, 27
  - surface layers on, 35
  - thickness contours in, 475
  - x-ray topographs of, 175
- Silicon carbide, etch pattern on, 451
- Silver, determination of, 227, 303
- sulfiding of, 30
- Silver alloys, stacking faults in, 554
- Silver bromide, dislocations in, 429
- Silver-indium alloys, stacking faults in, 502
- Slip traces, contrast at, 508
- Sodium hydroxide, purification of, 396
- storage of, 425
- Sorption, in storage of solutions, 393
- Spark, analysis with micro, 150
- surface analysis by, 138
- Spark source, ionization pattern in, 360
- secondary products in, 352
- Spark source mass spectra, molecular, 381
- Spark source mass spectrometry, 348
- accuracy of, 358, 377, 378
  - background in, 351, 355
  - capabilities of, 348
  - computer use in, 381
  - detection limits, 351
  - effect of gases in, 358
  - electrical detection in, 349, 383
  - emulsion calibration in, 360
  - energy distribution of ions in, 362
  - factors affecting, 351, 372
  - future of, 373
  - integration of intensity in, 360
  - ion charge distribution in, 381
  - ion fluctuations in, 370
  - ion samples in, 362
  - precision of ion measurements in, 366
  - quantitative, 358, 382
  - relative sensitivity in, 361
  - resolving power of, 356
  - sample handling in, 378
  - sample homogeneity in, 366, 370
  - sample volatility in, 379
  - selective ion transmission in, 379
  - sensitivity coefficients for, 362, 382
  - standards in, 371
  - suppression of fogging in, 353
- Specific ion electrodes, 102, 117, 119
- Spectrofluorimetry (*see* Fluorimetry, Fluorescence)
- Spectrograph resolving power, effect of, 159
- Spectrographic analysis (*see* Emission spectroscopy)
- Spectrophotometry (*see also* Fluorimetry, Fluorescence)
- amplification reactions in, 232
  - applications of, 304
  - catalytic reactions in, 233
  - compared to fluorimetry, 252
  - detection limits in, 232
  - future of, 237
  - high-precision, 305
  - masking in, 230
  - radioactive light sources for, 305
  - reagents for, 219
  - selectivity of, 217

sensitivity of reactions, 230  
ternary complexes in, 224  
Spin ordering, effect of, 527  
Stacking fault energy, climb rate technique for, 508  
for tetrahedron technique, 508  
measurement of, 501  
Stacking fault fringes, 496  
Stacking fault method, for loop character, 521  
Stacking faults, 441, 490  
antiphase boundaries, 493  
determination in crystals, 498, 554  
effects on electron diffraction, 537  
types of, 490  
x-ray diffraction topography of, 179  
Stacking fault tetrahedra, 514  
Standard reference materials, homogeneity of, 363, 370, 382  
in mass spectrometry, 362, 382  
need for, 326, 371, 383  
Statistics, for "not detected" results, 157  
Steel, determination of vanadium in, 304  
Steric effects, in complexes, 221, 256  
Storage of reagents, 425  
Strain, caused by traces, 205  
role in x-ray images, 173  
Stress, caused by impurities, 188  
Stress field, 437  
Stripping analysis, 96  
detection limits, 98  
electrode for, 115  
reverse electrolysis in, 100  
Structural defects, survey of, 431  
types of, 6  
Structural interstices, 204  
Structural transformation, 24  
Structure determination, historical survey of, 428  
Structure factors, determination by Pendellösung fringes, 196  
Subboundary geometry, decoration methods for, 465  
Sulfuric acid, storage of, 425  
Superconductors, effects of impurities in, 14  
Surface methods, in dislocation observation, 447  
Surfaces, analysis of, 92, 138, 150, 550  
cleaning of, 424  
properties of, 55

## T

Tantalum, domains in, 527  
Tantalum pentoxide, lattice fringes in, 532  
Tarnish reactions, 30  
Tast polarography, 78  
Tealite, boundaries in, 495  
Tellurium, determination of, 294  
Temperature, effect of flame, 126  
Tensile strength, effect of impurities on, 23  
Tetrahedron technique, for stacking fault energy, 508  
Thermally stimulated currents, analysis by, 63  
Thermoelectric effect, 71  
Thermoelectric power, application of, 73  
Thickness contour, 474  
Tilting method, to determine loop character, 520  
Tin disulfide, oscillatory contrast of, 487  
Titanium, domains in, 527  
Titanium dioxide, transition metals in, 214  
Titration, coulometric, 93  
Topographical methods, in x-ray diffraction, 166  
Topography, two-crystal, 206  
Trace analysis, defined, 152, 552  
function of, 207  
symposium on, 2  
Trace analysis methods, detection limits, 351  
Trace characterization, books on, 2  
definition of, 118  
requirements for, 1, 69  
Trace impurities, in highly perfect crystals, 180  
relation to properties, 7  
Tracer methods, evaluation of, 333  
Tracers, radioactive, 327  
use in research, 334  
Transformation in solids, types of, 24-28  
Transition probabilities, determination of, 131  
Triga reactor, use of, 316

## U

Uranium, determination of, 88  
determination of impurities in, 377

## V

Vacancies, in solids, 26  
 Van de Graff generator, 321  
 Vanadium, determination of, 304  
 Vaporization, losses in, 412  
 Volatilization, in arc, 131  
   separations by, 409  
 Voltammetry, 88, 114

## W

Washing, of laboratory ware, 395  
 Water, analysis of, 303, 421  
   determination of iodine in, 331  
   purification of, 395, 421  
   purity of, 43  
   storage of, 425  
 Whiskers, dislocations in, 467  
   properties of, 21  
 Wurtzite, stacking faults in, 501

## X

X-ray atomic scattering factors, 206  
 X-ray diffraction, camera for, 205  
   detection limits, 206  
   dislocation decoration in, 175  
   impurity effect on, 166, 193  
   relevance to trace characterization, 203  
   stacking faults by, 554  
 X-ray diffraction intensity, effect of  
   impurities on, 191  
 X-ray diffraction topography, assets and  
   limitations of, 199  
   contrast in, 171, 182

  crystal striations by, 188  
   detection limits, 185, 206  
   images in, 173  
   intensity mapping in, 166  
   methods in, 165, 166  
   Moiré patterns in, 189  
   stacking faults by, 179  
   stereo, 178  
   traverse (Lang) topographs, 171  
 X-ray fluorescence spectroscopy,  
   analytical curves in, 141  
   combined with electron microscopy, 540  
   detection limits, 139  
 X-ray intensity measurements, 206, 208  
 X-ray microscopy, terms in, 557  
 X-ray spectra, theory of excitation, 139  
 Xylenol orange, as spectrophotometric reagent, 235

## Y

Yield point, effect of impurities on, 21  
 Yttrium iron garnet, effect of impurities  
   in, 19

## Z

Zinc, determination of copper in, 305  
   loops in, 481, 519  
 Zinc oxide crystal, electron density  
   map of, 195  
 Zinc sulfide, interfaces in, 531  
   stacking faults in, 501  
 Zone melting, separation by, 412  
 Zone refining, resistivity measurement  
   in, 45







